Synthesis and Utilization of Naturally Occurring Functionalized Gamma Amino Acids in the Design of Hybrid Peptide Foldamers

A thesis

Submitted in partial fulfilment of the requirements

Of the degree of

Doctor of Philosophy

By

Anupam Bandyopadhyay

ID: 20083005

Indian Institute of Science Education and Research, Pune

Dedicated to

My family who encouraged me.

CERTIFICATE

This is to certify that the work incorporated in the thesis entitled **"Synthesis and Utilization of Naturally Occurring Functionalized Gamma Amino Acids in the Design of Hybrid Peptide Foldamers"** submitted by Anupam Bandyopadhyay carried out by the candidate at the Indian Institute of Science Education of Research (IISER), Pune, under my supervision. The work presented here or any part of it has not been included in any other thesis submitted previously for the award of any degree or diploma from any other University or institution.

10th December, 2012

Dr. Hosahudya N. Gopi
(Research Supervisor)
Assistant Professor, IISER, Pune
Pune-411008, India

Declaration

I hereby declare that the thesis entitled **"Synthesis and Utilization of Naturally Occurring Functionalized Gamma Amino Acids in the Design of Hybrid Peptide Foldamers"** submitted for the degree of Doctor of Philosophy in Chemistry at Indian Institute of Science Education of Research (IISER), Pune has not been submitted by me to any other University or Institution. This work was carried out at the, Indian Institute of Science Education of Research (IISER), Pune, India under supervision of Dr. Hosahudya N. Gopi.

10th December, 2012

Anupam Bandyopadhyay
ID: 20083005
Senior Research Fellow
Dept. of Chemistry, IISER-Pune
Pune - 411008

Acknowledgements

First of all I want to express my heartfelt sincere profound thanks to my supervisor Dr. Hosahudya N. Gopi in bringing me in the peptide field and pursuing good knowledge concerning peptides and foldamers. As a first Ph. D student, it gives me a great pleasure to express my deep sense of gratitude to my research supervisor for all his advice, guidance, support and encouragement in chemistry and its relevance in biological systems. His tireless enthusiasm was always a source of inspiration. Additionally, I revere his lessons on independent thinking, perfection soft skills and many more in shaping up the researcher in me. I am also thankful to for his valuable suggestions and advice at the time of difficulty on personal matters.

I thank our Director, Prof. K. N. Ganesh, for giving excellent research platform, financial support and facilities that I have been privileged with, during my research here at Indian Institute of science of Science, India. Beside that I gained many novel ideas and enthuse regarding how to become a great researcher at the initial stage when I have joined at IISER-Pune. Additionally, I would like to thank the director for several advices and mental support whenever I met. I am also thankful to the CSIR, India for my 5 years research fellowship. A special vote of thanks would be due for Dr. V. G. Anand and Dr. H. V. Thulasiram for their valuable suggestion in research advisory committee (RAC) meeting. I would like to acknowledge Dr. K. M. P. Raja (Madurai Kamaraj University) for NMR structure modeling, Dr. T. S. Mahesh for helping me with the 2D-NMR experiments, Dr. Kundan Sengupta for providing DLD1 colon cancer cell, and Dr. Rahul Banerjee for several suggestion in solving crystal structure. I am thankful to all the chemistry faculties in IISER-Pune for numerous help.

The research becomes boring if I would not have wonderful lab mates around. I am fortunate to have an excellent blend of talented and exceptional lab mates who can rise in any occasion in their own different way, in addition to being cooperative and helpful. They helped me a lot during my research work in different critical situation. My special thanks to Sachitanand M. Mali (Malia) and Sandip V. Jadhav (Sandy), who extended their moral support for solving my experimental problems in novel way. I also thank my labmates Mothukuri Ganesh Kumar (Gonesh), Shiva Shankar, Sushil N. Benke (Bhau) and Raajkumar Misra (Raz) for several kind of research support. As a new and young group we started work together at NCL Innovation Park (2008). Then we moved Sai Triniy Building (2009), followed by main campus. Always I got their full cooperation to shift my chemical and glass apparatus. The experiences in lab 101 Mandeleev Block (Dr. Gopi's lab) will also remain an unforgettable memory in my research life.

I must acknowledge the help from Puja Lunawat for recording NMR spectra, Archana for X-ray instrumental support, Swati M. Dixit for recording MALDI-TOF/TOF. I am also thankful to Biplab (X-

ray), Abhigyan (Fluorescence), Mahima (flurescence), Dr. Aritnakula (fluorescence microscopy), Somya (NMR), Avishek (NMR), Arvind ji (X-ray), A. V. R. Murthy (AFM), Smita (DLS) and Dr. Sahu (NCL). I am thankful to Naina & Mayuresh for administrative support, Zunjarrao for purchase support.

Further I thank my labmates, my roommate (Soumya), Biplab and Abhigyan for sharing many personal problems andthoughts. My friends (Somya, Biplab and Abhigyan) were always there for me whether I required some serious relaxation with frustrating results at Lab., or any enjoyable occasion. During my stay in HR2 (someswarbadi) cooking together with them at night, occasionally enjoying party with guitar and beer tend me to move forward afresh for good research thought. Also in last 3 years life was cheerful, enjoyable and pleasant with friends like Amar, Mali, Sandip, Murthy, Aurther, Sumanta (NCL), Partha (NCL), Kanika, Arvind, Abhishek, Abhik (Mota), Arindam, Aniruddha(Bio), Biplab (chotka) Sumit, Sohini, Somya (junior), as well as undergraduates Robins, Surojit and Sourav.

The thesis remains incomplete without mentioning the motivation blessings and love of my family. Their love support and credence have strengthened me for all my ventures in different ambits. At this point I would like to mention about the special person in my life Arunima Bandyopadhyay as this thesis would be incomplete if her encouragement, support and above all her patience would not have lingered up till now. She has been and would be my beloved wife, friend and soul mate as we move forward together for perpetuity.

Finally I pray to almighty Lord Shiva and Lord Ganesha, whose blessings made me able to complete the research work and submit this thesis for PhD degree.

Anupam Bandyopadhyay.

Contents

Chapter 1: Synthesis and crystal conformations of α, β-unsaturated γ^4-amino acids (E-vinylogous γ^4-amino acids) and their homooligomers

Chapter 2: Structural investigation of (E)-vinylogous γ-amino acids in hybrid β-hairpin and multi-strand β-sheets

Chapter 4: Synthesis of β-keto γ-amino acids and their Functionalization to coumarin and statin derivatives

Abbreviations

Ac = Acyl

Ac_2O = Acetic anhydride

AcOEt = Ethyl acetate

ACN = Acetonitrile

Ar = Aryl

Bn = Benzyl

Boc = tert-Butoxycarbonyl

$(Boc)_2O$ = Boc anhydride

Bu = Butyl

Bu^i- = Isobutyl

Bu^t- = Tertiary butyl

Calcd. = Calculated

Cbz = Benzyloxycarbonyl

CD = Circular Dichroism

COSY =Correlation spectroscopy

DCC = N, N'-Dicyclohexylcarbodiimide

DCM = Dichloromethane

DiPEA = Diisopropylethyl Amine

DMF = Dimethylformamide

DMP = Dess-Martin periodinane

DMSO = Dimethylsulfoxide

DNA = Deoxyribonucleic acid

EDC = Ethyl-N,N-dimethyl-3-aminopropylcarbodiimide

EtOH = Ethanol

EtOAc = Ethyl acetate

Fmoc = 9-Fluorenylmethoxycarbonyl

Fmoc-OSu = N-(9-Fluorenylmethoxycarbonyloxy) succinimide

g = gram

hrs = hours

HBTU = O-Benzotriazole-N,N,N',N'-tetramethyluronium hexafluorophosphate

HCl = Hydrochloric acid

HOBt = Hydroxybenzotriazol

HPLC = High Performance Liquid Chromatography

IBX = 2-Iodoxybenzoicacid

LAH = Lithium Aluminium Hydride

MALDI-TOF/TOF = Matrix-Assisted Laser Desorption /Ionization – Time of Flight

Me = Methyl

MeOH = Methanol

mg = miligram

min = Minutes

μL = Microliter

μM = Micromolar

mL = milliliter

mM = millimolar

mmol = millimoles

m.p. = Melting Point

MS = Mass Spectroscopy

MSA = Methanesulfonic acid

N = Normal

NHS = *N*-hydroxysuccinimide

NMP = N-methyl pyrrolidone

NMR = Nuclear Magnetic Resonance

NOE = Nuclear Overhauser Effect

PG = Protecting Group

ppm = Parts per million

Py = Pyridine

R_f = Retention factor

RMS = Root Mean Square

ROESY = Rotating Frame NOE Spectroscopy

RT = Room Temperature

TFA = Trifluoroacetic acid

THF = Tetrahydrofuran

TOCSY = TOtal Correlation SpectroscopY

Abstract

Designing synthetic protein structures from non-natural amino acids has immense importance not only to understand the protein folding but also from the perspective of medicinal chemistry. Significant progress has been achieved in this regard using the oligomers of β- and mixed sequences containing α/β hybrid peptides. However, the research in the area of γ^4-peptides containing proteinogenic amino acid side-chains (γ^4-amino acids, double homologated α-amino acids) is lagging behind that of β- and hybrid β-peptides, this in part probably due to the difficulty of obtaining stereochemically pure γ^4-amino acids. In contrast to the saturated γ^4-amino acids, backbone functionalized γ-amino acids such as α, β-unsaturated γ-amino acids, β-keto-γ-amino acids and β-hydroxy γ-amino acids have been frequently found in many biologically active peptide natural products. Inspired by the nature's selection, we explored whether or not these amino acids can be utilized to mimic protein secondary structures. Using these amino acids various secondary and super-secondary structures such as β-sheets, β-hairpins, helices and multi strand β-sheets were designed, synthesized and characterized in both solution and single crystals. Results of this investigation suggests that the α, β-unsaturated γ-amino acids are ideal candidates for the design of β-sheet structures, while the saturated γ-amino acids are found to be ideal for the constructions of helices with expanded H-bond pseudocycles. In contrast to the saturated γ-amino acids, the hybrid peptides containing β-hydroxy- γ-amino acids have showed little distorted helical structures. Further, we assessed the analogy of these hybrid secondary structures with natural protein secondary structures. In addition, the folding rules of the hybrid peptides were outlined. The conformational properties of these hybrid peptides, their folding rules and the analogy with protein structures can be utilized for the design of functional hybrid peptide foldamers.

Publications

1. α/γ^4-Hybrid peptide helices: Synthesis, crystal conformations and analogy with α-Helix. **Bandyopadhyay, A.**; Jadhav, S. V.; Gopi, H. N. *Chem. Commun.* **2012**, *48*, 7170-7072.
2. Hybrid Peptides: Direct Transformation of α/α, β-Unsaturated γ-Hybrid Peptides to α/γ-Hybrid Peptide 12-Helices. **Bandyopadhyay, A.**; Gopi, H. N. *Org. Lett.* **2012**, *14,* 2770-2773.
3. Synthesis and Structural Investigation of Functionalizable Hybrid β-Hairpin. **Bandyopadhyay, A.;** Mali, S. M.; Lunawat, P.; Raja, K. M. P.; Gopi, H. N. *Org. Lett.* **2011**, *13,*4482-4485.
4. A facile transformation of amino acids to functionalized coumarins. **Bandyopadhyay, A.**; Gopi, H. N. *Org. Biomol.Chem.* **2011**, *9,* 8089-8095.
5. Tin(II) chloride assisted synthesis of N-protected γ-amino β-keto esters through semipinacol rearrangement . **Bandyopadhyay, A.;** Agrawal, N.; Mali, S. M.; Jadhav, S. V.; Gopi, H. N. *Org. Biomol.Chem.* **2010**, *8,* 4855-4860.
6. Protein secondary structure mimetics: Crystal conformations of α/γ^4-hybrid peptide 12-helices with proteinogenic side chains and their analogy with α-and β-peptide helices, Jadhav, S. J.; **Bandyopadhyay, A.**; Gopi, H. N. *Org. Biomol. Chem.* **2012**, DOI: 10.1039/C2OB26805A (in press).
7. Thiazole-Carbonyl Interactions: A Case Study Using Phenylalanine Thiazole Cyclic Tripeptides, Mali, S. M.; Schneider, T. F.; **Bandyopadhyay, A.**; Jadhav, S. J.; Werz, D. B.; Gopi, H. N. *Cryst. Growth Des.* **2012**, *12*, 5643-5648.
8. Synthesis of α, β-unsaturated γ-amino esters with unprecedented high (E)-stereoselectivity and their conformational analysis in peptides. Mali, S. M.; **Bandyopadhyay, A.;** Jadhav, S. V.; Kumar, M. G.; Gopi, H. N., *Org. Biomol.Chem.* **2011**, *9,* 6566-6574.
9. A facile synthesis and crystallographic analysis of N-protected β-amino alcohols and short peptaibols. Jadhav, S. V.; **Bandyopadhyay, A.**; Benke, S. N.; Mali, S. M.; Gopi, H. N. *Org. Biomol.Chem.* **2011**, *9,* 4182-4187.

Chapter 1

Synthesis and crystal conformations of α, β-unsaturated γ^4-amino esters (*E*-vinylogous gamma amino esters) and their homooligomers

1.1 Introduction

The stability of protein 3-dimensional structures is fundamentally governed by many non-covalent interactions. Understanding the folding and self-assembly processes of proteins is of paramount importance in the *de novo* design of protein secondary structure elements.[1] Mimicking natural protein secondary structures using artificial molecules that are capable of forming specific and predictable secondary structures offer new possibilities in the field of molecular recognition, catalysis, and protein folding. The *de novo* design of the folded secondary structure from the artificial molecules is also very important from the perspective of designing biologically relevant peptidomimetics as inhibitors for proteases and protein-protein interactions.[2] This endeavour has been elegantly described in the design of the structured peptides from the homologated derivatives of α-amino acids such as β-, and γ-amino acids.[3] In mid 1990's, Seebach and colleagues have initiated a comprehensive and incisive analysis of the stereochemistry of β- and γ-peptide comprising single and double homologated α-amino acids, respectively.[4] At the same time Gellman and colleagues illustrated the crystallographic characterization of folded helical conformations from the homooligomers of *trans*-2-amino cyclopentanecarboxylic acid (ACPC) and *trans*-2-aminocyclohexanecarboxylicacid (ACHC), respectively.[5] Based on the substitution of the side chains, β-amino acids are classified as β^2-amino acids, β^3-amino acids, $\beta^{2,3}$-amino acids, $\beta^{2,2}$-amino acids and $\beta^{3,3}$-amino acids.[4a] In contrast to the naturally occurring α- and 3_{10}-helices, the homooligomers of β^2-and β^3-amino acids have shown to adopt 14-helical conformations. In addition, oligomers of γ^4-amino acids have shown to adopt 14-helical conformations.[4c] The oligomers of cyclic β-amino acids ACPC and ACHC have adopted 12- and 14-helical conformations, respectively. Interestingly, the H-bonding directionality and associated macrodipole of 12-helical and 14-helical conformations by cyclic β-amino acids and γ^4-amino acids respectively are analogous to that of α-peptide helices, while opposite directionality of the H-bonding and the associated macrodipole were observed in the case of 14-helical conformations from oligomers of homologated β-amino acids. In addition various groups have been utilising the different non-natural amino acids and organic templates to design foldamers that mimic the secondary structures of peptides and proteins. Balaram and colleagues reported folding patterns of hybrid peptides containing α- and ω-amino acids (β-, γ- and δ- amino acids).[3e,6] Sharma et al. utilized the carbo β- and γ-amino acids to design the hybrid helical peptides and reported various helical organizations using these amino acids.[7]

Reiser and colleagues explored the utilization of cyclic amino acids in the design of hybrid peptides.[8] Guichard et al. have incorporated urea bonds in the peptides and studied helical conformations.[9] Hamilton and colleagues adopted different strategy to mimic α-helices using non-peptidic organic templates such as Terphenyl, Terpyridine, Diphenylindane, Terephthalamide, Trispyridylamide, Phenylenaminones.[10] The list of selected amino acids and organic templates used in recent past to design foldamers are shown in the Figure 1. Enormous amount of literature is documented in the design of helical peptides using these amino acids and organic templates, however, very few reports are documented regarding the amino acids that favour the formation of β-sheets structures.

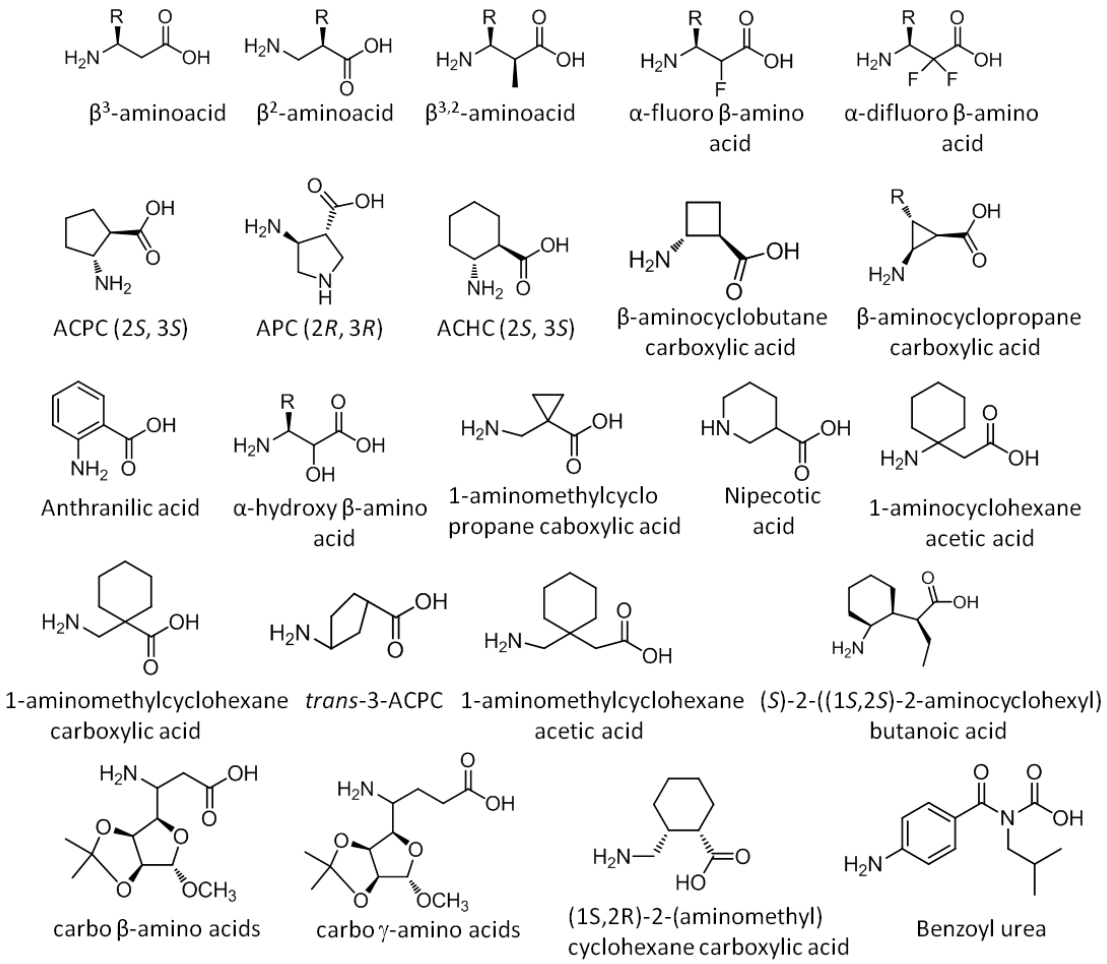

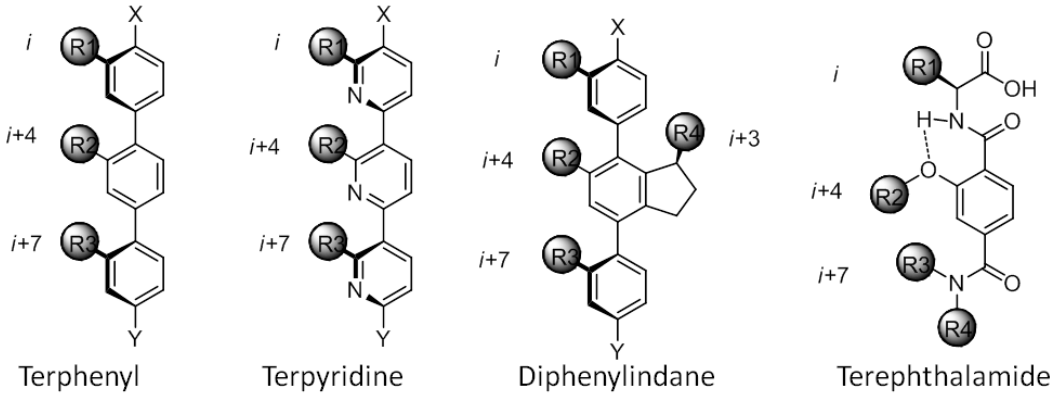

Figure 1: The list of selected amino acids and organic templates used in the design of foldamers.

1.1.1 Naturally occurring vinylogous amino acids and their Biological importance

α, β-Unsaturated γ-amino acids (insertion of –CH=CH– between $C_\alpha H$ and CO of α-amino acids, vinylogous amino acids) are highly versatile non-ribosomal amino acids have been frequently found in many peptide natural products, such as Cyclotheonamide (A, B, C, D, E), Miraziridine A, Gallinamide A (Figure 2).[11] These peptides have been shown as potent inhibitors against many proteases. Cyclotheonamide A and B cyclic peptides isolated from the Japanese marine sponge *Theonella swinhoei* are found to be potent thrombin inhibitor .[11e] These cyclic peptides are containing a vinylogous tyrosine residue, which is involved in binding to the thrombin.[11h] Cyclotheonamides are also found to be strong inhibitors of other trypsin and serine proteases. Schreiber and colleagues described a detailed mechanistic study of Cyclotheonamide A binding to a serine protease, bovine β-trypsin[11f] (Figure 2b). Miraziridine A, another naturally occurring hybrid peptide showed inhibition of the proteolytic activity of trypsin-like serine proteases, papain-like cysteine proteases, and pepsin-like aspartyl proteases.[11c] Gallinamide A isolated from marine cyanobacteria has also been showed as a potential anti-malarial agent.

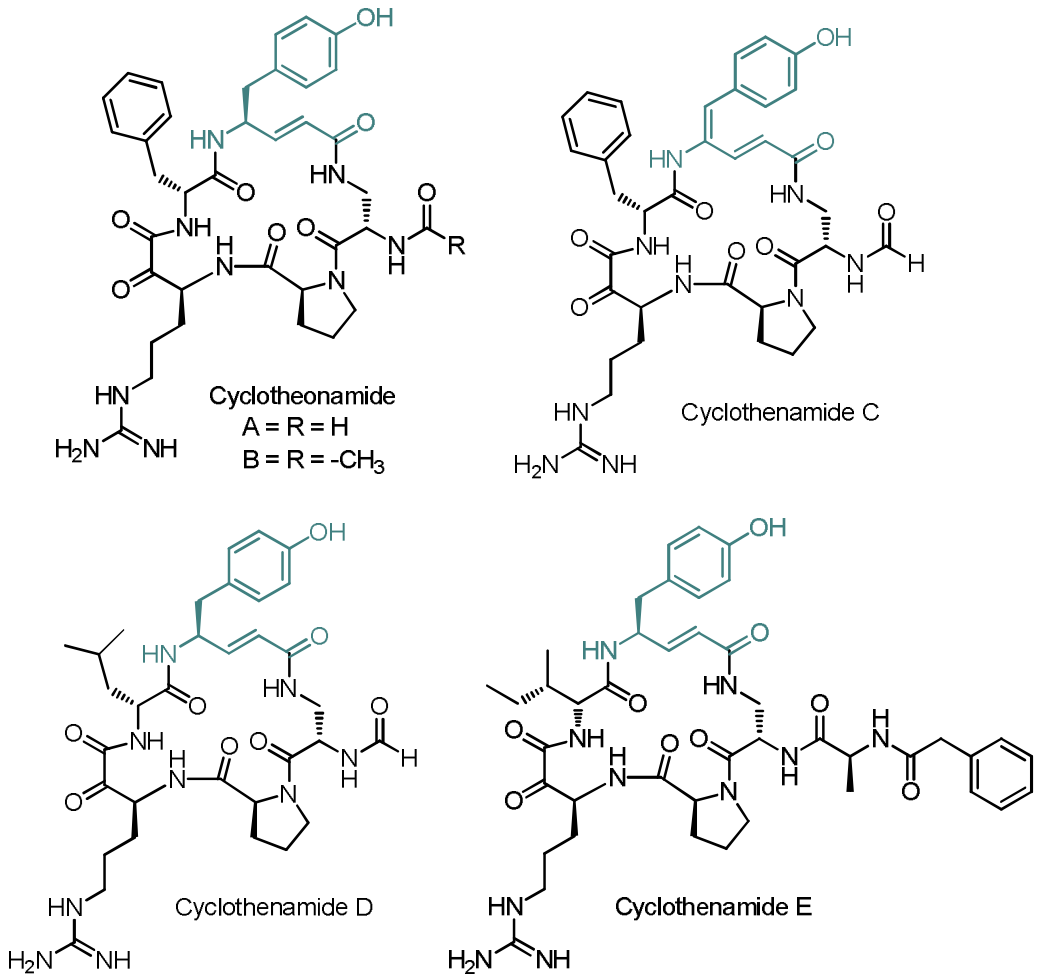
Cyclotheonamide
A = R = H
B = R = -CH3
Cyclothenamide C
Cyclothenamide D
Cyclothenamide E

a)

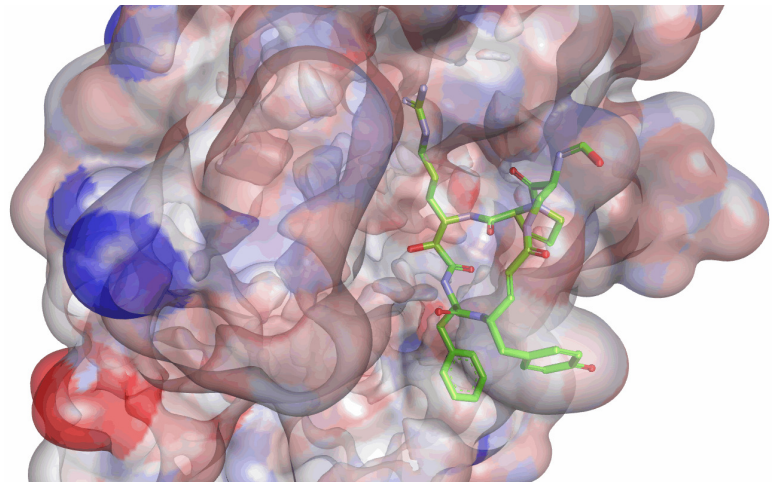

b)

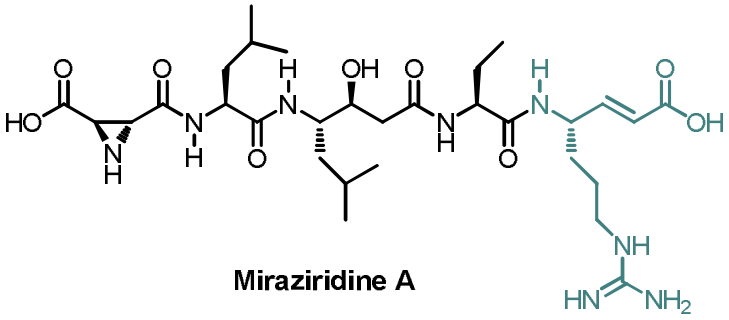

c)

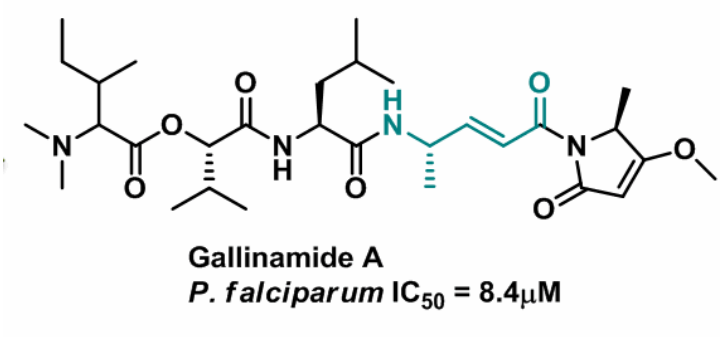

d)

Figure 2: a) The structures of Cyclothanimide derivatives, b) Crystal structure of Trypsin-Cyclotheonamide A Complex (PDB 1TYN), Chemical structures of c) Miraziridine A, d) Gallinamide A.

1.1.2 Peptides containing vinylogous amino acids as protease inhibitors

Inspired by the biological activity of naturally occurring peptides containing vinylogous amino acid residues, various groups have designed synthetic peptides containing vinylogous residues to target serine and cysteine proteases.[12] Peptidic substrates in which the scissile amide carbonyl is replaced by a Michael acceptor were pioneered by Hanzlik and colleagues in 1984.[12a] They have introduced a new class of peptidyl thiol protease inhibitor using vinylogous amino esters (3a).[12b] Further, Kong et al. have shown the potent inactivation of HRV 3C protease using vinylogous glutamine esters[12c] (Figure 3c). In addition, there are many reports of designed Michael acceptor based protease inhibitor and antiviral peptides using vinylogous residue (Figure 3d, e).[12d,e,f]

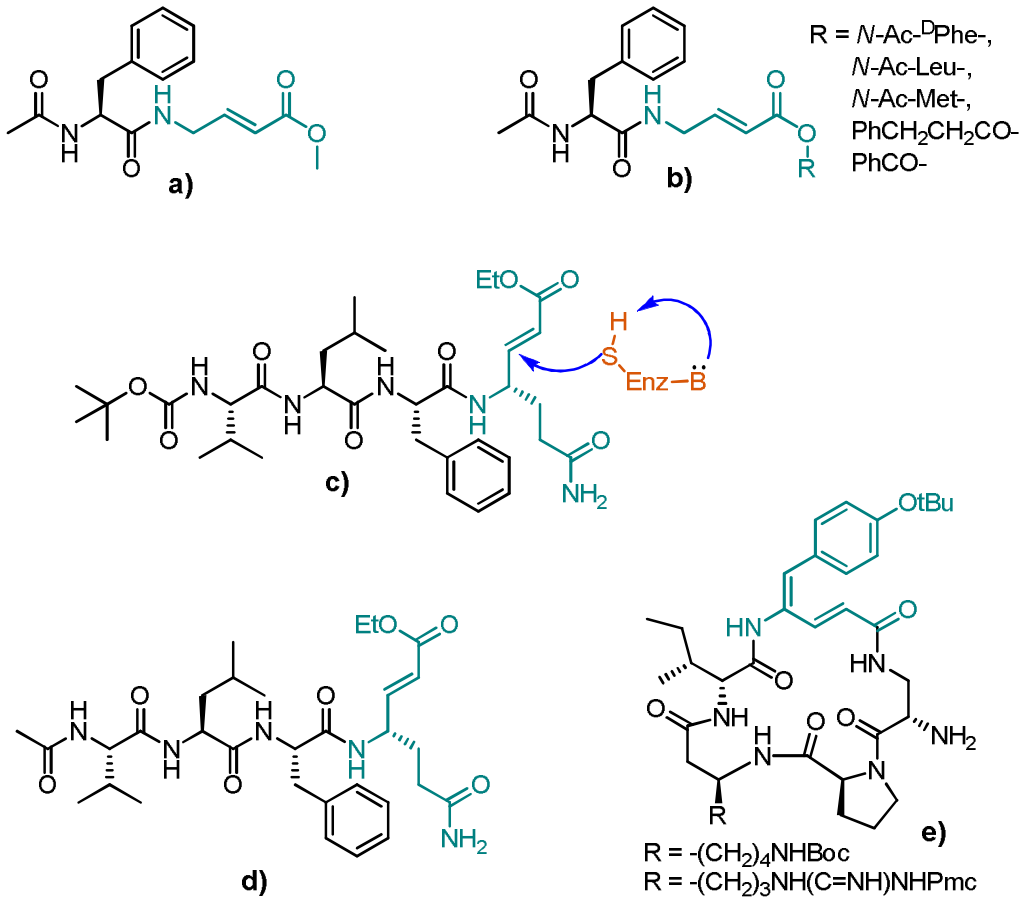

Figure 3: a) Inactivator of Thiol protease, b) Papain inhibitors, c) Michael Acceptor inhibitor of Human Rhinovirus 3C Protease, d) The peptide designed by Webber and co-workers showed antiviral activity,[12d] e) Human β-tryptase inhibitor (analogue of Cyclotheonamide)[12f].

1.1.3 Utilization of vinylogous resides in synthetic organic chemistry

Vinylogous amino acids have been used as starting materials for the synthesis of γ-amino acids[4b,c] as well as substrates in a variety of organic reactions including, 1,4-conjugate addition,[13] epoxidation,[14] and Diels-Alder reaction[15] to develop the functional derivatives of γ-amino acids (Scheme 1).

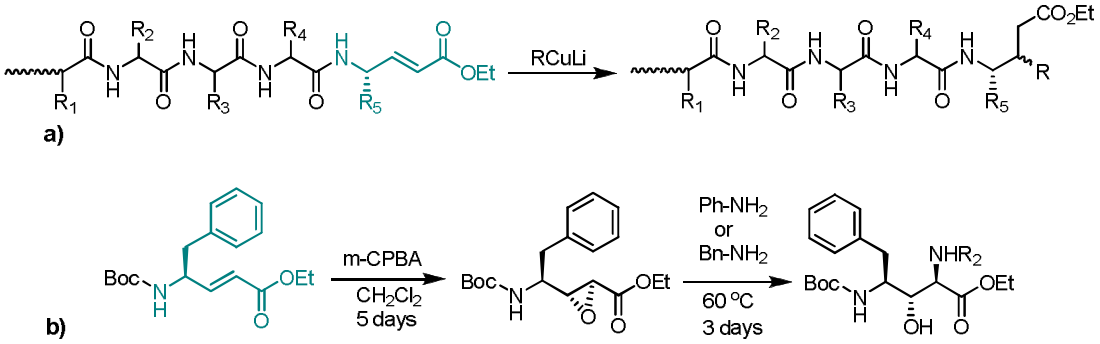

Scheme 1: a) Michael additions with RCuLi occur stereoselectively, depending upon the nature of the R group being transferred and on the configuration of the stereogenic centers along the peptide chain (by Reetz et al.), b) Transformation of vinylogous amino acid to statin (β-hydroxy γ-amino acid) analogue via epoxidation.

1.1.4 Vinylogous amino acids in designing foldamer

In spite of their utilization in the design of biologically active peptides and as starting materials for the synthesis of various γ- and functionalized γ-amino acids, the α, β-unsaturated γ-amino acids have been very little explored in the design of hybrid peptide foldamers. Nevertheless, preliminary work by Schreiber and colleagues gave an insight into the structures (Figure 4) that can be formed by the vinylogous residues. The crystallographic investigation of dipeptides and the hybrid hexapeptide containing *E*-vinylogous residues suggested the formation of parallel β-sheet type of structures and unusual helical type of structure, respectively.[16] Grison et al. reported the β-turn mimetics with a nine-membered hydrogen bond using (*Z*)-vinylogous amino acids.[17] Chakraborty et al. provided the detailed investigation on the utilization of *E*-vinylogous amino acids as revese trun inducers.[18] Recently, Hofmann et al. provided an overview of the helical structures formed by the vinylogous amino acids on the basis of a systematic computational analysis at various levels using ab initio MO theory.[19] These systematic analyses have performed using both *E* and *Z* geometry of the double bonds containing unsubstituted vinylogous amino acids. Theoretical studies suggest that vinylogous residues with (*E*)-double bonds favour helices with larger hydrogen bond pseudocycles starting from 14- up to 27-membered hydrogen-bonds, whereas the (*Z*)-configuration of the double bonds supports a distinct preference of helices with smaller seven- and nine-membered hydrogen bond pseudocycles. The stable helices of the (*E*)-vinylogous peptides with 22-, 24- and 27-membered hydrogen-bonded pseudocycles have

inner diameters as large enough to act as ion channel (Figure 5). Thus, they could be interesting model compounds for the design of membrane channels and monomolecular nanotubes. With this background regarding the structure and the functions of vinyologous residues motivated us to carry out the conformational analysis of vinyologus amino acids and their homooligomers.

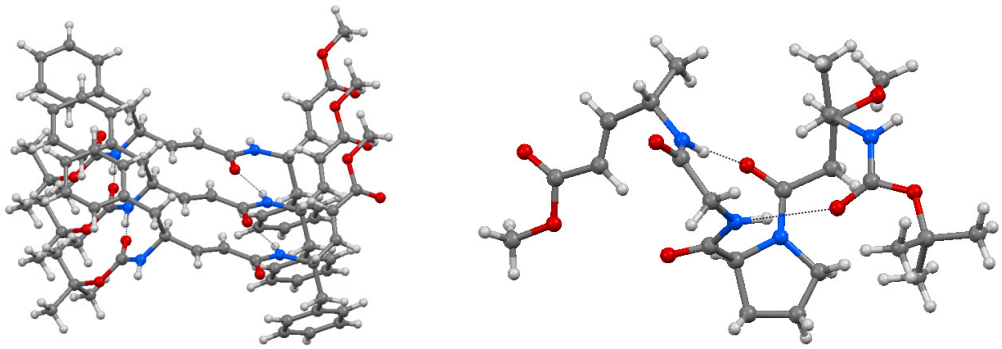

a) **b)**

Figure 4: a) Vinylogous dipeptide (Boc-dgF-dgF-OMe) adopted parallel sheet secondary structure, b) Boc-β-hydroxy γ-Ala-^{D}Pro-Gly-dgA-OMe adopted novel helical sheet structure.

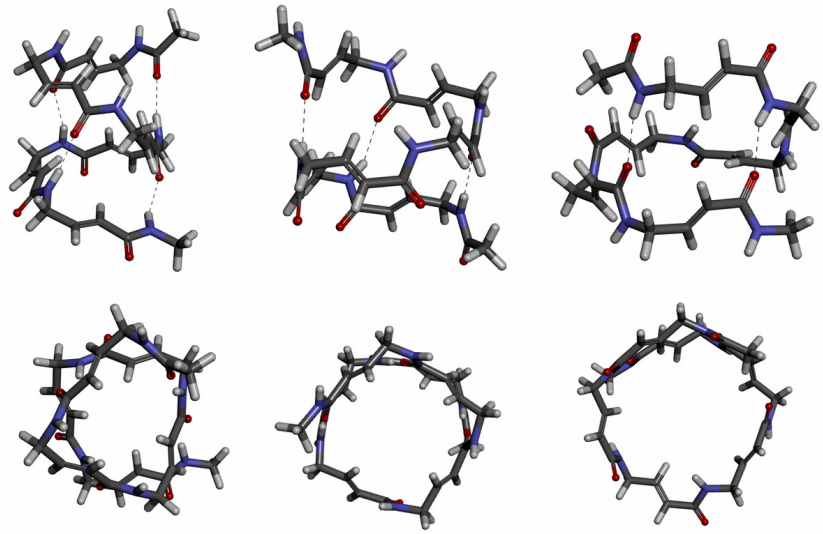

H_{19} H_{22} H_{27}

Figure 5: Most stable helices with hydrogen bonds of (*E*)-vinylogous-peptide hexamers. The structures are created from given co-ordinates in *J. Org. Chem.* **2005**, *70*, 5351 supporting information.

1.1.5 Earlier reports on vinylogous amino acid synthesis

A range of methodologies including Wittig,[20] Julia,[21] Horner-Wadsworth-Emmons reaction,[22] and Peterson[22] olefination have been reported for the synthesis of α, β-unsaturated esters. However, Horner-Wadsworth-Emmons reaction (Scheme 2), a variant of Wittig reaction has been extensively utilized for the synthesis of vinylogous amino acids.[4b,c, 24] In this reaction, alkali metal bases such as BuLi and NaH are commonly used to generate the reactive metalated phosphonate intermediate and to achieve the high levels of stereoselectivity, reactions are also performed in the presence of metal salts and organic bases.[25] Seebach and co-workers reported the synthesis of methyl esters of *N*-Boc-protected α, β-unsaturated γ-amino acids with the *E/Z* ratio of 3:1 to 7:1 *via* Horner-Wadsworth-Emmons reaction using NaH as a base.[4b,c] Grison and colleagues used Horner reagents as starting materials for the stereoselective synthesis of *E* and *Z* vinylogous amino acids.[17] To achieve the major *E*-selectivity, lithiated dianion derivative of 2-diethylphosphonopropanoic acid has been used, while *Z*-stereoselectivity has been achieved by KH/ethyl 2-bis(trifluoroethyl)-phosphonopropanoate or BuLi/ethyl 2-diethyl phosphonopropanoate. However, these procedures may not be compatible for the synthesis of vinylogous amino acids containing commonly used base labile Fmoc-protecting group.

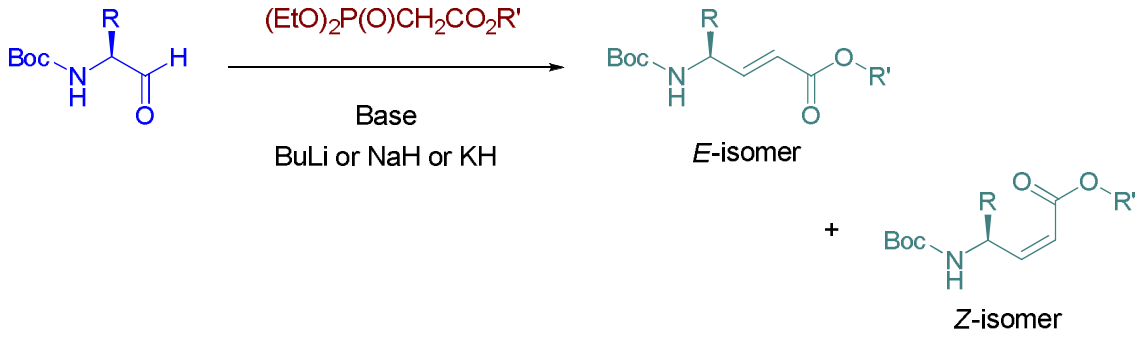

Scheme 2: Schematic representation of popular Horner-Wadsworth-Emmons reaction for synthesis of Vinylogous amino acids.

1.2 Aim and rationale of the present work

The naturally occurring and synthetic peptides containing α, β-unsaturated γ-amino acids have been utilized in a variety of biological applications. However, there is no detailed investigation regarding the conformations of these amino acids and the peptides containing these amino acids. The encouraging biological activities along with the functionalizable backbone double bonds motivated us to investigate the conformational properties of *E*-vinylogous amino acids and oligomers of these amino acids. In addition we would like to investigate the influence of the electronic effects on the conformations of the vinylogous amino acids.

Herein, we are reporting the synthesis of α, β-unsaturated γ-amino esters starting from the *N*-protected amino aldehydes using Wittig reaction with exceptional high *E*-selectivity and single crystal conformations of vinylogous amino ester, [(*S*, *E*)-ethyl 4-(tert-butoxycarbonylamino)-5-phenylpent-2-enoate (Boc-dgPhe-OEt or vinylogous phenylalanine)], solution [circular dichroism (CD) and 2D NMR (TOCSY, ROESY and COSY)] and crystal conformations of di and tripeptides. Further, we have assessed secondary structures adopted by vinylogous oligomers with natural α-peptide secondary structures.

1.3 Results and Discussion

1.3.1 Synthesis of *N*-Boc-α, β-unsaturated γ-amino esters (dgX)

As a part of our investigation to understand the structural features of vinylogous peptides, we sought to utilize the Wittig reaction, since the target vinylogous amino acids can be obtained at neutral conditions and it can be compatible with a variety of *N*-protecting groups including base labile Fmoc- group. To understand the efficacy and the stereochemical output of the Wittig reaction in the synthesis of vinylogous amino acids, initially, the Boc-alanal was subjected to the olefination reaction using the ylide, ethyl (triphenylphosphoranylidene)acetate in dry THF at room temperature. The Schematic representation of the synthesis is shown in Scheme 3. The Boc-amino aldehyde was synthesized from the LAH (Lithium aluminium hydride) reduction of the corresponding

Weinreb amide and subjected immediately to the Wittig reaction.[26] The corresponding Weinreb amide of amino acid was synthesized from the DCC mediated coupling reaction using Boc-Ala-OH and Weinreb amide hydrochloride in the presence of diisopropyl ethyl amine (DiPEA).

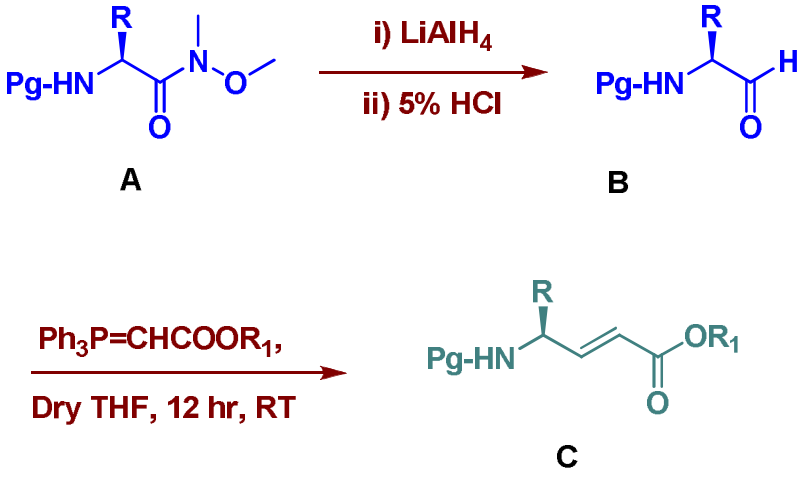

Scheme 3: Synthesis of α, β-unsaturated γ-amino acid esters using Wittig reaction.

Surprisingly, the analysis of the crude product reveals no trace of *Z* product in the reaction and 100% *E*-isomer (**1C**) was isolated in high yield (93%). Further, using same protocol various Wittig products (**2C-5C**) were isolated in high yields (>80%). The list of *E*-vinyologus amino acids isolated from the Wittig reaction is given the Table 1. Though it has been reported that the *E*- double bond is a major product in a verity of Wittig reactions, we are surprised to see unprecedented *E*-selectivity in the synthesis of vinylogous amino acids. All Wittig reactions of Boc-amino aldehydes proceeded very smoothly at room temperature in THF.

Table1: Synthesis of *N*-Boc-α, β-unsaturated γ-amino esters (dgX) using Wittig reaction

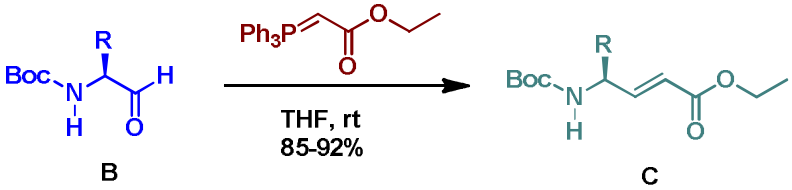

Entry	Aldehyde(B)	Product (C)	Yield (%)
1	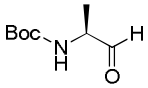	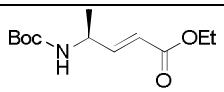 Boc-dgA-OEt	93
2	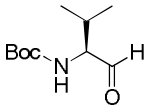	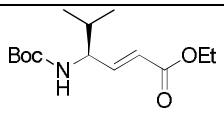 Boc-dgV-OEt	90
3	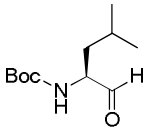	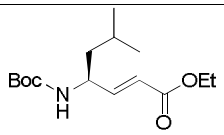 Boc-dgL-OEt	95
4	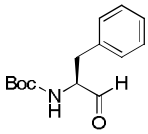	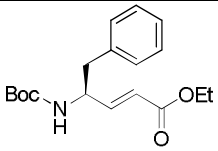 Boc-dgF-OEt	88
5	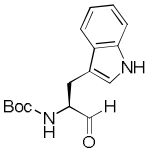	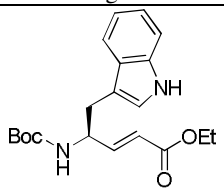 Boc-dgW-OEt	80

1.3.2 Crystal structure analysis of Boc-dgPhe-OEt

Out of all (*E*)-vinylogous amino esters in the Table 1, Boc-dgF-OEt (**4C**) was crystallized after slow evaporation of methanol solution at temperature ~ 23 ^{o}C. The crystal structure is shown in Figure 6a. The local conformation of these vinylogous residues were determined by introducing the additional torsional variables (Figure 6b) θ_1 (N-C$^{\gamma}$-C$^{\beta}$-C$^{\alpha}$) and θ_2 (C$^{\gamma}$-

$C^{\beta}=C^{\alpha}$-C) as described by the Hofmann and colleagues.[19] Crystal structure analysis of Boc-dgF-OEt (**4C**) reveals that θ_1 (125°), θ_2 (177°) and ψ (-170°) adopted extended conformation, where as ϕ (-80°) adopted semi extended conformation.

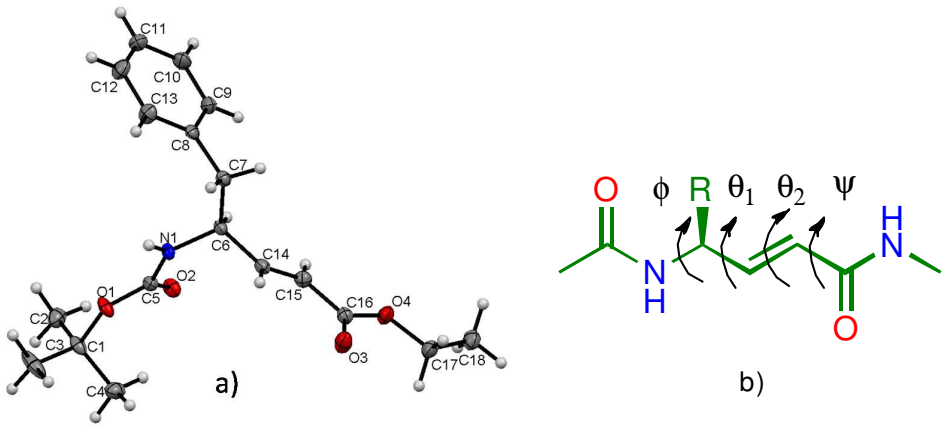

Figure 6: a) ORTEP diagram of Boc-dgPhe-OEt. Hydrogens are not labelled for clarity. b) Torsional variables for vinylogous amino acid.

1.3.3 Design and Synthesis of dipeptides

After understanding the single crystal conformation of *E*-vinylogous amino ester, we synthesized three dipeptides Boc-dgV-dgA-OEt (**P1**), Boc-dgV-dgL-OEt (**P2**) and Boc-dgF-dgA-OEt (**P3**) in solution phase to understand the conformations of *E*-vinylogous residues in peptides. The dipeptide Boc-dgV-dgA-OEt (**P1**) was synthesized by coupling of Boc-dgV-OH (vinylogous acid) and the free amine of Boc-dgA-OEt (**1C**) obtained after the saponification and the Boc-deprotection, respectively. The coupling reaction was mediated by HBTU (Scheme 4). The pure peptide **P1** was isolated in good yield after the silica gel column chromatography. By utilizing the same protocol peptide **P2** and **P3** were synthesized and purified.

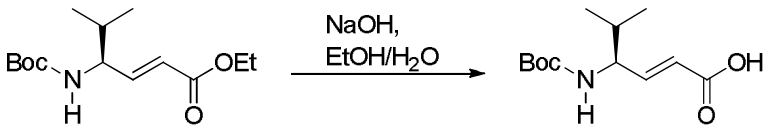

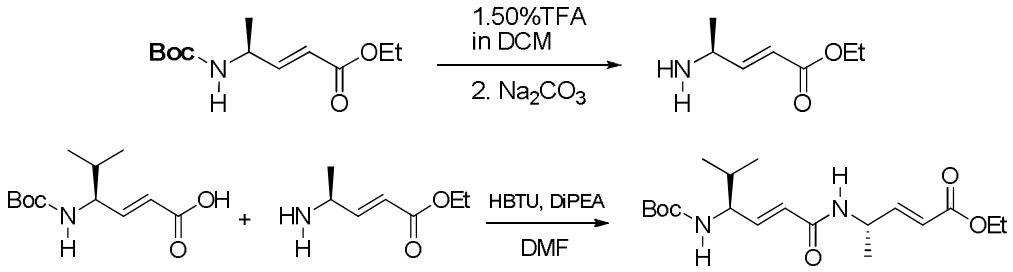

Scheme 4: Synthesis protocol of Boc-dgV-dgA-OEt (**P1**)

1.3.4 Crystal structure analysis of Boc-dgV-dgA-OEt (P1)

We have put efforts to crystallize all three dipeptides, out of them **P1** was crystallized after the slow evaporation of methanol solution. The X-ray structure of **P1** is shown in Figure 7a. Interestingly, the dipeptide adopted a β-sheet type of character in the crystal structure. No intramolecular H-bonds were observed in the peptide. Inspection of the torsional angles reveals that the molecule adopted an extended conformation similar to the amino acid dgF. The torsional values of the peptide are given in the Table 2. The analysis of crystal structure reveals that the dipeptide molecules are held together by two intermolecular H-bonding between the C=O and NH groups with N-H···O distances 2.035Å (N1H···O2) and 2.18Å (N2H···O3) with N-H···O angles 153° and 174°, respectively (Figure 7b). In addition, the dipeptide **P1** self-assembled into an infinite parallel β-sheet type of structure in the crystal packing mediated by the intermolecular H-bonds.

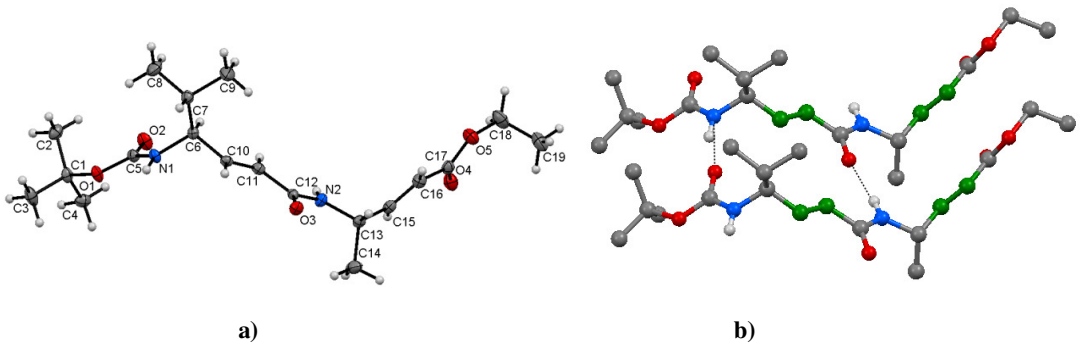

a) **b)**

Figure 7: a) ORTEP diagram of Boc-dgV-dgA-OEt (**P1**). Hydrogens are not labelled for clarity, b) Self-assembled parallel β-sheet structure exhibited by Boc-dgV-dgA-OEt (ball and stick model).

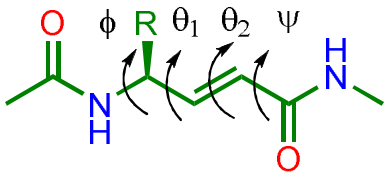

Table 2: Torsional variables (in deg) of Boc-dgV-dgA-OEt

Resd.	**φ**	**θ_1**	**θ_2**	**ψ**	**ω**
dgV	-125	116	176	176	174
dgA	-155	105	-179	170	-

1.3.5 Design and Synthesis of tripeptides and tetrapeptide

With these exciting results from the dipeptide **P1**, we further synthesized tri- and tetrapeptides to understand the conformational properties in higher ordered peptides. In addition, we would like to investigate whether helical type of structures can be induced in higher ordered peptides with intramolecular H-bonding. Two tripeptides Boc-dgV-dgA-dgL-OEt (**P4**), Boc-dgV-dgA-dgF-OEt (**P5**) and a tetrapeptide Boc-dgV-dgA-dgL-dgF-OEt (**P6**) were synthesized by solution phase method. The tripeptides were synthesized using 2+1 convergent strategy, while tetrapeptide was synthesized using 3+1 convergent strategy. In the case of tripeptides, the dipeptide Boc-dgV-dgA-OEt (**P1**) was hydrolysed and Boc-dgV-dgA-OH acid was coupled with the free amine of Boc-dgL-OEt (**3C**) and Boc-dgF-OEt (**4C**) to give tripeptides Boc-dgV-dgA-dgL-OEt (**P4**) and Boc-dgV-dgA-dgF-OEt (**P5**), respectively. The coupling reactions were mediated by HBTU (Scheme 5). After completion of reaction, the reaction mixture was diluted with ethyl acetate and immediately the peptides were separated as white precipitates from the reaction mixture indicating the formation of self-assemblies similar to the dipeptide **P1**, however, both peptides **P4** and **P5** are soluble in methanol. The white precipitate in the ethyl acetate layer was isolated after filtering through the sintered funnel. Further white powder was confirmed as expected peptide using 1H NMR (in $CDCl_3$) and MALDI-TOF/TOF mass.

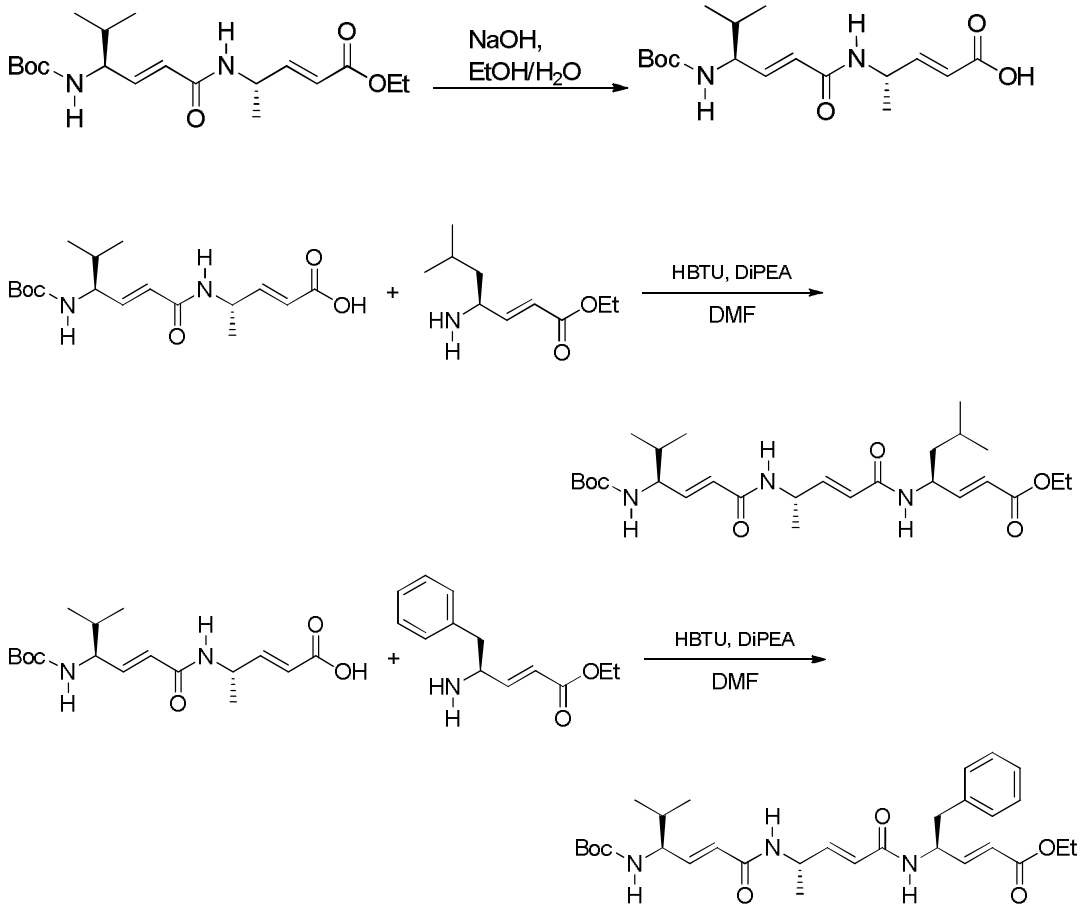

Scheme 5: Synthesis of tripeptides Boc-dgV-dgA-dgL-OEt (**P4**) and Boc-dgV-dgA-dgF-OEt (**P5**).

The tetrapeptide Boc-dgV-dgA-dgL-dgF-OEt (**P6**) was synthesized using 3+1 convergent strategy similar to the tripeptides. The Boc-dgV-dgA-dgL-OH (acid) was coupled to the free amine of Boc-dgF-OEt (**4C)** (Scheme 6) mediated by the coupling reagent HBTU. Instructively, white precipitate was observed within 30 min. After 3 hrs the white precipitate was collected after filtering through the sintered funnel. The peptide was confirmed by NMR and MALDI-TOF/TOF analysis. In contrast to the tripeptides **P4** and **P5**, peptide **P6** was sparingly soluble in methanol; however, it is completely soluble in DMF, DMSO and $CHCl_3$. Due to solubility problem, we are unable to extend synthesis of homooligomers beyond 4-residues of vinylogous amino acids.

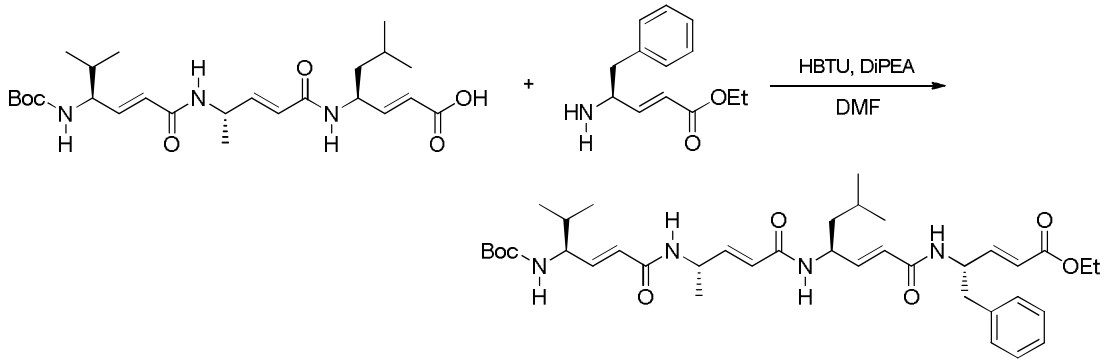

Scheme 6: Schematic diagram of tetrapeptide synthesis Boc-dgV-dgA-dgL-dgF-OEt (**P6**)

1.3.6 Crystal conformation analysis of P4 and P5

After slow evaporation of methanol solution, both tripeptides **P4** and **P5** yielded the single crystals suitable for X-ray diffraction. The crystal structures of **P4** and **P5** are shown in Figures 8 and 9. Instructively, no intramolecular H-bonds were observed in both peptides. The analysis of the X-ray structure of **P4** reveals that it adopted a β-sheet character. The torsion angles of **P4** are given in the Table 3. The residue dgV1 adopted a semi-extended conformation by having the ϕ value – 94°, however, the other torsion variables θ_1, θ_2 and ψ adopted extended conformations by having the values 109°, -176° and 167°, respectively. The second residue dgA2 adopted fully extended conformation by having the torsional values -116°, 113°, -179° and 165° for ϕ, θ_1, θ_2 and ψ, respectively. In case of dgL3, surprisingly, θ_1 is having value 0°, deviating from the β-sheet structure. However, the other torsional

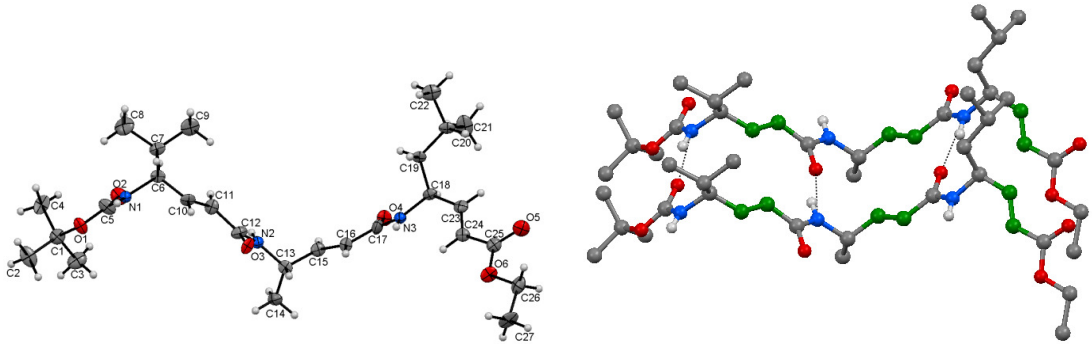

a) **b)**

Figure 8: a) ORTEP diagram of Boc-dgV-dgA-dgL-OEt. Hydrogens are not labelled for clarity, b) Self-assembled parallel β-sheet structure exhibited by Boc-dgV-dgA-dgL-OEt.

variables ϕ, θ_2 and ψ display the extended conformations. Inspection of the crystal structure reveals that the two tripeptide molecules of **P4** are held together by three intermolecular H-bonds. The H-bond parameters are tabulated in the Table 4. Overall the molecule is adopting parallel β-sheet type of structure stabilized by three intermolecular H-bonds.

In case of peptide **P5,** two different molecules were observed in asymmetric unit (Figure 9a) with slight variation in the torsional values. The analysis of the crystal structure reveals that one molecule adopted fully extended conformation, whereas another molecule adopted partially extended conformation by taking the torsional value θ_1 of dgF3 close to 0°. The torsional values of all vinylogous residues are given in the Table 3. Further, similar to the **P4** three intermolecular H-bonds were observed between the two tripeptide molecules. The H-bond parameters are tabulated in the Table 4. Instructively, both peptide molecules adopted a β-sheet character in the crystal structure. Further, crystal structures of **P4** and **P5** suggest that they self-assembled into infinite parallel β-sheet structures by three intermolecular H-bonding (Figure 9c). We tried to crystallize tetrapeptide **P6** in various combinations of solvents; however, we could not get the single crystals suitable for X-ray diffraction.

As **P1**, **P4** and **P5** have shown the β-sheet type of characters in single crystals, we subjected peptide **P4** to the solution structure analysis using 2D NMR to understand whether or not these peptides have same β-sheets character in solution.

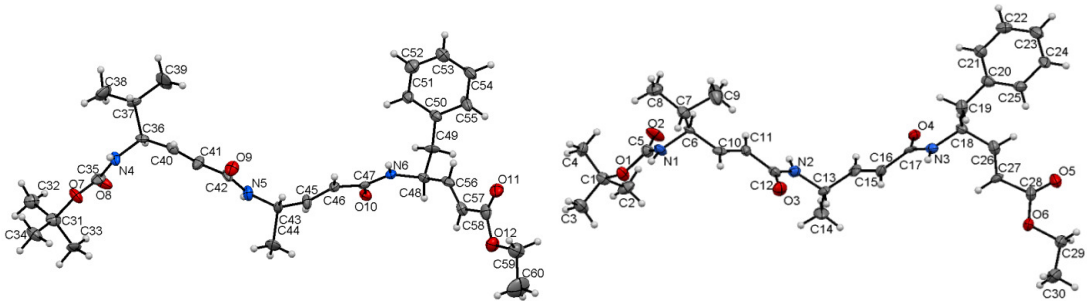

a)

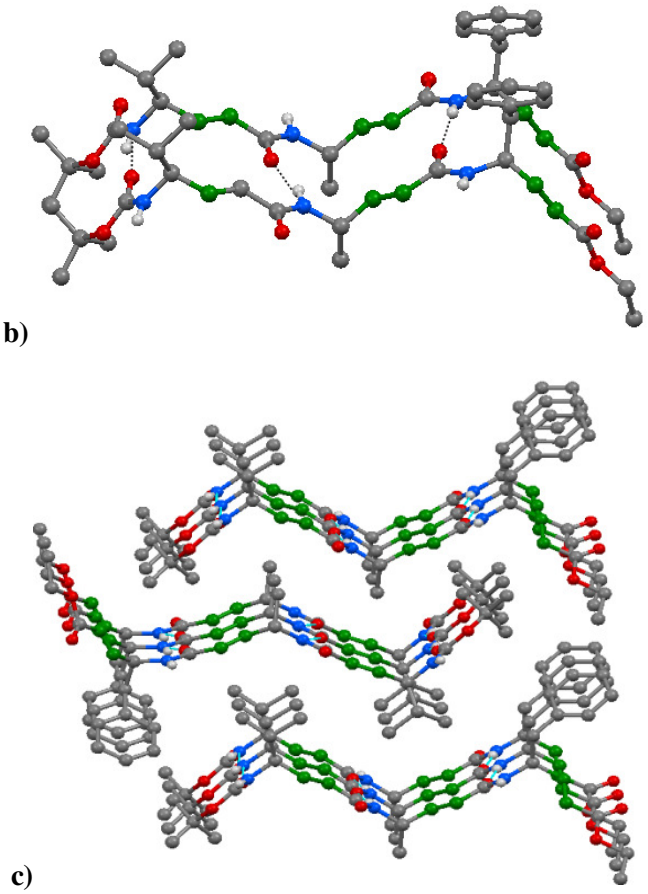

Figure 9: a) ORTEP diagram of Boc-dgV-dgA-dgF-OEt. Hydrogens are not labelled for clarity; two molecules are present in asymmetric unit, b) Self-assembled parallel β-sheet structure exhibited by Boc-dgV-dgA-dgF-OEt, c) Crystal packing.

Table 3: Torsional variables (in deg) of Boc-dgV-dgA-dgL-OEt (**P4**) and Boc-dgV-dgA-dgF-OEt (**P5**)

Pept.	Resd.	φ	θ_1	θ_2	ψ	ω
P4	dgV	-94	109	-176	167	179
	dgA	-116	113	-179	165	-168
	dgL	-141	0	-179	177	-
P5*	dgV	-101(-118)	114	-179(-175)	168(170)	-180(-179)
	dgA	-118(-134)	121(124)	-179(171)	169(-168)	-180(167)
	dgF	-109(-149)	-13(106)	-179(179)	173(171)	-

*two molecules are present in asymmetric unit.

Table 4: Hydrogen-Bond Parameters in Peptides Boc-dgV-dgA-dgL-OEt (**P4**) and Boc-dgV-dgA-dgF-OEt (**P5**)

Pept.	Donor (D)	Acceptor (A)	D···A (Å)	D-H···A (Å)	∠N-H···O (deg)	∠N···C=O (deg)
P4	N1(x,y,z)	O2(x,-1+y,z)	2.94	2.11	161.8	168
	N2(x,y,z)	O3(x,1+y,z)	2.87	2.05	156.5	165.8
	N3(x,y,z)	O4(x,-1+y,z)	3.04	2.20	168.2	175.6
P5*	N1(x,y,z)	O2(-1+x,y,z)	2.79	2.02	147.3	166.4
	N2(x,y,z)	O3(1+x,y,z)	2.89	2.03	177.0	175.1
	N3(x,y,z)	O4(-1+x,y,z)	2.95	2.10	173.4	170.2
	N4(x,y,z)	O8(-1+x,y,z)	2.75	1.95	154.6	168.8
	N5(x,y,z)	O9(1+x,y,z)	3.04	2.20	164.8	165.8
	N6(x,y,z)	O10(-1+x,y,z)	2.99	2.15	164.8	170.8

*two molecules are present in asymmetric unit.

1.3.7 Solution structures of P4 and P5

The 2D-NMR (TOCSY and ROESY) of **P4** in $CDCl_3$ were recorded at 300 K. The TOCSY spectrum of **P4** is shown in Figure 10a. Using sequential interactions of protons in the TOCSY spectrum, the vinylogous residues were indentified. Interestingly, the residues are positioned in the increasing order along the down field shift. The partial ROESY spectrum (NH-$C^{\gamma}H$, $C^{\gamma}H$-$C^{\beta}H/C^{\alpha}H$) of **P4** is given in the Figure 10b and 10c. All spatial interactions of protons observed in the ROESY spectrum were identified. Interestingly, no long range NOEs were observed. The critical NOEs observed in the ROESY spectrum are illustrated in the schematic diagram shown in Figure 10d. The characteristic sequential NH↔$C^{\alpha}H$ strong NOEs (blue colour) (Figure 10d) suggest that **P4** adopting an extended conformation in solution.

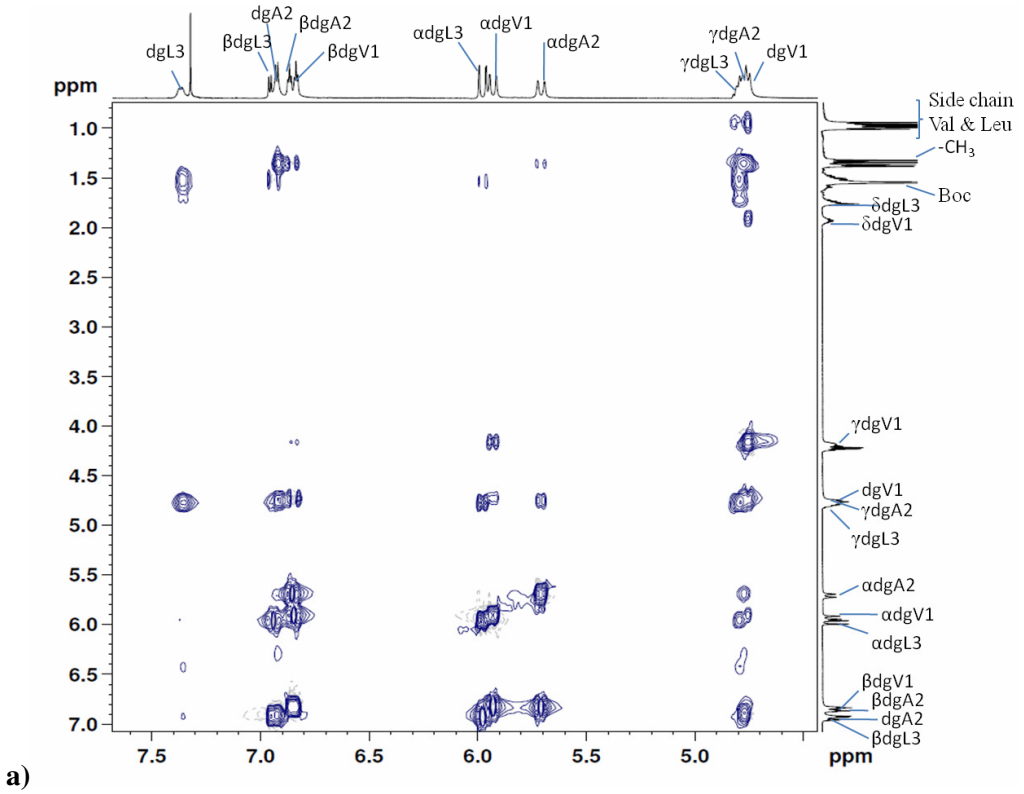
dgL3
dgA2
βdgA2
βdgL3
βdgV1
αdgL3
αdgV1
αdgA2
γdgA2
γdgL3
dgV1
Side chain
Val & Leu
-CH3
Boc
δdgL3
δdgV1
γdgV1
dgV1
γdgA2
γdgL3
αdgA2
αdgV1
αdgL3
βdgV1
βdgA2
dgA2
βdgL3
ppm

a)

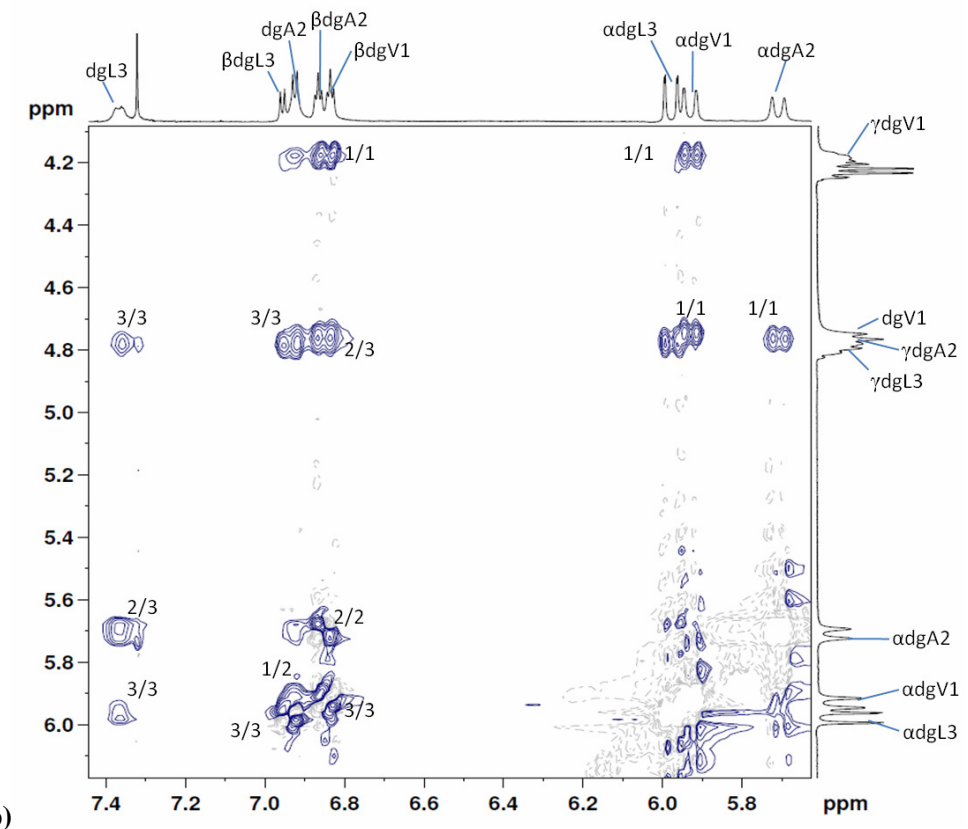
dgL3
dgA2
βdgA2
βdgL3
βdgV1
αdgL3
αdgV1
αdgA2
γdgV1
dgV1
γdgA2
γdgL3
αdgA2
αdgV1
αdgL3
1/1
3/3
2/3
2/2
1/2
ppm

b)

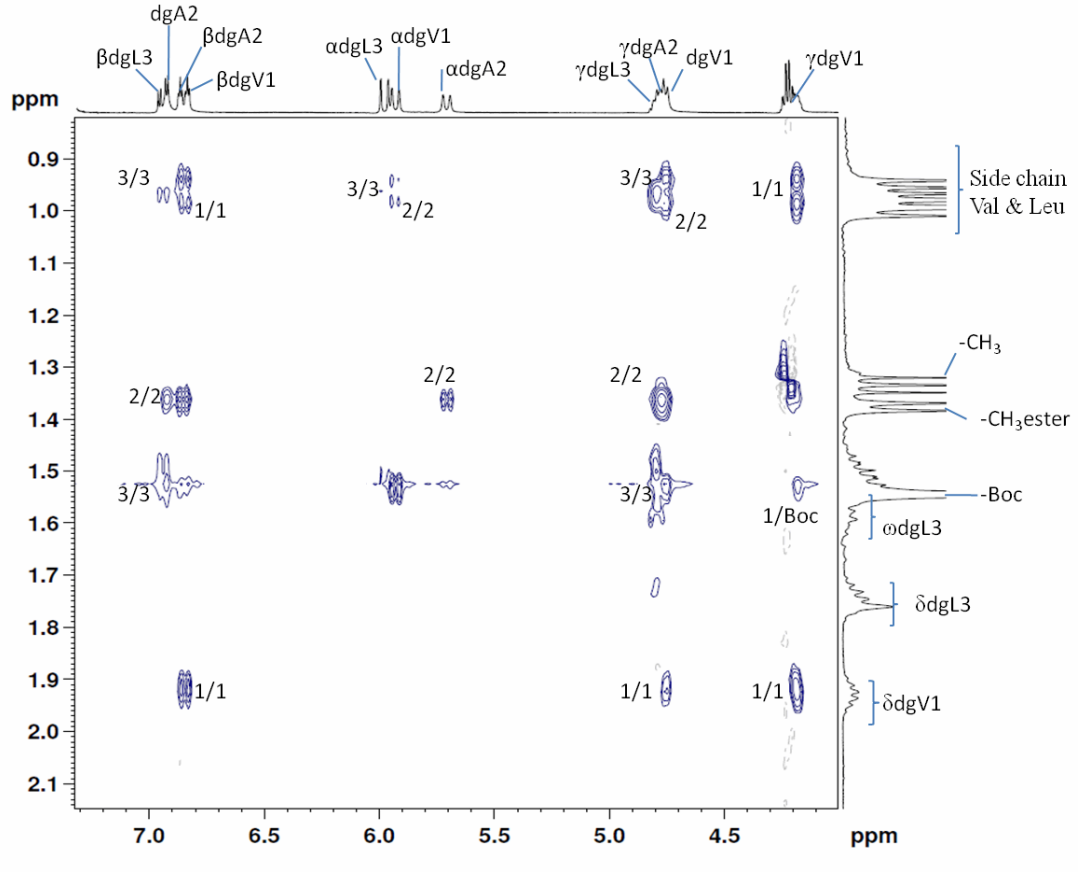

c)

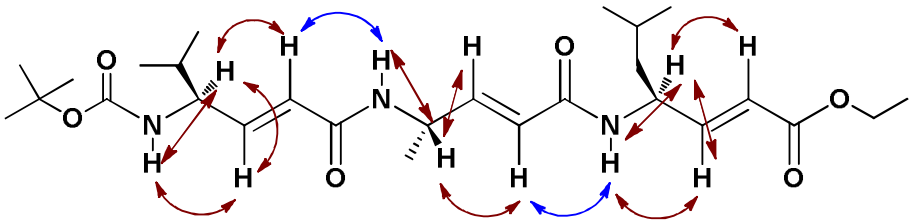

d)

Figure 10: a) TOCSY NMR spectrum of **P4** in $CDCl_3$. The sequential assignments of amino acids were performed using ROESY, b) Partial ROESY spectrum of **P4** showing sequential NOEs of NH↔ $C^{\alpha}H$, NH↔ $C^{\beta}H$, NH↔ $C^{\gamma}H$, $C^{\beta}H$ ↔ $C^{\gamma}H$ and $C^{\beta}H$ ↔ $C^{\alpha}H$, c) $C^{\alpha}H$↔Side chain, $C^{\beta}H$↔ Side chain and $C^{\gamma}H$↔ Side chain, d) Observed NOEs from ROESY spectrum of Boc-dgV-dgA-dgL-OEt (**P4**).

Further, to understand whether these peptides are self-assembled to parallel β-sheet (or anti parallel β-sheet) type of structures in solution, we subjected **P4** for gradual dilution experiments. The partial ^{1}H NMR spectra with gradual dilution with $CDCl_3$ is shown in Figure 11. Instructively, gradual upfield shift of amide proton with continuous dilution of **P4** with $CDCl_3$ was observed. These results suggest that the self assembling nature of **P4** β-sheet structures in solution.

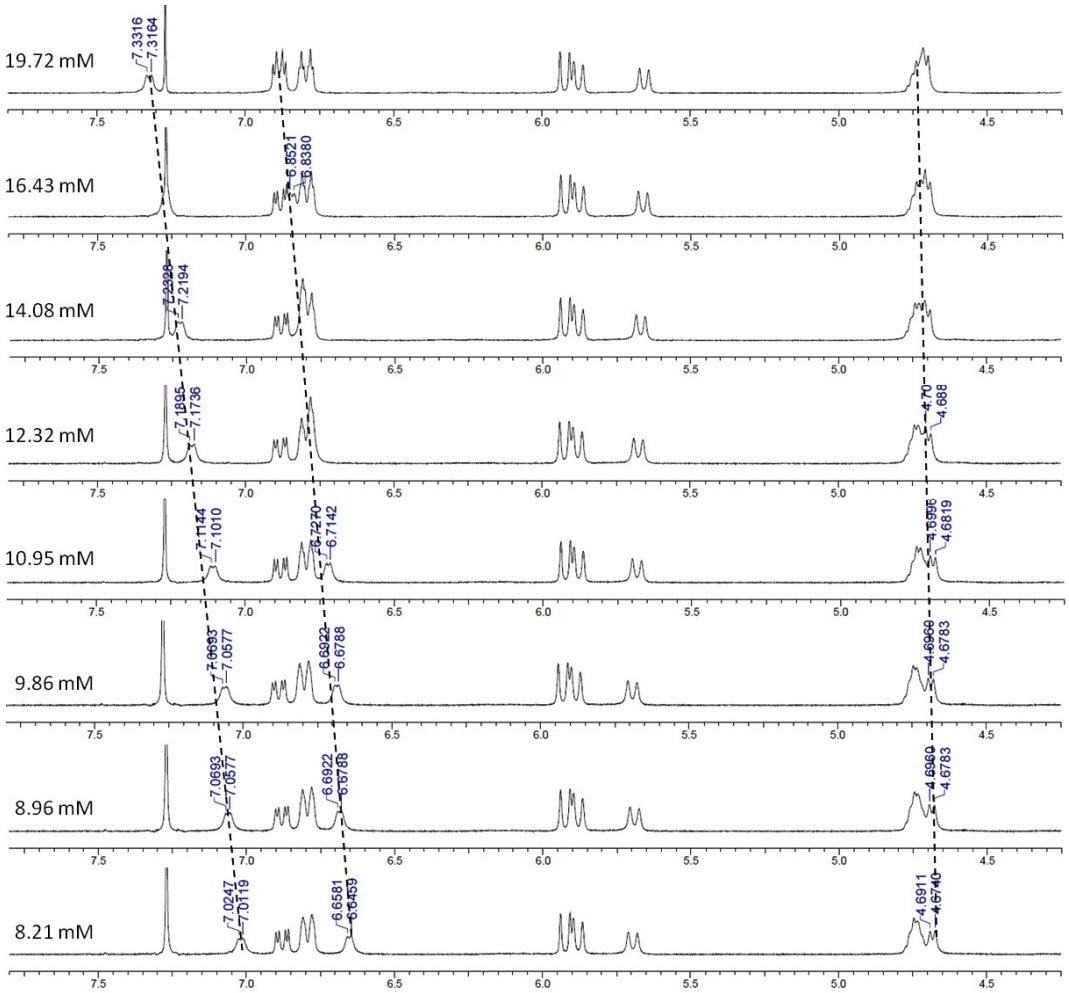

Figure 11: The partial ^{1}H-NMR spectra of Boc-dgV-dgA-dgL-OEt (**P4**), recorded with gradual dilution. The concentration is mentioned with each spectrum on the left side.

In order to investigate the conformations adopted by the tetrapeptide **P6,** we recorded the 2D NMR in $CDCl_3$. Partial TOCSY spectrum of **P6** is shown in Figure 12a. Using sequential proton interactions of TOCSY, all vinylogous residues were identified. Partial ROSEY spectrum of **P6** (NH-$C^{\gamma}H$, $C^{\gamma}H$-$C^{\beta}H/C^{\alpha}H$) is shown in Figures 12b and 12c. The critical NOEs observed in the ROESY spectrum are illustrated in the schematic diagram shown in Figure 12d. The characteristic sequential NH↔$C^{\alpha}H$ strong NOEs (blue colour) (Figure 12d) and absence of NH↔NH NOEs authenticate the adaptation of an extended sheet conformation by **P6**. There are no characteristic NOEs observed in spectrum which support helical or reverse turn conformation in **P6**.

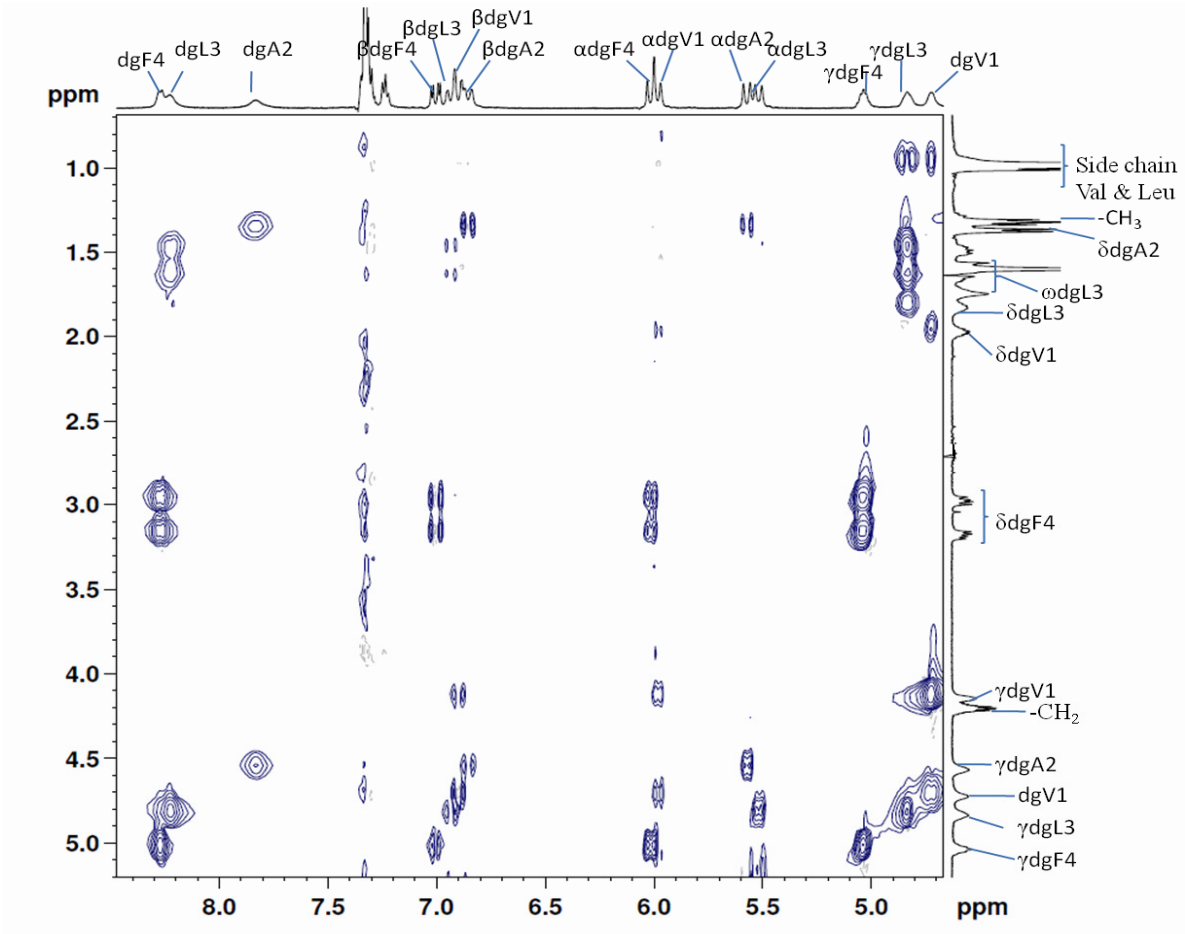

a)

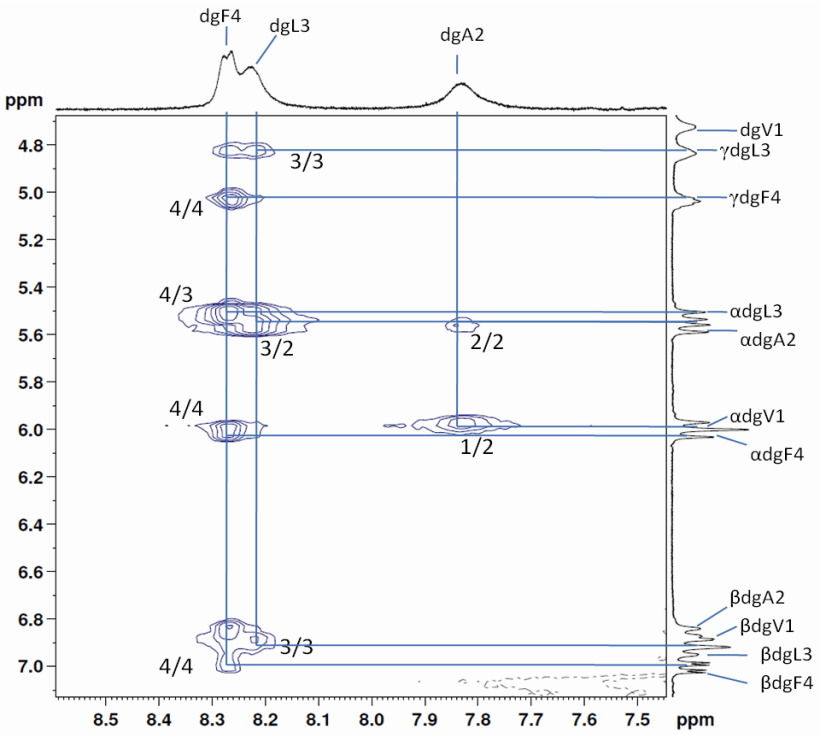
dgF4
dgL3
dgA2
ppm
dgV1
γdgL3
γdgF4
αdgL3
αdgA2
αdgV1
αdgF4
βdgA2
βdgV1
βdgL3
βdgF4
3/3
4/4
4/3
3/2
2/2
4/4
1/2
4/4
3/3
8.5 8.4 8.3 8.2 8.1 8.0 7.9 7.8 7.7 7.6 7.5 ppm

b)

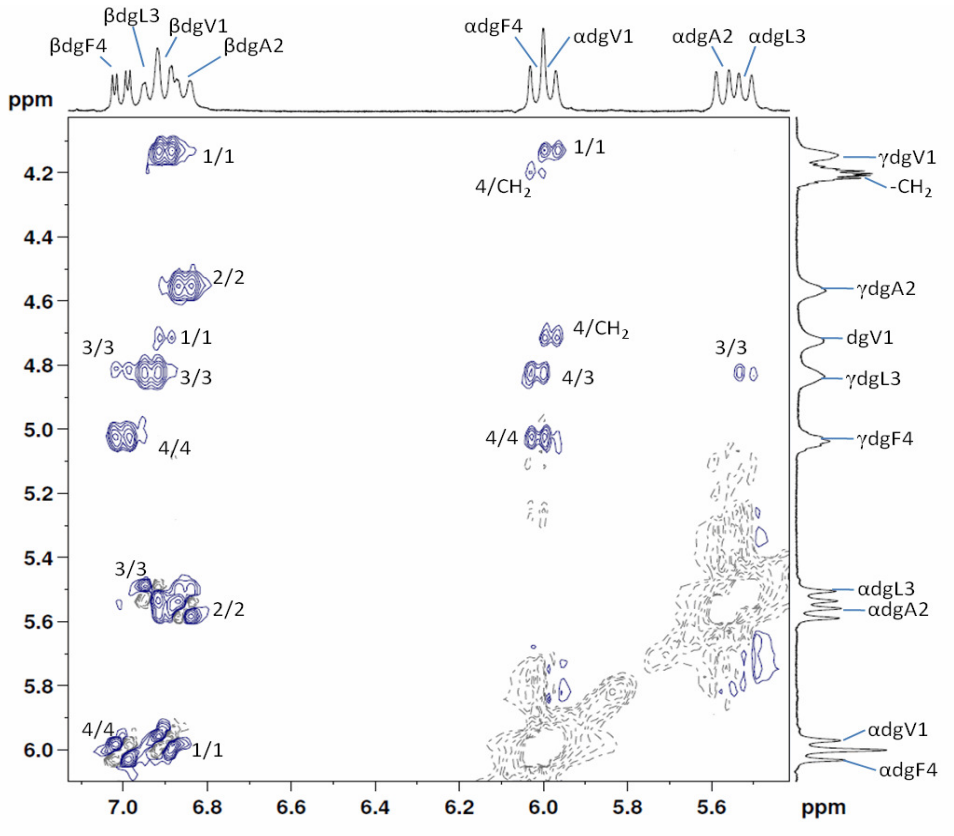
βdgL3
βdgV1
βdgF4
βdgA2
αdgF4
αdgV1
αdgA2
αdgL3
ppm
1/1
2/2
3/3
1/1
3/3
4/4
3/3
2/2
4/4
1/1
1/1
4/CH2
4/CH2
4/3
4/4
3/3
γdgV1
-CH2
γdgA2
dgV1
γdgL3
γdgF4
αdgL3
αdgA2
αdgV1
αdgF4
7.0 6.8 6.6 6.4 6.2 6.0 5.8 5.6 ppm

c)

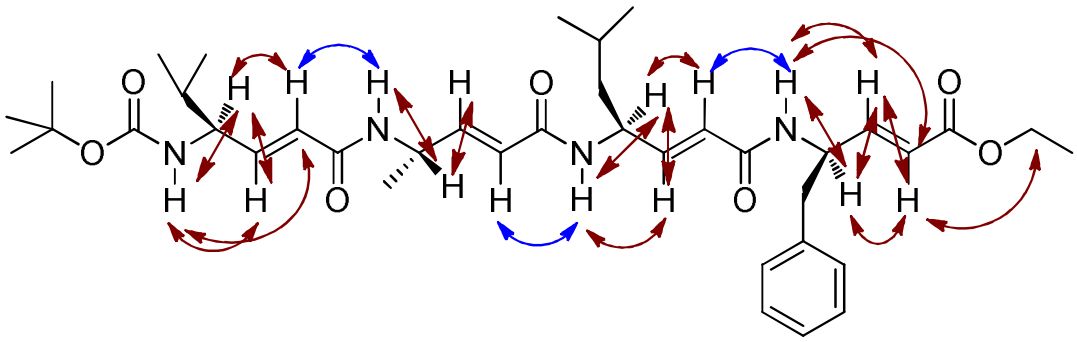

d)

Figure 12: a) TOCSY NMR spectrum of **P6** in $CDCl_3$, The sequential assignments of amino acids were performed using ROESY, b) Partial ROESY spectrum of **P6** showing sequential NOEs of NH↔ $C^{\alpha}H$, NH↔ $C^{\beta}H$, NH↔$C^{\gamma}H$, and c) $C^{\beta}H$ ↔ $C^{\alpha}H$, $C^{\beta}H$↔$C^{\gamma}H$ and $C^{\alpha}H$↔$C^{\gamma}H$, d) The critical NOEs of tetrapeptide (**P6**) observed in ROESY spectrum.

1.3.8 Parallel sheet stabilization by expanded hydrogen bond pseudocycle

In the backbone of protein structure, the β-sheet is one of the two regular scaffolds. The stereochemistry of the β-sheets was illustrated by Linus Pauling in 1951.[27] The β-sheets are composed of straight segments of the protein strand held together by intermolecular hydrogen bonds. Two types of β-sheets are observed in protein structure. They are classified as antiparallel and parallel β-sheet (Figure 13a, 13b). [27] It has been observed in natural β-sheets that antiparrallel β-sheets are stabilized through two cooperative hydrogen bonding psuodocycle, 10-membered and 14-membered (Figure 13a), whereas, parallel β-sheets are stabilized through continuous 12-membered hydrogen bonding psuodocycle (Figure 13b). In our investigation of the crystal structure of **P1**, **P4** and **P5**, we observed that vinylogous homooligomers adopted parallel β-sheet self assembled structures. Interestingly these vinylogous homooligomers are stabilized through 16-membered H-bonding pseudocycles (Figure 13c). In principle, the 16-membered hydrogen bond pseudocycles are less stable when compared to the 12-membered hydrogen bond pseudocycles observed in the natural parallel β-sheet structures. The question we ask that how these vinylogous homooligomers are stable as parallel β-sheets? Probably, the presence of geometrical restriction of double bonds present in the backbone and the availability of H-bonding partner with this particular

stable conformation lead them to assemble in a parallel β-sheet fashion. And the question still remains is that why only parallel β-sheets and not anti-parallel β-sheets?

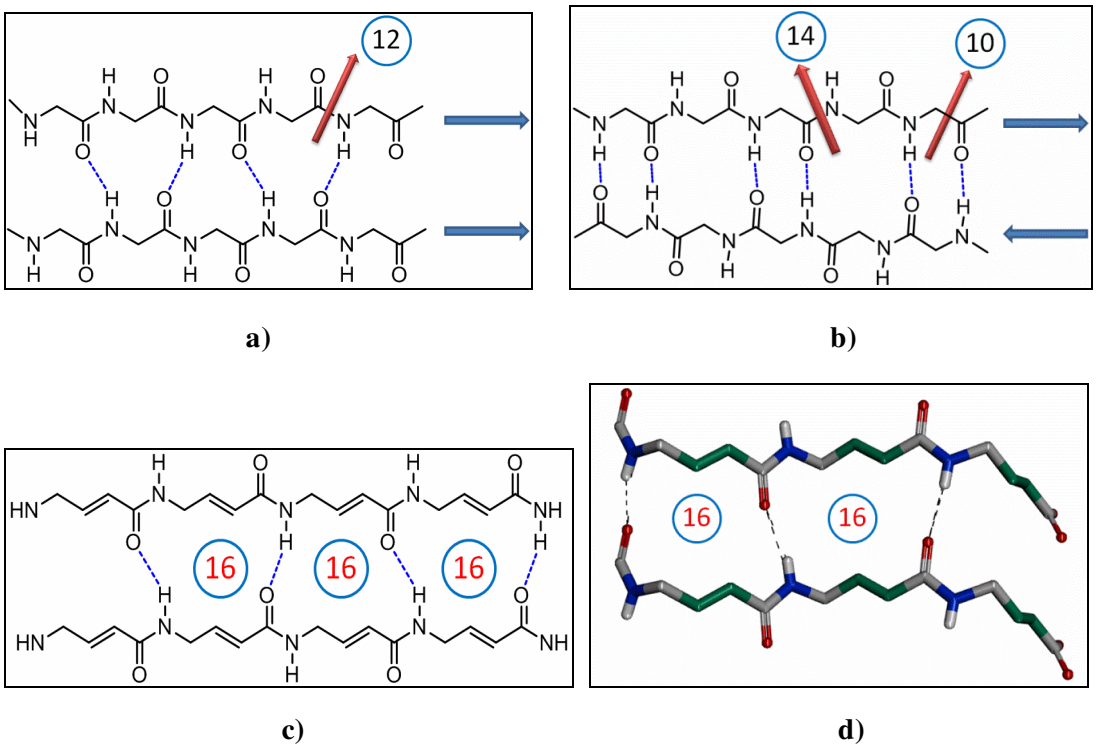

Figure 13: Schematic diagram H-bonding pseudocycles observed in a) parallel β-sheet, b) antiparallel β-sheet, c) Parallel β-sheet exhibited by vinylogous oligomers, d) Two 16-membered H-bonding pseudocycles observed in tripeptide crystal structure. Side chains are deleted for clarity.

1.3.9 Additional stability through C-H···O hydrogen bonding

In the antiparallel β-sheets, the C=O···H-N hydrogen bonds that grip the β-strands together are exactly perpendicular to the strands, as described by Pauling. Though, a several group of researchers found a shear in antiparallel and parallel β-sheets.[28] Ho & Curmi have shown that the only interaction consistent with the measured geometry of the shear is the formation of C^{α}-H···O hydrogen bond in the interface between the β-strands.[29] However, there is a debate on whether the C-H···O weak hydrogen bond is just an artefact in protein structures. Afterwards, Derewenda and co-workers found statistical evidence for the existence of C-H···O hydrogen bonds in protein structures.[30] The C=O···H-N hydrogen bond and the C^{α}-

H···O hydrogen bond form a network called the bifurcated hydrogen bond (Figure 14) where the O atom is common to the two hydrogen bonds. In the antiparallel β-sheet, the sheet is sheared to accommodate the bifurcated hydrogen bonds. In contrast, the parallel β-sheet as described by Linus Pauling, already places the C^{α}-H atoms in contact with the O atoms. This C^{α}-H···O hydrogen bond plays a significant role in determining both protein conformation[31] and stability[32], especially for parallel β-sheets.

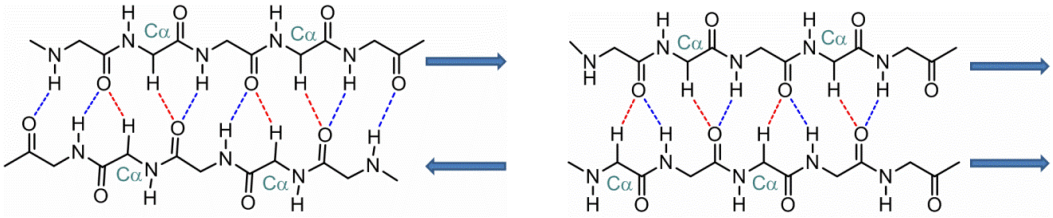

a) **b)**

Figure 14: The C=O···H-N (blue) and C^{α}-H···O (red) bifurcated hydrogen bond in a) antiparallel β-sheet, b) parallel β-sheet.

There are few examples of the exploitation of this interaction in the development of novel folded structures.[33] The careful analysis of crystal structures of **P1**, **P4** and **P5** reveals that the C^{α}-H···O hydrogen bond might be playing crucial role in stabilizing the parallel β-sheet structure of vinylogous polypeptide. The enhanced hydrogen bonding capabilities of this functional group may be attributed to the electron-withdrawing nature of carbonyl group as well as the acidic nature of the C-H which is directly attached to the sp^2 hybridized carbon (Figure 15). In all crystal structures, we observed the bifurcated hydrogen bond between N-H···O and C^{α}-H···O. Interestingly, the terminal ester C=O also participated in C^{α}-H···O hydrogen bond to favour β-sheet conformation. The bond angle and the distance criteria for CH···O hydrogen bonds are well satisfied in the vinylogous peptides.[34, 35] The bond angles and the distances of observed C-H···O H-bonds in the peptides **P1**, **P4** and **P5** are tabulated in Table 5. These values are in close agreement with the average values observed in proteins.

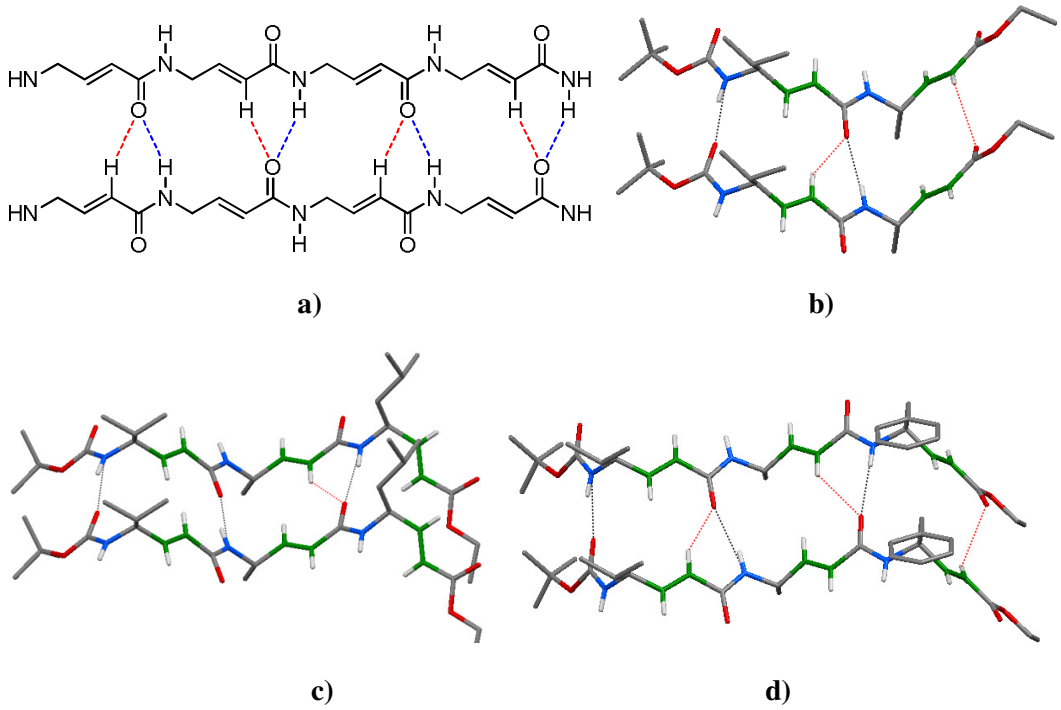

Figure 15: a) Schematic diagram of parallel β-sheet structure of vinylogous oligomer with C-H···O H-bonding (red). C-H···O H-bonding (red) shown along with NH···O=C H-bonding (black) in crystal structure of b) Boc-dgV-dgA-OEt (**P1**), c) Boc-dgV-dgA-dgL-OEt (**P4**), d) Boc-dgV-dgA-dgF-OEt (**P5**).

Table 5: Interstrand average CH···O hydrogen bond distances and angles for **P1**, **P4** and **P5**

Peptide	CH···O (Å)	C···O (Å)	∠N···C=O (deg)
P1	2.7	3.35	136.3
P4	2.85	3.60	143.2
P5	2.67	3.33	140.8

1.3.10 Circular dichroism (CD) spectra

Further, to understand the conformational signature of all the peptides in solution, we subjected them for CD analysis. The CD spectra of the all vinylogous peptides (**P1-P6**) in methanol are shown in Figure 16. Instructively, all peptides showed the CD negative maxima at ~ 228 nm, indicating a β-sheet character in solution. We speculate that the red shift of the CD negative maxima at 228 nm may be due to the conjugated enamides and esters of

vinylogous residues. Due to the similar CD minima observed in all the peptides, we conclude that **P2** and **P3** are also adpoting β-sheet character in solution.

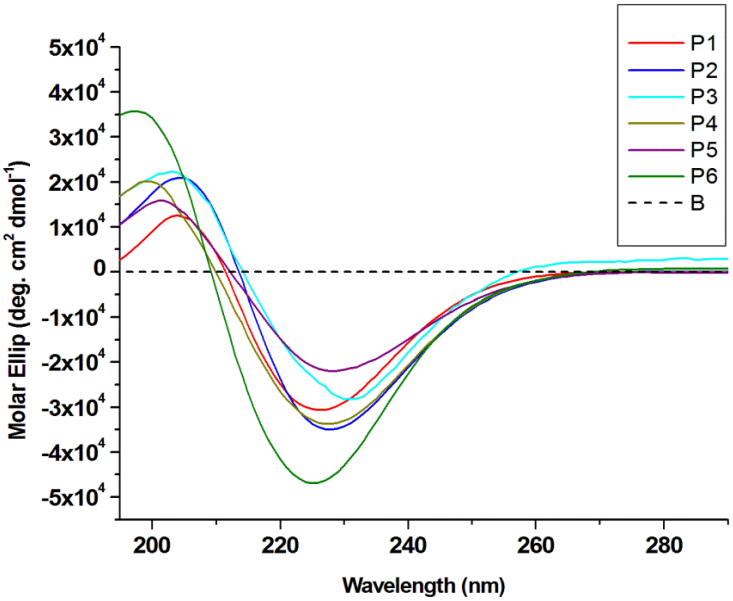

Figure 16: Circular Dichroism spectra of vinylogous peptides (**P1-P6**) recorded in MeOH.

1.3.11 Conformational analysis of the vinylogous residues

Surprised by the β-sheet structure adopted by vinylogous homooligomers, we sought to analyze the conformations adopted by the vinylogous residues in crystal structures. A careful analysis of the crystal structures of *E*-vinylogous residues reported earlier[16] and from the present work (Chapter 1, 2 and 3 containing vinylogous amino acid and peptides) revealed very intriguing results. From the analysis of total twenty four units of vinylogous residues in the single crystals of monomers and peptides, two lowest energy eclipsed conformations are observed (Scheme 7). The N-C_γ-C_β=C_α eclipsed conformation **A** (θ_1 = 0^o) is normally observed in the vinylogous esters, while H-C_γ-C_β=C_α eclipsed conformation **B** (θ_1 = ± 120^o) is observed in the vinylogous amides. In all the cases, θ_1 takes the value either close to 0 or ± 120^o. The conjugated carbonyl functional group mostly adapted local *s-cis* conformation (ψ = ~ ± 180^o) compared to the *s-trans* conformation (ψ = ~ ± 0^o). Results from the analysis reveal that vinylogous residues (amides) prefer the extended conformations and may serve as ideal candidates for the construction of β-sheet structures.

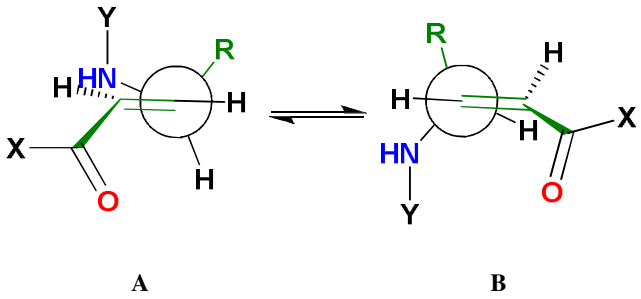

Scheme 7. The stable eclipsed conformers of vinylogous residues observed in the crystal structures.

The analysis of all crystal structures reveals that torsional variables θ_2 and ψ mostly adopted extended conformation with value ± 180°. Further, we plotted a two dimensional plot for the torsional variables θ_1 and φ by keeping θ_2 and ψ as constant. The two dimensional map of θ_1 and φ is shown in Figure 19. Nice correlation of vinylogous residues with the α-peptide β-sheet structure can be observed by comparing two dimensional plot (φ vs θ_1) of vinylogous residues with the classical Ramachandran Map[37] for α-peptides. Interestingly, the vinylogous ester in the C-terminal of the vinylogous peptides and the monomeric amino esters deviated from the β-sheet character. Analysis of these results suggests that the vinylogous amides are ideal candidates for the construction of β-sheet structures.

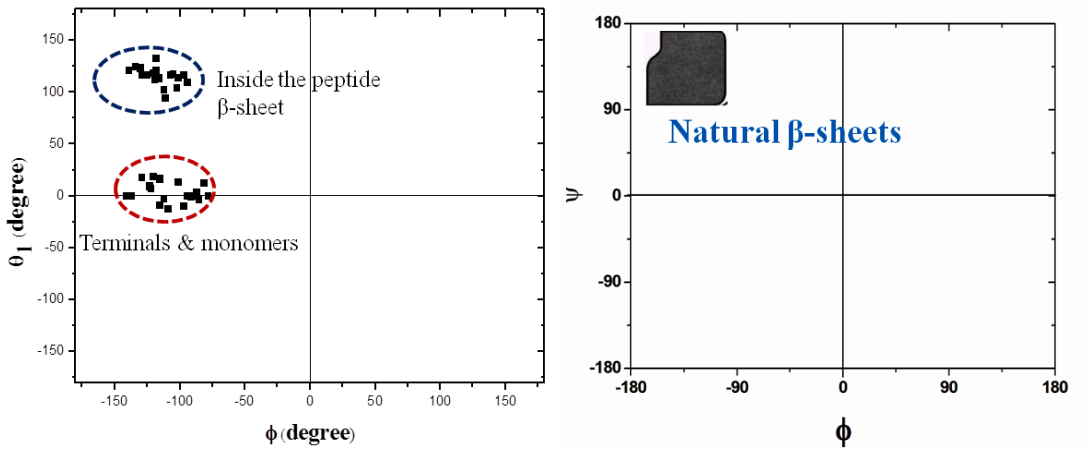

Figure 19: a) Two dimensional plot for vinylogous residues observed from crystal structures (listed in the next page), b) Ramachandran map; the position occupied by natural β-sheet is shown.

List of crystal structures used to plot the Figure 19a

Boc-dgA-OMe,[16] Boc-dgA-NHPr^{i},[16] Boc-dgF-dgF-OMe,[16] Boc-β-hydroxy γ-Ala-^{D}pro-Gly-dgA-OMe,[16] Boc-dgF-OEt, Boc-dgV-dgA-OEt, Boc-dgV-dgA-dgL-OEt, Boc-dgV-dgA-dgF-OEt, Ac-V-dgL-V-^{D}P-G-L-dgV-V-NH_2, Boc-Val-dgL-Val-^{D}Pro-Gly-Leu-dgV-Val-Ala-^{D}Pro-Gly-Leu-Val-dgL-Val-NH_2, Boc-U-dgF-U-dgF-OEt.

1.3.12 Analogy with Natural parallel β-sheets

The interesting results from the (*E*)-vinylogous oligomers **P1**, **P4** and **P5**, motivated us to evaluate the (*E*)-vinylogous homooligomers β-sheet structures with respect to the existing natural parallel β-sheets. The superimposition of the parallel β-sheets of **P5** with the natural parallel β-sheet of Pectate Lyase C [PBD CODE 1AIR, SEQUENCE Q-A-L-I-E (249-254) and T-W-V-L-K (275-289)][38] is shown in the Figure 20. Instructively, the backbone conformation of **P5** is well correlated with five residue natural β-sheet, except H-bonding pattern. The backbone correlation of (*E*)-vinylogous β-sheet structure with respect to the natural β-sheet suggests that these vinylogous peptides can be exploited as mimics of natural parallel β-sheets.

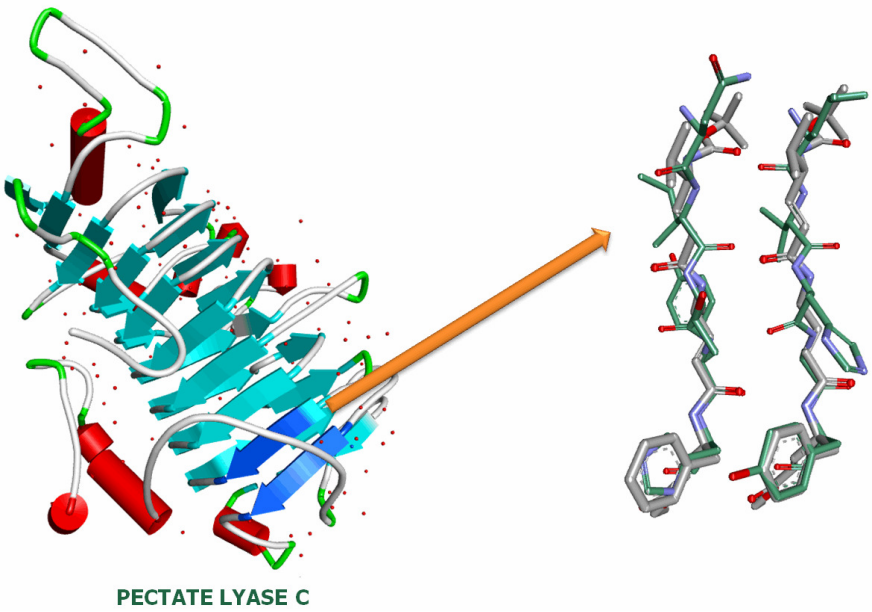

a) **b)**

Figure 20: a) Crystal structure of Pectate Lyase C protein (PDB 1AIR)[38], b) Superimposition of backbone conformation of the Boc-dgV-dgA-dgF-OEt peptide (gray) on the natural parallel β-sheet. All the backbone atoms of vinylogous tripeptide were used to overlay with pentapeptide of natural parallel β-sheet, RMSD = 0.91

1.4 Conclusion

We have demonstrated the facile synthesis of α, β-unsaturated γ-amino esters with exceptional *E*-stereoselectivity using Wittig reaction. Further, solution and the crystal conformations of vinylogous homooligomers suggested that they adopted stable β-sheet type of structures and self-assembled into infinite parallel β-sheets. Further the analogy of the vinylogous parallel β-sheet structures with respect to the natural α-peptide parallel sheets suggests that the tripeptide of vinylogous amino acids is sufficient to mimic the pentapeptide of the α-amino acids. Very nice backbone correlation has observed between α-pentapeptide and the vinylogous tripeptide except the H-bonding pattern. As compared to extensive investigations on the helix inducing amino acids/templates, there is a very little progress in the design of amino acid scaffolds that can induce the β-sheet conformations in peptides. Results from these findings reveal that *E*-vinylogous residues will serve as ideal candidates for the construction of β-sheet structures. The knowledge from this work can be further utilized to construct higher ordered structures of vinylogous residues as well as for the synthesis of biologically active peptides.

1.5 Experimental section

General Experimental Details

All amino acids, DiPEA, TFA, triphenylphosphine were purchased from Aldrich. THF, DCM, DMF, NaOH were purchased from Merck. Ethyl bromoacetate, HBTU, HOBt, EtOAc, NMP, Pet-ether (60-80 ^{o}C) were obtained from Spectrochem and used without further purification. THF and DiPEA were dried over sodium and distilled immediately prior to use. Column chromatographies were performed on Merck silica gel (120-200 mesh). The ^{1}H spectra were recorded on Bruker 500 MHz (or 125 MHz for ^{13}C) and Jeol 400 MHz (or 100 MHz for ^{13}C) using residual solvents signals as an internal reference [($CDCl_3$ δ_H, 7.26 ppm, δ_c 77.0 ppm) and CD_3OH δ_c 49.3 ppm]. The chemical shifts (δ) are reported in *ppm* and coupling constants (*J*) in Hz. MALDI-TOF/TOF mass spectra were obtained on Model 4800 (Applied Biosystems) instrument. X-Ray data were collected on Bruker APEX (II) DUO.

NMR spectroscopy: All 2D-NMR studies were carried out by using a Bruker 500 MHz and spectrometer at a probe temperature of 300 K. Resonance assignments were obtained by TOCSY and ROESY analysis. All two-dimensional data were collected in phase-sensitive mode, by using the time-proportional phase incrementation (TPPI) method. Sets of 1024 and 512 data points were used in the t_2 and t_1 dimensions, respectively. For TOCSY and ROESY analysis, 32 and 72 transients were collected, respectively. A spectral width of 6007 Hz was used in both dimensions. A spin-lock time of 256 ms was used to obtain ROESY spectra. Zero-filling was carried out to finally yield a data set of 2 K ×1 K. A shifted square-sine-bell window was used before processing.

Circular dichroism (CD) spectroscopy

CD spectrometry studies were carried out on JASCO J-815 spectropolarimeter using cylindrical, jacketed quartz cell (1 mm path length), which was connected to Julabo-UC-25 water circulator. Spectra were recorded with a spectral resolution of 1 nm, band width 1 nm at a scan speed of 50 nm/min and a response time 1 sec. All the spectra were corrected with MeOH solvent condition and are typically averaged over 3 scans.

Crystal structure analysis of Boc-dgF-OEt: Crystals were grown by slow evaporation from a solution of MeOH. A single crystal (0.35 × 0.23 × 0.18 mm) was mounted on loop with a small amount of the paraffin oil. The X-ray data were collected at 100K temperature on a Bruker AXS SMART APEX CCD diffractometer using Mo Kα radiation (λ = 0.71073 Å), ω-scans (2θ = 56.16), for a total of 4235 independent reflections. Space group *C2*, a = 21.719(3), b = 5.3179(7), c = 15.433(2), β = 90.208(5), V = 1782.5(4) Å^3, Monoclinic C, Z = 4 for chemical formula $C_{18}H_{25}NO_4$, with one molecule in asymmetric unit; ρ_{calcd} = 1.190 gcm^{-3}, μ = 0.084 mm^{-1}, *F*(000) = 688, R_{int} = 0.0230. The structure was obtained by direct methods using SHELXS-97.[39] The final R value was 0.0351 (*wR2* = 0.0905) 3987 observed reflections (F0 ≥ 4σ (|F0|)) and 212 variables, *S* = 1.133. The largest difference peak and hole were 0.197 and -0.214 eÅ^3, respectively.

Crystal structure analysis of (Boc-dgV-dgA-OEt) P1: Crystals of peptide were grown by slow evaporation from a solution of ethyl acetate. A single crystal (0.32 × 0.20 × 0.15 mm) was mounted in a loop with a small amount of the mother liquor. The X-ray data were collected at 100 K temperature on a Bruker AXS SMART APEX CCD diffractometer using

MoK_α radiation (λ = 0.71073 Å), ω-scans (2θ = 56.54°), for a total number of 5152 independent reflections. Space group *P2(1)*, *a* = 5.0377(9), *b* = 19.994(4), *c* = 10.408(2) Å, α = 90.00 , β = 95.693(5), γ = 90.00, *V* = 1043.2(3) $Å^3$, Monoclinic *P*, Z=2 for chemical formula $C_{19}H_{32}N_2O_5$, with one molecule in asymmetric unit; ρ_{calcd} = 1.173 g cm^{-3}, μ = 0.084 mm^{-1}, *F*(000) = 400, R_{int} = 0.0494. The structure was obtained by direct methods using SHELXS-97.[39] All non-hydrogen atoms were refined anisotropically. The hydrogen atoms were fixed geometrically in the idealized position and refined in the final cycle of refinement as riding over the atoms to which they are bonded. The final *R* value was 0.0494 (*wR2* = 0.1211) for 3804 observed reflections ($F_0 \geq 4\sigma$ ($|F_0|$)) and 242 variables, *S* = 0.834. The largest difference peak and hole were 0.185 and -0.213 $eÅ^3$, respectively.

Crystal structure analysis of (Boc-dgV-dgA-dgL-OEt) P4: Crystals of peptide were grown by slow evaporation from a solution of methanol. A single crystal (0.24 × 0.20 × 0.13 mm) was mounted in a loop with a small amount of the mother liquor. The X-ray data were collected at 100 K temperature on a Bruker AXS SMART APEX CCD diffractometer using MoK_α radiation (λ = 0.71073 Å), ω-scans (2θ = 50.34°), for a total number of 3075 independent reflections. Space group *P2(1)*, *a* = 17.12(4), *b* = 5.101(12), *c* = 17.59(4) Å, α = 90.00 , β = 98.34(3), γ = 90.00, *V* = 1520(6) $Å^3$, Monoclinic *P*, Z = 2 for chemical formula $C_{27}H_{45}N_3O_6$, with one molecule in asymmetric unit; ρ_{calcd} = 1.109 g cm^{-3}, μ = 0.078 mm^{-1}, *F*(000) = 552, R_{int} = 0.2011. The structure was obtained by direct methods using SHELXS-97.[39] All non-hydrogen atoms were refined anisotropically. The hydrogen atoms were fixed geometrically in the idealized position and refined in the final cycle of refinement as riding over the atoms to which they are bonded. The final *R* value was 0.0951 (*wR2* = 0.1797) for 1236 observed reflections ($F_0 \geq 4\sigma$ ($|F_0|$)) and 334 variables, *S* = 0.869. The largest difference peak and hole were 0.254 and -0.257 $eÅ^3$, respectively.

Crystal structure analysis of (Boc-dgV-dgA-dgF-OEt) P5: Crystals of peptide were grown by slow evaporation from a solution of methanol. A single crystal (0.34 × 0.30 × 0.10 mm) was mounted in a loop with a small amount of the mother liquor. The X-ray data were

collected at 100 K temperature on a Bruker AXS SMART APEX CCD diffractometer using MoK_α radiation (λ = 0.71073 Å), ω-scans (2θ = 56.56°), for a total number of 13291 independent reflections. Space group *P2(1)*, *a* = 4.9647(11), *b* = 50.644(11), *c* = 12.532(3) Å, α = 90.00 , β = 100.812(6), γ = 90.00, *V* = 3094.9(12) Å^3, Monoclinic *P*, Z = 2 for chemical formula $C_{60}H_{86}N_6O_{12}$, with two molecule in asymmetric unit; ρ_{calcd} = 1.163 g cm^{-3}, μ = 0.081 mm^{-1}, *F*(000) = 1168, R_{int} = 0.0990. The structure was obtained by direct methods using SHELXS-97.[39] All non-hydrogen atoms were refined anisotropically. The hydrogen atoms were fixed geometrically in the idealized position and refined in the final cycle of refinement as riding over the atoms to which they are bonded. The final *R* value was 0.0936 (*wR2* = 0.2003) for 5852 observed reflections ($F_0 \geq 4\sigma$ (|F_0|)) and 717 variables, *S* = 0.912. The largest difference peak and hole were 0.336 and -0.372 eÅ^3, respectively.

General procedure for the synthesis of ethyl ester of Boc-Protected α, β-unsaturated γ-amino acids

Boc-amino aldehyde (10 mmol) was dissolved in 30 mL of dry THF. The ylide (15 mmol, 5.22g) was added at RT. Reaction mixture was stirred for about 5hrs at RT. Completion of reaction was monitored by TLC. After completion, reaction mixture was quenched with 50 mL of 2*N* ammonium chloride solution. The product was extracted with EtOAc (3 × 80 mL). Combined organic layer was washed with brine (60 mL) and dried over anhydrous Na_2SO_4. Organic layer was concentrated under reduced pressure to give crude product, which was further purified on silica gel column chromatography using EtOAc/Pet-ether (60-80 °C) to get pure ethyl ester of Boc-protected α, β-unsaturated γ-amino acid.[36]

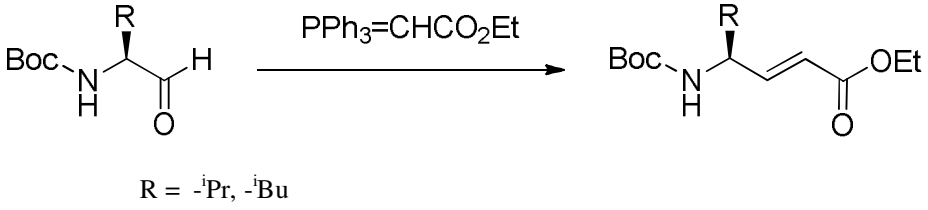

R = -^{i}Pr, -^{i}Bu

Scheme 6: Synthesis of ethyl ester of Boc-Protected α, β-unsaturated γ- amino acids

(*S*, *E*)-ethyl 4-(tert-butoxycarbonylamino)pent-2-enoate (1C)

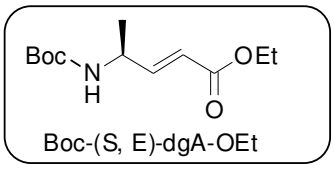

Physical state : Colourless Oil

Mol. Formula : $C_{12}H_{21}NO_4$

Yield : 93%, 2.25g

^{1}H NMR (400 MHz, $CDCl_3$) : δ_H 6.90-6.85 (dd, *J* = 14.7, *J* = 5.3, 1H vinylic β proton), 5.93-5.88 (d, *J* = 16.8, 1H vinylic α proton), 4.54 (br, NH), 4.44-4.38 (m, 1H, γ proton), 4.23-4.17 (q, *J* = 7.3 , -OC*H*$_2$), 1.45 (s, 9H, -C(CH_3)$_3$ Boc), 1.29-1.27 (m, 6H, -C*H*$_3$, -OCH_2CH_3);

^{13}C NMR (100 MHz $CDCl_3$) : δ_C 166.37, 154.87, 120.10, 79.75, 60.44, 46.98, 28.33, 20.32, 14.20;

MALDI TOF/TOF m/z : Calcd. $[M+Na]^+$ 266.1368, observed 266.1365.

(*S*, *E*)-ethyl 4-(tert-butoxycarbonylamino)-5-methylhex-2-enoate (2C)

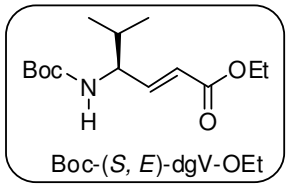

Physical state : Colourless crystalline

Mol. Formula : $C_{14}H_{25}NO_4$

Yield : 85%, 2.30g

^{1}H NMR (500 MHz, $CDCl_3$) : δ_H 6.88-6.84 (dd, *J* = 15.5, *J* = 4.5, 1H, C*H*=CHCO$_2$Et), 5.93-5.90 (d, *J* = 15.5, 1H, CH=C*H*CO$_2$Et), 4.57-4.56 (d, *J* = 8.5, 1H, NH), 4.21-4.17 (m, 3H, -OC*H*$_2$, C*H*-CH=CH), 1.89-1.85 (m, 1H, C*H*-(CH_3)$_2$), 1.45 (s, 9H, -(CH_3)$_3$ Boc), 1.30-1.28 (t, *J* = 7, 3H, -OCH_2CH_3), 0.95-0.90 (dd, *J* = 15.5, *J* = 7, 6H, CH-(C*H*$_3$)$_2$).

^{13}C NMR (100MHz, $CDCl_3$) : δ_C 166.24, 155.31, 147.34, 121.40, 79.61, 60.38, 56.61, 32.18, 28.29, 18.81, 17.94, 14.18.

MALDI TOF/TOF m/z : Calcd. for $[M+Na]^+$ 294.1681, observed 294.1606.

(*S*, *E*)-ethyl 4-(tert-butoxycarbonylamino)-6-methylhept-2-enoate (3C)

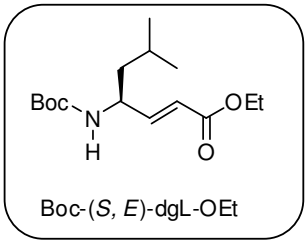

Physical state : Colourless crystalline

Mol. Formula : $C_{15}H_{27}NO_4$

Yield : 87%, 2.47g

^{1}H NMR (500 MHz, $CDCl_3$) : δ_H 6.85-6.80 (dd, *J* = 16, *J* = 5.5, 1H, C*H*=CHCO$_2$Et), 5.93-5.89 (d, *J* = 16, 1H, CH=C*H*CO$_2$Et), 4.49 (b, 1H, NH), 4.37-4.32 (m, 1H, C*H*-CH=CH), 4.21-4.16 (q, *J* = 7, 2H, -OC*H*$_2$), 1.72-1.67 (m, 1H, C*H*-(CH$_3$)$_2$), 1.44 (s, 9H, -(CH$_3$)$_3$ Boc), 1.40-1.37 (t, *J* = 7, 2H, C*H*$_2$CH-(CH$_3$)$_2$), 1.30-1.27 (t, *J* = 7, 3H, -OCH$_2$C*H*$_3$), 0.94-0.93 (d, *J* = 6.5, 6H, CH-(C*H*$_3$)$_2$).

^{13}C NMR (100MHz, $CDCl_3$) : δ_C 166.41, 155.05, 148.89, 120.35, 79.65, 60.40, 49.75, 43.78, 28.31, 24.67, 22.68, 22.14, 14.20.

MALDI TOF/TOF m/z : Calcd. $[M+Na]^+$ 308.1838, observed 308.1857.

(*S*, *E*)-ethyl 4-(*tert*-butoxycarbonylamino)-5-phenylpent-2-enoate (4C)

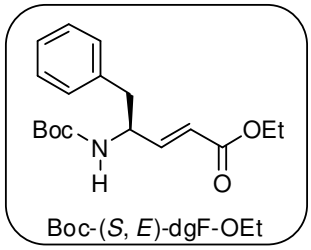

Physical state : White powder

Mol. Formula : $C_{18}H_{25}NO_4$

Yield : 84%, 2.67 g

^{1}H NMR (400 MHz, $CDCl_3$) : δ_H 7.30-7.14 (m, 5H, -Ph), 6.91-6.86 (dd, *J* = 5.04, *J* = 11, 1H, C*H*=CHCO$_2$Et), 5.85-5.81 (d, *J* = 17.4, 1H, CH=C*H*CO$_2$Et), 4.59 (b, 1H, NH), 4.52 (b, 1H, C*H*-CH=CH), 4.18-4.13 (q, *J* = 6.88, 2H, -OC*H*$_2$), 2.92-2.85 (m, 2H, C*H*$_2$-Ph), 1.37 (s, 9H, -(CH$_3$)$_3$ Boc), 1.27-1.23 (t, *J* = 7.3, 3H, -OCH$_2$C*H*$_3$).

^{13}C NMR (100MHz, $CDCl_3$) : δ_C 166.14, 154.91, 147.56, 136.33, 129.36, 128.54, 126.83, 121.04, 79.83, 60.44, 52.16, 40.82, 28.26, 14.18.

MALDI TOF/TOF m/z **:** Calcd. $[M+Na]^+$ 342.1681, observed 342.1657.

(*S*, *E*)-ethyl 4-(tert-butoxycarbonylamino)-5-(1H-indol-3-yl)pent-2-enoate (5C)

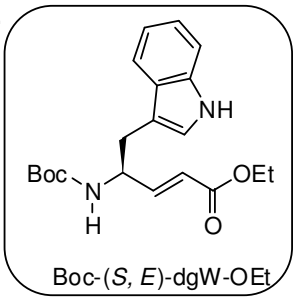

Boc-(*S, E*)-dgW-OEt

Physical state **:** White powder

Mol. Formula **:** $C_{20}H_{26}N_2O_4$

Yield **:** 80%, 2.86 g

^{1}H NMR (400 MHz, $CDCl_3$) **:** δ_H 8.169 (s, NH, indol ring), 7.60-6.95 (m, 6H, indol, C*H*=CHCO$_2$Et), 5.90-5.86 (d, *J* = 17.2, 1H, CH=C*H*CO$_2$Et), 4.67-4.62 (m, 2H, NH and C*H*-CH=CH), 4.20-4.14 (q, *J* = 6.9, 2H, -OC*H*$_2$), 3.08-3.07 (m, 2H, C*H*$_2$-indol), 1.41 (s, 9H, -(CH$_3$)$_3$ Boc), 1.28-1.24 (t, *J* = 7.2, 3H, -OCH$_2$C*H*$_3$) .

^{13}C NMR (100MHz, $CDCl_3$) **:** δ_C 166.27, 155.11, 148.44, 136.16, 122.83, 122.14, 120.86, 119.62, 118.88, 111.14, 110.51, 84.95, 79.74, 60.40, 28.29, 14.21.

MALDI TOF/TOF m/z **:** Calcd. For $[M+Na]^+$ 358.1893, observed 358.2425.

Synthesis of Dipeptide

(*Boc-dgV-dgA-OEt*) (P1)

Boc-dgV-OH: Boc-dgV-OEt (5 mmol, 1.35 g) was dissolved in ethanol (20 mL). Then 20 mL of 1(N) NaOH was added slowly to this solution. After completion of the reaction (~ 2 hrs), ethanol was evaporated from reaction mixture and the residue was acidified to *p*H ~ 3 using 5% HCl (5% volume in water) at cold condition after diluting with 50 mL of cold water. Product was extracted with ethyl acetate (3 × 70 mL). Combined organic layer was washed with brine (100 mL) and dried over anhydrous Na_2SO_4. Organic layer was concentrated under reduced pressure to give gummy product with quantitative yield 99% (4.95 mmol, 1.2 g).

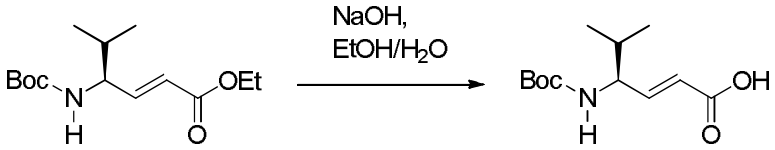

NH_2-dgA-OEt: (Boc-dgA-OEt) (5.5 mmol, 1.33 g) was dissolved in DCM (7 mL) and cooled the solution in ice bath. Then 7 mL neat TFA was added to this solution. After completion of the reaction (~ 30 min), TFA was removed from reaction mixture under *vacuum*. The residue was dissolved in water and the pH was adjusted to ~10 by the slow addition of solid Na_2CO_3 in ice cool condition. Then Boc deprotected free amine was extracted with ethyl acetate (3 × 40 mL). Combined organic layer was washed with brine (60 mL) followed by dried over Na_2SO_4 and concentrated under vacuum to *ca*. 2 mL and directly used for the coupling reaction in the next step.

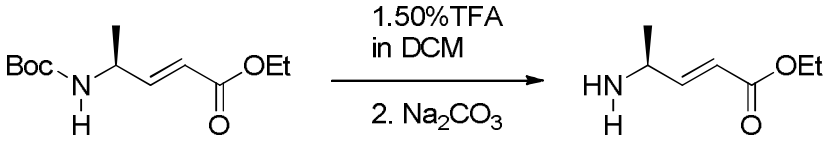

Boc-dgV-OH (4.95 mmol, 1.2 g) and NH_2-dgA-OEt were dissolved together in DMF (4 mL), followed by HBTU (5.5 mmol, 2.1 g) was added into the reaction mixture and cooled to 0 ^oC for 5 min. Then DiPEA (6 mmol, 1.08 mL) was added to the reaction mixture with stirring and the reaction mixture was allowed to come to room temperature. The progress of the reaction was monitored by TLC. After completion of the reaction (roughly 6hrs), reaction mixture was diluted with 300 mL of ethyl acetate and washed with 5% HCl (5 % by vol. in water, 2 × 80 mL), 10 % sodium carbonate solution in water (2 × 80 mL) and followed by brine (100 mL). The organic layer was dried over Na_2SO_4 and evaporated under reduced pressure to give gummy yellowish product, which was purified on silica gel column chromatography using DCM/MeOH solvent system to gummy product, which was further crystallized using EtOAc/Hexane. Overall yield 77% (3.8 mmol, 1.4 g).

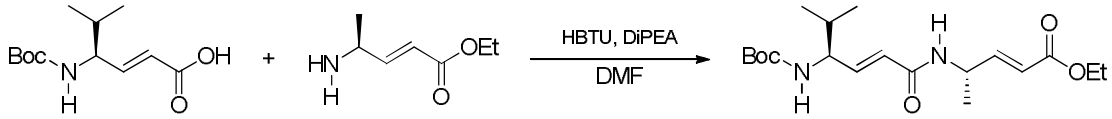

Boc-dgV-dgA-OEt (P1)

Physical state : White powder

Mol. Formula : $C_{19}H_{32}N_2O_5$

Yield : 77%, 1.4 g

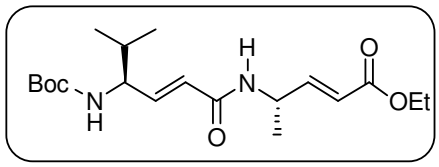

^{1}H NMR (400 MHz, $CDCl_3$) : δ_H 6.90-6.85 (dd, J = 5, J = 10.5, 1H, vinylic β proton), 6.75-6.70 (dd, J = 6.4, J = 8.7, 1H, vinylic β proton), 5.91-5.87 (d, 2H, vinylic α proton) , 5.78-5.76 (d, J = 7.8, 1H, NH), 4.82-4.77 (m, 1H, γ proton), 4.65-4.63 (d, J = 9.1, 1H, NH), 4.20-4.15 (q, J = 7, 2H, -OCH_2), 4.11-4.06 (m, 1H, γ proton), 1.87-1.79 (m, 1H),1.43 (s, 9H, C(CH_3)$_3$ Boc), 1.32-1.30 (d, J = 6.9, 3H, CH_3 side chain Ala), 1.29-1.25 (t, J = 7, 3H, -CH_2CH_3), 0.952-0.907 (m, 6H, CH-(CH_3)$_2$ Val side chain).

^{13}C NMR (100 MHz $CDCl_3$) : δ_C 166.27, 164.51, 155.39, 148.36, 143.58, 123.73, 120.62, 79.59, 60.49, 56.92, 45.61, 32.26, 28.34, 19.84, 18.84, 18.09, 14.16.

MALDI TOF/TOF m/z : Calcd. $[M+Na]^+$ 391.2209 Da, observed 391.2187 Da.

(*Boc-dgV-dgL-OEt*) (P2)

Boc-dgV-OH: Boc-dgV-OEt (5 mmol, 1.35 g) was dissolved in ethanol (20 mL). Then 20 mL of 1(N) NaOH was added slowly to this solution. After completion of the reaction (~ 2 hrs), ethanol was evaporated from reaction mixture and the residue was acidified to *p*H ~ 3 using 5% HCl (5% volume in water) at cold condition after diluting with 50 mL of cold water. Product was extracted with ethyl acetate (3 × 70 mL). Combined organic layer was washed with brine (100 mL) and dried over anhydrous Na_2SO_4. Organic layer was

concentrated under reduced pressure to give gummy product with quantitative yield 99% (4.95 mmol, 1.2 g).

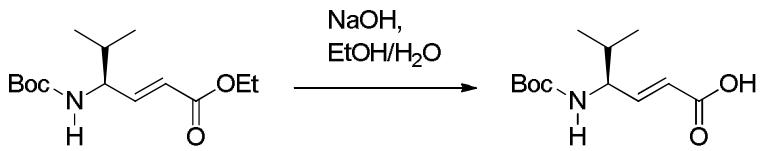

NH_2-dgL-OEt: (Boc-dgL-OEt) (5.5 mmol, 1.68 g) was dissolved in DCM (7 mL) and cooled the solution in ice bath. Then 7 mL neat TFA was added to this solution. After completion of the reaction (~ 30 min), TFA was removed from reaction mixture under *vacuum*. The residue was dissolved in water and the pH was adjusted to ~ 10 by the slow addition of solid Na_2CO_3 in ice cool condition. Then Boc deprotected free amine was extracted with ethyl acetate (3 × 40 mL). Combined organic layer was washed with brine (60 mL) followed by dried over Na_2SO_4 and concentrated under vacuum to *ca*. 2 mL and directly used for the coupling reaction in the next step.

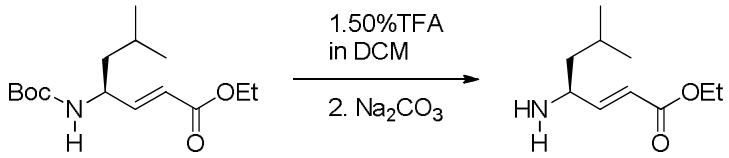

Boc-dgV-OH (4.95 mmol, 1.2 g) and NH_2-dgL-OEt were dissolved together in DMF (4 mL), followed by HBTU (5.5 mmol, 2.1 g) was added. The reaction mixture and cooled to 0 ^oC for 5 min. Then DiPEA (6 mmol, 1.08 mL) was added to the reaction mixture with stirring condition and the reaction mixture was allowed to come to room temperature. The progress of the reaction was monitored by TLC. After completion of the reaction (roughly 6hrs), reaction mixture was diluted with 300 mL of ethyl acetate and washed with 5% HCl (5 % by vol. in water, 2 × 80 mL), 10 % sodium carbonate solution in water (2 × 80 mL) and followed by brine (100 mL). The organic layer was dried over Na_2SO_4 and evaporated under reduced pressure to give gummy yellowish product, which was purified on silica gel column chromatography using DCM/MeOH solvent system to gummy product, which was further crystallized using EtOAc/Hexane. Overall yield 75% (3.6 mmol, 1.5 g).

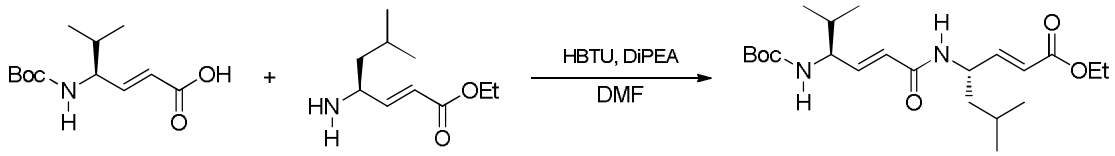

Boc-dgV-dgL-OEt (P2)

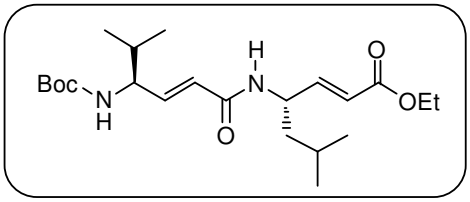

Physical state : White powder

Mol. Formula : $C_{22}H_{38}N_2O_5$

Yield : 75%, 1.5 g

^{1}H NMR (400 MHz, $CDCl_3$) : δ_H 6.85-6.80 (dd, *J* = 17.1, *J* = 2.7, 1H, vinylic β proton), 6.76-6.71(dd, *J* = 15.1, *J* = 2.9, 1H, vinylic β proton), 5.92-5.87(m, 2H, vinylic α proton), 5.48 (b, 1H, NH), 4.79 (m, 1H, γ proton), 4.59-4.57 (d, *J* = 8.7,1H, NH), 4.20-4.14 (q, *J* = 7.2, 2H, -OC*H*$_2$), 4.13-4.09 (m, 1H, γ proton), 1.87-1.79 (m, 1H), 1.71-1.58 (m, 3H), 1.44 (s, 9H, C(C*H*$_3$)$_3$ Boc), 1.29-1.25 (t, *J* = 7.1, 3H, -CH_2C*H*$_3$), 0.93-0.90 (m, 12H, CH-(C*H*$_3$)$_2$ Val & Leu side chains)

^{13}C NMR (100MHz, CD_3OH) : δ_C 168.74, 168.63, 158.8, 150.57, 145.71, 125.37, 122.08, 80.96, 62.35, 59.58, 44.62, 35.52, 34.38, 29.50, 27.48, 26.76, 24.00, 22.82, 20.32, 19.68, 15.25

MALDI TOF/TOF m/z : Calcd. $C_{22}H_{38}N_2O_5$ $[M+Na]^+$ 433.2678, observed 433.1865

(*Boc-dgF-dgA-OEt*) (P3)

Boc-dgF-OH: Boc-dgF-OEt (5 mmol, 1.59 g) was dissolved in ethanol (20 mL). Then 20 mL of 1(N) NaOH was added slowly to this solution. After completion of the reaction (~ 2 hrs), ethanol was evaporated from reaction mixture and the residue was acidified to *p*H ~ 3 using 5% HCl (5% volume in water) at cold condition after diluting with 50 mL of cold water. Product was extracted with ethyl acetate (3 × 70 mL). Combined organic layer was washed

with brine (100 mL) and dried over anhydrous Na_2SO_4. Organic layer was concentrated under reduced pressure to give gummy product with quantitative yield 99% (4.95 mmol, 1.56 g).

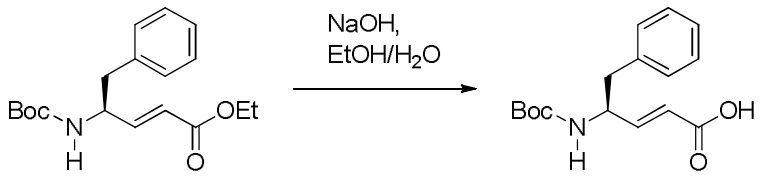

NH_2-dgA-OEt: (Boc-dgA-OEt) (5.5 mmol, 1.33 g) was dissolved in DCM (7 mL) and cooled the solution in ice bath. Then 7 mL neat TFA was added to this solution. After completion of the reaction (~ 30 min), TFA was removed from reaction mixture under *vacuum*. The residue was dissolved in water and the pH was adjusted to ~10 by the slow addition of solid Na_2CO_3 in ice cool condition. Then Boc deprotected free amine was extracted with ethyl acetate (3 × 40 mL). Combined organic layer was washed with brine (60 mL) followed by dried over Na_2SO_4 and concentrated under vacuum to *ca*. 2 mL and directly used for the coupling reaction in the next step.

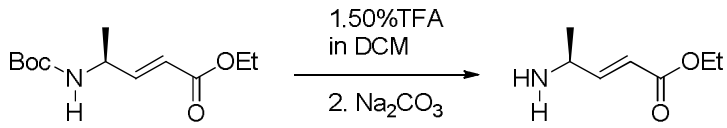

Boc-dgF-OH (4.95 mmol, 1.56 g) and NH_2-dgA-OEt were dissolved together in DMF (4 mL), followed by HBTU (5.5 mmol, 2.1 g) was added into the reaction mixture and cooled to 0 ^oC for 5 min. Then DiPEA (6 mmol, 1.08 mL) was added to the reaction mixture with stirring and the reaction mixture was allowed to come to room temperature. The progress of the reaction was monitored by TLC. After completion of the reaction (roughly 6hrs), reaction mixture was diluted with 300 mL of ethyl acetate and washed with 5% HCl (5 % by vol. in water, 2 × 80 mL), 10 % sodium carbonate solution in water (2 × 80 mL) and followed by brine (100 mL). The organic layer was dried over Na_2SO_4 and evaporated under reduced pressure to give gummy yellowish product, which was purified on silica gel column chromatography using DCM/MeOH solvent system to gummy product, which was further crystallized using EtOAc/Hexane. Overall yield 80% (4 mmol, 1.66 g).

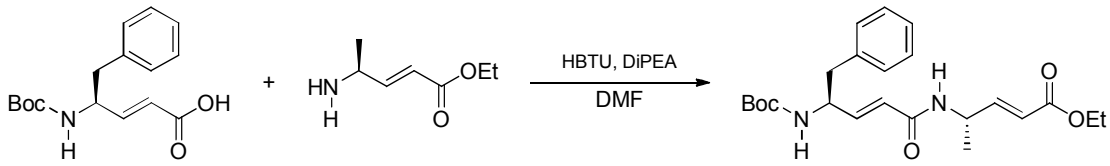

Boc-dgF-dgA-OEt (P3)

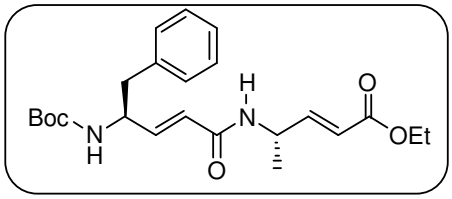

Physical state : White powder

Mol. Formula : $C_{23}H_{32}N_2O_5$

Yield : 80%, 1.66 g

^{1}H NMR (400 MHz, $CDCl_3$) : δ_H 7.33-7.17 (m, 5H, -Ph), 6.90-6.85 (dd, *J* = 5, *J* = 10.5, 1H, vinylic β proton), 6.82-6.78 (dd, *J* = 6.4, *J* = 8.7, 1H, vinylic β proton), 5.88-5.81 (d, *J* = 16.8, 1H, vinylic α proton) , 5.85-5.77 (d, *J* = 16.9, 1H, vinylic α proton), 5.57-5.56 (d, *J* = 7.5, 1H, NH), 4.83-4.74 (m, 1H, γ proton), 4.58 (b, 2H, NH and γ proton), 4.22-4.16 (q, *J* = 7, 2H, -OC*H*$_2$), 2.89-2.88 (d, *J* = 6.5, 2H, -C*H*$_2$-Ph),1.39 (s, 9H, -C(CH_3)$_3$ Boc), 1.31-1.27 (m, 6H, CH_3 side chain Ala and -CH_2C*H*$_3$)

MALDI TOF/TOF m/z : Calcd. $[M+Na]^+$ 439.2209Da, observed 439.1362Da.

Synthesis of Tripeptide

***Saponification of* Boc-dgV-dgA-OEt**

Boc-dgV-dgA-OH: Boc-dgV-dgA-OEt (3.8 mmol, 1.4 g) was dissolved in ethanol (15 mL). Then 15 mL of 1(N) NaOH was added slowly to this solution. After completion of the reaction (~ 2 hrs), ethanol was evaporated from reaction mixture and the residue was acidified to *p*H ~ 3 using 5% HCl (5% volume in water) at cold condition after diluting with 50 mL of cold water. Product was extracted with ethyl acetate (3 × 50 mL). Combined organic layer was washed with brine (80 mL) and dried over anhydrous Na_2SO_4. Organic

layer was concentrated under reduced pressure to give gummy product with quantitative yield 98% (3.72 mmol, 1.26 g). This dipeptide acid was further used to synthesize two tripeptides with different sequence.

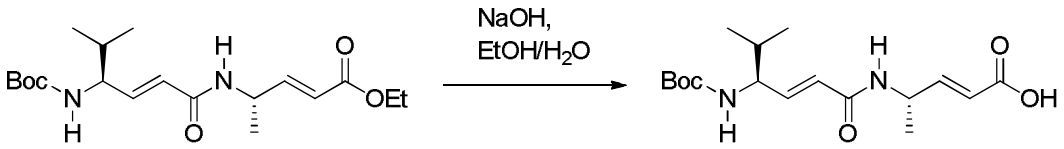

Boc-dgV-dgA-dgL-OEt (P4)

NH_2-dgL-OEt: (Boc-dgL-OEt) (1.25 mmol, 0.36 g) was dissolved in DCM (4 mL) and cooled the solution in ice bath. Then 4 mL neat TFA was added to this solution. After completion of the reaction (~ 30 min), TFA was removed from reaction mixture under vacuum. The residue was dissolved in water and the pH was adjusted to ~ 10 by slow addition of Na_2CO_3 in ice cold conditions. Then Boc deprotected free amine was extracted with ethyl acetate (3 × 20 mL). Combined organic layer was washed with brine (40 mL) followed by dried over Na_2SO_4 and concentrated under *vacuum* to *ca*.2 mL and directly used for coupling reaction in the next step.

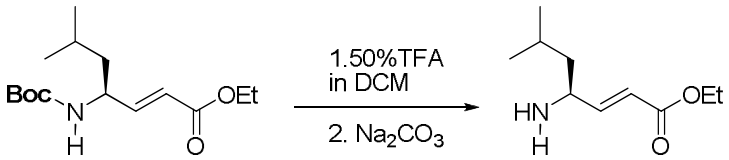

Boc-dgV-dgA-OH (1 mmol, 0.34 g) and NH_2-dgL-OEt were dissolved together in DMF (2 mL) and HBTU (1.1 mmol, 0.418 g) was added into the reaction mixture. Then reaction mixture was cooled to 0 ^oC for 5 min. Then DiEPA (1.25 mmol, 0.225 mL) was added to the reaction mixture and it was allowed to come in room temperature. The progress of the reaction was monitored by TLC. After completion of the reaction (roughly 6 hrs), peptide was precipitated out from reaction mixture. Then reaction mixture was diluted with 15 mL of ethyl acetate and it was observed that peptide is insoluble in ethyl acetate. Peptide was filtered out using sintered funnel and peptide was thoroughly washed with ethyl acetate (3 ×

20 mL). White powder peptide was collected and confirmed by analysing ^{1}H-NMR and MALDI TOF/TOF mass. Overall yield of the peptide 80% (0.8 mmol, 0.4 g).

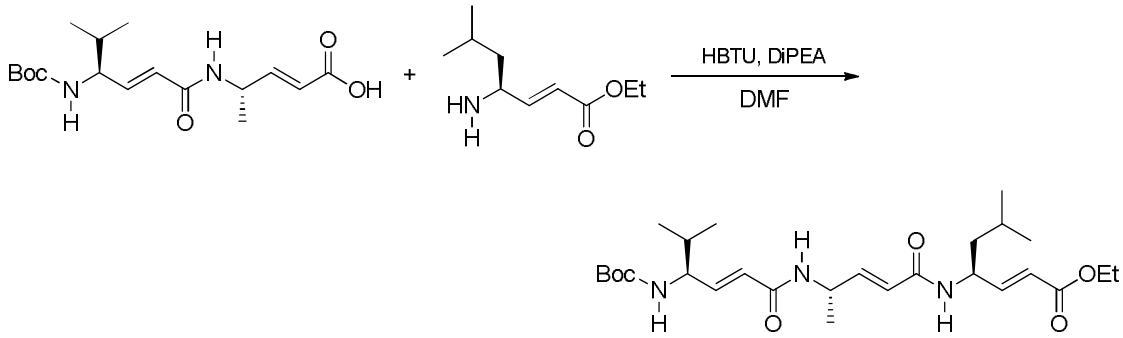

Boc-dgV-dgA-dgL-OEt (P4)

Physical state **:** White powder

Mol. Formula **:** $C_{27}H_{45}N_3O_6$

Yield **:** 80%, 0.4 g

^{1}H NMR (500 MHz, $CDCl_3$) **:** δ_H 7.31-7.29 (d, *J* = 7.9, 1H, NH of Leu), 6.90-6.77 (m, 4H, vinylic β proton, NH of Ala), 5.93-5.90 (d, *J* = 15.8, 1H, vinylic α proton), 5.89-5.86 (d, *J* = 15.2, 1H, vinylic α proton), 5.67-5.64 (d, *J* = 15.2, 1H, vinylic α proton), 4.75-4.70 (m, 3H, NH, γ proton), 4.19-4.12 (m, 3H, -OC*H*$_2$, γ proton), 1.89-1.85 (m, 1H), 1.69-1.67 (m, 1H), 1.49 (s, 9H, C(C*H*$_3$)$_3$ Boc), 1.48-1.46 (m, 2H), 1.32-1.28 (m, 6H, CH_3 side chain Ala, -CH_2C*H*$_3$), 0.95-0.88 (m, 12H, CH-(C*H*$_3$)$_2$ Val & Leu side chains)

MALDI TOF/TOF m/z **:** Calcd. $[M+Na]^+$ 530.3206 Da, observed 530.3857 Da.

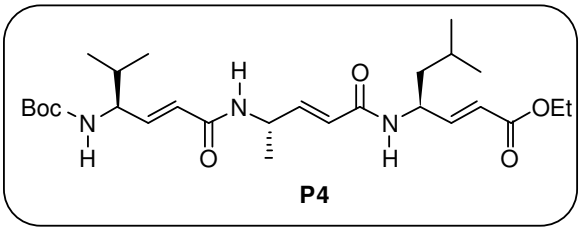

Boc-dgV-dgA-dgF-OEt (P5)

NH_2-dgF-OEt: Boc-dgF-OEt (1.25 mmol, 0.4 g) was dissolved in DCM (4 mL) and cooled the solution in ice bath. Then 4 mL neat TFA was added to this solution. After completion of the reaction (~ 30 min), TFA was removed from reaction mixture under *vacuum*. The residue was dissolved in water and the pH was adjusted to ~ 10 by the slow addition of solid Na_2CO_3 in ice cool condition. Then Boc deprotected free amine was extracted with ethyl acetate (3×20 mL). Combined organic layer was washed with brine (40 mL) followed by dried over Na_2SO_4 and concentrated under vacuum to *ca.* 2 mL and directly used for the coupling reaction in the next step.

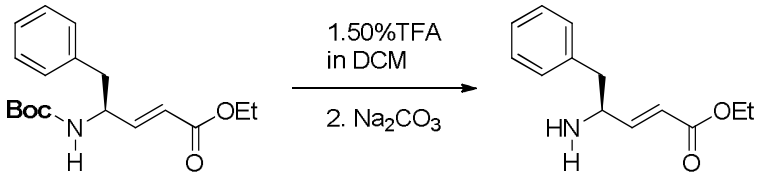

Boc-dgV-dgA-OH (1 mmol, 0.34 g) and NH_2-dgF-OEt were dissolved together in DMF (2 mL) followed by HBTU (1.1 mmol, 0.418 g) was added into the reaction mixture and cooled to 0 ^oC for 5 min. Then DiPEA (1.25 mmol, 0.225 mL) was added to the reaction mixture with stirring and the reaction mixture was allowed to come to room temperature. The progress of the reaction was monitored by TLC. After completion of the reaction (roughly 6hrs), reaction mixture was diluted with 15 mL of ethyl acetate and it was observed that the white precipitate is coming out from reaction mixture. We anticipated that peptide might be insoluble in ethyl acetate. The white precipitate was filtered out using sintered funnel and precipitate was thoroughly washed with ethyl acetate (3 ×20 mL). Further the precipitate was dried and by analysing ^{1}H-NMR and MALDI TOF/TOF mass suggested that, this is expected peptide. Overall yield of the peptide 78% (0.78 mmol, 0.44 g).

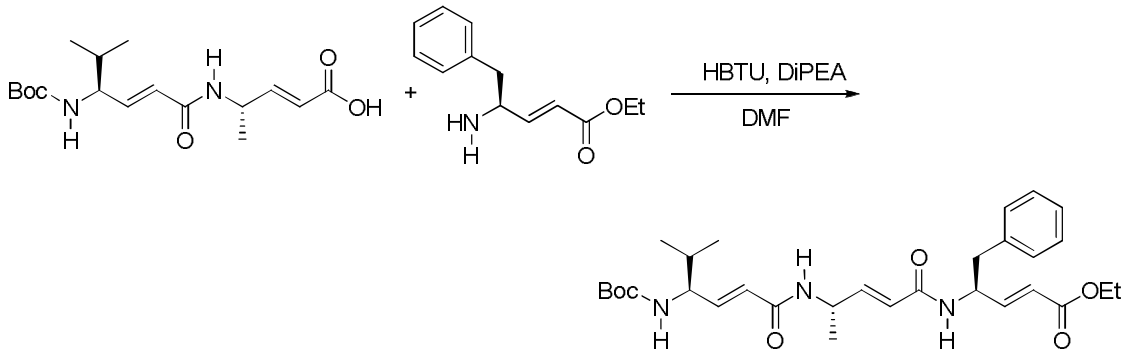

Boc-dgV-dgA-dgF-OEt (P5)

Physical state **:** White powder

Mol. Formula **:** $C_{30}H_{43}N_3O_6$

Yield **:** 78%, 0.44 g

^{1}H NMR (500 MHz, $CDCl_3$) **:** δ_H 7.62-7.61 (d, *J* = 5.8, 1H, NH), 7.27-7.20 (m, 5H, aromatic for –Ph), 6.93-6.90 (m, 2H, NH, vinylic β proton), 6.80-6.75 (dd, *J* = 5.3, *J* = 10.4, 1H, vinylic β proton), 6.71-6.66 (dd, *J* = 6.4, *J* = 8.7, 1H, vinylic β proton), 5.60-5.57 (d, *J* = 12.7, 2H, vinylic α proton), 5.85-5.82 (d, *J* = 12.4, 2H, vinylic α proton), 5.78-5.76 (d, *J* = 12.2, 1H, NH), 5.02-4.98 (m, 1H, γ proton), 4.71-4.69 (d, *J* = 6.8, 1H, NH), 4.17-4.09 (m, 3H, γ proton, -OC*H*$_2$), 3.06-2.87 (m, 2H, δ-proton of dgF), 1.88-1.82 (m, 1H), 1.49 (s, 9H, -C(CH_3)$_3$ Boc), 1.32-1.31 (d, *J* = 6.9, 3H, CH_3 side chain Ala), 1.27-1.24 (t, *J* = 7, 3H, -CH_2CH_3), 0.95-0.85 (m, 6H, CH-(C*H*$_3$)$_2$ Val side chain)

MALDI TOF/TOF m/z **:** Calcd. $[M+Na]^+$ 564.3050 Da, observed 564.3197 Da.

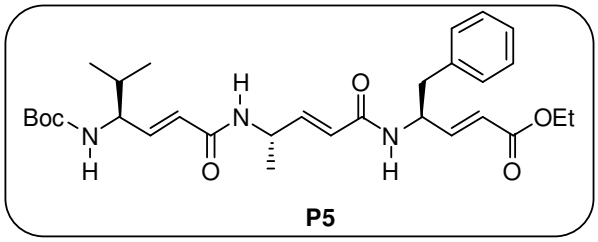

Synthesis of Tetrapeptide Boc-dgV-dgA-dgL-dgF-OEt (P6)

Boc-dgV-dgA-dgL-OH: Boc-dgV-dgA-dgL-OEt (0.5 mmol, 250 mg) was dissolved in ethanol (7 mL). Then 7 mL of 1(N) NaOH was added slowly to this solution. After completion of the reaction (~ 2 hrs), ethanol was evaporated from reaction mixture and the residue was acidified to *p*H ~ 3 using 5% HCl (5% volume in water) at cold condition after diluting with 30 mL of cold water. Product was extracted with ethyl acetate (3 × 30 mL). Combined organic layer was washed with brine (50 mL) and dried over anhydrous Na_2SO_4. Organic layer was concentrated under reduced pressure to give gummy product with quantitative yield 98% (0.49 mmol, 230mg).

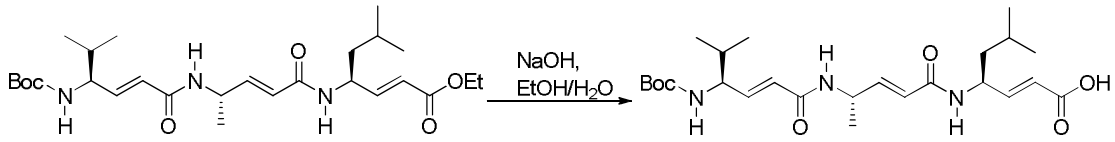

NH_2-dgF-OEt: Boc-dgF-OEt (0.75 mmol, 0.24 g) was dissolved in DCM (4 mL) and cooled the solution in ice bath. Then 4 mL neat TFA was added to this solution. After completion of the reaction (~ 30 min), TFA was removed from reaction mixture under *vacuum*. The residue was dissolved in water and the pH was adjusted to ~ 10 by the slow addition of solid Na_2CO_3 in ice cool condition. Then Boc deprotected free amine was extracted with ethyl acetate (3 × 20 mL). Combined organic layer was washed with brine (40 mL) followed by dried over Na_2SO_4 and concentrated under vacuum to *ca*. 2 mL and directly used for the coupling reaction in the next step.

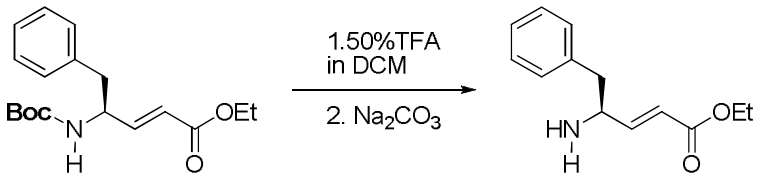

Boc-dgV-dgA-dgL-OH (0.49 mmol, 0.23 g) and NH_2-dgL-OEt were dissolved together in DMF (1.5 mL) and HBTU (0.52 mmol, 0.21 g) was added into the reaction mixture. Then reaction mixture was cooled to 0 ^oC for 5 min. Then DiPEA (0.75 mmol, 0.115 mL) was added to the reaction mixture and it was allowed to come in room temperature. The progress of the reaction was monitored by TLC. After completion of the reaction (roughly 6hrs), peptide was precipitated out from reaction mixture. Then reaction mixture was diluted with 15 mL of ethyl acetate and it was observed that peptide is insoluble in ethyl acetate. Peptide was filtered out using sintered funnel and peptide was thoroughly washed with ethyl acetate (3 × 20 mL). White powder peptide was collected and confirmed by analysing ^{1}H-NMR and MALDI TOF/TOF mass. Overall yield of the peptide 70% (0.343 mmol, 0.231 g).

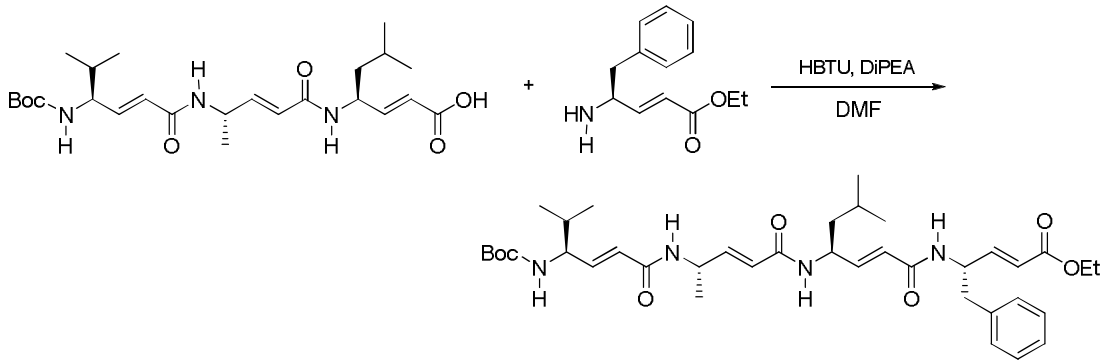

Boc-dgV-dgA-dgL-dgF-OEt (P6):

Physical state	**:**	White powder
Mol. Formula	**:**	$C_{19}H_{32}N_2O_5$
Yield	**:**	70%, 0.231 g

^{1}H NMR (500 MHz, $CDCl_3$) **:** δ_H 8.24-8.22 (d, *J* = 7.8, 1H, NH of dgF), 8.20-8.19 (d, *J* = 7.6, 1H, NH of dgL), 7.81 (b, 1H, NH of dgA), 7.29-7.18 (m, 5H, Ph), 6.97-6.82 (m, 4H, vinylic β proton), 5.98-5.94 (d, *J* = 15.6, 1H, vinylic α proton), 5.94-5.90 (d, *J* = 15.3, 1H, vinylic α proton), 5.53-5.49 (d, *J* = 15.2, 1H, vinylic α proton), 5.48-5.44 (d, *J* = 15.2, 1H, vinylic α proton), 5.01-4.97 (m, 1H, γ proton), 4.78 (b, 1H, γ proton), 4.67-4.66 (d, *J* = 7.2, 1H, NH), 4.51 (b, 1H, γ proton), 4.17-4.12 (q, *J* = 7, 2H, -OC*H*$_2$), 4.08 (b, 1H, γ proton), 3.13-2.88 (m, 2H, -C*H*$_2$Ph), 1.94-1.89 (m, 1H), 1.79-1.76 (m, 1H), 1.74-1.72 (m, 1H), 1.54 (s,

9H, $C(CH_3)_3$ Boc), 1.32-1.30 (d, J = 7, 3H, CH_3 side chain Ala), 1.29-1.25 (t, J = 7, 3H, -CH_2CH_3), 0.95-0.91 (m, 6H, CH-$(CH_3)_2$ Val & Leu side chains)

MALDI TOF/TOF m/z **:** Calcd. $C_{38}H_{56}N_4O_7$ $[M+Na]^+$ 703.4047 Da, observed 703.2796 Da.

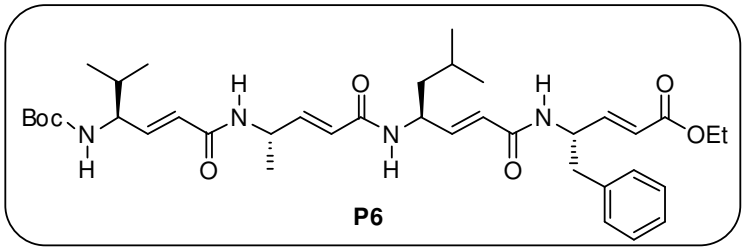

P6

1.6 References

1. a) DeGrado, W. F.; Summa, C. M.; Pavone, V.; Nastri, F.; Lombardi, A. *Annual Review of Biochemistry,* **1999**, *68*, 779-819. b) Hill, R. B.; Raleigh, D. P.; Lombardi, A.; Degrado, N. F. *Acc. Chem. Res.*, **2000**, *33*, 745-754. c) Gellman, S. H. *Curr. Opin. Chem. Biol.* **1998**, *2*, 717-725. d) Venkatraman, J.; Shankaramma, S. C.; Balaram, P. *Chem. Rev.* **2001**, *101*, 3131-3152.
2. a) Hill, D. J.; Mio, M. J.; Prince, R. B.; Hughes, T. S.; Moore, J. S. *Chem Rev.*, **2001**,*101*, 3893-4011. b) Gellman, S. H. *Acc. Chem. Res.,* **1998**, *31*, 173-180. c) Kim, I. C.; Hamilton, A. D. *Org. Lett.*, **2006**, *8*, 1751-1754. d) Brown, N. J.; Wu, C. W.; Seurynck-Servoss, S. L.; Barron, A. E. *Biochemistry,* **2008**, *47*, 1808-1818.
3. a) Seebach, D.; Gardiner, J. *Acc. Chem. Res.,* **2008**, *41*, 1366-1375. b) Horne, W. S.; Gellmann, S. H. *Acc. Chem. Res.*, **2008**, *41*, 1399-1408. c) Price, J. L.; Horne, W. S.; Gellman, S. H. *J. Am. Chem. Soc.*, **2010**, *132*, 12378-12387. d) Cheng, R. P.; Gellman, S. H.; DeGrado, W. F. *Chem. Rev.*, **2001**, *101*, 3219-3232. e) Vasudev, P. G., Chatterjee, S., Shamala, N., Balaram, P. *Chem. Rev.,* **2011**, *111*, 657-687.
4. a) Hintermann, T.; Gademann, K.; Jaun, B.; Seebach, D. *Helv. Chim. Acta*, **1998**, *81*, 983-1002. b) Seebach, D.; Beck, A. K.; Bierbaum, D. J. *Chem. Biodiv.,* **2004**, *1*, 1111-1239.
5. a) Appella, D. H.; Christianson, L. A.; Karle, I. L.; Powell, D. R.; Gellman, S. H. *J. Am. Chem. Soc.,* **1996**, *118*, 13071-13702. b) Appella, D. H.; Christianson, L. A.; Karle, I. L.; Powell, D. R.; Gellman, S. H. *J. Am. Chem. Soc.,* **1999**, *121*, 6206-6212. c) Appella, D. H.; Christianson, L. A.; Klein, D. A.; Richards, M. A.; Powell, D. R.; Gellman, S. H. *J. Am. Chem. Soc.,* **1999**, *121*, 7574-7581.
6. Chatterjee, S.; Roy, R. S.; Balaram, P. *J. R. Soc. Interface,* **2007***, 4,* 587-606
7. a) Sharma, G. V. M.; Reddy, R.; Krishna, P. R.; Ravi Sankar, A.; Narsimulu, K., Kumar, S. K.; Jayaprakash, P.; Jagannadh, B.; Kunwar, A. C. *J. Am. Chem. Soc.*, **2003**, *125*, 13670-13671. b) Sharma, G. V. M.; Babu, B. S.; Ramakrishna, K. V. S.; Nagendar, P.;. Kunwar, A. C.; Schramm, P.; Baldauf, C.; Hofmann, H. J. *Chem. Eur. J.,* **2009**, *15*, 5552-5566.c) Sharma, G. V. M.; Chandramouli, N.; Choudhary, M.; Nagendar, P.; Ramakrishna, K. V. S.; Kunwar, A. C.; Schramm, P.; Hofmann, H. -J. *J. Am. Chem. Soc.*, **2009**, *131*, 17335–17344.

8. a) Guitot, K.; Carboni, S.; Reiser, O.; Piarulli, U. *J. Org. Chem.,* **2009**, *74*, 8433-8436. b) De Pol, S.; Zorn, C.; Klein, C. D.; Zerbe, O.; Reiser, O. *Angew. Chem., Int. Ed. Engl.,* **2004**, *43*, 511-514.
9. a) Fischer, L.; Guichard, G. *Org. Biomol. Chem.,* **2010**, *8*, 3101-3117. b) Fremaux, J.; Fischer, L.; Arbogast, T.; Kauffman, B.; Guichard, G. *Angew. Chem., Int. Ed. Engl.,* **2011**, *50*, 11382-11385.
10. a) Davis, J. M.; Tsou, L. K.; Hamilton, A. D. *Chem. Soc. Rev.,* **2007**, *36*, 326-334. b) Adler, M. J.; Hamilton, A. D. *J. Org. Chem.* **2011**, *76*, 7040-7047.
11. a) Linington, R. G.; Clark, B. R.; Trimble, E. E.; Almanza, A.; Uren, L.-D.; Kyle, D. E.; Gerwick, W. H. *J. Nat. Prod.,* **2009**, *72*, 14-17. b) Coleman, J. E.; de Silva, E. D.; Kong, F.; Andersen, R. J.; Allen, T. M. *Tetrahedron*, **1995**, *51*, 10653-10662. c) Schaschke, N. *Bioorg. Med. Chem. Lett.,* **2004**, *14***,** 855–857. d) Lee, A. Y.; Hagihara, M.; Karmacharya, R.; Albers, M. W.; Schreiber, S. L.; Clardy, J. *J. Am. Chem. Soc.,***1993**, *115*, 12619-12620; e) Hagihara M.; Schreiber, S. L. *J. Am. Chem. Soc*., **1992**, *114*, 6570-6571. f) Lee, A. Y.; Hagihara, M.; Karmacharya, R.; Albers, M. W.; Schreiber, S. L.; Clardy, J. *J. Am. Chem. Soc.*, **1993**, *115*,12619-12620. g) Nieman, J. A.; Coleman, J. E.; Wallace, D. J.; Piers, E.; Lim, L. Y.; Roberge, M.; Andersen, R. J. *J. Nat. Prod*., **2003**, *66*, 183-199. h) Nakao, Y.; Matsunaga S.; Fusetani, N. *Bioorg. Med. Chem.* **1995**, *3*, 1115-1122. i) Fusetani, N.; Matsunaga, S.; Matsumoto, H.; Takebayashi, H. *J. Am. Chem. Soc.,* **1990**, *112*, 7051-7053.
12. a) Hanzlik, R. P.; Thompson, S. A. *J. Med. Chem.*, **1984**, *27*, 711-712. b) Liu, S.; Hanzlik, R. P. *J. Med. Chem.,* **1992**, *35*, 1067-1075. c) Kong, J-S.; Venkatraman, S.; Furness, K.; Nimkar, S.; Shepherd, T. A.; Wang, Q. M.; Aube, J.; Hanzlik, R. P. *J. Med. Chem.*, **1998**, *41*, 2579-2587. d) Santos, M. M. M.; Moreira, R. *Mini-Rev. Med. Chem. Lett*. **2007**, *7*, 1040-1050. e) Breuning, A.; Degel, B.; Schulz, F.; Buchold, C.; Stempka, M.; Machon, U.; Heppner, S.; Gelhaus, C.; Leippe, M.; Leyh, M.; Kisker, C.; Rath, J.; Stich, A.; Gut, J.; Rosenthal, P. J.; Schmuck, C.; Schirmeister, T. *J. Med. Chem.*, **2010**, *53*, 1951-1963. f) Schaschke N.; Sommerhoff, C. P. *ChemMedChem*, **2010**, *5*, 367-370.
13. Plummer, J. S.; Emery, L. A.; Stier, M. A.; Suto, M. J. *Tetrahedron Lett*., **1993**, *34*, 7529-7532.
14. Fu, Y.; Xu, B.; Zou, X.; Ma, C.; Yang, X.; Mou, K.; Fu, G.; Lu, Y.; Xu, P. *Bioorg. Med. Chem. Lett*., **2007**, *17*, 1102 – 1106.
15. Reetz, M. T. *Angew. Chem., Int. Ed. Engl.,* **1991**, *30*, 1531-1546.

16. Hagihara, M.; Anthony, N. J.; Stout, T. J.; Clardy J.; Schreiber, S. L. *J. Am. Chem. Soc.,* **1992**, *114*, 6568-6570.

17. a) Grison, C.; Coutrot, P.; Geńeve, S.; Didierjean, C.; Marraud, M. *J. Org. Chem*, **2005**, *70*, 10753-10764 b) Grison, C.; Geńeve, S.; Halbin, E.; Coutrot, P. *Tetrahedron,* **2001**, *57*, 4903-4923.

18. Chakraborty, T. K.; Ghosh, A.; Kumar, S. K.; Kunwar, A. C. *J. Org. Chem.,* **2003**, *68*, 6459-6462.

19. a) Baldauf, C.; Gunther, R.; Hofmann, H. J. *J. Org. Chem.*, **2005**, *70*, 5351-5361.

20. a) Wittig, G.; Geissler, G. *Liebigs Ann. Chem.,* **1953**, *580*, 44-68. b) Wittig, G.; Schollkopf, U. *Chem. Ber.,* **1954**, *87*, 1318-1330. c) Wittig, G. *Science,* **1980**, *210*, 600-604. d) Maerckar, A. *Org. React.,* **1965**, *14*, 270-490. d) Maryanoff, B. E.; Reitz, A. B. *Chem. Rev.,* **1989**, *89*, 863-927. e) Kolodiazhnyi, O. I. *Phosphorus Ylides, Chemistry and Application in Organic Synthesis*; Wiley-VCH: Weinheim, Germany, 1999. f) Vedejs, E.; Marth, C. F. *J. Am. Chem. Soc.,* **1990**, *112*, 3905–3909. g) El-Batta, A.; Jiang, C.; Zhao, W.; Anness, R.; Cooksy, A. L.; Bergdahl, M. *J. Org. Chem.*, **2007**, *72*, 5244-5259 and references sited therein.

21. a) Julia, M.; Paris, J. M. *Tetrahedron Lett.,* **1973**, *14*, 4833-4836. b) Baudin, J. B.; Hareau, G.; Julia, S. A.; Ruel, O.*Tetrahedron Lett.,* **1991**, *32*, 1175-1178. c) Kocienski, P. J. *Phosphorus Sulfur,* **1985**, *24*, 97-127. d) Blakemore, P. R. *J. Chem. Soc., Perkin Trans 1,* **2002**, 2563-2585.

22. a) Rotella, D. P. *J. Am. Chem. Soc.,* **1996**, *118*, 12246-12247. b) Oishi, S.; Kamano, T.; Niida, A.; Odagaki, Y.; Hamanaka, N.; Yamamoto, M.; Ajito, K.; Tamamura, H.; Otaka, A.; Fujii, N. *J. Org. Chem*., **2002**, *67*, 6162-6173. c) Chintareddy, V. R.; Ellern, A.; Verkade, J. G. *J. Org. Chem*., **2010**, *75*, 7166-7174 and references sited therein.

23. a) Peterson, D. J. *J. Org. Chem.,* **1968**, *33*, 780-784. b) Ager, D. J.; *Synthesis,* **1984**, 384-398. c) Ager, D. J. *Org. React.,* **1990**, *38*, 1-223.

24. Blasdel, L. K.; Myers, A. G. *Org. Lett.*, **2005**, *7*, 4281-4283.

25. a) Claridge, T. D. W.; Davies, S. G.; Lee, J. A.; Nicholson, R. L.; Roberts, P. M.; Russell, A. J.; Smith, A. D.; Toms, S. M. *Org Lett.*, **2008**, *10*, 5437-5440. b) Blanchette, M. A.; Choy, W.J.; Davis, T.; Essenfeld, A. P.; Masamune, S.; Roush, W. R.; Sakai, T. *Tetrahedron Lett.,* **1984**, *25*, 2183-2186. c) Rathke, M. W.; Nowak, M. *J. Org. Chem.,* **1985**, *50*, 2624-2626.

26. Bandyopadhyay, A.; Agrawal, N.; Mali, S. M.; Jadhav, S. V.; Gopi, H. N. *Org. Biomol. Chem.,* **2010**, *8*, 4855-4860.
27. Pauling, L.; Corey, R. B. *Proc. Natl. Acad. Sci. U. S. A.*, **1951**, *37*, 729-740.
28. a) Fraser, R. D. B.; MacRae, T. P. Academic Press, New York, 1973. b) Maccallum, P. H.; Poet,R.; Milner-White, E. J. *J. Mol. Biol.,* **1995**, *248*, 361-373. c) Wouters, M.A.; Curmi,P. M. G. *Proteins*: *Struct. Funct. Genet.* **1995**, *22*, 119-131.
29. Ho, B. K.; Curmi, P. M. *J. Mol. Biol.,* **2002**, *317*, 291-308.
30. Derewenda, Z.S.; Lee, L.; Derewenda, U. *J. Mol. Biol.,* **1995**, *252*, 248-262
31. Vargas, R.; Garza, J.; Dixon, D. A.; Hay, B. P. *J. Am. Chem. Soc.*, **2000**, *122*, 4750-4755.
32. Senes, A.; Ubarretxena-Belandia, I.; Engelman, D. M. *Proc. Natl. Acad. Sci. U. S. A.*, **2001**, *98*, 9056-9061.
33. a) Baures, P. W.; Beatty, A. M.; Dhanasekaran, M.; Helfrich, B. A.; Perez-Segarra, W.; Desper, J. *J. Am. Chem. Soc.*, **2002**, *124*, 11315-11323. b) Cheung, E. Y.; McCabe, E. E.; M. Harris, K. D.; Johnston, R. L.; Tedesco, E.; Raja, K. M. P.; Balaram, P. *Angew. Chem., Int. Ed.,* **2002**, *41*, 494-496. c) Sengupta, A.; Aravinda, S.; Shamala, N.; Raja, K. M. P.; Balaram, P. *Org. Biomol. Chem.*, **2006**, *4*, 4214-4222. d) Khurram, M.; Qureshi, N.; Smith, M. D. *Chem. Commun*. **2006**, 5006–5008
34. Steiner, T. *Angew. Chem., Int. Ed.*, **2002**, *41*, 48-76.
35. Steiner, T.; Saenger, W. *J. Chem. Soc., Perkin Trans.* **1998,** *2*, 371-388.
36. Mali, S. M.; Bandyopadhyay, A.; Jadhav, S. V.; Kumar, M. G.; Gopi, H. N.; *Org. Biomol. Chem.* **2011**, *9,* 6566-6574.
37. Ramachandran, G.N. &Sasisekharan, V. *Advan. Protein Chem.*, **1968**, 23, 283-437.
38. Lietzke, S.E.; Scavetta, R.D.; Yoder, M.D.; Jurnak, F. *Plant physiol.* **1996**, *111*, 73-92
39. SHELXS-97: Sheldrick, G. M. *Acta Crystallogr. Sect A*, **1990**, *46*, 467-473, b) Sheldrick, G. M. SHELXL-97, Universität Göttingen (Germany) 1997.

1.7 Appendix I: Characterization Data of Synthesized Compounds

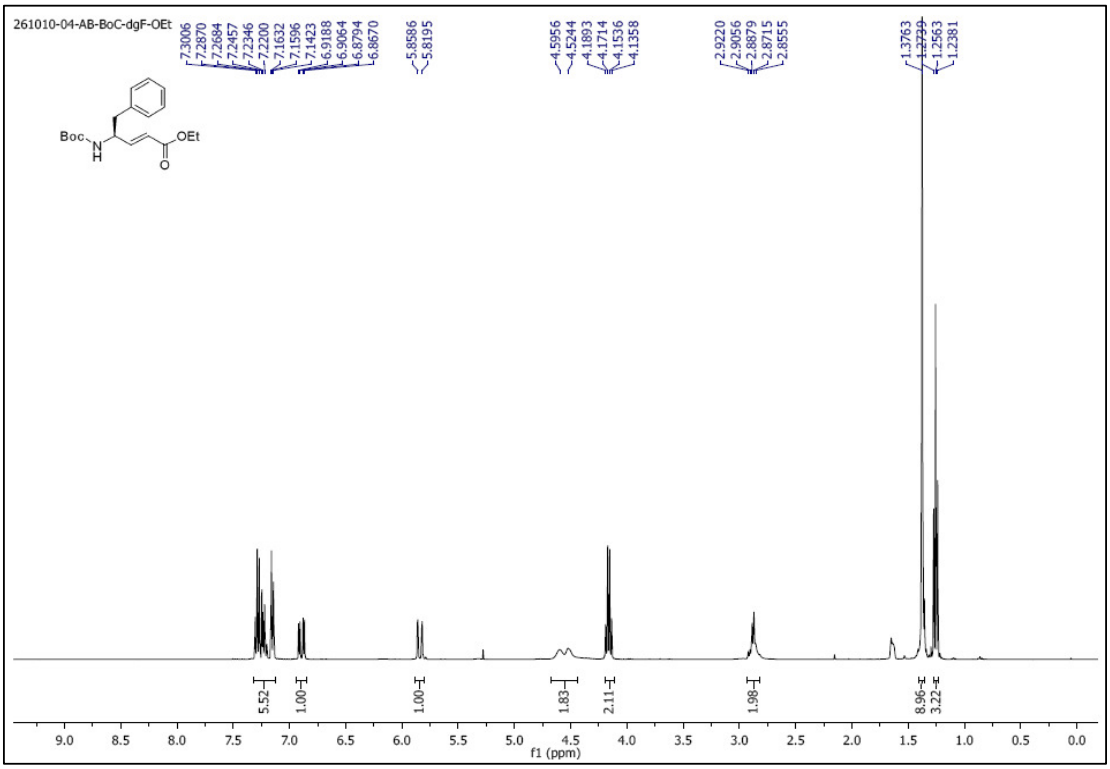
261010-04-AB-BoC-dgF-OEt
Boc
N
H
OEt
O
f1 (ppm)

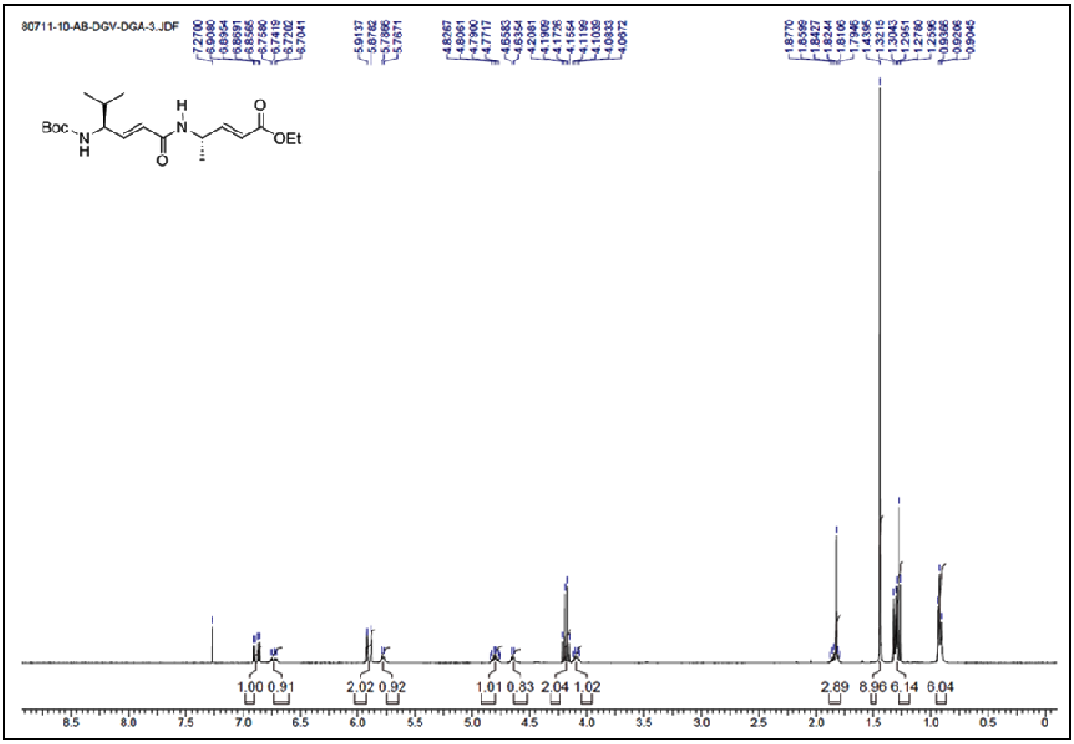
80711-10-AB-DGV-DGA-3..IDF
Boc
N
H
O
N
H
O
OEt

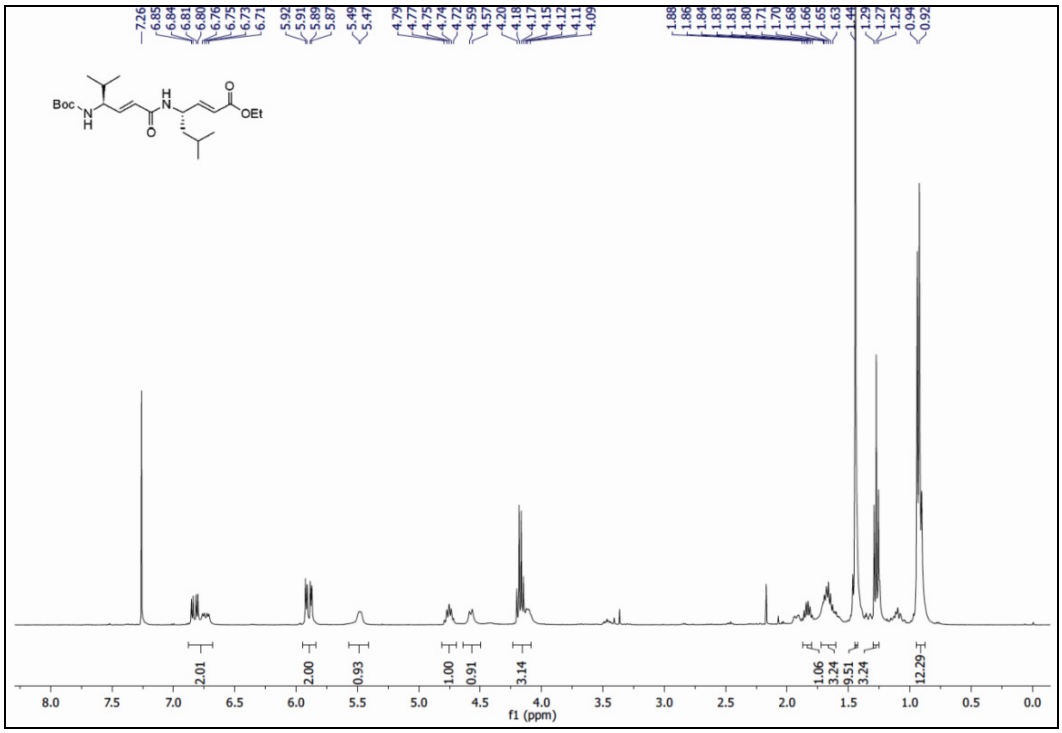
Boc
N
H
H
N
O
O
OEt
f1 (ppm)

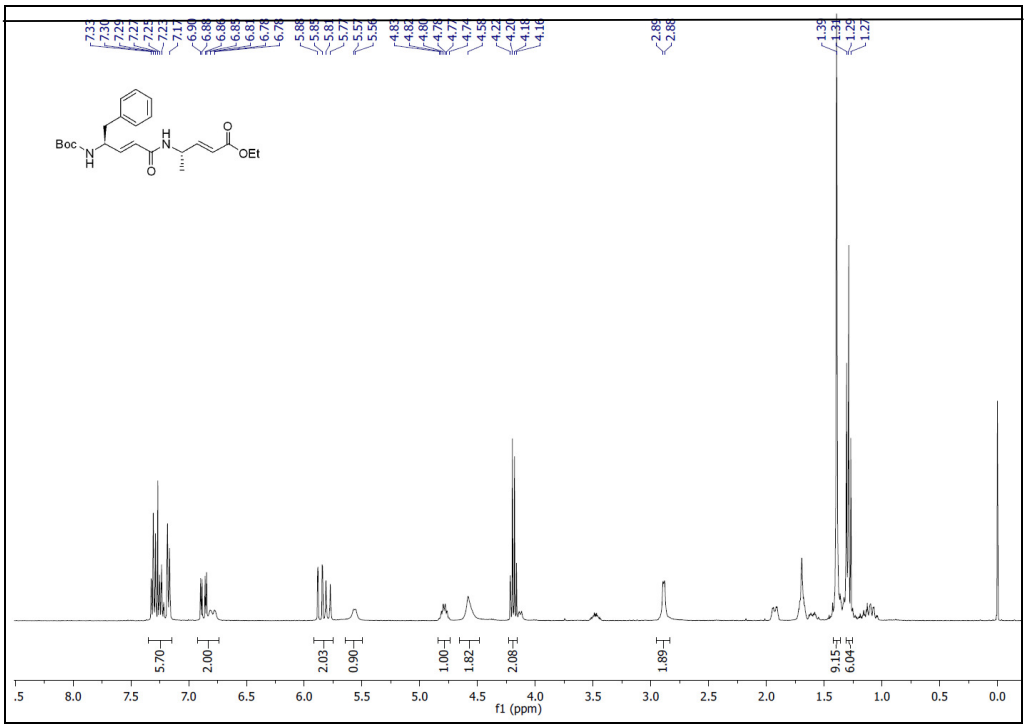
Boc
N
H
H
N
O
O
OEt
f1 (ppm)

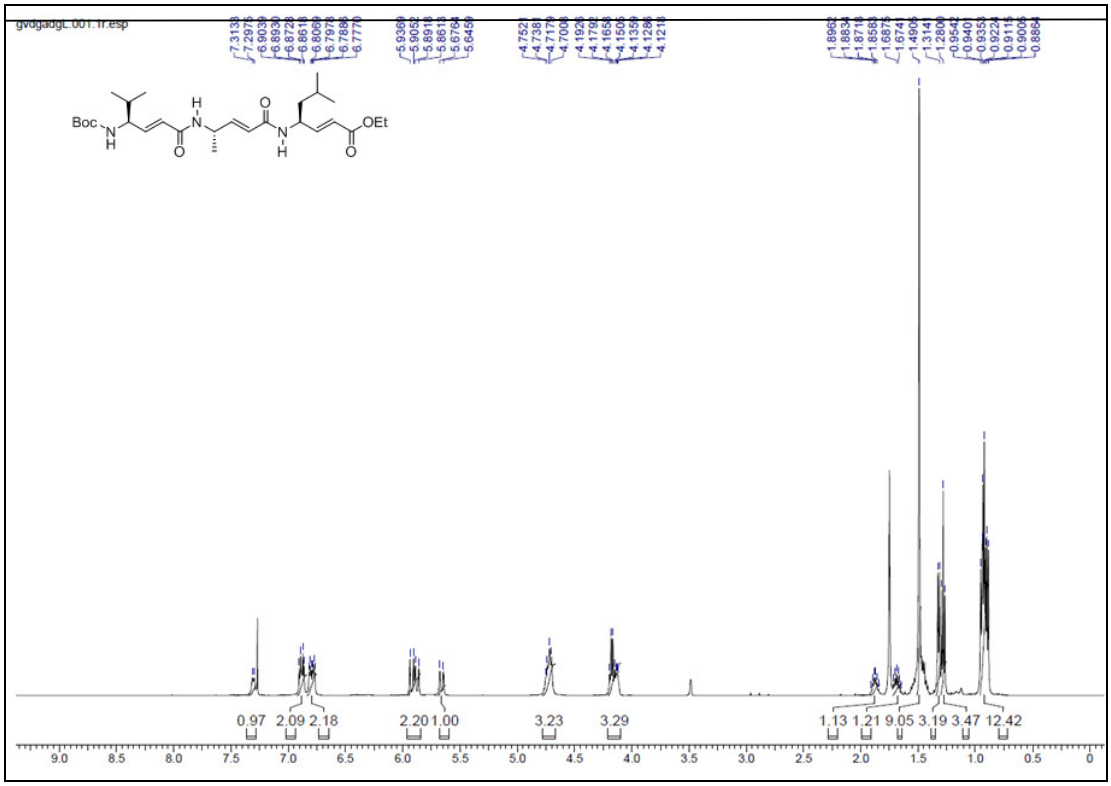
Boc
OEt
0.97 2.09 2.18 2.20 1.00 3.23 3.29 1.13 1.21 9.05 3.19 3.47 12.42

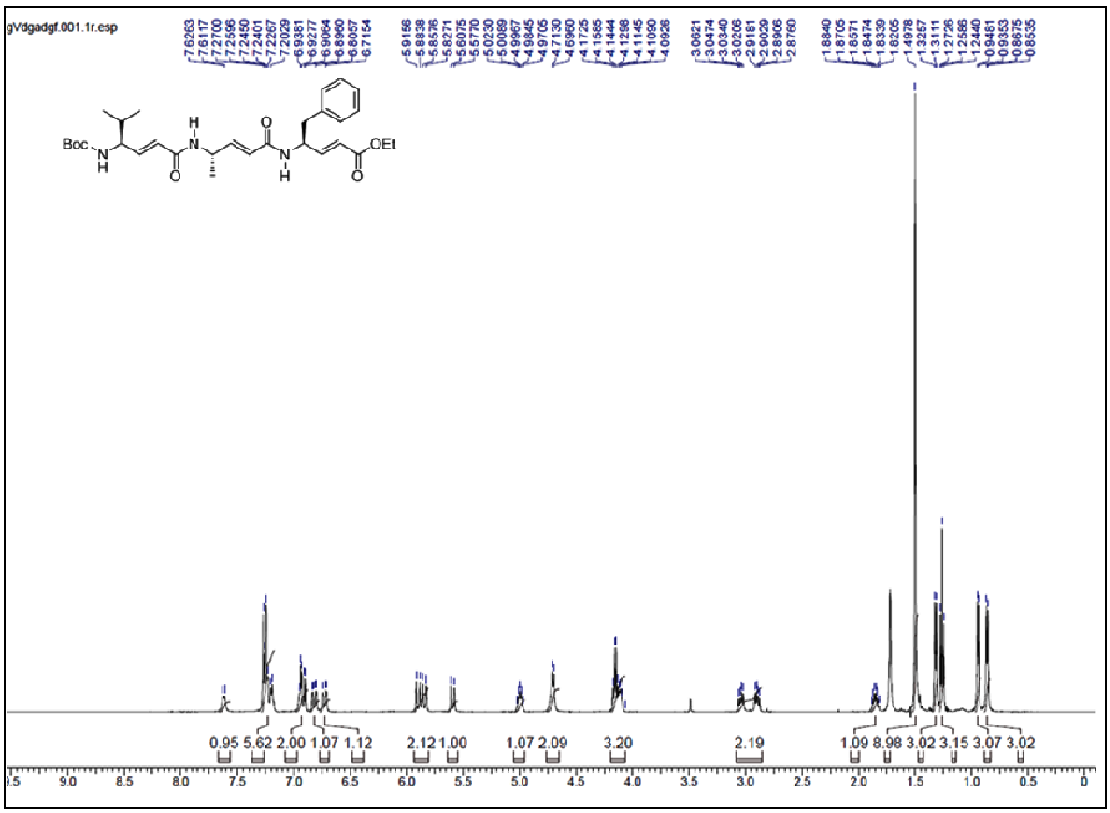
Boc
OEt
0.95 5.62 2.00 1.07 1.12 2.12 1.00 1.07 2.09 3.20 2.19 1.09 8.98 3.02 3.15 3.07 3.02

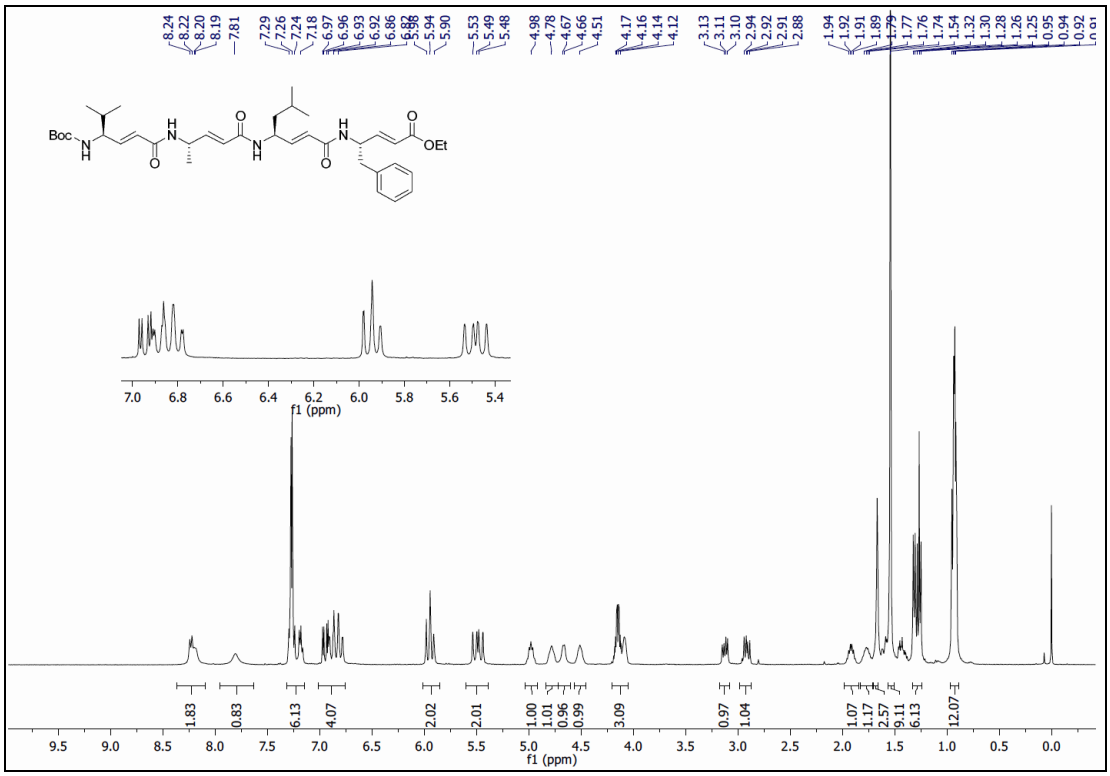
Boc
N
H
O
H
N
O
H
N
O
O
OEt
8.24
8.22
8.20
8.19
7.81
7.29
7.26
7.24
7.18
6.97
6.96
6.93
6.92
6.86
5.94
5.90
5.53
5.49
5.48
4.98
4.78
4.67
4.66
4.51
4.17
4.16
4.14
4.12
3.13
3.11
3.10
2.94
2.92
2.91
2.88
1.94
1.92
1.91
1.89
1.79
1.77
1.76
1.74
1.54
1.32
1.30
1.28
1.26
1.25
0.95
0.94
0.92
7.0
6.8
6.6
6.4
6.2
6.0
5.8
5.6
5.4
f1 (ppm)
1.83
0.83
6.13
4.07
2.02
2.01
1.00
1.01
0.96
0.99
3.09
0.97
1.04
1.07
1.17
2.57
9.11
6.13
12.07
9.5
9.0
8.5
8.0
7.5
7.0
6.5
6.0
5.5
5.0
4.5
4.0
3.5
3.0
2.5
2.0
1.5
1.0
0.5
0.0
f1 (ppm)

Chapter 2

Structural investigation of (*E*)-vinylogous γ-amino acids in hybrid β-hairpin and multi-strand β-sheets

2.1 Introduction

β-hairpins are one of the simplest supersecondary structures and they are extensively found in globular proteins (Figure 1). Unlike helical geometries, the extended conformations can be classified as parallel and antiparallel β-sheets.[1] The two extended sheets are connected by a reverse turn leading to β-hairpin structures. The β-turns are the most economical polypeptide geometry that can link two extended segments of polypeptide chain with reversal direction. The β-turn is the simplest defined loop structure with conformational characteristics determined by residues at two positions (*i*+1 and *i*+2) of the turn segment. The β-turns are further classified based on the torsional angles of *i*+1 and *i*+2 residues.[2] A β-strand typically consists of 3 to 10 amino acids. In their survey, Sibanda and Thornton[3] have found that 70% of β-hairpins are less than 7 residues in length with the two-residue tight turns. In contrast to the type I ($\phi_{i+1} = -60^o$ $\psi_{i+1} = -30^o$, $\phi_{i+2} = -90^o$, $\psi_{i+1} = 0^o$) and type II ($\phi_{i+1} = -60^o$ $\psi_{i+1} = 120^o$, $\phi_{i+2} = 80^o$, $\psi_{i+1} = 0^o$) turns, their mirror images type I′ ($\phi_{i+1} = 60^o$ $\psi_{i+1} = 30^o$, $\phi_{i+2} = 90^o$, $\psi_{i+1} = 0^o$) and type II′ turns ($\phi_{i+1} = 60^o$ $\psi_{i+1} = -120^o$, $\phi_{i+2} = -80^o$, $\psi_{i+1} = 0^o$), respectively, have been found predominantly in protein structures.

Many proteins often constitute a β-hairpin scaffold for biomolecular recognitions.[4] The β-hairpin scaffolds have been used to structurally mimic the epitopes of antibodies and cytokine receptors.[5] Recently, Robinson et al. have investigated the structural mimicry of canonical conformation in antibody Hypervariables loops using cyclic peptides containing a heterochiral diprolin template (Figure 2b). They have been used as inhibitors for protein-protein and protein-nucleic acid interactions, which have proven difficult targets for small molecule drugs,[6] as well synthetic vaccine design.[7] Naturally occurring β-hairpin scaffolds have proved their potential as antimicrobial and antiviral candidates.[8] The antimicrobial peptides are generally cationic and they possess β-hairpin structure stabilized by disulfide bridges, including the protegrins, polyphemusins, and tachyplesin (Figure 3). These peptides show broad-spectrum of antimicrobial activity against Gram-positive and Gram-negative bacteria. In their pioneering work, Robinson and colleagues have studied the first β-hairpin mimetic inhibitor for the bovine immunodeficiency virus (BIV) TAR-Tat domain.[6a]

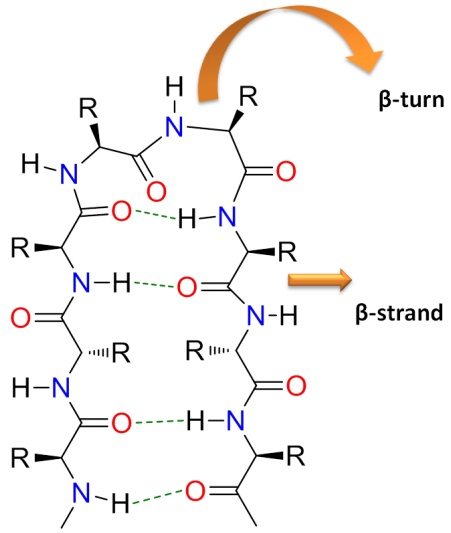

Figure 1: Schematic representation of β-hairpin.

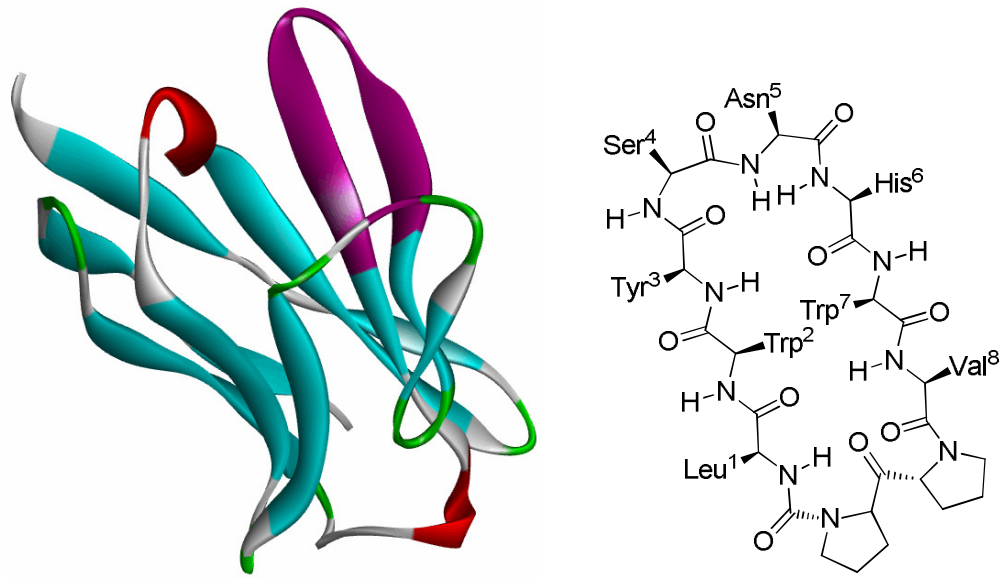

a) **b)**

Figure 2: a) Hairpin mimetics based on antibody CDR loops. The antibody domains are shown with the CDR loops purple, and b) The hairpin mimetic.

In addition, β-hairpins are also being used to obtain self-assembling biomaterials with gel and hydrogel properties.[9] These peptide based gels and hydrogels have been utilized in tissue

engineering and controlled drug release application. Moreover, designed β-hairpins have also been exploited as chiral catalysts in a variety of organic reactions.[10]

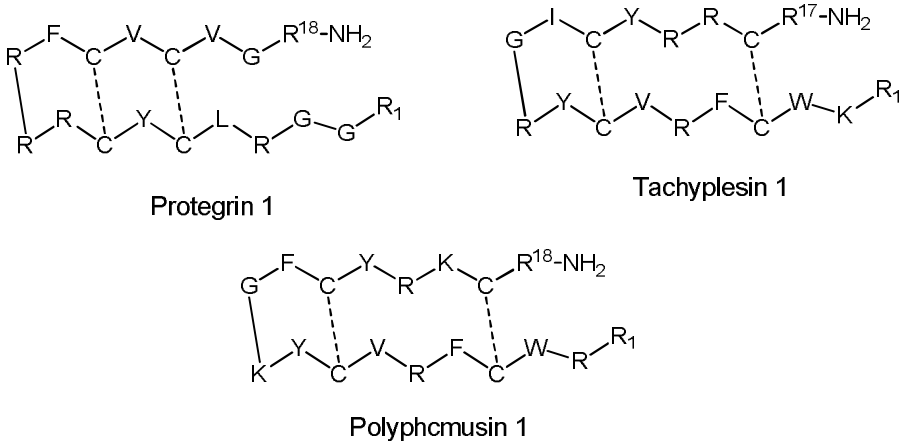

Figure 3: Hairpin, cationic antimicrobial peptides.

2.1.1 β-hairpins as catalyst in organic reactions

The discovery of new and effective small-molecule catalysts is a challenging process. Peptide-based catalysts have become important players in this area for a variety of reasons, in particular, due to their modularity and tunability.[11] In this context, designed β-hairpins have been exploited as asymmetric catalysts in a variety of organic reactions.[10] Miller and colleagues showed the utility of β-hairpin mimetic catalysts in selective acylation (Scheme 1), phosphorylation, conjugate addition, asymmetric C-C bond formation and other site specific reactions.

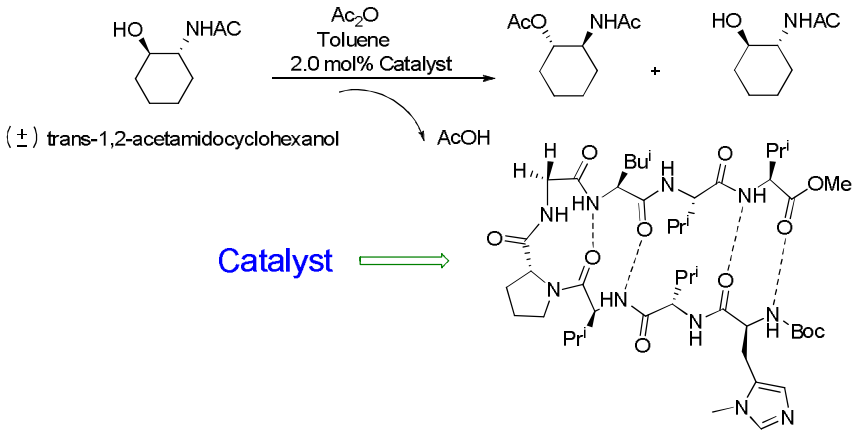

Scheme 1: Schematic diagram of asymmetric acylation reactions with β-hairpin peptide-based catalysts.[10c]

2.1.2 β-hairpin peptidomimetic using non-ribosomal amino acids

The remarkable and widespread properties of β-hairpins in both biology and synthetic organic chemistry have attracted synthetic chemists and structural biologists to design stable β-hairpins using non-natural amino acids.[12] Because in contrast to α-peptides, β-peptides and higher homologue oligomers have proven better proteolytic and metabolic stability and the prospect of intracellular delivery.[13] Unlike α-helical peptides, where the structure is stabilized by intramolecular 13-atoms H-bond, β-strand requires a structural context for the stabilization. The design of β-hairpins using non-natural amino acids with stabilized β-strands with tight turn is a challenging task for a chemist as well as biochemist. Recent advances that improved β-hairpin stabilities outside the protein context, thus far, have the sequences ^{D}Pro-Xxx (Xxx is Gly, Ala, Pro, Aib etc.,), Asn-Gly, Aib-Gly, Aib-^{D}Ala at the turn segment.[6a,11a,11b,14] The β-strand residues modulate the β-hairpin stability depending upon their intrinsic β-sheet propensities through both cross strand and diagonal side chain-side chain interactions. In this context, Gellman et al.,[14] Balaram and colleagues,[11d,11e,14] have investigated the β-hairpin structures by inserting a variety of non-natural amino acids as

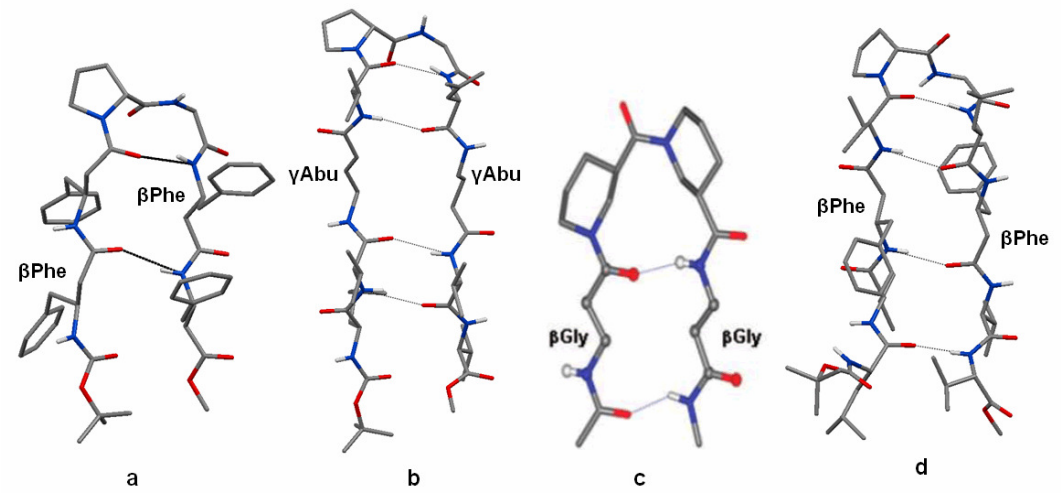

Figure 4: Crystal structures of β-hairpins containing non-natural amino acids a) Boc-β^{3}Phe-β^{3}Phe-^{D}Pro-Gly-β^{3}Phe-β^{3}Phe-OMe,[11d] b) Boc-Leu-Val-γAbu-Val-^{D}Pro-Gly-Leu-γAbu-Val-Val-OMe,[11e] c) Ac-βGly-Nip-Nip-βGly-NHMe,[16a] d) Boc-Leu-Val-β^{3}Phe-Val-^{D}Pro-Gly-Leu-β^{3}Phe-Val-Val-OMe.[15a]

guest into the host β-strands. They have shown that β^3-amino acids,[11d,15] γ-Abu (4-amino butyric acid),[11e] α,β-disubstituted β- amino acids ,[16a] *trans*-3-aminocyclopentanecarboxylic acid (*trans*-3-ACPC)[16b] can be incorporated into a canonical β-hairpin structure. The crystal conformations of some of these hybrid peptide β-hairpins are shown in the Figure 4.

2.1.4 Multi-stranded β-sheets

Besides the design of β-hairpins, efforts were also been taken in the design of multi-stranded β-sheets to understand the protein folding with little extension compared to β-hairpins. However, Balaram and colleagues[17] and Gellman et al.[18] have designed three, four and five stranded β-sheets by utilizing ^{D}Pro-Xxx sequences at the turn segments and studied their solution conformations. The turn sequence ^{D}Pro-Xxx can adopt either type I′ or type II′ conformations. Serrano et al., [19] reported a 20-residue polypeptide (named Betanova) adopting a three-stranded, antiparallel β-sheet using Asn-Gly in the turn segment. Kelly et al. have extensively investigated the role H-bonds in stabilizing the three stranded β-sheet conformations.[20] Recently, Schneider and colleagues showed the folding, self-assembly and bulk material properties of designed three stranded β-sheet hydrogels.[21] The major hurdle in the design of multi-stranded β-sheet structures is aggregation of the β-sheets in solutions, which is the major cause for many diseases such as Alzheimer's,[22] Parkinson's,[23] Huntington[24] diseases etc,. Understanding the nucleation and process of the β-sheet aggregation is of paramount importance in designing inhibitors for these diseases. However, thus far there are no reports regarding crystallographic charecterization of multi-stranded β-sheet structures.

2.2 Aim and rationale of the present work

The intriguing results of vinylogous amino acids and their tendency to adopt extended β-sheet structures in their homooligomers enable us to ask the question that whether it is possible to generate stable β-hairpins by incorporating these vinylogous amino acids as guest molecules into the host α-peptide β-hairpin structures. We anticipate that stable hybrid β-

hairpins and multi-stranded β-sheets can be generated by utilizing the conformational restrictions of the vinylogous amino acids. In order to understand the conformational properties of *E*-vinylogous amino acids in the α-peptide β-hairpin sequence, an octapeptide **P1** (Ac-Val-dgLeu-Val-^{D}Pro-Gly-Leu-dgVal-Val-$CONH_2$) and a 15-mer three stranded β-sheet (double β-hairpin, Boc-Val-dgL-Val-^{D}Pro-Gly-Leu-dgV-Val-Ala-^{D}Pro-Gly-Leu-Val-dgL-Val-NH_2) **P2** were designed by incorporating vinylogous amino acids at the opposite faces of the anti-parallel β-strands. The dipeptide segment ^{D}Pro-Gly[11a, 11b, 14] was used to induce β-turn in both β-hairpin and three stranded β-sheet. In addition, we speculate that the corresponding hybrid γ-peptides can be generated using single step catalytic hydrogenation. This strategy provides a unique opportunity to understand the conformational properties and stabilities of hybrid peptides containing unsaturated and saturated γ-amino acids.

2.3 Results and Discussion

2.3.1 Design and synthesis of Octapeptide β-hairpin

In order to understand the conformational behaviour of *E*-vinylogous residues in hybrid peptide β-hairpin, we designed an octapeptide (Ac-Val-dgL-Val-^{D}Pro-Gly-Leu-dgV-Val-NH_2) (**P1**). The *E*-vinylogous amino acids **dgL** and **dgV** were inserted at facing positions 2 and 7 in such a way that it should not disturb the interstrand H-bonding pattern in the designed β-hairpin (Figure 5). The ^{D}Pro-Gly segment was used to nucleate reverse turn. It has been proved that the ^{D}Pro-Gly dipeptide segment can adopt either type I' or type II' β-turns. The vinylogous hybrid octapeptide **P1** (Figure 5) was synthesized using solid phase method by standard Fmoc chemistry on Rink amide resin. The corresponding vinylogous amino acids, Fmoc-(*S,E*)-dgL-OH and Fmoc-(*S,E*)-dgV-OH were synthesized using Wittig reaction[25] starting from Boc-protected amino aldehydes as shown in Scheme 2. The Schematic representation of solid phase synthesis is shown in Scheme 3. After completion of the syntheis, the peptide was cleaved from resin using TFA/water cocktail mixture and isolated as solid white crude product after precipitation with chloroform/pet-ether solvent systems. The peptide was purified using reverse phase HPLC on C18 column using MeOH/H_2O as solvent systems.

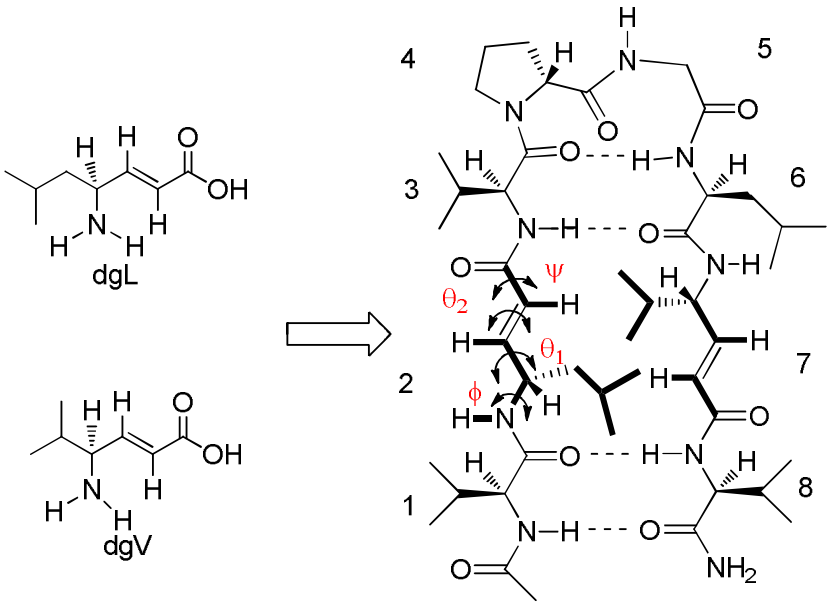

Figure 5: Model hybrid β-hairpin containing α, β-dehydro γ-amino acids (dg) at facing positions of the antiparallel β-strands.

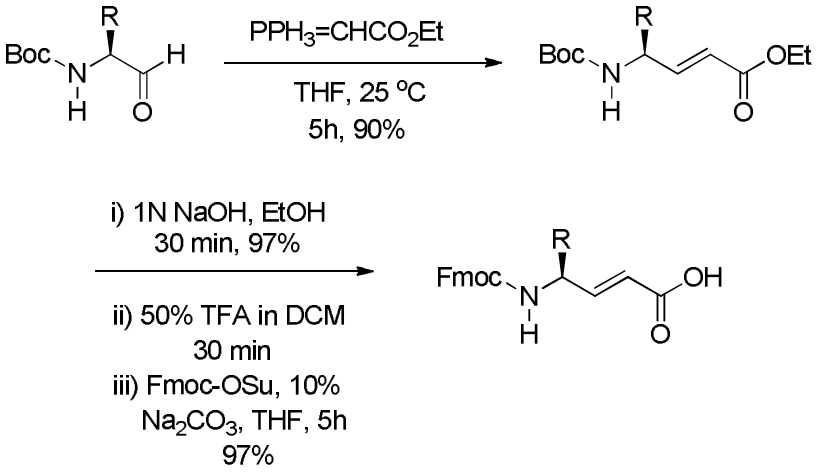

Scheme 2: Synthesis of Fmoc-*N*-vinylogous amino acid.

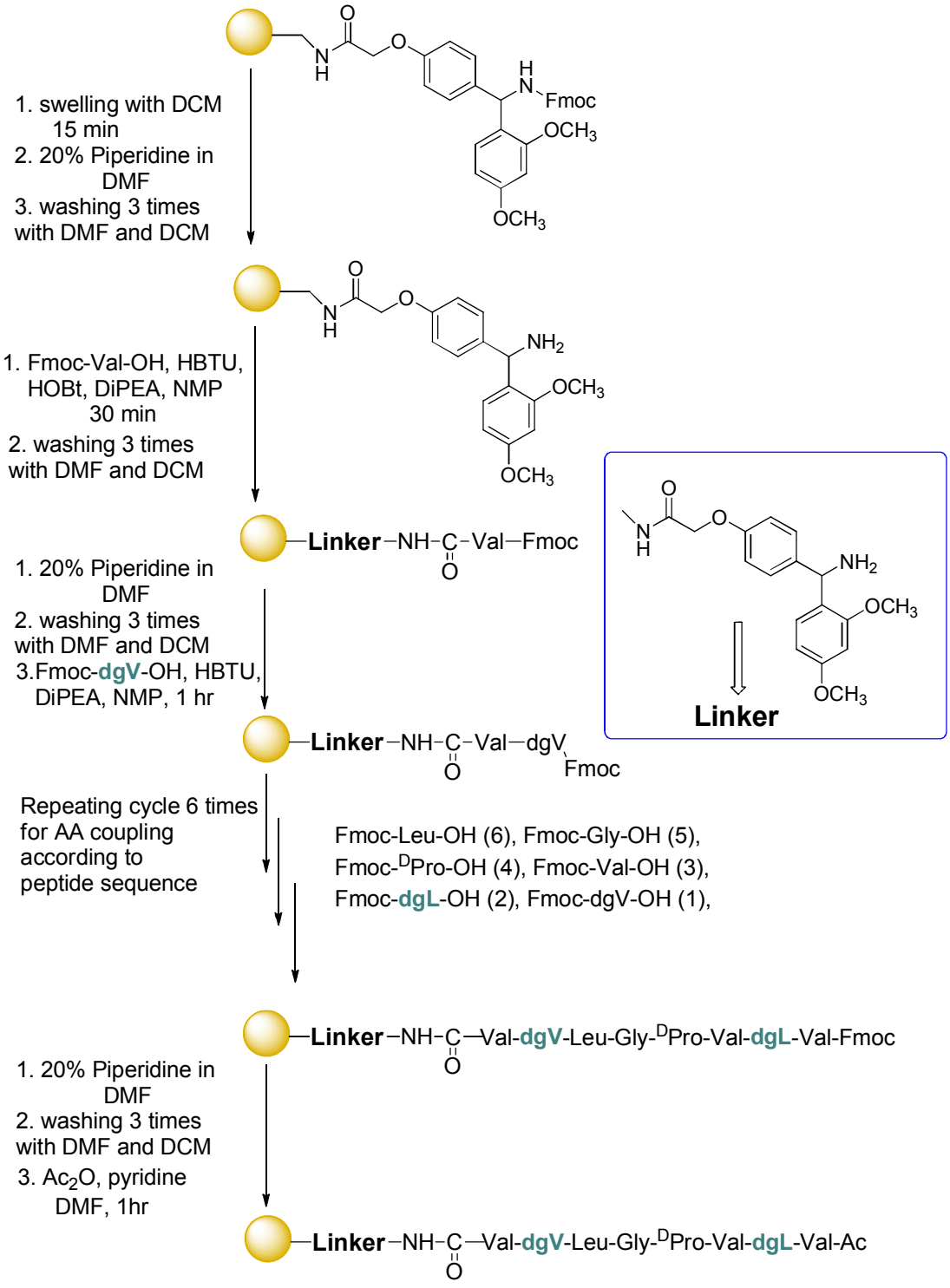

Scheme 3: Solid phase synthesis of peptide Ac-Val-dgL-Val-^{D}Pro-Gly-Leu-dgV-Val-NH_2

2.3.2. Structural analysis of P1 in solution

The ^{1}H NMR of **P1** in CD_3OH reveals that the wide dispersion of backbone NH and $C^{\gamma}H$ along with vinylic protons chemical shifts signalling a well structured peptide in solution. In addition, circular dichroism (CD) spectrum of **P1** (110 µM) in methanol shown in Figure 6a indicating the β-sheet structure in solution. We speculate that the red shift of the CD minima at 234 nm may be due to the conjugated enamides of vinylogous residues. Partial TOCSY spectrum of the **P1** is given Figure 7A. Using the sequential proton interactions from TOCSY, all residues in the β-hairpin were indentified. The order of amino acid residues in the sequence were established using ROESY spectrum. The chemical shifts of **P1** are tabulated in Table 1. As anticipated, the 2D NMR (ROESY) analysis showed the characteristic turn and the cross-strand NOEs of antiparallel β-strands confirming a β-hairpin structure in solution. The critical NOEs observed in the ROESY spectrum are illustrated in the schematic diagram shown in Figure 6b.

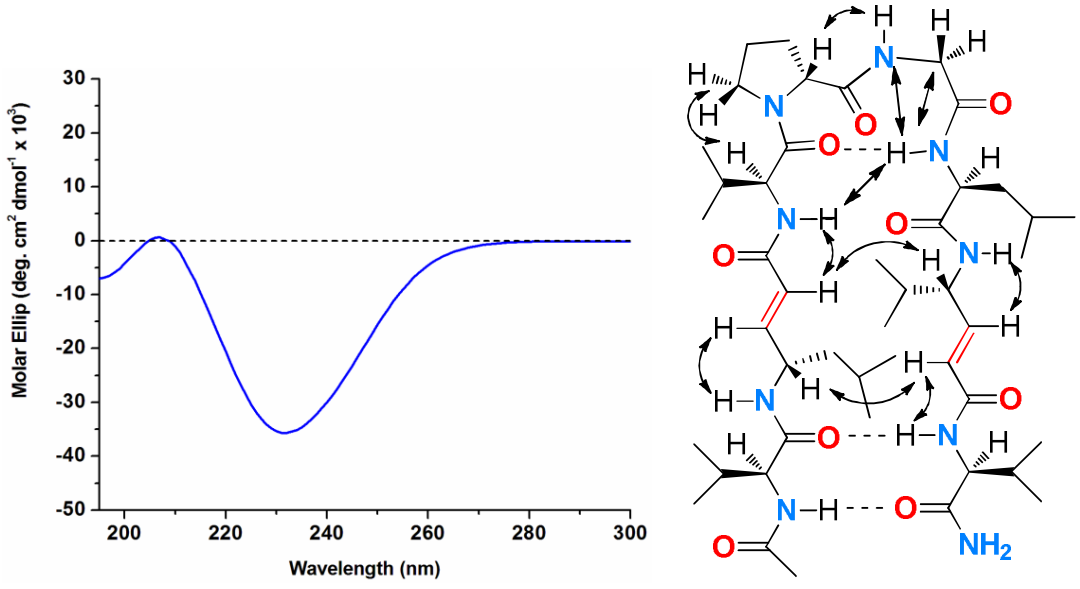

Figure 6: a) Circular dichroism (CD) spectrum of vinylogous hybrid β-hairpin **P1** in methanol, b) the observed NOEs of the peptide **P1** in the ROESY are schematically shown by double headed arrows.

The characteristic sequential NH↔$C^{\alpha}H$, cross-strand NH↔NH and $C^{\alpha}H \leftrightarrow C^{\gamma}H$ NOEs of facing vinylogous residues observed in the ROESY spectrum are shown in Figure 7B, 7C and 7D. The strong $C^{\alpha}H \leftrightarrow C^{\gamma}H$ NOEs between the interstrand vinylogous residues in **P1** indicating the stable and the well folded antiparallel β-sheet character in solution. In addition, the linear temperature dependence of β-strand amide NHs observed in vt NMR (temperature ranging from -20 to 35 ^{o}C), suggesting the strong registry of the antiparallel β-sheets (Figure 8a). The temperature coefficient of chemical shifts (dδ/dT) for amide protons are tabulated in Table 1. The analysis of (dδ/dT) reveals that NH proton Leu3 is less exposed in solvent compared to other NH protons of **P1** involved in internal H-bonding. In addition, the (dδ/dT) value (-4.8 ppb K^{-1}) for dgL2 amide proton (NH) suggests the involvement in an internal H-bond.The deuterium exchange of amide NHs was carried out in CD_3OD. Strikingly, it was found that the slower exchange rate of dgL2NH and dgV7NH even after 4.5 hrs (Figure 8b), indicating that the NHs are being shielded from the solvent by the extended antiparallel β-sheets of β-hairpins held together by strong intermolecular H-bonding.

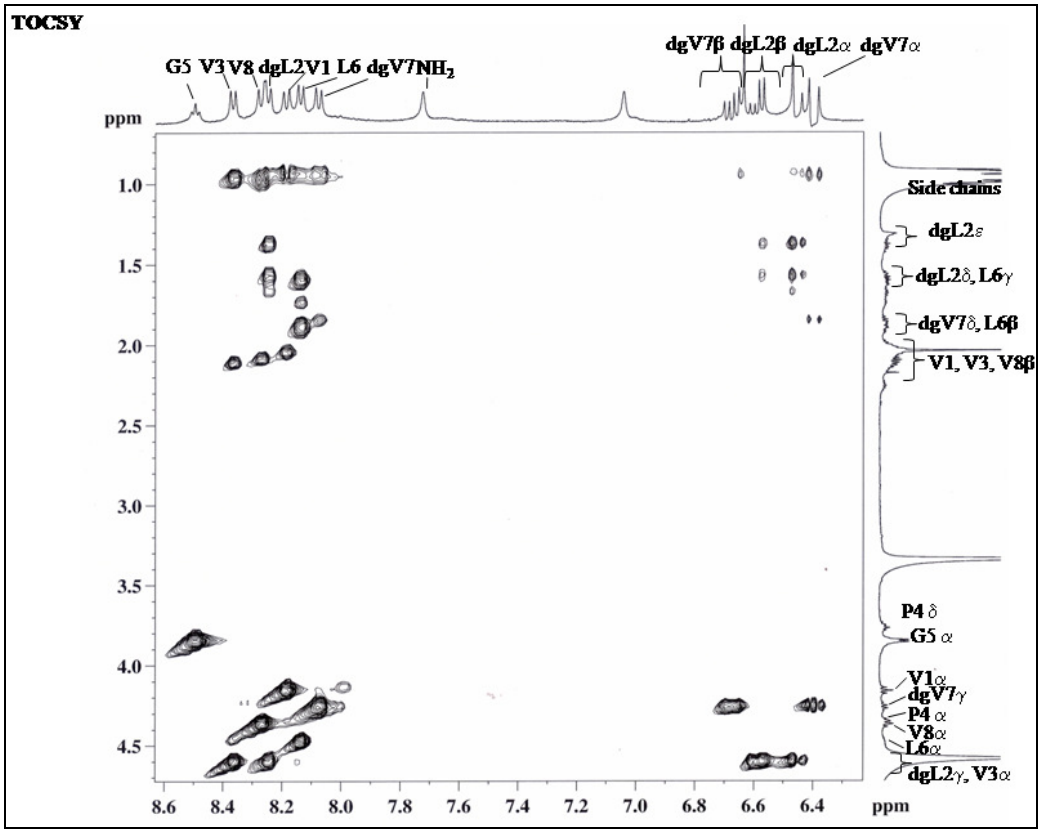

A

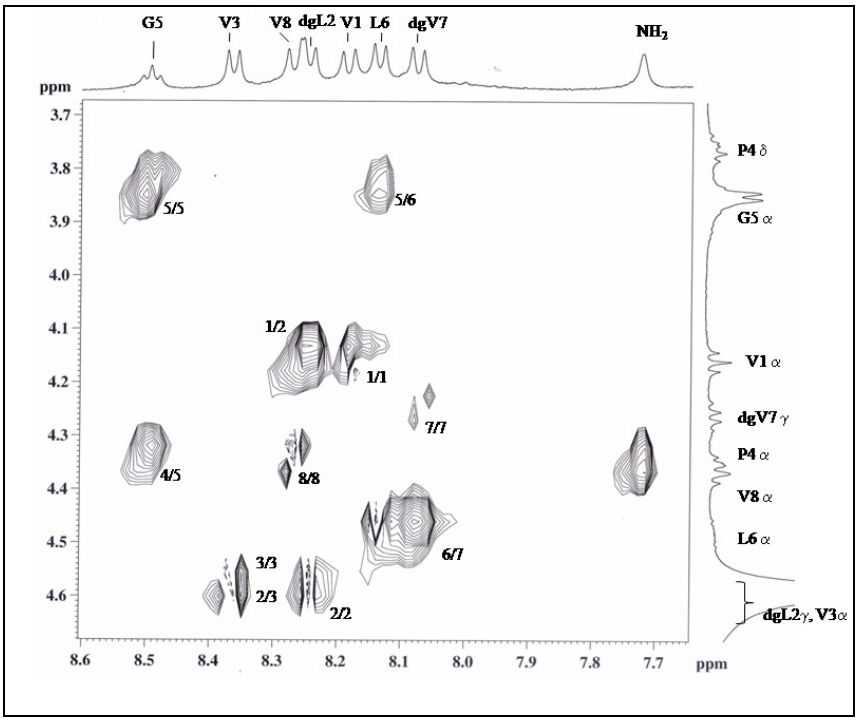
G5
V3
V8
dgL2
V1
L6
dgV7
NH2
ppm
P4 δ
G5 α
V1 α
dgV7 γ
P4 α
V8 α
L6 α
dgL2γ, V3α
5/5
5/6
1/2
1/1
7/7
4/5
8/8
6/7
3/3
2/3
2/2
8.6
8.5
8.4
8.3
8.2
8.1
8.0
7.9
7.8
7.7
ppm

B

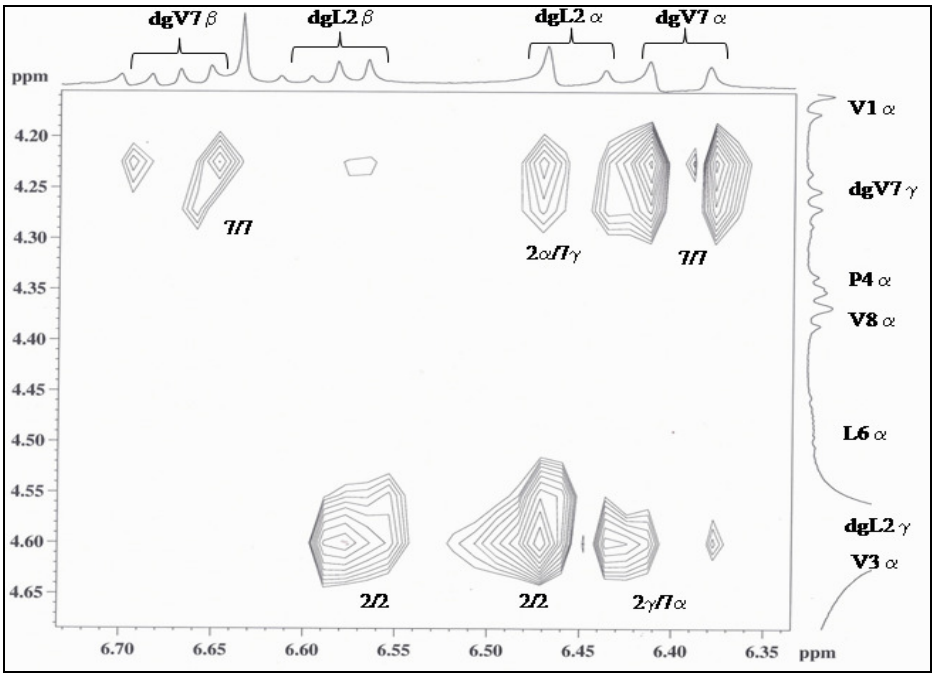
dgV7 β
dgL2 β
dgL2 α
dgV7 α
ppm
V1 α
dgV7 γ
P4 α
V8 α
L6 α
dgL2 γ
V3 α
7/7
2α/7γ
7/7
2/2
2/2
2γ/7α
6.70
6.65
6.60
6.55
6.50
6.45
6.40
6.35
ppm

C

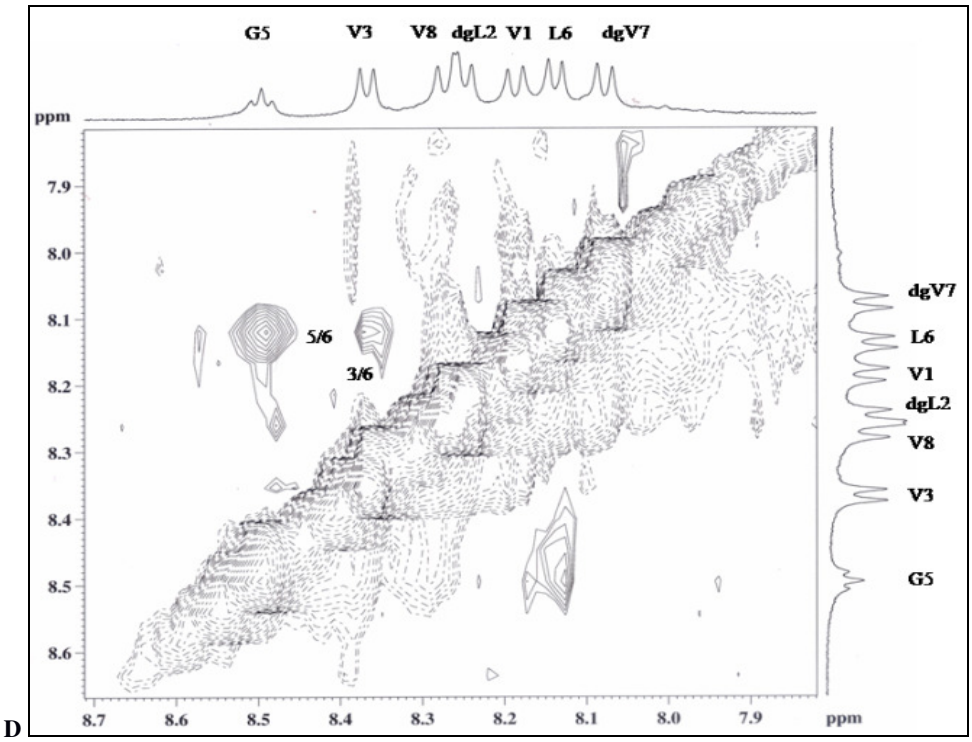

D

Figure 7: A) TOCSY NMR spectrum of **P1** in CD_3OH. The sequential assignments of amino acids were performed using ROESY. B) Partial ROESY spectra of **P1** showing cross-strand NOEs of NH↔ $C^{\alpha}H$, NH↔ $C^{\gamma}H$, C) $C^{\alpha}H$↔ $C^{\gamma}H$, $C^{\beta}H$↔ $C^{\gamma}H$ of antiparallel β-strand residues, and D) NH↔NH.

Table 1: Chemical Shifts of unsaturated hybrid octapeptide **P1**

Residue	Chemical Shifts (ppm)							dδ/dT	$^{3}J_{NHC^{\alpha}H}$
	NH	$C^{\alpha}H$	$C^{\beta}H$	$C^{\gamma}H$	$C^{\delta}H$	$C^{\omega}H$	Others	(ppb/K)	(Hz)
Val1	8.18	4.25	2.02	1.00-0.93	-	-	-	-7.59	8.6
dgLeu2	8.22	6.47*	6.59#	4.57	1.6	1.36-1.37	1.00-0.95	-6.6	8.72
Val3	8.35	4.61	2.1	1.00-0.93	-	-	-	-3.93	9.04
^{D}Pro4	-	4.48	2.21-1.98	2.18-2.01	3.78	-	-	-	-
Gly5	8.49	3.94	-	-	-	-	-	-6.61	5.88
Leu6	8.12	4.54	1.9	1.6	1.00-0.95	-	-	-7.22	8.36
dgVal7	8.07	6.40*	6.67#	4.27	1.85	1.00-0.94	-	-4.8	8.4
Val8	8.26	4.42	2.05	1.00-0.93	-	-	-	-6.49	9.04

* Alpha hydrogen of backbone in amino acid next to C=O (CH=C***H***-C=O). # Beta hydrogen of backbone in amino acid (C***H***=CH-C=O)

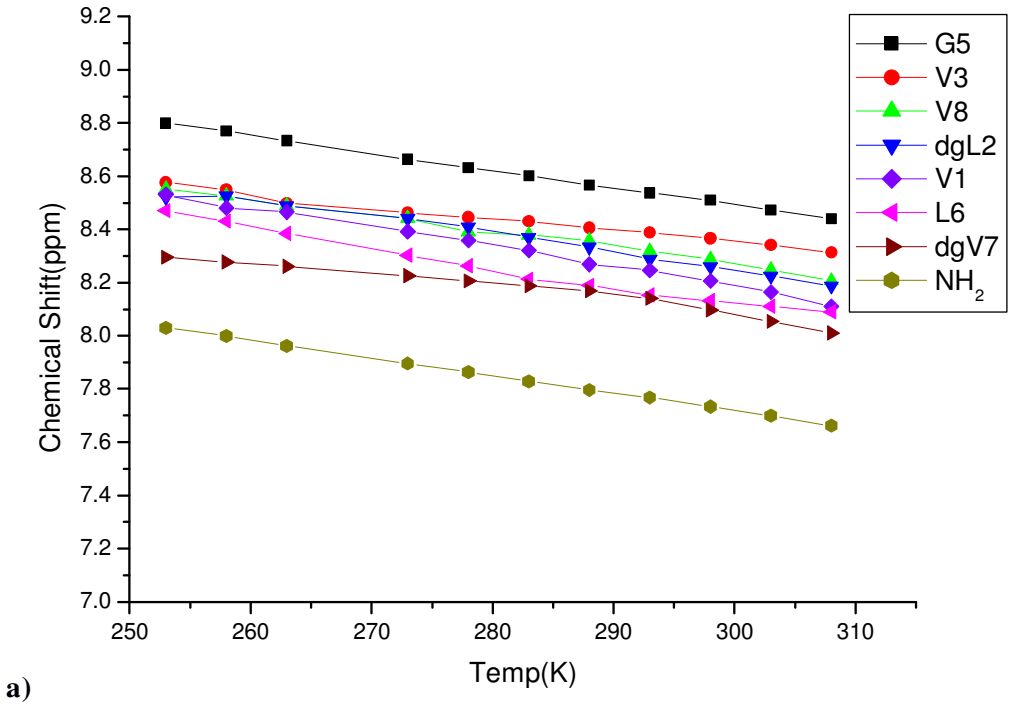

a)

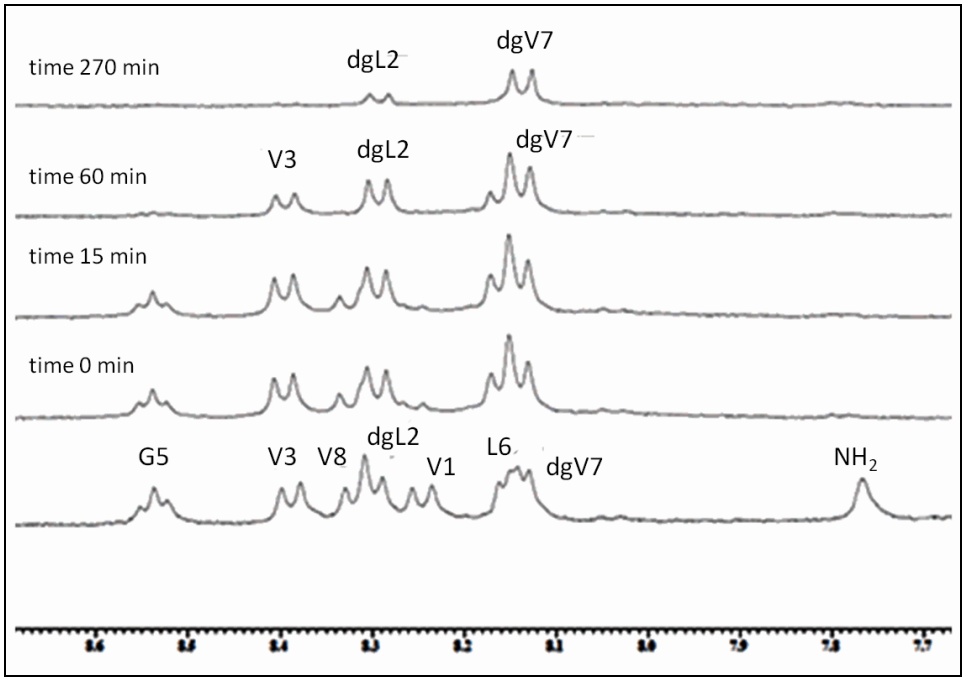

b)

Figure 8: a) Plot of amides chemical shift with the various temperatures, b) ^{1}H NMR spectra showing the exchange of amide NHs of **P1** with deuterium in CD_3OD. The pure peptide **P1** was dissolved in CD_3OD and subjected for time course experiment to probe the H-bonding and solvent accessibility.

2.3.3 Solid state structure of peptide P1

Single crystals of **P1** obtained in methanol solution after slow evaporation yield the structure shown in Figure 9. Indeed, hybrid peptide **P1** adopted a well folded β-hairpin conformation in crystals. The torsional variables are given in the Table 2. Examination of the torsional angles at ^{D}Pro-Gly segment reveals that it adapts a type II′ β-turn conformation [Standard ($\phi_{i+1} = 60^{o}$ $\psi_{i+1} = -120^{o}$, $\phi_{i+2} = -80^{o}$, $\psi_{i+1} = 0^{o}$), observed ($\phi_{i+1} = 61^{o}$ $\psi_{i+1} = -130^{o}$, $\phi_{i+2} = -75^{o}$, $\psi_{i+1} = -10^{o}$)]. All α-residues in strands adapted characteristic conformations of a β-sheet. Both vinylogous amino acids dgL(2) ($\phi = -118^{o}$, $\theta_1 = 132^{o}$, $\theta_2 = 174^{o}$, and $\psi = 174^{o}$) and dgV(7) ($\phi = -130^{o}$, $\theta_1 = 123^{o}$, $\theta_2 = 179^{o}$, and $\psi = 176^{o}$) were accommodated into the β-sheets with a very similar characteristic backbone conformations (Figure 7b). The torsional angles θ_2, ψ and ω all have extended geometry with a value approximately (±)180^{o}. The extended conformation of vinylic -C$^{\beta}$=C$^{\alpha}$- and -C$^{\alpha}$-CO- (*s-cis*) of enamide facilitates the

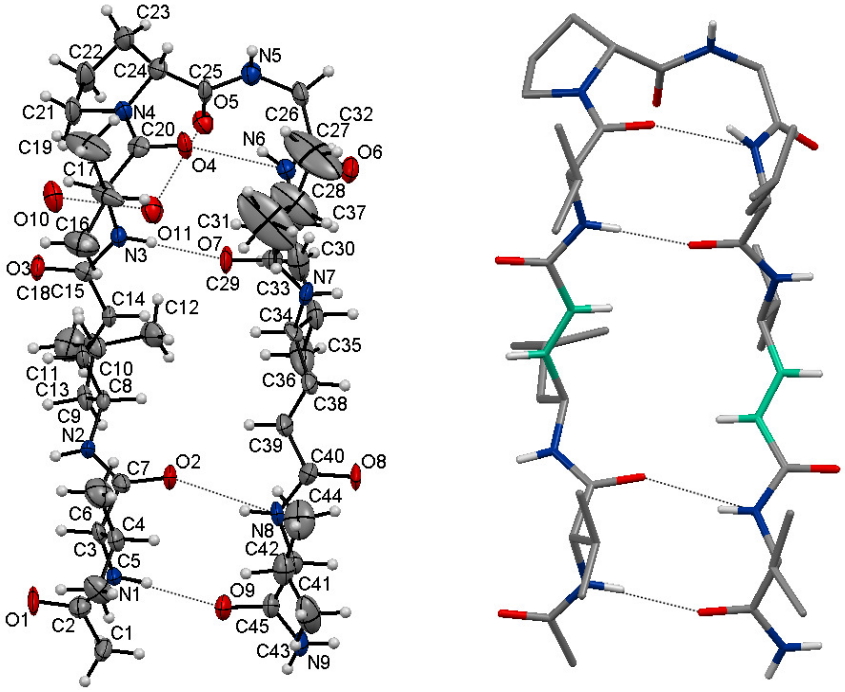

a) **b)**

Figure 9: a) The ORTEP diagram of hybrid octapeptide β-hairpin (**P1**) containing α, β-unsaturated γ-amino acids. H-atoms are not labelled for clarity. All four intramolecular hydrogen bonds are represented by dotted lines. The two water molecules O10 and O11 are also shown, b) capped stick model of **P1**, and for clarity some of the H-atoms are not shown.

accommodation of vinylogous residues into the backbone conformation without disturbing the canonical β-hairpin structure. Interestingly, the values of ϕ and θ_1 of vinylogous amino acids have values very similar to the ϕ and ψ of α-residues. In addition, the β-hairpin conformation in crystal is further stabilized by four cross strand intra molecular hydrogen bonds (Figure 10a). The characteristic hydrogen bond parameters are given in the Table 3. Both dgL2 and dgV7 are not involved in intramolecular hydrogen bonding as they are incorporated at the non-hydrogen bonding positions of antiparallel β-strands. After careful observation reveals that two water molecules O10 and O11 are involved in the head-to-head connection of two independent β-hairpins through H-bonding (Figure 10b). In addition they are self assembled through extended β-sheets connected by intermolecular hydrogen bonding (Figure 10a).

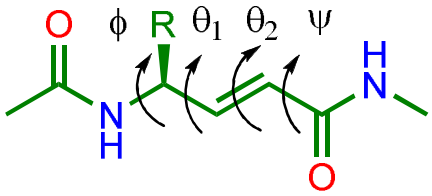

Torsional variables of vinylogous residues

Table 2: Backbone torsional variables (in deg) of vinylogous hybrid octapeptide β-hairpin (**P1**)

Residues	ϕ	θ_1	θ_2	ψ	ω
Val1	-118	---	---	114	178
dgL2	-118	132	174	174	-179
Val3	-141	---	---	103	178
^{D}Pro4	61	---	---	-130	178
Gly5	-75	---	---	-10	178
Leu6	-75	---	---	124	-178
dgV7	-130	123	179	176	-173
Val8	-137	---	----	130	---

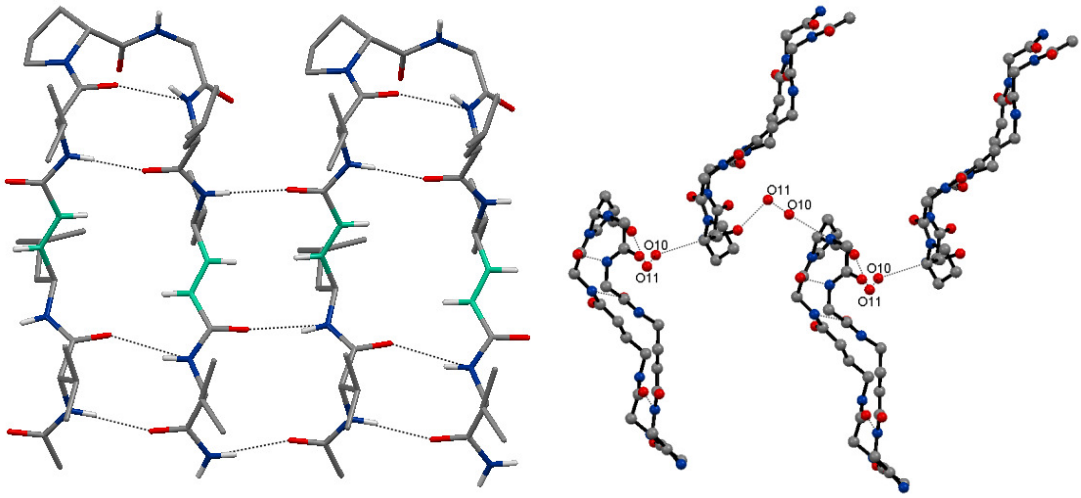

a) **b)**

Figure 10: a) The extended β-sheets connected by intermolecular hydrogen bonding, b) The side view of **P1** in crystal structure. The side chains are deleted for clarity. Two water molecules O10 and O11 are involved in the head-to-head connection of two independent β-hairpins through H-bonding.

Table 3: Hydrogen bonding parameters of octapeptide β-hairpin (**P1**)

Type	Donar [D]	Acceptor [A]	D···A [Å]	H···A [Å]	∠D-H···A [deg]	∠D···O=C [deg]
Intramol.	N1	O9	2.913	2.060	172	158
Intermol.	N2	O8[¶]	2.804	1.977	161	174
Intramol.	N3	O7	3.062	2.237	161	143
Pro	N4(Pro)	---	---	---	---	---
P1---Sol.	N5	O10(W1)[§]	2.915	2.058	175	---
Intramol.	N6	O4	2.892	2.124	148	135
Intramol.	N8	O2	2.932	2.125	156	154
Intermol.	N9	O1[*]	2.894	2.043	170	156
P1---Sol.	W2(O11)	O5	2.70	----	----	---
Sol---Sol.	W1	W2	2.825	----	----	---

Intermol.; intermolecular, intramol.; intramolecular, P1-Sol; Peptide-solvent, #Symmetry equivalent 1-x,-1/2+y, 1-z, †Symmetry equivalent –x, -1/2+y, 2-z, ¶Symmetry equivalent 1+x, y, z, §Symmetry equivalent 1-x, -1/2+y,-z, *Symmetry equivalent -1+x, y, z. a: Hydrogen bonding parameters of molecule A2B in the asymmetric unit.

2.3.4 Transformation of vinylogous hybrid Peptide P1 (Ac-V-dgL-V- ^{D}Pro-Gly-L-dgV-V-NH_2) to its saturated hybrid γ-peptide analogue P2 (Ac-V-γL-V- ^{D}Pro-Gly-L-γV-V-NH_2)

Further, we examined the feasibility of the transformation of an unsaturated β-hairpin to its saturated γ-peptide analogue **P2** (Ac-Val-γLeu-Val-^{D}Pro-Gly-Leu -γVal-Val-NH_2), using catalytic hydrogenation. The pure **P1** was subjected to catalytic hydrogenation using 10% Pd/C in ethanol. The reaction was monitored by MALDI-TOF and HPLC. Noticeably, complete conversion of **P1** to **P2** was observed in 6 hrs (Scheme 4). The pure hybrid γ-peptide was isolated in 95% yield. The transformation of vinylogous hybrid β-hairpin to its saturated analogue proceeds very smoothly. The completely assigned ^{1}H NMR of **P1** and **P2** (amide region) is shown in Figure 11. The redistribution of amide NHs and the complete disappearance of all vinylic protons are observed in hybrid γ-peptide analogue. Surprisingly, the up field chemical shifts were observed for all β-strand residues (Figure 11).

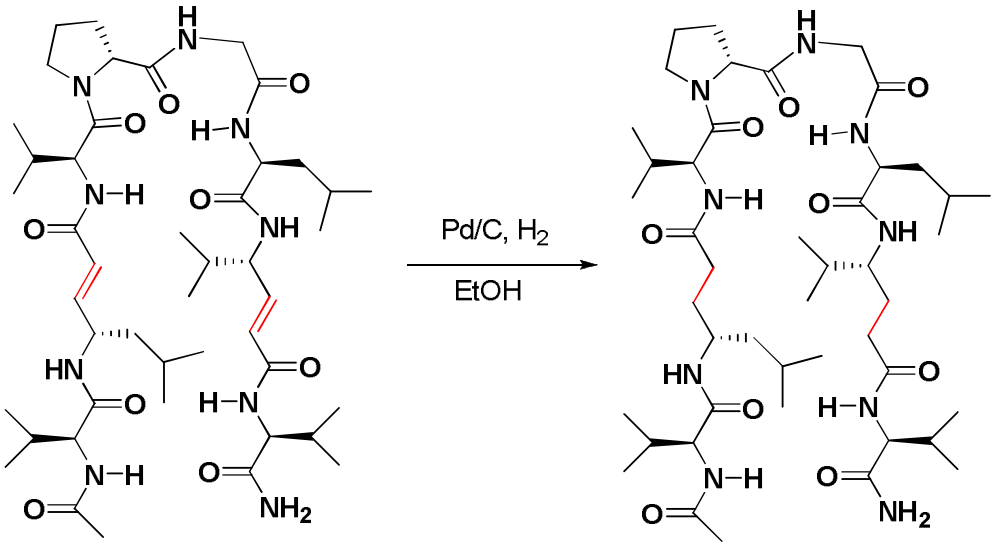

Scheme 4: Transformation of vinylogous hybrid octapeptide β-hairpin (**P1**) to its γ-hybrid peptide analogue (**P2**).

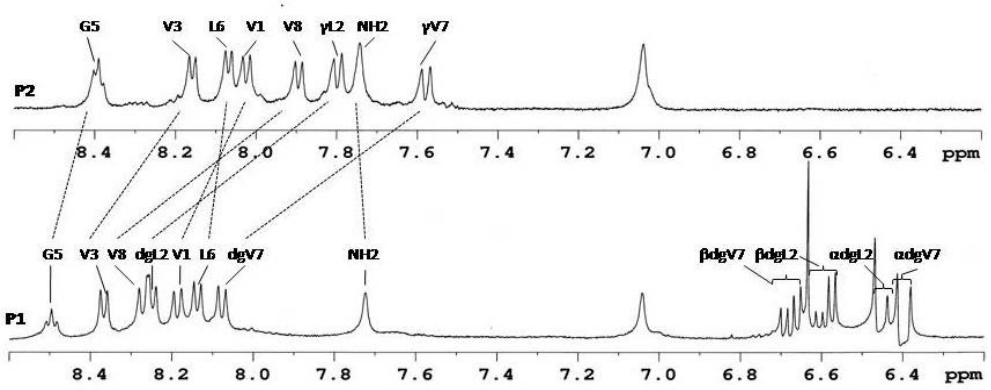

Figure 11: Assigned partial ^{1}H NMR spectra of **P1** and **P2**. A well dispersed amide and vinylic protons of **P1** are shown in the bottom spectrum. The disappearance of vinylic protons and the reshuffled amide protons of saturated peptide **P2** are shown in top spectrum. The sequential assignment of all amide protons were carried out using 2D NMR (TOCSY and ROESY).

2.3.5 Structural analysis of P2 in solution

In contrast to **P1**, saturated **P2** shows the anomalous CD spectrum with negative maxima at 200 and 225 nm (Figure 12). We made several attempts to crystallize **P2** in different solvents; however, we could not get X-ray diffract able quality crystals. Further, to understand the conformational behaviour of **P2** in solution, we subjected hybrid γ-peptide to 2D NMR analysis. The TOCSY spectrum used to identify the amino acid residues in **P2** is shown Figure 14A. The order of amino acid residues in the sequence were established using ROESY spectrum. The chemical shifts of **P2** are tabulated in Table 4. The NOEs observed from 2D NMR (ROESY) are schematically shown in Figure 13a. Interestingly, in contrast to **P1**, we did not observe any characteristic cross-strand NH↔NH and CH↔CH interactions in **P2**. However, the sequential NOEs of 5NH↔6NH (weak) and 6NH↔7NH (medium) indicating that the lack of proper β-strand registry of hairpin in solution. This may be due to the conformational freedom around the saturated C^{α}-C^{β} bond of γ-residues. However, a strong NOE between the side chains of γ-Leu2 to $C^{\gamma}H$ of γ-Val7 is observed. Using the experimentally deduced NOEs for **P2**, the ensemble of structures is obtained by distance restrained molecular dynamic simulations (Insight II 2005, Accelrys Inc.).[26] The overlay of ten low energy conformers of NMR calculated structures are shown in Figure13b. The NMR model reveals that the

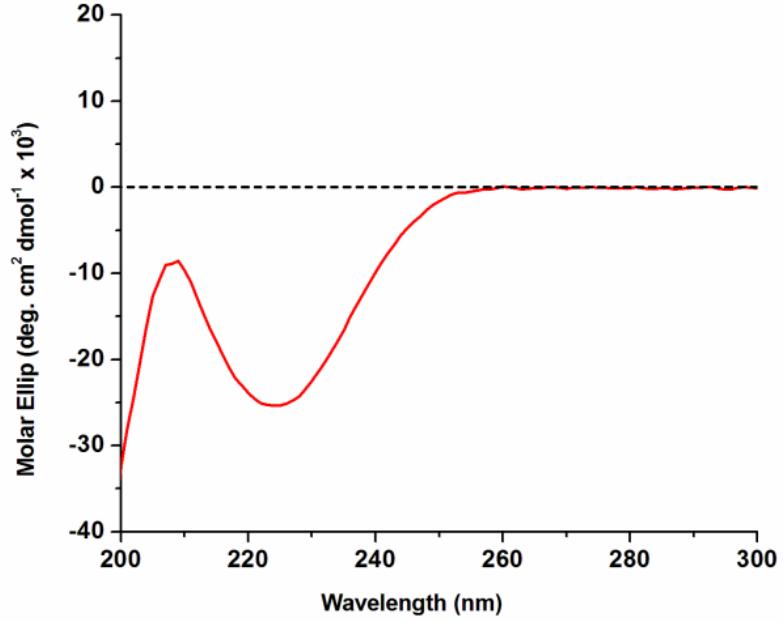

Figure 12: CD spectrum of **P2** recorded in methanol.

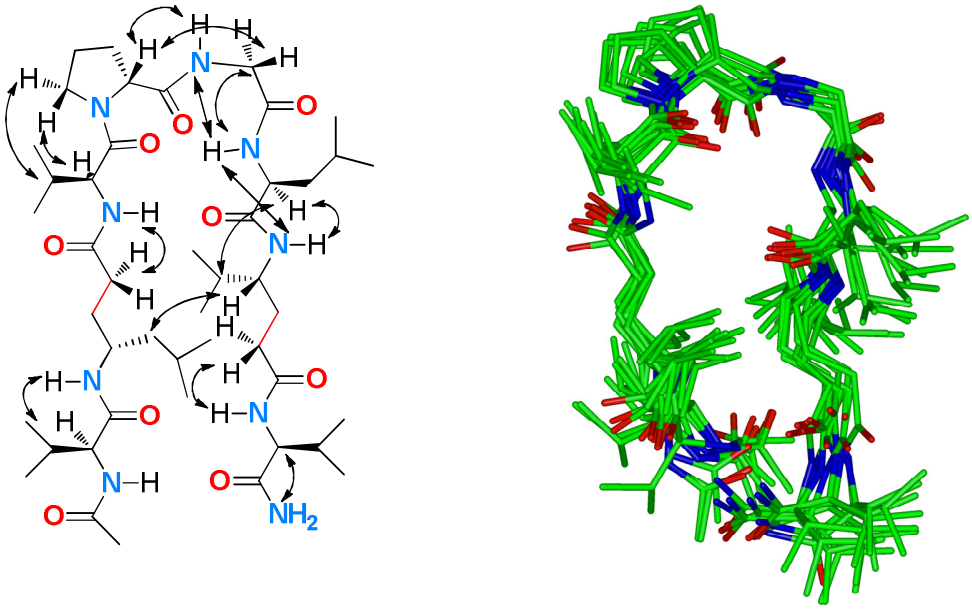

a) **b)**

Figure 13: a) the observed NOEs of the peptide **P2** in the ROESY are schematically shown by double headed arrows, b) The solution conformation of the peptide **P2** in methanol. The ensemble of ten low energy structures is calculated based on the observed NOEs. Hydrogens are omitted for clarity.

saturation of vinylic double bond introduces the additional freedom in the backbone and breaks the proper strand registry of β-hairpin. Overall, the hybrid γ-peptide **P2** adapted a folded β-hairpin conformation with poor β-strand registry in solution. It is interesting to notice that a well folded β-hairpin structure of hybrid vinylogous peptide **P1** transformed to a distorted β-hairpin conformation of **P2** after the catalytic hydrogenation. These results are suggesting that insertion of saturated γ-residues may lead to the distorted hairpin structures.

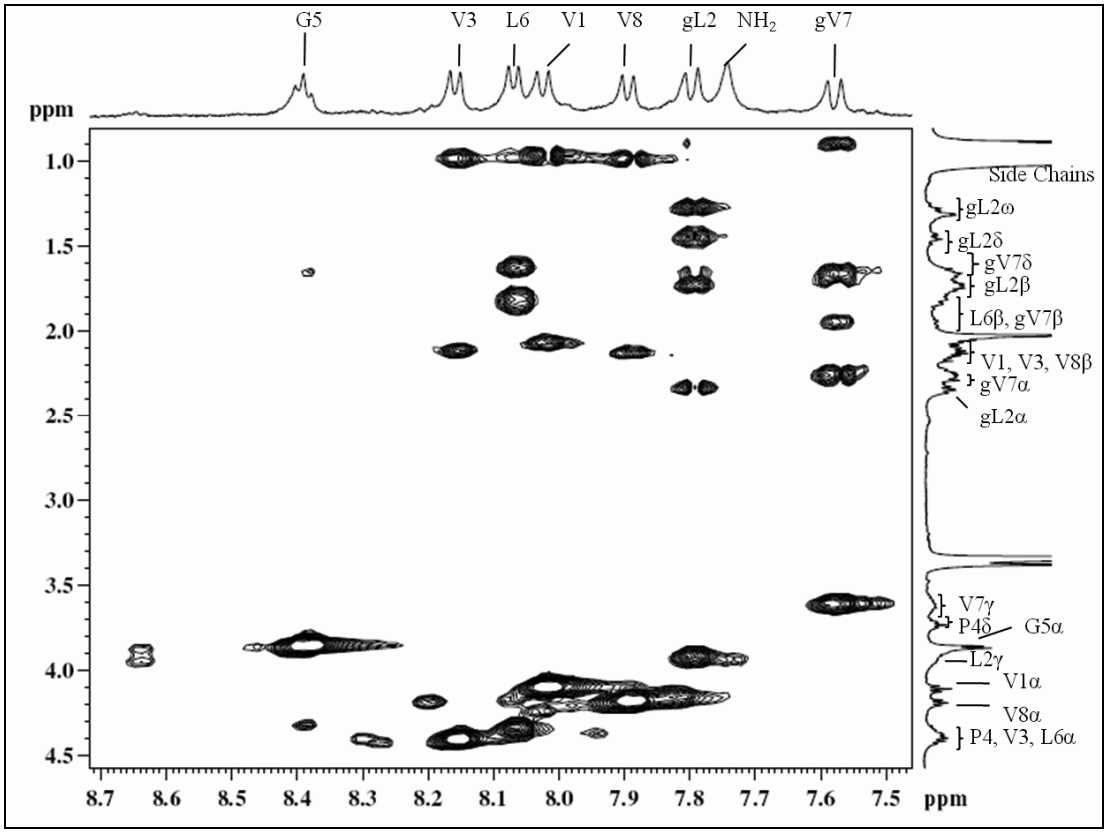

A

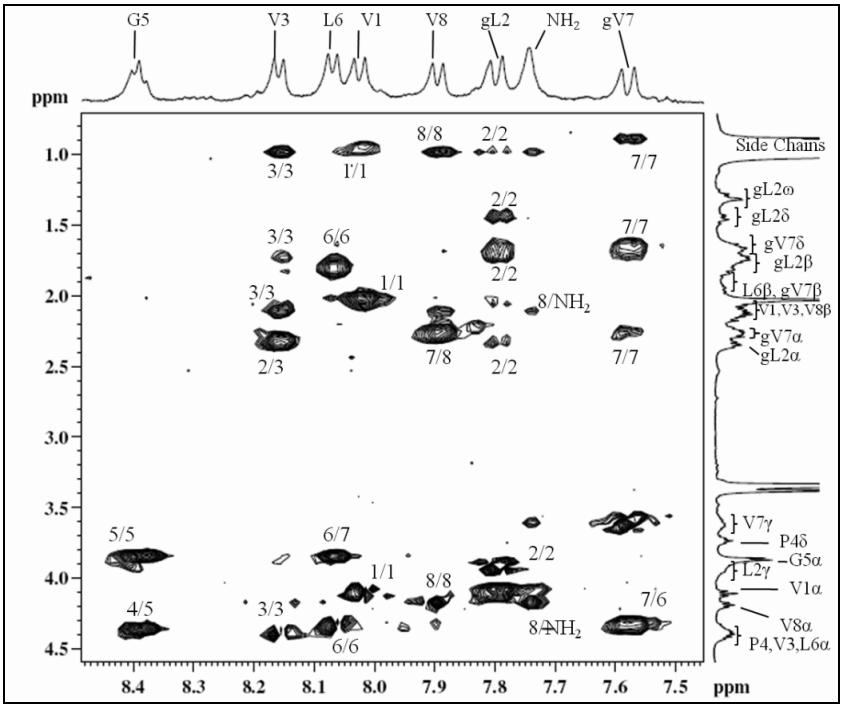
G5
V3
L6
V1
V8
gL2
NH2
gV7
ppm
Side Chains
gL2ω
gL2δ
gV7δ
gL2β
L6β, gV7β
V1,V3,V8β
gV7α
gL2α
V7γ
P4δ
G5α
L2γ
V1α
V8α
P4,V3,L6α
8.4
8.3
8.2
8.1
8.0
7.9
7.8
7.7
7.6
7.5
ppm

B

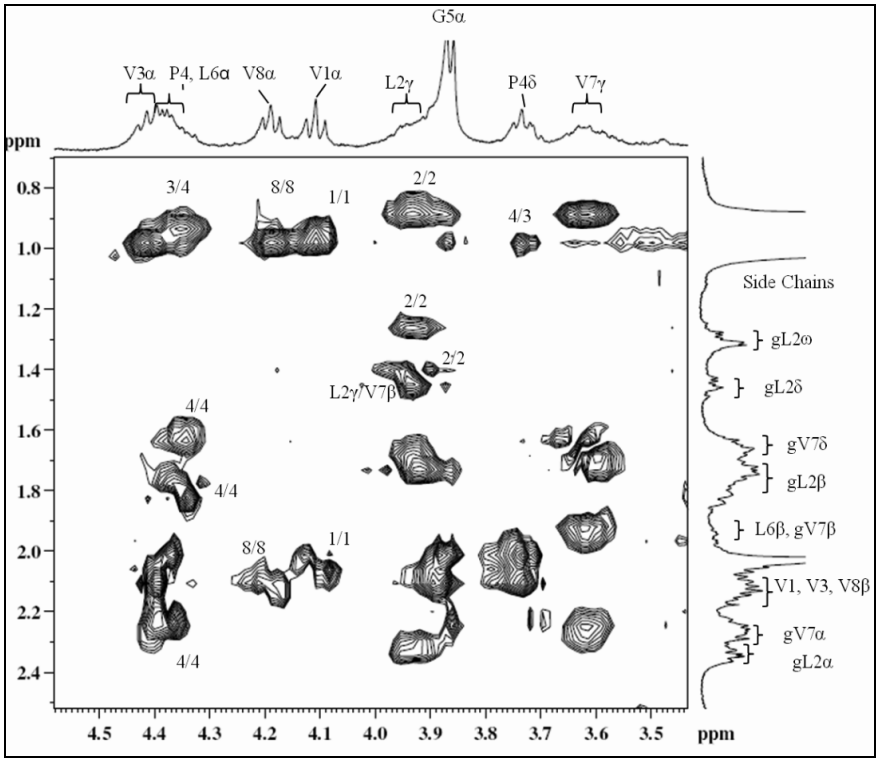
G5α
V3α
P4, L6α
V8α
V1α
L2γ
P4δ
V7γ
ppm
Side Chains
gL2ω
gL2δ
gV7δ
gL2β
L6β, gV7β
V1, V3, V8β
gV7α
gL2α
4.5
4.4
4.3
4.2
4.1
4.0
3.9
3.8
3.7
3.6
3.5
ppm

C

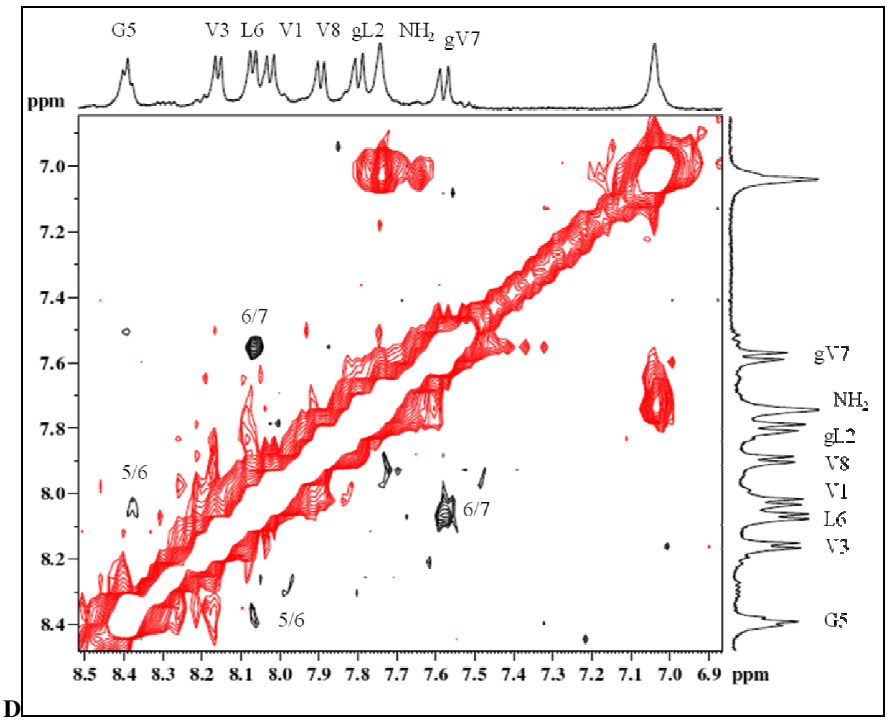

Figure 14: A) TOCSY NMR spectrum of **P2** in CD_3OH. The sequential assignments of amino acids were performed using ROESY. B) Partial ROESY spectra of **P2** in CD_3OH showing sequential and the cross-strand NOEs of NH↔$C^{\alpha}H$, NH↔$C^{\beta}H$ and NH↔$C^{\gamma}H$ of antiparallel β-strand residues, C) CH↔CH and D) NH↔NH.

Table 4: Chemical Shifts of saturated hybrid octapeptide **P2**

Residue	Chemical Shifts (ppm)							$^{3}J_{NHC^{\alpha}H}$
	NH	$C^{\alpha}H$	$C^{\beta}H$	$C^{\gamma}H$	$C^{\delta}H$	$C^{\omega}H$	Others	(Hz)
Val1	8.01	4.14	2.12	1.09-0.94	-	-	-	8.4
gLeu2	7.78	2.31*	1.73#	3.95	1.42	1.32	1.09-0.94	8.5
Val3	8.13	4.38	2.12	1.09-0.94	-	-	-	9.0
^{D}Pro4	-	4.38	2.21-1.98	2.18-2.01	3.73	-	-	-
Gly5	8.38	3.85	-	-	-	-	-	5.67
Leu6	8.05	4.38	1.84-1.93	1.6	1.00-0.95	-	-	8.2
gVal7	7.55	2.28*	1.84-1.93#	3.6	1.45-1.67	1.09-0.94	-	8.6
Val8	7.89	4.2	2.12	1.09-0.94	-	-	-	8.7

*Alpha hydrogen of backbone in amino acid next to C=O (CH_2-C***H_2**-C=O), # Beta hydrogen of backbone in amino acid (C***H_2***-CH_2-C=O)

2.3.6 Design and synthesis of 3-stranded antiparallel β-sheet

Exciting results from the vinylogous hybrid β-hairpin provoke us extend similar strategy to higher ordered super secondary structures. To understand whether or not the stable three stranded β-sheet structures can be generated by incorporating these *E*-vinylogous amino acids similar to the octapeptide β-hairpin **P1**, we designed a 15 residues three stranded β-sheet, Boc-Val-dgL-Val-^{D}Pro-Gly-Leu-dgV-Val-Ala-^{D}Pro-Gly-Leu-Val-dgL-Val-NH_2, **P3**. The anticipated three stranded structure is shown in Scheme 5. Similar to the **P1**, the dipeptide segment ^{D}Pro-Gly was used to induce either type I′ or type II′ β-turns in **P3**. Vinylogous residues, dgL, dgV and dgL were incorporated at facing positions of anti-parallel β-strands at positions 2, 7 and 14 respectively. The hybrid peptide was synthesized using solid phase method using standard Fmoc chemistry on Rink amide resin. After completion of the synthesis the peptide was cleaved from resin using TFA/water cocktail mixture and isolated as solid white crude product after precipitation with ethyl acetate/pet-ether solvent systems. The pure peptide was isolated after subjecting the crude product to reverse phase HPLC prurification on C18 column using MeOH/H_2O solvent systems. The purity of the peptide was confirmed by passing through analytical C18 column in reverse phase HPLC using same solvent system.

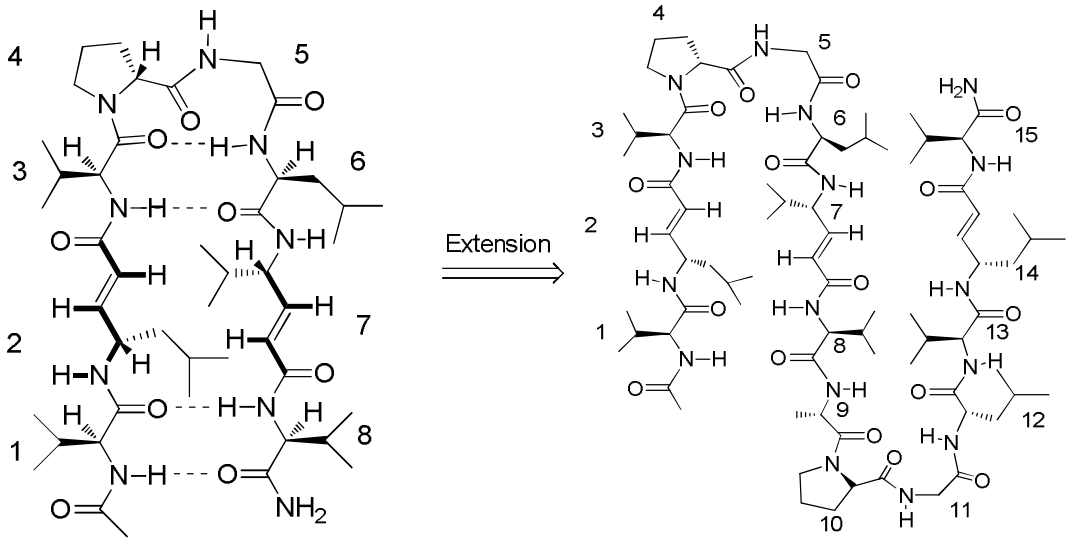

Scheme 5: Extension of octapeptide hybrid β-hairpin (**P1**) to 3-stranded β-sheets (**P3**).

2.3.7 Solution structure of P3

The circular dichroism (CD) spectrum of **P3** (100 μM) recorded in methanol is shown in Figure 15 along with peptide **P1.** The CD singnature of the **P3** in methanol suggested that the peptide adopted a regular β-sheet character in solution. In contrast to the **P1**, **P3** showed the CD minima at ~ 228 nm. The ^{1}H NMR of **P3** is shown in Figure 16. The ^{1}H NMR of **P3** in CD_3OH reveals that the wide dispersion of backbone NH and $C^{\gamma}H$ along with vinylic protons chemical shifts signalling a well structured peptide in solution. Further to evaluate the solution structure, we recorded 2D NMR (TOCSY and ROESY). Using TOCSY spectrum, amino acids residues were indentified. Fully assigned TOCSY spectrum is shown in Figure 18A. Using ROESY spectrum the order of the amino acid sequence was established. The chemical shifts of peptide **P3** are tabulated in Table 5. Critical NOEs observed in the ROESY spectrum are illustrated in the schematic diagram shown in Figure 17.

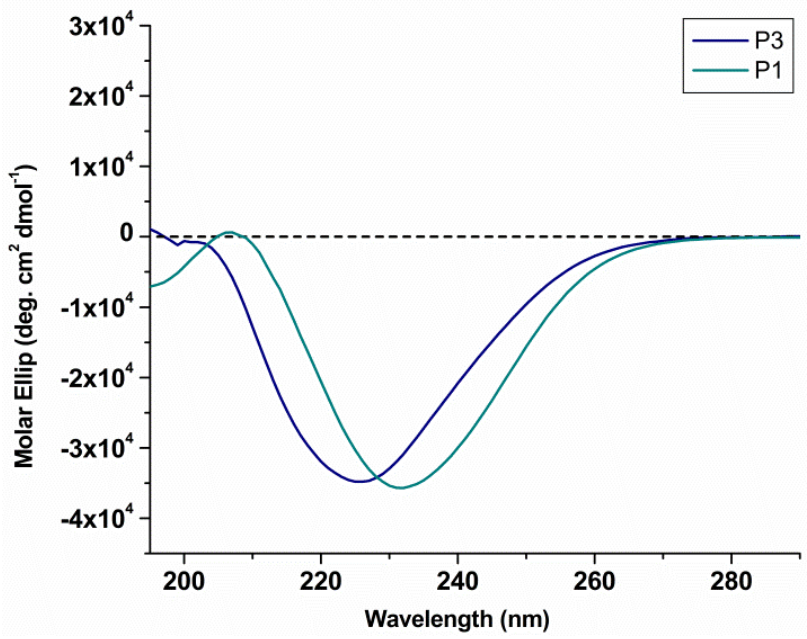

Figure 15: Circular dichroism (CD) spectra of vinylogous hybrid β-hairpin **P1** (navy blue) and 3-stranded β-sheet **P3** (cyan) in methanol.

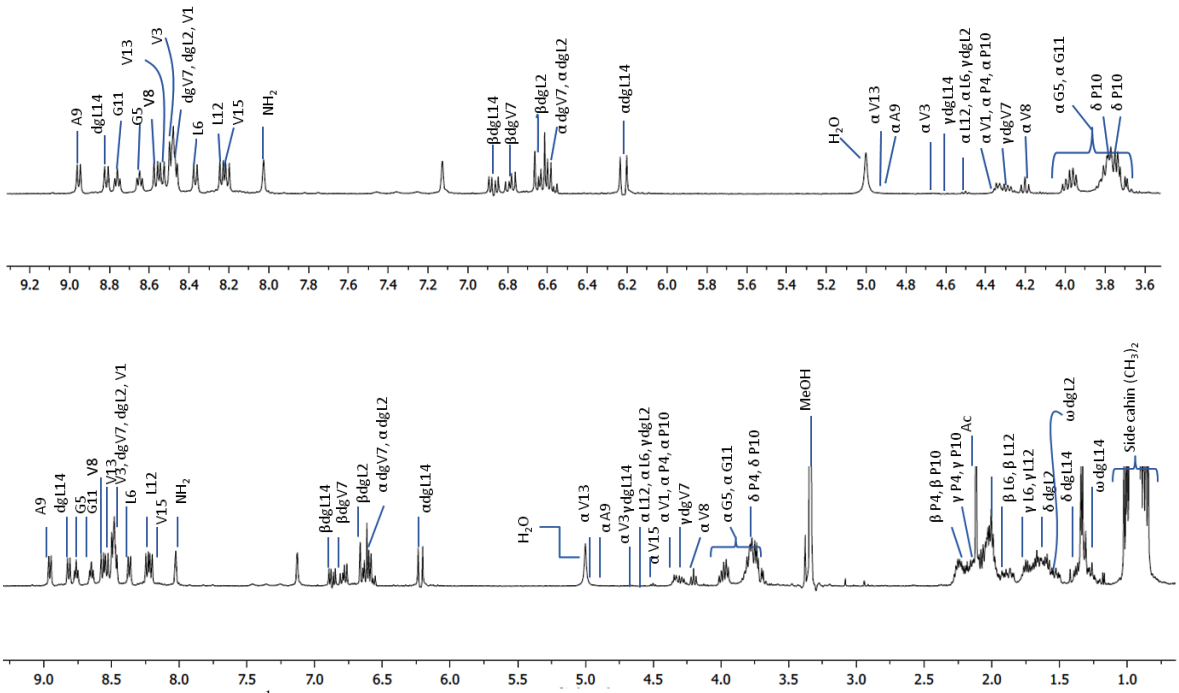

Figure 16: Fully assigned ^{1}H-NMR spectrum of **P3** (Bottom) recorded in CD_3OH. Expansion of NH, vinyl, $C^{\alpha}H$ and $C^{\gamma}H$ proton region (Top). The sequential assignments of amino acids were performed using TOCSY and ROESY spectra.

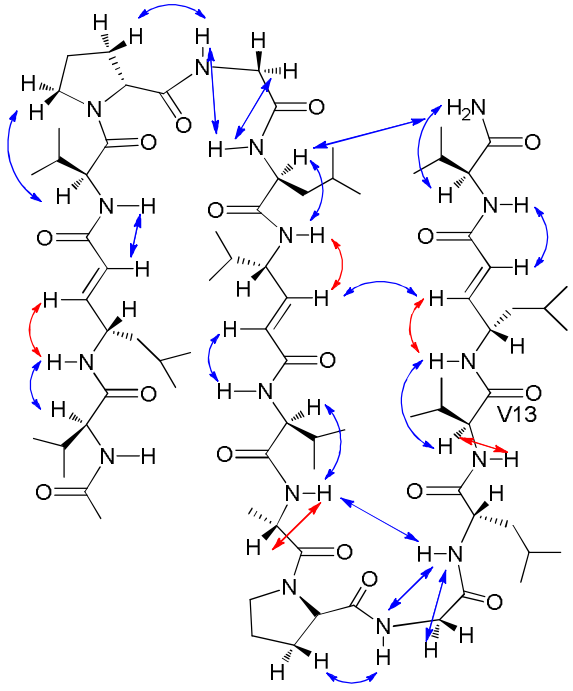

Figure 17: The observed NOEs of the peptide **P3** in the ROESY are schematically shown by double headed arrows, blue for inter-residue and red for intra-residue.

The strong sequential NOEs between the C^{α}-H(i+1) and NH(i) in the strand sequences are suggesting the β-sheet character. The characteristic sequential NH↔C^{α}H, cross-strand C^{β}H↔C^{β}H and NH↔NH NOEs of facing vinylogous residues observed in the ROESY spectrum are shown in Figure 18B, 18C and 18D, respectively. The long range NOEs between the Lue6 C^{α}H and NH_2(ter-amide) of Val 15 (C^{α}H↔NH_2) , dgL7 C^{β}H to dgL14C^{β}H (C^{β}H↔ C^{β}H) and Ala 9 NH to Leu 13 NH (NH↔NH) suggested the folded nature of the β-sheets 2 and 3. However, no cross strand NOEs were identified between the strands 1 and 2 as NHs were closely positioned in the ^{1}H NMR spectrum. The NH↔NH NOEs in Figure 18D gave the clear support that, in the two turns the i + 2 residue must adopted local helical conformations. Further to understand whether or not amide NHs are involved in the intermolecular H-bonding as well as to undersand the stability of β-strands we subjected **P3** for varaible temperature NMR. A plot of NH chemical shifts versus temperature is shown Figure 19. The linear temperature dependence of β-strand amide NHs in vt NMR (temperature ranging from -20 to 30 ^{o}C) are suggesting the strong registry of the antiparallel β-sheets. The temperature coefficient of chemical shifts (dδ/dT) for amide protons are tabulated in Table 5. The measured dδ/dT values are spread over the range -2.91 to -7.80 ppb K^{-1}. The analysis of (dδ/dT) reveals that NH protons of Val1, Leu6, dgV7, Ala9 and dgL14 are less exposed in solvent compared to other NH protons (dδ/dT value > -6 ppb K^{-1}) of **P3** involved in internal H-bonding. Further, Ala9 and dgL14 found to be strong involvement of internal H-bond in the 3-strand with (dδ/dT) values -2.91 and -3.38 ppb K^{-1}, respectively. In addition, the (dδ/dT) values for dgL2 and Val15 amide protons (NH) -4.83 and -3.31 ppb K^{-1}, respectively suggest the involvement in internal H-bond. The NH groups of residue Gly5 and Gly11, which are anticipated to be solvent exposed, have higher dδ/dT values with -7.8 and -6.85, respectively.

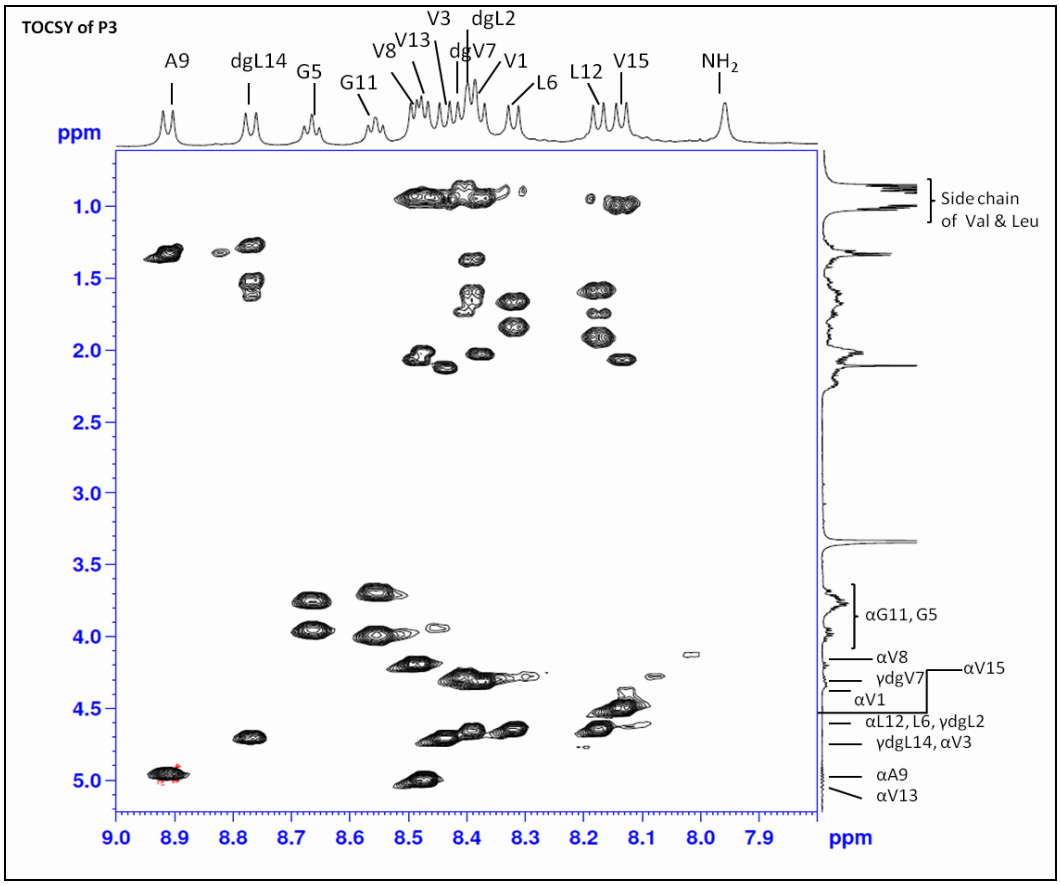
TOCSY of P3
A9
dgL14
G5
G11
V8
V13
V3
dgL2
dgV7
V1
L6
L12
V15
NH2
ppm
1.0
1.5
2.0
2.5
3.0
3.5
4.0
4.5
5.0
9.0
8.9
8.8
8.7
8.6
8.5
8.4
8.3
8.2
8.1
8.0
7.9
ppm
Side chain
of Val & Leu
αG11, G5
αV8
γdgV7
αV1
αV15
αL12, L6, γdgL2
γdgL14, αV3
αA9
αV13

A

B

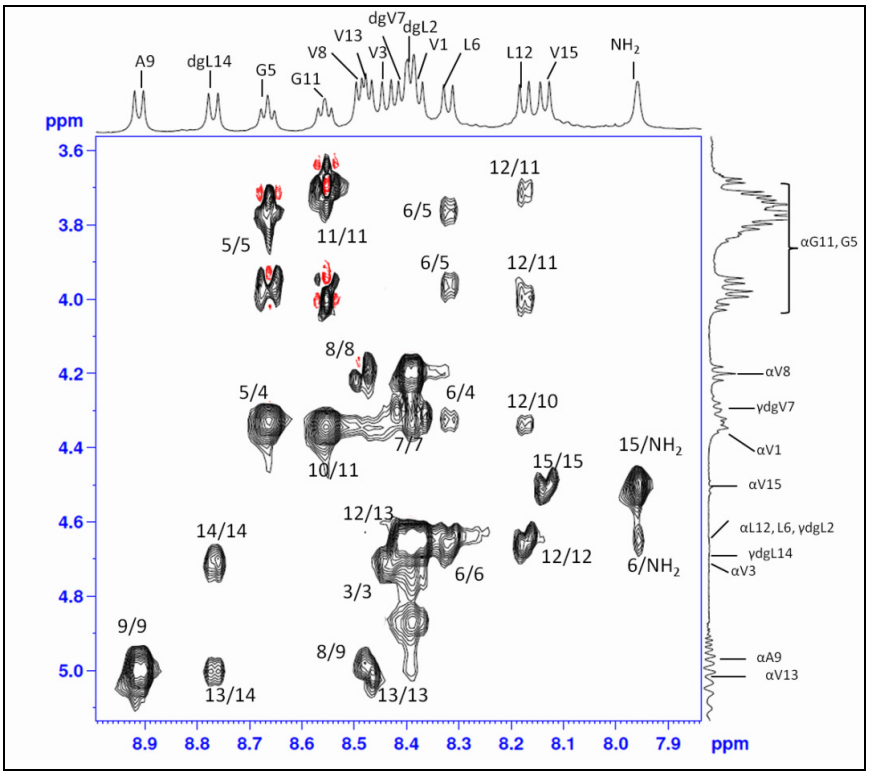
A9
dgL14
G5
G11
V8
V13
V3
dgV7
dgL2
V1
L6
L12
V15
NH2
ppm
3.6
3.8
4.0
4.2
4.4
4.6
4.8
5.0
12/11
6/5
5/5
11/11
6/5
12/11
8/8
5/4
6/4
12/10
7/7
10/11
15/NH2
15/15
12/13
14/14
12/12
6/6
6/NH2
3/3
9/9
8/9
13/14
13/13
αG11, G5
αV8
γdgV7
αV1
αV15
αL12, L6, γdgL2
γdgL14
αV3
αA9
αV13
8.9
8.8
8.7
8.6
8.5
8.4
8.3
8.2
8.1
8.0
7.9
ppm

C

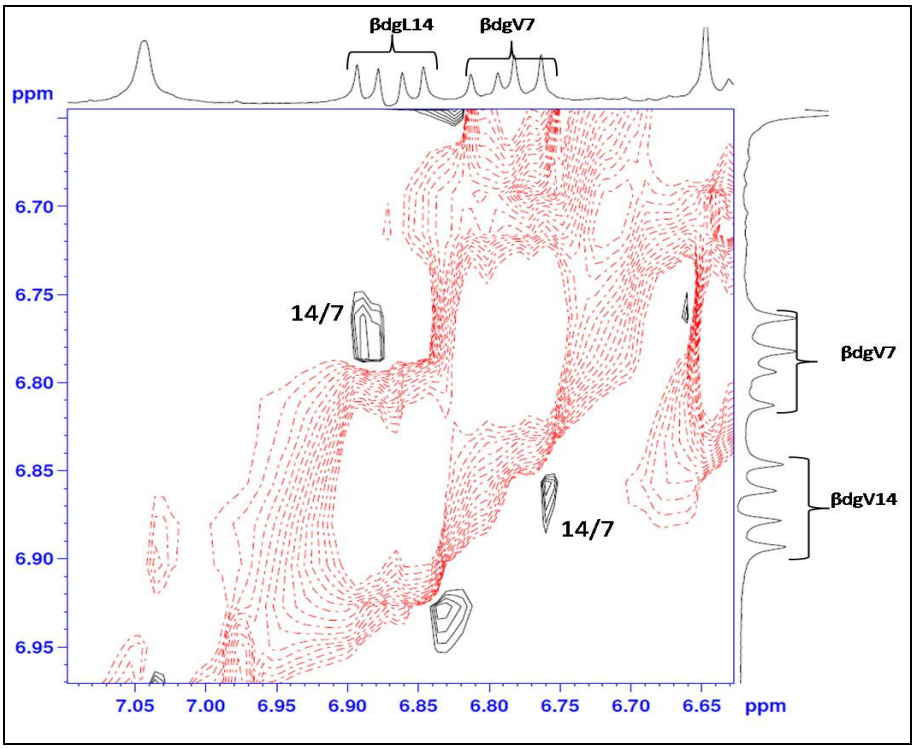
βdgL14
βdgV7
ppm
6.70
6.75
6.80
6.85
6.90
6.95
14/7
14/7
βdgV7
βdgV14
7.05
7.00
6.95
6.90
6.85
6.80
6.75
6.70
6.65
ppm

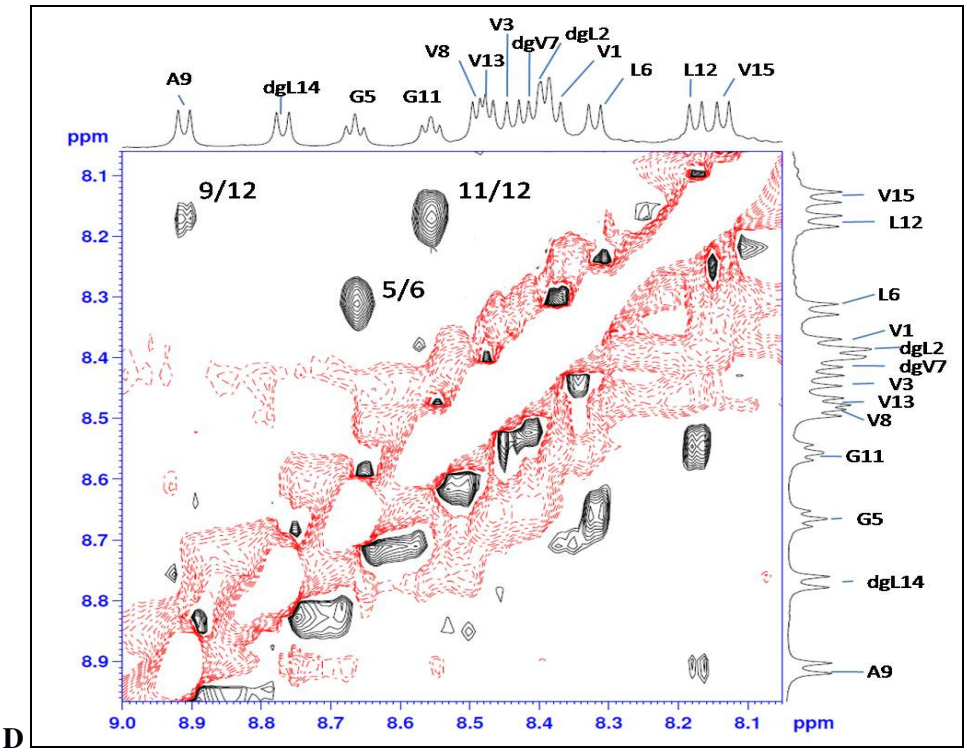

D

Figure 18: A) TOCSY NMR spectrum of **P3** in CD_3OH. The sequential assignments of amino acids were performed using ROESY, Partial ROESY spectra of **P3** showing cross-strand NOEs of B) NH↔ NH, C) vinylogous $C^{\beta}H \leftrightarrow C^{\beta}H$, and D) NH-$C^{\alpha}H$, NH-$C^{\gamma}H$ and NH-$C^{\delta}H$.

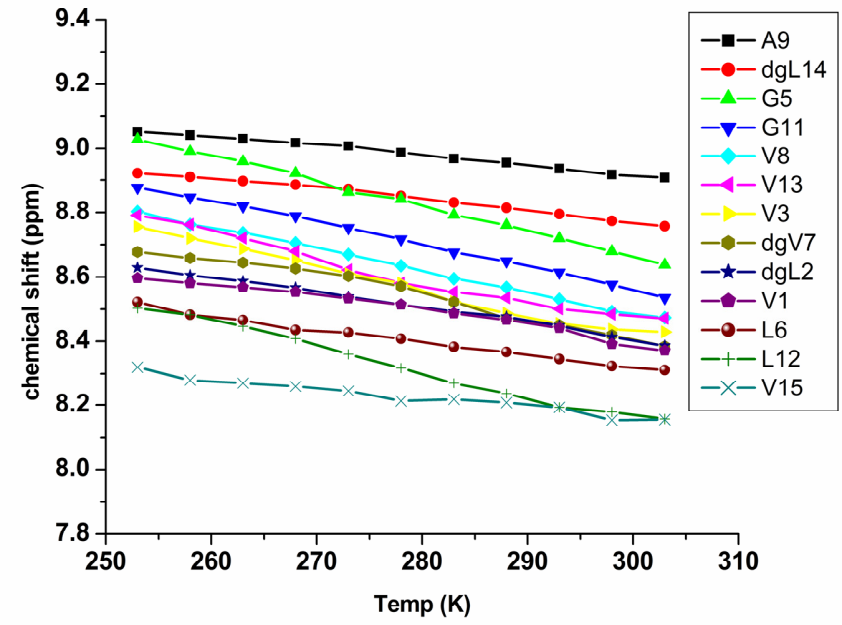

Figure 19: Plot of amides chemical shift with the various temperatures for **P3**

Table 5: Chemical Shifts of hybrid peptide **P3**

Residue	Chemical Shifts (ppm)							$^{3}J_{NHC^{\alpha}H}$	dδ/dT
	NH	$C^{\alpha}H$	$C^{\beta}H$	$C^{\gamma}H$	$C^{\delta}H$	$C^{\omega}H$	Others	(Hz)	ppb/K
Val1	8.38	4.39	2.03	0.8-0.6	-	-	-	9.15	-4.49
dgLeu2	8.39	6.61	6.64	4.62	1.36	1.63	0.8-0.6	8.85	-4.83
Val3	8.44	4.74	2.12	0.8-0.6	-	-	-	9.25	-6.48
^{D}Pro4	-	4.33	2.19-1.96	2.17-2.01	3.78	-	-	-	-
Gly5	8.66	3.79-3.98	-	-	-	-	-	6.1	-7.80
Leu6	8.32	4.6	1.88	1.72	0.8-0.6	-	-	8.55	-4.22
dgVal7	8.40	6.62	6.80	4.30	1.72	0.8-0.6		8.9	-5.86
Val8	8.48	4.18	2.08	0.8-0.6	-	-	-	9.15	-6.47
Ala9	8.91	4.92	1.32	-	-	-	-	7.95	-2.91
Pro10	-	4.35	2.24-2.02	2.17-2.01	3.76	-	-	-	-
Gly11	8.55	3.69-4.03	-	-	-	-	-	6.4	-6.85
Leu12	8.17	4.61	1.92	1.71	0.8-0.6	-	-	9.15	-6.92
Val13	8.47	5.02	2.03	0.8-0.6	-	-	-	9.15	-6.40
dgLeu14	8.77	6.22	6.87	4.75	1.58	1.28	0.8-0.6	8.55	-3.28
Val15	8.13	4.52	2.12	0.8-0.6	-	-	-	8.5	-3.31

* Alpha hydrogen of backbone in amino acid next to C=O (CH=C***H***-C=O), # Beta hydrogen of backbone in amino acid (C***H***=CH-C=O)

2.3.8 Solid state structure of peptide P3

We were able to get single crystals of **P3** after slow evaporation in aqueous methanol solution. The X-ray structure of **P3** is shown in Figure 20. As anticipated the hybrid peptide **P3** adopted a well folded 3-stranded β-sheet conformation in single crystals. Noticeably, this is first example of designed three stranded β-sheet structure in single crystals, though there are many reports in literature regarding the design of three stranded β-sheets. All α-residues in the strands adopted the characteristic conformations of a β-sheet. Three vinylogous amino acids dgL(2) (ϕ = -112°, θ_1 = 102°, θ_2 = 168°, and ψ = 161°), dgV(7) (ϕ = -102°, θ_1 = 104°, θ_2 = -170°, and ψ = -178°) and dgL(14) (ϕ = -111°, θ_1 = 94°, θ_2 = -177°, and ψ = 171°), accommodated into the β-sheets with a very similar characteristic backbone conformations. The local *s-cis* conformation is observed in all enamides of the vinylogous residues. Similar to **P1,** the extended conformation of vinylic -C_{β}=C_{α}- and -C_{α}-CO- (*s-cis*) of enamide

facilitates the accommodation of vinylogous residues into the backbone conformation without disturbing the overall fold of the molecule. The torsional angles θ_2, ψ and ω all have extended geometry with a value approximately (±) 180°. Interestingly, the values of ϕ and θ_1 of vinylogous amino acids have values very similar to the ϕ and ψ of α-residues. The torsional variables of all amino acids are given in the Table 6. The analysis of the crystal structure reveals that the peptide is stabilized by eight strong cross-strand intramolecular C=O···H-N H-bonds (Figure 20a). According to design the vinylogous residues dgL2 and dgV7 are not involved in intramolecular hydrogen bonding as they are incorporated at the non-hydrogen bonding positions of the antiparallel β-strands, however, dgV(7) and dgL(14) are involvoved in intramolecular H-bonding as they are placed in the H-bonding positions in antiparallel β-strands 2 and 3. Surprisingly, ideally positioned Ala9 NH and the Leu 13 C=O are not involved in the intramolecular H-bonds as their N-H···O distance exceeds (2.32Å) the normal H-bonding distances. In addition, all exposed NHs and the C=O groups are involved in the intermolecular H-bonding. The characteristic hydrogen bond parameters are given in

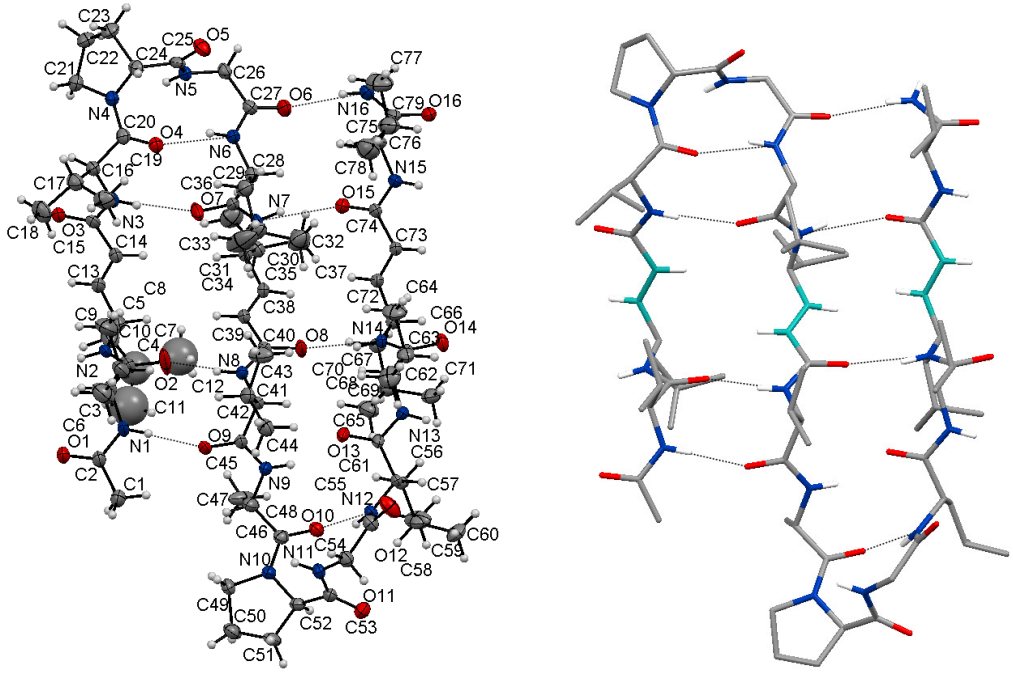

a) **b)**

Figure 20: a) The ORTEP diagram of hybrid 3-stranded β-sheet (**P3**) containing α, β-unsaturated γ-amino acids. H-atoms are not labelled for clarity. All four intramolecular hydrogen bonds are represented in dotted lines, b) capped stick model of **P3**, and for clarity some of the H-atoms are not shown.

the Table 7. All H-bonding distances and angles are within the limits of standard H-bonding parameters.[27]

Careful analysis of torsional angles at the turn ^{D}Pro-Gly segments reveals that they both adopted type I′ β-turn conformation [Standard (ϕ_{i+1} = 60° ψ_{i+1} = 30°, ϕ_{i+2} = 90°, ψ_{i+1} = 0°), observed ^{D}Pro4-Gly5 (ϕ_{i+1} = 66° ψ_{i+1} = 25°, ϕ_{i+2} = 88°, ψ_{i+2} = 1°) and ^{D}Pro10-Gly11 (ϕ_{i+1} = 57° ψ_{i+1} = 30°, ϕ_{i+2} = 86°, ψ_{i+2} = -15°)]. In contrast to the ^{D}Pro-Gly segment in octapeptide **P1** which adopted type II′ conformation, similar octapeptide (1-8 residues) adopted type I′ conformation in **P3**. After extending the β-strand lengths a smooth transition from type II′ to type I′ is observed. It has been observed that type I′ β-turn is the most abundant two residue β-turn in protein structures. The crystal structures of both **P1** and **P3** provide the unique opportunity to elucidate and understand the stereochemical properties of type I′ and type II′ β-hairpin structures.

Table 6: Torsional variables (in deg.) of Ac-Val-dgLeu-Val-^{D}Pro-Gly-Leu-dgVal-Val-Ala-^{D}Pro-Gly-Leu-Val-dgLeu-Val-NH_2 (**P3**)

Resd.	ϕ	θ_1	θ_2	ψ	ω
Val1	-119	-	-	114	170
dgLeu2	-112	102	168	161	173
Val3	-147	-	-	139	162
^{D}Pro4	66	-	-	25	-177
Gly5	88	-	-	1	174
Leu6	-104	-	-	120	168
dgVal7	-102	104	-170	-178	-175
Val8	-127	-	-	116	-173
Ala9	-152	-	-	137	179
^{D}Pro10	57	-	-	30	-178
Gly11	86	-	-	-15	-174
Leu12	-80	-	-	138	171
Val13	-100	-	-	103	-176
dgLeu14	-111	94	-177	171	176
Val15	-98	-	-	136	-

Table 7: Hydrogen bonding parameters of 3-stranded β-sheet **Ac-Val-dgLeu-Val-^{D}Pro-Gly-Leu-dgVal-Val-Ala-^{D}Pro-Gly-Leu-Val-dgLeu-Val-NH_2 (P3)**.

Type	Donar [D]	Acceptor [A]	D···A [Å]	H···A [Å]	D-H···A [deg]	D···O=C [deg]
Intramol.	N1	O9	2.85	1.99	176	156
Intermol.	N2	O14[¶]	2.78	1.98	157	169
Intramol.	N3	O7	2.97	2.20	148	157
Pro	N4(Pro)	---	---	---	---	---
Intermol.	N5	O12[*]	2.71	1.97	144	168
Intramol.	N6	O4	2.96	2.13	159	128
Intramol.	N7	O15	2.98	2.17	155	157
Intramol.	N8	O2	2.79	1.96	161	154
Intramol.	N9	O13	3.09	2.32	148	146
Pro	N10(Pro)	---	---	---	---	---
Intermol.	N11	O16[#]	2.92	2.18	156	149
Intramol.	N12	O10	2.87	2.06	157	124
Intermol.	N13	O1	2.88	2.04	164	164
Intramol.	N14	O8	2.77	1.97	157	169
Intermol.	N15	O3[§]	3.00	2.15	172	175
Intramol.	N16	O6	2.91	2.06	167	165
Intermol.	N16	O9[†]	3.01	2.15	175	110

Intermol.; intermolecular, intramol.; intramolecular, #Symmetry equivalent x, y, 1+z, †Symmetry equivalent x, y, -1+z, ¶Symmetry equivalent -1+x, -1+y, z, §Symmetry equivalent 1+x, 1+y,1+z, *Symmetry equivalent -1+x, -1+y, -1+z.

2.3.9 Expanded H-bond pseudocycles

In our investigation parallel β-sheet structurs of vinylogous hybrid peptides revealed that the parallel β-sheets are stabilized by continous intermolecular 16 membered H-bonding pseudocycles. Inspection of the vinylogous segments in the three stranded β-sheet revealed that the structure is stabilized by 14 and 16 membered H-bond psuedocyles along with the regular 10 and 14 memberd H-bond psuedocycles in anti-parallel sheets. The three stranded β-sheets are interconnecting in parallel sheets fassion through intermolecular H-bonding between the sheet 3 and 1. The infinite β-sheet assembly of three stranded β-sheets is shown in Figure 21a. In addition, the crystal structure analysis reveals that three independent 3-

strand β-sheet molecules are involved in the head-to-tail fashion through three intermolecular H-bonding as shown in Figure 21b.

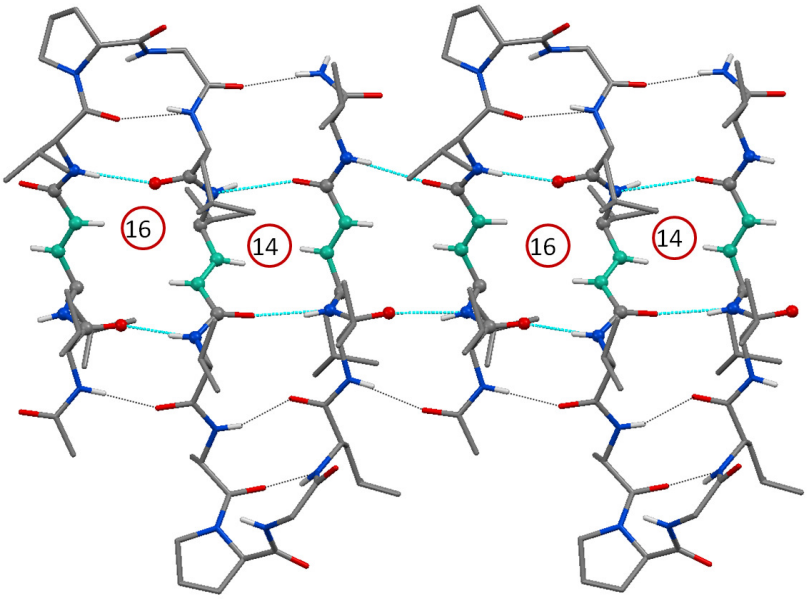

a)

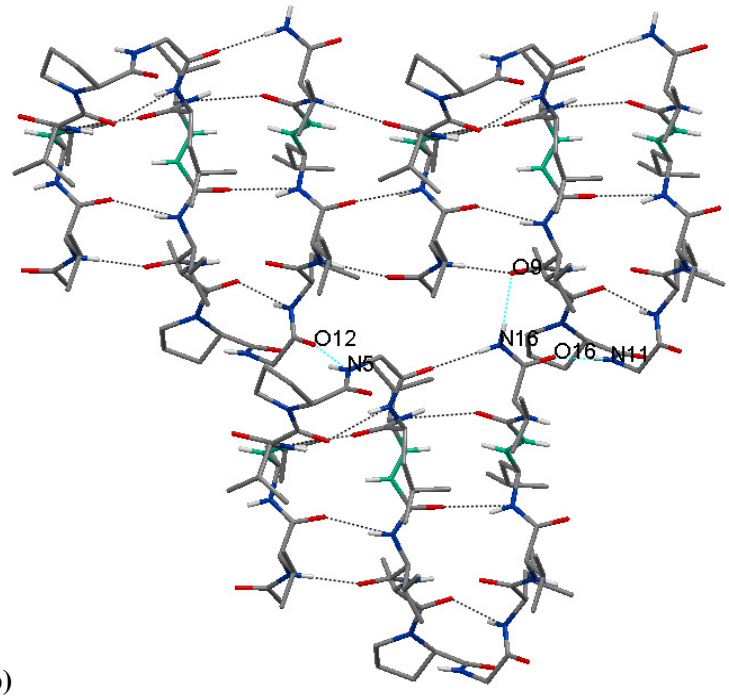

b)

Figure 21: a) The extended β-sheets connected by intermolecular hydrogen bonding, b) three independent 3-strand β-sheet molecules are involved in the head-to-tail connection through three intermolecular H-bonding (shown with cyan wireframe).

2.3.10 Analysis of β-haripins containing type I′ and type II′ β-turns

Crystal structures of **P1** and **P3** provides realistic examples to analyze the context free isolated β-hairpin secondary structures containing type I′ and type II′ β-turns. The sequence of **P1** is similar to the 1-8 residues of three stranded β-sheet, however, **P1** adopted a type II′ β-turn, while the same sequence adopted type I′ β-turn in **P3**. The intramolecular H-bonding distances between the anti-parallel β-strands suggested that the H-bond lengths are shorter in the hairpins are conatining type I′ β-turn. In addition we measured the atom to atom distances between the anti-parallel β-strands of the two hairpin models. The H-bond distances and the distances between the backbone to backbone atoms are given the Table 8 and Table 9 respectively. These results suggested that the β-strands are more compactly packed in the type I′ β-hairpins compared to the type II′ hairpins.

Table 8: Comparison between H-bond distances (Å) observed in **P1** and **P3**

	β-hairpin **P1**		3-stranded **P3**		Difference (**P1 - P3**) D-H···A (Å)	Difference (**P1 - P3**) D···A (Å)
	D-H···A (Å)	D···A (Å)	D-H···A (Å)	D···A (Å)		
Val1NH···O=CVal8	2.080	2.933	1.996	2.855	0.084	0.078
Val1C=O···HNVal8	2.213	2.929	1.960	2.791	0.253	0.128
Val3NH···O=CLeu6	2.246	3.069	2.206	2.972	0.040	0.097
Val3C=O···HNLeu6	2.111	2.880	2.139	2.960	-0.028	-0.08

Table 9: Comparison between cross-strand backbone atom to atom distance (Å) observed in **P1** and **P3**

Cross-strand backbone Atom↔Atom	β-hairpin **P1** (Å)	3-stranded **P3** (Å)	Difference (**P1 - P3**) (Å)
Val1N↔C(O)Val8	4.120	4.026	0.094
Val1C_α↔C_αVal8	5.097	5.072	0.015
Val1C(O)↔NVal8	4.102	3.945	0.157
dgL2N↔C(O)dgV7	5.721	5.523	0.198
dgL2C_γ↔$C_\alpha$dgV7	4.751	4.477	0.274
dgL2C_β ↔$C_\beta$dgV7	5.900	5.608	0.292
dgL2C_α↔$C_\gamma$dgV7	4.937	4.502	0.435
dgL2C(O)↔NdgV7	5.791	5.601	0.190
Val3N↔C(O)Leu6	4.113	4.153	-0.040
Val3C_α↔C_αLeu6	5.024	5.407	-0.383
Val3C(O)↔NLeu6	3.887	3.849	0.038

2.3.11 Overlay of hybrid three stranded β-sheets over α-peptide β-sheets

This interesting result of three stranded β-sheet structure motivated us to assess its structural similarities with native protein structures. In this regard, we randomly selected the alpha-cobra toxin venom from Naja naja[28] (PBD CODE 2CTX). The overlay of the peptide **P3** with cobra toxin is shown in Figure 22. Instructively, the backbone conformation of **P3** is well correlated with the multi-strand β-sheet motif. These results suggest that three-stranded β-sheet (**P3**) can be utlized in mimicking the native chemical domain of natural β-sheets or toxin molecules. In addition, the alpha and α, β-unsaturated hybrid multi-stranded β-sheet might provide useful route to design many functionally targeted theraputics as well as inhibitors for protein-protein interactions.

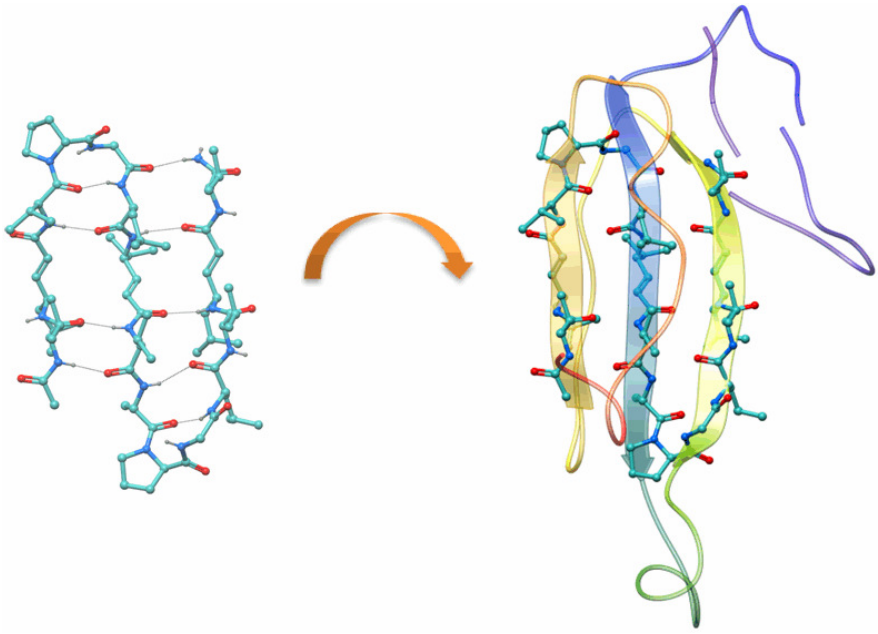

Figure 22: Overlay structure of **P3** with β-sheet rich region of Cobra toxin venom protein (PDB 2CTX)[27] from Naja naja.

2.4 Conclusion

In conclusion, we have shown the effective incorporation of the vinylogous amino acids into the cannonical β-hairpin and 3-stranded β-sheets. The solution and solid state structural analysis reveals that the peptide **P1** adopted a stable and regular β-hairpin and **P3** adopted a multiple β-hairpin structure. In addition, we have demonstrated the effective incorporation of functionalizable vinylogous amino acids into the β-hairpin and 3-stranded β-sheet without disturbing the overall fold of the molecule. Also we have described a single step conversion of vinylogous hybrid peptide into its saturated analogue. The hybrid γ-peptide adapted a distorted β-hairpin conformation with poor strand registry in solution. It is worth noting that appropriate geometry for the proper interstrand registry of β-hairpin peptide **P1** is dictated by the double bonds of vinylogous γ-residues. This geometrical constrain is lacking in **P2**, which leads to the non-registry of interstrands, altering its conformation. This present study envisages that the choice of these α,β-unsaturated γ-amino acids at appropriate positions could be used to design a well folded β-hairpin and multi-strand β-sheet with proper strand registry.

2.5 Experimental section

General Experimental Details

All amino acids, DiPEA, TFA, Triphenylphosphine were purchased from Aldrich. THF, DCM, DMF, NaOH were purchased from Merck. Ethyl bromoacetate, HBTU, HOBt, EtOAc, NMP, Pet-ether (60-80 ^{o}C) were obtained from Spectrochem and used without further purification. THF and DiPEA were dried over sodium and distilled immediately prior to use. Column chromatographies were performed on Merck silica gel (120-200 mesh). Final peptides were purified on reverse phase HPLC (Waters 600) (C18 column, MeOH/H_2O 65:35- 95:5 as gradient, 1.25 mL flow per min). The ^{1}H spectra were recorded on Bruker 500 MHz (or 125 MHz for ^{13}C) and Jeol 400 MHz (or 100 MHz for ^{13}C) using residual solvents signals as an internal reference ($CDCl_3$ δ_H, 7.26 ppm, δ_c 77.3 ppm and CD_3OH δ_H 3.31 ppm, δ_c 49.0 ppm). The chemical shifts (δ) are reported in *ppm* and coupling constants (*J*) in Hz. Mass was recorded on MALDI TOF/TOF (Applied Biosystem) and CD was recorded on JASCO (*J*-815). X-Ray data were collected on Bruker APEX II DUO.

NMR spectroscopy: All NMR studies were carried out by using a Bruker AVANCE^{III}-500 MHz spectrometer at a probe temperature of 300 K. Resonance assignments were obtained by TOCSY and ROESY analysis. All two-dimensional data were collected in phase-sensitive mode, by using the time-proportional phase incrementation (TPPI) method. Sets of 1024 and 512 data points were used in the t_2 and t_1 dimensions, respectively. For TOCSY and ROESY analysis, 32 and 72 transients were collected, respectively. A spectral width of 6007 Hz was used in both dimensions. A spin-lock time of 256 ms was used to obtain ROESY spectra. Zero-filling was carried out to finally yield a data set of 2 K × 1 K. A shifted square-sine-bell window was used before processing.

Molecular Dynamics: Model building and molecular dynamics simulation of P2 was carried out using Insight II (97.0) / Discover program on a Silicon Graphics Octane workstation. [28] The cvff force field with default parameters was used throughout the simulations. Minimization's were done first with steepest decent, followed by conjugate gradient methods for a maximum of 1000 iterations each or RMS deviation of 0.001 kcal/mol, whichever was earlier. The energy-minimized structures were then subjected to MD simulations. A number of inter atomic distance constraints obtained from NMR data were used as restraints in the minimization as well as MD runs. For MD runs, a temperature of 300 K was used. The molecules were initially equilibrated for 50 ps and subsequently subjected to a 1 ns dynamics with a step size of 1 fs, sampling the trajectory at equal intervals of 10 ps. In trajectory 50 samples were generated and the best structures were again energy minimized with above protocol and superimposed these structures.

Circular dichroism (CD) spectroscopy:

CD spectrometry study was carried out on JASCO J-815 spectropolarimeter using cylindrical, jacketed quartz cell (1 mm path length), which was connected to Julabo-UC-25 water circulator. Spectra were recorded with a spectral resolution of 0.05 nm, band width 1 nm at a scan speed of 50 nm/min and a response time 1 sec. All the spectra were corrected for methanol solvent and are typically averaged over 3 scans.

List of NOEs used in the MD calculation

Residue	H-atom	Residue	H-atom	NOE observed
Val(1)	NH	Val(1)	αH	Strong
Val(1)	NH	Val(1)	βH	Strong
Val(1)	αH	γLeu(2)	NH	Strong
Val(1)	αH	C-terminal NH_2	NH_2	Weak
Val(1)	βH	γLeu(2)	NH	Weak
γLeu(2)	NH	γLeu(2)	βH	Strong
γLeu(2)	NH	γLeu(2)	γH	Medium
γLeu(2)	NH	γLeu(2)	αH	Weak
γLeu(2)	NH	γLeu(2)	δH	Medium
γLeu(2)	NH	γLeu(2)	$-(CH_3)_2$	Weak
γLeu(2)	αH	γLeu(2)	γH	Strong
Val(3)	NH	γLeu(2)	αH	Strong
Val(3)	NH	γLeu(2)	βH	Weak
Val(3)	NH	Val(3)	αH	Medium
Val(3)	NH	Val(3)	βH	Medium
Val(3)	NH	Val(3)	γH	Medium
Val(3)	αH	Pro(4)	δH	Medium
Val(3)	βH	Pro(4)	δH	Medium
Pro(4)	αH	Pro(4)	δH	Strong
Pro(4)	αH	Gly(5)	αH	Strong
Pro(4)	βH	Pro(4)	δH	Strong

Pro(4)	βH	Gly(5)	αH	Medium
Gly(5)	NH	Pro(4)	αH	Strong
Gly(5)	NH	Gly(5)	αH	Strong
Gly(5)	NH	Leu(6)	NH	Weak
Gly(5)	αH	Leu(6)	NH	Strong
Leu(6)	NH	Leu(6)	αH	Medium
Leu(6)	NH	Leu(6)	βH	Strong
Leu(6)	NH	γVal(7)	NH	Medium
Leu(6)	αH	γVal(7)	δH	Medium
Leu(6)	αH	γVal(7)	NH	Strong
γVal(7)	NH	γVal(7)	αH	Weak
γVal(7)	NH	γVal(7)	βH	Strong
γVal(7)	NH	γVal(7)	γH	Medium
γVal(7)	γH	γVal(7)	αH	Strong
γVal(7)	γH	γLeu(2)	δH	Strong
γVal(7)	βH	γLeu(2)	γH	Medium
Val(8)	NH	γLeu(2)	αH	Strong
Val(8)	NH	Val(8)	γH	Medium
Val(8)	NH	Val(8)	βH	Weak
Val(8)	NH	Val(8)	αH	Medium
Val(8)	αH	C-terminal NH_2	NH_2	Medium
Val(8)	βH	C-terminal NH_2	NH_2	Weak

Structure Solution and Refinement

The initial cell constants were obtained from three series of ω scans at different starting angles. Each series consisted of 12 frames collected ω with the exposure time of 10 seconds per frame. Obtained reflections were successfully indexed by an automated indexing routine built in the SMART program.

The data were collected by using the full sphere data collection routine to survey the reciprocal space to the extent of a full sphere to a resolution of 0.75 Å, with an exposure time 10 sec per frame. The data integration and reduction were processed with SAINT [29] software. A multi-scan absorption correction was applied to the collected reflections.

The systematic absences in the diffraction data were uniquely consistent for the space group that yielded chemically reasonable and computationally stable results of refinement.[30] A successful solution by the direct methods provided most non-hydrogen atoms from the E-map. The remaining non-hydrogen atoms were located in an alternating series of least-squares cycles and difference Fourier maps. All non-hydrogen atoms were refined with anisotropic displacement coefficients. All hydrogen atoms were included in the structure factor calculation at idealized positions and were allowed to ride on the neighbouring atoms with relative isotropic displacement coefficients.

Crystal structure analysis of P1 (Ac-Val-dgLeu-Val-^{D}Pro-Gly-Leu-dgVal-Val-NH_2)

Crystals of peptide **P1** were grown by slow evaporation from a solution of methanol. A single crystal (0.25 × 0.20 × 0.10 mm) was mounted in a loop with a small amount of the mother liquor. The X-ray data were collected at 200 K temperature on a Bruker AXS SMART APEX II CCD diffractometer using MoK_α radiation (λ = 0.71073 Å), ω-scans (2θ = 52.52°), for a total number of 5661 independent reflections. Space group *P2(1)* , a = 9.758(6), b = 13.043(8), c = 20.820(13) Å, α = 90.00 , β = 92.986(8), γ = 90.00, V= 2646(3) $Å^3$, Monoclinic *P*, Z=2 for chemical formula $C_{45}H_{77}N_9O_9.2\text{-}H_2O$, with one molecule in asymmetric unit; ρ_{calcd} = 1.155 g cm^{-3}, μ = 0.083 mm^{-1}, F(000) = 1004, R_{int} = 0.2279. The structure was obtained by direct methods using SHELXS-97.[30] All non-hydrogen atoms were refined anisotropically. The hydrogen atoms were fixed geometrically in the idealized position and refined in the final cycle of refinement as riding over the atoms to which they

are bonded. The final *R* value was 0.0747 (*wR2* = 0.1130) for 2828 observed reflections ($F_0 \geq 4\sigma(|F_0|)$) and 599 variables, *S* = 1.075. The largest difference peak and hole were 0.208 and -0.201 e Å^3, respectively. [CCDC 802256]

Crystal structure analysis of P3 (Ac-Val-dgLeu-Val-^{D}Pro-Gly-Leu-dgVal-Val-Ala-^{D}Pro-Gly-Leu-Val-dgLeu-Val-NH_2)

Crystals of peptide were grown by slow evaporation from a solution of methanol. A single crystal (0.18 × 0.14 × 0.11 mm) was mounted in a loop with a small amount of the mother liquor. The X-ray data were collected at 100 K temperature on a Bruker AXS SMART APEX II CCD Duo diffractometer using MoK_α radiation (λ = 0.71073 Å), ω-scans (2θ = 56.56°), for a total number of 21007 independent reflections. . Space group P1, *a* = 12.367(3), *b* = 13.818(3), *c* = 16.091(5) Å, α = 105.224(6) , β = 97.197(6), γ = 113.827(4), V = 2342.2(10) Å^3, Triclinic P, Z = 1 for chemical formula ($C_{79}H_{134}N_{16}O_{16}$), with one molecule in asymmetric unit; ρ_{calcd} = 1.117 g cm^{-3}, μ = 0.078 mm^{-1}, *F*(000) = 854, R_{int} = 0.0472. The structure was obtained by direct methods using SHELXS-97.[30] All non-hydrogen atoms were refined anisotropically. The hydrogen atoms were fixed geometrically in the idealized position and refined in the final cycle of refinement as riding over the atoms to which they are bonded. The final *R* value was 0.0705 (*wR2* = 0.1939) for 14462 observed reflections ($F_0 \geq 4\sigma$ ($|F_0|$)) and 1009 variables, *S* = 1.041. The largest difference peak and hole were 1.192 and -0.500 e Å^3, respectively.

During the refinement it was observed that, C10, C11 and C12 atoms are disordered with two site occupancy (where C10 with 50:50, C11 with 60:40 and C12 with 60:40). A significant amount of time was invested to refine the disordered atoms anisotropically using constrains to fix them. But due to huge disorder property of C10, C11 and C12 atoms were refined isotropically and it was observed that the absolute value of parameter shift to su ratio is 4.25.

General procedure for the synthesis of Fmoc-α, β-unsaturated γ- amino acids

Boc-α, β-unsaturated γ-amino acid: Ethyl ester of Boc-α, β-unsaturated γ- amino acid (2 mmol) was dissolved in 5 mL of ethanol. Then 5 mL of 1*N* NaOH was added slowly to the reaction mixture. After completion of the reaction (~ 30 min), ethanol was evaporated from the reaction mixture and residue was acidified using 10 mL of 5% HCl (5% volume in water) at cold conditions. The product was extracted with ethyl acetate (3 × 40 mL). Combined organic layer was washed with brine (30 mL) and dried over anhydrous Na_2SO_4. The solvent was concentrated under reduced pressure to give Boc-α, β-unsaturated γ-amino acid as gummy product in a quantitative yield.

The Boc-α, β-unsaturated γ-amino acid (1 mmol) was dissolved in 5 mL of DCM and cooled to 0 ^oC in ice bath followed by 5 mL of neat TFA was added to the reaction mixture. After 30 min, TFA was removed from reaction mixture under *vacuum*. Residue was dissolved in 15 mL of water (15 mL) and the pH was adjusted to ~ 10 by the slow addition of solid Na_2CO_3. The solution of Fmoc-OSu (1 mmol) in 10 mL of THF was added slowly to the reaction mixture. Reaction mixture was stirred overnight at RT. After completion of the reaction, the reaction mixture was acidified with 20 mL of 20% HCl (20% volume in water) in cold condition. Product was extracted with ethyl acetate (3 × 50 mL). Combined organic layer was washed with brine (30 mL) and dried over anhydrous Na_2SO_4. The solvent was concentrated under reduced pressure to give gummy product, which was recrystallized using EtOAc/Pet-ether. The pure white solid of Fmoc- α, β-unsaturated γ-amino acid was subjected for SPPS. The schematic representation of the synthesis is shown below.

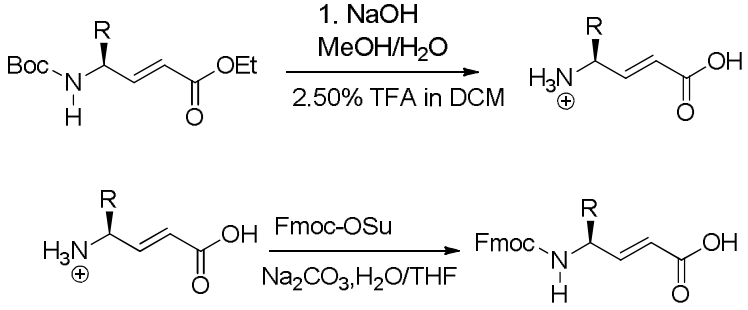

R = -^{i}Pr, -^{i}Bu

(*S*, *E*)-4-(((9H-fluoren-9-yl)methoxy)carbonylamino)-5-methylhex-2-enoic acid

Physical state : white powder

Mol. Formula : $C_{22}H_{23}NO_4$

Yield : 0.590 g, 90%

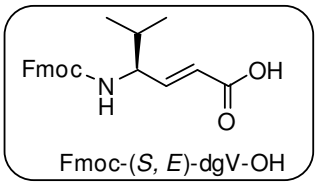

Fmoc-(*S, E*)-dgV-OH

^{1}H NMR (400 MHz, $CDCl_3$) : δ_H 7.7814-7.3095 (m, 8H, -Fmoc aromatic) 6.9853-6.9349 (dd, *J* = 9.6, *J* = 5.34, 1H, C*H*=CHCO$_2$Et), 5.9154-5.8730 (d, *J* = 16, 1H, CH=C*H*CO$_2$Et), 4.8123-4.7871 (d, *J* = 9.1,1H, NH), 4.4881-4.4732 (d, *J* = 6.1, 2H, -OCH_2-Fmoc), 4.3174-4.2086 (m, 2H, C*H*-CH=CH,-C*H*(of Fmoc)), 1.9360-1.8524 (m, 1H, C*H*-(CH$_3$)$_2$), 0.9543-0.9096 (m, 6H, CH-(CH_3)$_2$).

^{13}C NMR (100 MHz, $CDCl_3$) : δ_C 170.6868, 155.8987, 149.3389, 143.7707, 141.3298, 127.7430, 127.0661, 124.9017, 121.0402, 119.9819, 66.6454, 57.2825, 47.2902, 32.1112, 18.8772, 18.0191.

MALDI-TOF/TOF m/z : Calcd. $[M+Na]^+$ 388.1525, observed 388.1581

(*S*, *E*)-4-(((9H-fluoren-9-yl)methoxy)carbonylamino)-6-methylhept-2-enoic acid

Physical character : white powder

Mol. Formula : $C_{23}H_{25}NO_4$

Yield : 0.60 g, 89%

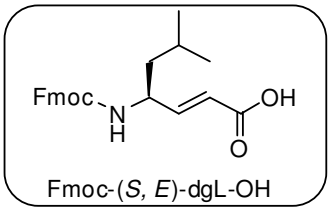

Fmoc-(*S, E*)-dgL-OH

^{1}H NMR (400 MHz, $CDCl_3$) : δ_H 7.7754-7.3033 (m, 8H, -Fmoc aromatic) 6.9482-6.8955 (dd, *J* = 10.5, *J* = 5.4, 1H, C*H*=CHCO$_2$Et), 5.9069-5.8680 (d, *J* = 15.5, 1H, CH=C*H*CO$_2$Et), 4.6859-4.6652 (d, *J* = 8.2,1H, NH), 4.4842-4.4686 (d, *J* = 6.2, 2H, -OCH_2-Fmoc)), 4.4281-4.3926 (t, *J* = 4.7, 1H, C*H*-CH=CH), 4.2277-4.1967 (t, *J* = 4.1, 1H,-C*H*(of Fmoc), 1.6824-1.6033 (m, 2H, CH_2-CH-(CH$_3$)$_2$), 1.4281-1.3926 (t, *J* = 4.7, 3H, C*H*-(CH$_3$)$_2$), 0.9372-0.9218 (d, *J* = 6.1, 6H, CH-(CH_3)$_2$).

^{13}C NMR (100 MHz, $CDCl_3$) **:** δ_C 170.7535, 155.6031, 150.8358, 143.7325, 141.3298, 127.7335, 127.0661, 124.9017, 119.9724, 66.5501, 50.3032, 47.29.02, 43.4669, 24.6742, 22.7196, 22.0331.

MALDI-TOF/TOF m/z **:** Calcd. $[M+Na]^+$ 402.1681, observed 402.1662.

SPPS peptide synthesis of (Ac-V-dgL-V-^{D}Pro-Gly-L-dgV-V-NH_2) (P1)

P1 peptide was synthesized at 0.2 mmol scale on Rink Amide resin using standard Fmoc-chemistry. HBTU/HOBT was used as coupling agents. The coupling reactions were monitored by Kaiser Test. After completion of the synthesis, peptide was cleaved from the resin using 15 mL of TFA/thioanisole/H_2O (98:1.5:0.5) cocktail mixture. After cleavage, the resin was filtered and washed with TFA. The cleavage mixture was evaporated under reduced pressure to give gummy product. Peptide was further recrystallized using EtOAc/Hexane. Peptide was filtered and purified through reverse phase HPLC on C_{18} column using MeOH/H_2O gradient. Homogeneity of peptide was further confirmed using analytical C_{18} column in same MeOH/H_2O gradient system. The HPLC profile is given below. The mass of the peptide was confirmed using **MALDI TOF/TOF** Mass Calcd. for $C_{45}H_{77}N_9O_9$ [M+Na] 910.5742 Da, observed 910.4104 Da.

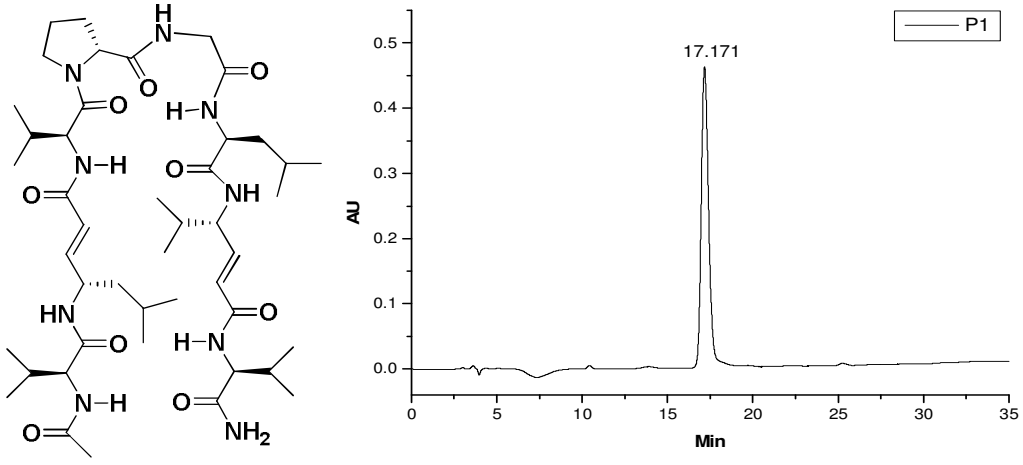

a) **b)**

Figure 23: a) Schematic view of **P1**. b) Reverse Phase HPLC profile of peptide P1. Methanol/ H_2O were used as a solvent system at a flow rate of 1.25 mL /min.

Transformation of vinylogous hybrid Peptide P1 (Ac-V-dgL-V- ^{D}Pro-Gly-L-dgV-V-NH_2) to its saturated hybrid γ-peptide analogue (Ac-V-γL-V- ^{D}Pro-Gly-L-γV-V-NH_2) P2

Ac-V-dgL-V-^{D}Pro-Gly-L-dgV-V-NH_2 (**P1**) (0.0225 mmol, 20 mg) was dissolved in EtOH (5 mL), and was treated with 20 mg of Pd/C. The hydrogen gas was supplied through balloon. The schematic representation is shown below. The reaction mixture was stirred under hydrogen atmosphere for about 6 hrs. The completion of the reaction was monitored by MALDI TOF/TOF and HPLC. After the completion, the reaction mixture was diluted with EtOH (10 mL) and it was centrifuged at 4000 rpm for about 20 min. The Pd/C was precipitated out and the supernatant was collected and evaporated under reduced pressure. Peptide was purified by reverse phase HPLC using the same protocol mentioned above. Overall, the γ-hybrid peptide was isolated in 95% yield (19 mg, 0.0214mmol). The mass of the peptide was confirmed using **MALDI TOF/TOF** m/z Calcd. for $C_{45}H_{81}N_9O_9$ [M+Na] 914.6055Da, observed 914.3443Da;

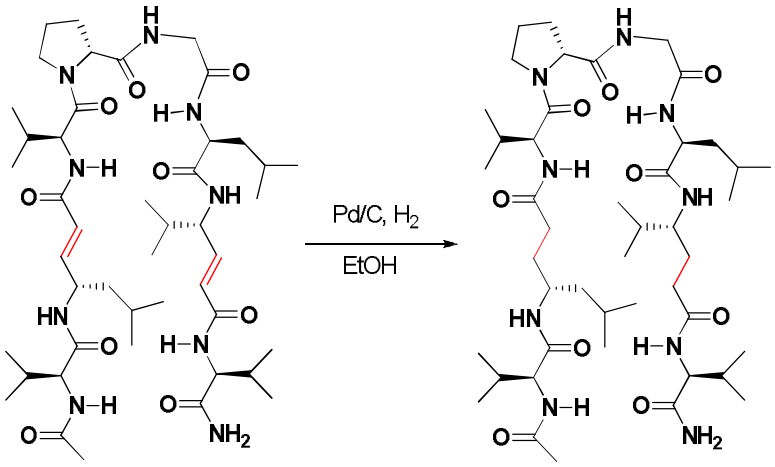

HPLC profile of P2

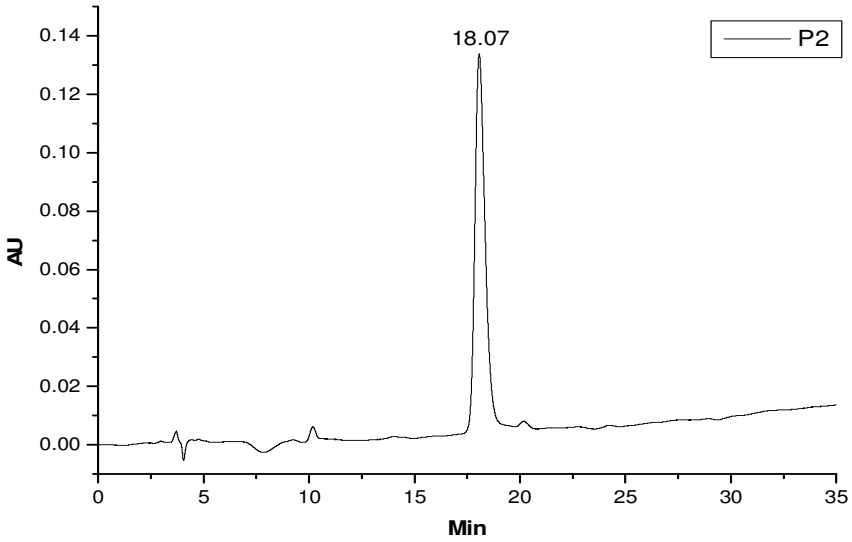

SPPS peptide synthesis of (Ac-Val-dgLeu-Val-^{D}Pro-Gly-Leu-dgVal-Val-Ala-^{D}Pro-Gly-Leu-Val-dgLeu-Val-NH_2) P3

P3 peptide was synthesized at 0.2 mmol scales on Rink Amide resin using standard Fmoc-chemistry. HBTU/HOBT was used as coupling agents for alpha amino acids and only HBTU was used as coupling agent for vinylogous γ-amino acids. Fmoc deprotections were facilitated using 20% piperidine in DMF. *N*-terminal of peptide was capped with acetyl group. The coupling reactions were monitored by Kaiser Test. After completion of the synthesis, peptide was cleaved from the resin using 15 mL of TFA/thioanisole/H_2O (98:1.5:0.5) cocktail mixture. After cleavage, the resin was filtered and washed with TFA. The cleavage mixture was evaporated under reduced pressure to give gummy product. Peptide was further recrystallized using EtOAc/Hexane. Peptide was filtered and finally it was purified on reverse phase HPLC (Waters 600), with C_{18} column (XBridge^{TM} Prep BEH 130, C_{18} 5µm, dimension 10 × 250 mm column) using MeOH/H_2O (system MeOH/H_2O 65:35- 95:5 as gradient, 1.25 mL flow per min)gradient system. Homogeneity of peptide was further confirmed using analytical (XBridge^{TM} BEH 130, C_{18} 5µm, dimension 4.6 × 250 mm column) C_{18} column in same MeOH/H_2O (system MeOH/H_2O 65:35- 95:5 as gradient, 0.75 mL flow per min) gradient system. The HPLC profile is given below. The mass of the

peptide was confirmed using **MALDI TOF/TOF** Mass Calcd. for $C_{79}H_{134}N_{16}O_{16}$ $[M+Na]^+$ 1586.0061 Da, observed 1586.3785 Da.

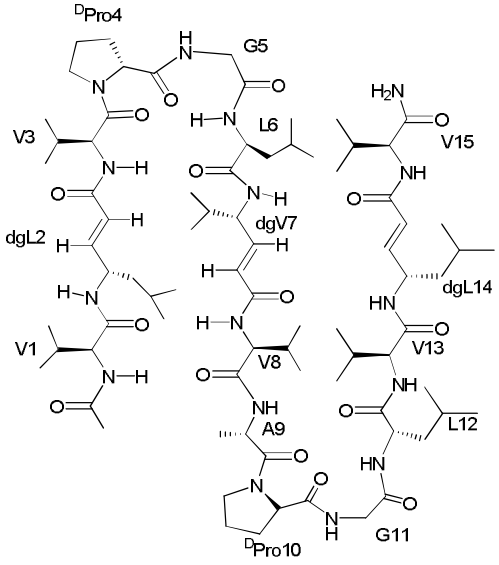

A

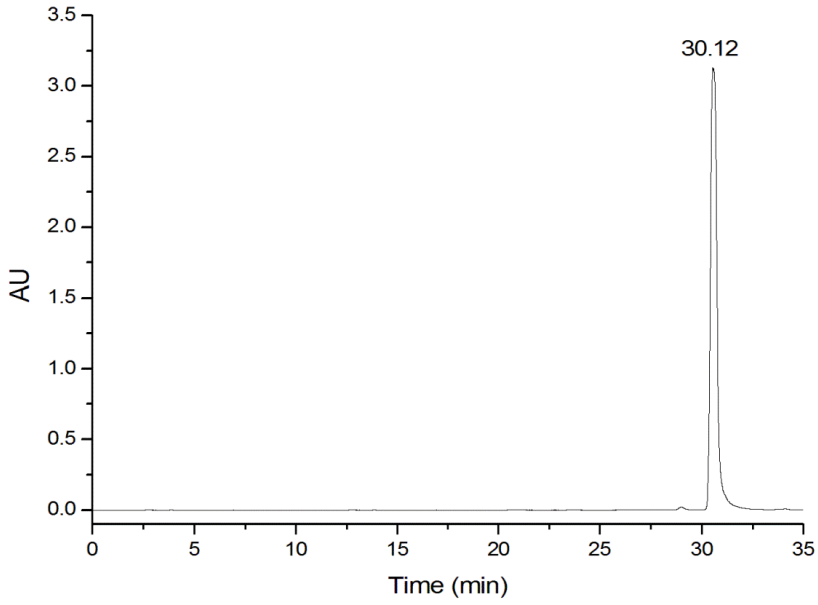

B

Figure 23: A: Schematic view of **P3**. **B**. Reverse phase HPLC profile of 3-stranded β-sheet (**P3**). Methanol/ H_2O were used as a solvent system at a flow rate of 1.25 mL /min.

2.6 References

1. Pauling, L.; Corey, R. B. *Proc. Natl. Acad. Sci. U. S. A.* **1951**, *37*, 729-740.
2. a) Venkatachalam, C. M. *Biopolymers* **1968**, *6*, 1425-1436. b) Lewis, P.N.; Momany, F.A.; Scheraga, H. A. *Biochim. Biophys. Acta* **1973**, *303*, 211-229.
3. Sibanda, B.L.; Thornton, J.M. *Nature* **1985**, *316*, 170-174.
4. a) Hillier, B. J.; Christopherson, K. S.; Prehoda, K. E.; Bredt, D. S.; Lim, W. A. *Science* **1999**, *284*, 812-815. b) Gajiwala, K. S.; Chen, H.; Cornille, F.; Roques, B. P.; Reith, W.; Mach, B.; Burley, S. K. *Nature* **2000**, *403*, 916-921. c) Zavala-Ruiz, Z.; Strug, I.; Walker, B. D.; Norris, P. J.; Stern, L. J. *Proc. Natl. Acad. Sci. USA* **2004**, *101*, 13279-13284. d) Berisio, R.; Schluenzen, F.; J. Harms, J.; Bashan, A.; Auerbach, T.; Baram, D.; Yonath, A. *Nat. Struct. Biol.* **2003**, *10*, 366-370. e) M. A. Schumacher, M. A.; Hurlburt, B. K.; Brennan, R. G. *Nature* 2001, *409*, 211-215. f) Muller, Y. A.; Li, B.; Christinger, H. W.; Wells, J. A.; Cunningham, B. C.; de Vos, A. M. *Proc. Natl. Acad. Sci. USA* **1997**, *94*, 7192-7197.
5. a) Russell, S. J.; Cochran, A. G. *J. Am. Chem. Soc.* **2000**, *122*, 12600-12601. b) Jager, M.; Dendle, M.; A. A. Fuller, A. A.; Kelly, J. W. *Protein Sci.* **2007**, *16*, 2306-2313. c) Favre, M.; Moehle, K.; Jiang, L.; Bfeiffer, B.; Robinson, J. A. *J. Am. Chem. Soc.* **1999**, *121*, 2679-2685. d) Jiang, L.; Moehle, K.; Dhanapal, B.; Obrecht, D.; Robinson, J. A. *Helv. Chim. Acta* **2001**, *83*, 3097-3112.
6. a) Robinson, J. A. *Acc. Chem. Res.* **2008**, *41*, 1278-1288. b) Pantoja-Uceda, D.; Santiveri, C. M.; Jimenez, M. A. *Methods Mol. Biol.* **2006**, *340*, 27-51. c) Maynard, A. J.; Sharman, G. J.; Searle, M. S. *J. Am. Chem. Soc.* **1998**, *120*, 1996-2007. d) Arkin, M. R.; Wells, J. A. *Nat. Rev. Drug Discov* **2004**, *3*, 301-317.
7. Robinson, J. A. *Chimia* **2007**, *61*, 84-92.
8. a) Brogden, K. A. *Nat. Rev. Microbiol.* **2005**, *3*, 238-250. b) Cole, A. M.; W. Wang, W.; Waring, A. J.; Lehrer. R. I. *Curr. Protein Pept. Sci.* **2004**, *5*, 373-381.
9. a) Nagarkar, R. P.; Hule, R. A.; Pochan, D. J.; Schneider, J. P. *J. Am. Chem. Soc.* **2008**, *130*, 4466-4474. b) Branco, M. C.; Pochan, D. J.; Wagner, N. J.; Schneider, J. P. *Biomaterials* **2009**, *30*, 1339-1347.
10. a) Miller, S. J. *Acc. Chem. Res.* **2004**, *37*, 601-610. b) Lewis, C. A.; Miller, S. J. *Angew. Chem., Int. Ed.* **2006**, *45*, 5616-5619. c) Blank T. J.; Miller, S. J. *Biopolymers* **2006**, *84*, 38-47.

11. a) Dalko, P. I.; Moisan, L. *Angew. Chem. Int., Ed.* **2004**, *43*, 5138–5175. b) Berkessel, A. *Curr. Opin. Chem. Biol.* **2003**, *7*, 409–419. c) Jarvo, E. R.; Miller, S. J. *Tetrahedron* **2002**, *58*, 2481–2495. d) List, B. *Tetrahedron* **2002**, *58*, 5573–5590.
12. a) Gellman, S. H. *Curr. Opin. Chem. Biol.* **1998**, *2*, 717-725. b) Venkatraman, J.; Shankaramma, S. C.; Balaram, P. *Chem. Rev.* **2001**, *101*, 3131-3152. c) Woll, M. G.; Lai, J. R.; Guzei, I. A.; Taylor, S. J. C.; Mark E. B. Smith, M. E. B.; Gellman, S. H. *J. Am. Chem. Soc.* **2001**, *123*, 11077-11078. d) Karle, I. L.; Gopi, H. N.; Balaram, P. *Proc. Natl. Acad. Sci. USA*. **2002**, *99*, 5160-5164. e) Roy, R. S.; Gopi, H. N.; Raghothama, S.; Karle, I. L.; Balaram, P. *Chem. Eur. J.* **2006**, *12*, 3295-3302. f) Lengyel, G. A.; Frank, R. C.; Horne W. S. *J. Am. Chem. Soc.* **2011**, *133*, 4246-4249.
13. a) Frackenpohl, J.; Arvidsson, P. I.; Schreiber, J. V., Seebach, D. *ChemBioChem* **2001**, *2*, 445-455. b) Wiegand, H.; Wirz, B.; Schweitzer, A.; Camenisch, G. P.; Perez, M. I. R.; Gross, G.; Woessner, R.; Voges, R.; Arvidsson, P. I.; Frackenpohl, J.; Seebach, D. *Biopharm. Drug Disp.* **2002**, *23*, 251-262. c) Potocky, T. B.; Menon, A. K.; Gellman, S. H. *J. Am. Chem. Soc.* **2005**, *127*, 3686-3692.
14. a) Haque, T. S.; Little, J. C.; Gellman, S. H. *J. Am. Chem. Soc.* **1994**, *116*, 4105-4106. b) Karle, I. L.; Awasthi, S. K.; Balaram, P. *Proc. Natl. Acad. Sci. U.S.A.* **1996***, 93***,** 8189-8193. c) Ramirez-Alvarado, M.; Blanco, F. J.; Serrano, L. *Nat. Struct. Biol.* **1996**, *3*, 604-612. d) Masterson, L. R.; Etienne, M. A.; Porcelli, F.; Barany, G.; Hammer, R. P.; Veglia, G. *Biopolymers* **2007**, *88*, 746-753. e) Aravinda, S.; Shamala, N.; Rajkishore, R.; Gopi, H. N.; Balaram, P. *Angew. Chem. Int. Ed. Engl*. **2002**, *41*, 3863-3865.
15. a) Karle, I. L.; Gopi, H. N.; Balaram, P. *Proc. Natl. Acad. Sci. U. S. A.* **2001**, *98*, 3716-3719. b) Gopi, H. N.; Roy, R. S.; Raghothama, S.; Karle, I. L.; Balaram, P. *Helv. Chim. Acta* **2002**, *85*, 3313-3330.
16. a) Chung, Y. J.; Huck, B., R.; Christianson, L. A.; Stranger, H. E.; Krauthauser, S.; Powell, D. R.; Gellman, S. H. *J. Am. Chem. Soc.* **2000**, *122*, 3995-4004. b) Woll, M. G.; Lai, J. R.; Guzei, I. A.; Taylor, S. J. C.; Smith, M. E. B.; Gellman, S. H. *J. Am. Chem. Soc.* **2001**, *123*, 11077-11078.
17. a) Das, C.; Raghothama, S.; Balaram, P. *J. Am. Chem. Soc.* **1998**, *120*, 5812-5813; b) Das, C.; Raghothama, S.; Balaram, P. *Chem. Commun*. **1999**, 967–968; c) Venkatraman, J.; Naganagowda, G. A.; Sudha, R.; P. Balaram, *Chem. Commun.* **2001**, 2660-2661. d) Venkatraman, J.; Naganagowda, G. A.; Sudha, R.; Balaram, P. *J. Am, Chem. Soc.* **2002**, *124*, 4987-4994.

18. Schenck, H. L.; Gellman, S. H. *J. Am. Chem. Soc.* **1998**, *120*, 4869-4870.
19. Kortemme, T.; Ramirej-Alvarado, M.; Serrano, L. *Science* **1998**, *281*, 253–256.
20. Deechongkit, S.; Dawson, P. E.; Jeffery, K. W. *J. Am. Chem. Soc.* **2004**, *126*, 16762-16771.
21. Rughani, R. V.; Salick, D. A.; Lamm, M. S.; Yucel, T.; Pochan, D. J.; Schneider, J. P. *Biomacromolecules* **2009**, *10*, 1295-1304.
22. a) Berchtold, N. C.; Cotman, C. W. *Neurobiol. Aging*. **1998**, *19*, 173-189. b) Chiang, P. K.; Lam, M. A.; Luo, Y. *Curr. Mol. Med.* **2008**, *8*, 580-584.
23. Irvine, G. B.; El-Agnaf, O. M.; Shankar, G. M.; Walsh, D. M. *Mol. Med.* (*Cambridge, Mass.*) **2008**, *14,* 451-464.
24. Truant, R.; Atwal, R. S.; Desmond, C.; Munsie, L.; Tran, T. *FEBS jour.* **2008**, *275,* 4252-4262.
25. Mali, S. M.; Bandyopadhyay, A.; Jadhav, S. V.; Ganesh Kumar, M.; Gopi, H. N. *Org. Biomol. Chem.* **2011**, *9*, 6566-6574.
26. Shankaramma, S. C.; Kumar Singh, S.; Sathyamurthy, A.; Balaram, P, *J. Am. Chem. Soc.* **1999**, *121*, 5360-5363.
27. Desiraju, G. R.; Steiner, T. The "*Weak Hydrogen Bond in Structural Chemistry and Biology*" Oxford Science Publication: Oxford, 1999.
28. Betzel, C.; Lange, G.; Pal, G.P.; Wilson, K.S.; Maelicke, A.; Saenger, W. *J. Biol. Chem.* **1991**, *266*, 21530-21536.
29. *SAINT Plus*, (Version 7.03); Bruker AXS Inc.: Madison, WI, 2004.
30. a) SHELXS-97: G. M. Sheldrick, *Acta Crystallogr. Sect A* **1990**, *46*, 467-473, b) G. M. Sheldrick, SHELXL-97, Universität Göttingen (Germany) 1997.

2.7 Appendix I: Characterization Data of Synthesized Compounds

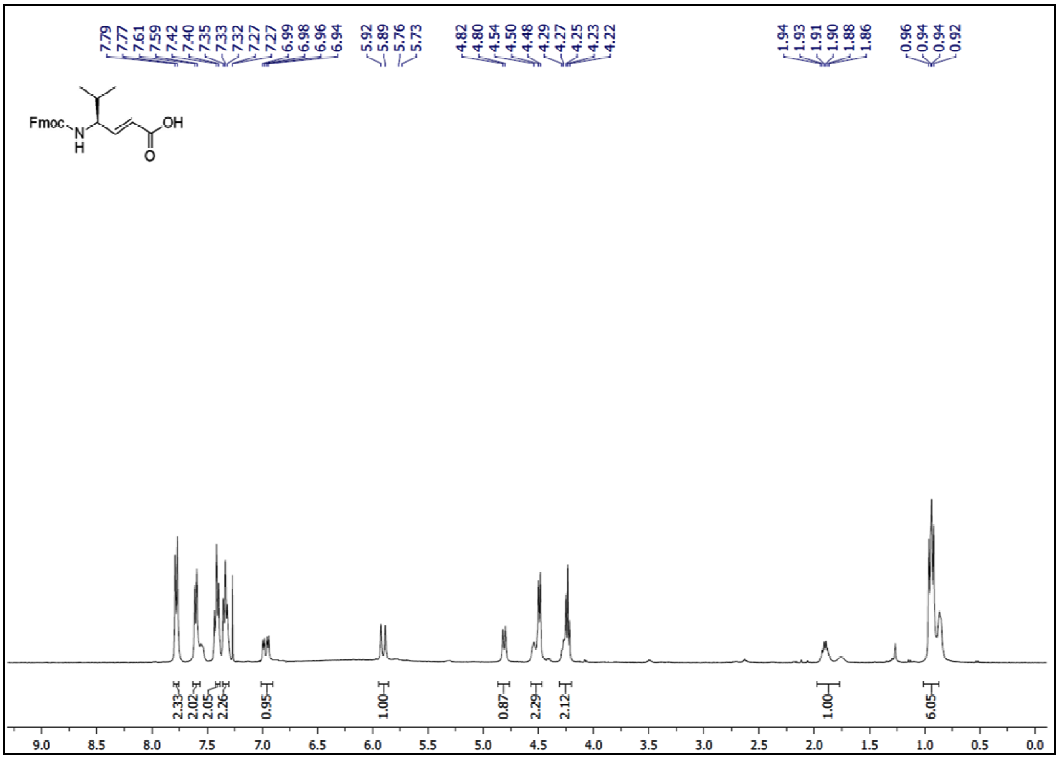
7.79
7.77
7.61
7.59
7.42
7.40
7.35
7.33
7.32
7.27
7.27
6.99
6.98
6.96
6.94
5.92
5.89
5.76
5.73
4.82
4.80
4.54
4.50
4.48
4.29
4.27
4.25
4.23
4.22
1.94
1.93
1.91
1.90
1.88
1.86
0.96
0.94
0.94
0.92
Fmoc
N
H
OH
O
2.33
2.02
2.05
2.26
0.95
1.00
0.87
2.29
2.12
1.00
6.05
9.0
8.5
8.0
7.5
7.0
6.5
6.0
5.5
5.0
4.5
4.0
3.5
3.0
2.5
2.0
1.5
1.0
0.5
0.0

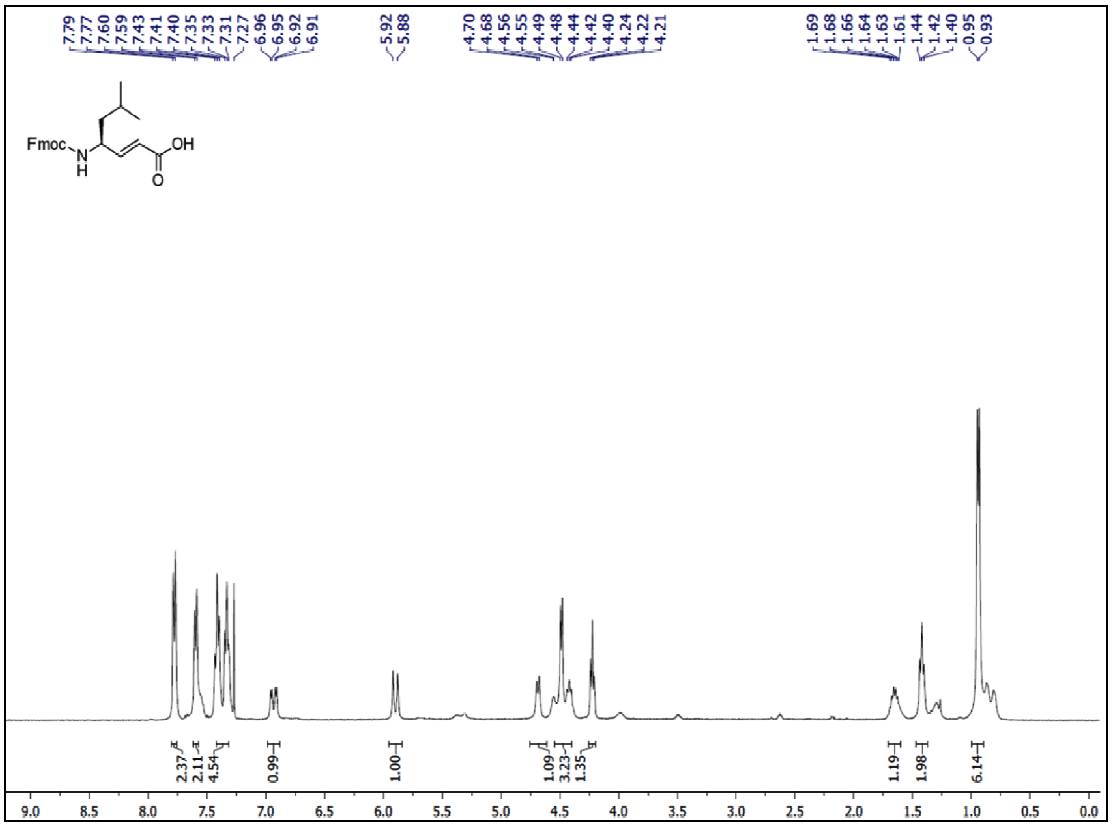
7.79
7.77
7.60
7.59
7.43
7.41
7.40
7.35
7.33
7.31
7.27
6.96
6.95
6.92
6.91
5.92
5.88
4.70
4.68
4.56
4.55
4.49
4.48
4.44
4.42
4.40
4.24
4.22
4.21
1.69
1.68
1.66
1.64
1.63
1.61
1.44
1.42
1.40
0.95
0.93
Fmoc
N
H
OH
O
2.37
2.11
4.54
0.99
1.00
1.09
3.23
1.35
1.19
1.98
6.14
9.0
8.5
8.0
7.5
7.0
6.5
6.0
5.5
5.0
4.5
4.0
3.5
3.0
2.5
2.0
1.5
1.0
0.5
0.0

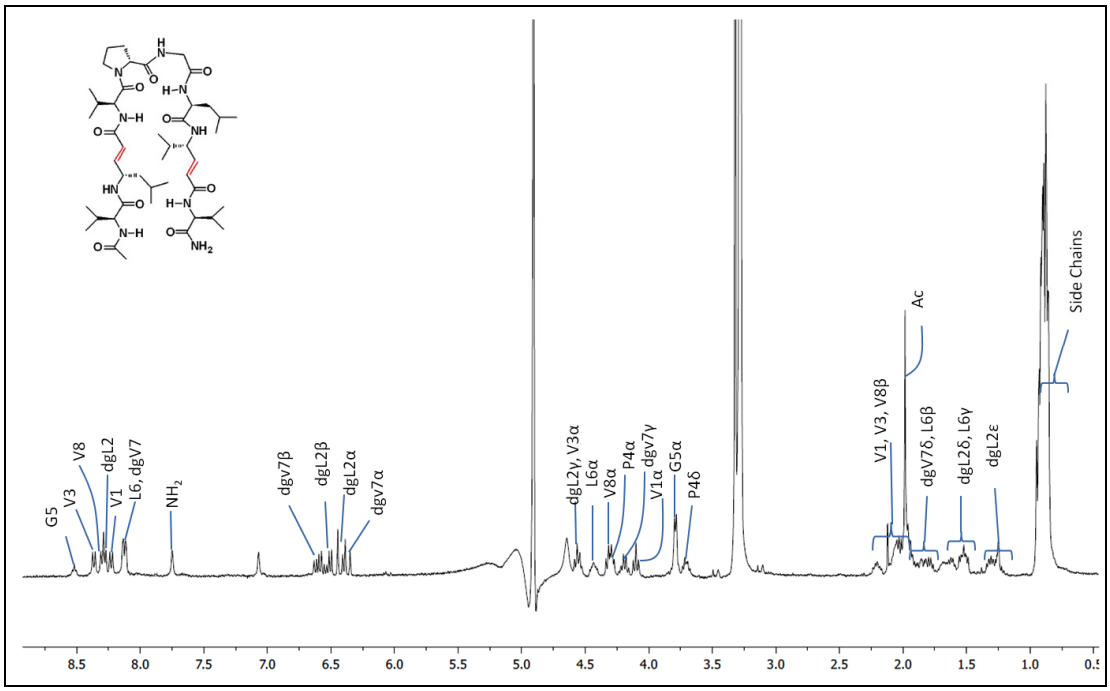
G5
V3
V8
dgL2
V1
Lδ, dgV7
NH2
dgv7β
dgL2β
dgL2α
dgv7α
dgL2γ, V3α
L6α
V8α
P4α
dgv7γ
V1α
G5α
P4δ
V1, V3, V8β
Ac
dgV7δ, L6β
dgL2δ, L6γ
dgL2ε
Side Chains
8.5
8.0
7.5
7.0
6.5
6.0
5.5
5.0
4.5
4.0
3.5
3.0
2.5
2.0
1.5
1.0
0.5

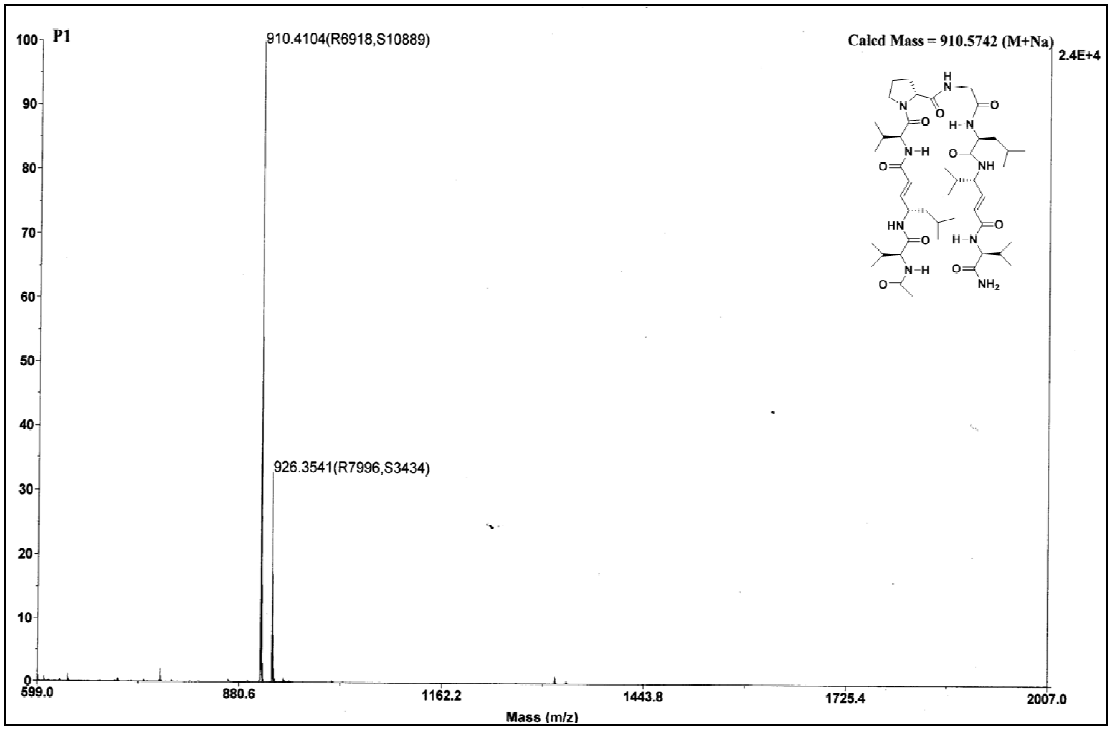
P1
910.4104(R6918,S10889)
Calcd Mass = 910.5742 (M+Na)
2.4E+4
926.3541(R7996,S3434)
100
90
80
70
60
50
40
30
20
10
0
599.0
880.6
1162.2
1443.8
1725.4
2007.0
Mass (m/z)

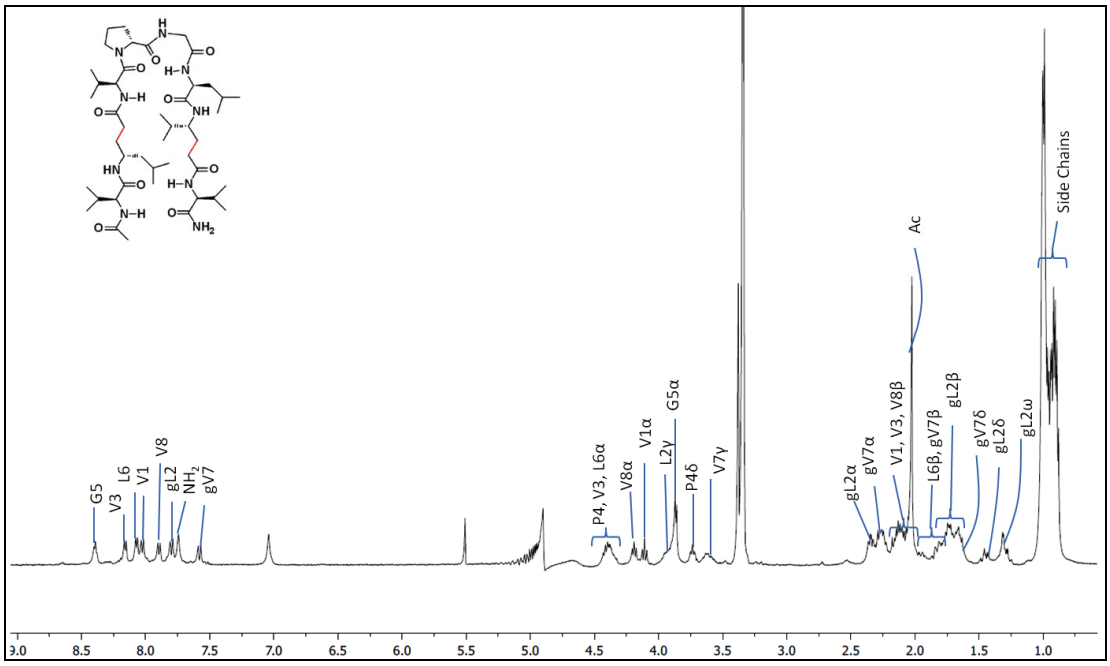
G5
V3
L6
V1
V8
gL2
NH2
gV7
P4, V3, L6α
V8α
V1α
L2γ
G5α
P4δ
V7γ
gL2α
gV7α
V1, V3, V8β
Ac
L6β, gV7β
gL2β
gV7δ
gL2δ
gL2ω
Side Chains
9.0
8.5
8.0
7.5
7.0
6.5
6.0
5.5
5.0
4.5
4.0
3.5
3.0
2.5
2.0
1.5
1.0

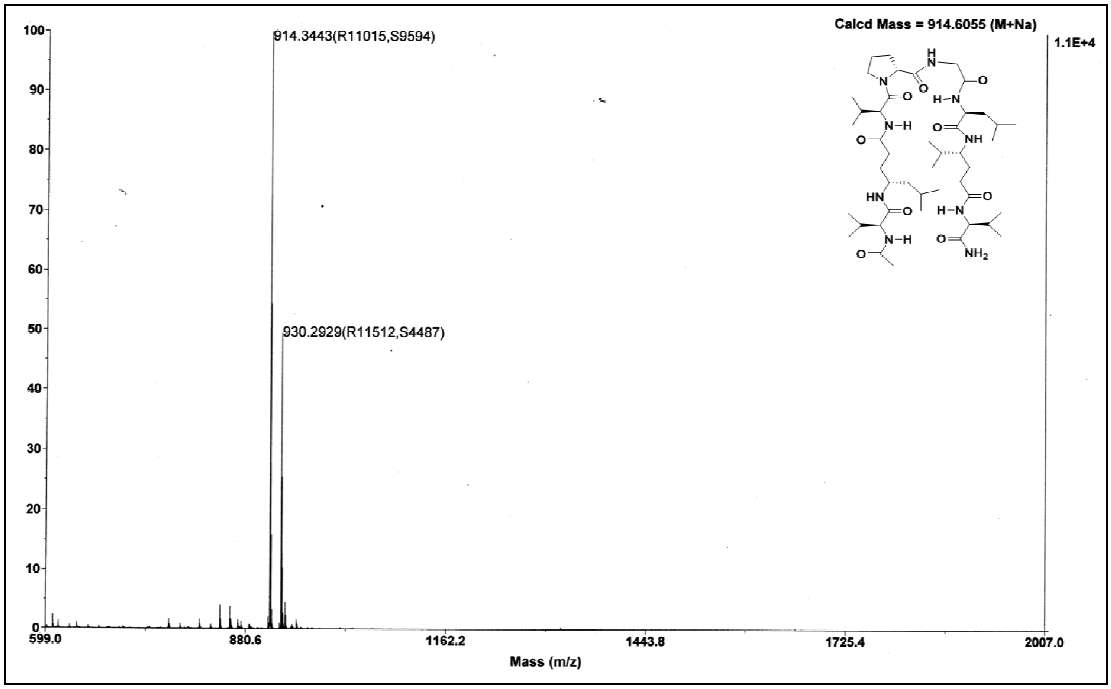
914.3443(R11015,S9594)
930.2929(R11512,S4487)
Calcd Mass = 914.6055 (M+Na)
1.1E+4
100
90
80
70
60
50
40
30
20
10
0
599.0
880.6
1162.2
1443.8
1725.4
2007.0
Mass (m/z)

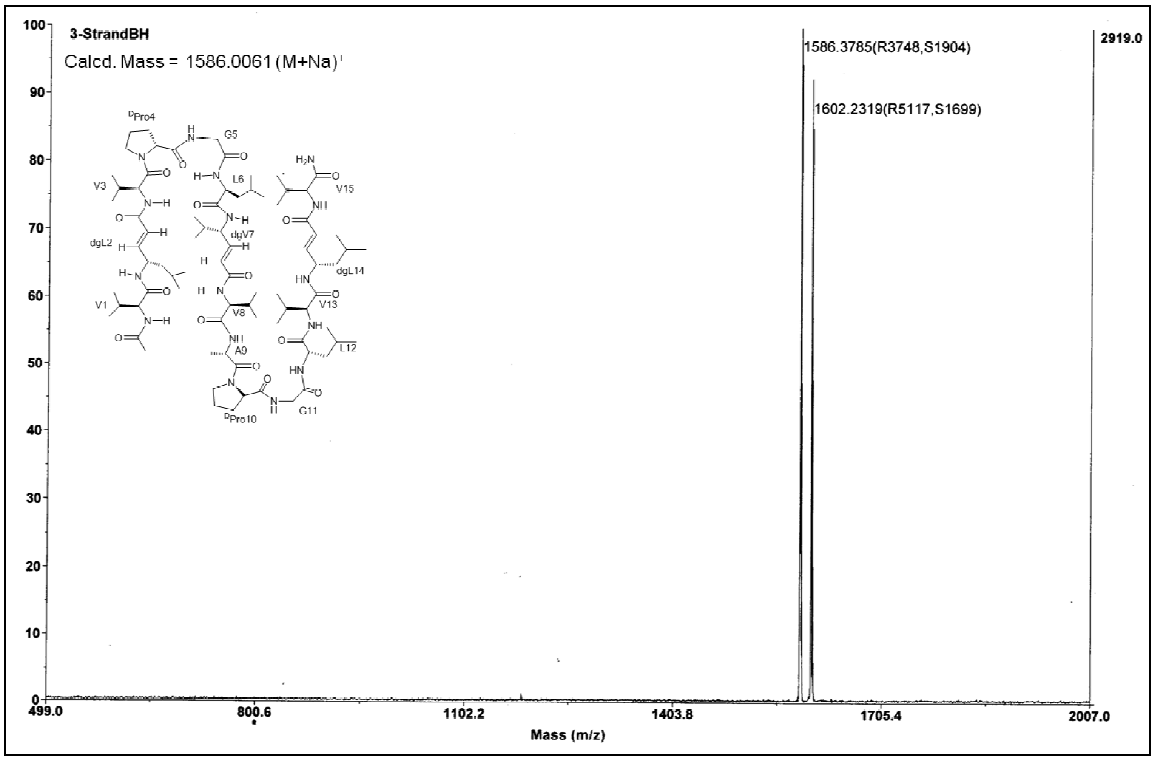
3-StrandBH
Calcd. Mass = 1586.0061 (M+Na)+
1586.3785(R3748,S1904)
1602.2319(R5117,S1699)
2919.0
100
90
80
70
60
50
40
30
20
10
0
499.0
800.6
1102.2
1403.8
1705.4
2007.0
Mass (m/z)

Chapter 3

α/γ^4-hybrid peptide helices: Direct transformation of α/α, β-unsaturated γ-hybrid peptides to α/γ^4-hybrid peptide 12-helices and analogy with α-helix

3.1 Introduction

The deconstruction of a protein leads to a limited number of secondary structural elements, such as β-strands, helices, and turns. Among these secondary structures, the helix is most prevalent. The helical secondary structures of α-peptides can be recognized as C_{13}-helix (or α- helix) and C_{10}-helix (3_{10}-helix) by the nature of the internal hydrogen bonding pattern.[1,2] In both the cases, the directionality of the hydrogen bond with respect to the chain direction (C←N) is the same. The α-helix plays fundamental roles in various biological and physiological processes.[4] α-Helix in natural peptides and proteins is induced by consecutive intramolecular hydrogen bonds between the carbonyl group of amino acid residue *i* and the amide proton in the residue *i* + 4 (Figure 1a) with 3.6 residues per turn. There are 13 atoms involved to form intramolecular hydrogen bond through the backbone. The backbone conformation of α-helix can be described by the three torsion angles ϕ, ψ and ω (Figure 1b) and α-helix possesses average torsional values $\phi = -57^{o}$ and $\psi = -47^{o}$.

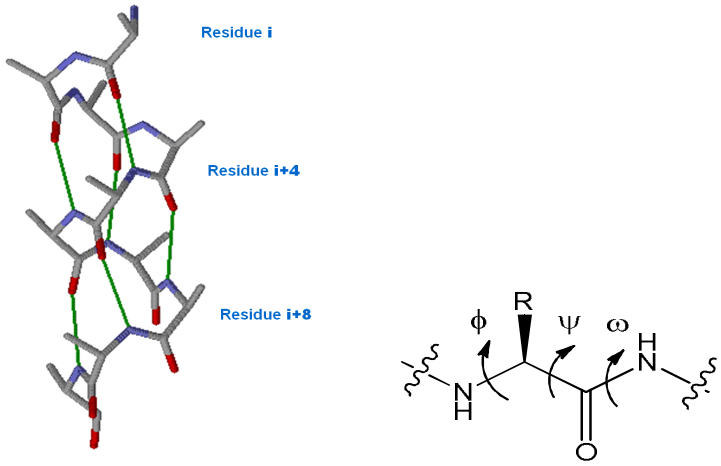

a) **b)**

Figure 1: a) Molecular model for right-handed α-helix. Intramolecular hydrogen bonds are shown with green wireframes, b) Three torsion angles to describe the backbone conformation of α-helix.

α-Helix is a basic building block for many protein structures such as the helix bundles[5] and coiled coils.[6] It has been hypothesized that in the process of protein folding, α-helix forms at the early stage and subsequently induces other processes.[7,8] α-Helix also acts as the basic receptor-binding element in many peptide hormones, including neuropeptide Y[9], calcitonin,[10]

and often serves as the recognition site in the DNA-protein interactions[11] and other protein-protein interactions, such as p53/HDM2[12] and Bak/Bcl-xL.[13] As helical secondary structures have been involved in various biomolecular protein-protein interactions, enormous efforts have been made to design the α-helical structures outside the protein context. In the past two decades, foldamer chemistry has attracted chemists and biologists to design the α-helical mimetics.[14] In this regard a good deal of success has been achieved using non-natural amino acid or higher homologous of α-amino acids such as β-amino acids and γ-amino acids.

3.2 Helical structure mimicry using higher homologous of α-amino acids

3.2.1 Homooligomers of β- and γ-amino acids

It has been shown that in contrast to α-peptides, β-peptides and higher homologue oligomers have proved the proteolytic and metabolic stability in the prospect of intracellular delivery.[15] These properties make β-peptides and higher homologue oligomers very attractive from a biomedical perspective. The design of helical peptides containing non-natural amino acids has been achieved by several research groups. The major achievements in designing of several types of helical conformations using β-amino acids and γ-amino acids homooligomers has been documented by Seebach et al.,[14a] Gellman's group[16] and Balaram et al.[14b] Seebach and colleagues utilized the homologated α-amino acids in their study, while Gellman et al. utilized the cyclic β- and γ-amino acids. In addition, Sharma et al. demonstrated the helical folding patterns from carbohydrate modified β- γ-and δ-amino acids.[17] The oligomers of homologated β^3- and β^2-amino acids have been shown to adopt left handed 14-helical (the helix is made up of a 14-membered H-bridged ring; three amino acid units make a turn) conformation. Interestingly, helicity and the macrodipole of β^3-peptide helix are opposite to that of α-helix. The schematic representation of 14-helix adopted by (H-βhVal-βhAla-βhLeu-βhVal-βhAla-βhLeu-OH) is shown in Figure 2a. Further Seebach et al. have investigated and shown that (*S*)-β^2-oligomers also adopt left handed 14-helical structure. In contrast, peptides containing alternatively β^3- and β^2-residues were found to form a right-handed 12/10-helix consisting of alternating 12- and 10-membered hydrogen-bonded rings (Figure 2b).

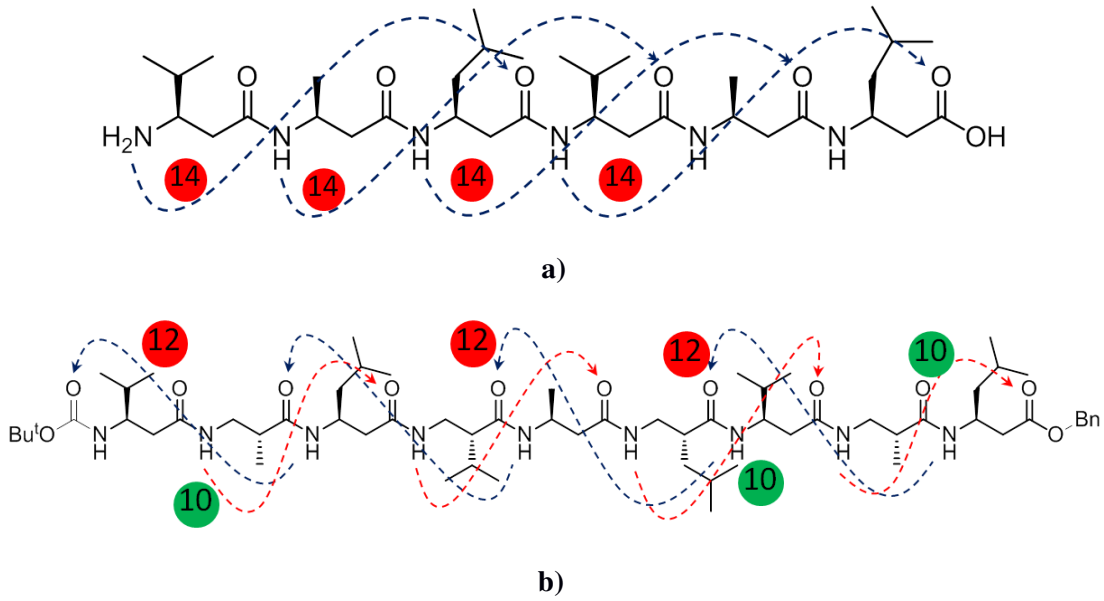

Figure 2: a) The 3_{14}-helix of the β^3-hexapeptide TFA H-(β^3hVal-β^3hAla-β^3hLeu)$_2$-OH in MeOH, b) the 12/10-helix of β^3/β^2-mixed peptide Boc-β^3hVal-β^2hAla-β^3hLeu-β^2hVal-β^3hAla-β^2hLeu-β^3hVal-β^2hAla-β^3hLeu-OBn and schematic presentation of the 12- (blue) and 10- (red) membered hydrogen-bonded rings.

The first crystallographic characterization of novel helices in oligopeptides was demonstrated by Gellman and colleagues using cyclic β-amino acids *trans*-2-aminocyclopentanecarboxylicacid (ACPC) and *trans*-2-aminocyclohexanecarboxylic acid (ACHC).[16] The oligomers of *trans*-ACHC adopted the right handed stable 14-helical conformation where the hydrogen bond direction is N←C (Figure 3a), whereas the oligomers of *trans*-ACPC adopted a stable right handed 12-helical structure (Figure 3b). According to crystal structure of oligomers of *trans*-ACPC the hydrogen bond direction and the associated macrodipole are analogous to that of α-helix. The interesting observation in this is that the backbone dihedral angle θ is close to the gauche form, which induces the helical folding. However, Fulop et al. reported $C_{10/12}$ helix from the oligomers of *cis*-2-Aminocyclohex-3-ene carboxylic acid (*cis*-ACHEC) residues with alternating backbone configuration (figure 3c).[18] In 2010 Aitken and colleague studied the 12-helical conformations in cyclobutane β-amino acid[19] oligomers in both solution and solid state (figure 3d).

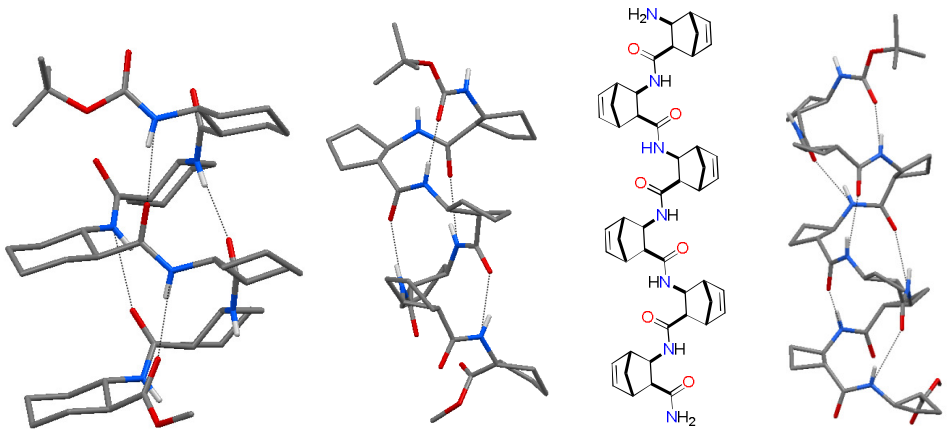

Figure 3: Crystal structure of a) *trans*-ACHA oligomer, b) *trans*-ACPC oligomer, c) schematic representation of *cis*-ACHEC oligomer, d) crystal structure of cyclobutane β-amino acid oligomers.

The lessons that have been learnt, thus far, from the growing body of work on β-peptide helices is the helices with novel H-bonding patterns can be generated along with reversal of directionality of donors and acceptors, and reversal of the sense of helix twist.

In comparison with β-peptides and β-amino acids, the folding patterns of oligomers of γ-amino acids are less explored probably due to the difficulty of obtaining stereochemically pure γ^4-amino acids. Nevertheless, Seebach and colleagues[20] and Hanessain et al.[21] in their pioneering work recognized the formation of 14-helical conformations of the oligomers of the γ^4-amino acids. The schematic representation of H-γ^4Val-γ^4Ala-γ^4Leu-γ^4Val-γ^4Ala-γ^4Leu-OH with 14-membered H-bonding is shown in Figure 4. In contrast to the β-peptide 14-helix generated from the β-amino acids, the directionality of H-bonding and associated macrodipole of the γ-peptide helix is analogous to that of α-helix. Sharma et al. have shown

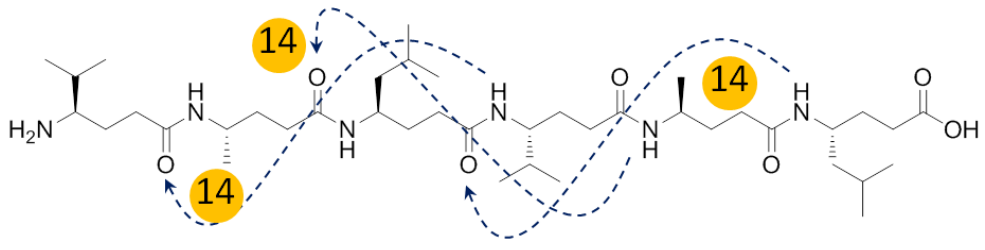

Figure 4: The C_{14}-helix of the γ^4-hexapeptide H-γ^4Val-γ^4Ala-γ^4Leu-γ^4Val-γ^4Ala-γ^4Leu-OH

left handed C_9-helix in gamma peptides using dipeptide repeats of carbo-γ^4 amino acid and γ-amio butyric acid.[17b] In their investigation, Balaram et al. demonstrated the formation of novel C_9-helix in a short tetrapeptide[22] containing β,β′-disubstituted γ-amino acid residue,1-(aminomethyl) cyclohexaneacetic acid, gabapentin (Figure 5a and 5b). It has been argued that the presence of geminal substituents at the C_β carbon restricts the torsion angles θ_1 and θ_2 primarily to gauche conformations. In addition, recently Gellman et al.,[23] have demonstrated the right handed 14-helical conformation (Figure 5d) adopted by the homooligomers of cyclic γ-amino acids.

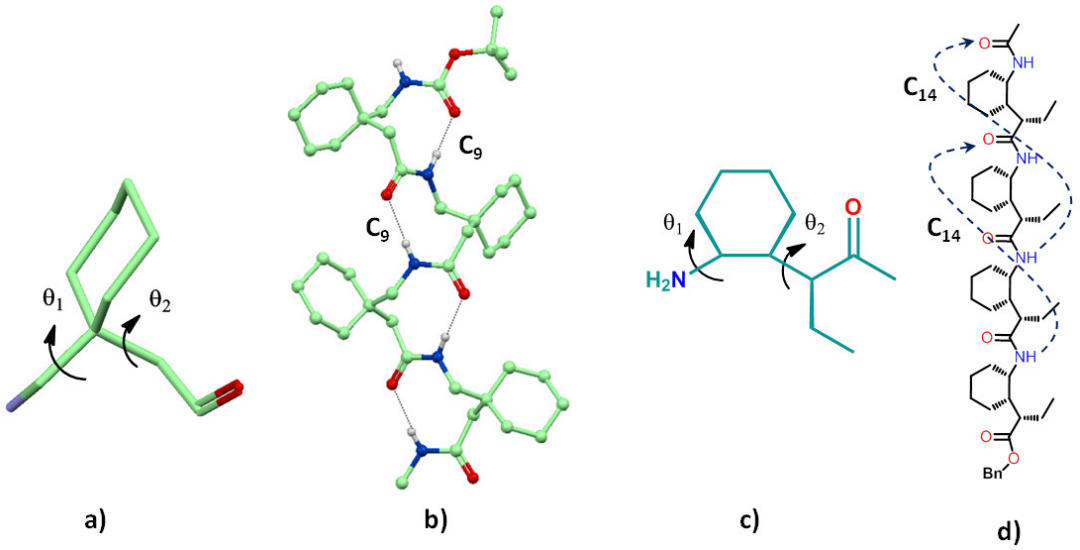

Figure 5: a) Gabapentin residue, b) Gabapentin oligomer C_9-helix, c) $\gamma^{2,3,4}$-trisubstituted amino acid residue, d) $\gamma^{2,3,4}$-trisubstituted oligomer 14-helix.

3.2.2 Hybrid peptide helices and their biological applications

In addition to the β-and γ-peptide homooligomers, another very attractive area of research in the foldamers is the hybrid peptides. Hybrid peptides are heterooligomers composed of different combination of α/β, β/γ and α/γ amino acids. By varying the sequence combinations and the composition various ordered helical patterns can be generated with different H-bonding pseudocycles.[24] This aspect of heterooligomers have several advantages over that of their homooligomers counterparts, including access to many new conformational diversity based on the variation in the stoichiometries and patterns of the residues

combination. Further, heterooligmers have been shown to be more effective than homo-oligomers in the context of inhibitions of protein-protein interactions.[24]

Based on the 4→1 and 5→1 hydrogen bonding patterns, the 1:1 alternating hetero amino acid sequences in the hybrid peptides different types of hybrid helices can be derived. The different types of helices formed in the heterooligomeric peptides are tabulated in the Tables 1a, and 1b based on 4→1 and 5→1hydrogen bonding patterns, respectively.

Table 1: Schematic diagram showing the number of atoms involved in the a) two-residue hydrogen bonded turns (4→1) and b) three residue hydrogen bonded turns (5→1) for α, β, γ and their hybrid peptides.

a) $4\rightarrow1(CO_i\cdots HN_{i+3})$

	α	β	γ	δ
α	10	11	12	13
β	11	12	13	14
γ	12	13	14	15
δ	13	14	15	16

b) $5\rightarrow1(CO_i\cdots HN_{i+4})$

	αα	αβ/βα	αγ/γα	ββ	βγ/ γβ	γγ
α	13	14	15	15	16	17
β	14	15	16	16	17	18
γ	15	16	17	17	18	19

The hypothesis of the hybrid peptide concept was demonstrated by Balaram and colleagues in the crystal structure of hybrid peptide containing unsubtituted β-and γ-amino acids.[25] Subsequently, Reiser and co-workers,[26] and Gellman et al.[27] conducted the structural studies of hybrid α/β peptides. Further, Sharma and co-workers provided the evidences of variety of 'mixed' H-bonding pattern in α/β hybrid peptides such as $C_{9/11}$[17a] and $C_{14/15}$[17e] helices. Seebach et al. concluded the α/β hybrid peptides containing Aib and β^3-residue can adopt 14/15-helix-like conformation in solution,[28] however, recently Balaram and colleagues provided the crystallographic evidence for the formation of 14/15-helical conformation.[29] Some of the examples of hybrid peptide helices are shown in Figure 6.

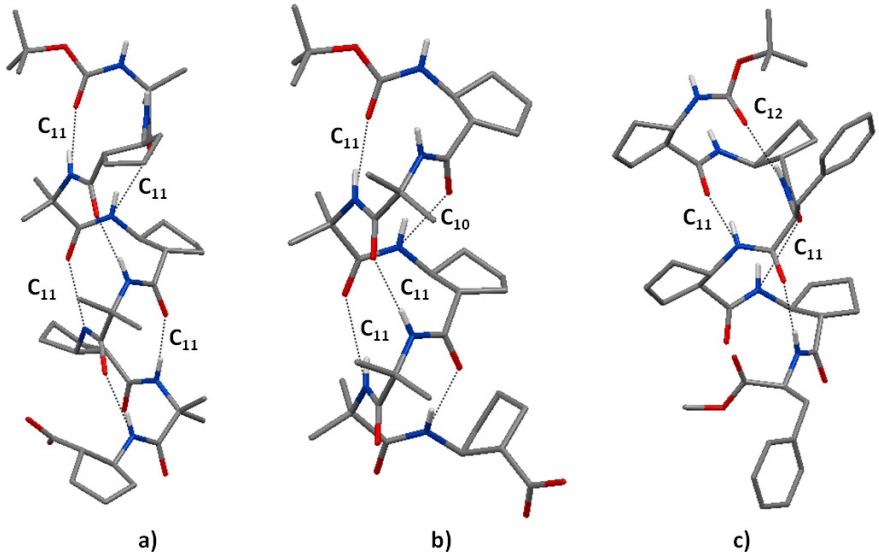

Figure 6: Examples of experimentally characterized hybrid peptides a) αβ Boc-Aib-ACPC-Aib-ACPC-Aib-ACPC-Aib-ACPC-OBn, b) ααβ with 10/11/11 helix, Boc-ACPC-Aib-Aib-ACPC-Aib-Aib-ACPC-OBn, c) ββα 12/11/11 helix, Boc-ACPC-ACPC-Phe-ACPC-ACPC-Phe-OBn,

Creating foldamers which can adopt distinct tertiary structure is also a challenging job to develop potential inhibitor for protein-protein interactions. Gellman's group has shown the formation of three and four helix bundle by systematic α→ β^3 substitution at selected positions in the peptides from yeast protein GCN4-p1(33-residue α-peptide) and GCN4-pLI (Figure 7).[30] Each β^3-residue bears the side chain of the α-residue. The crystallographic data of these two peptides provided first high-resolution insight for heterogeneous backbone that can adopt helix bundle structure. Further, the same group has demonstrated the formation of heterohelix quaternary bundle.[31]

a) Ac-RMKQLEDKVEELLSKNYHLENEVARLKKLVGER-OH

b) Ac-RMKQI EDKLEE I LSKLYH IENELARI KKLLGER-OH

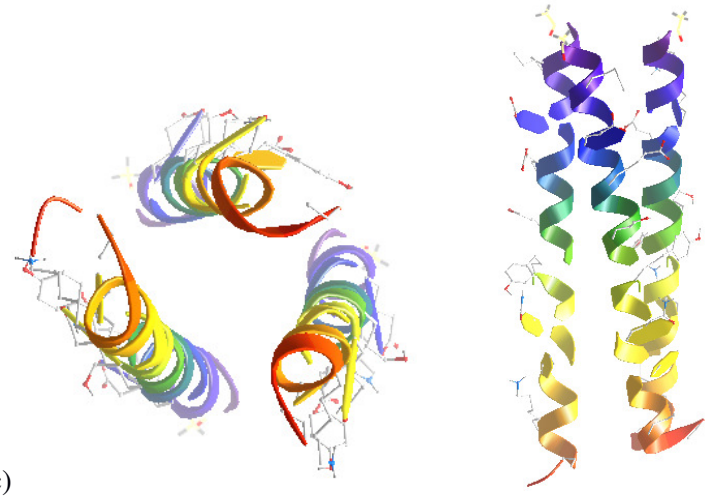

c)

Figure 7: Primary sequence of a) GCN4-p1and b) GCN4pLI. Blue colour residue indicates substitution α-amino acid with the corresponding β^3-amino acid. c) Three helix bundle from the crystal structure of α/β-hybrid peptide (PDB-2OXJ).

In contrast to the α/β-hybrid peptides, α/γ hybrid have received little attention. However, Hoffmann and colleagues provided the overview of the formation of various ordered helical conformations in 1:1 alternating α- and γ- acids using ab initio calculations.[32] Nevertheless, Balaram and colleagues[33] and Gellman et al.[34] have demonstrated the formation of stable

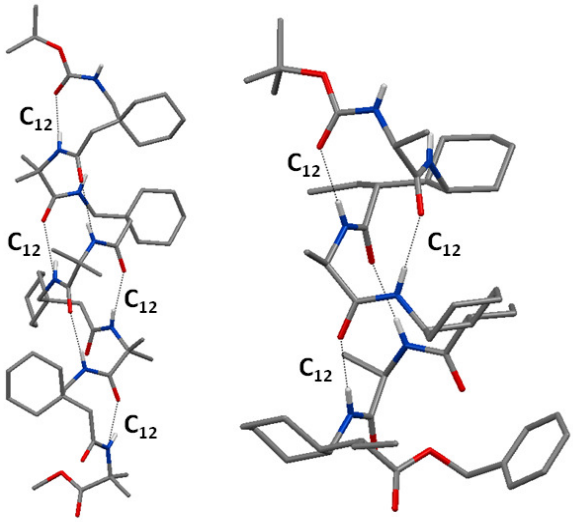

a) **b)**

Figure 8: Crystal structure of 12 helical α/γ-hybrid peptides a) Boc-(Gpn-Aib)$_4$-OMe and b) Boc-(Ala-$\gamma^{2,3,4}$ AA)$_3$-OBn

right handed 12-helical conformations using 3, 3-dialkyl γ-amino acids (Figure 8a) and cyclic γ-amino acids (Figure 8b), respectively. In addition, Sharma et al. reported the 10/12 mixed helix formation using C-linked carbo γ-amino acids in α/γ-mixed hybrid peptides.[35] However, helical conformations of α/γ-hybrid peptides containing γ^4-amino acid having proteinogenic side chains has not been much explored.

3.3 Aim and rationale of the present work

In continuation of our studies in the design of hybrid peptides containing *E*-vinylogous amino acids, we sought to understand the conformational behavior of vinylogous amino acids in the presence of conformationally constrained, helix favoring Aib residues. In addition, as the vinylogous amino acids containing the functionalizable double bonds we sought to investigate whether or not these hybrid peptides can be transformed into their saturated γ-peptide analogues. We anticipate that this approach provides an unprecedented opportunity to analyze and understand the conformational preferences of both α, β-unsaturated and saturated γ^4-amino acids in hybrid oligopeptides. To understand the conformational behaviour of α, β-unsaturated γ-amino acids as well as γ-amino acids in hybrid peptides, various 1:1 alternating α- and α, β-unsaturated γ-amino acids were synthesized and subjected for the analysis.

3.4 Results and Discussion

3.4.1 Synthesis of α/α, β-unsaturated γ-amino acids (vinylogous amino acids) hybrid tetrapeptides

In order to test our hypothesis, three tetrapeptides (Boc-Aib-dgF-Aib-dgF-OEt) **D1**, (Boc-Ala-dgF-Aib-dgF-OEt) **D2** and (Boc-Aib-dgF-Leu-dgF-OEt) **D3** (Scheme 1) containing alternative α and vinylogous amino acids were synthesized in solution phase. The *N*-terminal was protected with the Boc- group, while the C-terminal was protected with ethyl ester. The two Aib residues of **D1** were alternatively replaced with Ala and Leu in **D2** and **D3**,

respectively. The *E*-vinylogous amino acid dgF [dgF = α, β-dehydro γ-phenylalanine] was synthesized using Wittig reaction.[36] First the dipeptide Boc-Aib-dgF-OEt (**A1**) was synthesized by coupling of Boc-Aib-OH and the free amine of Boc-dgF-OEt obtained after the Boc-deprotection. The coupling reaction was mediated by HBTU (Scheme 1a). Further Boc-Aib-dgF-OEt was purified using silica gel column chromatography. Similarly, other two dipeptides Boc-Ala-dgF-OEt (**A2**) and Boc-Leu-dgF-OEt (**A3**) were synthesized using the same protocol. The tetrapeptides were synthesized using through [2+2] convergent strategy (Scheme 1b).

a)

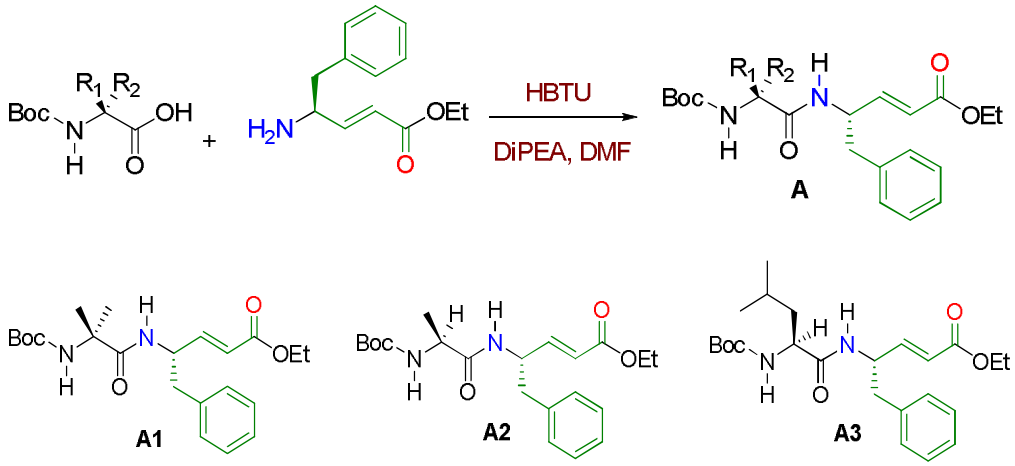

b)

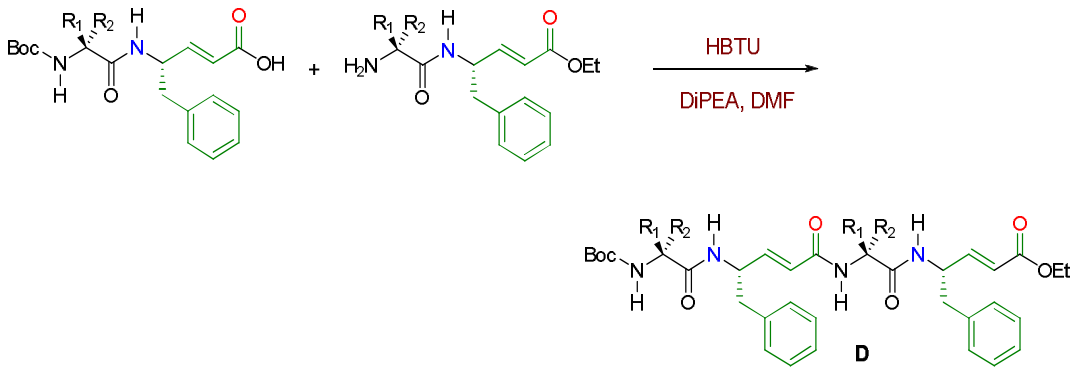

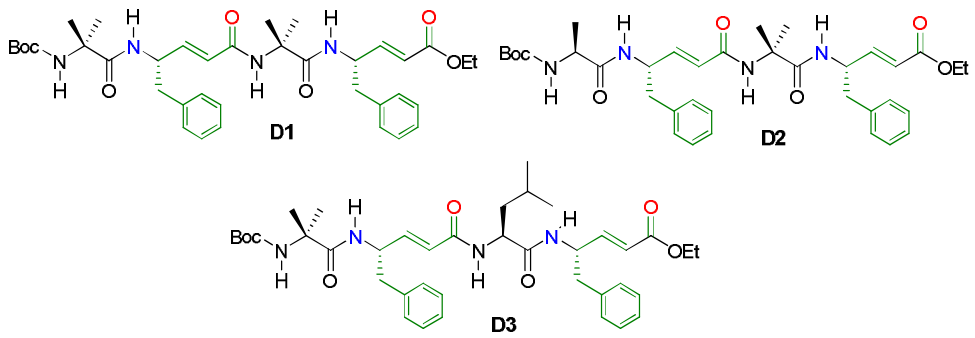

Scheme 1: Schematic representation of a) synthesis of **A1, A2** and **A3** dipeptide, b) synthesis of **D1**, **D2** and **D3**.

3.4.2 Crystal structure analysis of D1

In order to understand the conformations of these hybrid peptides in single crystals, we tried to crystallize all α/vinylogous hybrid peptides in the various combinations of solvents. Out of all the peptides we were able to get the single crystals of **D1** from the slow evaporation of methanol/toluene solution. X-ray structure of **D1** shown in Figure 9a. Interestingly, the **D1** adopted an unusual planar structure in crystalline state and as anticipated did not show any protein secondary structural properties. No intramolecular H-bonding is observed in the crystal structure. Examination of the torsional angles of α-residues reveals that both residues adopted opposite right and left handed helical conformations with the ϕ and ψ values -51^{o}, -48^{o}, and 64^{o} and 52^{o} respectively. The local conformations of the vinylogous residues were determined by introducing additional torsional variables θ_1 (N–C_γ–C_β=C_α) and θ_2 (C_γ–C_β=C_α–C) as shown in Figure 9c. The vinylogous residue dgF2 adopted a fully extended conformation by having the torsional angles $\phi = -139^{o}$, $\theta_1 = 121^{o}$, $\theta_2 = 178^{o}$ and $\psi = -161^{\circ}$. Interestingly, another vinylogous residue, dgF4 adopted N–C_γ–C_β=C_α eclipsed conformation by having θ_1 close to 0°. Further, the torsional angle ϕ adapted a semi-extended conformation with the value – 81° and the other torsional variables θ_2 and ψ of dgF4 showed the extended conformations by having the values 180^{o} and –168°, respectively. In addition, the local *s-cis* conformations (ψ = ~180°) of conjugated ester (dgF4) and the amide (dgF2), favouring the extended planar structures. The torsional variables are tabulated in Table 2.

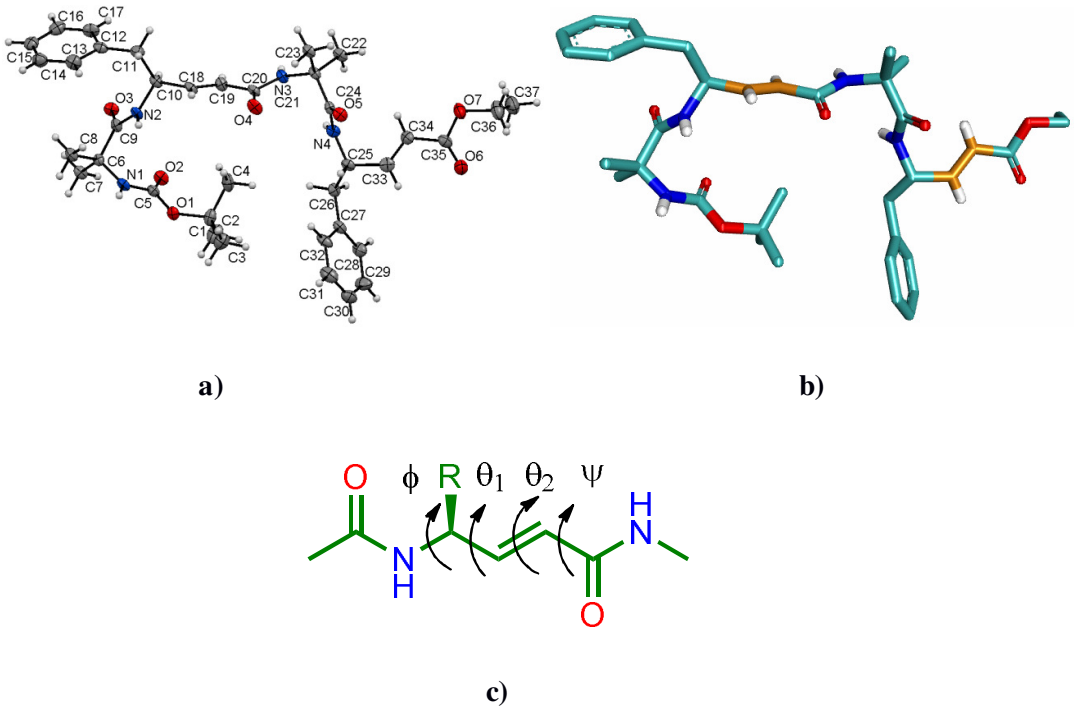

Figure 9: The crystal structure of Boc-Aib-dgF-Aib-dgF-OEt (**D1**) a) ORTEP diagram, H-atoms are not labelled for clarity, b) capped stick model, c) Torsional variables of vinylogous amino acids.

Table 2. Torsion angle variables (in deg) of Boc-Aib-dgF-Aib-dgF-OEt (**D1**)

Resd.	φ	θ_1	θ_2	ψ	ω
Aib	-51	-	-	-48	179
dgPhe	-139	121	178	-161	165
Aib	64	-	-	52	178
dgPhe	-81	12	180	-168	-

3.4.3 Structural analysis using 2D-NMR spectra

Further, we investigated whether peptide **D1** adopted the similar conformation in solution or not. We recorded 2D NMR (TOCSY, ROESY) of **D1** in $CDCl_3$ at 300K. The ^1H NMR shows the wide dispersion of NH and vinylic protons. Using the TOCSY, the amino acid residues were indentified in the sequence. Partial TOCSY spectrum is shown in Figure 10A. Subsequently, the order of the amino acids in the peptide sequence is determined using ROESY. Fully assigned ROESY spectrum is shown in the Figures 10B and 10C.

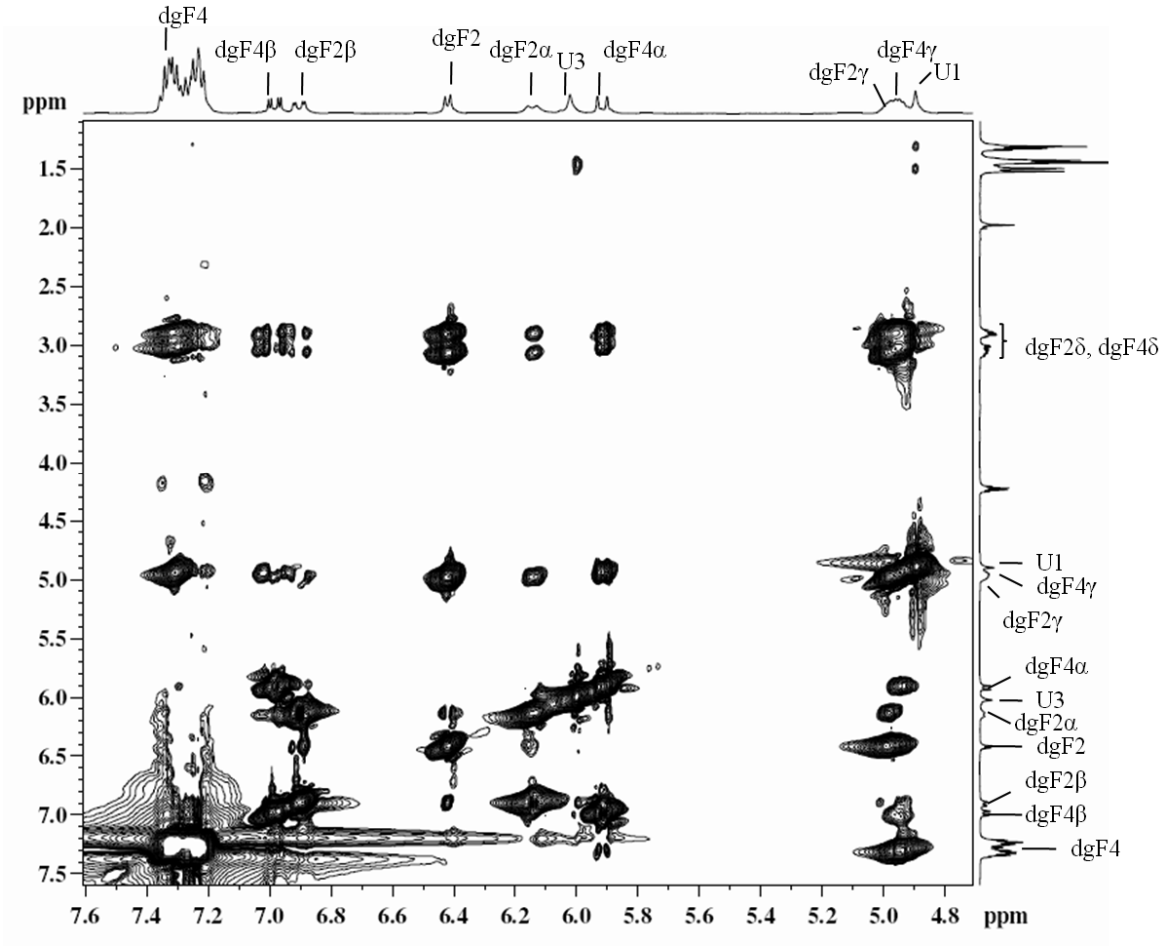

A

Surprisingly, ROESY analysis reveals that no characteristic intramolecular NOEs corresponding to either the helix, sheet or reverse turn conformations, indicating that no secondary structure in the hybrid peptide. The observed NOEs in the ROESY spectrum are shown in the crystal structure of **D1** and the NOEs match satisfactorily in the observed conformation of **D1** crystal structure (Figure 11). Similarly, 2D NMR analysis of **D2** and **D3** suggests no secondary structure present in the hybrid peptide containing 1:1 alternating α and *E*-vinylogous amino acids.

Full ROESY Spectrum

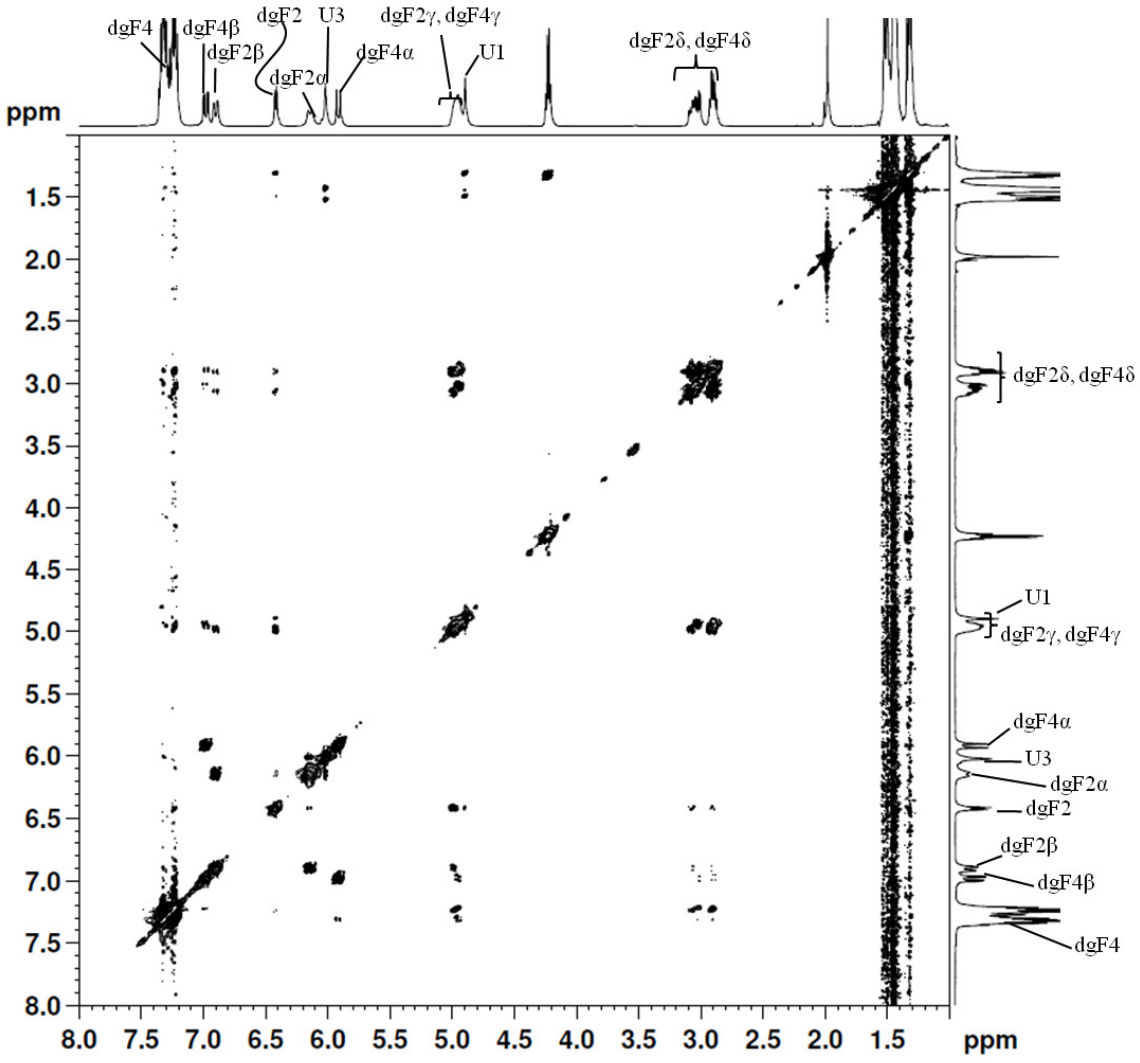

B

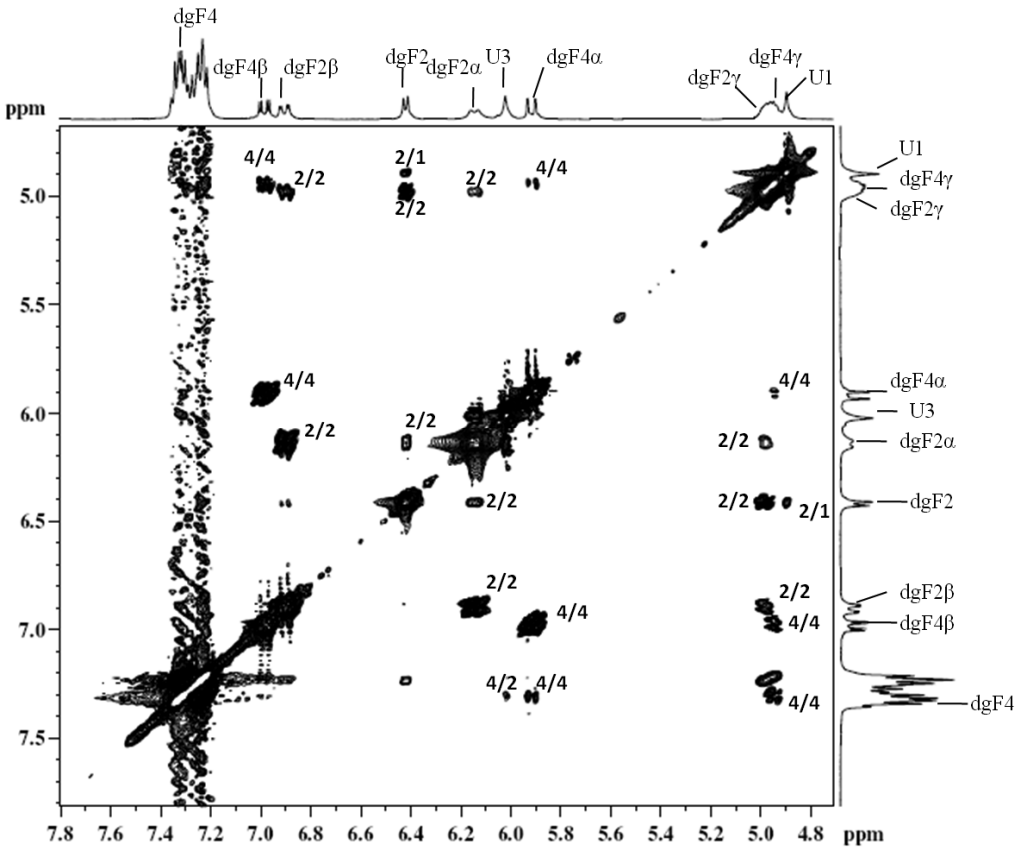

C

Figure 10: a) TOCSY NMR spectrum of peptide **D1** in $CDCl_3$. The sequential assignments of amino acids were performed using ROESY, b) The full ROESY spectra of peptide **D1**, c) Partial ROESY spectra of peptide **D1** showing sequential NOEs of NH↔NH, $C^{\alpha}H$, NH↔$C^{\beta}H$, NH↔$C^{\gamma}H$, $C^{\alpha}H$↔$C^{\beta}H$, $C^{\alpha}H$↔$C^{\gamma}H$ and $C^{\beta}H$↔$C^{\gamma}H$.

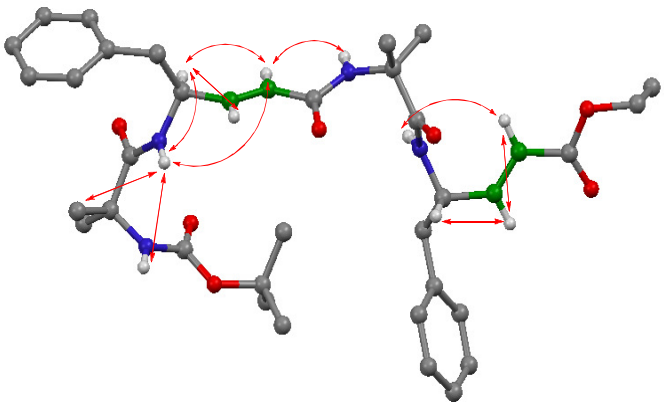

Figure 11: The observed NOEs from ROESY spectra of peptide **D1** are highlighted in the crystal structure.

3.4.4 Circular dicroism spectra of α/vinylogous peptides D1, D2 and D3

Further, CD spectra of all hybrid peptides **D1**, **D2**, and **D3** recorded in MeOH are given in the Figure 12. The CD spectra of the α/vinylogous peptides **D1**, **D2** and **D3** showed similar kind of CD signature with negative maxima at ~ 209 nm. The results from CD spectra further confirmed that all the hybrid peptides **D1, D2** and **D3** adopted similar structure in solution.

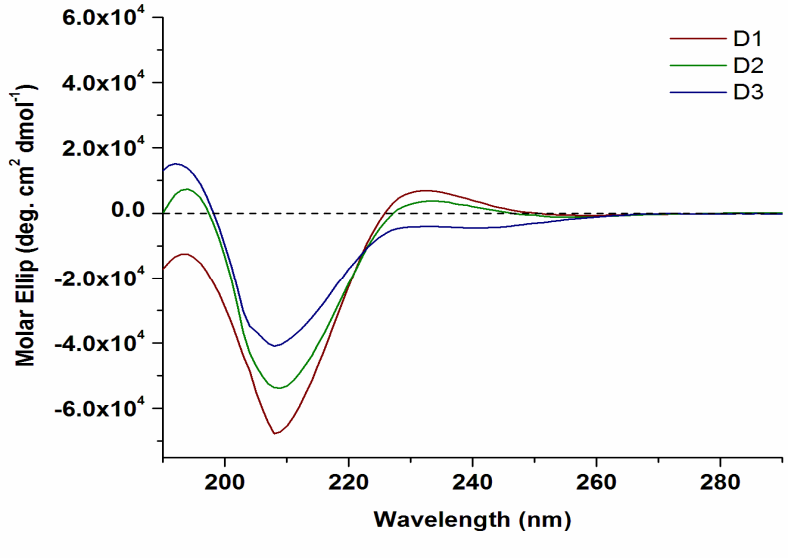

Figure 12: Circular dichroism (CD) spectra of α/vinylogous hybrid peptides **D1**, **D2** and **D3**.

3.4.5 Direct transformation of α/vinylogous hybrid peptides to α/γ^4-hybrid peptides and their analysis

Indeed surprised by the unusual planar structure of **D1**, which is probably due to the conformational restrictions of the double bonds provoke us to release the conformational strain through the catalytic hydrogenation. We anticipate that the conformational flexibility provided by the saturated γ^4-amino acids in hybrid peptides may lead to the ordered structures through intramolecular H-bonding. The types of possible intramolecular H-bonding in the α/γ-hybrid peptides are depicted in the Scheme 2. In the case of backward H-bonding a 12-helix may prevail due to presence of two C_{12} H-bond pseudocycles compared to the other or a C_{10}-helix may dominate in the case forward H-bonding due to the presence of three C_{10} H-bond pseudocycles. We anticipate that the α/γ^4-hybrid tetrapetides may adopt either C_{10} or

C_{12} or the combination of C_{10}/C_{12} H-bonded structures as reported in the literature for other γ-amino acids such as 3,3-dialkyl γ-amino acids,[33] carbo γ-amino acids[35] and cyclic γ-amino acids.

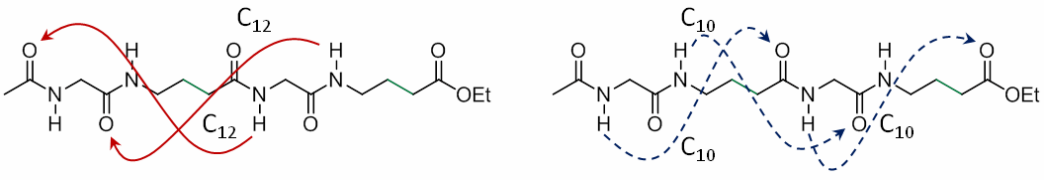

a) **b)**

Scheme 2: Schematic representation of possible a) backward, and b) forward CO···NH H-bonds in α/γ-hybrid peptides.

We further investigated the possibilities of transforming hybrid unsaturated peptide to its saturated analogue using catalytic hydrogenation. The pure peptide **D1** was subjected to catalytic hydrogenation using 20% Pd/C in ethanol. The reaction was monitored by MALDI-TOF/TOF and HPLC. The complete conversion of peptide **D1** to peptide (Boc-Aib-γ^4Phe-Aib-γ^4Phe-OEt) **G1** was achieved within six hours and the pure α/γ^4-hybrid peptide was isolated in 95% yield (Scheme 3a). The transformation of hybrid unsaturated peptide to its saturated analogue proceeds very smoothly. Fully assigned ^{1}H NMR (amide and vinylic region) before and after the catalytic hydrogenation of **D1** is shown in Scheme 3b.

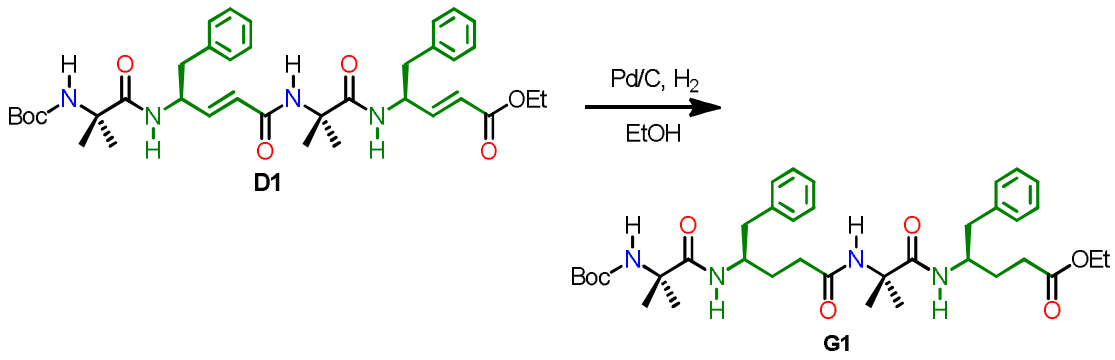

a)

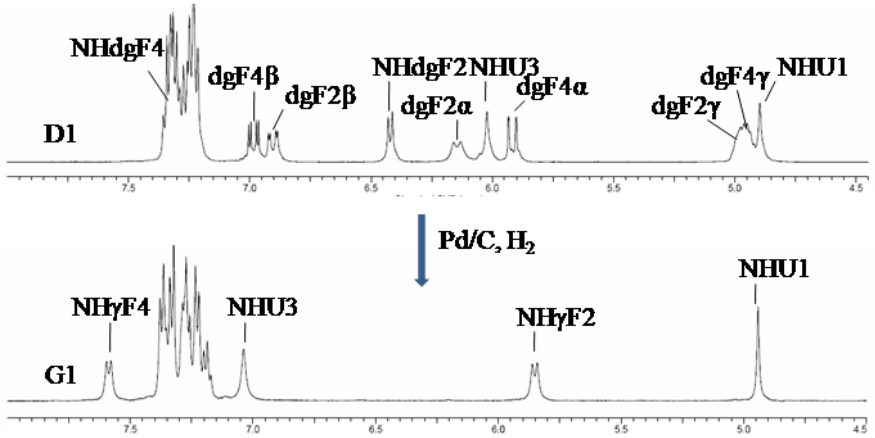

b)

Scheme 3: a) Transformation of hybrid unsaturated peptide **D1** (Boc-Aib-dgF-Aib-dgF-OEt) to its saturated analogue **G1** (Boc-Aib-γ^4Phe-Aib-γ^4Phe-OEt) using catalytic hydrogenation, b) The ^{1}H NMR spectra of peptides before (**D1**) and after (**G1**) the catalytic hydrogenation.

Single crystals of α/γ^4-hybrid peptide **G1** obtained from the slow evaporation of ethanol solution yielded the structure shown in Figure 13. Four molecules were observed in the asymmetric unit with slight variation in the torsional values. The ORTEP diagram of **G1** has shown in Figure 13a. Instructively, the peptide adopted a right-handed 12-helical [12-atom ring H-bonds of C=O(i)···H–N(i+3), C_{12}] conformation in the crystalline state. The analysis of the crystal structure reveals that the two cooperative twelve membered backward (1←4) H-bonds (Scheme 2a) C=O(Boc)···NH(3) [C=O···H–N dist. 2.064Å, O···N dist. 2.920Å and ∠O···H–N 172°] and C=O(1)···NH(4) [C=O···H–N dist. 1.984 Å, O···N dist. 2.819Å and ∠O···H–N 163°] stabilizing the helical conformation (Figure 17b). The torsion angle variables are tabulated in Table 3.

Further, we investigated whether the peptide **G1** adopted similar conformation in solution using 2D NMR. The observed NOE patterns of the peptide are highlighted in crystal conformation (Figure 14c). The NOEs between the protons of inter-residues within the peptide molecule provide the evidence of the strong population of compact helical conformations in solution. The TOCSY and partial ROESY spectra are shown in Figure15.

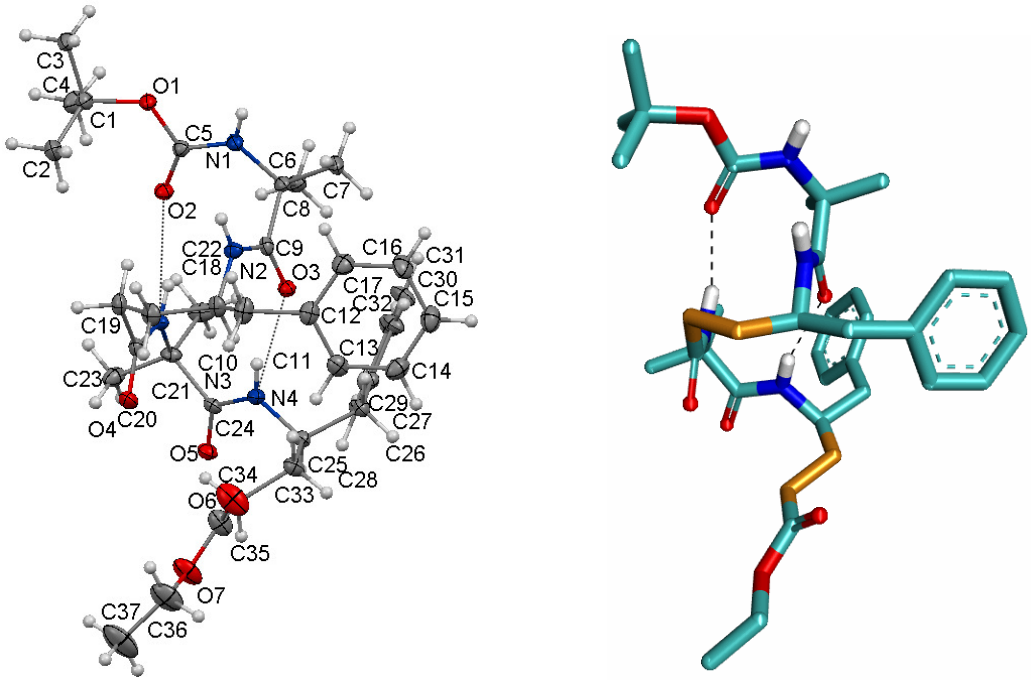

Figure 13: a) ORTEP diagram of α/γ^4-hybrid peptide Boc-Aib-γ^4Phe-Aib-γ^4Phe-OEt (**G1**), b) capped stick model of **G1.**

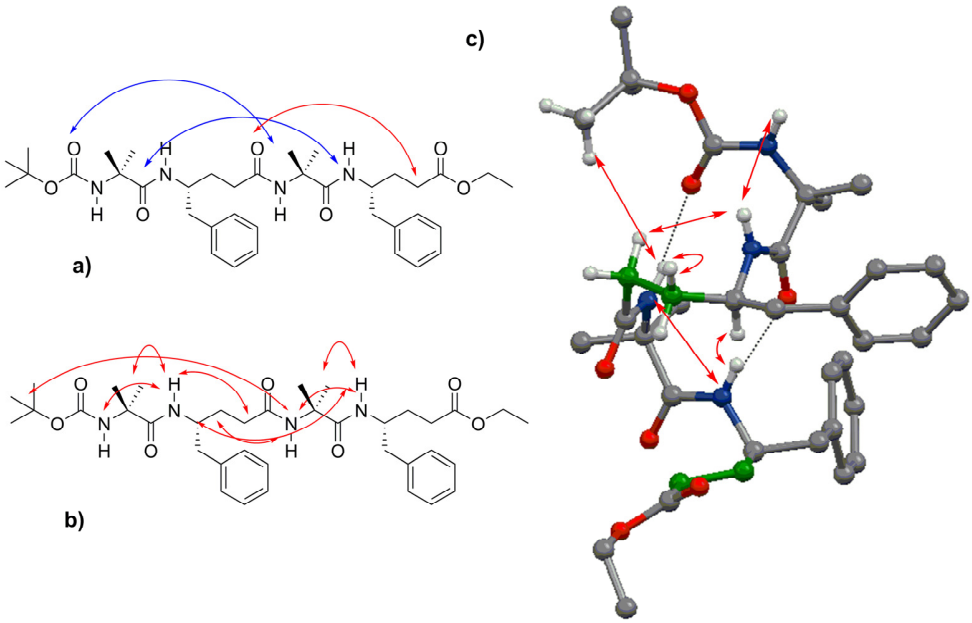

Figure 14. a) The H-bonds observed in the crystal structure of G1. The C–H···O hydrogen bond is highlighted using red colour. b) The NOEs observed in the ROESY spectrum. c) The observed NOEs are highlighted in the crystal structure.

Among the unambiguous NOEs involving in the backbone protons of peptide **G1**, the strong NOEs were observed between protons of NH(1)↔NH(2), $C^{\beta}H(2)$↔NH(3), *tert*-butyl↔NH(3), NH(4)↔$C^{\gamma}H(3)$ and NH(3)↔NH(4) with the distances less than 3.0 Å are shown in Figure 14B and 14C. Overall, the α/γ^4-hybrid peptide **G1** adopted helical conformation in crystals as well as in solution.

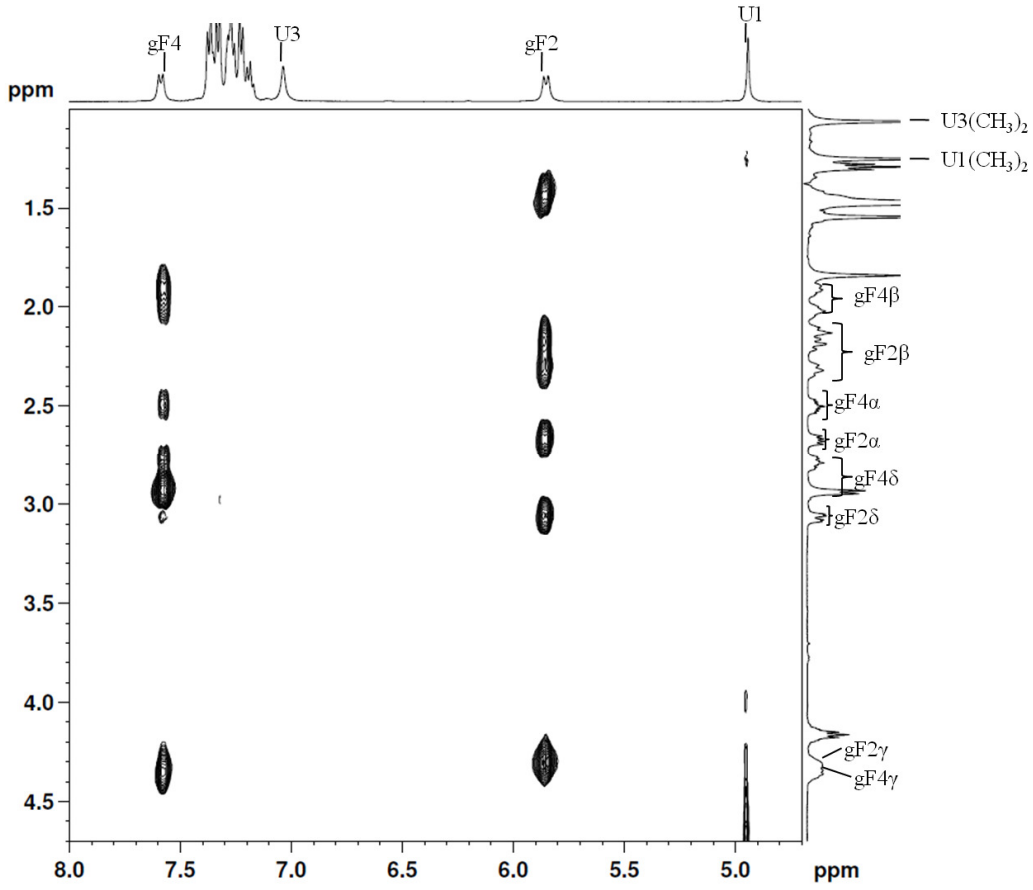

A

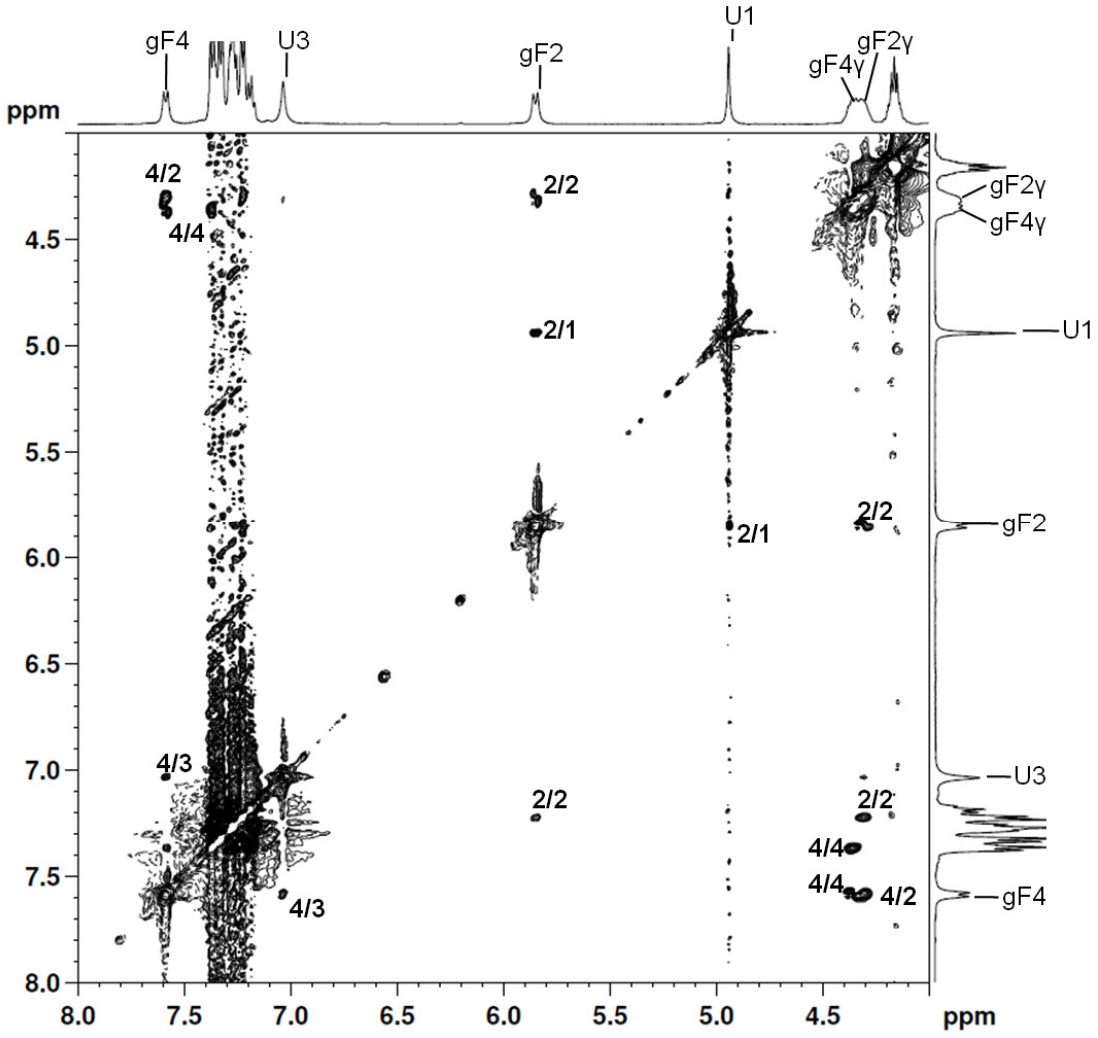
gF4
U3
gF2
U1
gF4γ
gF2γ
ppm
4/2
4/4
2/2
2/1
4/3
2/2
2/1
2/2
4/4
4/4
4/2
4/3
gF2γ
gF4γ
U1
gF2
U3
gF4
8.0
7.5
7.0
6.5
6.0
5.5
5.0
4.5
ppm

B

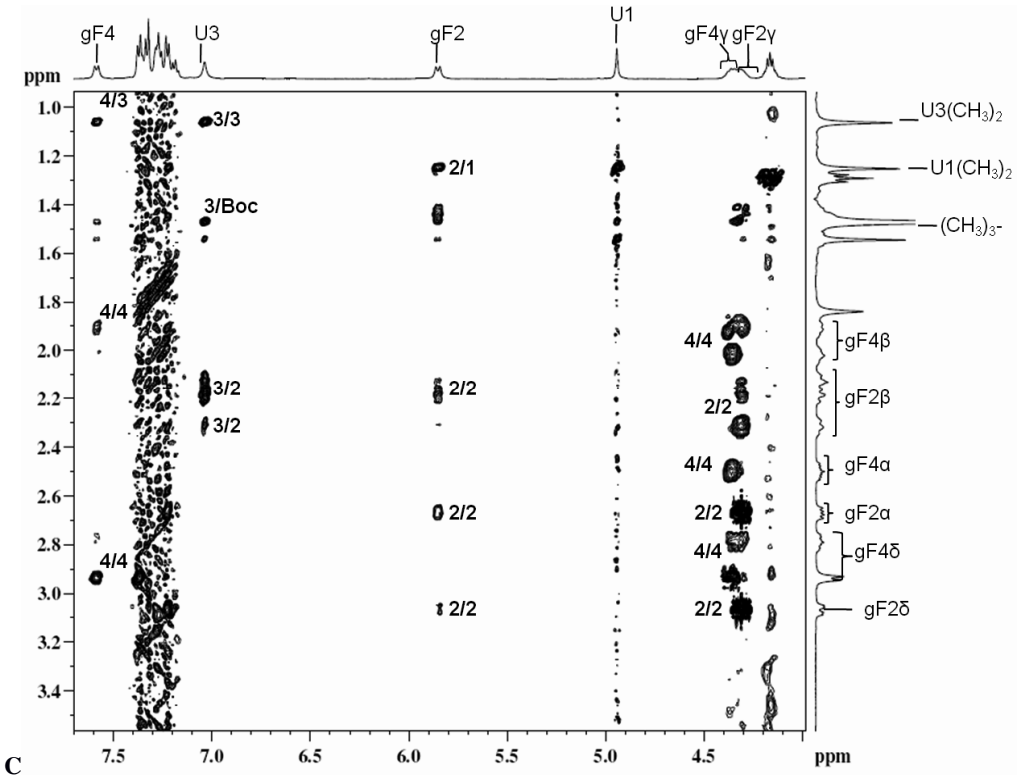

C

Figure 15: A) TOCSY NMR spectrum of peptide **D1** in $CDCl_3$. The sequential assignments of amino acids were performed using ROESY, B) Partial ROESY spectra of peptide **G1** showing sequential NOEs of NH↔NH and NH↔$C^{\gamma}H$, C) Partial ROESY spectra of peptide **G1** showing sequential NOEs of NH↔$C^{\alpha}H$, NH↔$C^{\beta}H$, NH↔$C^{\delta}H$, $C^{\gamma}H$ ↔ $C^{\alpha}H$, $C^{\gamma}H$↔$C^{\beta}H$ and $C^{\gamma}H$↔$C^{\delta}H$.

The transformation of **D1** to **G1** providing a unique example of converting a non-folded to folded state of peptides. Inspired by the 12-helical conformation of **G1**, we further subjected **D2** and **D3** to the catalytic hydrogenation to give saturated peptides **G2** (Boc-Ala-γ^4Phe-Aib-γ^4Phe-OEt) and **G3** (Boc-Aib-γ^4Phe-Leu-γ^4Phe-OEt), respectively (Scheme 4).

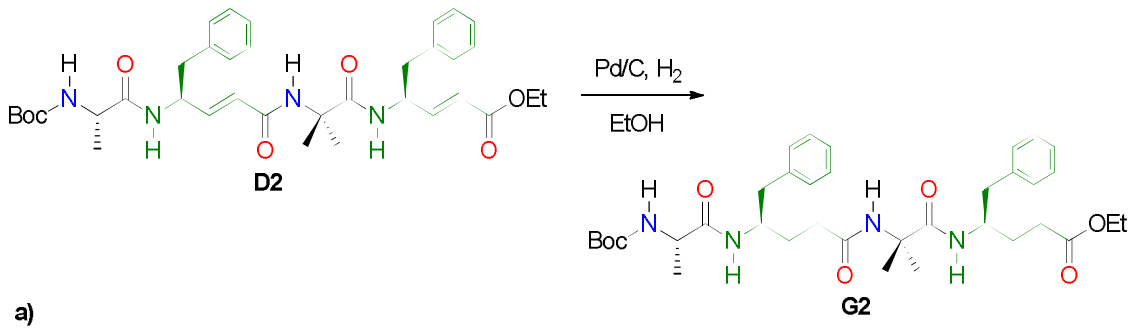

a)

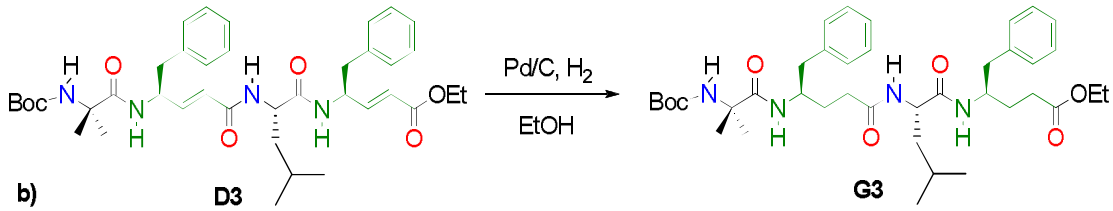

Scheme 4: Schematic representation of transformation of hybrid unsaturated peptide to its saturated analogue using catalytic hydrogenation: a) **D2** (Boc-Ala-dgF-Aib-dgF-OEt) to **G2** (Boc-Ala-γ^4Phe-Aib-γ^4Phe-OEt), b) **D3** (Boc-Aib-dgF-Leu-dgF-OEt) to **G3** (Boc-Aib-γ^4Phe-Leu-γ^4Phe-OEt).

Single crystals of **G2** and **G3** were obtained from the slow evaporation of peptides solutions in ethanol and methanol, respectively. The crystal structures of **G2** and **G3** is shown in Figure 16a and 17a, respectively. The crystal structure analysis reveals that similar to **G1** both peptides **G2** and **G3** adopted 12-helical conformations. Along with **G2,** one ethanol molecule was observed in the asymmetric unit. As shown in Figure 16c, ethanol played very important role in the inter-connecting two independent helical molecules through head-to-tail interactions.

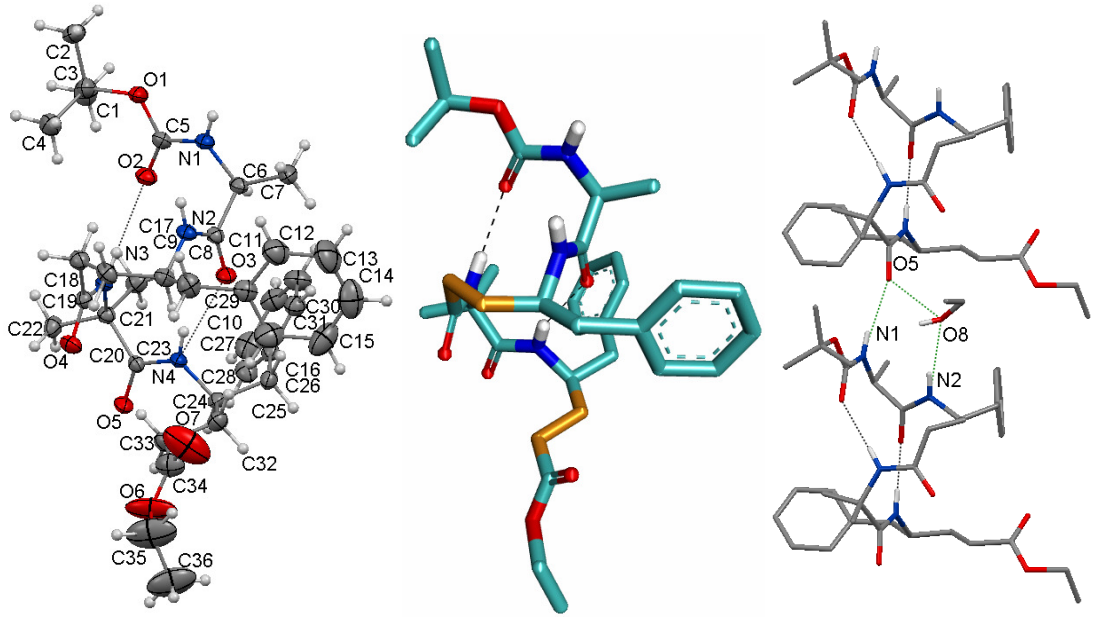

Figure 16: a) ORTEP diagram of Boc-Ala-γ^4Phe-Aib-γ^4Phe-OEt (**G2**), b) capped stick model of **G2,** c) interconnection of two different **G2** molecules in head-to-tail fashion with the help of an ethanol molecule. Interconnected H-bonds are shown with green colour.

The analysis of the crystal structure reveals that the similar to the **G1**, two cooperative twelve membered backward hydrogen bonds (1←4) are stabilizing the helical conformations. In the case of **G3,** two molecules are present in the asymmetric unit along with two methanol molecules. The two different molecules in asymmetric unit are interconnected with other independent helix with the help of methanol in a head-to-tail fashion (Figure 17c) similar to **G2**. The hydrogen bonding parameters of all hybrid peptides **G1, G2** and **G3** are tabulated in Table 3.

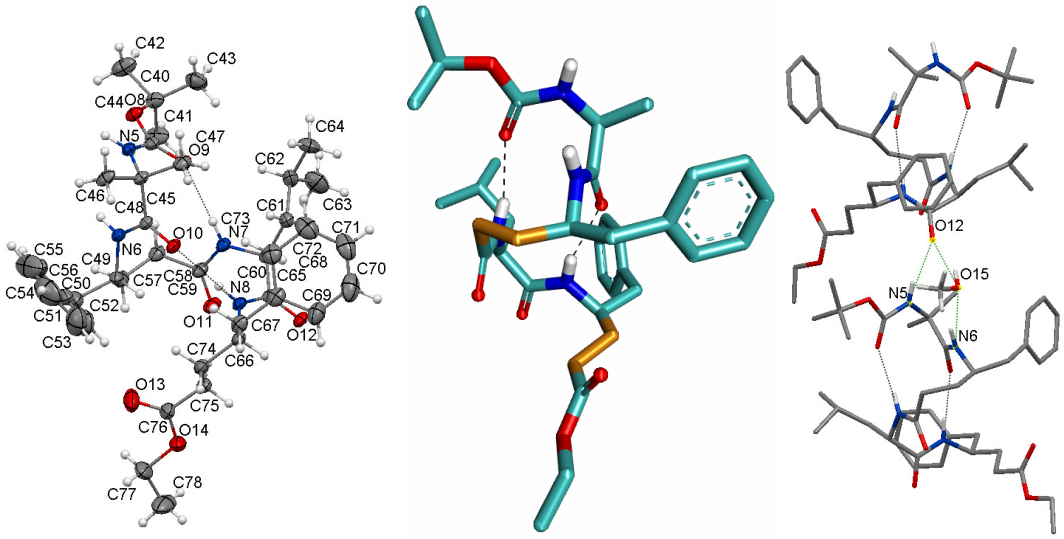

a) **b)** **c)**

Figure 17: a) ORTEP diagram of Boc-Aib-γ^4Phe-Leu-γ^4Phe-OEt (**G3**), b) capped stick model of **G3,** c) interconnection of two different **G3** molecules in head-to-tail fashion with the help of a methanol molecule. Interconnected H-bonds are shown with green colour.

In contrast to peptide **D1**, α-residues in **G1-G3** showed the right handed helical conformations by having average ϕ and ψ values –58 ± 3° and –39 ± 5°, respectively. The torsion angle variables are tabulated in Table 3. The stereochemical analysis of γ^4-residues in **G1, G2** and **G3** reveal that, γ^4Phe2 adopted *gauche*$^+$, *gauche*$^+$ (g^+, g^+, $\theta_1 \approx \theta_2 \approx 60°$) local conformation about the C_β–C_γ and C_α–C_β bonds, while the C-terminal γ^4Phe4 residues displayed *gauche*$^+$ (C_β–C_γ), *anti* (C_α–C_β) conformation due to the lack of terminal H-bond donor (NH). We anticipate that g^+, g^+ conformation can be induced in the terminal γ-amino acid by introducing H-bond donor (NH) at the C-terminus. Peptide **G4** (Boc-Ala-γ^4Phe-Aib-

γ^4Phe-CONHMe) was synthesized from **G2** to evaluate the hypothesis. The treatment of aqueous methyl amine to the *N*-hydroxy succinimidyl ester of **G2** leads to formation **G4** (Scheme 5)**.** After the slow evaporation of 5% MeOH solution in DCM **G4** was crystallized and its X-ray structure is shown in Figure 18. As anticipated, the terminal γ^4-residue adopted g^+, g^+ conformation and accommodated into the helix. The torsion variables of **G4** are tabulated in Table 3. The helical structure is stabilized by three consecutive intramolecular backward C_{12} H-bonds. The hydrogen bonding parameters of **G1-G4** are shown in Table 4. The H-bonding between the 1←4 residues in all α/γ^4 hybrid peptides indicating the backbone expanded version of a 3_{10}-helix.

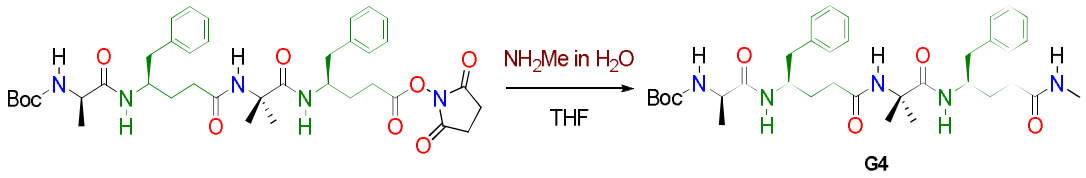

Scheme 5: Schematic representation of synthesis of Boc-Ala-γ^4Phe-Aib-γ^4Phe-CONHMe (**G4**).

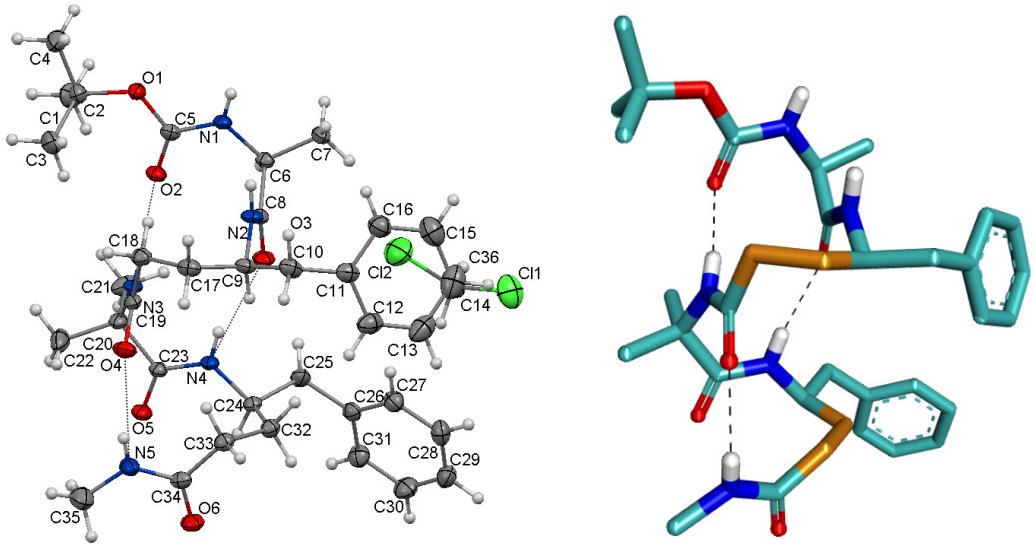

Figure 18: X-ray structure of α/γ^4-hybrid peptides Boc-Ala-γ^4Phe-Aib-γ^4Phe-CONHMe (**G4**) a) ORTEP diagram, and b) capped stick model.

Table 3: Backbone torsional variables (in deg) of α/γ^4-hybrid tetrapeptides

Pept.	Resd.	φ	θ_1	θ_2	ψ	ω
G1	Aib1	-59±1	-	-	-38±3	-172±5
	γPhe2	-127±6	50±3	62.5±0.5	-117±7	-175±3
	Aib2	-58±3	-	-	-39±5	-178±4
	γPhe4	-104±3	61±2	-175±3	-155±7	-
G2	Ala1	-65	-	-	-39	-177
	γPhe2	-123	51	63	-123	-172
	Aib3	-58	-	-	-40	-169
	γPhe4	-113	57	-177	-130	-
G3	Aib1	-60±1	-	-	-36±1	-175
	γPhe2	-126±3	50±2	63±3	-111±4	-175±0.5
	Leu3	-63±2	-	-	-37±1	-177±1
	γPhe4	-108±7	62±2	-176/179	-142/65	-
G4	Ala1	-67	-	-	-46	179
	γPhe2	-117	49	68	-125	-172
	Aib3	-63	-	-	-30	-176
	γPhe4	-111	43	56	-137	177

Table 4: Hydrogen-Bond Parameters in Peptides **G1**, **G2**, **G3** and **G4**

Type of H-bonds	Donar (D)	Acceptor (A)	D····A (Å)	D-H····A (Å)	∠N-H···O (deg)
Boc-Aib-γ^4Phe-Aib-γ^4Phe-OEt (G1)					
1←4	N3	O0(Boc)	3.03	2.18	168.7
1←4	N4	O1	2.84	2.03	156.5
Boc-Ala-γ^4Phe-Aib-γ^4Phe-OEt (G2)					
1←4	N3	O0(Boc)	3.00	2.14	178.2
1←4	N4	O1	2.86	2.06	155.8
Boc-Aib-γ^4Phe-Leu-γ^4Phe-OEt (G3)					
1←4	N3	O0(Boc)	2.95	2.10	161.0
1←4	N4	O1	2.90	2.07	155.8
Boc-Ala-γ^4Phe- Aib-γ^4Phe-NHMe (G4)					
1←4	N3	O0(Boc)	2.88	2.02	173.5
1←4	N4	O1	2.94	2.13	156.6
1←4	N5	O2	2.92	2.16	147.5

3.4.6 Synthesis and crystal structure analysis of α/γ^4-hybrid hexapeptides

Further, to exploit the same methodology and to understand the conformational behaviour of α/γ^4-hybrid helix containing vinylogous amino acids, a hexapeptide **D4** (Boc-Aib-γ^{4}Phe-Leu-γ^{4}Phe-Aib-dgF-OEt) was synthesized from **G3** through [4+2] convergent strategy. It is noteworthy to mention that pure **D4** was crystallized within 30 min in many solvents including acetone and ethyl acetate/hexane. The single crystals of **D4** in ethyl acetate/hexane yield the structure shown in Figure 19. The crystal structure analysis reveals that the 12-helical structure is stabilized by four consecutive backward 1←4 hydrogen bonds. Surprisingly, the C-terminal vinylogous residue nicely accommodated into the helix (top view Figure 19b) through a 10 membered weak C-H···O H-bonding between the dgF6 C_α-H and the carbonyl of γPhe4 (1←3). In contrast to the **D1**, the vinylogous amino acid in **D4** displayed the torsional angle 23° for θ_1 and the conjugated ester adopted local *s-trans* conformation with the ψ value 28°. It is interesting to notice the little distortion in the structure of vinylogous amino acid in the helix terminal compared β-sheet structures observed earlier.

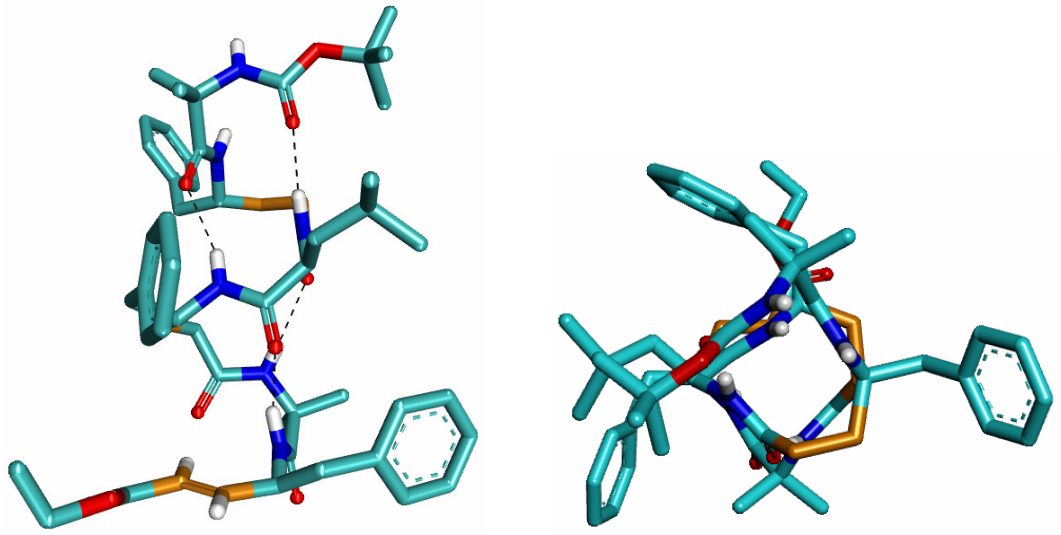

a) **b)**

Figure 19: a) X-ray structure of Boc-Aib-γ^{4}Phe-Leu-γ^{4}Phe-Aib-dgF-OEt (**D4**) (capped stick model). Non-polar H-atoms are not shown for clarity, b) top view of **D4.**

Two independent **D4** molecules (along with a solvent water molecule) are present in the asymmetric unit with slight variation in the torsional values. The two helices are independently interconnected with the other helices in a head-to-tail fashion (Figure 20) through four intermolecular H-bonds with the help of water molecule, NH(7)···O(6) [NH···O dist. 2.132Å, N···O dist. 2.927 Å and ∠N-H···O = 154°], NH(8)···O(8) [NH···O dist. 2.235 Å, N···O dist. 3.062 Å and ∠N-H···O = 161°], NH(1)···O15 [NH···O dist. 2.210 Å, N···O dist. 2.921 Å and ∠N-H···O = 155°], and NH(2)···O17 [NH···O dist. 2.225 Å, N···O dist. 3.061 Å and ∠N-H···O = 164°].

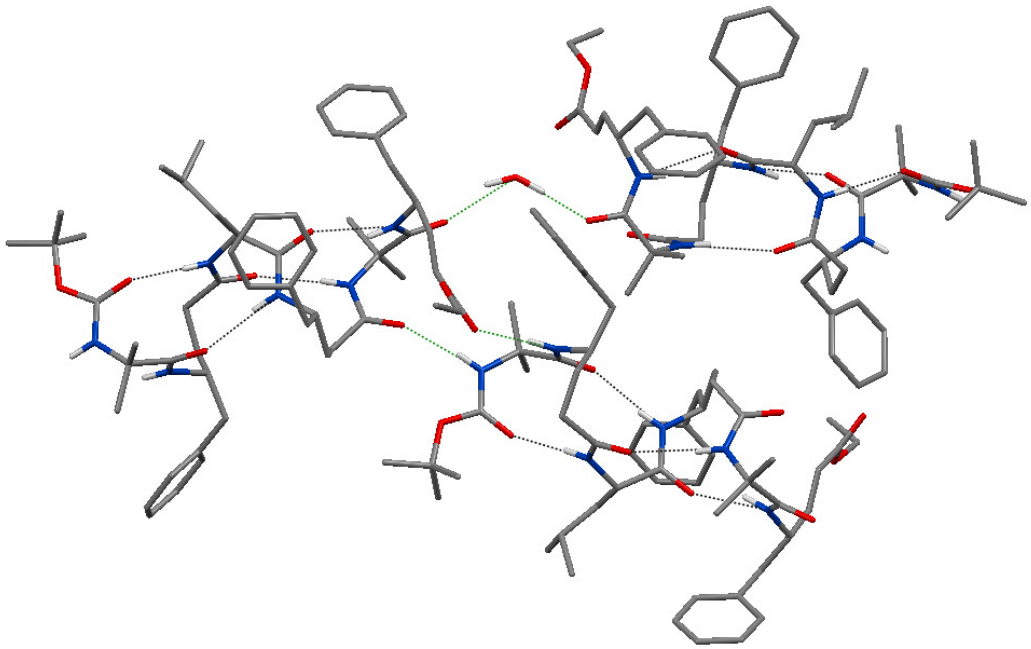

Figure 20: The two independent helix molecules of **D4** are interconnected with the other helices in a head-to-tail fashion through four intermolecular H-bonds with the help of water molecule.

Further, **D4** was transformed to its saturated analogue **G5** (Boc-Aib-γ^4Phe-Leu-γ^4Phe-Aib-γ^4Phe-OEt) using catalytic hydrogenation and its X-ray structure is shown in Figure 21. The analysis reveals the 12-helical structure of **G5** in single crystals is stabilized by four consecutive C_{12} intramolecular 1←4 H-bonds. Similar to **G1**, **G2**

and **G3**, the C-terminal γ-amino ester in **G5** adopted g^+, t^- conformation. The torsion angles of **D4** and **G5** are tabulated in Table 6. In addition, a weak 10 membered C–H···O H-bond between the acidic α-hydrogens and the C=O of preceding γPhe residue (1←3) was observed in all hybrid peptides containing C-terminal γ-amino ester (**G1-G3** and **G5**). The H-bond parameters of peptides **D4** and **G5** are tabulated and given in the Table 5. The two peptide molecules of **G5** (**a** and **b**) (along with a solvent water molecule) are present in the asymmetric unit with slight variation in the torsional values and displayed antiparallel orientation.

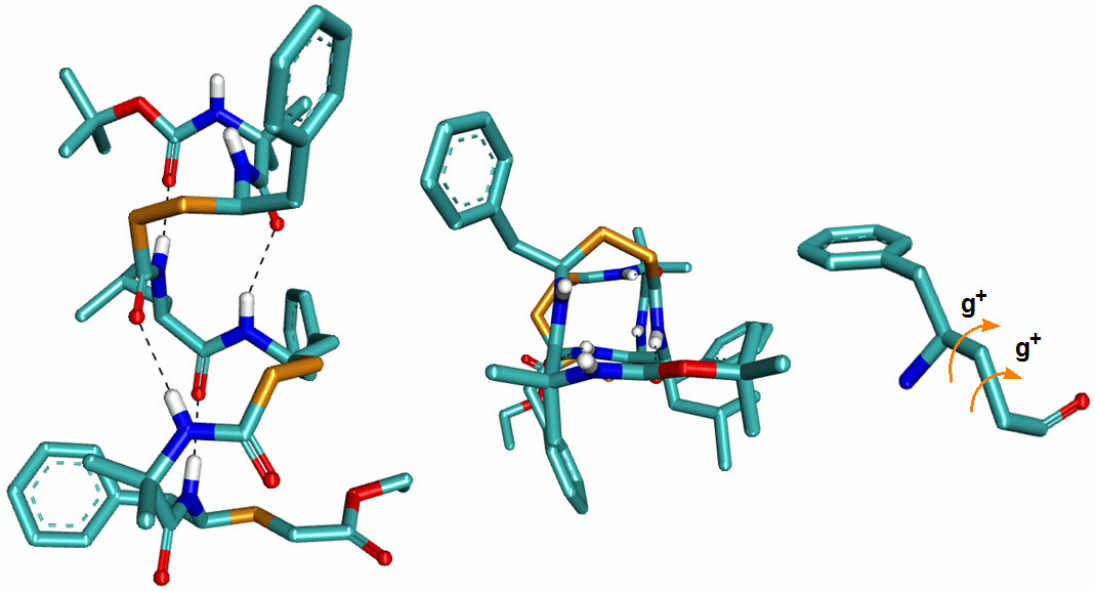

a) **b)** **c)**

Figure 21: a) X-ray structures of Boc-Aib-γ^{4}Phe-Leu-γ^{4}Phe-Aib-γ^{4}Phe-OEt (**G5**), b) top view of **G5** showing the distinct projections of amino acid side-chains, c) helix favouring the g^+, g^+ conformation adopted by the γ^{4}Phe residue in 12-helices.

In contrast to **D4**, the two peptide molecules in **G5** are interconnected through the intermolecular C-H···π interaction between the aromatic side-chains of γPhe2 (**a**) and γPhe4 (**b**) [C-H···π dist. 2.898 Å] along with water mediated CH(70)···O(19) [CH···O dist. 2.457Å, C···O dist. 3.264 Å and ∠C-H···O = 145^o] and O(7)···H-O(19) [O···OH dist. 1.764 Å, O···O dist.2.807 Å and ∠O-H···O = 170^o] H-bonds. The two peptides (**a** and **b**) in the asymmetric

unit are independently interacting with other helices in a head-to-tail fashion through two intermolecular H-bonds (Figure 22). In the molecule **a,** NH(1)···O(6) [NH---O dist. 2.114 Å, N···O dist. 2.889 Å and ∠N-H···O = 150^{o}] and NH(2)---O(8) [NH---O dist. 2.151 Å, N---O dist. 2.959 Å and ∠N-H···O = 156^{o}] are involved in the intermolecular H-bonding, while in the molecule **b,** NH(7)---O(15) [NH---O dist. 2.226 Å, N---O dist. 3.050 Å and ∠N-H···O = 160^{o}] and NH(8)---O(17) [NH---O dist. 2.069 Å, N---O dist. 2.882 Å and ∠N-H···O = 157^{o}] are involved in the intermolecular H-bonding.

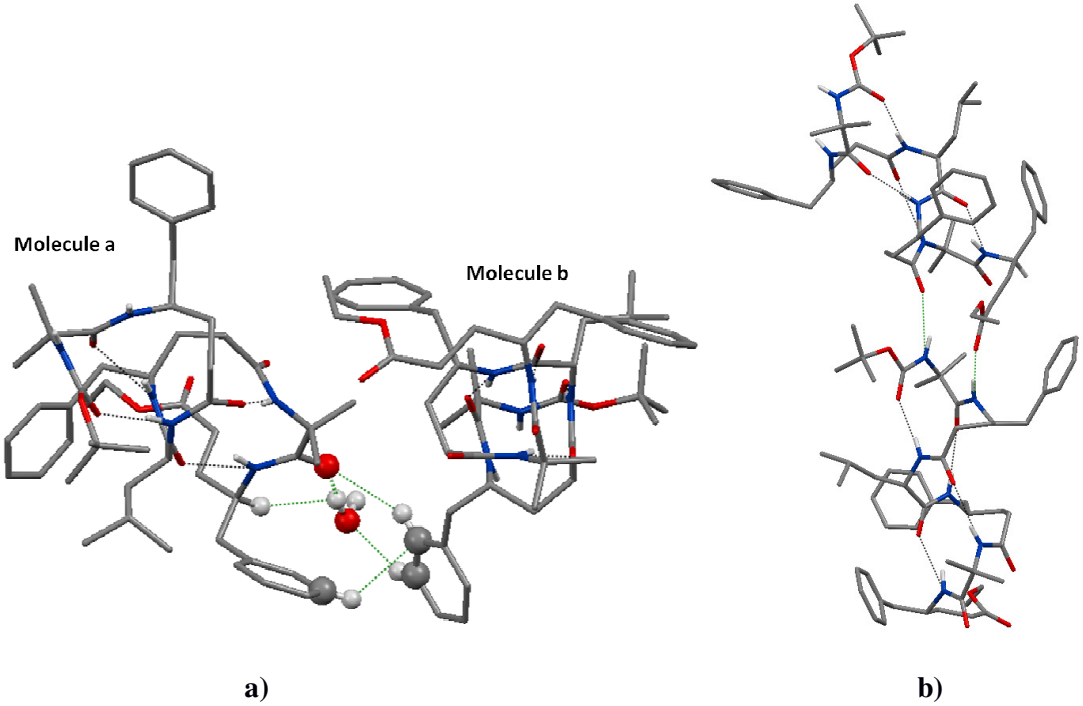

Figure 22: a) The packing of two independent molecules in asymmetric unit through C-H···π interaction along with water molecule, b) interconnection of two different **G5** molecules in head-to-tail fashion. Interconnected H-bonds are shown with green colour.

Table 5: Hydrogen-Bond Parameters in Peptides **D4** and **G5**

Type of H-bonds	Donar (D)	Acceptor (A)	D···A (Å)	D-H···A (Å)	∠N-H···O (deg)
Boc-Aib-γ^{4}Phe-Leu-γ^{4}Phe-Aib-dgPhe-OEt (D4)					
1←4	N3	O0(Boc)	2.89	2.03	176.3
1←4	N4	O1	2.95	2.14	156.5
1←4	N5	O2	3.03	2.18	172.1
1←4	N6	O3	2.80	2.01	152.8
Boc-Aib-γ^{4}Phe-Leu-γ^{4}Phe-Aib-γ^{4}Phe-OEt (G5)					
1←4	N3	O0(Boc)	2.87	2.01	174.2
1←4	N4	O1	2.96	2.18	150.7
1←4	N5	O2	2.98	2.12	174.5
1←4	N6	O3	2.80	2.00	153.4

Table 6: Backbone torsional variables (in deg) of α/γ^4-hybrid Hexapeptides **D4** and **G5**

Pept.	Resd.	φ	θ_1	θ_2	ψ	ω
D4	Aib1	-55.5±2	-	-	-49±0.5	-175
	γPhe2	-137.5±1	61.5±1	59	-115±1	-176
	Leu3	-64±1	-	-	-33±1	-175±1
	γPhe4	-123±2	49±1	63±1	-120±3	-170±1
	Aib5	-61.5±1	-	-	-32.5±1	-173±1
	dgPhe6	-113	24.5±1	173±1	29.5±1.5	-
G5	Aib1	-58	-	-	-47	-175.5±0.5
	γPhe2	-135	59±1	61	-114±1	-176
	Leu3	-66±1	-	-	-31±2	-176
	γPhe4	-122.5±2.5	46.5±2.5	63.5±2.5	-127±3	-171
	Aib5	-60±2	-	-	-35.5±1.5	-175.5±2.5
	γPhe6	-116±3	55±1	177.5±0.5	24.5±0.5	-

3.4.7 Solution structure Boc-Aib-γ^4Phe-Leu-γ^4Phe-Aib-γ^4Phe-OEt (G5)

Further, we investigated whether or not the peptide **G5** adopted similar conformation in solution using 2D NMR. Fully assigned TOCSY spectrum is shown in Figure 24A. The partial ROESY spectra assigned with NOEs are shown in Figure 24B and 24C. The observed NOE patterns of the peptide obtained from the ROESY spectrum are highlighted in Figure 23a. In the ROESY spectrum the NOEs were observed between protons of NH(1)↔NH(2), $C^{\beta}H(1)\leftrightarrow NH(2)$, $C^{\alpha}H(2)\leftrightarrow NH(3)$, NH(3)↔NH(4), $C^{\gamma}H(2)\leftrightarrow NH(4)$, $C^{\beta}H(3)\leftrightarrow NH(4)$, $C^{\alpha}H(3)\leftrightarrow NH(5)$, $NH(5)\leftrightarrow C^{\beta}H(2)$, NH(5)↔NH(6), $NH(6)\leftrightarrow C^{\gamma}H(4)$ and $C^{\beta}H(5)\leftrightarrow NH(6)$. The NOEs between the protons of inter-residues within the peptide molecule provide the evidence of the strong population of compact helical conformations in solution. The observed NOEs are shown in the crystal structure of **G5** (Figure 23c) and they are well correlated with the helical conformation observed in crystal structure (Figure 23c). Overall, the α/γ^4-hybrid peptide **G5** adopted helical conformation in crystals as well as in solution.

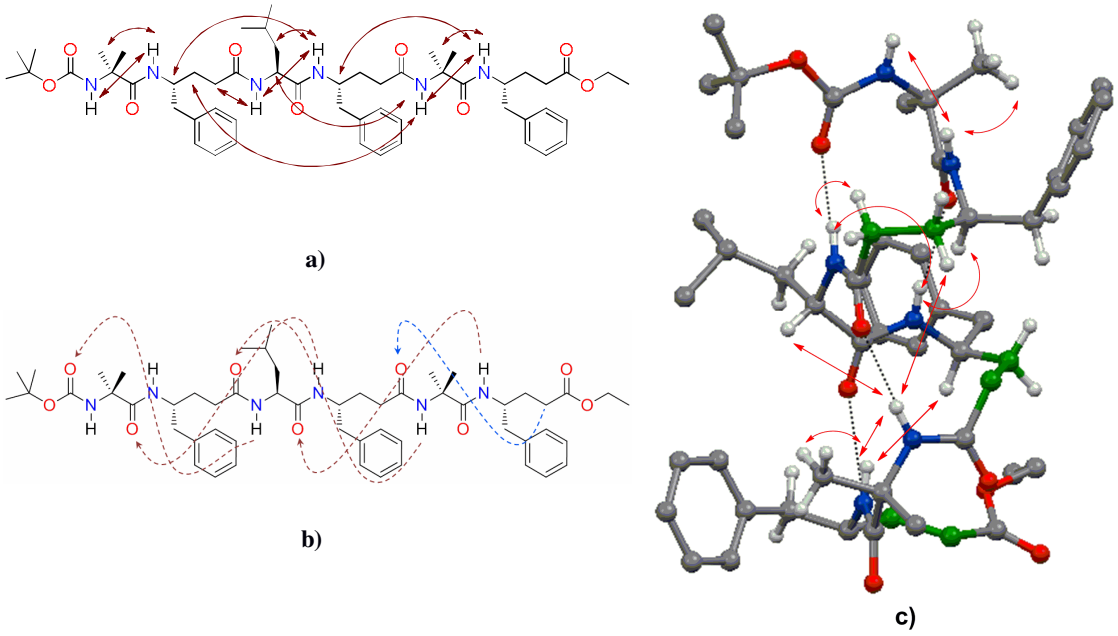

Figure 25: a) The NOEs observed in the ROESY spectrum, b) The H-bonds observed in the crystal structure of **G5**. The C–H···O hydrogen bond is highlighted using blue colour arrow, c) The observed NOEs are highlighted in the crystal structure.

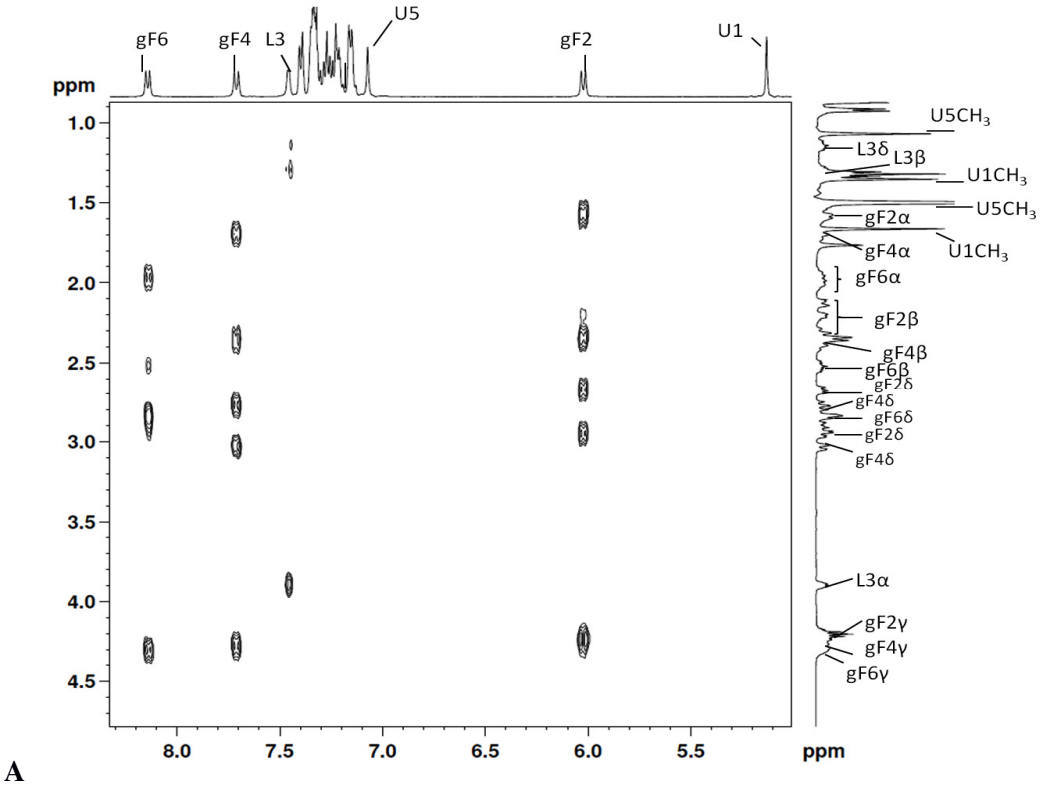
gF6
gF4
L3
U5
gF2
U1
ppm
U5CH3
L3δ
L3β
U1CH3
U5CH3
gF2α
gF4α
U1CH3
gF6α
gF2β
gF4β
gF6β
gF2δ
gF4δ
gF6δ
gF2δ
gF4δ
L3α
gF2γ
gF4γ
gF6γ
8.0
7.5
7.0
6.5
6.0
5.5
ppm

A

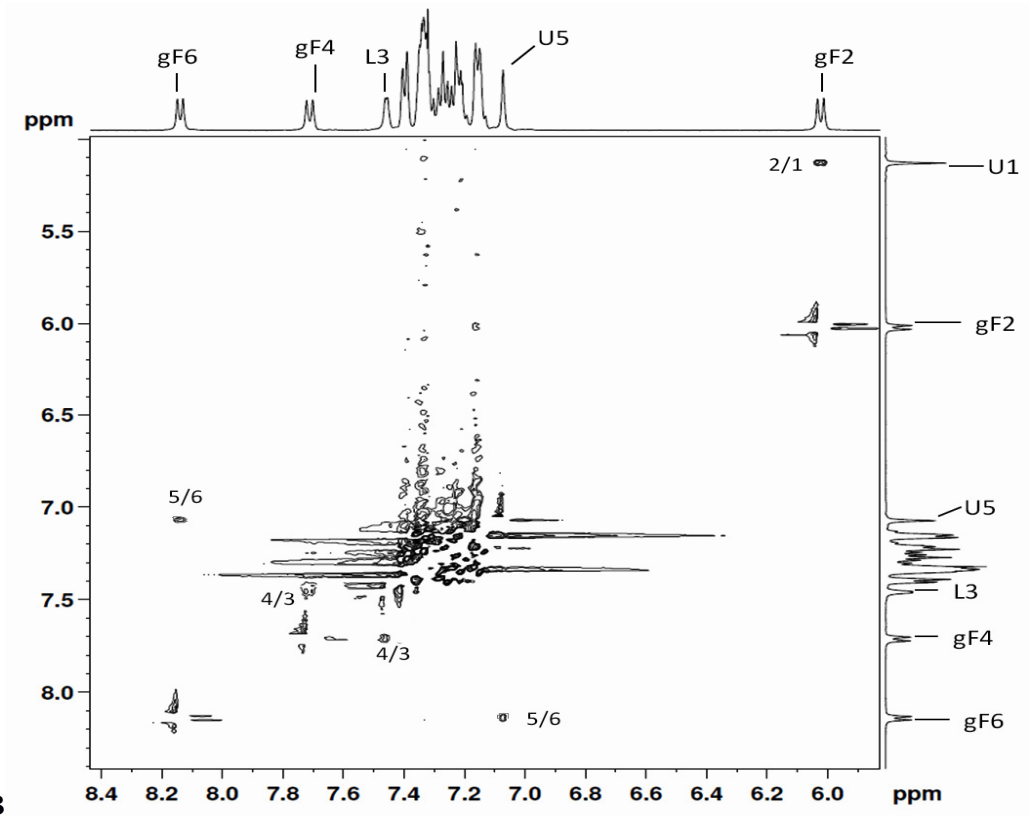
gF6
gF4
L3
U5
gF2
ppm
2/1
U1
gF2
5/6
4/3
4/3
5/6
U5
L3
gF4
gF6
8.4
8.2
8.0
7.8
7.6
7.4
7.2
7.0
6.8
6.6
6.4
6.2
6.0
ppm

B

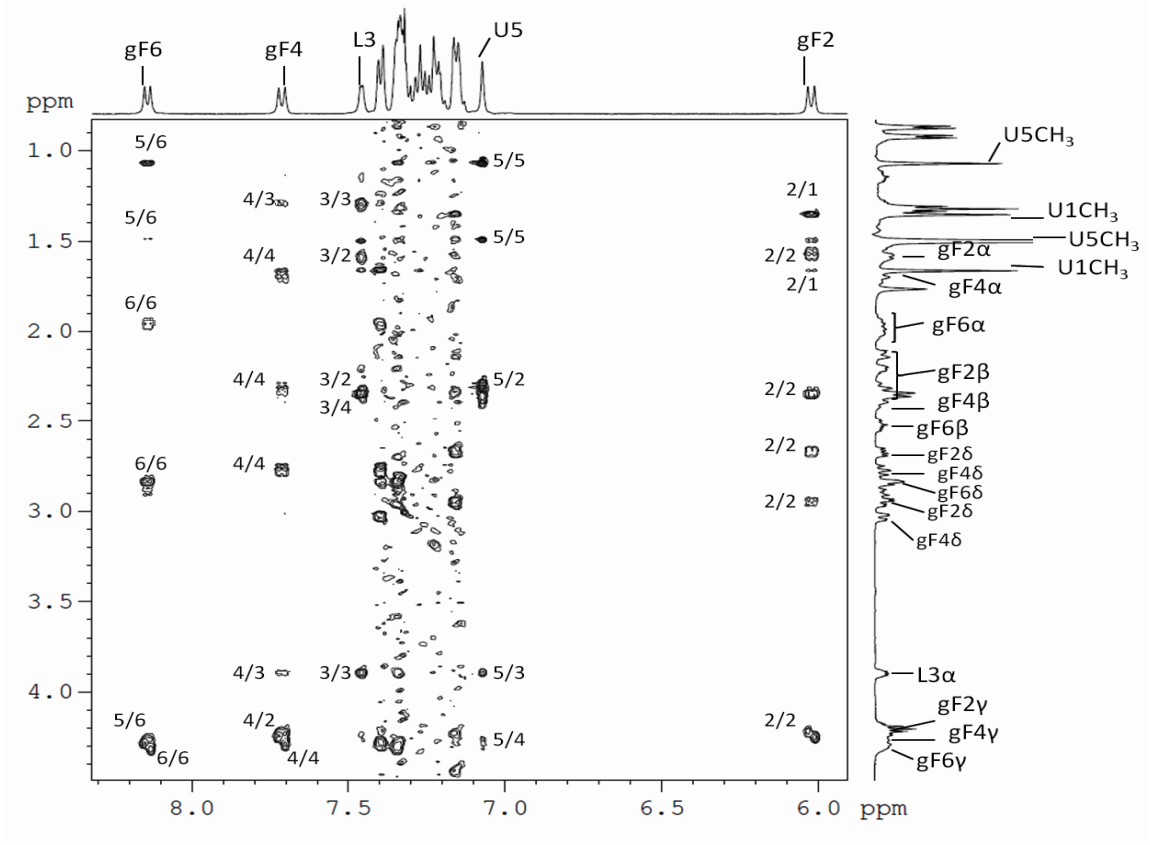

C

Figure 24: A) TOCSY spectrum of **G5** in $CDCl_3$. The sequential assignments of amino acids were performed using ROESY, B) Partial ROESY spectra of peptide **G5** showing sequential NOEs of NH↔NH, C) Partial ROESY spectra of peptide **G5** showing sequential NOEs of $NH\leftrightarrow C^{\alpha}H$, $NH\leftrightarrow C^{\beta}H$, $NH\leftrightarrow C^{\gamma}H$

3.4.8 Ramachandran type plot for α/γ^4-hybrid peptides

From the analysis of the crystal structures of all α/γ^4-hybrid peptides (**G1-G5** and **D4**) reveal that the α-residues adopted right handed helical conformations by having average ϕ and ψ values –59 ± 5° and –38 ± 5°, respectively. In addition, we observed that all γ^4-amino acid residues participated in the 12-helical structures adopted g^+, g^+ conformations with torsional angles $\theta_1 \approx \theta_2 \approx 60°$. Keeping θ_1 and θ_2 as a constant, two distinct regions in the left quadrant of the Ramachandran map[1] can be recognized for γ-and α-residues. The average ϕ and ψ values for all γ^4-residues participated in the helix were found to be -126 ± 10° and -118 ± 10°, respectively. A plot of ϕ and ψ angles of all residues in peptides **G1-G5** and **D4** is

shown in Figure 25, except the C-terminal ester residues which are not participated in the canonical helical structures with regular CO···HN bonds. This plot may be useful in the design of functional α/γ^4-hybrid foldamers similar to the α/β-hybrid peptides.

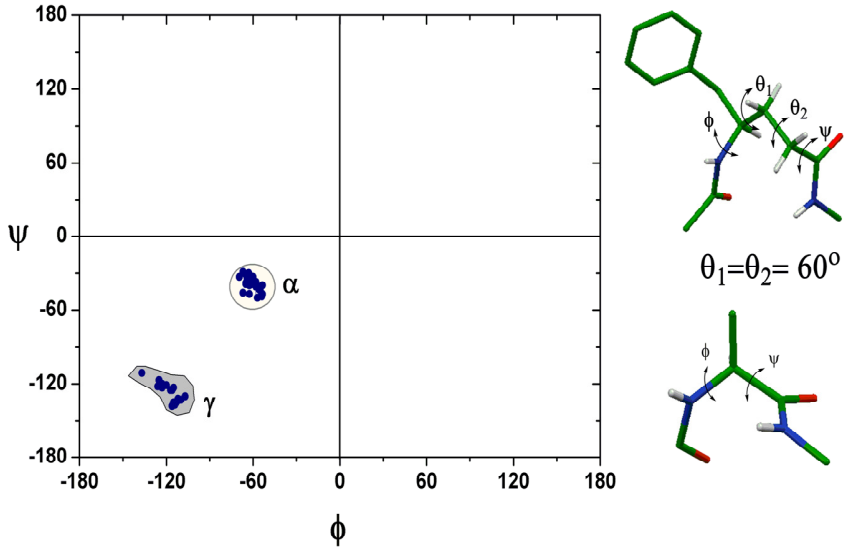

Figure 25: A plot depicting the ϕ and ψ values in the α/γ^4-hybrid peptides. The C-terminal γ^4-residues are not considered.

3.4.9 Circular Dichroism spectra of α/γ^4-hybrid peptide 12-helices

In order to understand the CD signature of α/γ^4-hybrid peptide 12-helices, we recorded circular dichroism spectra of all α/γ^4-hybrid peptides **G1**, **G2**, **G3**, **G4**, **G5** and **D4** in methanol solution (200 μM). The CD spectra of the all peptides are shown in Figure 26. A typical CD signature was observed for all peptides with CD maxima at ~ 205 nm and weak minima with at ~ 218 nm. Recent work on C_{12}-helices containing cyclic β-amino acid, Gellman et al. and Aitken et al. also observed the similar CD signature for 12-helices.[18, 37] Comparably, **D4** displayed a little distorted CD spectrum with the CD maxima at 204 nm and minima at 218 nm, may be due to the interference of C-terminal α,β-unsaturated ester.

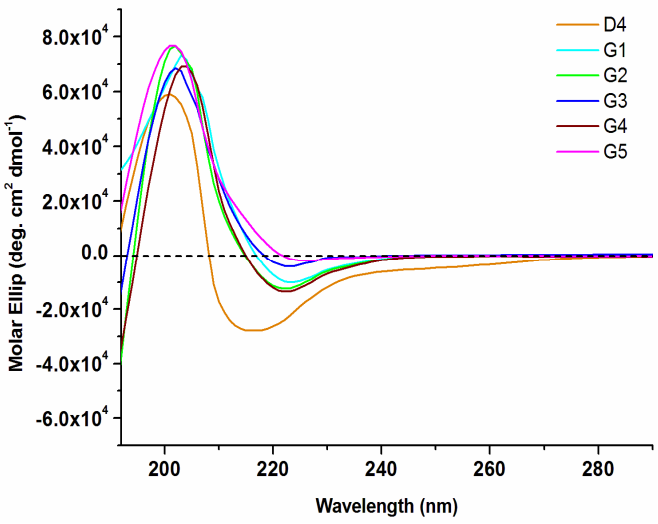

Figure 26: Circular dichroism spectra of α/γ^4-hybrid peptides **G1-G5** and **D4** in MeOH.

3.4.10 Analogy with α-helix

The intriguing results from the hybrid α/γ^4-hybrid peptides **G1**-**G5**, encouraged us to assess the hybrid 12-helical structure with respect to the predominantly existing natural α-helix. The superimposition of the backbone conformations of **G5** (Boc-Aib-γ^4Phe-Leu-γ^4Phe-Aib-γ^4Phe-OEt) with the α-helix of chicken egg white lysozime (PBD CODE 1HEL, SEQUENCE C-E-L-A-A-A-M-K, 6-13)[38] is shown in the Figure 27a. Instructively, the backbone conformation of hybrid hexapeptide **G5** is well correlated with eight residue α-helix, except the H-bonding pattern. However, the internal H-bonding orientation and the macrodiople of α/γ^4-hybrid peptides are analogous to the α-peptide helix. The top view of the superimposed **G5** and the α-helix signify the projection of the amino acid side-chains (Figure 27a). The backbone correlation and the side-chain projections of α/γ^4-hybrid peptide helcies with respect to the α-helix suggest that these hybrid peptides can be exploited as possible mimics of α-peptide helices. Further, with the availability of broad side-chain diversity in both α-and γ^4-amino acids, these α/γ^4-hybrid peptides stand unique than the other α/γ-hybrid peptides.

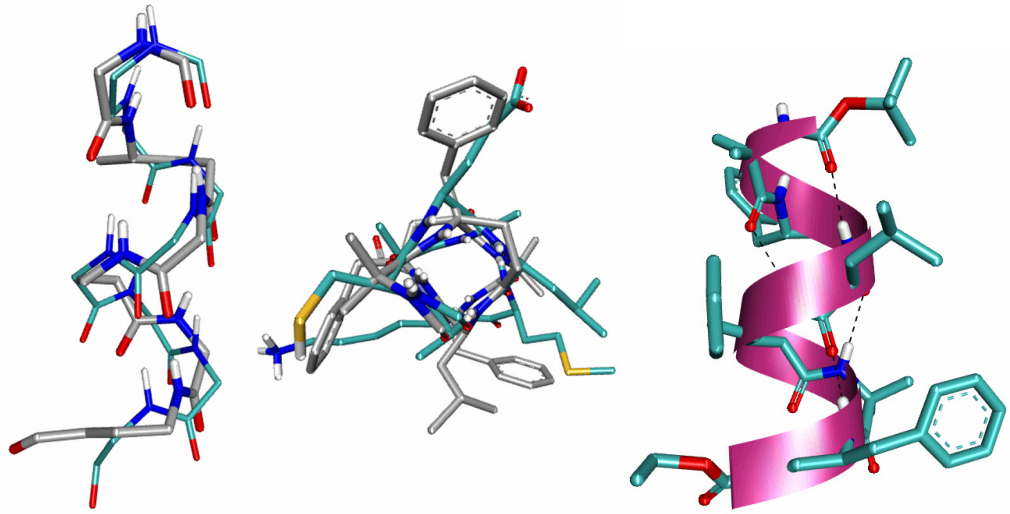

a) **b)**

Figure 27: a) Superposition of backbone conformation of the α/γ-hybrid peptide on the α-helix. All the backbone atoms of α/γ^4 hybrid peptide were used to overlay with octapeptide of α-helix, RMSD = 0.81 b) **G5** (Boc-Aib-γ^4Phe-Leu-γ^4Phe-Aib-γ^4Phe-OEt) cryastal structure, along with ribbon representation of **G5**.

3.4 Conclusion

In conclusion, we presented the stereochemical analysis of hybrid α/α, β-unsaturated γ-peptides and their smooth transformation to α/γ^4-hybrid peptides. Though there is a possibility of conceiving different types of H-bond pseudocycles, the atomic resolution data of a series of α/γ^4-hybrid peptides revealed the unprecedented 12-helical conformations. The strategy described here provides an opportunity to study the conformational preferences of both vinylogous and saturated γ^4-amino acids in hybrid oligopeptides. The presence of geometrical constrains of the double bonds in the hybrid vinylogous peptides enforcing the molecules to adopt unusual planar conformations. After releasing the geometrical constrains of the double bonds, the H-bond strength overrode the conformational flexibility of the saturated γ^4-amino acids to accommodate into the helical conformations. The conformational analysis and the unique side-chain projections of α/γ^4-hybrid peptides presented here may provide basic information for the structure-based designs with specific functions.

3.5 Experimental section

All amino acids, DIPEA, TFA, Triphenylphosphine were purchased from Aldrich. THF, DCM, DMF, NaOH were purchased from Merck. Ethyl bromoacetate, $MeNH_2$ solution in water, HOSu, HBTU, HOBT, EtOAc, Pet-ether (60-80 ^oC) were obtained from Spectrochem and used without further purification. THF and DIPEA were dried over sodium and distilled immediately prior to use. Column chromatographies were performed on Merck silica gel (120-200 mesh). The ^1H, ^{13}C and 2D spectra were recorded on Jeol 400 MHz (or 100 MHz for ^{13}C) and Bruker 500 MHz using residual solvents signals as an internal reference ($CDCl_3$ δ_H, 7.26 ppm and δ_C, 77.00). The chemical shifts (δ) are reported in *ppm* and coupling constants (*J*) in Hz. Mass was recorded on MALDI TOF/TOF (Applied Biosystem) and CD was recorded on JASCO (*J*-815). X-Ray data were collected on Bruker APEX (II) DUO.

NMR spectroscopy: All 2D NMR studies were carried out by using a Bruker AVANCE^{III}-500 MHz spectrometer at a probe temperature of 300 K. Resonance assignments were obtained by TOCSY and ROESY analysis. All two-dimensional data were collected in phase-sensitive mode, by using the time-proportional phase incrementation (TPPI) method. Sets of 1024 and 512 data points were used in the t_2 and t_1 dimensions, respectively. For TOCSY and ROESY analysis, 32 and 72 transients were collected, respectively. A spectral width of 6007 Hz was used in both dimensions. A spin-lock time of 256 ms was used to obtain ROESY spectra. Zero-filling was carried out to finally yield a data set of 2 K ×1 K. A shifted square-sine-bell window was used before processing.

Circular dichroism (CD) spectroscopy:

CD spectrometry study was carried out on JASCO J-815 spectropolarimeter using cylindrical, jacketed quartz cell (1 mm path length), which was connected to Julabo-UC-25 water circulator. Spectra were recorded with a spectral resolution of 0.05 nm, band width 1 nm at a scan speed of 50 nm/min and a response time 1 sec. All the spectra were corrected for methanol solvent and are typically averaged over 3 scans.

Crystal structure analysis of (Boc-Aib-dgF-Aib-dgF-OEt) D1: Crystals of peptide were grown by slow evaporation from a solution of methanol/toluene. A single crystal (0.32 × 0.18 × 0.11 mm) was mounted in a loop with a small amount of the mother liquor. The X-ray data were collected at 100 K temperature on a Bruker AXS SMART APEX CCD diffractometer using MoK_α radiation (λ = 0.71073 Å), ω-scans (2θ = 56.56°), for a total number of 9672 independent reflections. Space group *P2(1)*, *a* = 9.541(8), *b* = 12.369(10), *c* = 18.060(14) Å, α = 90.00 , β = 95.405(17), γ = 90.00, *V* = 2122(3) $Å^3$, Monoclinic *P*, Z = 2 for chemical formula $C_{37}H_{50}N_4O_7.C_7H_8$, with one molecule in asymmetric unit; ρ_{calcd} = 1.182 g cm^{-3}, μ = 0.080 mm^{-1}, *F*(000) = 812, R_{int} = 0.1006. The structure was obtained by direct methods using SHELXS-97.[39] All non-hydrogen atoms were refined anisotropically. The hydrogen atoms were fixed geometrically in the idealized position and refined in the final cycle of refinement as riding over the atoms to which they are bonded. The final *R* value was 0.0866 (*wR2* = 0.1815) for 4850 observed reflections ($F_0 \geq 4\sigma(|F_0|)$) and 505 variables, *S* = 0.973. The largest difference peak and hole were 0.682 and -0.504 e $Å^3$, respectively.

Crystal structure analysis of (Boc-Aib-γ^{4}Phe-Aib-γ^{4}Phe-OEt) G1: Crystals of peptide were grown by slow evaporation from a solution of ethanol. A single crystal (0.58 × 0.43 × 0.38 mm) was mounted in a loop with a small amount of the mother liquor. The X-ray data were collected at 100 K temperature on a Bruker AXS SMART APEX CCD diffractometer using MoK_α radiation (λ = 0.71073 Å), ω-scans (2θ = 56.56°), for a total number of 36899 independent reflections. . Space group *P2(1)*, *a* = 19.123(10), *b* = 20.644(11), *c* = 20.129(11) Å, α = 90.00 , β = 98.135(11), γ = 90.00, *V* = 7866(7) $Å^3$, Monoclinic *P*, Z = 4 for chemical formula $2(C_{37}H_{54}N_4O_7).C_2H_6O$, with two molecule in asymmetric unit; ρ_{calcd} = 1.165 g cm^{-3}, μ = 0.081 mm^{-1}, *F*(000) = 2984, R_{int} = 0.0450. The structure was obtained by direct methods using SHELXS-97.[39] All non-hydrogen atoms were refined anisotropically. The hydrogen atoms were fixed geometrically in the idealized position and refined in the final cycle of refinement as riding over the atoms to which they are bonded. The final *R* value was 0.063 (*wR2* = 0.1527) for 24459 observed reflections ($F_0 \geq 4\sigma(|F_0|)$) and 1819 variables, *S* = 1.048. The largest difference peak and hole were 0.967 and -0.619 e $Å^3$, respectively.

Crystal structure analysis of (Boc-Ala-γ^{4}Phe-Aib-γ^{4}Phe-OEt) G2: Crystals of peptide were grown by slow evaporation from a solution of ethanol. A single crystal (0.34 × 0.30 × 0.28 mm) was mounted in a loop with a small amount of the mother liquor. The X-ray data

were collected at 100 K temperature on a Bruker AXS SMART APEX CCD diffractometer using MoK_α radiation (λ = 0.71073 Å), ω-scans (2θ = 56.56°), for a total number of 7324 independent reflections. Space group *P2(1)*, *a* = 10.591(4), *b* = 9.065(4), *c* = 21.005(9) Å, α = 90.00 , β = 92.232(11), γ = 90.00, V = 2015.2(15) $Å^3$, Monoclinic *P*, Z = 2 for chemical formula $C_{36}H_{53}N_4O_7.C_2H_6O$, with one molecule in asymmetric unit; ρ_{calcd} = 1.152 g cm^{-3}, μ = 0.081 mm^{-1}, *F*(000) = 756, R_{int}= 0.0624. The structure was obtained by direct methods using SHELXS-97.[39] All non-hydrogen atoms were refined anisotropically. The hydrogen atoms were fixed geometrically in the idealized position and refined in the final cycle of refinement as riding over the atoms to which they are bonded. The final *R* value was 0.0535 (*wR2* = 0.1290) for 4583 observed reflections ($F_0 \geq 4\sigma(|F_0|)$) and 460 variables, *S* = 1.026. The largest difference peak and hole were 0.269 and -0.259 e $Å^3$, respectively.

Crystal structure analysis of (Boc-Aib-γ^{4}Phe-Leu-γ^{4}Phe-OEt) G3: Crystals of peptide were grown by slow evaporation from a solution of methanol. A single crystal (0.42 × 0.35 × 0.32 mm) was mounted in a loop with a small amount of the mother liquor. The X-ray data were collected at 100 K temperature on a Bruker AXS SMART APEX II CCD Duo diffractometer using MoK_α radiation (λ = 0.71073 Å), ω-scans (2θ = 56.56°), for a total number of 14908 independent reflections. . Space group *P2(1)*, *a* = 10.132(2), *b* = 20.141(4), *c* = 21.010(4) Å, α = 90.00 , β = 99.384(5), γ = 90.00, V = 4230.1(14) $Å^3$, Monoclinic P, Z = 4 for chemical formula $(C_{39}H_{58}N_4O_7).CH_4O$, with two molecule in asymmetric unit; ρ_{calcd} = 1.141 g cm^{-3}, μ = 0.079 mm^{-1}, *F*(000) = 1576, R_{int} = 0.0699. The structure was obtained by direct methods using SHELXS-97.[39] All non-hydrogen atoms were refined anisotropically. The hydrogen atoms were fixed geometrically in the idealized position and refined in the final cycle of refinement as riding over the atoms to which they are bonded. The final *R* value was 0.0574 (*wR2* = 0.1331) for 6991 observed reflections ($F_0 \geq 4\sigma(|F_0|)$) and 958 variables, *S* = 0.929. The largest difference peak and hole were 0.256 and -0.212 e $Å^3$, respectively. Strange C-O-H Geometry (C-O .LT. 1.25 Ang…….O15) is reported in check cif. This is due to the disordered over two sites occupancy of oxygen atom (O15) in methanol solvent molecule.

Crystal structure analysis of (Boc-Ala-γ^{4}Phe-Aib-γ^{4}Phe-NHMe) G4: Crystals of peptide were grown by slow evaporation from a solution of DCM and methanol. A single crystal (0.34 × 0.32 × 0.28 mm) was mounted in a loop with a small amount of the mother liquor. The X-ray data were collected at 100 K temperature on a Bruker AXS SMART APEX CCD diffractometer using MoK_α radiation (λ = 0.71073 Å), ω-scans (2θ = 57.12°), for a total number of 8813 independent reflections. . Space group *P 2(1)*, *2(1)*, *2(1)*; *a* = 10.5245(18), *b* = 16.382(3), *c* = 22.095(4) Å, α = 90.00 , β = 90.00, γ = 90.00, *V* = 3809.4(11) Å^3, Orthorhombic *P*, Z = 4 for chemical formula $(C_{35}H_{50}N_5O_6).CH_2Cl_2$, with one molecule in asymmetric unit; ρ_{calcd} = 1.258 g cm^{-3}, μ = 0.220 mm^{-1}, *F*(000) = 1540, R_{int} = 0.0343. The structure was obtained by direct methods using SHELXS-97.[39] All non-hydrogen atoms were refined anisotropically. The hydrogen atoms were fixed geometrically in the idealized position and refined in the final cycle of refinement as riding over the atoms to which they are bonded. The final *R* value was 0.0511 (*wR2* = 0.1180) for 8813 observed reflections ($F_0 \geq 4\sigma(|F_0|)$) and 449 variables, *S* = 1.015. The largest difference peak and hole were 0.280 and -0.262 e Å^3, respectively.

Crystal structure analysis of (Boc-Aib-γ^{4}Phe-Leu-γ^{4}Phe-Aib-dgF-OEt) D4: Crystals of peptide were grown by slow evaporation from a solution of ethylacetate and hexane. A single crystal (0.35 × 0.28 × 0.16 mm) was mounted in a loop with a small amount of the mother liquor. The X-ray data were collected at 100 K temperature on a Bruker AXS SMART APEX II CCD Duo diffractometer using MoK_α radiation (λ = 0.71073 Å), ω-scans (2θ = 56.56°), for a total number of 28846 independent reflections. . Space group *P2(1)*, *a* = 14.850(6), *b* = 18.173(7), *c* = 24.075(9) Å, α = 90.00 , β = 107.254(7), γ = 90.00, V = 6204(4) Å^3, Monoclinic *P*, Z = 4 for chemical formula $2(C_{54}H_{76}N_6O_9).H_2O$, with two molecule in asymmetric unit; ρ_{calcd} = 1.029 g cm^{-3}, μ = 0.071 mm^{-1}, *F*(000) = 2072, R_{int} = 0.0660. The structure was obtained by direct methods using SHELXS-97.[39] All non-hydrogen atoms were refined anisotropically. The hydrogen atoms were fixed geometrically in the idealized position and refined in the final cycle of refinement as riding over the atoms to which they are bonded. The final *R* value was 0.0576 (*wR2* = 0.1400) for 13821 observed reflections ($F_0 \geq 4\sigma(|F_0|)$) and 1272 variables, *S* = 0.788. The largest difference peak and hole were 0.215 and -0.197 e Å^3, respectively.

There were partially occupied molecules of some solvent also present in the asymmetric unit. A significant amount of time was invested in identifying and refining the disordered

molecules. It was observed that one hexane and EtOAC molecule, which tend to host disordered solvent molecules. Bond length restraints were applied to model the molecules but the resulting isotropic displacement coefficients suggested the molecules were highly mobile. In addition, the refinement was computationally unstable. Option SQUEEZE of program PLATON[40] was used to correct the diffraction data for diffuse scattering effects and to identify the solvent molecule. PLATON calculated the upper limit of volume that can be occupied by the solvent to be 1149.4Å^3, or 18.5% of the unit cell volume. The program calculated 60 electrons in the unit cell for the diffuse species. No data are given for the diffusely scattering species.

Crystal structure analysis of (Boc-Aib-γ^{4}Phe-Leu-γ^{4}Phe-Aib-γ^{4}Phe-OEt) G5: Crystals of peptide were grown by slow evaporation from a solution of acetone. A single crystal (0.42 × 0.32 × 0.18 mm) was mounted in a loop with a small amount of the mother liquor. The X-ray data were collected at 100 K temperature on a Bruker AXS SMART APEX II CCD Duo diffractometer using MoK$_\alpha$ radiation (λ = 0.71073 Å), ω-scans (2θ = 56.56^o), for a total number of 27803 independent reflections. . Space group *P 2(1)*, *2(1)*, *2(1)*; *a* = 17.910(3), *b* = 24.339(4), *c* = 26.446(4) Å, α = 90.00 , β = 90.00, γ = 90.00, V = 11528(3) Å^3, Orthorhombic *P*, Z = 4 for chemical formula 2($C_{54}H_{78}N_6O_9$).H_2O, with two molecule in asymmetric unit; ρ_{calcd} = 1.111 g cm^{-3}, μ = 0.076 mm^{-1}, *F*(000) = 4168, R_{int} = 0.0661. The structure was obtained by direct methods using SHELXS-97.[39] All non-hydrogen atoms were refined anisotropically. The hydrogen atoms were fixed geometrically in the idealized position and refined in the final cycle of refinement as riding over the atoms to which they are bonded. The final *R* value was 0.0927 (*wR2* = 0.2457) for 11730 observed reflections ($F_0 \geq 4\sigma(|F_0|)$) and 1258 variables, *S* = 1.074. The largest difference peak and hole were 0.720 and -0.331 e Å^3, respectively.

There were partially occupied molecules of some solvent also present in the asymmetric unit. A significant amount of time was invested in identifying and refining the disordered molecules. It was observed that two acetone molecules, which tend to host disordered solvent molecules. Bond length restraints were applied to model the molecules but the resulting isotropic displacement coefficients suggested the molecules were highly mobile. In addition, the refinement was computationally unstable. Option SQUEEZE of program PLATON[40] was used to correct the diffraction data for diffuse scattering.

Synthesis of Dipeptide

Boc-Aib-dgF-OEt:

(*S*, *E*)-ethyl 4-(*tert*-butoxycarbonylamino)-5-phenylpent-2-enoate (Boc-dgF-OEt) (11 mmol, 3.15 g) was dissolved in DCM (10 mL) and cooled the solution in ice bath. Then, 10 mL of neat TFA was added slowly to this solution. After completion of the reaction (~ 30 min), TFA was removed from the reaction mixture under *vacuum*. The residue was dissolved in water and the pH was adjusted to ~ 10 by the slow addition of solid Na_2CO_3 in ice cold conditions. Then Boc deprotected free amine was extracted with ethyl acetate (3 × 40 mL). The combined organic layer was washed with brine (60 mL), dried over Na_2SO_4, concentrated under *vacuum* to *ca*. 2 mL and directly used for the coupling reaction in the next step.

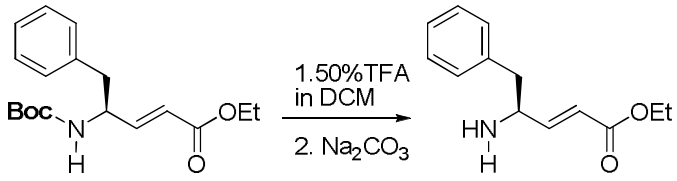

Boc-Aib-OH (10 mmol, 2 g) and NH_2-dgF-OEt were dissolved together in DMF (6 mL), followed by HBTU (11 mmol, 4.2 g) was added to the reaction mixture and cooled to 0 ^oC for 5 min. Then, DiPEA (12 mmol, 2.15 mL) was added to the reaction mixture with stirring and the reaction mixture was allowed to come to room temperature. The progress of the reaction was monitored by TLC. After completion

(roughly 6 hrs), the reaction mixture was diluted with 400 mL of ethyl acetate and washed with 5% HCl (2 × 150 mL), 10 % sodium carbonate solution in water (2 × 150 mL) and followed by brine (130 mL). The organic layer was dried over anhydrous Na_2SO_4 and evaporated under reduced pressure to give gummy yellowish product, which was purified on silica gel column chromatography using EtOAc/Petether (60-80 ^oC) to get white crystalline product. Overall yield 75% (3.25 g, 7.5 mmol).

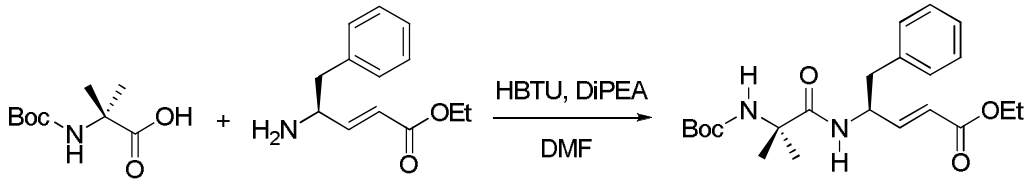

Boc-Aib-dgF-OEt

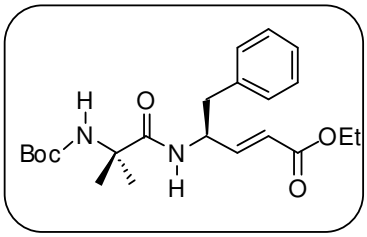

Physical state **:** white powder

Mol. Formula **:** $C_{22}H_{32}N_2O_5$

Yield **:** 75%, 3.25g

^{1}H NMR (400 MHz, $CDCl_3$) **:** δ_H δ 7.31-7.17 (m, 5H, -Ph), 6.96-6.91 (dd, *J* = 5.04, *J* = 11.3, 1H, C*H*=CHCO$_2$Et), 6.69 (b, 1H, NH), 5.94-5.90 (d, *J* = 16.8, 1H, CH=C*H*CO$_2$Et), 4.98-4.91 (m, 1H, C*H*-CH=CH), 4.81 (s, 1H, NH), 4.19-4.13 (q, *J* = 6.88, 2H, -OC*H*$_2$), 2.99-2.84 (m, 2H, C*H*$_2$-Ph), 1.44 (s, 15H, -(CH$_3$)$_3$ Boc, -(CH$_3$)$_2$ Aib), 1.27-1.24 (t, *J* = 7.3, 3H, -OCH$_2$C*H*$_3$).

^{13}C NMR (100 MHz, $CDCl_3$) **:** δ_C 173.37, 166.30, 154.98, 147.18, 136.55, 129.37, 128.63, 126.94, 121.21, 80.95, 60.44, 56.93, 50.76, 40.64, 28.36, 25.22, 14.27.

MALDI TOF/TOF m/z **:** Calcd. $[M+Na]^+$ 427.2209, observed 427.2511

(Boc-Ala-dgF-OEt):

(*S*, *E*)-ethyl 4-(tert-butoxycarbonylamino)-5-phenylpent-2-enoate (Boc-dgF-OEt) (5.5 mmol, 1.57 g) was dissolved in DCM (5 mL) and cooled the solution in ice bath. Then 5mL neat TFA was added to this solution. After 30 min reaction was completed, monitored by TLC. Then TFA was removed from reaction mixture under vacuum. The residue was dissolved in water and the pH was adjusted to ~10 by the slow addition of solid Na_2CO_3 in ice cold conditions. Then Boc deprotected free amine was extracted with ethyl acetate (3 × 40 mL). Combined organic layer was washed with brine (60 mL) followed by dried over Na_2SO_4 and concentrated under vacuum to *ca*.2 mL for coupling.

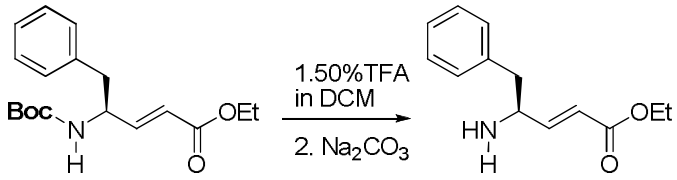

Boc-Ala-OH (5 mmol, 0.95 g) and NH_2-dgF-OEt were dissolved together in DMF (4 mL) and HBTU (5.5 mmol, 2.1 g) was added into the reaction mixture. Then reaction mixture was cooled to 0 ^oC for 5 min. Then DiEPA (6 mmol, 1.05 mL) was added to the reaction mixture and it was allowed to come in room temperature. The progress of the reaction was monitored by TLC. After completion of the reaction (roughly 6 hrs), reaction mixture was diluted with 300 mL of ethyl acetate and washed with 5% HCl (5 % by vol. in water, 2 × 100 mL), 10 % sodium carbonate solution in water (2 × 100 mL) and followed by brine (100 mL). The organic layer was dried over Na_2SO_4 and evaporated under reduced pressure to get gummy yellowish product, which was purified on silica gel column chromatography using EtOAc/Pet-ether (60-80 ^oC) to get gummy product. Overall yield 88% (1.72 g, 4.4 mmol).

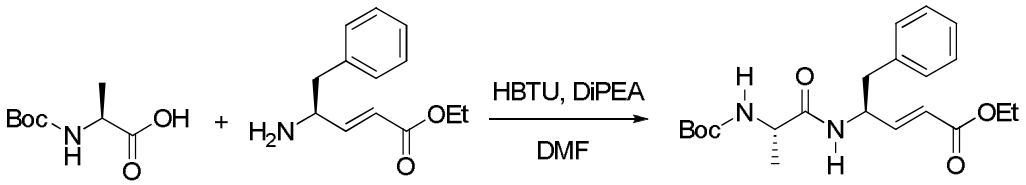

Boc-Ala-dgF-OEt

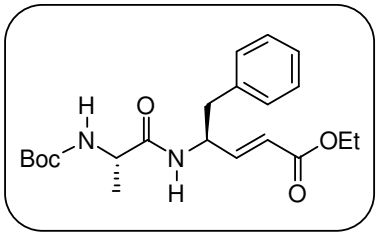

Physical state **:** colourless gummy

Mol. Formula **:** $C_{21}H_{30}N_2O_5$

Yield **:** 88%, 1.72g

^{1}H NMR (400 MHz, $CDCl_3$) **:** δ_H 7.31-7.15 (m, 5H, -Ph), 6.94-6.88 (dd, *J* = 4.8, *J* = 10.8, 1H, C*H*=CHCO$_2$Et), 6.34-6.32 (d, *J* = 7.84, 1H, NH), 5.87-5.82 (d, *J* = 17.4, 1H, CH=C*H*CO$_2$Et), 4.94-4.89 (m, 1H, α-H of Ala), 4.84-4.83 (d, *J* = 6.16, 1H, NH), 4.19-4.07 (m, 3H, -OC*H*$_2$, C*H*-CH=CH), 2.97-2.84 (m, 2H, C*H*$_2$-Ph), 1.44 (s, 9H, -(CH$_3$)$_3$ Boc), 1.28-1.24 (m, 6H, -OCH$_2$C*H*$_3$, -C*H*$_3$).

^{13}C NMR (100 MHz, $CDCl_3$) **:** δ_C 171.94, 166.03, 146.60, 136.18, 129.26, 128.58, 126.94, 121.32, 79.68, 60.46, 50.57, 40.41, 28.25, 25.22, 14.17.

MALDI TOF/TOF m/z **:** Calcd. $[M+Na]^+$ 413.2052, observed 413.2655.

(Boc-Leu-dgF-OEt)

(*S*, *E*)-ethyl 4-(tert-butoxycarbonylamino)-5-phenylpent-2-enoate (Boc-dgF-OEt) (5.5 mmol, 1.57 g) was dissolved in DCM (5 mL) and the solution was cooled in ice bath. Then, 5 mL of neat TFA was added slowly to the solution. After completion of the reaction (30 min.), the TFA was removed from reaction mixture under reduced pressure. The residue was dissolved in water and the pH was adjusted to ~10 by the slow addition of solid Na_2CO_3 in ice cold conditions. The Boc deprotected free amine was extracted with ethyl acetate (3 × 40 mL). The combined organic layer was washed with brine (60 mL), dried over anhydrous Na_2SO_4 and concentrated under *vacuum* to *ca*. 2 mL and directly used for coupling reaction.

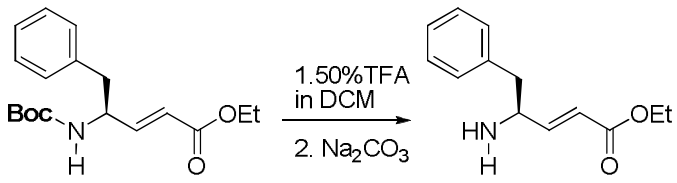

Boc-Leu-OH (5 mmol, 1.15 g) and NH_2-dgF-OEt were dissolved together in DMF (4 mL) and HBTU (5.5 mmol, 2.1 g) was added into the reaction mixture. The reaction mixture was cooled to 0 ^oC for 5 min.Then DiPEA (6 mmol, 1.05 mL) was added to the reaction mixture and allowed to come to room temperature. The progress of the reaction was monitored by TLC. After completion of the reaction (roughly 6 hrs), the reaction mixture was diluted with 300 mL of ethyl acetate and washed with 5%

HCl (2 × 100 mL), 10 % sodium carbonate solution in water (2 × 100 mL) followed by brine (100 mL). The organic layer was dried over anhydrous Na_2SO_4 and evaporated under reduced pressure to get gummy yellowish product, which was purified via silica gel column chromatography using EtOAc/Petether (60-80 ^oC) to get white solid product. Overall yield 78% (1.68 g, 3.9 mmol).

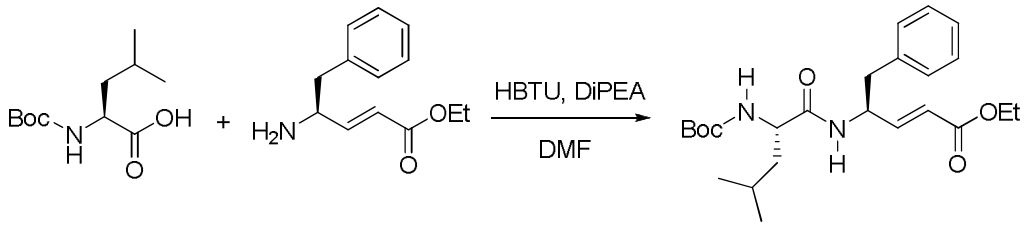

Boc-Leu-dgF-OEt

Physical state **:** white powder

Mol. Formula **:** $C_{24}H_{36}N_2O_5$

Yield **:** 78%

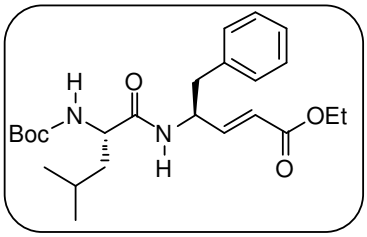

^{1}H NMR (400 MHz, $CDCl_3$) **:** δ_H 7.31-7.16 (m, 5H, -Ph), 6.94-6.88 (dd, *J* = 4.9, *J* = 10.9, 1H, C*H*=CHCO$_2$Et), 6.34-6.31 (d, *J* = 8.8, 1H, NH), 5.86-5.82 (d, *J* = 16.9, 1H, CH=C*H*CO$_2$Et), 4.08-4.90 (m, 1H, α-H of Leu), 4.74-4.73 (d, *J* = 5.8, 1H, NH), 4.20-4.14 (q, *J* = 7.1, 2H, -OC*H*$_2$), 4.08-3.99 (m, 1H, C*H*-CH=CH), 2.97-2.85 (m, 2H, C*H*$_2$-Ph), 2.08-2.05 (m, 2H, β-H of Leu), 1.63-1.54 (m, 1H, γ-H of Leu), 1.44 (s, 9H, -(CH$_3$)$_3$ Boc), 1.28-1.25 (t, *J* = 7.1, 3H, -OCH$_2$C*H*$_3$), 0.92-0.90 (d, *J* = 6.9, 3H).

^{13}C NMR (100 MHz, $CDCl_3$) **:** δ_C 171.95, 166.05, 155.74, 146.57, 136.18, 129.29, 128.58, 126.94, 121.35, 80.42, 60.47, 50.62, 40.43, 31.57, 28.24, 24.69, 22.88, 14.17.

MALDI TOF/TOF m/z **:** Calcd. $[M+Na]^+$ 455.2522, observed 455.3341.

Synthesis of Tetrapeptide

(Boc-Aib-dgF-Aib-dgF-OEt) (D1)

Boc-Aib-dgF-OH: Boc-Aib-dgF-OEt (2 mmol, 0.810 g) was dissolved in ethanol (5 mL). Then 5 mL of 1(N) NaOH was added slowly to this solution. After completion of the reaction (~ 2 hrs), ethanol was evaporated from reaction mixture and residue was acidified to *p*H ~ 3 using 5% HCl (5% volume in water) at cold conditions after diluting with 50 mL cold water. Product was extracted with ethyl acetate (3 × 30 mL). Combined organic layer was washed

with brine (40 mL) and dried over anhydrous Na_2SO_4. Organic layer was concentrated under reduced pressure to give gummy product with quantitative yield 98% (1.96 mmol, 0.742 g).

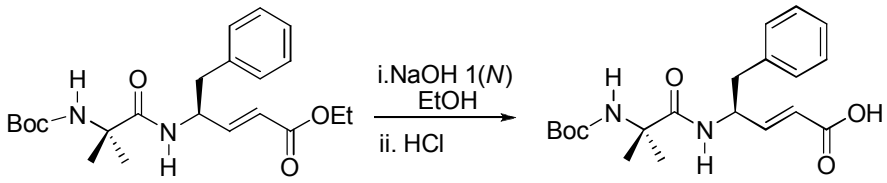

NH_2-Aib-dgF-OEt: Boc-Aib-dgF-OEt (2.2 mmol, 0.90 g) was dissolved in DCM (5 mL) and cooled the solution in ice bath. Then 5 mL neat TFA was added to the solution. After completion of the reaction (~ 30 min), TFA was removed from reaction mixture under vacuum. The residue was dissolved in water and the pH was adjusted to ~ 10 by the slow addition of solid Na_2CO_3 in ice cold conditions. Then Boc deprotected dipeptide was extracted with ethyl acetate (3 × 40 mL). Combined organic layer was washed with brine (60 mL) followed by dried over Na_2SO_4 and concentrated under vacuum to *ca*.2 mL and used for coupling reaction in the next step.

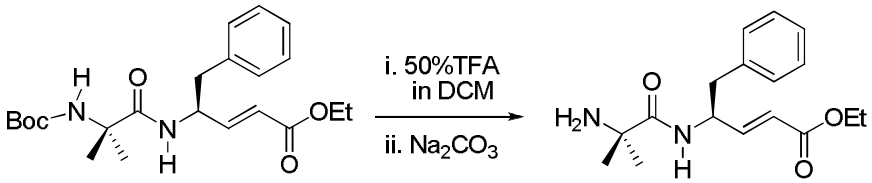

Boc-Aib-dgF-OH (1.96 mmol, 0.742 g) and NH_2-Aib-dgF-OEt were dissolved together in DMF (5 mL) followed by HBTU (2.2 mmol, 0.820 g) was added. The reaction mixture was cooled to 0 ^oC for 5 min. Then DiEPA (2.5 mmol, 0.45 mL) was added to the reaction mixture and it was allowed to come in room temperature at constant stirring. The progress of the reaction was monitored by TLC. After completion of the reaction (roughly 4hrs), reaction mixture was diluted with 200 mL of ethyl acetate and washed with 5% HCl (5 % by vol. in water, 2 × 80 mL), 10 % sodium carbonate solution in water (2 × 80 mL) and followed by brine (80 mL). The organic layer was dried over Na_2SO_4 and evaporated under reduced pressure to give gummy yellowish product, which was purified on silica gel column chromatography using DCM/MeOH solvent system to get gummy product, which was further crystallized using EtOAc/Hexane. Overall yield 70% (1.4 mmol, 0.861 g).

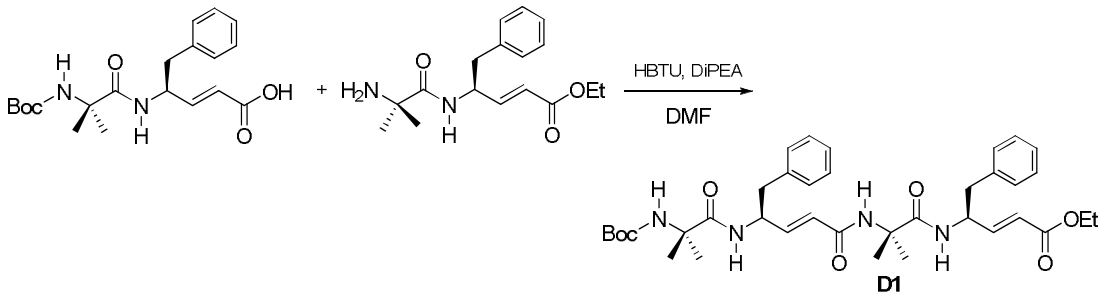

Boc-Aib-dgF-Aib-dgF-OEt (D1)

Physical state : white crystalline powder

Mol. Formula : $C_{37}H_{50}N_4O_7$

Yield : 70%, 0.861g

^{1}H NMR (500 MHz, $CDCl_3$) : δ_H 7.36-7.21 (m, 11H, -Ph, NH), 7.00-6.97 (dd, *J* = 5.04, *J* = 11, 1H, C*H*=CH), 6.92-6.89 (dd, *J* = 4.84, *J* = 10.7, 1H, C*H*=CH), 6.42-6.41 (d, *J* = 8.45, 1H, NH), 6.15-6.13 (d, *J* = 14.4, 1H, CH=C*H*), 6.02 (s, 1H, NH), 5.93-5.90 (d, *J* = 15, 1H, CH=C*H*), 4.98-4.92 (m, 2H, C*H*-CH=CH), 4.90 (s, 1H, NH), 4.25-4.21 (q, *J* = 6.88, 2H, -OCH_2), 3.05-2.88 (m, 4H, CH_2-Ph), 1.52 (s, 3H, -$(CH_3)_2$), 1.50 (s, 3H, -$(CH_3)_2$), 1.43 (s, 12H, -$(CH_3)_3$ Boc, -$(CH_3)_2$ Aib), 1.34-1.31 (m, 6H, -OCH_2CH_3, -$(CH_3)_2$ Aib).

MALDI TOF/TOF m/z : Calcd. $[M+Na]^+$ 685.3620, observed 685.4178.

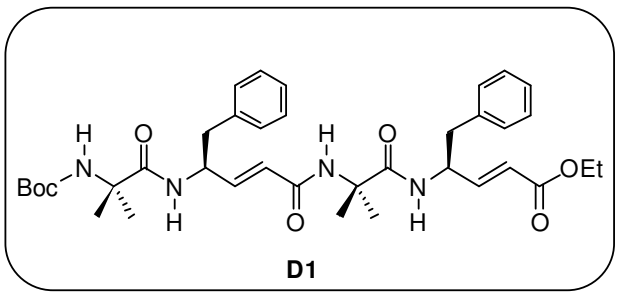

(*Boc-Ala-dgF-Aib-dgF-OEt*) (D2)

Boc-Ala-dgF-OH: Boc-Ala-dgF-OEt (2 mmol, 0.780 g) was dissolved in ethanol (7 mL). Then 5 mL of 1(N) NaOH was added slowly to this solution. After completion of the reaction (~ 2 hrs), ethanol was evaporated from reaction mixture and residue was acidified to *p*H ~ 3

using 5% HCl (5% volume in water) at cold conditions after diluting with 50 mL cold water. Product was extracted with ethyl acetate (3 × 30 mL). Combined organic layer was washed with brine (40 mL) and dried over anhydrous Na_2SO_4. Organic layer was concentrated under reduced pressure to give gummy product with quantitative yield 99% (1.98 mmol, 0.716 g).

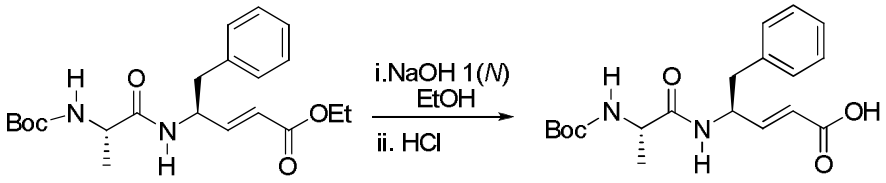

NH_2-Aib-dgF-OEt: Boc-Aib-dgF-OEt (2.2 mmol, 0.810 g) was dissolved in DCM (5 mL) and cooled the solution in ice bath. Then 5 mL neat TFA was added to the solution. After completion of the reaction (~ 30 min), TFA was removed from reaction mixture under vacuum. The residue was dissolved in water and the pH was adjusted to ~ 10 by the slow addition of solid Na_2CO_3 in ice cold conditions. Then Boc deprotected dipeptide was extracted with ethyl acetate (3 × 40 mL). Combined organic layer was washed with brine (60 mL) followed by dried over Na_2SO_4 and concentrated under vacuum to *ca*.2 mL and used for coupling reaction in the next step.

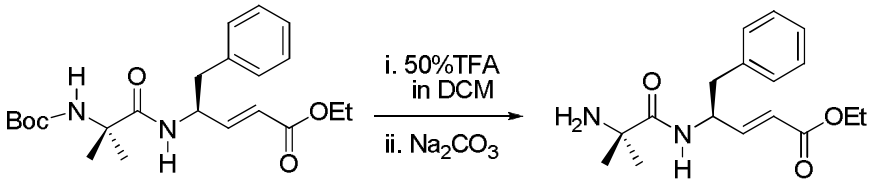

Boc-Ala-dgF-OH (1.83 mmol, 0.742 g) and NH_2-Aib-dgF-OEt were dissolved together in DMF (5 mL) followed by HBTU (2.2 mmol, 0.820 g) was added. The reaction mixture was cooled to 0 ^oC for 5 min. Then DiEPA (2.5 mmol, 0.45 mL) was added to the reaction mixture and it was allowed to come in room temperature at constant stirring. The progress of the reaction was monitored by TLC. After completion of the reaction (roughly 4hrs), reaction mixture was diluted with 200 mL of ethyl acetate and washed with 5% HCl (5 % by vol. in water, 2 × 80 mL), 10 % sodium carbonate solution in water (2 × 80 mL) and followed by

brine (80 mL). The organic layer was dried over Na_2SO_4 and evaporated under reduced pressure to give gummy yellowish product, which was purified on silica gel column chromatography using DCM/MeOH solvent system to get gummy product, which was further crystallized using EtOAc/Hexane. Overall yield 73% (1.46 mmol, 0.946 g).

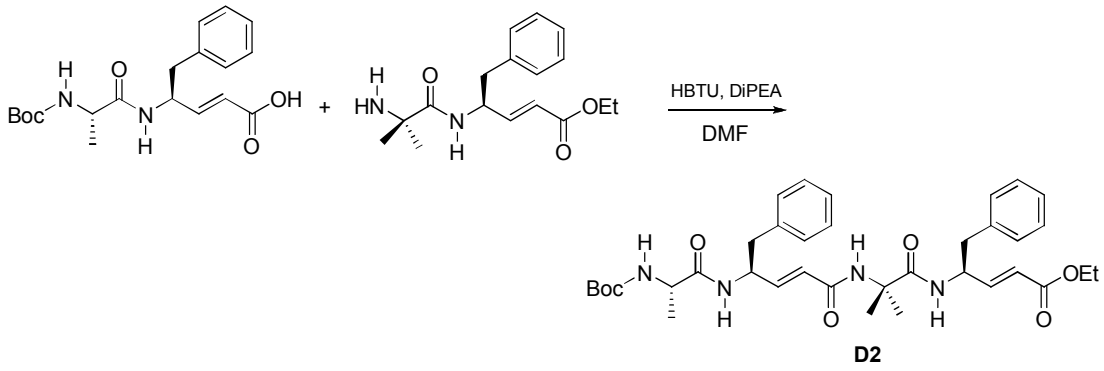

Boc-Ala-dgF-Aib-dgF-OEt (D2)

Physical state **:** white crystalline powder

Mol. Formula **:** $C_{36}H_{48}N_4O_7$

Yield **:** 73%, 0.716 g

^{1}H NMR (500 MHz, $CDCl_3$) **:** δ_H 7.31-7.15 (m, 11H, -Ph, NH of dgF), 6.96-6.91 (dd, *J* = 5, *J* = 10.8, 1H, C*H*=CH), 6.85-6.80 (dd, *J* = 4.7, *J* = 10.8, 1H, C*H*=CH), 6.35-6.33 (b, 1H, NH), 5.95 (b, 1H, NH) 5.90-5.83 (m, 2H, CH=C*H*), 4.93-4.88 (m, 2H), 4.82-4.79 (d, *J* = 9.47, 1H, NH), 4.20-4.15 (q, *J* = 7.1, 2H, -OCH_2), 4.10-4.07 (m, 2H), 3.00-2.81 (m, 4H, CH_2-Ph), 1.46 (s, 3H, -$(CH_3)_2$), 1.41 (s, 9H, -$(CH_3)_3$ Boc), 1.40 (s, 3H, -$(CH_3)_2$) Aib), 1.29-1.25 (m, 6H, -OCH_2CH_3, -$(CH_3)_2$ Aib).

MALDI TOF/TOF m/z **:** Calcd. $[M+Na]^+$ 671.3421, observed 671.4699

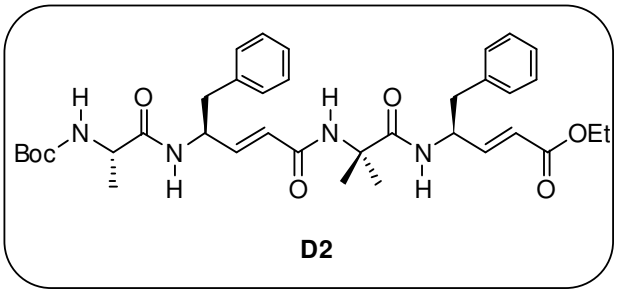

Boc-Aib-dgF-Leu-dgF-OEt (D3)

Boc-Aib-dgF-OH: Boc-Aib-dgF-OEt (2 mmol, 0.810 g) was dissolved in ethanol (5 mL). Then 5 mL of 1(N) NaOH was added slowly to this solution. After completion of the reaction (~ 2 hrs), ethanol was evaporated from reaction mixture and the residue was acidified to *p*H ~ 3 using 5% HCl (5% volume in water) at cold conditions after diluting with 50 mL of cold water. Product was extracted with ethyl acetate (3 × 30 mL). Combined organic layer was washed with brine (40 mL) and dried over anhydrous Na_2SO_4. Organic layer was concentrated under reduced pressure to give gummy product with quantitative yield 98% (1.83 mmol, 0.742 g).

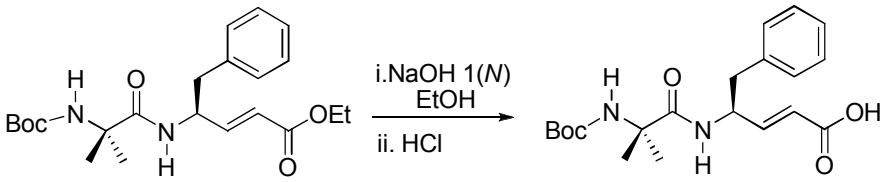

NH_2-Leu-dgF-OEt: Boc-Leu-dgF-OEt (2.2 mmol, 0.870 g) was dissolved in DCM (5 mL) and cooled the solution in ice bath. Then 5 mL of neat TFA was added to the solution. After completion of the reaction (~ 30 min), TFA was removed from reaction mixture under *vacuum*. The residue was dissolved in water and the pH was adjusted to ~ 10 by the slow addition of solid Na_2CO_3 in ice cold conditions. Then Boc deprotected dipeptide was extracted with ethyl acetate (3 × 40 mL). Combined organic layer was washed with brine (60 mL), dried over anhydrous Na_2SO_4, concentrated under *vacuum* to *ca*. 2 mL and directly used for coupling reaction in the next step.

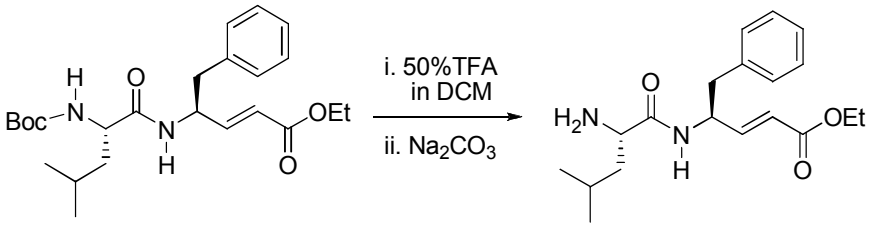

Boc-Aib-dgF-OH (1.83 mmol, 0.742 g) and NH_2-Leu-dgF-OEt were dissolved together in DMF (5 mL) followed by HBTU (2.2 mmol, 0.820 g) was added. The reaction mixture was cooled to 0 ^oC for 5 min. Then DiPEA (2.5 mmol, 0.45 mL) was added to the reaction

mixture and it was allowed to come to room temperature at constant stirring. The progress of the reaction was monitored by TLC. After completion of the reaction (roughly 4hrs), the reaction mixture was diluted with 200 mL of ethyl acetate and washed with 5% HCl (2 × 80 mL), 10 % sodium carbonate solution in water (2 × 80 mL) and followed by brine(80 mL). The organic layer was dried over anhydrous Na_2SO_4 and evaporated under reduced pressure to give gummy yellowish product, which was purified on silica gel column chromatography using DCM/MeOH solvent system to get gummy product, which was further crystallized using EtOAc/Hexane. Overall yield 68% (1.36 mmol, 0.938 g).

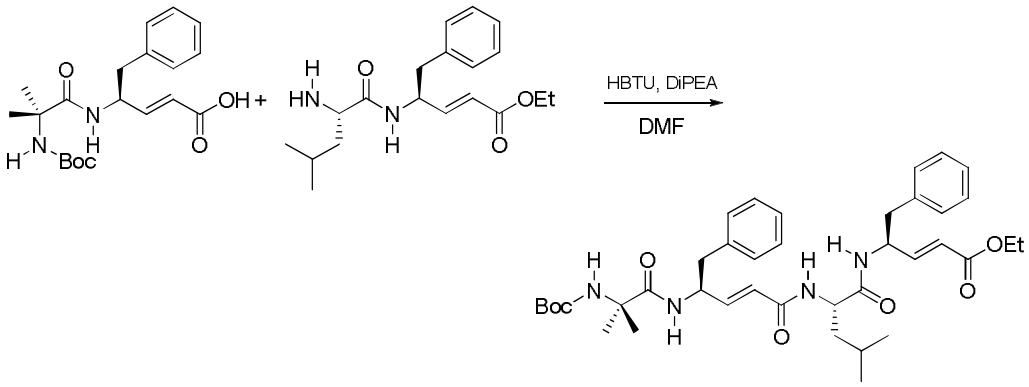

Boc-Aib-dgF-Leu-dgF-OEt (D3)

Physical state **:** white crystalline powder

Mol. Formula **:** $C_{39}H_{54}N_4O_7$

Yield **:** 68%, 0.938 g

^{1}H NMR (500 MHz, $CDCl_3$) **:** δ_H 7.31-7.10 (m, 10H, -Ph), 6.92-6.84 (m, 2H, C*H*=CH), 6.66-6.84 (d, *J* = 8.5, 1H, NH), 6.44-6.42 (d, *J* = 8.5, 1H, NH), 6.06-6.02 (d, *J* = 15.5, 1H, CH=C*H*), 5.88-5.83 (d, *J* = 17.4, 1H, CH=C*H*), 5.80-5.78 (d, *J* = 7.8, 1H, NH), 5.00-4.95 (m, 2H), 4.91-4.84 (m, 1H, -CH-), 4.81 (s, 1H, NH), 4.46-4.40 (m, 1H, -CH-), 4.20-4.15 (q, *J* = 7, 2H, -OCH_2), 3.03-2.77 (m, 4H, CH_2-Ph), 1.71-1.52 (m, 3H, α and β-H of Leu), 1.47 (s, 3H, -$(CH_3)_2$ Aib), 1.39 (s, 9H, -$(CH_3)_3$ Boc), 1.29-1.26 (t, *J* = 7.1, 3H, -OCH_2CH_3), 1.27 (s, 3H, -$(CH_3)_2$ Aib), 0.90-0.88 (d, *J* = 6.8, 3H, -CH_3 of Leu), 0.87-0.86 (d, *J* = 6.8, 3H, -CH_3 of Leu).

MALDI TOF/TOF m/z **:** Calcd. $[M+Na]^+$ 713.3890, observed 713.4538.

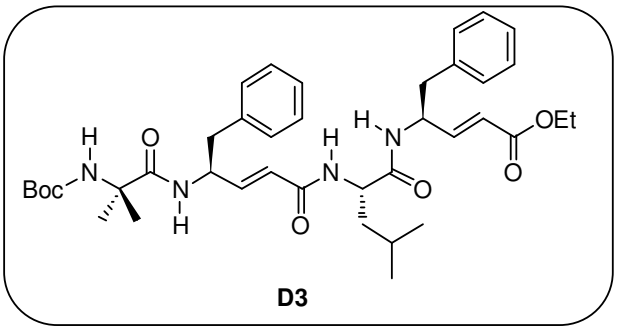

D3

General procedure for transformation of Vinylogous hybrid tetra peptide to its saturated hybrid γ^4-peptide analogue

Vinylogous hybrid tetra peptide (0.5 mmol) was dissolved in EtOH (5 mL), and was treated with 60 mg of Pd/C. The hydrogen gas was supplied through balloon. The schematic representation is shown below. The reaction mixture was stirred under hydrogen atmosphere for about 6 hrs. The completion of the reaction was monitored by MALDI TOF/TOF and HPLC. After the completion of reaction, the reaction mixture was diluted with EtOH (30 mL) and it was filtered through sintered funnel using celite bed and celite bed was washed with EtOH (3 × 25mL). The filtrate was evaporated under vacuum to get white crystalline pure product. Overall, the γ-hybrid peptide was isolated with quantitative yield.

a) Boc-Aib-γ^4Phe-Aib-γ^4Phe-OEt:

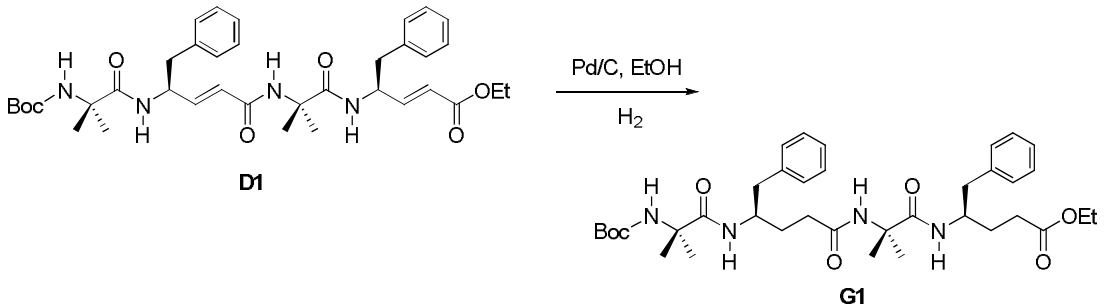

D1 **G1**

Boc-Aib-γ⁴Phe-Aib-γ⁴Phe-OEt (G1)

Physical state : white crystalline powder

Mol. Formula : $C_{37}H_{54}N_4O_7$

Yield : 95%

^{1}H NMR (500 MHz, $CDCl_3$) : δ_H 7.59-7.58 (d, *J* = 9, 1H, NH of γF), 7.38-7.20 (m, 10H, -Ph), 7.03 (s, 1H, NH of U), 5.86-5.84 (d, *J* = 9.4, 1H, NH of γF), 4.94 (s, 1H, NH of U), 4.37-4.30 (m, 2H, C*H*-CH_2-CH_2), 4.19-4.15 (q, *J* = 7, 2H, -OC*H*$_2$), 3.08-2.71 (m, 4H, C*H*$_2$-Ph), 2.69-2.46 (m, 4H, C*H*$_2$-C=O), 2.34-1.98 (m, 4H, C*H*$_2$-CH_2-C=O), 1.54 (s, 3H, -$(CH_3)_2$ Aib), 1.47 (s, 12H, -$(CH_3)_3$ Boc, -$(CH_3)_2$ Aib), 1.30-1.27 (t, *J*=7, 3H, -OCH_2CH_3), 1.25 (s, 3H, -$(CH_3)_2$ Aib), 1.06 (s, 3H, -$(CH_3)_2$ Aib).

MALDI TOF/TOF m/z : Calcd. $[M+Na]^+$ 689.3890, observed 689.4219.

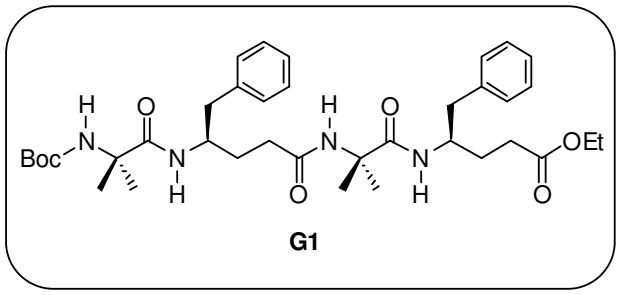

G1

b) Boc-Ala-γ⁴Phe-Aib-γ⁴Phe-OEt (G2):

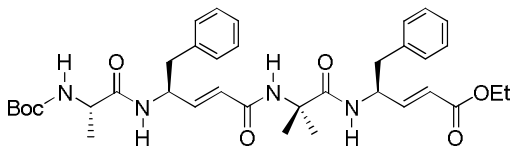

D2

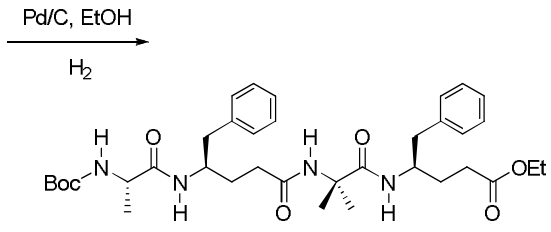

G2

Boc-Ala-γ^4Phe-Aib-γ^4Phe-OEt (G2)

Physical state : white crystalline powder

Mol. Formula : $C_{36}H_{52}N_4O_7$

Yield : 97%

^{1}H NMR (500 MHz, $CDCl_3$) : δ_H 7.30-7.15 (m, 11H, NH, -Ph), 6.74 (b, 1H, NH), 6.00 (b, 1H, NH), 4.92 (b, 1H, NH), 4.27-4.21 (m, 1H, -CH-), 4.15-4.08 (m, 3H, -OC*H*$_2$, -CH-), 3.97-3.94 (m, 1H, -CH-), 2.97-2.60 (m, 5H, C*H*$_2$-Ph, -C*H*$_2$-), 2.44-2.38 (m, 1H, -C*H*$_2$-), 2.24-1.72 (m, 6H, -C*H*$_2$-), 1.45 (s, 3H, -$(CH_3)_2$ Aib), 1.43 (s, 9H, -$(CH_3)_3$ Boc), 1.26-1.21 (m, 6H, -OCH_2CH_3, -CH_3 of Ala), 1.11 (s, 3H, -$(CH_3)_2$ Aib

MALDI TOF/TOF m/z : Calcd. $[M+Na]^+$ 675.3734, observed 675.4694

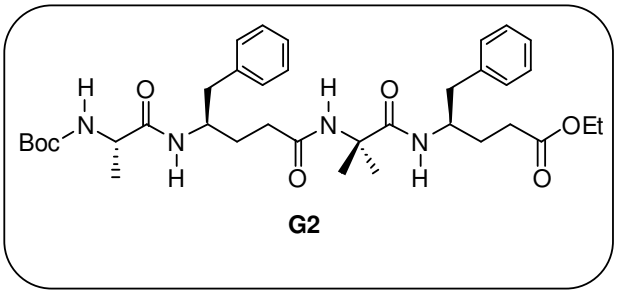

G2

c) Boc-Aib-γ^4Phe-Leu-γ^4Phe-OEt:(G3):

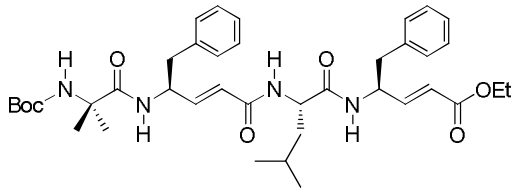

D3

Pd/C, EtOH

H_2

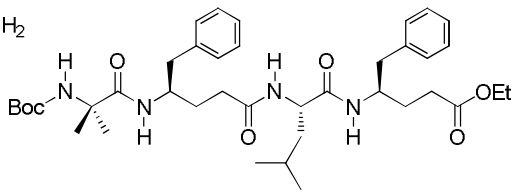

G3

Boc-Aib-γ^4Phe-Leu-γ^4Phe-OEt (G3)

Physical state : white crystalline powder

Mol. Formula : $C_{39}H_{58}N_4O_7$

Yield : 96%

^{1}H NMR (500 MHz, $CDCl_3$) : δ_H 7.49-7.47 (d, *J* = 8.7, 1H, NH), 7.29-7.13 (m, 10H, -Ph), 6.76 (s, 1H, NH), 5.85-5.83 (d, *J* = 9.28, 1H, NH), 4.93 (s, 1H, NH), 4.30-4.18 (m, 2H, -C*H*-), 4.12-4.07 (m, 3H, -OCH_2, -C*H*-), 3.00-2.80 (m, 4H, CH_2-Ph), 2.65-2.60 (m, 1H, CH_2-Ph), 2.57-2.36 (m, 2H, -CH_2-), 2.30-2.10 (m, 3H, -CH_2-), 1.97-1.72 (m, 14H, -CH_2-), 1.60-1.53 (m, 1H, γ-H of Leu), 1.48 (s, 3H, -$(CH_3)_2$ Aib), 1.41 (s, 9H, -$(CH_3)_3$ Boc), 1.26-1.22 (t, *J* = 7, 3H, -OCH_2CH_3), 1.22 (s, 3H, -$(CH_3)_2$ Aib), 0.84-0.82 (d, *J* = 6.6, 3H, -CH_3 of Leu), 0.80-0.79 (d, *J* = 6.9, 3H, -CH_3 of Leu).

MALDI TOF/TOF m/z : Calcd. $[M+Na]^+$ 717.4203, observed 717.5516.

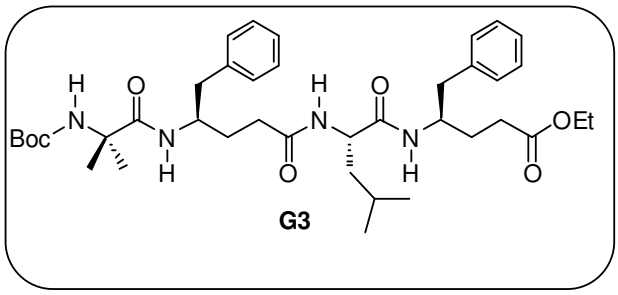

Synthesis of (Boc-Ala-γ^4Phe-Aib-γ^4Phe-NHMe) (G4)

Boc-Ala-γ^4Phe-Aib-γ^4Phe-OH: Boc-Ala-γ^4Phe-Aib-γ^4Phe-OEt (0.33 mmol, 0.210 g) was dissolved in ethanol (4 mL). Then 5 mL of 1(N) NaOH was added slowly to this solution. After completion of the reaction (~ 2 hrs), ethanol was evaporated from reaction mixture and residue was acidified to *p*H ~ 3 using 5% HCl (5% volume in water) at cold conditions after diluting with 50 mL cold water. Product was extracted with ethyl acetate (3 × 20 mL). Combined organic layer was washed with brine (40 mL) and dried over anhydrous Na_2SO_4. Organic layer was concentrated under reduced pressure to give gummy product with quantitative yield 98% (0.323 mmol, 0.200 g).

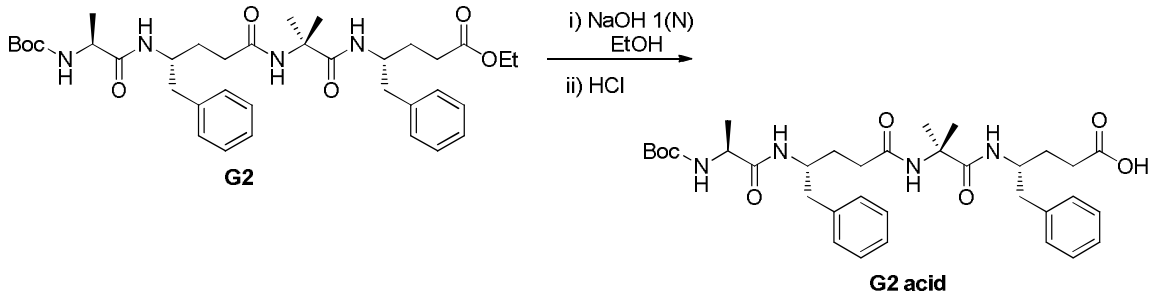

Boc-Ala-γ⁴Phe-Aib-γ⁴Phe-OSu: Boc-Ala-γ⁴Phe-Aib-γ⁴Phe-OH (0.323 mmol, 0.2 g) and *N*-hydroxysuccinimide were dissolved together in DMF (3 mL) followed by HBTU (0.4 mmol, 0.151 g) was added. The reaction mixture was cooled to 0 ^{o}C for 5 min. Then DiEPA (0.5 mmol, 0.09 mL) was added to the reaction mixture and it was allowed to come in room temperature at constant stirring. The progress of the reaction was monitored by TLC. After completion of the reaction (roughly 8 hrs), reaction mixture was diluted with 50 mL of ethyl acetate and washed with 10 % sodium carbonate solution in water (2 × 25 mL) and followed by brine (30 mL). The organic layer was dried over Na_2SO_4 and evaporated under reduced pressure to give gummy product, which was used for next step without further purification. Overall yield 78% (0.25 mmol, 0.180 g).

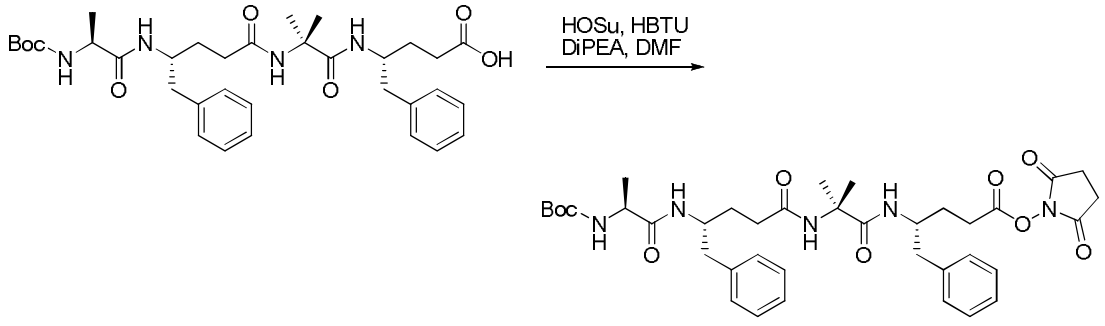

Boc-Ala-γ⁴Phe-Aib-γ⁴Phe-NHMe: Boc-Ala-γ⁴Phe-Aib-γ⁴Phe-OSu (0.25mmol, 0.180 g) was dissolved in 10 mL THF. Then the solution was cooled to 0^{o} C for 5 min. Methyl amine solution in water (roughly 10 mL) was added to the reaction and reaction mixture was kept for 5hrs to complete the reaction. After completion of reaction, methyl amine was evaporated

from reaction mixture. Then the solid residue was dissolved in ethyl acetate (70 mL) and organic layer was washed with 5% HCl (5 % by vol. in water, 2 ×40 mL), followed by brine (40 mL). The organic layer was dried over Na_2SO_4 and evaporated under reduced pressure to give white solid product, which was purified on silica gel column chromatography using DCM/MeOH (product was eluted at 4.5% MeOH in DCM) solvent system to get solid white powder product. Overall yield 85% (0.21 mmol, 0.135 g).

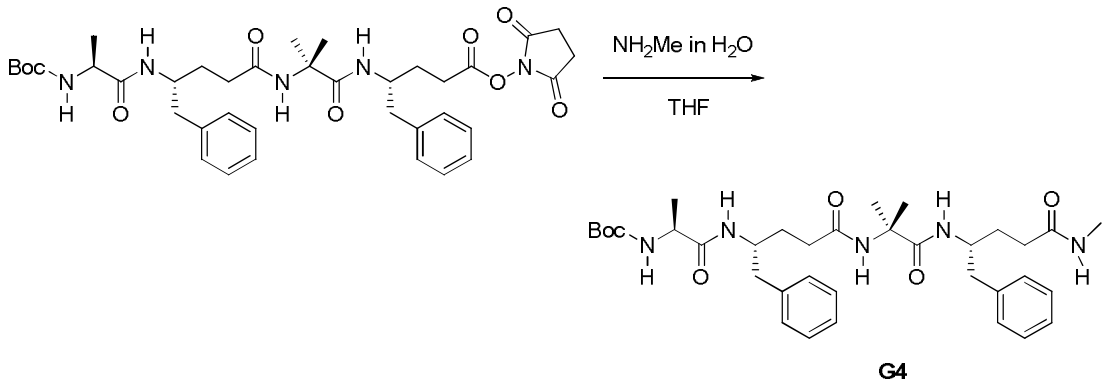

Boc-Ala-γ[4]Phe-Aib-γ[4]Phe-NHMe (G4)

Physical state : white crystalline powder

Mol. Formula : $C_{35}H_{51}N_5O_6$

Yield : 85%, 0.135 g

^{1}H NMR (500 MHz, $CDCl_3$) : δ_H 7.46-7.44 (d, *J* = 7.4, 1H, NH), 7.27-7.10 (m, 11H, -Ph, NH), 6.95 (s, 1H, NH), 6.05-6.03 (d, *J* = 8.2, 1H, NH), 5.01 (b, 1H, NH), 4.25-4.22 (m, 1H, -C*H*-), 4.15-4.10 (m, 1H, -C*H*$_2$-), 3.96-3.90 (m, 1H, -C*H*-), 2.87-2.60 (m, 4H, -C*H*$_2$-Ph), 2.79-2.78 (d, *J* = 3.7, 3H, -NHMe), 2.39-1.87 (m, 8H, -C*H*$_2$-), 1.44 (s, 9H, -$(CH_3)_3$ Boc), 1.39 (s, 3H, -$(CH_3)_2$ Aib), 1.27-1.26 (d, *J* = 5.84, 3H, -C*H*$_3$ of Ala), 0.99 (s, 3H, -$(CH_3)_2$ Aib).

MALDI TOF/TOF m/z : Calcd. $[M+Na]^+$ 660.3737, observed 660.4789

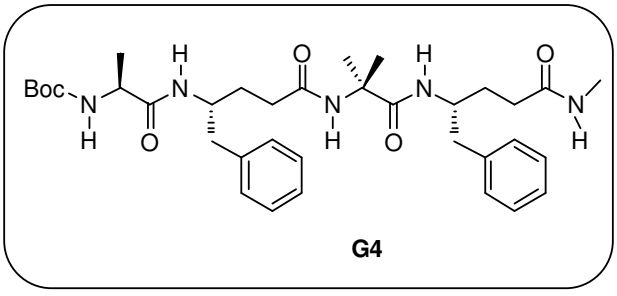

Synthesis of Hexapeptide (Boc-Aib-γ⁴Phe-Leu-γ⁴Phe-Aib-dgF-OEt) (D4)

Boc-Aib-γ⁴Phe-Leu-γ⁴Phe-OH: Boc-Aib-γ⁴Phe-Leu-γ⁴Phe-OEt (0.4 mmol, 0.286 g) was dissolved in ethanol (4 mL). Then 5 mL of 1(N) NaOH was added slowly to this solution. After completion of the reaction (~ 2 hrs), ethanol was evaporated from reaction mixture and residue was acidified to *p*H ~ 3 using 5% HCl (5% volume in water) at cold conditions after diluting with 50 mL cold water. Product was extracted with ethyl acetate (3 × 25 mL). Combined organic layer was washed with brine (40 mL) and dried over anhydrous Na_2SO_4. Organic layer was concentrated under reduced pressure to give gummy product with quantitative yield 98% (0.392 mmol, 0.261 g).

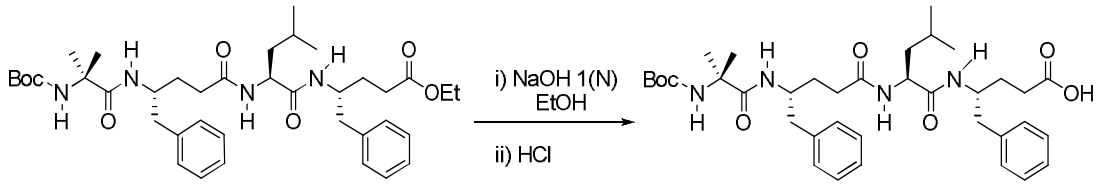

G3 G3 acid

NH_2-Aib-dgF-OEt: Boc-Aib-dgF-OEt (0.5 mmol, 0.210 g) was dissolved in DCM (3 mL) and cooled the solution in ice bath. Then 3 mL of neat TFA was added to the solution. After completion of the reaction (~ 30 min), TFA was removed from reaction mixture under vacuum. The residue was dissolved in water and the pH was adjusted to ~10 by the slow addition of solid Na_2CO_3 at ice cold conditions Then Boc
deprotected dipeptide was extracted with ethyl acetate (3 × 25 mL). Combined organic layer was washed with brine (40 mL), dried over Na_2SO_4 and concentrated under *vacuum* to *ca.* 2 mL and directly used for the coupling reaction in the next step.

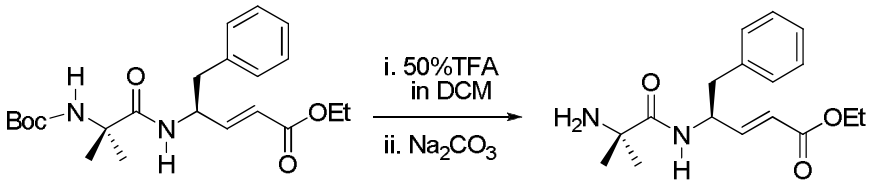

Boc-Aib-γ^4Phe-Leu-γ^4Phe-OH (0.392 mmol, 0.261 g) and NH_2-Aib-dgF-OEt were dissolved together in DMF (2 mL) followed by HBTU (0.5 mmol, 0.190 g) was added. The reaction mixture was cooled to 0 ^oC for 5 min. Then DiPEA (0.7 mmol, 0.12 mL) was added to the reaction mixture and it was allowed to come to room temperature at constant stirring. The progress of the reaction was monitored by TLC. After completion of the reaction (roughly 8 hrs), the reaction mixture was diluted with 100 mL of ethyl acetate. The organic layer was washed with 5% HCl (2 × 40 mL), 10 % sodium carbonate solution in water (2 × 40 mL) and brine (50 mL). The organic layer was dried over Na_2SO_4 and evaporated under reduced pressure to give gummy yellowish product, which was purified on silica gel column chromatography using EtOAc/Pet-ether (product was eluted at 90% EtOAc in pet-ether) solvent system to get gummy product, which was further crystallized using EtOAc/Hexane. Overall yield 60% (0.231 mmol, 0.220 g).

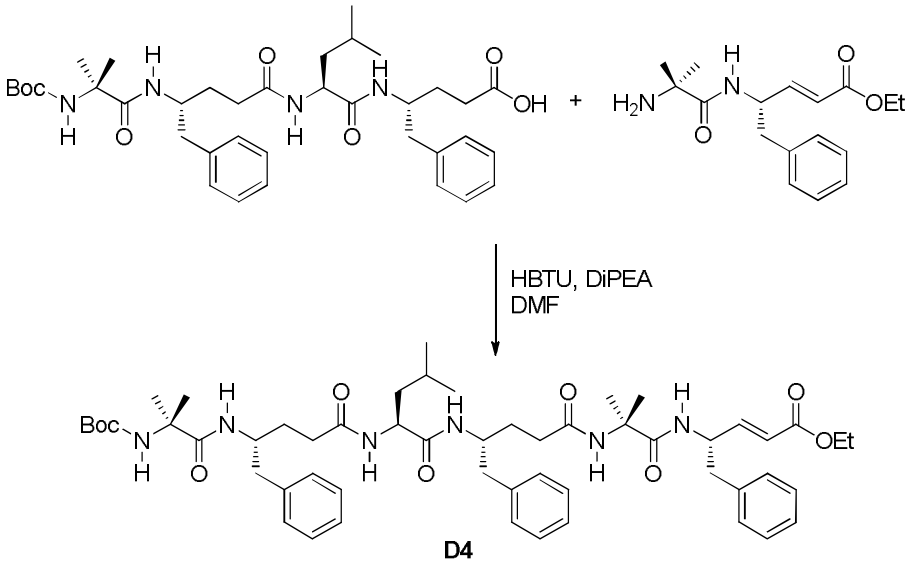

D4

Boc-Aib-γ^4Phe-Leu-γ^4Phe-Aib-dgF-OEt (D4)

Physical state : white crystalline powder

Mol. Formula : $C_{54}H_{76}N_6O_9$

Yield : 60%

^{1}H NMR (500 MHz, $CDCl_3$) : δ_H 8.59-8.57 (d, *J* = 8.3, 1H, NH), 7.70-7.68 (d, *J* = 10.2, 1H, NH), 7.48-7.47 (d, *J* = 3.85, 1H, NH), 7.48-7.07 (m, 17H, -Ph, NH, -C*H*-(β) of dgF), 6.53-6.49 (dd, *J* = 17.7, *J* = 2.1, 1H, -CH= -C*H* α of dgF), 6.07-6.05 (d, *J* = 10.3, 1H, NH),

5.23 (s, 1H, NH), 5.13-4.97 (m, 1H, γ-C*H*- of dgF), 4.26-4.13 (m, 4H γ-C*H*- of γPhe, -OCH_2), 3.80-3.76 (m, 1H, α-C*H*- of Leu), 2.98-2.60 (m, 6H, -CH_2-Ph), 2.29-2.10 (m, 4H, α-CH_2- of γPhe), 1.76 (s, 3H, -$(CH_3)_2$ for Aib),1.71-1.65 (m, 2H, β-CH_2- of γPhe), 1.59 (s, 3H, -$(CH_3)_2$ for Aib), 1.55-1.48 (m, 2H, β-CH_2- of γPhe), 1.45 (s, 3H, -$(CH_3)_2$ for Aib), 1.43 (s, 9H, -$(CH_3)_3$ Boc), 1.30 (s, 3H, -$(CH_3)_2$ for Aib), 1.29-1.26 (t, *J* = 7, 3H, -OCH_2CH_3), 1.20-1.14(m, 2H, β-CH_2- of Leu), 0.99 (s, 3H, -$(CH_3)_2$ for Aib), 0.94-0.88 (m, 2H, γ-CH_2- of Leu), 0.83-0.82 (d, *J* = 6.6, 3H, -CH_3 of Leu), 0.78-0.77 (d, *J* = 6.7, 3H, -CH_3 of Leu).

MALDI TOF/TOF m/z **:** Calcd. $[M+Na]^+$ 975.5571, observed 975.9615.

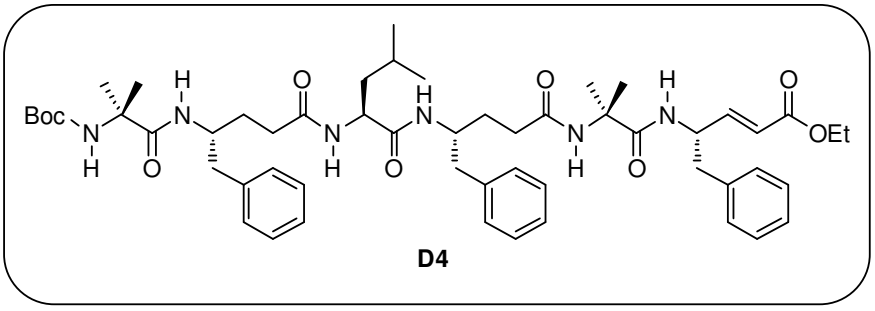

D4

Transformation of α-γ-Vinylogous hybrid hexapeptide Boc-Aib-γ^{4}Phe -Leu-γ^{4}Phe-Aib-dgF-OEt (D4) to its saturated hybrid γ^4-peptide analogue Boc-Aib-γ^{4}Phe-Leu-γ^{4}Phe-Aib-γ^{4}Phe-OEt (G5)

Boc-Aib-γ^{4}Phe -Leu-γ^{4}Phe-Aib-dgF-OEt (D4) (0.10 mmol, 100 mg) was dissolved in EtOH (4 mL), and was treated with 20 mg of 20% Pd/C. The hydrogen gas was supplied through balloon. The schematic representation is shown below. The reaction mixture was stirred under hydrogen atmosphere for about 6 hrs. The completion of the reaction was monitored by MALDI-TOF/TOF (m/z Calcd. For $C_{54}H_{78}N_6O_9$ $[M+Na]+$ 977.5728, observed 977.8813) and HPLC. After the completion of the reaction, the reaction mixture was diluted with EtOH (10 mL) and it was filtered through sintered funnel using celite bed and celite bed was washed with EtOH (3 × 15 mL). The filtrate was evaporated under *vacuum* to get white crystalline

pure product. Overall, the α/γ^4-hybrid peptide was isolated in 97% yield (97 mg, 0.097 mmol).

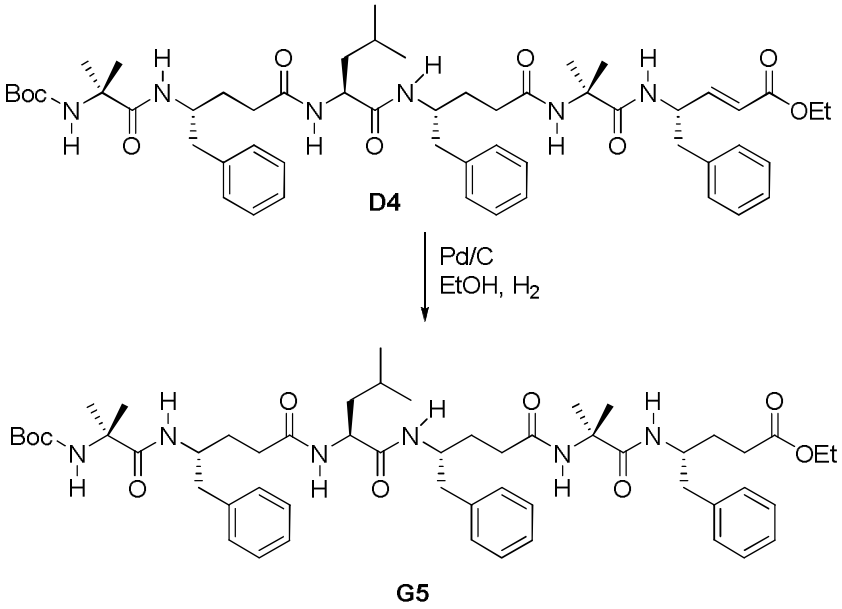

Boc-Aib-γ^4Phe-Leu-γ^4Phe-Aib-γ^4Phe-OEt (G5)

Physical state **:** White crystalline powder

Mol. Formula **:** $C_{54}H_{78}N_6O_9$

Yield **:** 97%, 97 mg

^{1}H NMR (500 MHz, $CDCl_3$) **:** δ_H 8.08-8.06 (d, *J* = 9.25, 1H, NH), 7.66-7.64 (d, *J* = 10.2, 1H, NH), 7.39-7.38 (d, *J* = 4, 1H, NH), 7.39-7.09 (m, 15H, -Ph), 7.01 (s, 1H, NH), 5.96-5.94 (d, *J* = 10.3, 1H, NH), 5.05 (s, 1H, NH), 4.26-4.13 (m, 5H, -OC*H*$_2$, -C*H*-(γ) of γPhe), 3.85-3.82 (m, 1H, α -C*H*- of Leu), 2.99-2.59 (m, 6H, C*H*$_2$-Ph), 2.49-2.02 (m, 6H, -C*H*$_2$-(α) of γPhe), 1.99-1.83(m, 6H, -C*H*$_2$-(β) of γPhe), 1.72-1.58(m, 6H, -C*H*$_2$-(β) of γPhe), 1.56-1.48(m, 6H, -C*H*$_2$-(β) of γPhe), 1.60 (s, 3H, -$(CH_3)_2$ for Aib), 1.44 (s, 9H, -$(CH_3)_3$ Boc), 1.43 (s, 3H, -$(CH_3)_2$ for Aib), 1.29 (s, 3H, -$(CH_3)_2$ for Aib), 1.27-1.22 (m, 5H, -OCH_2CH_3, C*H*$_2$-, β-H of Leu), 1.13-1.05 (m, 1H, γ-H of Leu), 1.00 (s, 3H, -$(CH_3)_2$ for Aib), 0.86-0.85 (d, *J* = 6.6, 3H, -C*H*$_3$ of Leu), 0.81-0.80 (d, *J* = 6.7, 3H, -C*H*$_3$ of Leu).

MALDI TOF/TOF m/z **:** Calcd. $[M+Na]^+$ 977.5728, observed 977.8813.

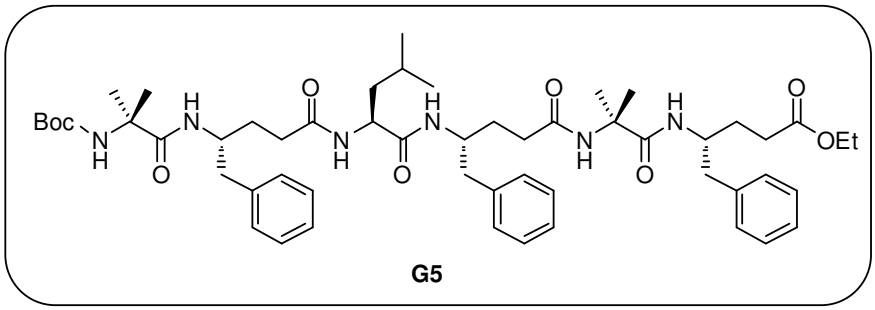

G5

3.6 References

1. Ramachandran, G.N. &Sasisekharan, V. *Advan. Protein Chem.*, **1968**, 23, 283-437.
2. Creighton, T.E. *Proteins Structures and Molecular Properties*. **1993** W.H. Freeman and Company, New York
3. Barlow, D. J.; Thornton, J. M. *J. Mol. Biol.* **1988**, *201*, 601-619.
4. Andrews, M. J. I.; Tabor, A. B. *Tetrahedron* **1999**, *55*, 11711-11743.
5. Mott, H. R.; Campbell, I. D. *Curr. Opin.Struct. Biol.* **1995**, *5*, 114-12.
6. Lupas, A. *Trends Biol. Sci.* **1996**, *21*, 375-382.
7. Karplus, M.; Weaver, D. L. *Protein Sci.* **1994**, *3*, 650-668.
8. Kim, P. S.; Baldwin, R. L. *Annu. Rev. Biochem.* **1990**, *59*, 631-660.
9. Beck-Sickinger, A. G.; Jung, G. *Biopolymers* **1995**, *37*, 123-142.
10. Motta, A.; Morell, M. A. C.; Gons, N.; Temussi, P. A. *Biochemistry* **1989**, *28*, 7996-8002.
11. a) Struhl, K. *Trends Biol. Sci.* **1989**, *14*, 137-140. b) Brennan, R. G.; Mattbews, B. W. *Trends Biol. Sci.* **1989**, *14*, 286-290. c) Ellenberger, T. E.; Brandl, C. J.; Struhl, K.; Harrison, S. C. *Cell* **1992**, *71*, 1223-1237.
12. Kussie, P. H.; Gorina, S.; Marechal, V.; Elenbaas, B.; Moreau, J.; Levine, A. J.; Pavletich, N. P. *Science* **1996**, *274*, 948-953.
13. Sattler, M.; Liang, H.; Nettesheim, D.; Meadows, R. P.; Harlan, J. E.; Eberstadt, M.; Yoon, H. S.; Shuker, S. B.; Chang, B. S.; Minn, A. J.; Thompson, C. B.; Fesik, S. W. *Science* **1997**, *275*, 983-986.
14. a) Seebach, D., Beck, A. K., Bierbaum, D. J. *Chemistry & Biodiversity,* **2004**, *1*, 1111-1239. b) Vasudev, P. G., Chatterjee, S., Shamala, N., Balaram, P. *Chem. Rev.* **2011**, *111*, 657-687.

15. a) Frackenpohl, J.; Arvidsson, P. I.; Schreiber, J. V.; Seebach, D. *ChemBioChem* **2001**, *2*, 445-455. b) Wiegand, H.; Wirz, B.; Schweitzer, A.; Camenisch, G. P.; Perez, M. I. R.; Gross, G.; Woessner, R.; Voges, R.; Arvidsson, P. I.; Frackenpohl, J.; Seebach, D. *Biopharm. Drug Disp.* **2002**, *23*, 251-262. c) Potocky, T. B.; Menon, A. K.; Gellman, S. H. *J. Am. Chem. Soc.* **2005**, *127*, 3686-3692.

16. Cheng, R. P.; Gellman, S. H.; DeGrado, W. F. *Chem. Rev*. **2001**, *101*, 3219-3232.
17. a) Sharma, G. V. M.; Nagendar, P.; Jayaprakash, P.; Krishna, P. R.; Ramakrishna, K. V. S.; Kunwar, A. C. *Angew. Chem., Int. Ed.* **2005**, *44*, 5878-5882. b) Sharma, G. V. M.; Jayaprakash, P.; Narsimulu, K.; Sankar, A. R.; Reddy, K. R.; Radha, Krishna, P.; Kunwar, A. C. *Angew. Chem., Int. Ed.* **2006**, *45*, 2944-2947. c) Sharma, G. V. M., Chandramouli, N.; Choudhary, M.; Nagendar, P.; Ramakrishna, K. V.; Kunwar, A. C.; Schramm, P.; Hofmann, H. J. *J. Am. Chem. Soc.* **2009**, *131*,17335-17344. d) Schramm, P.; Sharma, G. V. M.; Hofmann, H. J. *Biopolymers*, **2010**, *94*, 279-291. e) Sharma, G. V. M.; Yadav, T. A.; Choudhary, M.; Kunwar, A. C. *J. Org. Chem.* **2012**, *77*, 6834-6848.
18. Mandity, I. M.; Fulop, L.; Vass, E; Toth, G. K.; Martinek, T. A.; Fulop F. *Org. Lett.* **2010**, *12*, 5584-5587.
19. Fernandes, C.; Faure, S.; Pereira, E.; Thery, V.; Declerck, V.; Guillot, R. Aitken, D. J. *Org. Lett.* **2010**, *12*, 3606-3609
20. Hintermann, T.; Gademann, K.; Jaun, B.; Seebach, D. *Helv. Chim. Acta* **1998**, *81*, 893–1002.
21. Hanessian, S.; Luo, X.; Schaum,R.; Michnick, S. *J. Am. Chem. Soc* .**1998**, *120*, 8569–8570.
22. Vasudev, P. G.; Ananda, K.; Shamala, N.; Balaram, P. *Angew. Chem.,Int. Ed.* **2005**, *44*, 4968-4972.
23. a) Guo, L.; Almeida, A. M.; Zhang, W.; Reidenbach, A. G.; Choi, S. H.; Guzei, I. A.; Gellman, S. H. *J. Am. Chem. Soc.* **2010**, *132*, 7868-7869. b) Guo, L.; Zhang, W.; Reidenbach, A. G.; Giuliano, M. W.; Guzei, I. A.; Spencer, L. C.; Gellman, S. H. *Angew. Chem.Int. Ed*. **2011**, *50*, 5843–5846.
24. Horne W. S.; Gellman, S. H. *Acc. Chem. Res.* **2008**, *41*, 1399-1408.
25. Karle, I. L.; Pramanik, A.; Banerjee, A.; Bhattacharjya, S.; Balaram, P. *J. Am. Chem. Soc.* **1997**, *119*, 9087-9095.

26. De Pol, S.; Zorn, C.; Klein, C. D.; Zerbe, O.; Reiser, O. *Angew. Chem., Int. Ed.* **2004**, *43*, 511–514.
27. a) Hayen, A.; Schmitt, M. A.; Ngassa, F. N.; Thomasson, K. A.; Gellman, S. H. *Angew. Chem., Int. Ed.* **2004**, *43*, 505–510. b) Schmitt, M. A.; Choi, S. H.; Guzei, I. A.; Gellman, S. H. *J. Am. Chem. Soc.* **2005**, *127*, 13130-13131. c) Schmitt, M. A.; Choi, S. H.; Guzei, I. A.; Gellman, S. H. *J. Am. Chem. Soc.* **2006**, *128*, 4538-4539.
28. Seebach, D.; Jaun, B.; Sebesta, R.; Mathad, R. I.; Flogel, O.; Limbach, M.; Sellner, H.; Cottens, S. *Helv. Chim. Acta* **2006**, *89*, 1801–1825.
29. Basuroy, K.; Dinesh, K.; Shamala, N.; Balaram P. *Angew. Chem., Int. Ed.* **2012**, *51*, 8736-8739
30. Horne, W.S.; Price, J.L.; Keck, J.L.; Gellman, S.H. *J. Am. Chem. Soc.* **2007**, *129*, 4178-4180.
31. Price, J. L.; Horne, W. S.; Gellman, S. H. *J. Am. Chem. Soc.* **2007**, *129*, 6376-6377.
32. Baldauf, C.; Gunther, R.; Hofmann, H.-J. *J. Org. Chem.* **2006**, *71*, 1200-1208.
33. Chatterjee, S.; Vasudev, P. G.; Raghothama, S.; Ramakrishnan, C.; Shamala, N.; Balaram, P. *J. Am. Chem. Soc.* **2009**, *131*, 5956-5965.
34. a) Guo, L.; Zhang, W.; Guzei, I. A.; Spencer, L. C.; Samuel H. Gellman, S. H. *Org. Lett*. **2012**, *14*, 2582-2585. b) Guo, L.; Chi, Y.; Almeida, A. M.; Guzei, I. A.; Parker, B. K.; Gellman, S. H. *J. Am. Chem. Soc.* **2009**, *131*, 16018-16020.
35. Sharma, G. V. M.; Jadhav, V. B.; Ramakrishna, K. V. S.; Jayaprakash, P.; Narsimulu, K.; Subash, V.; Kunwar, A. C. *J. Am. Chem. Soc.* **2006**, *128*, 14657–14668.
36. Mali, S. M.; Bandyopadhyay, A.; Jadhav, S. V.; Ganesh Kumar, M.; Gopi, H. N. *Org. Biomol. Chem.* **2011**, *9*, 6566-6574.
37. a) Park, J. S.; Lee, H. S.; Lai, J. R.; Kim, B. M; Gellman, S. H. *J. Am. Chem. Soc.* **2003**, *125*, 8539-8545. b) Porter, E. A.; Wang, X.; Schmitt, M. A.; Gellman, S. H. *Org. Lett.* **2002**, *4*, 3317-3319
38. Wilson, K. P.; Malcolm, B. A.; Matthews, B. W. *J. Biol. Chem.* **1992**, *267*, 10842-10849
39. a) SHELXS-97: G. M. Sheldrick, *Acta Crystallogr. Sect A*, **1990**, *46*, 467-473, b) G. M. Sheldrick, SHELXL-97, Universität Göttingen (Germany) **1997**.
40. A.L. Spek (**1990**) Acta Cryst. A46, C34.

3.7 Appendix I: Characterization Data of Synthesized Compounds

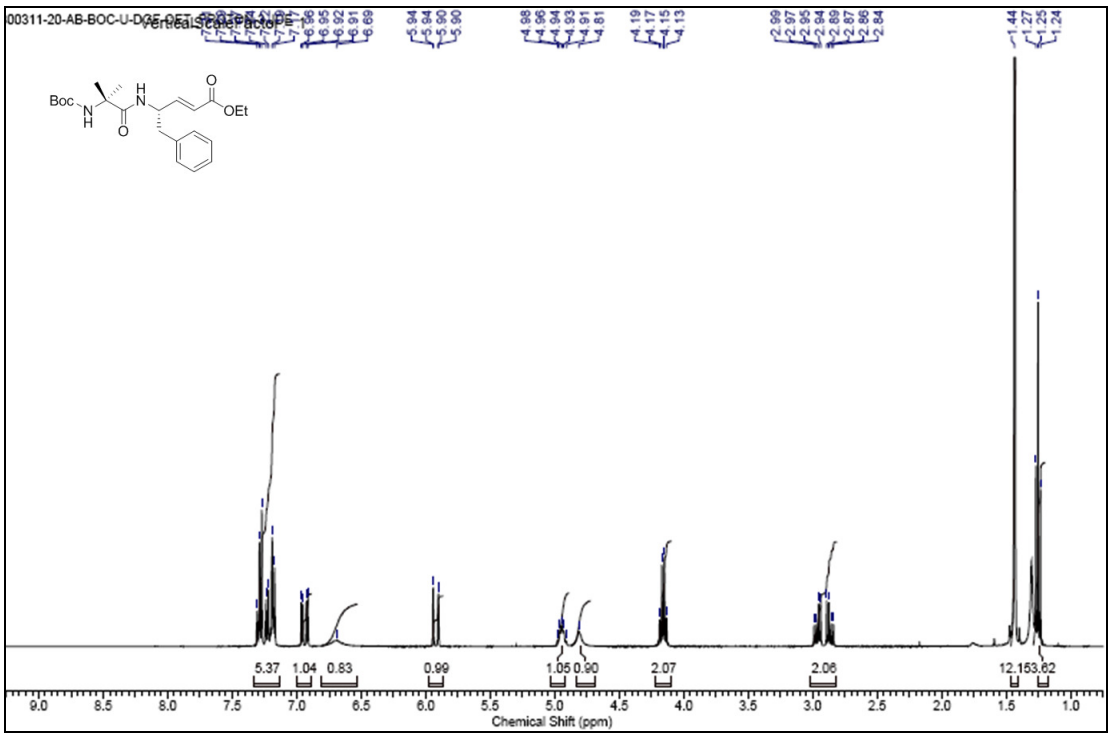
Boc
N
H
O
N
H
O
OEt
5.37
1.04
0.83
0.99
1.05
0.90
2.07
2.06
12.15
3.62
Chemical Shift (ppm)

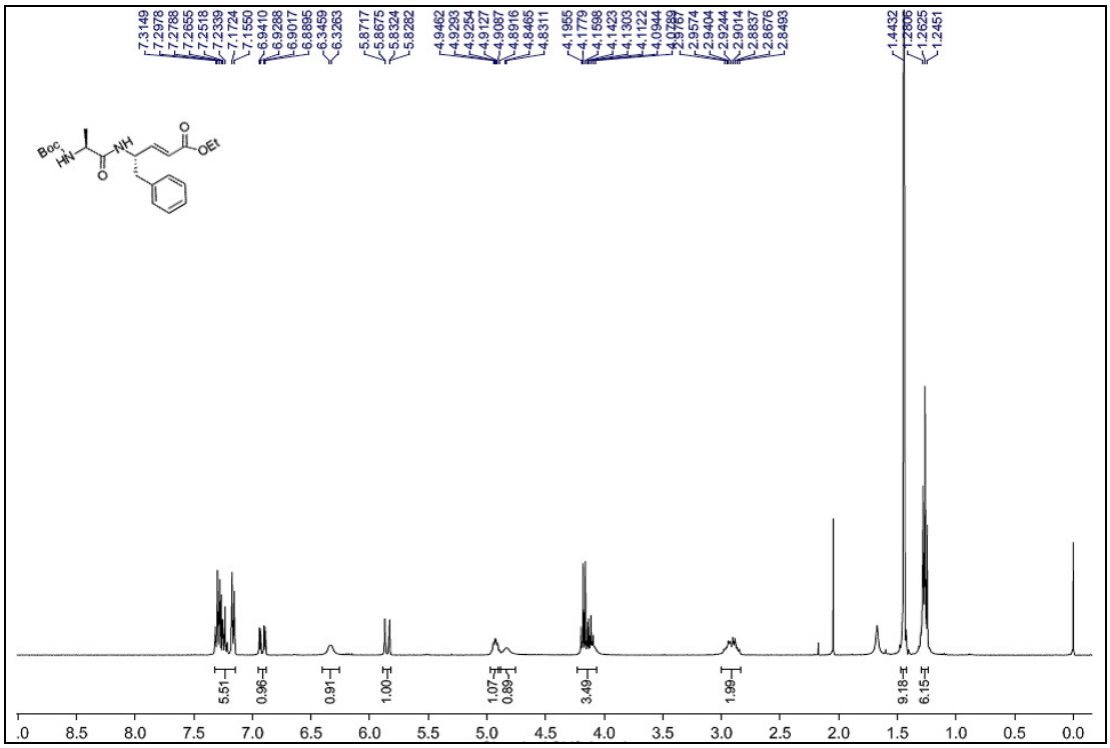
Boc
HN
NH
O
OEt
5.51
0.96
0.91
1.00
1.07
0.89
3.49
1.99
9.18
6.15

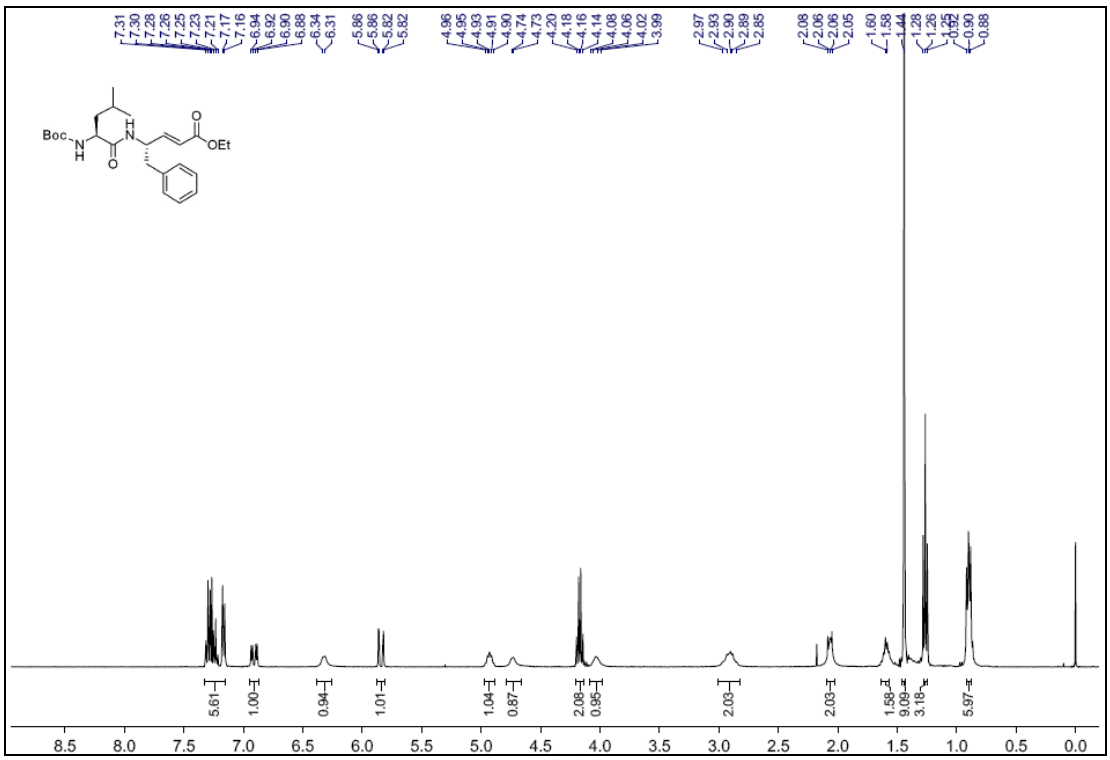
Boc
N
H
O
H
N
O
OEt
5.61
1.00
0.94
1.01
1.04
0.87
2.08
0.95
2.03
2.03
1.58
9.09
3.18
5.97

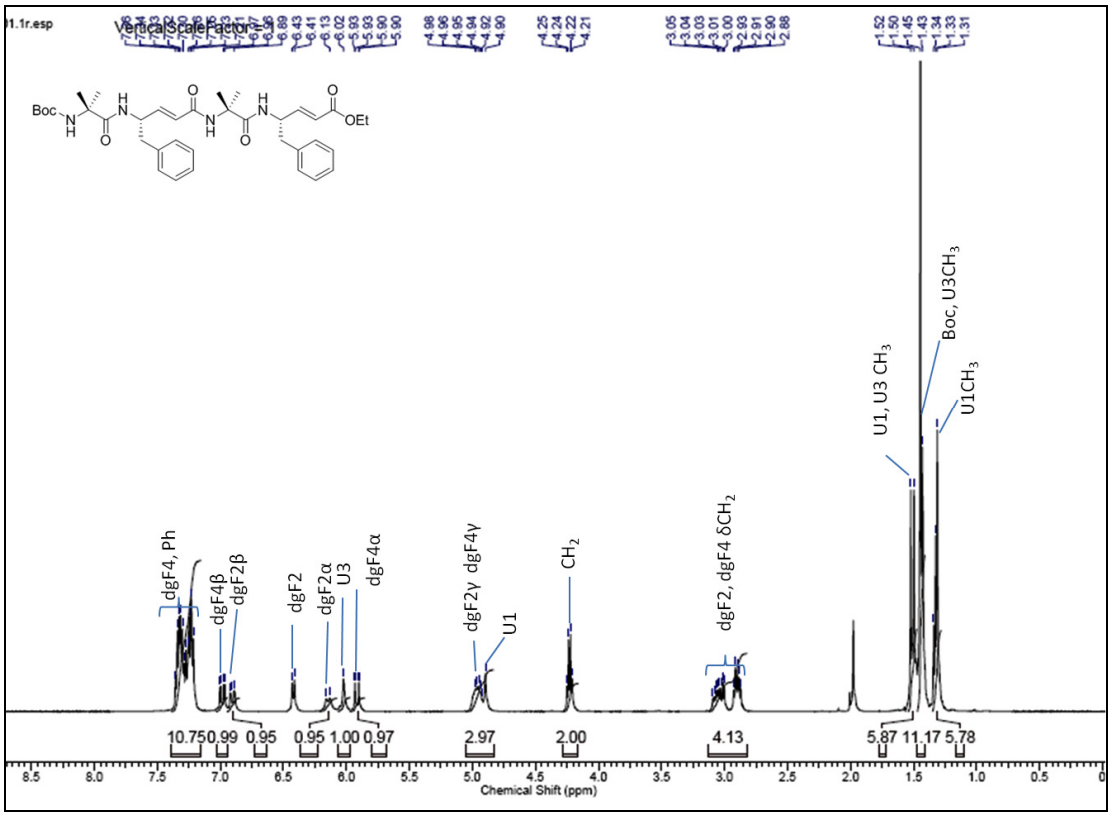
VerticalScaleFactor=1
Boc
N
H
O
H
N
O
H
N
O
OEt
dgF4, Ph
dgF4β
dgF2β
dgF2
dgF2α
U3
dgF4α
dgF2γ dgF4γ
U1
CH2
dgF2, dgF4 δCH2
U1, U3 CH3
Boc, U3CH3
U1CH3
10.75
0.99
0.95
0.95
1.00
0.97
2.97
2.00
4.13
5.87
11.17
5.78
Chemical Shift (ppm)

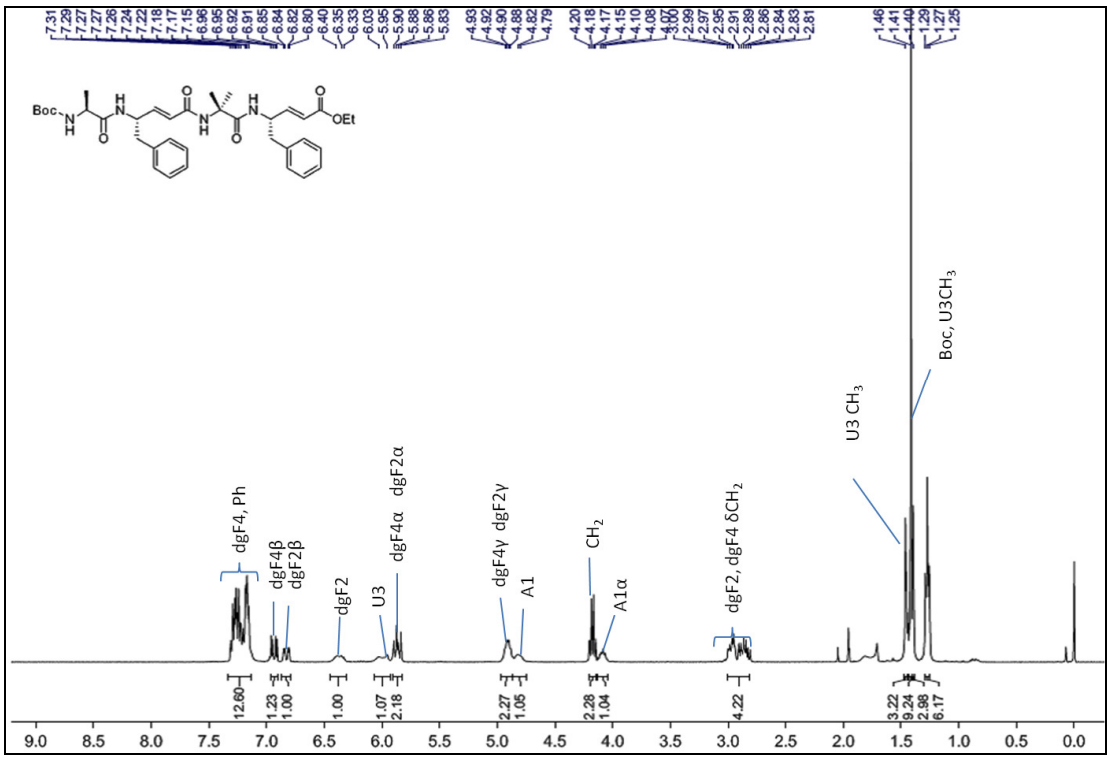
dgF4, Ph
dgF4β
dgF2β
dgF2
U3
dgF4α
dgF2α
dgF4γ dgF2γ
A1
CH2
A1α
dgF2, dgF4 δCH2
U3 CH3
Boc, U3CH3

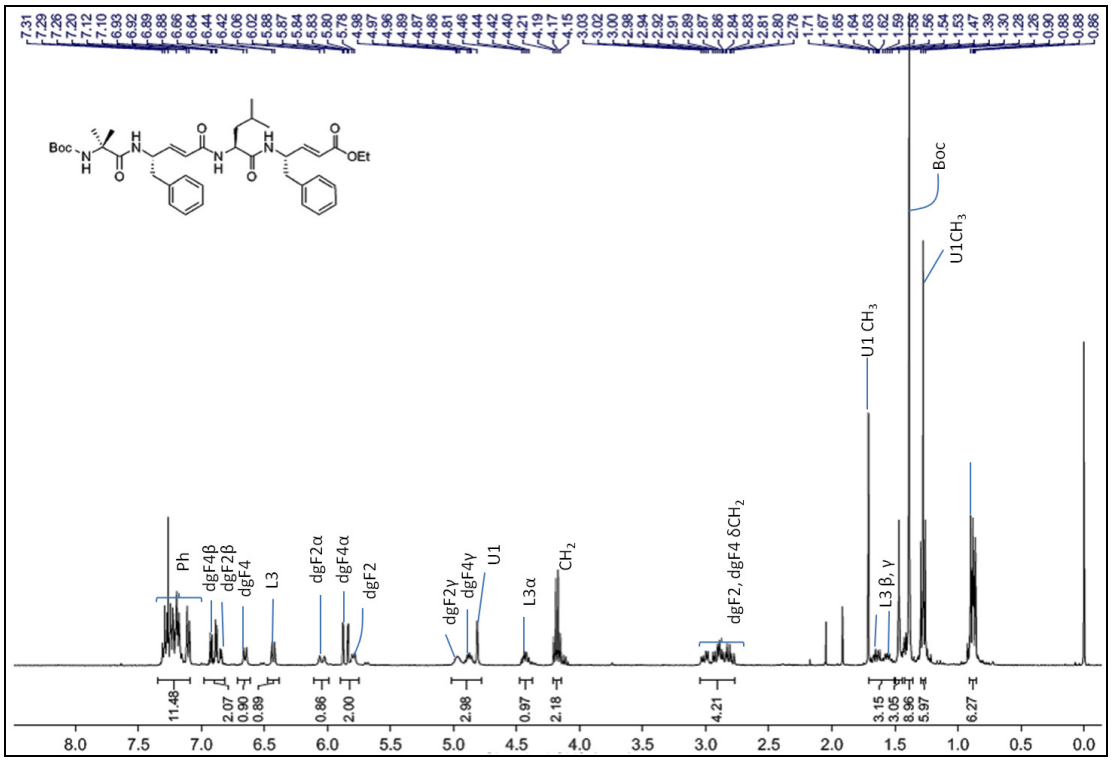
Ph
dgF4β
dgF2β
dgF4
L3
dgF2α
dgF4α
dgF2
dgF2γ
dgF4γ
U1
L3α
CH2
dgF2, dgF4 δCH2
U1 CH3
L3 β, γ
Boc
U1CH3

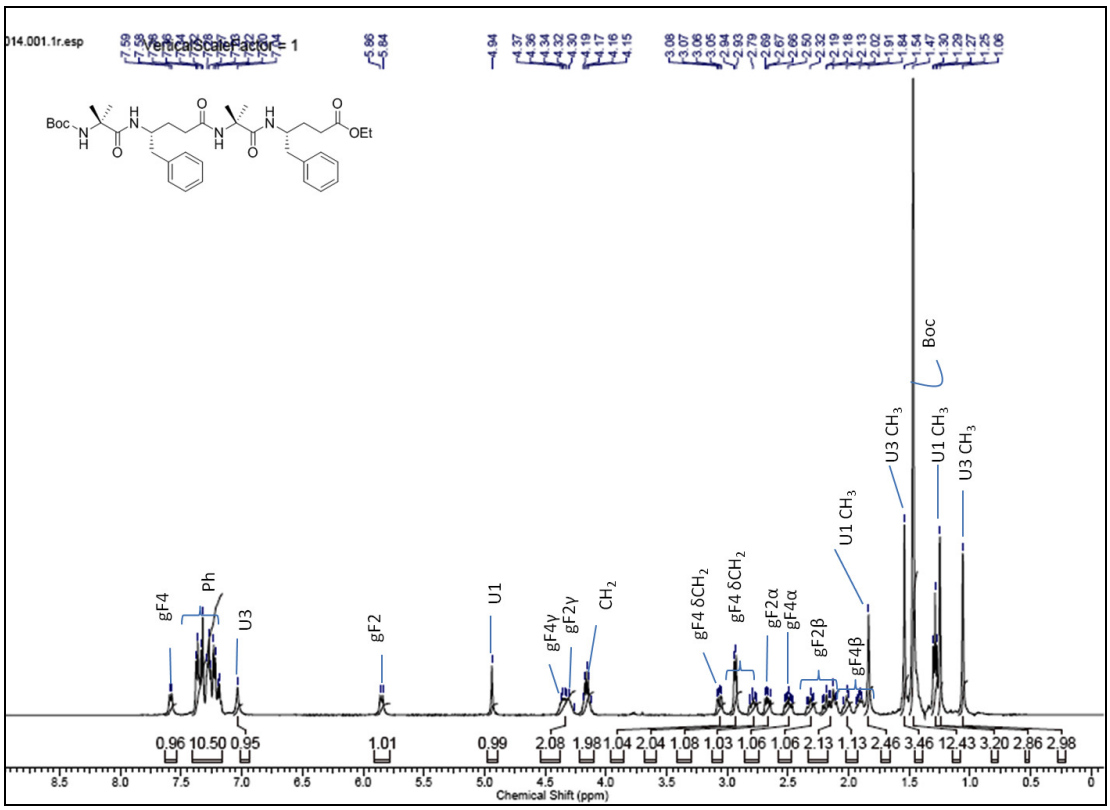
014.001.1r.esp
VerticalScaleFactor = 1
Boc
OEt
gF4
Ph
U3
gF2
U1
gF4γ
gF2γ
CH2
gF4 δCH2
gF4 δCH2
gF2α
gF4α
gF2β
gF4β
U1 CH3
U3 CH3
U1 CH3
U3 CH3
Boc
0.96 10.50 0.95 1.01 0.99 2.08 1.98 1.04 2.04 1.08 1.03 1.06 1.06 2.13 1.13 2.46 3.46 12.43 3.20 2.86 2.98
Chemical Shift (ppm)

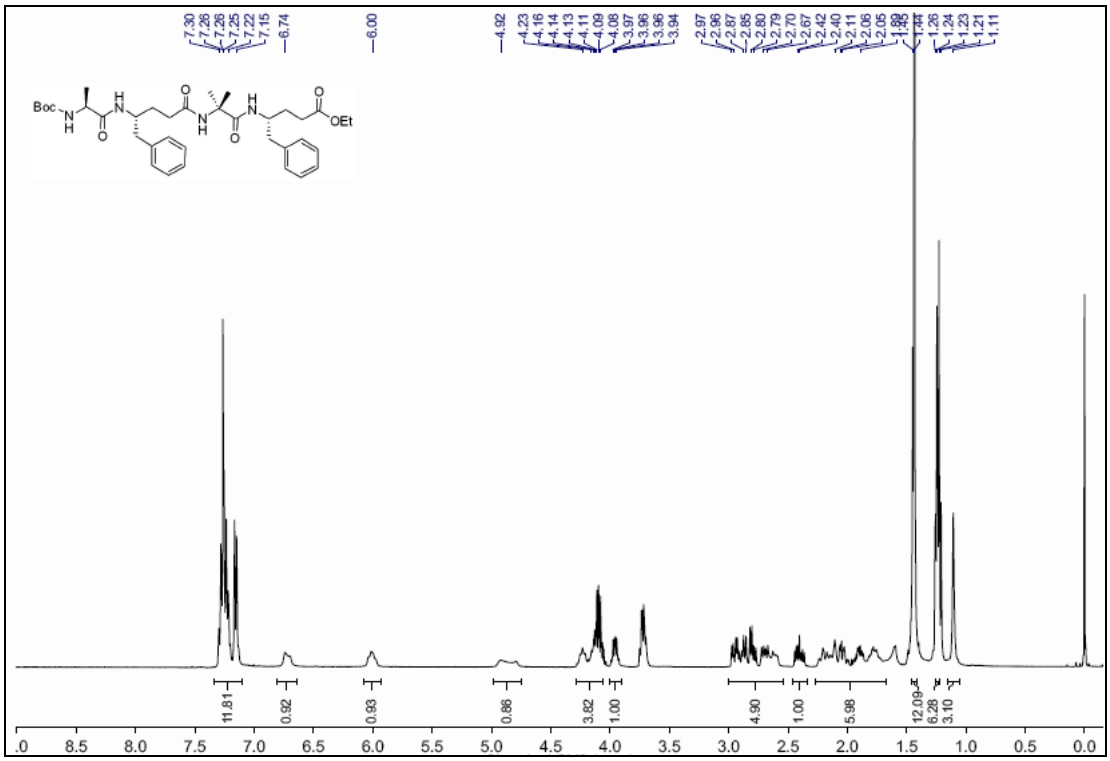
Boc
OEt
11.81 0.92 0.93 0.86 3.82 1.00 4.90 1.00 5.98 12.09 6.28 3.10

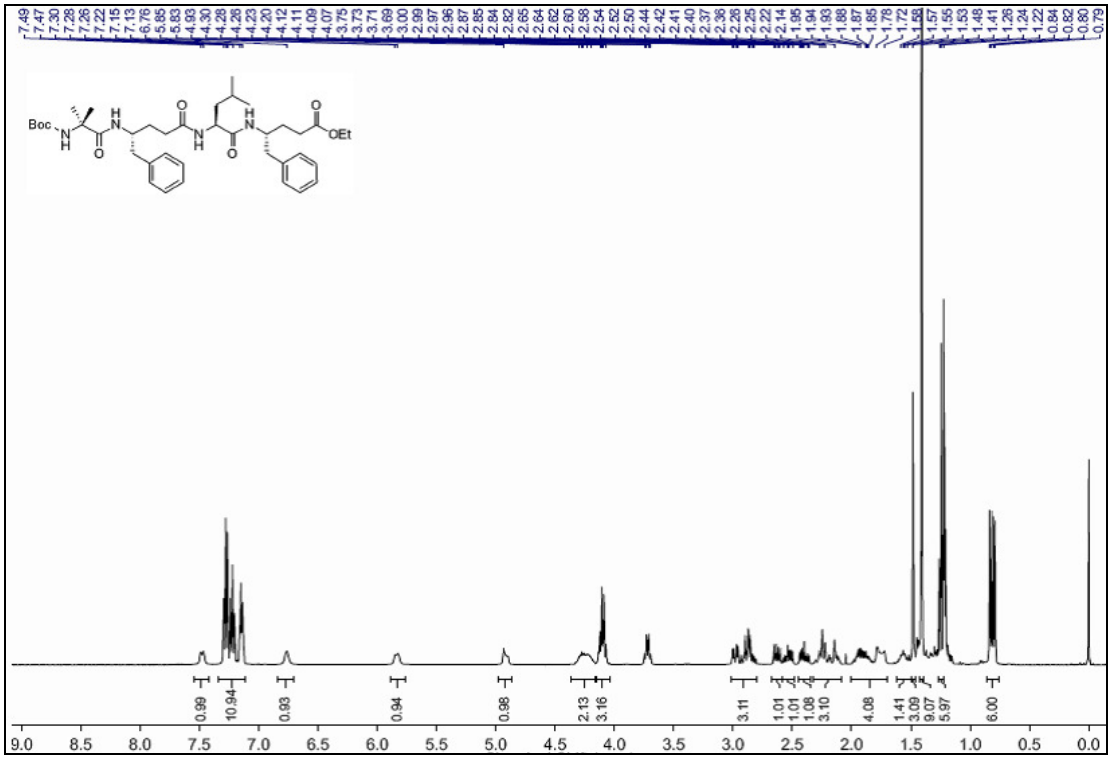
Boc
OEt

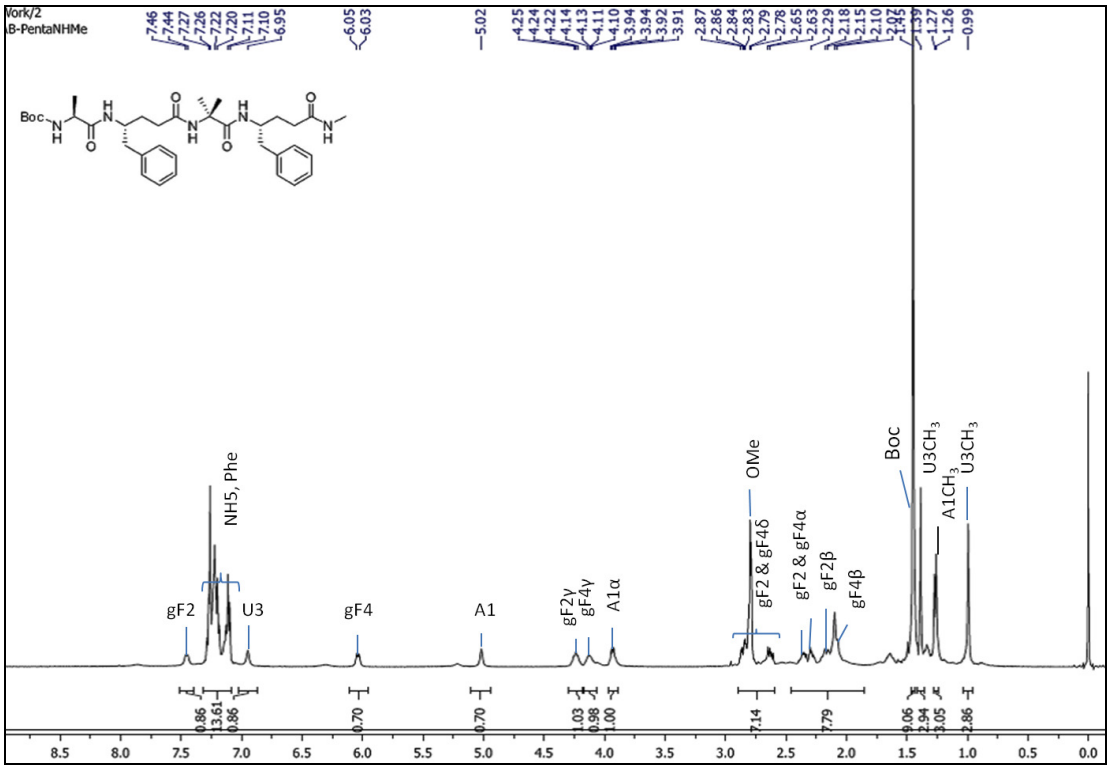
Boc
gF2
NH5, Phe
U3
gF4
A1
gF2γ
gF4γ
A1α
OMe
gF2 & gF4δ
gF2 & gF4α
gF2β
gF4β
Boc
U3CH3
A1CH3
U3CH3

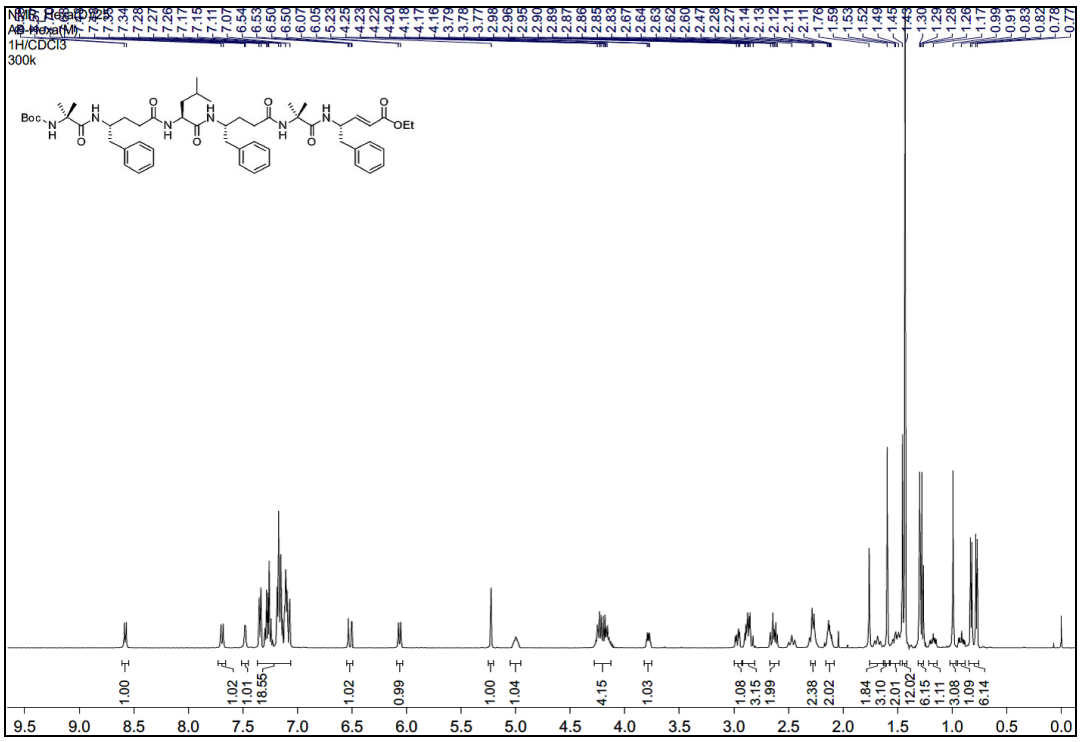
1H/CDCl3
300k
Boc
OEt

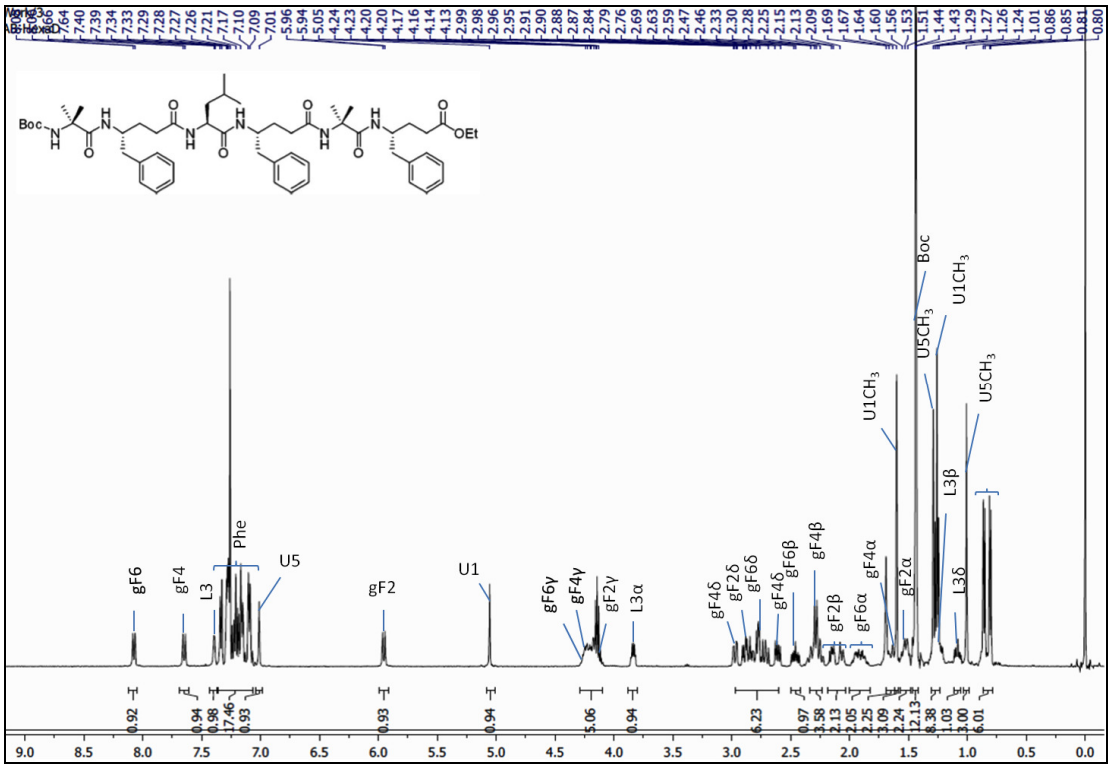
Boc
OEt
gF6
gF4
L3
Phe
U5
gF2
U1
gF6γ
gF4γ
gF2γ
L3α
gF4δ
gF2δ
gF6δ
gF4δ
gF6β
gF4β
gF2β
gF6α
gF4α
gF2α
U1CH3
U5CH3
Boc
U1CH3
L3β
L3δ
U5CH3

Chapter 4

Synthesis of β-keto γ-amino acids and their Functionalization to coumarin and statin derivatives

Section 4A : Tin(II) Chloride Assisted Synthesis of *N*-protected γ- amino β-keto esters through Semipinacol Rearrangement

4A.1 Introduction

In the previous three chapters we have discussed regarding the synthesis and utilization of naturally occurring vinylogous γ-amino acids in hybrid peptides. In addition to the α,β-unsaturated γ-amino acids, the γ-amino β-keto acids, (insertion of $–C(O)CH_2–$ between $C_\alpha H$ and CO of α-amino acids) another highly versatile non-natural amino acids frequently found in several biologically active peptides, such as Nostopeptolide, MajusculamideC, Desmethoxymajusculamide C, Dolastatin etc. (Figure 1) .[1, 2] Gamma-amino β-keto esters have been widely used as intermediates for the synthesis of many biologically relevant molecules such as statins,[3a,b] ketomethylene dipeptide isosteres,[3c] β-lactams,[3d] tricarbonyl compounds,[3e] rhodopeptins[3f], substituted pyridines,[3g] fluorescent amino acid tags,[3h,i] cholecystokinin (CCK) receptor antagonists,[3j] γ-amino α, β-unsaturated esters,[3k] and α-azo-β carbonyl compounds.[3l] Several methods exist for the synthesis of γ-amino β-keto esters.[4] The most commonly used method involves the Claisen ester type condensation of activated carboxylic acid followed by nucleophilic substitution either with lithium enolate of alkyl acetates[3b, 5a-c] or magnesium enolates of alkyl malonates [3a, 3l] or mono alkyl malonates in the presence of magnesium chloride.[5d,] *N, N'*-Carbonyldiimidazole (CDI) is normally used for the carbonyl activation.[6] The other carbonyl activating groups such as pentafluorophenyl esters[5a], *N*-carboxy anhydrides (NCAs),[7a,b] and mixed anhydrides[5b] of *N*-protected amino acids are also utilized in the Claisen ester type condensation. Similarly, C-acylation of protected amino acids with Meldrum's acid *via* mixed anhydride method followed by the hydrolysis leading to the β-keto esters has also been reported.[8] The success of these methods varies for the reasons including functional group compatibility, multistep procedures for nucleophile preparation, poor yields, harsh reaction conditions and longer duration of reactions. Consequently, there is a need for the development of new and efficient methods for the synthesis of γ-amino β-keto-esters.

Reaction between diazomethane and aldehydes leading to ketones is a classic organic reaction.[9] The versatility of metal mediated diazocoupling reactions is well explored in

organic synthesis.[10] Participation of diazoacetates in aldol[11] and Mannich[12] type reactions, and diazoacetamides as well as diazoacetates in Darzens[13] and aziridination[14] reactions in the presence of Lewis acid catalysts are well documented. In addition, in their accidental discovery, Holmquist and Roskamp reported a facile Lewis acid mediated synthesis of rearranged β-keto-esters using aliphatic and aromatic aldehydes with ethyl diazoacetate.[15]

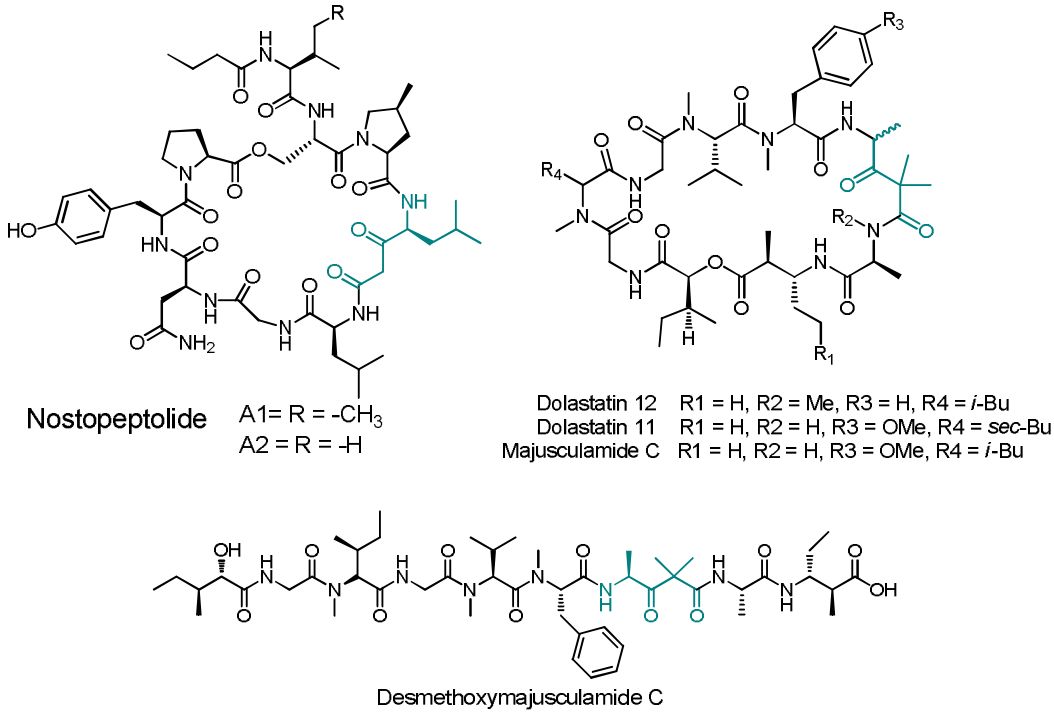

Figure 1: Representative examples of β-keto γ-amino acid in peptide natural products.

4A.2 Aim and rationale of the present work

We have been interested in the synthesis and conformational analysis of non-natural amino acid containing peptide foldamers and their biological activities. Being a chemist, we always look forward to develop a new methodology for biologically active non-natural amino acid or small molecule. Developing a new protocol with better yield and compatible with different protecting groups and functional groups is a challenging task for synthesis of non-natural amino acids. In our presumption regarding the earlier reported synthetic methodologies[3,4,5,6]

is that they may not be compatible with Fmoc-*N*-protecting group and other base labile functional groups as well as protecting groups. We envisioned that γ-amino β-keto acids could be obtained from the reaction between *N*-protected amino aldehyde and ethyl diazoacetate in the presence of catalytic amount of anhydrous tin (II) chloride at ambient temperature. Also we anticipated this reaction condition could be compatible for Boc-, Cbz-, and Fmoc- *N*-protecting groups as well as other side chain protecting groups. Here we are reporting the mild and efficient synthetic methodology for synthesis of *N*-protectected γ-amino β-keto- esters and possible mechanism that is involved in the reaction. Further, utilization of these γ-amino β-keto- acids for the synthesis of functionalized coumarins and β-hydoxy γ-amino acids is described in the following section **4B** and **4C**, respectively.

4A.3 Results and Discussion

To explore the feasibility of this method we began with *N*-Boc-protected amino aldehydes. The schematic representation of the synthesis of β-keto γ-amino esters starting from *N*-protected α-amino acids is shown in Scheme 1**.** As shown in the Scheme 1, The *N*- protected amino acid **1** was converted to Weinreb amide **2** using the reported procedure.[16] Then column purified Weinreb amides were subjected to LAH reduction to give corresponding aldehydes **3**. All the aldehyde products are

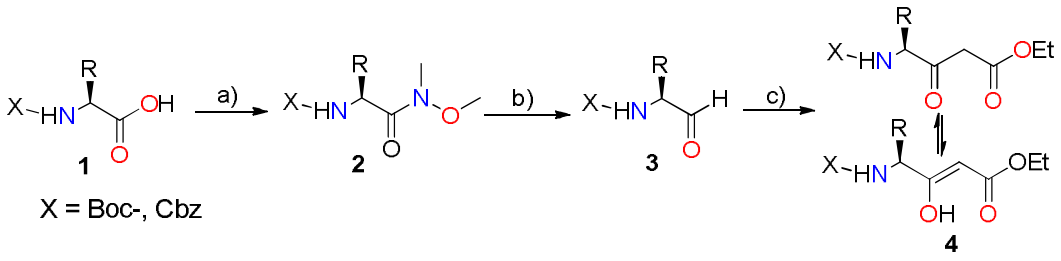

Reagents and Conditions:(a) HBTU, HOBt, DiPEA, HCl.NH(OMe)Me, 2h, 93-97%; (b) LAH, THF, 0 ^{o}C, 30 min, 86-92%; (c) Ethyl diazoacetate, DCM, 20 mol% $SnCl_2$, 76-84%;

Scheme 1: Synthesis of *N*-protected γ-amino β-keto esters from the coupling reaction between amino aldehydes and ethyl diazoacetate in the presence of tin(II) chloride.

Table 1: List of *N*-protected amino aldehydes synthesized from the *N*-protected Weinreb amides.

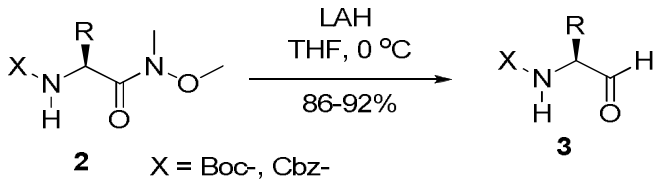

Products	Yield (%)
Boc-Ala-H (**3a**)	89
D-Boc-Ala-H (**3b**)	90
Boc-Val-H (**3c**)	90
Boc-Leu-H (**3d**)	92
Boc-Phe-H (**3e**)	92
Boc-Ile-H (**3f**)	86
Boc-Pro-H (**3g**)	89
Boc-Tyr-H (**3h**)	90
Cbz-Ala-H (**3i**)	88
Cbz-Val-H (**3j**)	91
Cbz-Leu-H (**3k**)	87

shown in Table 1. These amino aldehydes were directly used for the next step without further purification. In an initial reaction, we subjected Boc-alanal, **3a** to the coupling reaction with ethyl diazoacetate. In a typical reaction procedure, **3a** was dissolved in dichloromethane and pre-activated by adding 20 mol% of anhydrous tin (II) chloride at room temperature. To this, ethyl diazoacetate was added slowly. We observed immediate evolution of nitrogen gas after the addition of ethyl diazoacetate, and it was ceased within 30 minutes indicating the complete consumption of aldehyde. In the course of the reaction, we found that 20 mol% catalyst is optimum for the reaction to get good to excellent yield. Different Lewis acid catalysts such as $ZnCl_2$, BF_3, $GeCl_2$ and $TiCl_4$ were also reported in the similar type of reaction, however, we restricted our reactions to tin(II) chloride catalyst.[15,17,18] Because, $TiCl_4$ and zinc Lewis acid catalysts have also been used in the Mukaiyama-aldol type reactions[19] with aldehydes and diazoacetates. In addition, though BF_3 has been used as a catalyst for the

synthesis of Boc-protected γ- amino β-keto esters, however yields were lower than the tin (II) chloride assisted systhesis.[20] Reactions using tin chloride were found to be insensitive to the atmosphere and all reactions were performed in open flasks. In a control reaction **3a** with ethyl diazoacetate in the absence of catalyst no reaction occurred, and we isolated starting aldehyde. We further extended this reaction to other Boc-protected amino aldehydes, **3b-h**. The reactions were instantaneous and all Boc- protected β-keto esters, **4a-h**, were isolated in good yields (76-84%) and purity after simple aqueous work-up, and are given in Table 2. Yields are better or comparable to the nucleophilic substitution reactions.[3,5,6] Having identified mild conditions for the synthesis of Boc-protected γ-amino β-keto esters, the scope and generality of the reaction was further examined with Cbz- and Fmoc- protected amino acids. We observed quantitative conversion of **2** to **4** in the case of Cbz-protected amino acids; however, in the case of Fmoc-protected amino acids yields were lower than expected. We synthesized Cbz-protected β-keto esters **4i-k**, starting from Cbz-protected amino aldehydes **3i-k**, using the same protocol as described for Boc-amino aldehydes (Table 2).

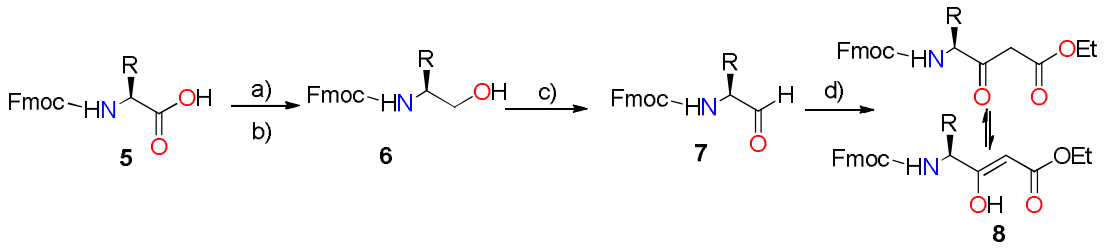

Reagents and Conditions: (a) Isobutyl chloroformate, DiPEA, THF; (b) NaBH4, H_2O, 90-98%; (c) Dess-Martin periodinane, DCM, 84-95%; (d) Ethyl diazoacetate, DCM, 20 mol% $SnCl_2$, 76-84%

Scheme 2: Synthesis of *N*-Fmoc protected γ-amino β-keto esters from the coupling reaction between amino aldehydes and ethyl diazocaetate in the presence of tin(II) chloride.

We anticipated that lower yields in the case of Fmoc-amino Weinreb amides may be due to the untimely cleavage of Fmoc- group in the presence of LAH.[21] This was further confirmed by the ninhydrin test of the reaction mixture. To avoid pre-mature departure of Fmoc-group in the LAH reduction, we adopted different strategy for the

Table 2. List of *N*-protected γ-amino β-keto esters synthesized from the *N*-protected amino aldehydes and ethyl diazoacetate in the presence of 20 mol% tin (II) chloride.

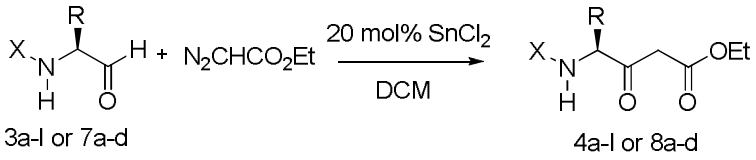

Entry	substrate	product	yield(%)	entry	substrate	product	yield(%)
1.	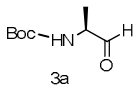 3a	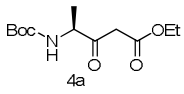 4a	76	9.	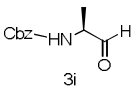 3i	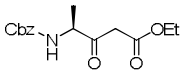 4i	80
2.	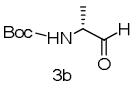 3b	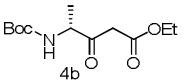 4b	78	10.	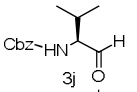 3j	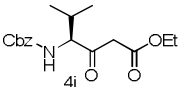 4j	75
3.	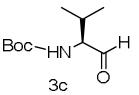 3c	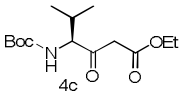 4c	84	11.	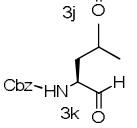 3k	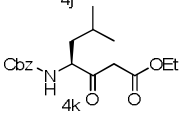 4k	83
4.	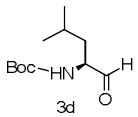 3d	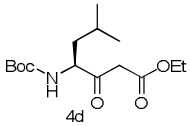 4d	79	12.	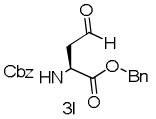 3l	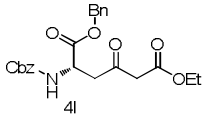 4l	69
5.	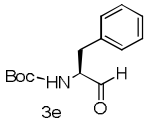 3e	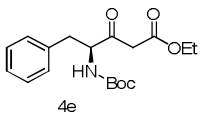 4e	78	13.	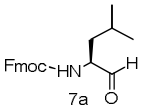 7a	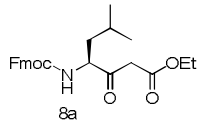 8a	77
6.	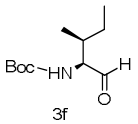 3f	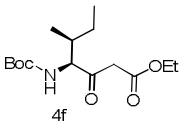 4f	76	14.	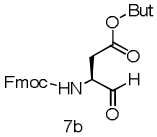 7b	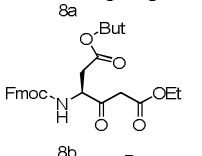 8b	77
7.	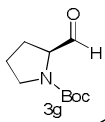 3g	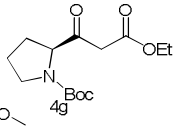 4g	78	15.	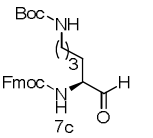 7c	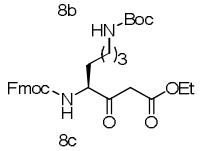 8c	80
8.	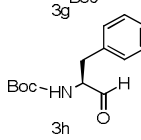 3h	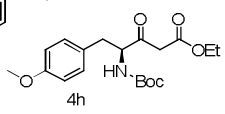 4h	80	16.	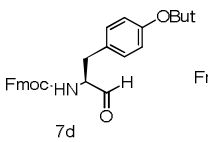 7d	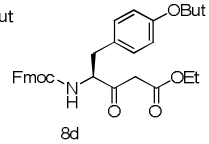 8d	83

synthesis of *N*-Fmoc amino aldehyde **7**. The schematic representation is shown in Scheme 2 for synthesis of *N*-Fmoc amino aldehyde **7**. The Fmoc-amino alcohol **6** was readily synthesized starting from *N*-Fmoc amino acid **5** through the mild $NaBH_4$ reduction of corresponding mixed anhydride.[22] The Fmoc-amino alcohol **6** was then subjected to Dess-Martin periodinane (DMP) oxidation[23] to obtain **7a-d** in quantitative yield. The Fmoc-protected amino aldehydes were directly used for the next step without purification. Fmoc-γ-amino β-keto esters, **8a-d**, were isolated in good yields similar to Boc- and Cbz- amino esters, and are given in the Table 2. Similar protocol of DMP oxidation was used for the synthesis of compound Cbz-Asp(CHO)-OBzl (**3l,** Table 2, entry 12) from the corresponding side chain alcohol Cbz-Asp(CH_2OH)-OBzl. All β-keto esters were purified through silica gel column chromatography using ethyl acetate/pet ether as eluent. Notably, all *N*-protected β-keto esters were isolated in comparable yields indicating that reaction was insensitive to the protecting groups. Out of all β-keto esters **4e, 4h, 4l** and **8c** were isolated as solids and other compounds were isolated as oils. The melting points for all solid compounds were recorded. The specific rotations were given in the experimental section. Out of all solid products, Boc-phenylalanine β-keto ester (**4e**) was crystallized in ethyl acetate on standing (in the round bottom flask). The X-ray structure of **4e** is shown in Figure 2. Similar to the vinylogous and γ-amino acids two additional torsion variables were introduced to analyse the conformational properties of Boc-phenylalanine β-keto ester. Crystal structure analysis reveals that ϕ and θ_2 adopted extended conformation with -135 and 162° respectively, whereas θ_1 and Ψ have taken the values 35 and 93°, respectively.

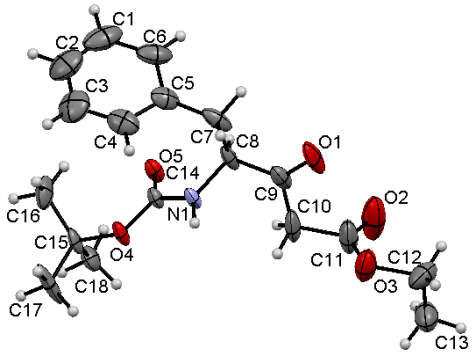

Figure 2: The ORTEP diagram of Boc-phenylalanine β-keto esters (**4e**)

The ^{1}H and ^{13}C NMR of the *N*-protected γ-amino β-keto esters were recorded in $CDCl_3$. We observed a doublet of doublet for α-active methylene protons in AB coupling pattern at δ 3.5

ppm along with two distinct and common peaks at around δ 5.5 and δ 12 ppm for en-ol protons, respectively. The ratio of keto/en-ol form was found to be ≥10:1. Notably, we did not observe any change in the ratio of keto/en-ol tautomers even with range of temperatures from -40 to 30 ^{o}C (Figure 3). Interestingly, no en-ol form of the β-keto ester is observed even in the solid state structure of Boc-phenylalanine β-keto ester (**4e)** as C9-C10 bond distance showing the single bond character.

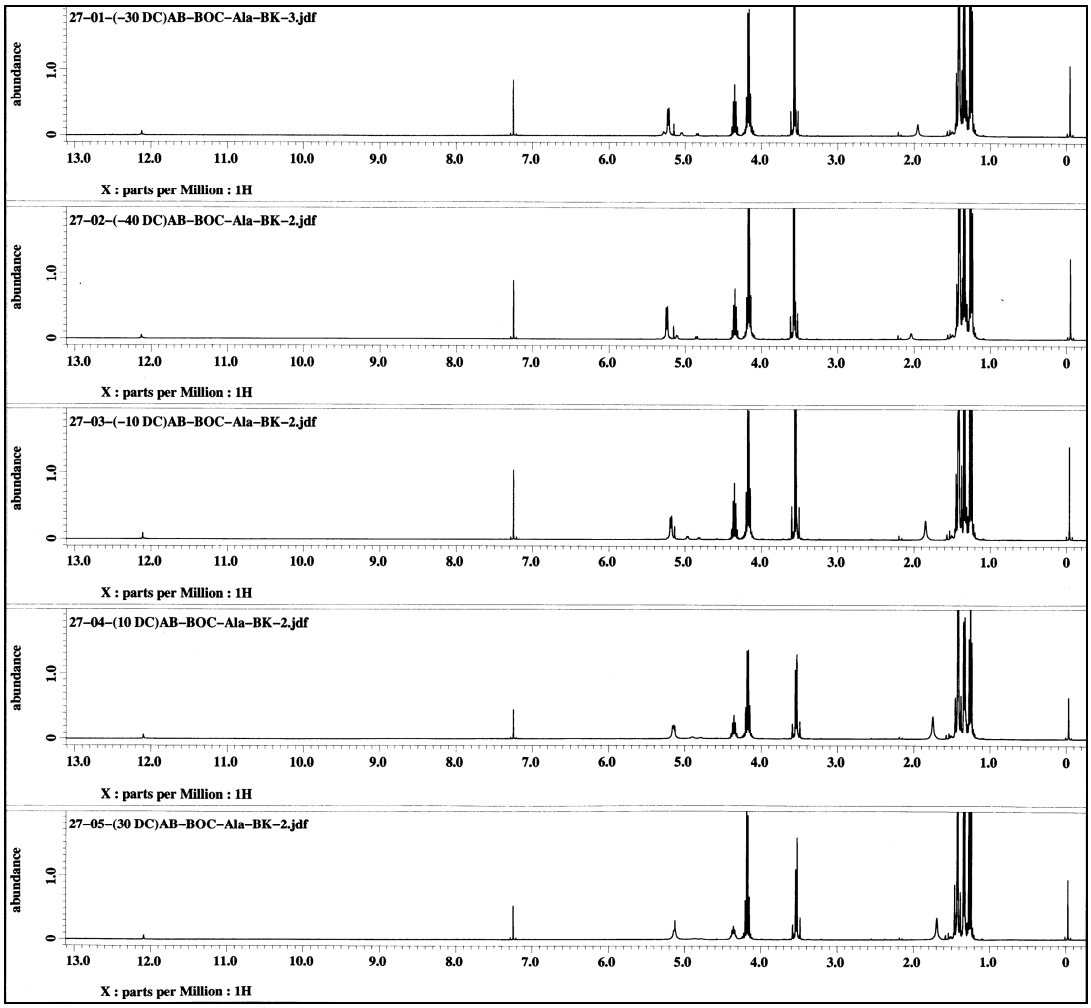

Figure 3: Temperature Experiment of **4a** in $CDCl_3$: The peak at δ ~ 12.1 ppm indicating the existence of enol from of β-keto ester at various temperatures.

On the basis of results observed from this work and the results reported in the literature,[19] we propose a plausible reaction mechanism for the formation of β-keto esters (Scheme 3).

We anticipate that formation of protected γ-amino β-keto esters proceeds *via* β-hydroxy-α-diazo ester intermediate. Activation of aldehyde by coordination with the tin (II) chloride and subsequent *re* or *si*-face nucleophilic addition of ethyl diazoacetate leads to the favourable formation of intermediate II or II', respectively. To achieve this, diazogroup must proceed with gauche conformation with the R group as shown in I or I'. The gauche conformation may be stabilized by ionic interactions between the charged intermediates. Further, the intermediate II or II' subsequently loses nitrogen followed by 1, 2-hydride shift to give β-keto esters. Overall, the formation of β-keto esters proceeds through the semipinacol rearrangement.

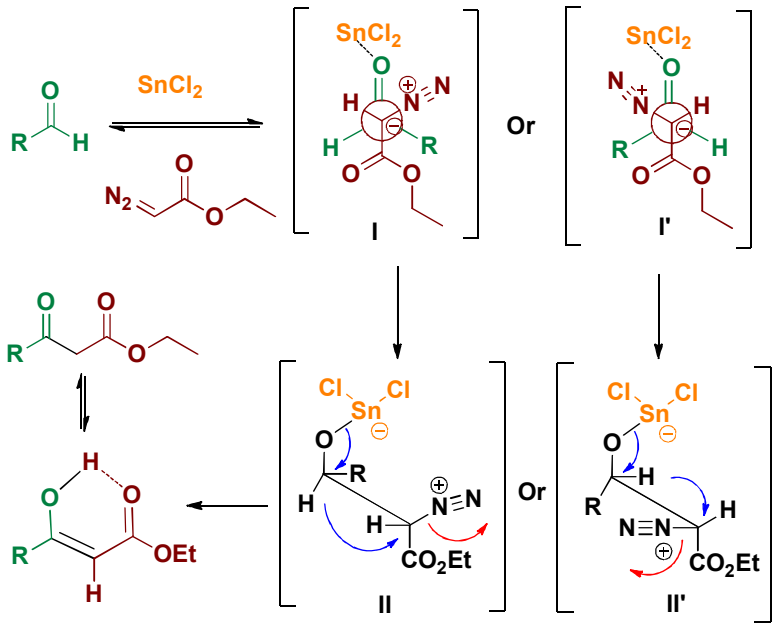

Scheme 3: Proposed mechanism for the formation of β-keto ester from aldehyde and ethyl diazoacetate.

4A.4 Conclusions

In conclusion, we have described the facile synthesis of *N*-protected γ-amino β-keto esters from readily accessible amino aldehydes and commercially available ethyl diazoacetate. The reaction is insensitive to the Boc-, Cbz- and Fmoc- protecting groups as well as atmospheric conditions. We further utilized these amino acids for the synthesis of coumarins and β-hydroxy γ-amino acids.

Section 4B: A Facile Transformation of Amino acids to Functionalized Coumarins

4B.1 Introduction

Coumarins are widely occurring class of compounds isolated from a variety of plant sources.[24] High concentration of coumarins are present in the tonka bean (*Dipteryx odorata*), vanilla grass (*Anthoxanthum odoratum*), sweet woodruff (*Galium odoratum*), mullein (*Verbascum spp.*), sweet grass (*Hierochloe odorata*), cassia cinnamon (*Cinnamomum aromaticum*), melilot (*Melilotus ssp.*), Panicum Clandestinum, sweet clover (*Fabaceae spp.*) so on.[24] Natural and synthetic derivatives of coumarins have been shown to possess remarkable array of pharmacological and biomedical properties including anticancer, anticoagulant, antimicrobial, anti-inflammatory and antioxidant activities.[25] The wide pharmacological properties of coumarins and their ability to interact more than one target is the significant source of inspiration for synthetic chemists to design

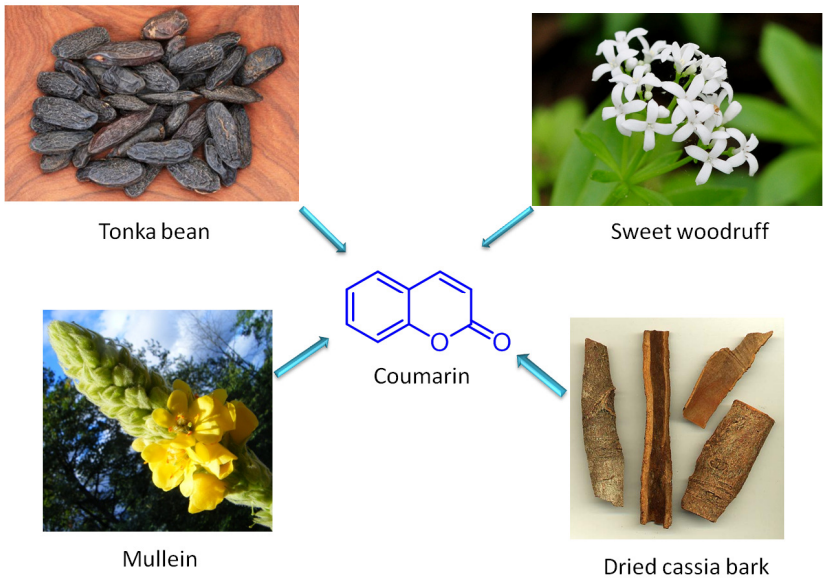

Figure 4: Schematic representation of coumarin moiety with different plant sources of coumarin.

structural analogues with improved or entirely different pharmacological properties.[24, 26] The functionalized coumarins also find applications as dyes in laser technology,[27] in perfumery industry[28] and more importantly as fluorescent tags.[29] Due to the broad spectrum properties in both biology and material science, without surprising, considerable effort has been made

towards the synthesis of coumarins and functionalized coumarins using traditional Pechmann, Perkin, Reformatsky, Knoevenagel, Wittig, Claisen and other methods.[29,30]

4B.2 Aim and rationale of the present work

Various procedures have been reported for the synthesis of coumarin and their derivatives. However, so far there is no report regarding the synthesis of coumarins functionalized with proteinogenic amino acid side chains in the literature. These proteinogenic amino acid side chain functionalized coumarins may be more relevant from the pharmacological and biomedical perspective. In this regard, we sought to investigate whether the α-amino acids can be directly transformed to chiral coumarins. In the earlier section (**4A)** we have discussed the facile and straightforward procedure to synthesis of *N*-protected β-keto ester. We sought to utilize these β-keto-esters for the synthesis of chiral coumarin with proteinogenic side chains using simple Pechmann reaction condition. Herein we are reporting the synthesis of *N*-Boc protected protienogenic side chain containing coumarin amine and coumarin side chain containing amino acid starting from *N*-protected β-keto-esters. In addition, we have also studied solid state structure of Boc-alanyl coumarin and Boc-prolyl coumarin. Further we have examined their fluorescent properties by incorporating into peptide sequences.

4B.3 Results and Discussion

4B.3.1 Method for synthesis of functionalized coumarin

We choose the simplest and widely used Pechmann reaction for the synthesis of functionalized coumarins. Pechmann reaction involves phenol condensation with a β-ketoester in the presence of a variety of Bronsted and Lewis acids.[31] We used Lewis acid-catalyzed protocol for the transformation of α-amino acids to γ-amino β- keto esters as described earlier in the section **4A**.[32] In the initial reaction, to verify whether or not these β-keto-γ-amino acids can undergo von Pechmann condensation to give functionalized coumarins, we subjected ethyl ester of Boc-protected-β-keto-γ-alanine (**3a**) for the condensation reaction with 3-methoxyphenol in the presence of methanesulfonic acid

(MSA).[33] The schematic representation of the synthesis is shown in Scheme 4. To our surprise, the yield was lower than the expected when compared to the simple ethyl acetoacetate. We speculate that Boc-group may be responsible for the unexpected impurities in the reaction. To circumvent the formation of impurities, the Boc- group was removed from **3a** prior to the reaction using TFA. The trifluoroacetate salt of free amine was isolated and subjected to the Pechmann condensation. The functionalized free amino coumarin derivative of **4a** was isolated as red salt after the condensation with 3-methoxyphenol. The free amine of the coumarin was again protected with the Boc-group after neutralizing the methanesulfonate salt with Na_2CO_3. The pure **4a** was isolated in modest yield (72%) after column chromatography. The successful isolation of Boc-alanylcoumarin has led us to subject other γ-amino β-keto esters (**3b-3f**) to the Pechmann condensation. The list of functionalized coumarins (**4b-4f**) synthesized from the Boc-γ-amino β-keto esters is given in the Table 3.

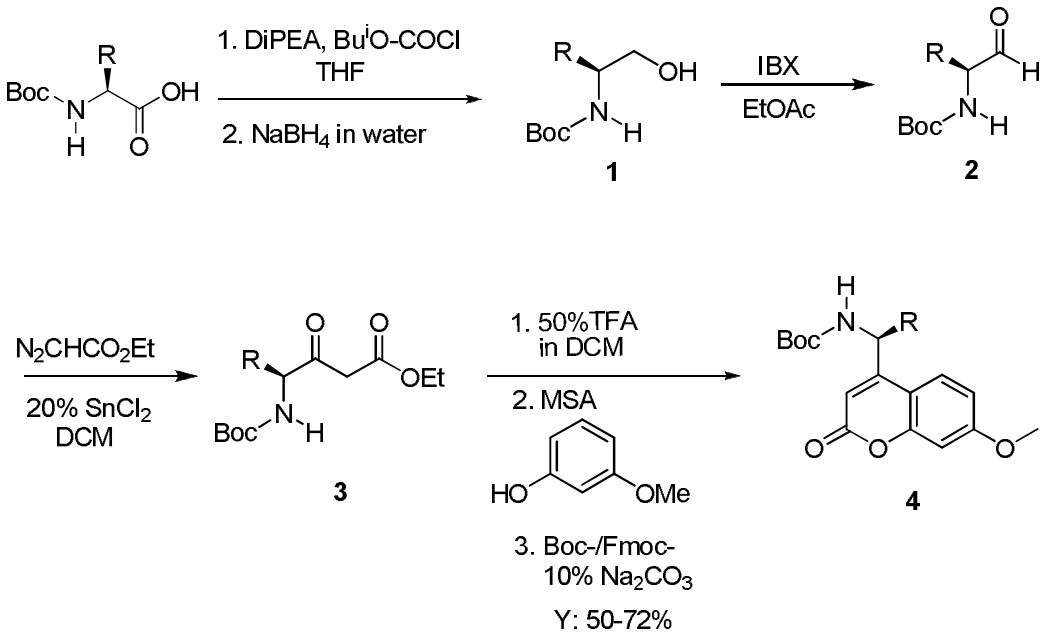

Scheme 4: Synthesis of 4-substituted chiral coumarins.

Table 3: List of functionalized coumarins synthesized from ethyl esters of β-keto-γ-amino acids.

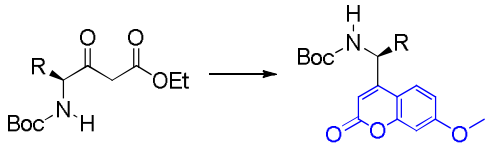

3 **4**

No.	β-keto ester(**3**)	Coumarin(**4**)	Yield (%)
a	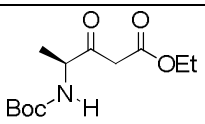	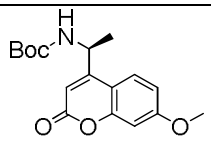	**72**
a1	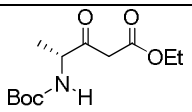	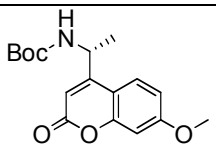	**72**
b	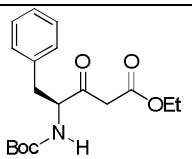	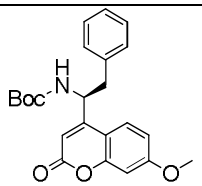	**70**
c	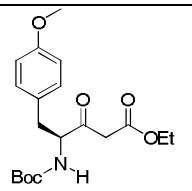	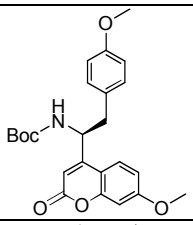	**68**
d	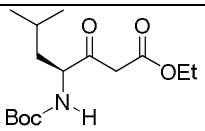	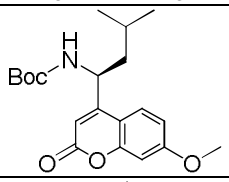	**63**
e	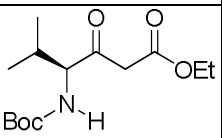	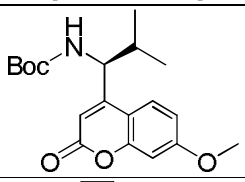	**50**
f	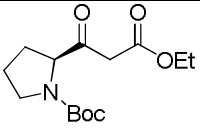	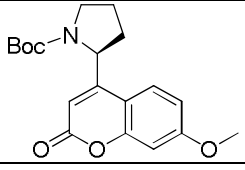	**71**

4B.3.2 Synthesis of side chain coumarin amino acid

With these encouraging results we thought to incorporate coumarin as a side chain on an amino acid backbone. To incorporate coumarin as a side chain on an amino acid backbone, we adapted a different strategy. The coumarin amino acid, **4g**, was synthesized starting from the commercially available Cbz-Asp(OH)-OBzl. The free carboxylic acid was converted to aldehyde [Cbz-Asp(CHO)-OBzl] through the oxidation of corresponding alcohol using DMP.[23] The aldehyde was transformed to β-keto ester (**3g**) by reacting with ethyl diazoacetate in the presence of $SnCl_2$ catalyst. The Pechmann condensation of **3g** with 3-methoxyphenol in the presence of MSA led to the formation of methanesulfonate salt of amino acid coumarin. The free amino group was again protected with Fmoc- after neutralizing with Na_2CO_3. The protected amino acid coumarin (**4g**) was isolated in moderate yield after aqueous work-up and the column chromatography. The Scheme 5 represents the synthesis steps of **4g** from Cbz-Asp(CH_2OH)-OBzl.

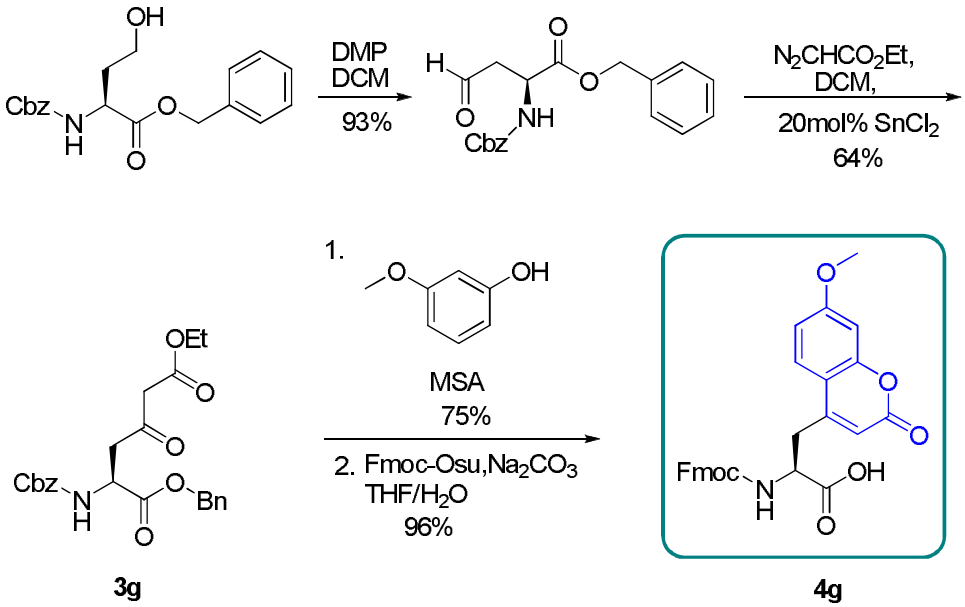

Scheme 5: Synthesis of side chain coumarin amino acid.

4B.3.3 Fluorescence spectra and solid state structures

In order to understand the fluorescence properties of coumarins, the UV absorption spectra were recorded for all coumarins (**4a-4g**) and the absorption maxima were observed at around 324 nm. The fluorescence spectra of all coumarins were recorded after exciting at 324 nm and are shown in the Figure 5. Further, out of all chiral coumarins, we were able to obtain single crystals for the compounds **4a** and **4f** after slow evaporation in methanol solution. The X-ray structures are shown in Figure 6. Examination of the crystal structure of **4a** reveals that the coumarins are connected by intermolecular H-bonding between the amide NH and CO groups as well as C9H and CO. Interestingly, a remarkable organic framework is observed in the crystal structure of **3f** (Figure 6c). Inspection of crystal structure reveals that the crystal packing is stabilized by CH···O, C-H···π and lone pair···π interactions.[34]

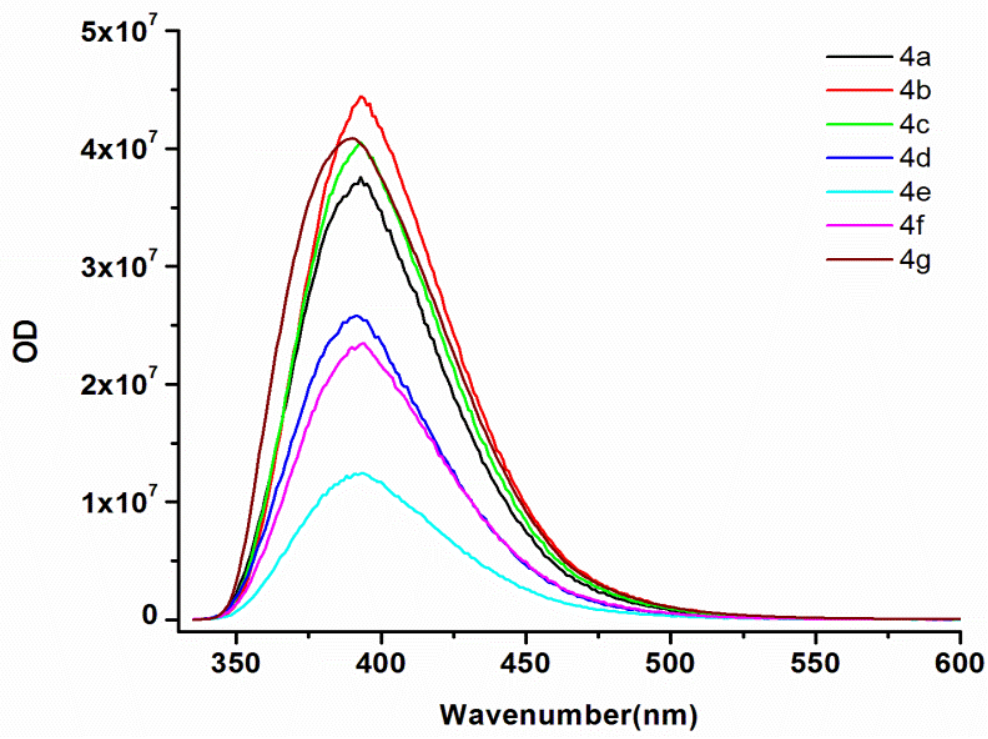

Figure 5: The fluorescence emission spectra of functionalized coumarins (**4a-4g**).

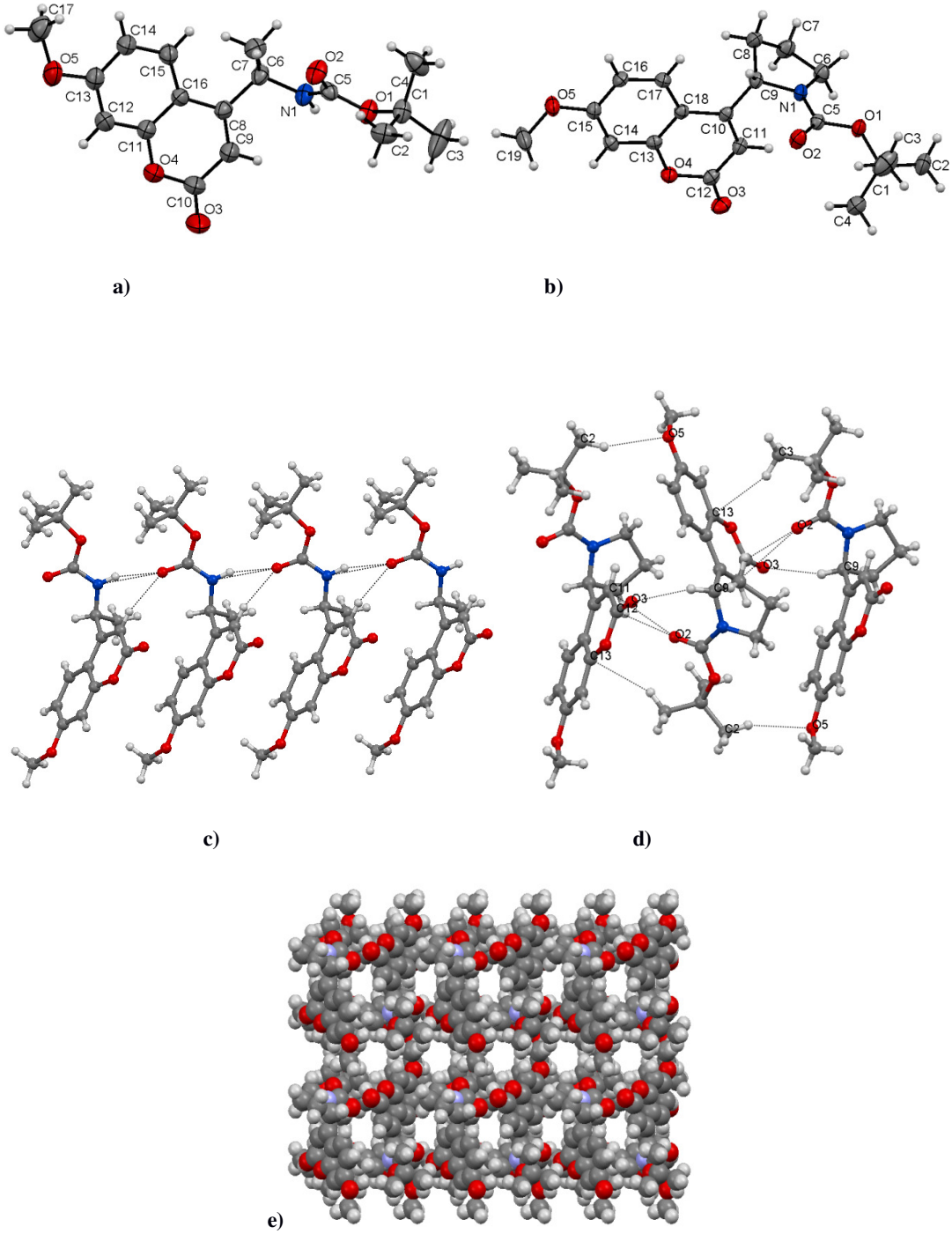

Figure 6: ORTEP diagram of a) Boc-alanylcoumarin, b) Boc-prolylcoumarin; H-atoms are not labled for clarity. c) The extended sheet type assembly of Boc-alanylcoumarin, d) The crystal packing depicting the non-covalent interactions in Boc-prolylcoumarin, e) The space filled model depicting the organic frame work observed in the crystal packing of Boc-prolylcoumarin.

4B.3.4 Experiment for racemization during synthesis

In order to understand racemisation during the coumarin synthesis, we synthesized **4a1** and (±)DL alanylcoumarins starting from Boc-D-Ala and Boc-(±)DL-Ala, respectively. The compounds **4a**, **4a1** and Boc-(±)DL alanylcoumarins were subjected to chiral HPLC using Daicel CHIRALPAK-AI column and is shown in Figure 7. The compounds **4a** and **4a1** gave the single peaks with the t_R 11.62 and 7.85, respectively. The Boc-(±)DL alanylcoumarins gave two peaks with the t_R corresponding to the **4a** and **4a1**. These results indicate that no racemization has occurred during the transformation of amino acids to coumarins.

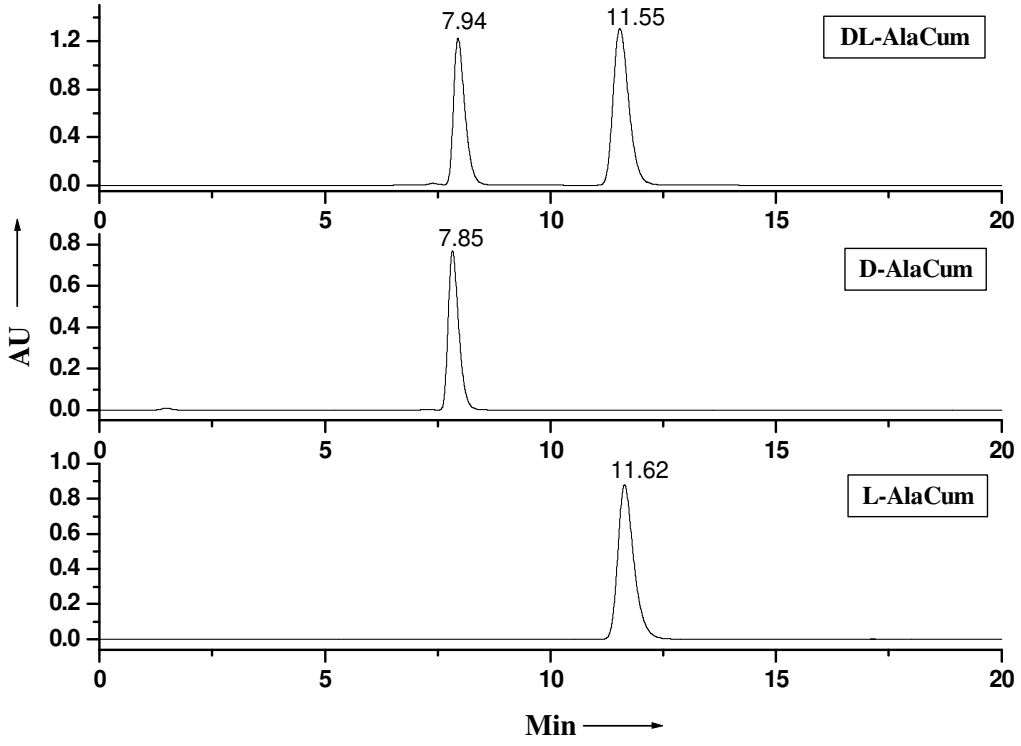

Figure 7: Chiral HPLC of L, D and (±)DL Boc-AlaCum. The HPLC was performed on chiral pack AD column using 90% isopropanol in n-hexane as a solvent system at isocratic mode with the flow rate of 1 mL/ min: a) HPLC profile of (±)DL Boc-AlaCum b) HPLC profile of Boc-D-AlaCum and c) HPLC profiles for the Boc-L-AlaCum.

4B.3.5 Incorporation of functionalized chiral coumarin to HIV-1 TAT peptide sequence and study of its cell permeability

To investigate whether these functionalized chiral fluorescent coumarins could be used in the biological studies, we synthesized cell permeable HIV-1 TAT peptide[35] GRKKKRRQRRRPPQ (**P1**) by incorporating coumarin **4b** at the C-terminal of the peptide using solid phase synthesis. The advantage is that the coumarins can be directly incorporated into the peptides along with amino acid side chain without using additional linkers. However, except **4g**, all coumarins are lack of carboxylic acid at

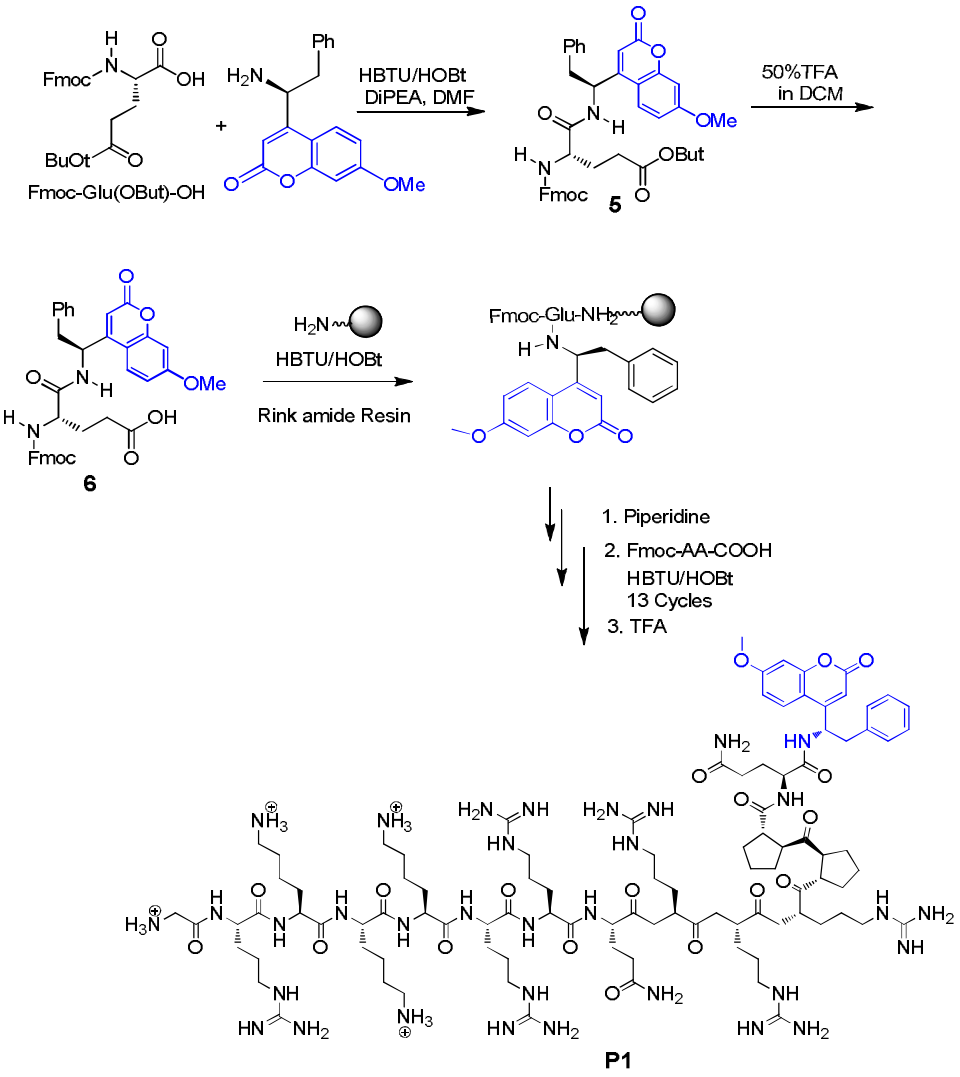

Scheme 6: Incorporation of chiral coumarin into HIV-1 TAT peptide (**P1**).

the C-terminal to incorporate into the peptides. To insert these coumarins into peptides, we developed a new protocol as shown in Scheme 6. The free carboxylic acid [Fmoc-Glu(OH)-PheCum] of dipeptide **5** was coupled to the Rink amide resin and the peptide synthesis was continued by stepwise addition of Fmoc-amino acids using standard HBTU/HOBt couplings. Finally, the peptide was released from the resin and purified by reverse phase HPLC. The pure peptide was incubated with DLD-1 colon cancer cells and the internalization was visualized by fluorescence laser scanning microscopy. The fluorescence image of the cells is shown in Figure 8. Overall, we have demonstrated the effective incorporation of amino acid side chain functionalized coumarins into peptides as fluorescent tags.

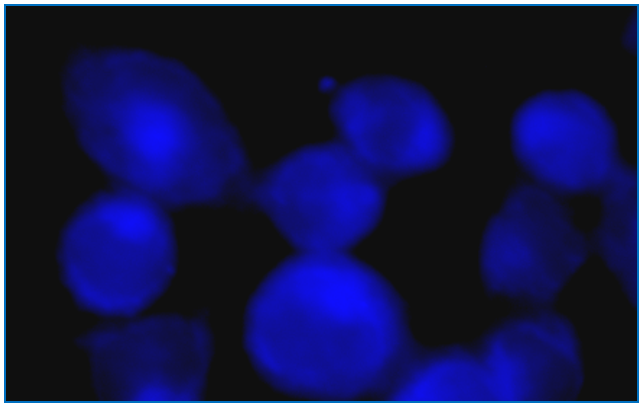

Figure 8: Fluorescence image of **P1** in DLD-1colon cancer cells.

4B.4 Conclusions

In conclusion, we have demonstrated the facile transformation of amino acids to novel coumarins functionalized with amino acid side chains and their incorporation into peptides using solid phase synthesis. The Boc-prolylcoumarin showed the remarkable organic framework in the crystal structure. The biological properties of these chiral coumarins and their organic framework will be further investigated.

Section 4C: Conformational analysis of β-hydroxy γ-amino acid (Statin) in hybrid peptides

4C.1 Intorduction

In recent years, *syn*- and *anti*-β-hydroxy γ-amino acids (Figure 9) have received much attention since these compounds are found to be key components of many peptidomimetic protease inhibitors.[36] Interestingly in the β-hydroxy γ-amino acids, the hydroxyl group mimics the tetrahedral transition state for peptide bond hydrolysis, which has been found to be essential for their bioactivity. In addition β-hydroxy γ-amino acids are widely present in many peptide natural products.[37] Representative examples of β-hydroxy γ-amino acids with (*S*, *S*) configuration can be found in the bioactive depsipeptides didemnins A-C[38], tamadarin B[39] and hapalosin[40] inter alia. Some of these peptide natural products are shown in Figure 9.

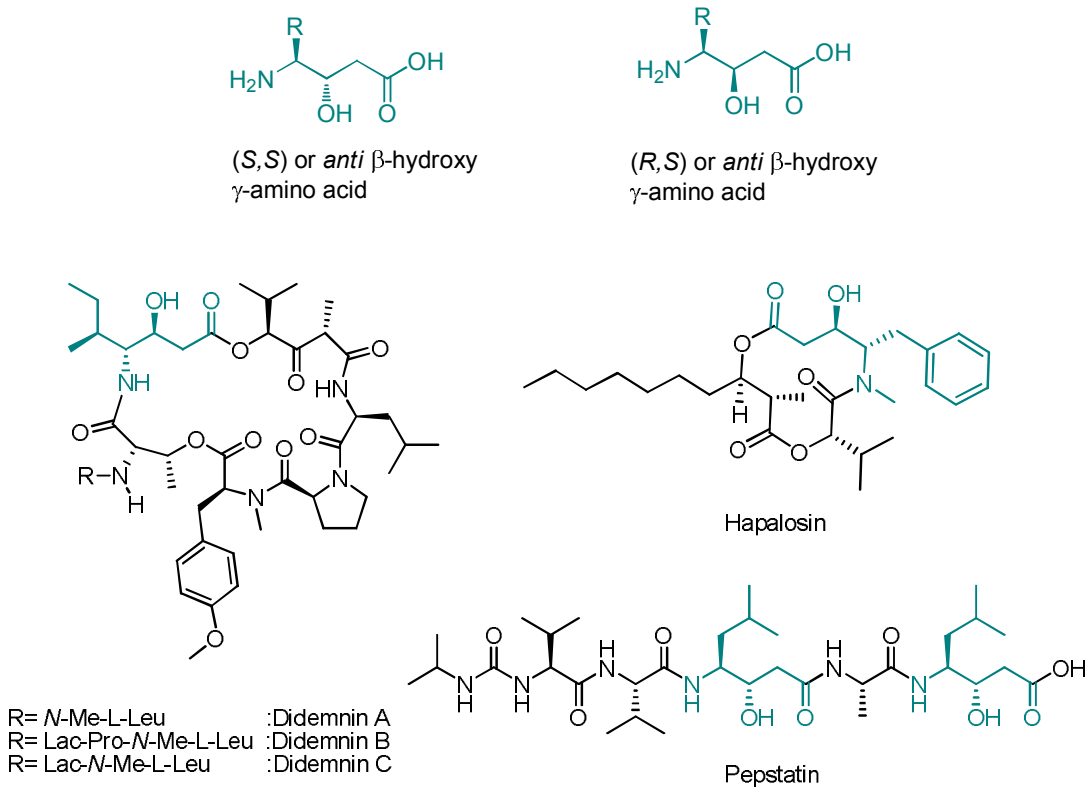

Figure 9: Representative examples of β-hydroxy γ-amino acids in peptide natural products.

In addition, both *syn*- and *anti* configurations of hydroxyl group with respect to the amino acid side-chain are important constituents of many natural products including paclitaxel (taxol), the immunological response modifier bestatin, metabolites isolated from lithistid sponges,[41] and other protease inhibitors.[42] A very well known naturally occurring peptide Pepstatin (Figure 9) acts as carboxyl protease inhibitor discovered by Umezawa.[43] Inspired by the tremendous biological applications of naturally occurring β-hydroxy γ-amino acids various peptides have been designed and synthesized.[44] Though there has been several reports regarding the synthesis of β-hydroxy γ-amino acids and natural products and peptides, however, very little is known regarding the conformation of β-hydroxy γ-amino acids in designed peptides.

4C.2 Aim and rationale of the present work

Natural occurrence and their excellent biologically activity inspired us to design functional hybrid foldamers containing β-hydroxy γ-amino acids. As there are no reports regarding the utilization of these amino acids in the design of hybrid peptides in the literature, we sought to investigate the conformational behaviour of these amino acids in the hybrid peptides. We anticipate that β-keto-γ-amino esters can serve as starting materials for the synthesis of β-hydroxy γ-amino acids. In addition we speculate that stable hybrid helix can be generated the presence of β-hydroxy group as there is a possibility of additional 15 membered H-bonding to strengthen the helix interior (Figure 10). In this section, we describe the synthesis of β-hydroxy γ-amino acids through mild reduction of β-keto esters as well as their incorporation into peptides. The conformational properties of the designed 1:1 alternating hybrid peptides containing the α- and β-hydroxy γ-amino acids are studied in single crystals.

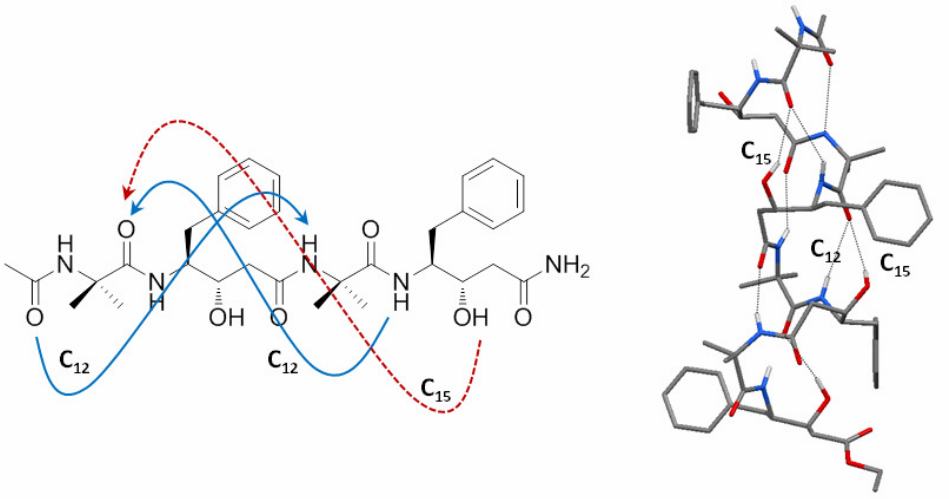

a) **b)**

Figure 10: a) Schematic representation of possible CO···NH (12 membered) and CO···OH (15 membered) H-bonds in α/(*S, S*) β-hydroxy γ-amino acid hybrid peptides, b) model octapeptide of α/ (*S, S*) β-hydroxy γ-amino acid hybrid peptide based on α/γ^4 12-helical backbone conformation.

4C.3 Result and Discussion

4C.3.1 Synthesis of Boc-*N*-β-hydroxy-γ-amino ester (Statin)

The β-keto-γ-amino esters were subjected to the mild reduction using the $NaBH_4$ in THF similar to the protocol described by Rich et al.[3a] The list of β-keto-γ-amino esters used in this study is given the Table 4. To understand the stereochemcial output of the $NaBH_4$ reduction, we initially subjected Boc-*N*-β-keto γ-amino ester [26a] of Valine (**1a**). The reduction was carried out in dry THF at -75 ^oC. The schematic representation of the keto group reduction is shown in Scheme 7. The product Boc-*N*-β-hydroxy-Val-γ-amino ester was isolated as diastereoisomers as confirmed by the TLC. These diastereoisomers (*S, S*) and (*R, S*) were separated using normal silica-gel column chromatography. Instructively, the diastereoisomer with (*R*, *S*) configuration was found to be the major product and (*S, S*) diastereoisomer was found to be the minor product. With these encouraging results, we subjected other β-keto-γ-amino esters **1b-1e** (Table 4) for $NaBH_4$ reduction. Using this protocol we have isolated diastereoisomeric products of **1b-1e**. All the diastereoisomer products we have separated

using column chromatography. Out of all the products, we observed the diastereoisomers of **1e** have very close R_f values in TLC. Similar to **1a**, compounds **1b, 1c, 1d** and **1e** gave (*S, S*)

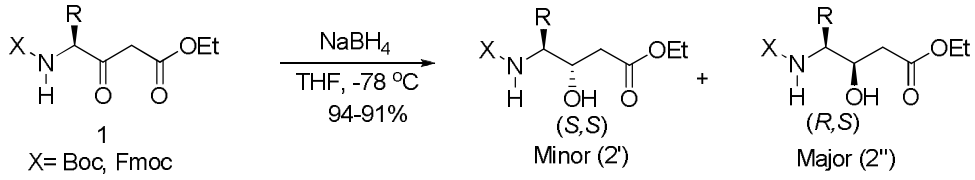

Scheme 7: Conversion of *N*-protected β-keto γ-amino ester to *N*-protected *syn*- and *anti*-β-hydroxy γ-amino ester diastereoisomers.

Table 4: List of functionalized *N*-protected *syn*- and *anti*-β-hydroxy γ-amino ester diastereoisomers.

Entry	Substrate (**1**)	Product (**2**)		Total Yield (%)
		(*S,S*) or *trans*	(*R,S*) or *cis*	
a	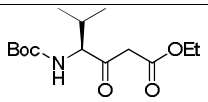	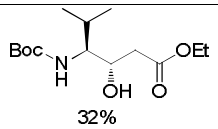 32%	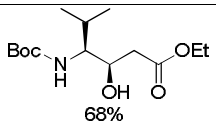 68%	93
b	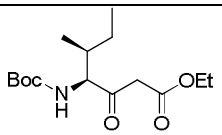	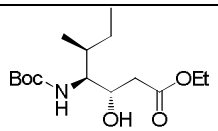 32%	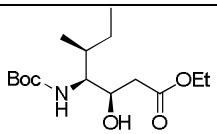 68%	90
c	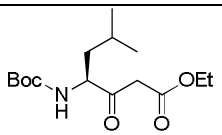	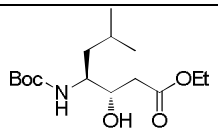 36%	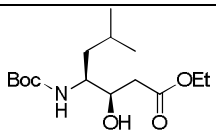 64%	92
d	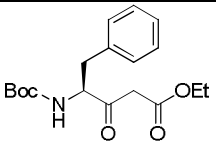	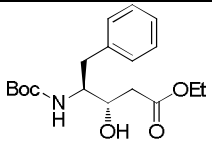 35%	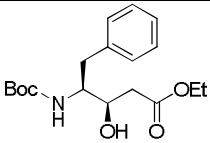 65%	95
e	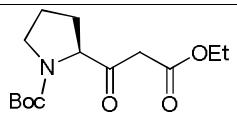	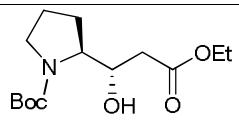 42%	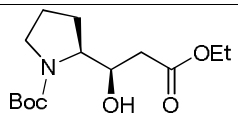 58%	91

as a minor and (*R, S*) as a major products after the reduction. Out of all diastereoisomers, (*R, S*)-Boc-*N*-β-hydroxy-Phe-γ-amino ester was crystallized in methanol solution. The crystal structure is shown in Figure 11a. Similar to the other γ-amino acids, two additional torsional variables θ_1 and θ_2 were introduced to understand the conformations of β-hydroxy γ-amino acids. The stereochemical analysis reveals that ϕ, Ψ and θ_2 adopted extended conformation with -130 -169 and -171° respectively, whereas, θ_1 adopted *gauche*$^+$ conformation with torsional value 59°.

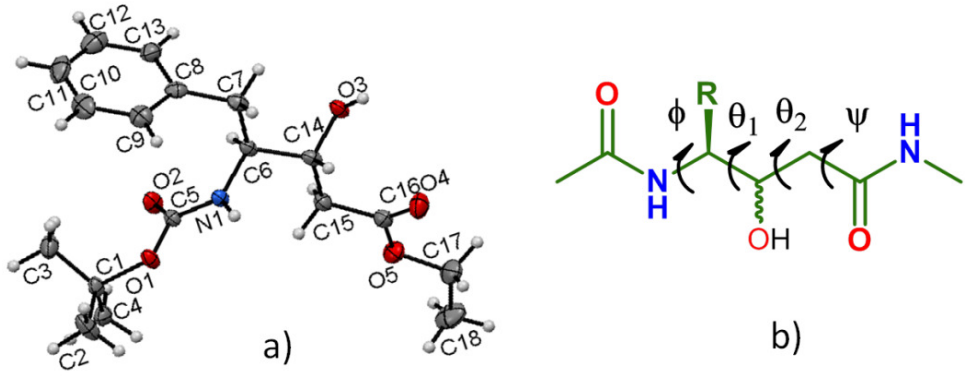

Figure 11: a) ORTEP diagram of (*R, S*)-Boc-*N*-β-hydroxy-Phe-γ-amino ester, b) Torsional variables of β-hydroxy- γ-amino ester.

4C.3.2 Design and synthesis of α/(*S, S*) β-hydroxy γ-amino acid hybrid peptides, and their conformational analysis

In order to understand the conformational properties of β-hydroxy γ-amino acids, we designed two peptides **P1** (Boc-Aib-(*S, S*)-γPhe-Aib-(*S, S*)-γPhe-OEt) and **P2** (Boc-Aib-(*S, S*)-γPhe-Aib-(*S, S*)-γPhe-Aib-OMe) [(*S, S*)-Phe = *anti-β*-hydroxy phenylalanine-γ-amino acids]. We used (*S, S*) diastereoisomers for conformational studies as they are predominantly present in many biologically active peptides compared to (*R, S*) diastereoiosmers. The peptides **P1** and **P2** ware synthesized using in solution phase chemistry using 2+2 and 4+1 convergent strategies, respectively. HBTU was used as coupling agent in all coupling reactions. To confirm whether the free hydroxyl group will interfere in the coupling reaction,

initially synthesized a dipeptide [Boc-Aib-(*S, S*)-Phe-OEt [(*S, S*)-Phe = *anti*-β-hydroxy phenylalanine-γ-amino acids]. The dipeptide was isolated with moderate yield (76%) and no other ester or any cyclic products were observed in the coupling reaction suggesting that no interference of –OH group in the coupling reaction. This result suggested that no need of protection of the hydroxyl group in the peptides while performing coupling reactions. Using similar peptide coupling reactions we synthesized both tetra and pentapeptides without protecting of β-hydroxy group. The schematic representation of the synthesis is shown in the Scheme 8. After the synthesis, peptides were purified using normal silica gel chromatography and subjected for the further analysis.

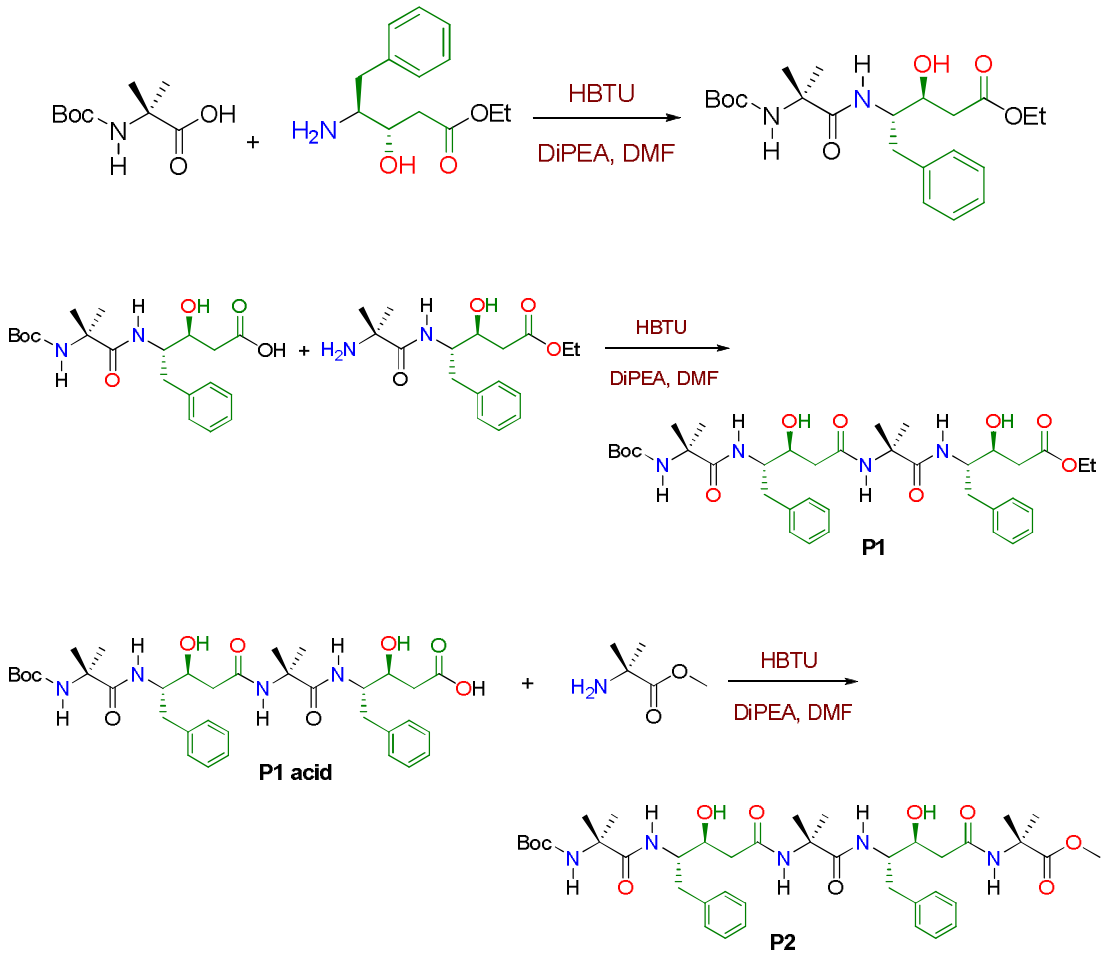

Scheme 8: Synthesis protocol of α/(*S, S*) β-hydroxy γ-amino acid hybrid peptides.

4C.3.3 Solid phase synthesis of heptapeptide (Ac-Ala-(*R, S*)-γPhe-Aib-(*R, S*)-γPhe-Ala-(*R, S*)-γPhe-Aib-NH_2) (P3)

To understand whether these β-hydroxy γ-amino acids can be used in the solid phase peptide synthesis, we synthesized solid phase compatible *N*- Fmoc protected β-hydroxy γ-amino acids. The schematic representation of the synthesis is shown in Scheme 9. We utilized (*R, S*)-γPhe for the solid phase synthesis. The Fmoc-(*R, S*)-γPhe-OH was synthesized starting from Boc-(*R, S*)-γPhe-OEt. Using Fmoc-(*R, S*)-γPhe-OH we synthesized a hepta peptide Ac-Ala-(*R, S*)-γPhe-Aib-(*R, S*)-γPhe-Ala-(*R, S*)-γPhe-Aib-NH_2) (**P3**) (Figure 12) on Rink amide resin using HBTU as coupling agent. Further the peptide was cleaved from resin using TFA/water cocktail mixture and isolated as solid white crude after precipitation with chloroform/pet-ether solvent systems. Then the peptide was purified using reverse phase HPLC using MeOH/H_2O as solvent systems. Results suggests that β-hydroxy γ-amino acids can be incorporated into peptides using solid phase synthesis without any hydroxy group protections.

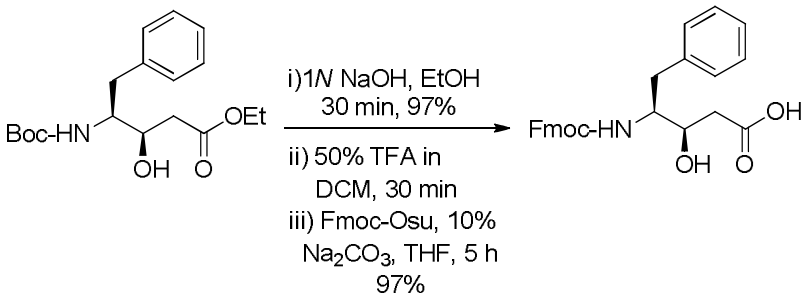

Scheme 3: Synthesis of Fmoc-*N*-(*R, S*)-γPhe-OH amino acids.

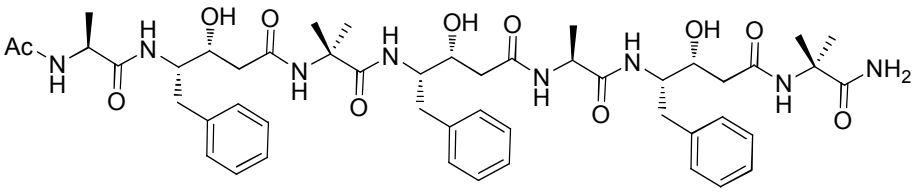

Figure 12: Schematic representation of hepta peptide **P3** (Ac-Ala-(*R, S*)-γPhe-Aib-(*R, S*)-γPhe-Ala-(*R, S*)-γPhe-Aib-NH_2).

4C.3.4 Single crystal conformations of P1 and P2

In order to understand the conformational properties of β-hydroxy-γ-amino acids in peptides we subjected both peptides **P1** and **P2** for crystallization in various solvent combinations. Single crystals of peptide **P1** obtained from the slow evaporation of methanol/H_2O solution yield the structure shown in Figure13. The crystal structure analysis reveals that, **P1** adopted a 12-helical conformation similar to α/γ^4 hybrid peptides.[41] Two molecules of **P1** were observed in the asymmetric unit with slight variation in the torsional values. The conformational analysis of β-hybroxy-γ-Phe residues reveals (*S, S*)-Phe2 adopted *gauche*$^+$, *gauche*$^+$ (g^+, g^+, $\theta_1 \approx \theta_2 \approx 60°$) local conformation about the C_β–C_γ and C_α–C_β bonds, while the C-terminal (*S, S*)-Phe4 residue display extended conformation with θ_1 = 178 and θ_2 = 168. The torsion angles of **P1** are tabulated in Table 6. The two cooperative intramolecular 12-membered backward (1←4) H-bonds C=O(Boc)···NH(3) [C=O···H–N dist. 2.119Å, O···N dist. 2.972Å and ∠O···H–N 170°] and C=O(1)···NH(4) [C=O···H–N dist. 2.004 Å,

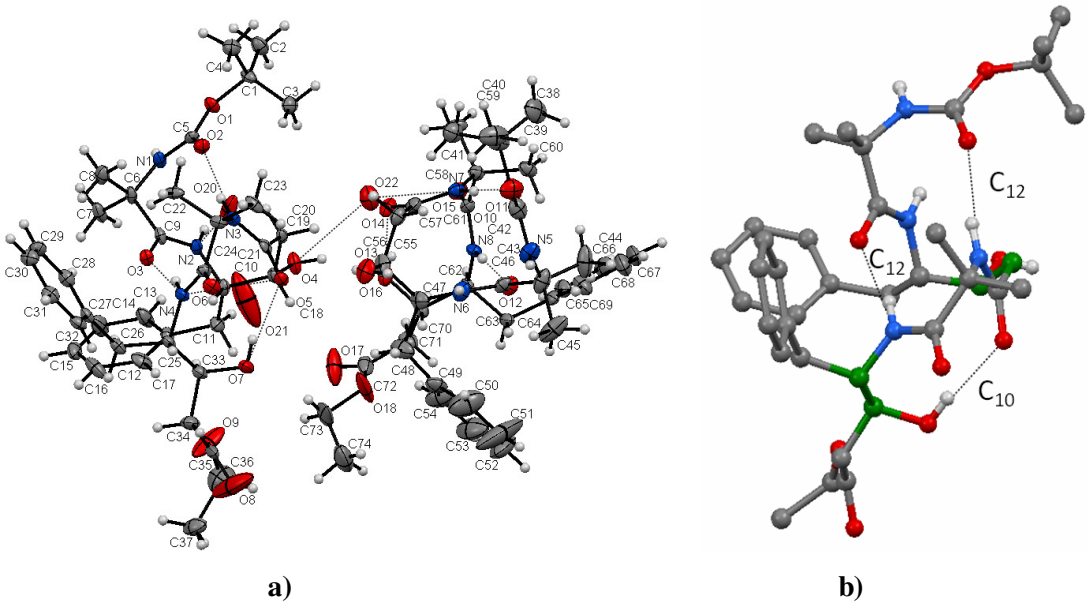

a) **b)**

Figure 13: a) ORTEP diagram of Boc-Aib-(*S, S*)-γPhe-Aib-(*S, S*)-γPhe-OEt (**P1**). Two molecules are present in asymmetric unit with three water molecules, b) Single molecule shown with ball and stick model with three intramolecular H-bond (black wireframe).

O···N dist. 2.847Å and ∠O···H–N 166°] stabilizing the helical conformation (Figure 13b). The H-bonding parameters are tabulated in Table 5. Due to the lack of donor NH group at the C-terminal, we observed a 10-membered intramolecular H-bonding through β-OH group of (*S, S*)-Phe4 and C=O of (*S, S*)-Phe2 [C=O(2)··· β-OH4, C=O···H–O dist. 1.99 Å, C=O···O dist. 2.78 Å and ∠O···H–O 163°].

The pure peptide **P2** was crystallized as rod shaped morphology (Figure 14c) from the slow evaporation of ethanol/H_2O solution. Similar to **P1**, the pentapeptide **P2** also adopted the helical conformation however with little distortion at the C-terminal. The crystal structure of **P2** is shown in Figure14b. The crystal analysis of β-hybroxy-γ-Phe residues in **P2** reveal that (*S, S*)-Phe2 adopted *gauche*$^+$, *gauche*$^+$ (g^+, g^+, $\theta_1 \approx \theta_2 \approx 60°$) local conformation about the C_β–C_γ and C_α–C_β bonds and surprisingly (*S, S*)-Phe4 adopted an extended conformation due to intra-residue 6-membered H-bonding of C=O(4)···β-OH4 [C=O(4)··· β-OH4, C=O···H–O dist. 2.02 Å, C=O···O dist. 2.70 Å and ∠O···H–O 139.5°] even though it is possible to have another 1←4 hydrogen bond between the C=O(i+2) to the NH of terminal Aib5. In contrast to the α/γ^4-hybrid peptides reported earlier, the conformation adopted by the(*S, S*)-Phe4 is quite unusual. The torsion angles are tabulated in Table 5. Further the helical conformation is stabilized by two cooperative 12-membered backward (1←4) H-

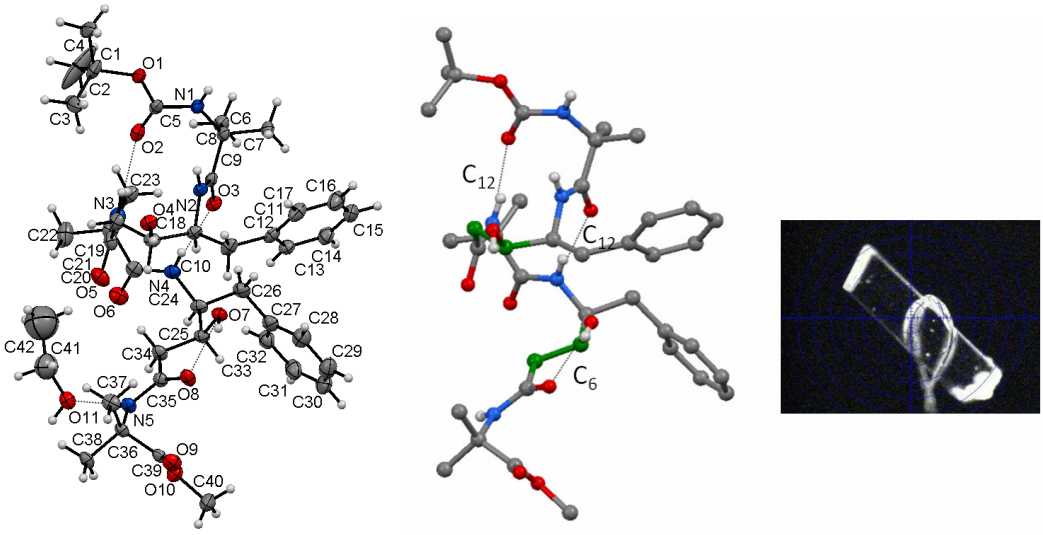

a) **b)** **c)**

Figure 14: ORTEP diagram of Boc-Aib-(*S, S*)-γPhe-Aib-(*S, S*)-γPhe-Aib-OMe (**P2**) with one ethanol molecules, b) **P2** shown with ball and stick model with three intramolecular H-bond (black wireframe), c) rod shapped crystal of **P2** formed in the solution of ethanol/water system.

bonds. The hydrogen bonding parameters of **P2** are tabulated in Table 7. All Aib residues in the peptide adopted right handed helical conformation with ϕ = ~ -55 and Ψ = ~ - 40. Overall the peptide **P2** adapted a distorted helical structure. These results suggest that anti-β-hydroxy γ-amino acids can adopt helical as well as extended conformation in the hybrid peptides.

Table 5: Hydrogen bonding parameters in Boc-Aib-(*S, S*)-γPhe-Aib-(*S, S*)-γPhe-OEt (**P1**).
(two molecules are present in asymmetric unit with three water molecules)

Type of H-bonds	Donar (D)	Acceptor (A)	D····A (Å)	D-H····A (Å)	∠X-H···O (deg), X = N or O	∠X···O=C (deg) X = N or O
Intramol.	N3	O0(Boc)	2.97	2.11	170.6	145.1
Intramol.	N4	O1	2.84	2.00	166.1	138.9
Intramol.	O(7)H	O5	2.78	1.99	162.7	128.8
Intramol.	N7	O11	2.95	2.09	175.59	143.1
Intramol.	N8	O12	2.87	2.02	169.0	141.4
Intramol.	O(16)H	O14	2.82	2.02	164.87	128.38
Intermol.	N5†	O15†	2.90	2.07	164.9	157.9
Intermol.	N2	O20 (H_2O)	2.95	2.13	159.3	-
Intermol.	O6	O20 (H_20)‡	2.74	-	-	126.8
Intermol.	O13	O20 (H_20)‡	2.74	-	-	-
Intermol.	O7	O21 (H_20)‡	2.92	-	-	-
Intermol.	O4	O22 (H_20)	2.93	2.30	134	-
Intermol.	N6†	O22 (H_20)	2.92	2.13	152.2	-
Intermol.	O13	O22 (H_20)	2.74	-	-	-
Intermol.	O15†	O22 (H_20)†	2.93	2.30	-	125.9

Two peptide and three water molecules are present in asymmetric unit with symmetry x,y,z; Intermol.; intermolecular, intramol.; intramolecular; ‡Symmetry equivalent x,-1+y, z; †Symmetry equivalent x,1+y,z.

Table 6: Torsional variables (in deg) of Boc-Aib-(*S, S*)-γPhe-Aib-(*S, S*)-γPhe-OEt (**P1**) and Boc-Aib-(*S, S*)-γPhe-Aib-(*S, S*)-γPhe-Aib-OMe (**P2**)

Pept.	Resd.	ϕ	θ_1	θ_2	ψ	ω
P1*	Aib1	-62/-61	-	-	-35/-42	-173/-174
	(S, S)γPhe2	-125/-124	48/53	63/60	-120/-121	-173/-173
	Aib2	-53/-51	-	-	-37/-43	176/-179
	(S, S)γPhe4	-106/-102	176/171	168/177	-51/-52	-
P2	Aib1	-58	-	-	-38	-170
	(S, S)γPhe2	-124	47	66	-114	-176
	Aib2	-54	-	-	-43	-176
	(S, S)γPhe4	-103	59	-175	-159	-173
	Aib3	-55	-	-	-44	-

*two molecules are present in the asymmetric unit

Table 7: Hydrogen bonding parameters in Boc-Aib-(*S, S*)-γPhe-Aib-(*S, S*)-γPhe-Aib-OMe (**P2**)

Type of H-bonds	Donar (D)	Acceptor (A)	D⋯A (Å)	D-H⋯A (Å)	∠X-H⋯O (deg), X = N or O	∠X⋯O=C (deg) X = N or O
Boc-Aib-(*S, S*)-γPhe-Aib-(*S, S*)-γPhe-Aib-OMe (P2)						
Intramol.	N3	O0(Boc)	2.90	2.05	169.4	152.1
Intramol.	N4	O1	2.88	2.05	163.8	142.6
Intramol.	O(7)H	O8	2.70	2.02	139.51	87.68
Intermol.	N2	O11[#]	2.98	2.19	153.0	-
Intermol.	N5[#]	O11[#]	2.86	2.01	167.7	-
Intermol.	O(4)H	O11[#]	2.73	1.94	161.8	-
Intermol.	N1	O6[#]	2.02	2.86	166.0	176.1
Intermol.	O(4)H	O9[‡]	2.73	1.94	161.8	-

Intermol.= intermolecular, intramol.= intramolecular; # Symmetry equivalent x, 1+y, z, ‡ Symmetry equivalent ½-x, ½+y, 1-z.

4C.4 Conclusion

We have demonstrated the facile synthesis of β-hydroxy γ-amino acids starting from β-keto-γ-amino esters. In addition we showed the smooth incorporation of statin amino acid residues into peptides without protection of β-hydroxy group in both solution and solid phase protocols. The stereochemical analysis of statin amino acids in hybrid peptides suggests they can be incorporated into helical structures, however with caution, as they preferred extended conformations due to the formation of intraresidue H-bonding. These results may provide basic information for the structure-based designs of hybrid peptides containing β-hydroxy γ-amino acids.

4.2 Experimental section

4.2.1 General Experimental Details

All amino acids, ethyl diazoacetate, LAH, DiPEA, Tin(II) chloride, TFA , DMP, Cs_2CO_3, Cbz-Cl were purchased from Aldrich. THF, DCM, DMF, were purchased from Merck. Isobutyl chloroformate, $NaBH_4$, HBTU, HOBT, Methanesulfonic acid, di-tert-butyl dicarbonate, Fmoc-OSu, 3-Methoxy phenol, Benzyl bromide were obtained from spectrochem and used without further purification. THF and DiPEA were dried over sodium and distilled immediately prior to use. Column chromatographies were performed on Merck silica gel (120-200 mesh) and using flash chromatography (Combi Flash R_f). The ^1H spectra were recorded Brucker 500 MHz (or 125 MHz for ^{13}C) and Jeol 400 MHz (or 100 MHz for ^{13}C) spectrometers using residual solvents signals as an internal reference ($CDCl_3$ δ_H, 7.26 ppm, δ_c 77.0 ppm). The chemical shifts (δ) are reported in *ppm* and coupling constants (J) in Hz. Specific rotations were recorded using MeOH as a solvent (Rudolph Analytical Research). UV and Fluorescence data were performed on Thermo Scientific and Fluorolog (Horiba Jobin Yvin) spectrophotometers, respectively. High-resolution mass spectra obtained from HRMS-ESI (waters), LCMS/MS (waters) and MALDI TOF/TOF (Applied Biosciences). X-Ray data were collected on Bruker APEX (II) DUO.

4.2.2 Synthesis procedure and compound characterization for Section 4A

General procedure for the synthesis of Cbz-/Boc-Weinreb amides

We used the reported procedure for the synthesis of Weinreb amides.[16] In a typical experiment, the protected amino acid (15 mmol) was dissolved in dry DCM (30 mL) and then treated with HBTU (15 mmol, 5.68 g) and DiEPA (45 mmol , 4.54 g), the reaction mixture was cooled to 0 ^{o}C. After stirring for 5 min hydrochloride salt (18 mmol, 1.74g) of *N, O*- dimethylhydroxylamine was added. The progress of the reaction was monitored by TLC. After completion of the reaction (roughly 2hrs), DCM was evaporated and the residue was diluted with 150 mL of ethyl acetate and washed with 5% HCl (5 % by vol. in water, 2 x 30 mL), 10 % sodium carbonate solution in water (2 × 40 mL) and followed by brine (30 mL). The organic layer was dried over Na_2SO_4 and evaporated under reduced pressure. The pure Boc-Weinreb amides were isolated after column chromatography using EtOAc/ pet.ether (60-80 ^{o}C) solvent system.

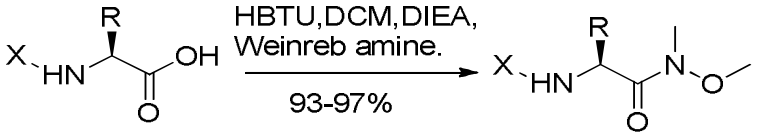

X= -Boc, -Cbz Amino acid = Ala, Val, Leu, Ile, Phe, Tyr, Pro.

General procedure for the synthesis of Cbz-/Boc-amino aldehydes

The *N*-Protected Weinreb amide (15 mmol) was dissolved in 120 mL of dry THF under N_2 atmosphere, cooled to 0 ^{o}C, and then $LiAlH_4$ (18.75 mmol, 0.712 g) was added slowly during 10 min. Reaction was stirred for another 20 min to complete the reaction. Reaction was quenched with 5% HCl (5 % by volume in water) very slowly in ice cool condition (*p*H 3). THF was evaporated from the reaction mixture and the *N*-protected amino aldehyde was extracted with ether (3 × 80 mL). Combined ether layer was washed with brine (40 mL) and dried over anhydrous Na_2SO_4. Organic layer was concentrated under reduced pressure to get oily product and immediately used for next step without purification.

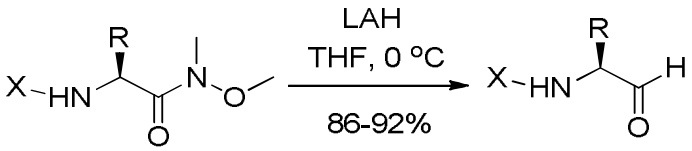

X= -Boc, -Cbz. Amino acid = Ala, Val, Leu, Ile, Phe, Tyr, Pro.

General procedure for the synthesis of Fmoc-amino alcohol

The Fmoc-protected amino acid (10 mmol) was dissolved in dry THF (20 mL) under nitrogen atmosphere, and cooled -15 ^{o}C , and then treated with DiPEA (10.2 mmol, 1.32g) followed by isobutyl chloroformate (10 mmol, 1.366g). White hydrochloride salt of DiPEA was precipitated out immediately after addition of isobutyl chloroformate. The reaction was continued to stir for another 10 min. The hydrochloride salt of DiPEA was filtered and washed with THF (2 × 10 mL). The filtrate was again cooled to -15 ^{o}C under nitrogen atmosphere, and then a solution of $NaBH_4$ (20 mmol, 720 mg) in 3mL of water was added with vigorous stirring. Immediate evolution of gas was observed after the addition. THF was evaporated from the reaction mixture and diluted with EtOAc (150 mL). The organic layer was washed with 5% HCl (5 % by volume in water, 2 × 50 mL), 5 % sodium carbonate solution in water (2 x 50 mL), followed by brine (50 mL). Organic layer was dried over anhydrous Na_2SO_4 and evaporated under reduced pressure. The Fmoc-alcohol was purified using column chromatography and used for the next step.

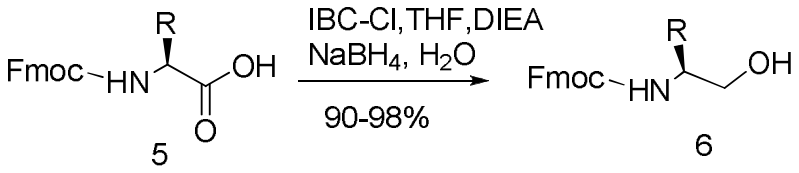

R = -^{i}Bu, -(CH$_2$)-NH-Boc, -CH$_2$CO$_2$^{t}Bu, -CH$_2$-Ph-O^{t}Bu

Product	Yield
(*S*)-(9H-fluoren-9-yl)methyl (1-hydroxy-4-methylpentan-2-yl)carbamate (**6a**)	92% (3.123g)
(*S*)-*tert*-butyl 3-((((9H-fluoren-9-yl)methoxy)carbonyl)amino)-4-hydroxybutanoate (**6b**)	90% (3.572g)
(*S*)-(9H-fluoren-9-yl)methyl *tert*-butyl (6-hydroxyhexane-1,5-diyl)dicarbamate (**6c**)	98% (4.443g)
(*S*)-(9H-fluoren-9-yl)methyl (1-(4-(*tert*-butoxy)phenyl)-3-hydroxypropan-2-yl) (**6d**)	91% (4.045g)

Carbamate

General procedure for the synthesis of Fmoc-amino aldehydes

The Fmoc-amino alcohol (5mmol) was dissolved in 50 mL of DCM at rt and then 2.1 g (7.5mmol) Dess-Martin periodinane (DMP) was added . Resulting reaction mixture was stirred for 1hr; the progress of the reaction was monitored by TLC. Reaction mixture was diluted with diethylether (50mL) followed by 10% Na_2CO_3 solution (50mL) with vigorous stirring. After 10 min organic layer was separated and washed with 10% Na2CO3 solution (50 mL × 2) and brine. Organic layer was dried over anhydrous Na_2SO_4 and concentrated under reduced pressure to get Fmoc-amino aldehyde and it was immediately used in the next step without purification.

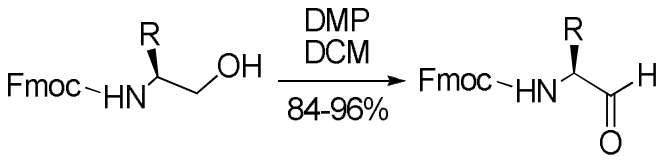

R= -iBu, -(CH_2)-NH-Boc, -$CH_2CO_2{}^tBu$, -CH_2-Ph-O^tBu

Compound	Yield
(*S*)-(9H-fluoren-9-yl)methyl (4-methyl-1-oxopentan-2-yl)carbamate **(7a)**	92% (1.55gm)
(*S*)-*tert*-butyl 3-((((9H-fluoren-9-yl)methoxy)carbonyl)amino)-4-oxobutanoate **(7b)**	88% (1.73gm)
(*S*)-(9H-fluoren-9-yl)methyl *tert*-butyl (6-oxohexane-1,5-diyl)dicarbamate **(7c)**	96% (2.16gm)
(*S*)-(9H-fluoren-9-yl)methyl(1-(4-(*tert*-butoxy)phenyl)-3-oxopropan-2-yl)carbamate **(7d)**	84% (1.85gm)

General procedure for the synthesis of *N*-protected γ-amino β-keto ester

The *N*-protected amino aldehyde (2.0 mmol) was dissolved in 15 mL of DCM at room temperature (20-25 ^{o}C) and then 0.0756 g (20 mol %) of tin (II) chloride was added followed by 0.239 g (2.1 mmol) of ethyl diazoacetate. Immediate gas evolution was observed. The reaction mixture was stirred and the progress of the reaction was monitored by TLC. After completion of the reaction, it was quenched with 10 mL of 0.5N HCl and the reaction mixture was extracted with DCM (30 mL x 3). The combined organic layer was washed with 20 mL of brine, dried over anhydrous sodium sulfate and concentrated under reduced pressure to get greenish oily crude product which was purified on silica gel column chromatography.

(*S*)-ethyl 4-(tert-butoxycarbonylamino)-3-oxopentanoate (4a)

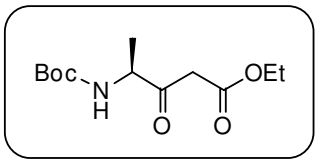

Physical state : colourless liquid

Mol. Formula : $C_{12}H_{21}NO_5$

Yield : (0.398g, 76%)

$[\alpha]_D$ ^{25} : -35.69 (c = 1, MeOH)

^{1}H NMR (500 MHz, $CDCl_3$) : δ_H 12.13 (s, 1H enolic 3.5%), 5.17 (b, s, 1H, NH), 4.43-4.37 (m, 1H, CH), 4.24-4.20 (q, *J* = 7, 2H, OCH_2), 3.62-3.54 (dd, *J* = 14.5, *J* =10.5 2H, CH_2, AB coupling), 1.46 (s, 9H, $C(CH_3)_2$, Boc), 1.38-1.36 (d, *J* =6.5, 3H, CH_3), 1.31-1.28 (t, *J* = 7, 3H, CH_3).

^{13}C NMR (125 MHz, $CDCl_3$) : δ_C 202.50, 166.96, 155.19, 80.14, 61.57, 55.42, 45.91, 28.32, 17.11, 14.11.

ESI-MS m/z : Calcd. $[M+Na]^+$ 282.1317, observed 282.1317.

(*R*)-ethyl 4-(*tert*-butoxycarbonylamino)-3-oxopentanoate (4b)

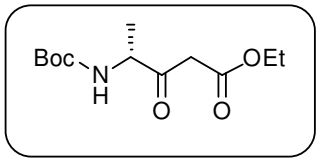

Physical state : colourless liquid

Mol. Formula : $C_{12}H_{21}NO_5$

Yield : 0.405 g, 78%

$[\alpha]_D^{25}$: +35.16 (c = 1, MeOH)

^{1}H NMR (400 MHz, $CDCl_3$) : δ_H 12.09 (s, 1H enolic 7.5%), 5.11-5.12(d, *J* = 5.5 Hz, 1H, NH), 4.48-4.33 (m, 1H, CH), 4.20 -4.15 (q, *J* = 7.3 Hz, 2H, CH_2), 3.58-3.48 (dd, *J* = 14.5 Hz, *J* = 10.5 Hz, 2H, CH_2, AB coupling), 1.42 (s, 9H, $C(CH_3)_3$, Boc-), 1.34-1.32 (d, *J* = 7.3 Hz, 3H, CH_3), 1.27-1.23 (t, *J* = 7.3 Hz, 3H, CH_3).

^{13}C NMR (100 MHz, $CDCl_3$) : δ_C 202.55, 167.02, 155.24, 80.19, 61.63, 55.48, 45.96, 28.37, 17.17, 14.16

ESI-MS m/z : Calcd. $[M+Na]^+$ 282.1317, observed 282.1321.

(*S*)-ethyl 4-(*tert*-butoxycarbonylamino)-5-methyl-3-oxohexanoate (4c)

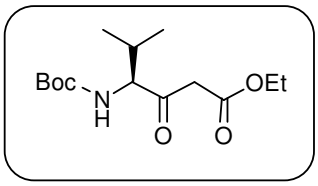

Physical state : colourless liquid

Mol. Formula : $C_{14}H_{25}NO_5$

Yield : 0.48g, 84%

$[\alpha]_D^{25}$: - 32.64 (c = 1, MeOH)

^{1}H NMR (500 MHz, $CDCl_3$) : δ_H 12.11 (s, 1H enolic form 6.5%), 5.06 (s, b, 1H, NH), 4.35-4.32 (m, 1H, CH), 4.22- 4.18 (q, *J* = 7 Hz, 2H, $-OCH_2$), 3.57-3.50 (dd, *J* = 15.5 Hz, *J* = 3 Hz, 2H, CH_2, AB coupling), 2.27-2.23 (m, 1H, $CH(CH_3)_2$), 1.44 (s, 9H, $C(CH_3)_3$, Boc-), 1.29-1.26 (t, *J* = 7 Hz, 3H, CH_3), 1.02-0.82 (m, 6H, $C(CH_3)_2$).

^{13}C NMR (125 MHz, $CDCl_3$) : δ_C 202.23, 166.75, 155.86, 80.03, 64.38, 61.55, 47.14, 29.56, 28.31, 19.84, 16.67, 14.10.

ESI-MS m/z : Calcd. $[M+Na]^+$ 310.1630, observed 310.1620.

(*S*)-ethyl 4-(*tert*-butoxycarbonylamino)-6-methyl-3-oxoheptanoate (4d)

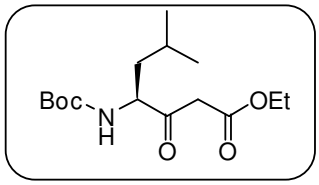

Physical state : light yellowish liquid

Mol. Formula : $C_{15}H_{27}NO_5$

Yield : 0.476g, 79%

$[\alpha]_D^{25}$: - 53.70 (c = 1, MeOH)

^{1}H NMR (500 MHz, $CDCl_3$) : δ_H 12.10 (s, 1H, enolic 5.5 %), 4.96- 4.94 (d, *J* = 9.5 Hz, 1H, NH), 4.40-4.36 (m, 1H, CH), 4.24-4.20 (q, *J* = 7 Hz, 2H, -OCH_2), 3.63-3.53 (dd, *J* = 16.0 Hz, *J* = 18.5Hz, 2H, CH_2, AB coupling), 1.74-1.67 (m, 3H, CH_2, CH), 1.46 (s, 9H, $C(CH_3)_3$, Boc-), 1.32-1.29 (t, *J* = 7 Hz, 3H, CH3), 0.97 (b, s, 6H, $C(CH_3)_2$).

^{13}C NMR (125 MHz, $CDCl_3$) : δ_C 203.02, 167.07, 155.55, 80.15, 61.51, 58.19, 46.35, 39.90, 28.31, 24.83, 23.28, 21.59, 14.12.

ESI-MS m/z : Calcd. $[M+Na]^+$ 324.1786, observed 324.1784.

(*S*)-ethyl 4-(*tert*-butoxycarbonylamino)-3- oxo-5-phenylpentanoate (4e)

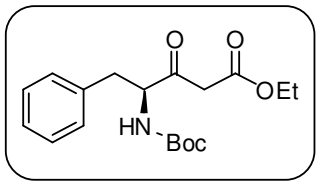

Physical state : white crystalline

Mol. Formula : $C_{18}H_{25}NO_5$

Yield : 0.521 g, 78%

$[\alpha]_D^{25}$: - 54.5 (c = 0.6, MeOH)

M. P. : 61.4 ^oC

^{1}H NMR (400 MHz, $CDCl_3$) : δ_H 12.16 (s, 1H, enolic 17%), 7.24-7.15 (m, 5H, C_6H_5), 5.03-5.01 (d, *J* = 7.3 Hz, 1H, NH), 4.57-4.52 (q, *J* = 6.4 Hz, 1H, CH), 4.18-4.12 (q, *J* = 7.2 Hz, 2H, -OCH_2), 3.51-3.40 (dd, *J* = 16 Hz, *J* = 11.4 Hz, 2H, CH_2, AB coupling), 3.15-2.95 (m, 2H, CH_2Ph), 1.38 (s, 9H, $C(CH_3)_3$), 1.26-1.22 (t, *J* = 7.2 Hz, 3H, CH_3).

^{13}C NMR (100 MHz, $CDCl_3$) : δ_C 201.96, 166.86, 155.18, 136.04, 129.24, 128.67, 127.00, 80.21, 61.45, 60.43, 46.86, 36.89, 28.20, 14.02.

ESI-MS m/z **:** Calcd. $[M+Na]^+$ 358.1630, observed 358.1633.

(*4S, 5R*)-ethyl 4-((*tert*-butoxycarbonyl)amino)-5-methyl-3-oxoheptanoate (4f)

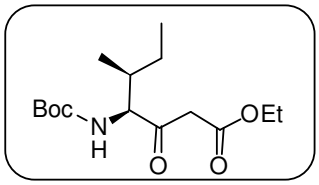

Physical state **:** colourless liquid

Mol. Formula **:** $C_{15}H_{27}NO_5$

Yield **:** 0.453g, 76%

$[\alpha]_D^{25}$ **:** - 25.08 (c = 1, MeOH)

^{1}H NMR (400 MHz, $CDCl_3$) **:** δ_H 12.09 (s, 1H, enolic 7.5%), 5.03-5.01(d, *J* = 8.24 Hz,1H, NH), 4.31-4.28 (m, 1H, CH), 4.19-4.13 (q, *J* = 6.88 Hz, 2H, $-OCH_2$), 3.51(s, 2H, αCH_2), 1.97-1.90 (m, 1H, CH), 1.63-1.57 (m, 2H, CH_2),1.41 (s, 9H, $C(CH_3)_3$, Boc-), 1.27-1.23 (t, *J* = 7.2 Hz, 3H,CH_3), 0.97-0.95 (dd, *J* = 3.64 Hz, *J* = 3.24 Hz, 3H, CH_3), 0.89-0.85 (t, *J* = 6.9 Hz, 3H, CH_3)

^{13}C NMR (100 MHz, $CDCl_3$) **:** δ_C 202.38, 166.72, 155.74, 79.99, 64.26, 61.47, 47.28, 36.28, 28.25, 24.00, 16.02, 14.05, 11.60

ESI-MS m/z **:** Calcd. $[M+Na]^+$ 324.1787, observed 324.1709

(*S*)-*tert*-butyl 2-(3-ethoxy-3-oxopropanoyl)pyrrolidine-1-carboxylate (4g)

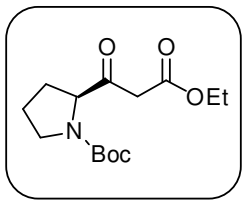

Physical state **:** colourless liqiuid

Mol. Formula **:** $C_{14}H_{23}NO_5$

Yield **:** 0.445 g, 78%

$[\alpha]_D^{25}$ **:** - 64.34 (c = 0.6, MeOH)

^{1}H NMR (400 MHz, $CDCl_3$) **:** δ_H 4.31-4.26 (m, 1H, C*H*), 4.1265-4.06 (m, 2H, $-OCH_2$), 3.66-3.53 (dd, *J* = 13.64 Hz, *J* = 22.4 Hz, 2H, CH_2, AB coupling), 3.34-3.31 (m, 2H, δCH_2),

2.07-2.05 (m, 1H, one proton of βCH_2), 1.91-1.68 (m, 3H, γCH_2, and one proton of βCH_2), 1.40 (s, 9H, $C(CH_3)_3$), 1.20-1.17 (t, J = 7.2 Hz, 3H, CH_3).

^{13}C NMR (100 MHz, $CDCl_3$) **:** δ_C 203.49, 167.41, 154.31, 153.31, 79.71, 65.34, 61.14, 47.11, 46.99, 46.07, 45.84, 29.45, 28.51, 28.31, 24.45, 23.60, 14.53

MALDI-TOF/TOF m/z **:** Calcd. $[M+Na]^+$ 308.1474, observed 308.1439.

(*S*)-ethyl 4-(*tert*-butoxycarbonylamino)-5-(4-methoxyphenyl)-3-oxopentanoate (4h)

Physical state **:** semi solid

Mol. Formula **:** $C_{19}H_{27}NO_6$

Yield **:** 0.586 g, 80%

$[\alpha]_D^{25}$ **:** - 56.32 (c = 1, MeOH)

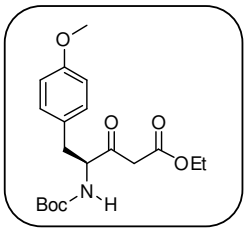

^{1}H NMR (400 MHz, $CDCl_3$) **:** δ_H 12.15 (s, 1H, enolic 10%), 7.07–7.05 (d, J = 8.68, 2H, aromatic), 6.82–7.80 (d, J = 8.65, 2H, aromatic), 5.01-4.99 (d, J = 7.6 Hz, 1H, NH), 4.53-4.48 (q, J = 7 Hz, 1H, CH), 4.17-4.12 (q, J = 7.2 Hz, 2H, $-OCH_2$), 3.76 (s, 3H, $-OCH_3$), 3.49-3.38 (dd, J = 16 Hz, J = 11.4 Hz, 2H, CH_2, AB coupling), 3.07-2.88 (m, 2H, CH_2Ph), 1.38 (s, 9H, $C(CH_3)_3$), 1.25-1.22 (t, J = 7.2 Hz, 3H, CH_3).

^{13}C NMR (100 MHz, $CDCl_3$) **:** δ_C 202.11, 166.85, 158.60, 155.18, 130.26, 127.82, 114.07, 80.17, 61.45, 60.55, 46.93, 36.12, 28.22, 14.04

MALDI-TOF/TOF m/z **:** Calcd. $[M+Na]^+$ 388.1736, observed 388.1783.

(*S*)-ethyl 4-(benzyloxycarbonylamino)-3-oxopentanoate (4i):

Physical state **:** colourless liquid

Mol. Formula **:** $C_{15}H_{19}NO_5$

Yield **:** 0.469g, 80%

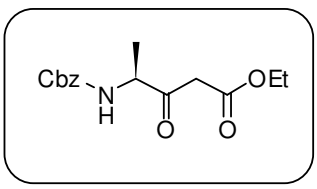

$[\alpha]_D^{25}$ **:** - 14.06 (c = 1, MeOH)

^{1}H NMR (500 MHz, $CDCl_3$) **:** δ_H 12.20 (s, 1H, enolic 4.5%), 7.40 (s, 5H, C_6H_5), 5.53 (b, s, 1H, NH), 5.14 (s, 2H, OCH_2Ph), 4.54-4.48 (m, 1H, CH), 4.23-4.18 (q, *J* = 7.5 Hz, 2H, OCH_2), 3.63-3.55 (dd, *J* = 16.5 Hz, *J* = 11.5 Hz, 2H, CH_2, AB coupling), 1.43-1.42 (d, *J* = 7 Hz, 3H, CH_3), 1.31-1.28 (t, *J* = 7 Hz, 3H, CH_3).

^{13}C NMR (125 MHz, $CDCl_3$) **:** δ_C 201.83, 166.74, 155.68, 136.16, 128.60, 128.29, 128.16, 67.09, 61.69, 55.84, 45.93, 17.26, 14.09.

LC-MS m/z **:** Calcd. $[M+K]^+$ 332.0900, observed 332.0912.

(*S*)-ethyl 4-(benzyloxycarbonylamino)-5-methyl-3-oxohexanoate (4j)

Physical state **:** yellowish liqiuid

Mol. Formula **:** $C_{17}H_{23}NO_5$

Yield **:** 0.481g, 75%

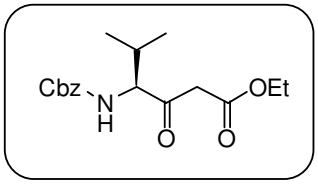

$[\alpha]_D^{25}$ **:** - 24.37 (c = 1, MeOH)

^{1}H NMR (500 MHz, $CDCl_3$) **:** δ_H 12.12 (s, 1H, enolic 6.5%), 7.367 (s, 5H, C_6H_5), 5.38-5.36 (d, *J* = 8.5 Hz, 1H, NH), 5.11 (s, 2H, -OCH_2Ph), 4.47-4.44 (m, 1H, CH), 4.21-4.17 (q, *J* = 7 Hz, 2H, CH_2, OCH_2), 3.54-3.54 (m, 2H, CH_2, AB coupling), 2.30-2.26 (m, 1H, CH), 1.286-1.25 (t, *J* = 7 Hz, 3H, CH_3), 1.05 - 0.81 (m, 6H, $CH(CH_3)_2$)

^{13}C NMR (125 MHz, $CDCl_3$) **:** δ_C 201.72, 166.60, 156.48, 136.17, 128.60, 128.29, 128.15, 127.00, 67.20, 64.81, 61.64, 47.13, 29.67, 19.85, 16.55, 14.08

MALDI-TOF/TOF m/z **:** Calcd. $[M+K]^+$ 360.1213, observed 360.125

(*S*)-ethyl 4-(benzyloxycarbonylamino)-6-methyl-3-oxoheptanoate (4k)

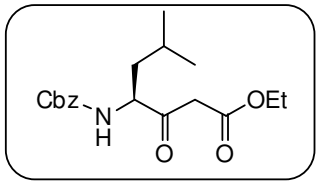

Physical state **:** colourless liquid

Mol. Formula **:** $C_{18}H_{25}NO_5$

Yield **:** 0.554g, 83%

$[\alpha]_D^{25}$ **:** -32.50 (c = 1, MeOH)

^{1}H NMR (500 MHz, $CDCl_3$) **:** δ_H 12.11 (s, 1H enolic 6%), 7.37 (s, 5H, C_6H_5), 5.33-5.32 (d, *J* = 7 Hz, 1H, NH), 5.13 (s, 2H, -OCH_2Ph), 4.51-4.47 (m, 1H, CH), 4.23-4.19 (q, *J* = 7, 2H, -OCH_2), 3.62-3.53 (dd, *J* = 15.75 Hz, *J* = 13.5 Hz, 2H, CH_2, AB coupling), 1.80-1.66 (m, 2H, CH_2), 1.46-1.42 (t, *J* = 11 Hz, 1H, CH), 1.30-1.27 (t, *J* = 7 Hz, 3H, CH_3), 0.99-0.95 (dd, *J* = 6.2 Hz, *J* = 8 Hz, 6H, $CH(CH_3)_2$).

^{13}C NMR (125 MHz, $CDCl_3$) **:** δ_C 202.48, 166.89, 156.15, 136.16, 128.59, 128.28, 128.11, 67.16, 61.60, 58.60, 46.41, 39.98, 24.81, 23.29, 21.54, 14.09

MALDI-TOF/TOF m/z **:** Calcd. $[M+K]^+$ 282.1317, observed 282.1317.

(*S*)-1-benzyl 6-ethyl 2-(benzylcarbonylamino)-4-oxohexanedioate (4l):

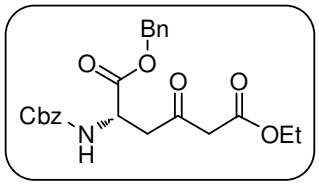

Physical state **:** white solid

Mol. Formula **:** $C_{23}H_{25}NO_7$

Yield **:** 0.589 g, 69%

$[\alpha]_D^{25}$ **:** - 16.30 (c = 1, MeOH)

M. P. **:** 68.3 ^oC

^{1}H NMR (400 MHz, $CDCl_3$) **:** δ_H 12.06 (s, 1H, enolic), 7.33-7.28 (m, 10H, aromatic), 5.75-5.72 (d, *J* = 8.2 Hz, 1H, NH), 5.63-5.59 (m, 1H, CH), 5.14 (s, 2H, -OCH_2Ph), 5.08 (s, 2H, -OCH_2Ph), 4.17-4.11 (q, *J* = 7 Hz, 2H, -OCH_2Me), 3.39 (s, 2H, CH_2, AB coupling), 3.33-3.10 (m, 2H, CH_2), 1.24-1.21 (t, *J* = 7.1 Hz, 3H, CH_3)

^{13}C NMR (100 MHz, $CDCl_3$) **:** δ_C 200.78, 170.51, 166.42, 155.99, 136.02, 135.10, 128.57, 128.50, 128.42, 128.21, 128.03, 67.57, 67.08, 61.59, 49.88, 49.07, 44.59, 14.01

MALDI-TOF/TOF m/z **:** Calcd. $[M+K]^+$ 466.1268, observed 466.1276

(*S*)-ethyl 4-(((9H-fluoren-9-yl)mehtoxy)carbonylamino)-6-methyl-3-oxoheptanoate (8a)

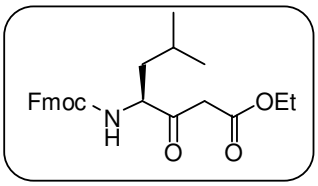

Physical state **:** colourless liquid

Mol. Formula **:** $C_{25}H_{29}NO_5$

Yield **:** 0.651g, 77%

$[\alpha]_D^{25}$ **:** -28.9 (c = 1, MeOH)

^{1}H NMR (500 MHz, $CDCl_3$) **:** δ_H 12.16 (s, 1H, enolic), 7.80-7.79 (d, *J* = 7.5 Hz, 2H, aromatic, Fmoc-), 7.63-7.61 (t, *J* = 6.5 Hz, 2H, aromatic, Fmoc-), 7.44-7.42 (t, *J* = 7.5 Hz, 2H, aromatic, Fmoc-), 7.36-7.33 (t, *J* = 7.5 Hz, 2H, aromatic, Fmoc-), 5.26-5.24 (d, *J* = 8 Hz, 1H, NH), 4.50-4.45 (m, 3H, CH, CH_2), 4.26-4.21 (m, 3H,-OCH_2, CH-Fmoc), 3.59-3.50 (dd, *J* = 16 Hz, *J* = 13 Hz, 2H, CH_2, AB coupling), 1.71-1.68 (m, 2H, CH_2), 1.47-1.43 (m, 1H, CH), 1.34-1.30 (t, *J* = 7 Hz, 3H, CH_3), 1.00-0.97 (m, 6H, $C(CH_3)_2$).

^{13}C NMR (125 MHz, $CDCl_3$) **:** δ_C 202.54, 166.91, 156.13, 143.72, 141.38, 127.78, 127.11, 125.08, 120.05, 66.87, 61.63, 58.56, 47.28, 46.35, 39.93, 24.80, 23.33, 21.54, 14.13

MALDI-TOF/TOF m/z **:** Calcd. $[M+K]^+$ 462.1683, observed 462.1631.

(*S*)-1-*tert*-butyl 6-ethyl 3-(((9H-fluoren-9-yl)methoxy)carbonylamino)-4-oxohexanedioate (8b)

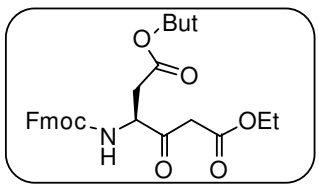

Physical state **:** colourless liquid

Mol. Formula **:** $C_{27}H_{31}NO_7$

Yield **:** 0.742g, 77.2%

$[\alpha]_D^{25}$ **:** 1.43 (c = 1, MeOH)

^{1}H NMR (500 MHz, $CDCl_3$) **:** δ_H 12.11 (s, 1H, enolic 5.5%), 7.78-7.32 (m, 8H, aromatic, Fmoc), 5.91 (b, s, 1H, NH), 4.60-4.51 (m, 2H, CH_2), 4.45-4.41(m, 1H, CH), 4.24-4.18 (m, 3H,- OCH_2, CH-Fmoc), 3.56 (s, 2H, αCH_2), 2.94-2.69 (dd, *J* = 16.5 Hz, *J* = 13.8 Hz, 2H, $-CH_2CO_2{}^tBu$), 1.44 (s, 9H, $-OC(CH_3)_3$), 1.28-1.25 (t, *J* = 7.3 Hz, CH_3)

^{13}C NMR (125 MHz, $CDCl_3$) **:** δ_C 201.05, 170.52, 166.87, 156.00, 143.67, 141.39, 127.83, 127.11, 125.08, 120.09, 82.17, 67.13, 61.57, 56.70, 47.23, 46.03, 36.57, 28.035, 14.10.

ESI-MS m/z **:** Calcd. $[M+Na]^+$ 520.1738, observed 520.1722

(*S*)-ethyl 4-(((9H-fluoren-9-yl) mehtoxy) carbonylamino)-8-(*tert*-butoxycarbonylamino)-3-oxooctanoate (8c)

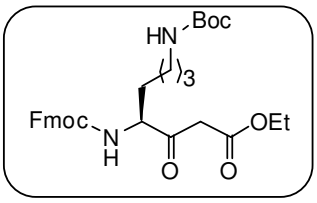

Physical state **:** white solid

Mol. Formula **:** $C_{30}H_{38}N_2O_7$

Yield **:** 0.862g, 80.2%

$[\alpha]_D$ ^{25} **:** -81.53(c = 1, MeOH)

M. P. **:** 114 ^oC

^{1}H NMR (400 MHz, $CDCl_3$) **:** δ_H 12.11 (s, 1H, enolic), 7.760-7.28 (m, 8H, aromatic, Fmoc-), 5.57-5.56 (d, *J* = 7.3 Hz, 1H, NH-Fmoc), 4.59 (s, b,1H, NH-Boc), 4.45-4.39 (m, 3H, CH, CH_2), 4.21-4.16 (m, 3H, $-OCH_2$, CH-Fmoc), 3.55-3.45 (dd, *J* = 15.6 Hz, *J* = 9.16 Hz, 2H , CH_2, AB coupling), 3.12-3.02 (q, *J* = 7.3 Hz, 2H, CH_2NH-Boc), 1.95-1.84 (m, 2H, CH_2), 1.71-1.41 (m, 4H, $-CH_2-CH_2-$), 1.37 (s, 9H, $C(CH_3)_3$, Boc), 1.27-1.23 (t, *J* = 7.1 Hz, 3H, CH_3).

^{13}C NMR (100 MHz, $CDCl_3$) **:** δ_C 201.96, 166.89, 156.27, 143.80, 141.41, 127.84, 127.18, 125.12, 120.09, 79.34, 67.00, 61.74, 60.01, 47.28, 46.27, 39.86, 30.34, 29.78, 28.50, 22.19, 14.18.

ESI-MS m/z **:** Calcd. $[M+Na]^+$ 561.2576, observed 561.2577.

(*S*)-ethyl 4-(((9H-fluoren-9-yl)methoxy)carbonylamino)-5-(4-*tert*-butoxyphenyl)-3-oxopentanoate (8d)

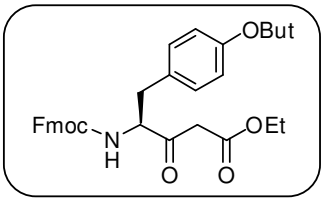

Physical state : colourless gummy

Mol. Formula : $C_{32}H_{35}NO_6$

Yield : 0.88g, 83.3%

$[\alpha]_D$ [25] : -37.45 (c = 1, MeOH)

^{1}H NMR (400 MHz, $CDCl_3$) : δ_H 12.17 (s, 1H, enolic), 7.75-7.28 (m, 8H, aromatic, Fmoc-), 7.03-7.01 (d, *J* = 8.3 Hz, 2H, aromatic, Ph-), 6.90-6.88 (d, *J* = 8.3 Hz, 2H, aromatic, Ph-), 5.33-5.31 (d, *J* = 7.8 Hz, 1H, NH), 4.64-4.587 (m, 1H, CH-), 4.39-4.38 (d, *J* = 6.9 Hz, 2H, CH_2), 4.19-4.10 (m, 3H, -OCH_2, CH-Fmoc), 3.44-3.34 (dd, *J* = 16 Hz, *J* = 11.4 Hz, 2H, CH_2, AB coupling), 3.09-2.94 (m, 2H, -CH_2Ph-O^{t}Bu), 1.30 (s, 9H, -$C(CH_3)_3$, O^{t}Bu), 1.25-1.22 (t, *J* = 7.1 Hz, 3H, CH_3).

^{13}C NMR (100 MHz, $CDCl_3$) : δ_C 201.51, 166.62, 155.66, 154.49, 143.61, 141.29, 130.39, 129.69, 127.73, 1.27.68, 127.04, 124.97, 124.36, 124.24, 124.19, 119.97, 78.87, 66.90, 61.54, 60.81, 47.14, 46.97, 36.43, 28.77, 14.04

ESI-MS m/z : Calcd. $[M+Na]^+$ 552.2362, observed 552.2363.

Crystal structure analysis of Boc-Phe-βK-OEt: Crystals were grown by slow evaporation from a solution of MeOH. A single crystal (0.21× 0.14 × 0.10 mm) was mounted on loop with a small amount of the paraffin oil. The X-ray data were collected at 100K temperature on a Bruker APEX DUO CCD diffractometer using Mo K_α radiation (λ = 0.71073 Å), ω-scans (2θ = 47.08), for a total of 2772 independent reflections. Space group P21, a = 9.562(3), b = 9.127(3), c = 10.911(3), β = 92.657(7), V= 951.1(5) Å^3, Monoclinic P, Z = 2 for chemical formula C_{18} H_{25} N O_4, with one molecule in asymmetric unit; ρ calcd = 1.171 gcm^{-3}, μ = 0.085mm^{-1}, F(000)= 360, R_{int} = 0.0371. The structure was obtained by direct methods using SHELXS-97.[42] The final R value was 0.0737 (wR2= 0.1148) 1811 observed reflections ($F_0 \geq 4\sigma$ ($|F_0|$)) and 222 variables, S = 1.281. The largest difference peak and hole were 0.532 and -0.262 eÅ^3, respectively.

4.2.3 Synthetic procedure and compound characterization for Section 4B

General procedure for the synthesis of Boc-protected coumarins functionalized with proteinogenic amino acid side chains

Trifluoroacetic acid (4 mL) was added to the cold solution of *N*-Boc-γ-amino-β-keto ester (2.0 mmol) in DCM (4 mL). After 30 min, the reaction mixture was evaporated to dryness to afford brown gummy product and then 3-methoxyphenol (3.5 mmol, 0.434 g) was added and cooled to 0 ^{o}C for 5 min. Further, the methanesulfonic acid (MSA) (50 mmol, 4.8 g) was added slowly to the reaction mixture and stirred for about 3 hrs. The progress of reaction was monitored by TLC. After completion of the reaction, it was diluted with diethyl ether (100 mL) and cooled to -15 ^{o}C. The ether layer was centrifuged (4000 rpm at 4 ^{o}C) and the red precipitate (methanesulfonate salt of coumarin) was separated. The red precipitate was dissolved in the solution of 30% Na_2CO_3 (20 mL) and THF (5 mL) and cooled to 0 ^{o}C. A solution of di-tert-butyl dicarbonate (0.460 g, 2.1 mmol) in THF (10 mL) was added slowly to the reaction mixture and stirred for about 5 hrs at room temperature. After completion of the reaction, it was extracted with ethyl acetate (50 mL × 3). The combined organic layer was washed with 5% HCl (50 mL × 2), brine (30 mL), dried over anhydrous sodium sulfate and concentrated under reduced pressure to give reddish gummy crude product which was further purified on silica gel column chromatography.

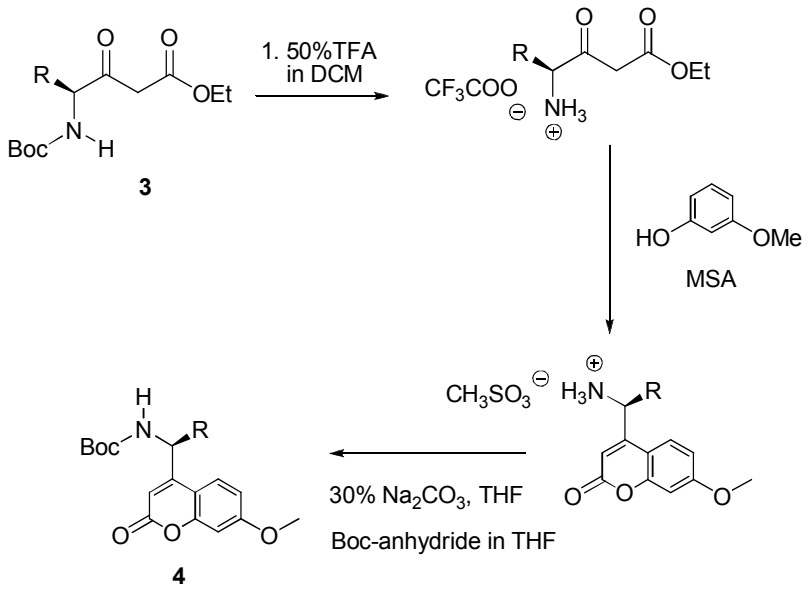

Products

(*S*)-*tert*-butyl1-(7-methoxy-2-oxo-2*H*-chromen-4-yl)ethylcarbamate (4a)

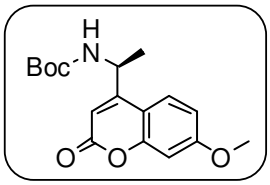

Physical state : White powder

Mol. Formula : $C_{17}H_{21}NO_5$

Yield : 0.460g, 72%

$[\alpha]_D$ [20] : -25.0 (c =1, MeOH)

M. P. : 168 ^oC

UV absorption (λ_{max}) : 323 nm

Fluorescen Emmision (λ_{max}) : 393 nm

^{1}H NMR (400 MHz, $CDCl_3$) : δ_H 7.58-7.56(d, *J* = 8.7, 1H, aromatic), 6.85-6.81(m, 2H, aromatic), 6.26 (s, 1H, C=C*H*), 5.12-5.05 (m, 1H, NH-C*H*), 4.84-4.82 (d, *J* = 6.4, 1H, -N*H*), 3.85 (s, 3H, -OCH_3),1.47-1.45 (d, *J* = 6.9 Hz, 3H, CH_3),1.41(s, 9H, -C(CH_3)$_3$).

^{13}C NMR (100 MHz, $CDCl_3$) : δ_C 162.64, 161.65, 157.76, 155.84, 154.67, 124.90, 112.58, 107.91, 101.14, 80.44, 55.75, 28.30, 20.83.

MALDI-TOF/TOF m/z : Calcd. $[M+Na]^+$ 342.1317, observed 342.1320.

(*R*)-*tert*-butyl1-(7-methoxy-2-oxo-2*H*-chromen-4-yl)ethylcarbamate (4a1)

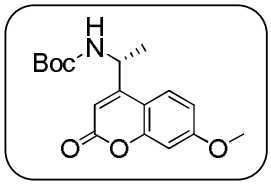

Physical state : colourless crystalline

Mol. Formula : $C_{17}H_{21}NO_5$

Yield : 0.460g, 72%

$[\alpha]_D^{20}$: -25.4 (c =1, MeOH)

M. P. : 167 ^oC

UV absorption (λ_{max}) : 323 nm

Fluorescen Emmision (λ_{max}) : 393 nm

^{1}H NMR (400 MHz, $CDCl_3$) : δ_H 7.58-7.56 (d, *J* = 8.7, 1H, aromatic), 6.85-6.81 (m, 2H, aromatic), 6.26 (s, 1H, C=C*H*), 5.08 (b, 1H, NH-C*H*), 4.84 (b, *J* = 6.4, 1H, -N*H*), 3.8469 (s, 3H, -OCH_3),1.46-1.44 (d, *J* = 6.9, 3H, CH_3),1.4109 (s, 9H, -C(CH_3)$_3$).

^{13}C NMR (100 MHz, $CDCl_3$) : δ_C 162.63, 161.66, 157.76, 155.79, 154.67, 124.91, 112.55, 111.23, 107.92, 101.14, 80.41, 55.74, 45.74, 28.29, 20.82.

MALDI-TOF/TOF m/z : Calcd. $[M+Na]^+$ 342.1317, observed 342.1392.

(*S*)-*tert*-butyl1-(7-methoxy-2-oxo-2H-chromen-4-yl)-2-phenylethylcarbamate (4b)

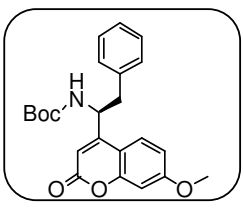

Physical state : white powder

Mol. Formula : $C_{23}H_{25}NO_5$

Yield : 0.550 g, 70%

$[\alpha]_D^{20}$: 21.67 (c = 1, MeOH)

M. P. : 175 ^oC

UV absorption (λ_{max}) : 324 nm

Fluorescen Emmision (λ_{max}) : 393 nm

^1H NMR (400 MHz, $CDCl_3$) : δ_H 7.63-7.61(d, *J* = 8.7, 1H, aromatic), 7.29-7.23 (m, 3H, Ph-group), 7.13-7.11 (d, *J* = 6.9, 2H, Phe-group), 6.85 (s, 1H, aromatic ring of coumarin), 6.83 (s, 1H, aromatic ring of coumarin), 6.13 (s, 1H, C=C*H*), 5.34-5.27 (q, *J* = 5.5, 1H, NH-C*H*), 4.85-4.84 (d, *J* = 7.8, 1H, -N*H*), 3.85 (s, 3H, -OCH_3), 3.22-2.88 (m, 2H, -CH_2-Ph), 1.34 (s, 9H, -C(CH_3)$_3$).

^{13}C NMR (100 MHz, $CDCl_3$) : δ_C 162.69, 161.39, 156.13, 155.75, 154.78, 135.79, 129.09, 128.79, 127.31, 124.77, 112.64, 111.25, 109.02, 101.25, 80.50, 55.77, 50.58, 40.46, 28.21.

MALDI-TOF/TOF m/z : Calcd. $[M+Na]^+$ 418.1630, observed 418.1649.

(*S*)-tert-butyl (1-(7-methoxy-2-oxo-2H-chromen-4-yl)-2-(4-methoxyphenyl)ethyl)carbamate (4c)

Physical state : white powder

Mol. Formula : $C_{24}H_{27}NO_6$

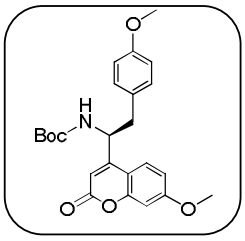

Yield : 0.580 g, 68%

$[\alpha]_D^{20}$: 51.57 (c =1, MeOH)

M. P. : 177 ^oC

UV absorption (λ_{max}) : 325 nm

Fluorescen Emmision (λ_{max}) : 391 nm

^{1}H NMR (400 MHz, $CDCl_3$) **:** δ_H 7.63-7.60 (d, *J* = 8.7, 1H, aromatic), 7.02-7.00 (d, *J* = 6.9, 2H, Phe-group), 6.86-6.80 (m, 4H, Ph-group, aromatic ring of coumarin), 6.09 (s, 1H, C=C*H*), 5.27-5.24 (q, *J* = 5.5, 1H, NH-C*H*), 4.83-4.81 (d, *J* = 6.9, 1H, -N*H*), 3.85 (s, 3H, -OCH_3), 3.76 (s, 3H, -OCH_3), 3.15-2.83 (m, 2H, -CH_2-Ph- OCH_3), 1.35 (s, 9H, -C(CH_3)$_3$).

^{13}C NMR (100 MHz, $CDCl_3$) **:** δ_C 162.65, 161.39, 158.80, 156.16, 155.74, 154.81, 130.16, 127.41, 124.78, 114.17, 112.62, 111.26, 109.01, 101.24, 80.47, 55.76, 55.25, 50.69, 39.49, 28.23.

MALDI-TOF/TOF m/z **:** Calcd. $[M+Na]^+$ 448.1736, observed 448.1786.

(*S*)-*tert*-butyl1-(7-methoxy-2-oxo-2H-chromen-4-yl)-3-methylbutylcarbamate (4d)

Physical state **:** white powder

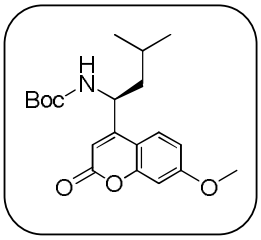

Mol. Formula **:** $C_{20}H_{27}NO_5$

Yield **:** 0.455 g, 63%

$[\alpha]_D^{20}$ **:** -48.33 (c = 1, MeOH)

M. P. **:** 101 ^oC

UV absorption (λ_{max}) **:** 323 nm

Fluorescen Emmision (λ_{max}) **:** 394 nm

^{1}H NMR (400 MHz, $CDCl_3$) **:** δ_H 7.59-7.57 (d, *J* = 8.7, 1H, aromatic), 6.86-6.81(m, 2H, aromatic), 6.22 (s, 1H, C=C*H*), 5.07-5.03 (m, 1H, NH-C*H*), 4.81-4.79 (d, *J* = 7.3, 1H, -N*H*), 3.84 (s, 3H, -OCH_3), 1.89-1.78 (m, 2H, -CH-CH_2), 1.62-1.56 (m, 1H, -C*H*-$(CH_3)_2$ 1.41 (s, 9H, -C(CH_3)$_3$), 1.07-1.05 (d, *J* = 6.4, 3H, CH-(CH_3)$_2$), 0.95-0.93 (d, *J* = 6.4, 3H, CH-(CH_3)$_2$).

^{13}C NMR (100 MHz, $CDCl_3$) **:** δ_C 162.63, 161.72, 157.83, 155.82, 154.99, 124.75, 112.56, 108.12, 101.21, 80.37, 55.74, 48.39, 44.25, 28.29, 25.34, 23.26, 21.53.

MALDI-TOF/TOF m/z **:** Calcd. $[M+Na]^+$ 384.1787, observed 384.1706.

(*S*)-*tert*-butyl1-(7-methoxy-2-oxo-2H-chromen-4-yl)-2-methylpropylcarbamate (4e)

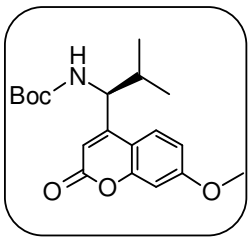

Physical state : white powder

Mol. Formula : $C_{19}H_{25}NO_5$

Yield : 0.361 g, 50%

$[\alpha]_D^{20}$: -42.6 (c = 1, MeOH)

M. P. : 99 ^oC

UV absorption (λ_{max}) : 323 nm

Fluorescen Emmision (λ_{max}) : 393 nm

^{1}H NMR (400 MHz, $CDCl_3$) : δ_H 7.58-7.55 (d, *J* = 8.7, 1H, aromatic), 6.85-6.82 (m, 2H, aromatic), 6.16 (s, 1H, C=C*H*), 4.89 (b, 2H, NH-C*H* , -N*H*), 3.84 (s, 3H, -OCH_3), 2.12-2.04 (m, 1H, -C*H*-$(CH_3)_2$ 1.41 (s, 9H, -C(CH_3)$_3$), 1.06-1.05 (d, *J* = 6.4, 3H, CH-(CH_3)$_2$), 0.89-0.87 (d, *J* = 6.4, 3H, CH-(CH_3)$_2$).

^{13}C NMR (100 MHz, $CDCl_3$) : δ_C 162.72, 161.53, 156.54, 155.74, 155.33, 125.11, 112.55, 111.81, 108.92, 101.18, 80.36, 55.75, 54.95, 31.49, 28.29, 20.30, 16.78.

MALDI-TOF/TOF m/z : Calcd. $[M+Na]^+$ 370.1630, observed 370.1666.

(*S*)-*tert*-butyl2-(7-methoxy-2-oxo-2H-chromen-4-yl)pyrrolidine-1-carboxylate (4f)

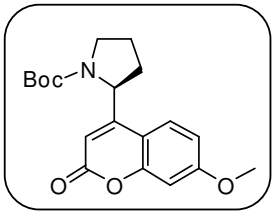

Physical state : white powder

Mol. Formula : $C_{19}H_{23}NO_5$

Yield : 0.486 g, 71%

$[\alpha]_D^{20}$: -42.6 (c = 1, MeOH)

UV absorption (λ_{max}) : 322 nm

Fluorescen Emmision (λ_{max}) **:** 391 nm

^{1}H NMR (400 MHz, $CDCl_3$) **:** δ_H 7.48-7.45 (d, *J* = 8.7, 1H, aromatic), 6.85-6.80 (m, 2H, aromatic), 6.07, 6.05 (s, 1H, C=C*H*), 5.23-5.20, 5.07-5.05 (d, *J* = 8.2, 1H, NH-C*H*), 3.85-3.84 (s, 3H, -OCH_3), 3.62-3.56, 3.51-3.44 (m, 2H, -CH_2), 2.41-2.30 (m, 1H, -CH_2), 1.93-1.84 (m, 2H, -CH_2), 1.44, 1.24 (s, 9H, -C(CH_3)$_3$).

^{13}C NMR (100 MHz, $CDCl_3$) **:** δ_C 162.50, 161.67, 156.38, 155.84, 154.30, 124.91, 124.62, 112.44, 112.38, 111.27, 107.79, 101.19, 101.03, 80.32, 80.18, 57.17, 56.84, 55.72, 47.01, 46.70, 32.93, 31.78, 28.42, 28.20, 28.20, 23.62, 23.02;

MALDI-TOF/TOF m/z **:** Calcd. $[M+Na]^+$ 368.1473, observed 368.1480.

Synthesis of Fmoc-Coumaryl amino acid

Compound 2g (0.427 g, 1 mmol) was treated with 3-methoxyphenol (0.615 g, 5 mmol) and the mixture was cooled to 0 ^oC under N_2 atmosphere. After stirring for 5 min, MSA (2.4 g, 25 mmol) was added slowly at constant stirring. The reaction mixture was allowed to come to room temperature and the stirring was continued for another 2 hrs. The progress of the reaction was monitored by TLC. After completion of the reaction (~ 2 hrs), it was diluted with diethyl ether (100 mL) and cooled to -15 ^oC. The ether layer was centrifuged (4000 rpm at 4 ^oC) and red precipitate (methanesulfonate salt of coumarin) was separated. The red precipitate was dissolved in the solution of 30% Na_2CO_3 (20 mL) and THF (5 mL) and cooled to 0 ^oC. A solution of Fmoc-OSu (0.370 g, 1.1 mmol) in THF (5 mL) was added to the reaction mixture and allowed to stir overnight to complete the reaction. After completion (monitored by TLC), it was washed with ether (20 mL × 2) and the aqueous layer was acidified with 3N HCl (up to pH 3) under ice cold condition. The combined organic layer was washed with 5% HCl (50 mL × 2), brine (30 mL), dried over anhydrous sodium sulfate and concentrated under reduced pressure to give reddish gummy crude product which was further purified on silica gel column chromatography to give pure white powder.

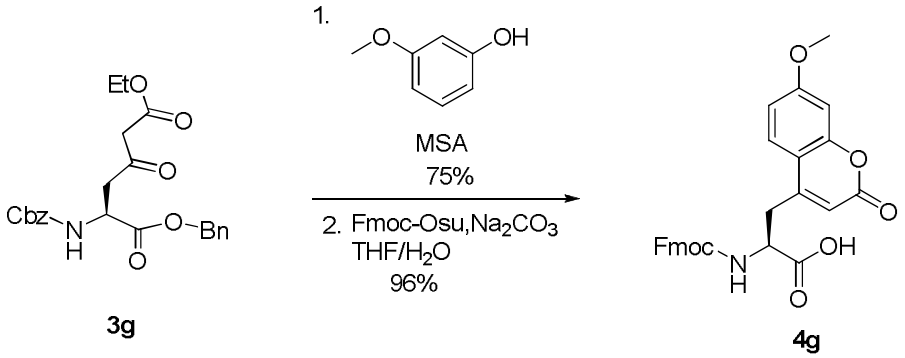

(*S*)-2-(((9H-fluoren-9-yl)mehtoxy)carbonylamino)-3-(7-methoxy-2-oxo-2*H*-chromen-4-yl)propanoic acid (4g)

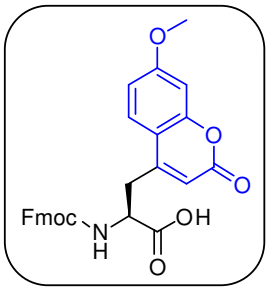

Physical state : white powder

Mol. Formula : $C_{28}H_{23}NO_7$

Yield : 0.315 g, (62%)

$[\alpha]_D^{20}$: 14.5 (c = 1, MeOH)

M. P. : 119 ^oC

UV absorption (λ_{max}) : 324 nm

Fluorescen Emmision (λ_{max}) : 384 nm

^{1}H NMR (400 MHz, DMSO) : δ_H 13.09 (s, b, 1H, -COO*H*), 7.88-7.86 (d, *J* = 7.32, 2H, aromatic Fmoc), 7.74-7.63 (d, *J* = 9.16, 1H, aromatic ring of coumarin), 7.63-7.59 (dd, *J* = 7.36, *J* = 3.64 2H, aromatic Fmoc), 7.41-7.37 (t, *J*= 7.56, 2H, aromatic Fmoc), 7.31-7.25 (dd, *J* = 7.32, *J*= 6.88, 2H, aromatic Fmoc), 7.02-6.979 (m, 2H, aromatic ring of coumarin), 6.24 (s, 1H, C=C*H*), 4.33-4.27 (m, 1H, Fmoc-C*H*), 4.23 - 4.14 (m, 3H, Fmoc-CH_2), 3.84 (s, 3H, -OCH_3), 3.34- 3.04 (m, 2H, CH-CH_2).

^{13}C NMR (100 MHz, DMSO) : δ_C 172.58, 162.38, 159.95, 155.94, 155.04, 152.62, 143.64, 140.66, 128.16, 127.64, 127.04, 125.83, 125.12, 120.12, 112.41, 112.03, 101.13, 65.74, 56.06, 52.76, 46.51, 32.60.

MALDI-TOF/TOF m/z : Calcd. $[M+Na]^+$ 508.1372, observed 508.2198.

Synthesis of Dipeptide Fmoc-Glu(OBu^t)-Phe-coumarin (5)

Trifluoroacetic acid (5 mL) was added to the cold solution of Boc-Phe-coumarin (0.396 g, 1 mmol) in DCM (5 mL), and the reaction mixture was stirred for about 30 min. in an ice bath. After completion of the deprotection, TFA was removed under reduced pressure and the residue was dissolved in water (50 mL). The pH of the solution was adjusted to ~10 by the addition of solid Na_2CO_3. The free coumaryl amine was extracted with ethyl acetate (30 mL x 3). The combined organic layer was washed with brine and concentrated to ~ 2-3 mL and immediately subjected to the coupling reaction.

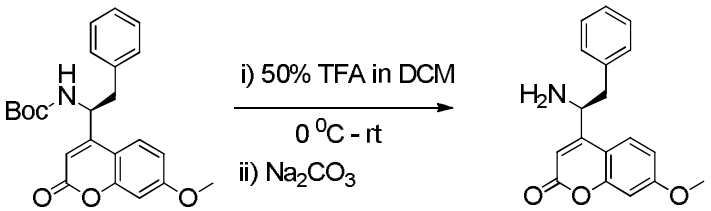

4b

The Fmoc-Glu(OBu^t)-OH (0.425 g, 1 mmol) was dissolved in DMF (4 mL) and NH_2-Phe-coumarin (in ~2-3 mL of EtOAc, obtained from the above step) was added to the solution followed by HBTU (0.416 g, 1.1 mmol) and HOBt (0.148 g, 1.1 mmol). The reaction mixture was cooled to 0 °C. After stirring for 5 min, DiEPA (0.35 mL, 2 mmol) was added to the reaction mixture and allowed to come to the room temperature. The progress of the reaction was monitored by TLC. After completion of the reaction (~ 5 hrs), it was diluted with100 mL of ethyl acetate, washed with 5% HCl (2 × 30 mL), 10 % Na_2CO_3 (2 × 40 mL) and followed by brine (30 mL). The organic layer was dried over anhydrous sodium sulphate and evaporated under reduced pressure to give gummy yellowish product, which was further purified on column chromatography. The pure peptide was isolated as solid white powder.

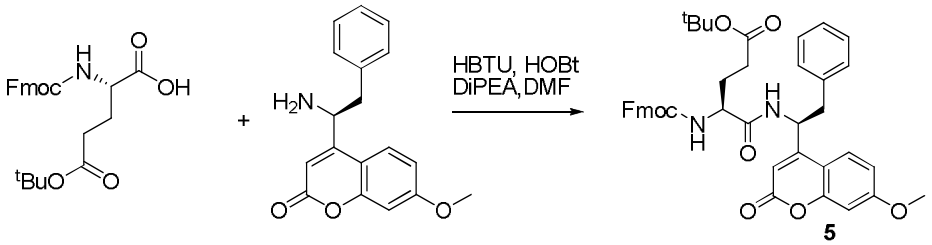

Fmoc-Glu(OBu^t)-Phe-coumarin (5)

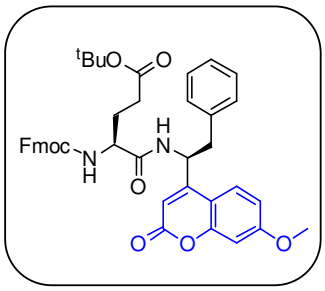

Physical state : white powder

Mol. Formula : $C_{42}H_{42}N_2O_8$

Yield : 0.5 g (78%)

$[\alpha]_D$ ^{20} : - 23.33 (c = 1, MeOH)

M. P. : 119 ^oC

UV absorption (λ_{max}) : 324 nm

Fluorescen Emmision (λ_{max}) : 384 nm

^{1}H NMR (400 MHz, DMSO) : δ_H 7.75-7.74 (d, *J* = 7.3, 2H, aromatic Fmoc), 7.64-7.62 (d, *J* = 8.5, 1H, aromatic ring of coumarin), 7.56-7.54 (d, *J* = 6.9, 2H, aromatic Fmoc), 7.38-6.80 (m, 10H, aromatic ring of Phenyl, aromatic Fmoc, -N*H*), 6.17 (s, 1H, C=C*H*), 5.65-5.63 (d, *J* = 7.3,1H, -N*H*), 5.58-5.52 (q, *J* = 7.3, 1H, NH-C*H*), 4.38-4.31 (m, 2H, Fmoc-C*H*, NH-C*H*), 4.14-4.07 (m, 2H, Fmoc-CH_2), 3.83 (s, 3H, -OCH_3), 3.22-2.94 (m, 2H, CH_2-Ph), 2.24-2.17 (m, 2H, -CH_2), 1.97-1.77 (m, 2H, -CH_2), 1.12 (s, 9H, -C(CH_3)$_3$).

^{13}C NMR (100 MHz, DMSO) : δ_C 170.97, 162.76, 161.23, 158.16, 155.72, 155.39, 143.66, 141.27, 135.76, 128.99, 128.70, 127.76, 127.07, 125.09, 125.04, 120.00, 112.70, 111.12, 109.36, 101.24, 100.60, 81.44, 67.08, 55.96, 49.43, 47.03, 40.24, 31.89, 29.75, 28.03.

MALDI-TOF/TOF m/z : Calcd. $[M+Na]^+$ 725.2838, observed 725.2869.

SPPS synthesis of H_2N-Gly-Arg-Lys-Lys-Lys-Arg-Arg-Gln-Arg-Arg-Arg-Pro-Pro-Gln-FCuM (P1)

Synthesis of Fmoc-Glu(OH)-Phe-coumarin (**6**): Trifluoroacetic acid (5 mL) was added to the cold solution of Fmoc-Glu(OBu^t)-Phe-coumarin (0.420 g, 0.6 mmol) in DCM (5 mL) and the mixture was stirred for 30 min. in an ice-bath. After the deprotection (~30 min.), TFA was removed from the reaction mixture under reduced pressure and the residue was diluted with EtOAc (100 mL), washed with water, brine and dried over anhydrous sodium sulfate. The organic layer was concentrated under reduced pressure to give gummy product which was further recrystallized using EtOAc/hexane to get white solid powder (**6**) and used for the synthesis of P1 using SPPS (solid phase peptide synthesis) without further purification. Peptide synthesis was carried out by manual stepwise solid-phase method using standard Fmoc-/Boc- chemistry at 0.1 mmol scale on Rink amide resin. In the initial step, the dipeptide acid **5** was coupled to the resin using standard coupling agents HBTU/HOBt. After the coupling, the Fmoc- deprotection was carried out using 25% piperidine in DMF. The peptide elongation was continued by successive addition of Fmoc-amino acids followed by Fmoc-deprotection. The final peptide (P1) was released from the resin using TFA/H_2O (19:1) (10 mL) cocktail mixture. Further, the peptide was purified through reverse phase HPLC using C_{18} column in Acetonitrile/H_2O gradients. Homogeneity of the peptide was confirmed by analytical reverse phase HPLC and MALDI TOF/TOF m/z Calcd. for $C_{99}H_{167}N_{33}O_{19}$ [M^{4+}+H^+] 2124.32 Da, observed 2124.79 Da.

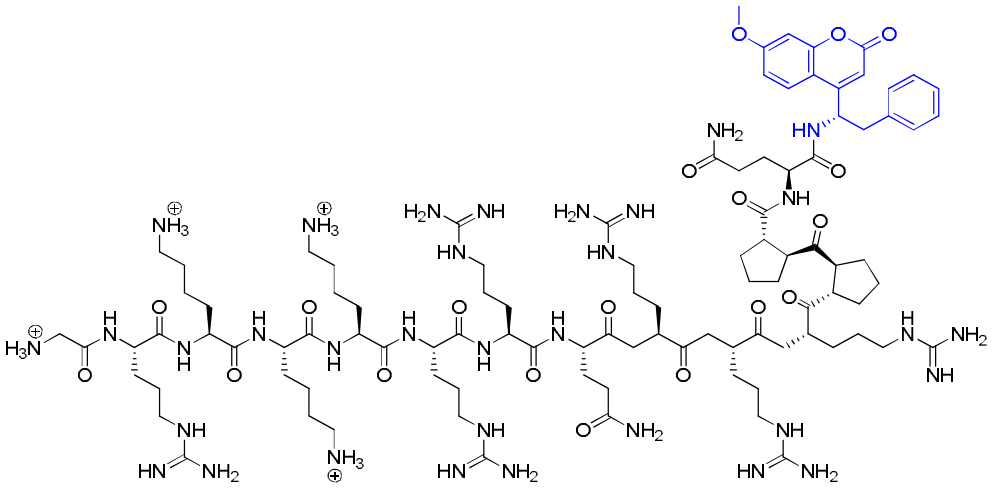

P1

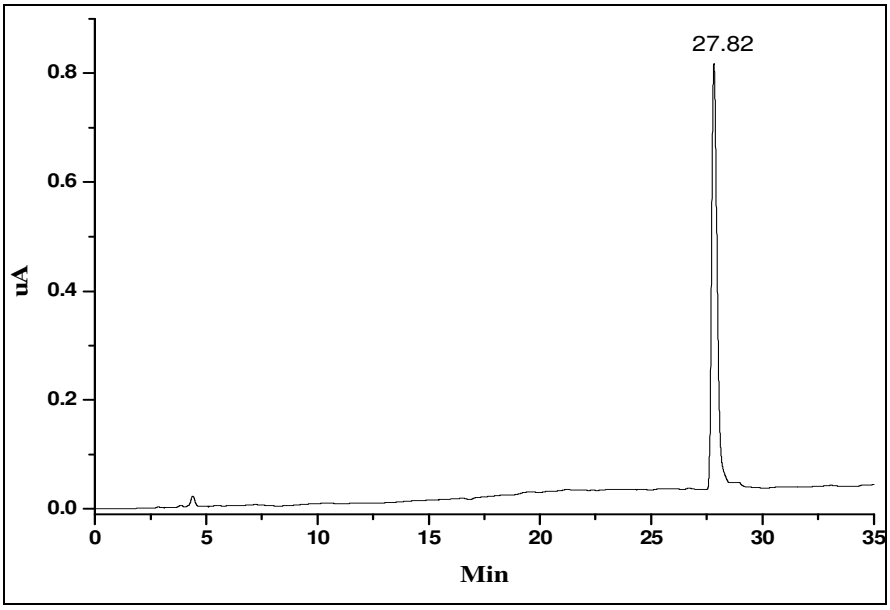

HPLC profile of Coumarin Tagged HIV-1 TAT Peptide

Peptide visualization in DLD-1 colon cancer cells

DLD1 cells were plated onto four-chamber culture slides and grown overnight in Dulbecco's minimum essential medium complemented with 10% fetal bovine serum and 100 units/ml penicillin/streptomycin in a 5% CO2 atmosphere at 37 °C. Cells were treated with 10 μM **P1** for 3hrs. Then the culture slides were washed twice with phosphate-buffered saline and the cells were fixed with 3% para formaldehyde at room temperature (30 min). The fixed cells were washed repeatedly with phosphate-buffered saline. Culture slides were mounted using anti-FAD fluorescent mounting medium and the fluorescence image recorded. Excitation was provided with a mercury ion laser set at 405 nm, and the emitted light was filtered with an appropriate long pass filter.

Crystal structure analysis Boc-Prolinyl Coumarin (4f)

Crystals were grown by slow evaporation from a solution of EtOAc/Hexane. A single crystal (0.38× 0.25 × 0.15 mm) was mounted on loop with a small amount of the paraffin oil. The X-

ray data were collected at 200K temperature on a Bruker APEX DUO CCD diffractometer using Mo K_α radiation (λ = 0.71073 Å), ω-scans (2θ = 56.56), for a total of 3198 independent reflections. Space group C2, a = 16.779(3), b = 10.0638(17), c = 11.0022(19), β = 103.905(4), V = 1803.4(5) $Å^3$, Monoclinic, Z = 4 for chemical formula $C_{19}H_{23}NO_5$, with one molecule in asymmetric unit; ρ calcd. = 1.272 gcm^{-3}, μ = 0.092mm^{-1}, F(000) = 736, R_{int} = 0.0216. The final R value was 0.0355 (wR2= 0.0896) 2882 observed reflections ($F_0 \geq 4\sigma$ ($|F_0|$)) and 230 variables, S = 1.052. The structure was obtained by direct methods using SHELXS-97.[42] All non-hydrogen atoms were refined anisotropically. The hydrogen atoms were fixed geometrically in the idealized position and refined in the final cycle of refinement as riding over the atoms to which they are bonded. The largest difference peak and hole were 0.169 and -0.202e$Å^3$, respectively.

Crystal structure analysis Boc-Alanyl Coumarin (4a)

Crystals were grown by slow evaporation from a solution of MeOH/water. A single crystal (0.35× 0.30 × 0.20 mm) was mounted on loop with a small amount of the paraffin oil. The X-ray data were collected at 200K temperature on a Bruker APEX DUO CCD diffractometer using Mo K_α radiation (λ = 0.71073 Å), ω-scans (2θ = 56.56), for a total of 3782 independent reflections. Space group P21, a = 5.122(3), b = 10.085(6), c = 16.501(10), β = 96.065(13), V = 847.6(8) $Å^3$, Monoclinic, Z = 2 for chemical formula $C_{17}H_{21}NO_5$, with one molecule in asymmetric unit; ρ calcd. = 1.251 gcm^{-3}, μ = 0.092 mm^{-1}, F(000) = 340, R_{int} = 0.0468. The final R value was 0.0537 (wR2= 0.1113) 1598 observed reflections ($F_0 \geq 4\sigma$ ($|F_0|$)) and 213 variables, S = 0.899. The structure was obtained by direct methods using SHELXS-97.[42] All non-hydrogen atoms were refined anisotropically. The hydrogen atoms were fixed geometrically in the idealized position and refined in the final cycle of refinement as riding over the atoms to which they are bonded. The largest difference peak and hole were 0.126 and -0.143 e$Å^3$, respectively.

4.2.5 Synthetic procedure and compound characterization for Section 4C

General procedure for the synthesis of *syn*- and *anti*-β-hydroxy γ-amino ester

The *N*-protected β-keto γ-amino ester (**1**) (1 mmol) was dissolved in 10 mL of dry THF under N_2 atmosphere, cooled to -78 ^oC, and then $NaBH_4$ (1.4 mmol, 0.142 g) was added in one portion. The reaction mixture was stirred for further 3 hrs to complete the reaction. The progress of the reaction was monitored by TLC. After completion of the reaction, it was quenched by pouring the mixture into ice-cold 1 N hydrochloric acid (10 mL). The aqueous phase was extracted with ethyl acetate (3 × 20 mL). Then the combined organic layers was washed with brine (60mL) and dried over anhydrous Na_2SO_4, and evaporated under reduced pressure. The diastereoisomer mixtures of **2a**, **2c** and **2d** (Table 4) were separated passing through normal silica gel column chromatography using pet- ether (60-80 ^oC)–ethyl acetate solvent system. The diastereoisomer mixture of **2b**, **2e** and **2f** (Table 4) are not separable in normal silica gel column chromatography.

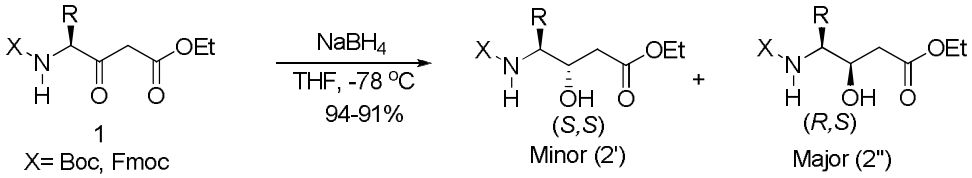

Spectroscopic data for *syn*- and *anti*-β-hydroxy γ-amino ester

(3*S*, 4*S*)-ethyl 4-(tert-butoxycarbonylamino)-3-hydroxy-5-methylhexanoate (2a')

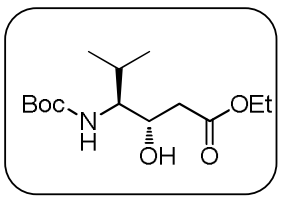

Physical state : colourless liquid

Mol. Formula : $C_{15}H_{29}NO_5$

Yield : 0.085g, 32%

$[\alpha]_D^{20}$: – 37.8 (c = 1, MeOH)

^{1}H NMR (400 MHz, $CDCl_3$) **:** δ_H 4.87-4.85 (d, *J* = 9.7, 1H, NH), 4.19-4.14 (q, *J* = 7.2, 2H, -OC*H*$_2$), 4.11-4.09 (d, *J* = 8, 1H,-C*H*-OH), 3.67-3.65 (m, 1H, -C*H*-), 3.26 (b, 1H, -OH), 2.50-2.44 (m, 2H, -C*H*$_2$CO), 1.84-1.79 (m, 1H, -δC*H*-), 1.41 (s, 9H, Boc -(C*H*$_3$)$_3$) ,1.28-1.24 (t, *J* = 7.2, 3H, -C*H*$_3$), 0.92-0.88 (m,6H, -(C*H*$_3$)$_2$).

^{13}C NMR (100 MHz, $CDCl_3$) **:** δ_C 173.63, 155.35, 79.87, 68.37, 64.28, 61.33, 39.26, 28.35, 26.89, 20.03, 14.15.

MALDI-TOF/TOF m/z **:** Calcd. $[M+Na]^+$ 312.1787, observed 312.1739.

(3*R*, 4*S*)-ethyl 4-(tert-butoxycarbonylamino)-3-hydroxy-5-methylhexanoate (2a'')

Physical state **:** colourless liquid

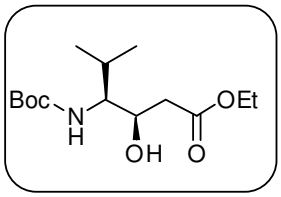

Mol. Formula **:** $C_{15}H_{29}NO_5$

Yield **:** 0.182g, 68%

$[\alpha]_D^{20}$ **:** – 23.6 (c = 1, MeOH)

^{1}H NMR (400 MHz, $CDCl_3$) **:** δ_H 4.64-4.62 (d, *J* = 9.8, 1H, NH), 4.18-4.13 (q, *J* = 7.1, 2H, -OC*H*$_2$), 4.09-4.07 (d, *J* = 8, 1H,-C*H*-OH), 3.62-3.58 (m, 1H, -C*H*-), 3.24 (b, 1H, -OH), 2.52-2.40 (m, 2H, -C*H*$_2$CO), 1.83-1.74 (m, 1H, -δC*H*-), 1.42 (s, 9H, Boc -(C*H*$_3$)$_3$) ,1.29-1.25 (t, *J* = 7.2, 3H, -C*H*$_3$), 0.93-0.86 (m, 6H, -(C*H*$_3$)$_2$).

^{13}C NMR (100 MHz, $CDCl_3$) **:** δ_C 173.13, 155.21, 79.82, 68.11, 63.93, 62.45, 38.79, 28.03, 26.32, 19.45, 14.07.

MALDI-TOF/TOF m/z **:** Calcd. $[M+Na]^+$ 312.1787, observed 312.1754.

(3*S*, 4*S*, 5*S*)-ethyl 4-((tert-butoxycarbonyl)amino)-3-hydroxy-5-methylheptanoate (2b')

Physical state **:** colourless liquid

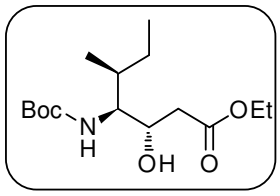

Mol. Formula **:** $C_{14}H_{27}NO_5$

Yield : 0.087g, 28.8%

$[\alpha]_D^{20}$: – 52.2 (c = 1, MeOH)

^{1}H NMR (500 MHz, $CDCl_3$) : δ_H 4.86-4.84 (d, *J* = 9.5, 1H, NH), 4.28-4.26 (d, *J* = 7.1, 2H, - C*H*-OH), 4.19-4.15 (t, *J* = 7.2, 1H,-OCH_2), 3.28 (b, 1H, -OH), 3.24-3.20 (t, *J* = 8.6, 1H, -C*H*-γ), 2.58-2.43 (m, 2H, -CH_2-α), 1.67-1.62 (m, 1H, -C*H*-δ), 1.58-1.54 (m, 2H, -CH_2-), 1.44 (s, 9H, Boc -(CH_3)$_3$) ,1.29-1.26 (t, *J* = 7.0, 3H, -CH_3), 0.97-0.96 (d, *J* = 5.3, 3H, -(CH_3)), 0.91-0.88 (t, *J* = 5.5, 3H, -(CH_3)).

MALDI-TOF/TOF m/z : Calcd. $[M+Na]^+$ 326.1943, observed 326.2314.

(3*R*, 4*S*, 5*S*)-ethyl 4-((tert-butoxycarbonyl)amino)-3-hydroxy-5-methylheptanoate (2b'')

Physical state : colourless liquid

Mol. Formula : $C_{15}H_{29}NO_5$

Yield : 0.184g, 61.2%

$[\alpha]_D^{20}$: - 22.7 (c = 1, MeOH)

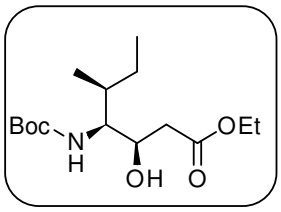

^{1}H NMR (500 MHz, $CDCl_3$) : δ_H 4.43-4.41 (d, *J* = 9.4, 1H, NH), 4.20-4.15 (q, *J* = 7.2, 2H, -OCH_2), 4.02-4.39 (t, *J* = 7.8, 1H,-C*H*-OH), 3.59-3.54 (m, 1H, -C*H*-γ), 3. 33 (b, 1H, -OH), 2.59-2.43 (m, 2H, -CH_2-α), 1.82-1.77 (m, 1H, -C*H*-δ), 1.60-1.53 (m, 2H, -CH_2-), 1.44 (s, 9H, Boc -(CH_3)$_3$) ,1.29-1.26 (t, *J* = 7.0, 3H, -CH_3), 0.95-0.91 (m, 6H, -(CH_3)$_2$).

MALDI-TOF/TOF m/z : Calcd. $[M+Na]^+$ 326.1943, observed 326.3148.

(3*S*, 4*S*)-ethyl 4-(tert-butoxycarbonylamino)-3-hydroxy-6-methylheptanoate (2c')

Physical state : colourless liquid

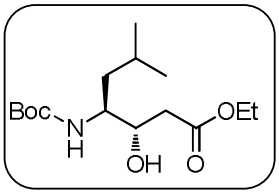

Mol. Formula : $C_{14}H_{27}NO_5$

Yield : 0.09g, 30.1%

$[\alpha]_D^{20}$: – 38.2 (c = 1, MeOH)

^{1}H NMR (400 MHz, $CDCl_3$) : δ_H 4.73-4.71 (d, *J* = 10, 1H, NH), 4.20-4.15 (q, *J* = 7.2, 2H, -OC*H*$_2$), 4.03-4.01 (d, *J* = 8, 1H,-C*H*-OH), 3.63-3.60 (m, 1H, -C*H*-), 3. 30 (b, 1H, -OH), 2.59-2.46 (m, 2H, -C*H*$_2$CO), 1.69-1.58 (m, 3H, -C*H*$_2$C*H*-), 1.44 (s, 9H, Boc -(C*H*$_3$)$_3$) ,1.30-1.26 (t, *J* = 7.2, 3H, -C*H*$_3$), 0.94-0.92 (m,6H, -(C*H*$_3$)$_2$).

^{13}C NMR (100 MHz, $CDCl_3$) : δ_C 173.55, 156.00, 79.18, 69.65, 51.93, 41.70, 38.67, 28.35, 24.73, 23.01, 22.24, 14.13.

MALDI-TOF/TOF m/z : Calcd. $[M+Na]^+$ 326.1943, observed 326.2034.

(3*R*, 4*S*)-ethyl 4-(tert-butoxycarbonylamino)-3-hydroxy-6-methylheptanoate (2c'')

Physical state : semisolid

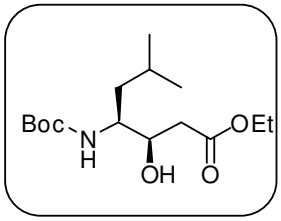

Mol. Formula : $C_{15}H_{29}NO_5$

Yield : 0.191g, 63.9%

$[\alpha]_D^{20}$: - 32.5 (c = 1, MeOH)

^{1}H NMR (400 MHz, $CDCl_3$) : δ_H 4.59-4.57 (d, *J* = 8.8, 1H, NH), 4.20-4.15 (q, *J* = 7, 2H, -OC*H*$_2$), 4.05-4.01 (m,1H, C*H*-OH), 3.70-3.63 (m, 1H, -C*H*), 3.45 (b, 1H, -OH), 2.48-2.42 (m, 2H, -C*H*$_2$CO-), 1.66-1.57 (m, 2H, -δC*H*$_2$-), 1.44 (s, 9H, Boc -(C*H*$_3$)$_3$), 1.34-1.31 (t, *J* = 6.8, -ωC*H*-) 1.29-1.26 (t, *J* = 7.2, 3H, -C*H*$_3$), 0.95-0.91 (m,6H, -(C*H*$_3$)$_2$).

^{13}C NMR (100 MHz, $CDCl_3$) : δ_C 172.84, 156.16, 79.57, 71.38, 60.82, 52.69, 38.84, 37.95, 28.35, 24.70, 23.65, 21.55, 14.14.

MALDI-TOF/TOF m/z : Calcd. $[M+Na]^+$ 326.1943, observed 326.2148.

(3*S*, 4*S*)-ethyl 4-((tert-butoxycarbonyl)amino)-3-hydroxy-5-phenylpentanoate (2d')

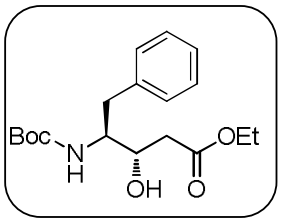

Physical state : white powder

Mol. Formula : $C_{18}H_{27}NO_5$

Yield : 0.134g, 40%

$[\alpha]_D^{20}$: – 36.2 (c = 1, MeOH)

^{1}H NMR (400 MHz, $CDCl_3$) : δ_H 7.31-7.22 (m, 5H, -Ph), 4.97-4.95 (d, *J* = 9.8, 1H, NH), 4.16-4.11 (q, *J* = 7.2, 2H, -OC*H*$_2$), 4.00-3.97 (d, *J* = 8, 1H,-C*H*-OH), 3.76-3.70 (m, 1H, -C*H*-), 3.52 (b, 1H, -OH), 2.93-2.91 (m, 2H, -C*H*$_2$-Ph), 2.63-2.35 (m, 2H, -C*H*$_2$CO), 1.42 (s, 9H, Boc -(C*H*$_3$)$_3$) ,1.27-1.25 (t, *J* = 7.0, 3H, -C*H*$_3$).

^{13}C NMR (100 MHz, $CDCl_3$) : δ_C 173.61, 155.81, 138.14, 129.41, 128.45, 126.36, 79.40, 66.94, 60.85, 55.34, 38.53, 29.68, 28.33, 14.09.

MALDI-TOF/TOF m/z : Calcd. $[M+Na]^+$ 360.1787, observed 360.1747.

(3*S*, 4*R*)-ethyl 4-((tert-butoxycarbonyl)amino)-3-hydroxy-5-phenylpentanoate (2d'')

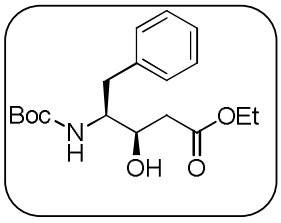

Physical state : white powder

Mol. Formula : $C_{18}H_{27}NO_5$

Yield : 0.196g, 60%

$[\alpha]_D^{20}$: –14.3 (c = 1, MeOH)

^{1}H NMR (400 MHz, $CDCl_3$) : δ_H 7.32-7.22 (m, 5H, -Ph), 4.56-4.54 (d, *J* = 9.8, 1H, NH), 4.21-4.16 (q, *J* = 7.2, 2H, -OC*H*$_2$), 4.00-3.99 (d, *J* = 6.5, 1H,-C*H*-OH), 3.90-3.84 (m, 1H, -C*H*-), 3.61 (b, 1H, -OH), 3.01-2.82 (m, 2H, -C*H*$_2$-Ph), 2.61-2.47 (m, 2H, -C*H*$_2$CO), 1.36 (s, 9H, Boc -(C*H*$_3$)$_3$) ,1.30-1.26 (t, *J* = 7.2, 3H, -C*H*$_3$).

^{13}C NMR (100 MHz, $CDCl_3$) **:** δ_C 173.01, 155.71, 137.60, 129.47, 128.45, 126.43, 79.60, 70.06, 60.89, 55.11, 38.12, 35.79, 28.24, 14.13.

MALDI-TOF/TOF m/z **:** Calcd. $[M+Na]^+$ 360.1787, observed 360.1732.

(*S*)-tert-butyl 2-((*S*)-3-ethoxy-1-hydroxy-3-oxopropyl)pyrrolidine-1-carboxylate (2e')

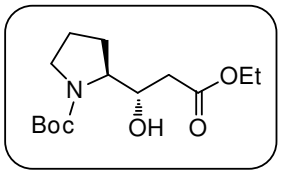

Physical state **:** colourless liquid

Mol. Formula **:** $C_{14}H_{25}NO_5$

Yield **:** 0.109g, 38.2%

$[\alpha]_D^{20}$ **:** – 37.8 (c = 1, MeOH)

^{1}H NMR (500 MHz, $CDCl_3$) **:** δ_H 4.96 (b, -βC*H*-OH, 1H), 4.19-4.14 (q, *J* = 7.2, 2H, -OCH_2), 4.04-4.02, 3.95-3.63 (m, 2H, -εCH_2-), 3.49 (b, 1H, -OH), 3.33-3.28 (m, 1H, -γC*H*-), 2.52-2.39 (m, 2H, -αCH_2-), 2.00-1.66 (m, 4H, -δ & ωCH_2-), 1.46, 1.26 (s, 9H, Boc -(CH_3)$_3$), 1.29-1.26 (t, *J* = 7.0, 3H, -CH_3).

MALDI-TOF/TOF m/z **:** Calcd. $[M+Na]^+$ 310.1630, observed 310.1867.

(*S*)-tert-butyl 2-((*R*)-3-ethoxy-1-hydroxy-3-oxopropyl)pyrrolidine-1-carboxylate (2e'')

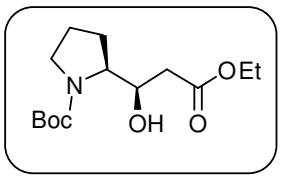

Physical state **:** colourless liquid

Mol. Formula **:** $C_{14}H_{25}NO_5$

Yield **:** 0.152g, 52.8%

$[\alpha]_D^{20}$ **:** – 21.6 (c = 1, MeOH)

^{1}H NMR (400 MHz, $CDCl_3$) **:** δ_H 4.49-4.44 (m, -βC*H*-OH, 1H), 4.19-4.16 (q, *J* = 7.0, 2H, -OCH_2), 4.18-4.15, 3.95-3.92 (m, 2H, -εCH_2-), 3.48 (b, 1H, -OH), 3.28-3.23 (m, 1H, -

C*H*-), 2.47-2.38 (m, 2H, -αCH_2-), 1.99-1.66 (m, 4H, -δ & ωCH_2-), 1.47, 1.26 (s, 9H, Boc -(CH_3)$_3$), 1.29-1.26 (t, *J* = 7.0, 3H, -CH_3).

MALDI-TOF/TOF m/z **:** Calcd. $[M+Na]^+$ 310.1630, observed 310.1845.

Synthesis of Dipeptide Boc-Aib-(S, S)-γPhe -OEt

(Boc-(*S, S*)-γPhe-OEt) (4 mmol, 1.35 g) was dissolved in DCM (4 mL) and cooled the solution in ice bath. Then, 4 mL of neat TFA was added slowly to this solution. After completion of the reaction (~ 30 min), TFA was removed from the reaction mixture under *vacuum*. The residue was dissolved in water and the pH was adjusted to ~ 10 by the slow addition of solid Na_2CO_3 in ice cold conditions. Then Boc deprotected free amine was extracted with ethyl acetate (3 × 20 mL). The combined organic layer was washed with brine (30 mL), dried over Na_2SO_4, concentrated under *vacuum* to *ca*. 2 mL and directly used for the coupling reaction in the next step.

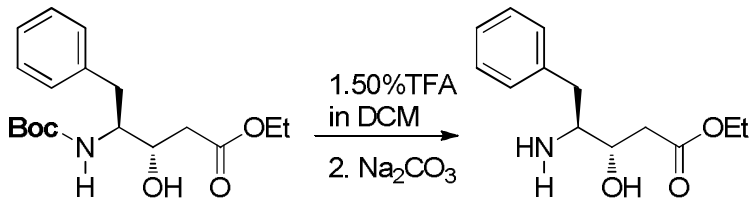

Boc-Aib-OH (3.5 mmol, 0.71 g) and NH_2-(*S, S*)-γPhe-OEt were dissolved together in DMF (2.5 mL), followed by HBTU (3.85 mmol, 1.46 g) was added to the reaction mixture and cooled to 0 ^oC for 5 min. Then, DiPEA (4.2 mmol, 0.75 mL) was added with stirring and the reaction mixture was allowed to come to room temperature. The progress of the reaction was monitored by TLC. After completion(roughly 6 hrs), the reaction mixture was diluted with 200 mL of ethyl acetate and washed with 5% HCl (2 ×100 mL), 10 % sodium carbonate solution in water (2 × 100 mL) and followed by brine (100 mL). The organic layer was dried over anhydrous Na_2SO_4 and evaporated under reduced pressure to give gummy yellowish

product, which was purified on silica gel column chromatography using EtOAc/Petether (60-80 ^{o}C) to get white crystalline product. Overall yield 76% (1.07 g, 2.66 mmol).

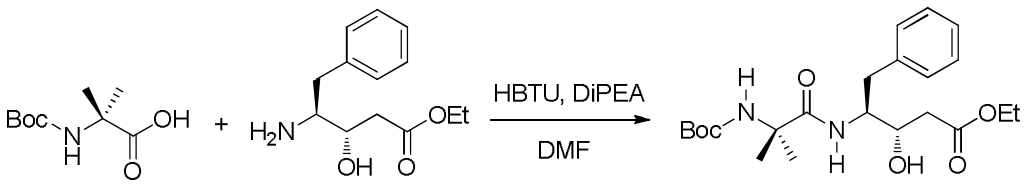

Boc-Aib-(*S*, *S*)-γPhe-OEt

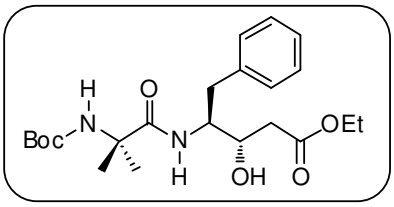

Physical state **:** gummy

Mol. Formula **:** $C_{22}H_{34}N_2O_6$

Yield **:** 76%

^{1}H NMR (500 MHz, $CDCl_3$) **:** δ_H 7.29-7.17 (m, 5H, -Ph), 6.68-6.66 (d, *J* = 8.5, 1H, NH), 4.86 (s, 1H, NH), 4.16-4.08 (m, 3H, -OC*H*$_2$, -γCH of (*S*, *S*) γPhe), 4.03-4.01 (d, J = 9.5, 1H, -βCH of (*S*, *S*) γPhe), 3.64 (b, 1H, -OH), 2.96-2.87 (m, 2H, C*H*$_2$-Ph), 2.71-2.34 (m, 2H, -αCH$_2$ of (*S*, *S*) γPhe), 1.45 (s, 3H, -$(CH_3)_2$ for Aib),1.42 (s, 9H, -$(CH_3)_3$ Boc), 1.29 (s, 3H, -$(CH_3)_2$ for Aib), 1.24-1.21 (t, *J* = 7, 3H, -OCH$_2$C*H*$_3$,).

MALDI TOF/TOF m/z **:** Calcd. $[M+Na]^+$ 422.2315, observed 445.3820.

Synthesis of tetrapeptide Boc-Aib-(*S*, *S*)-γPhe-Aib-(*S*, *S*)-γPhe-OEt

Boc-Aib-(*S, S*)-γPhe-OH: Boc-Aib-(*S, S*)-γPhe-OEt (1.2 mmol, 0.485 g) was dissolved in ethanol (5 mL). Then 5 mL of 1(N) NaOH was added slowly to this solution. After completion of the reaction (~ 2 hrs), ethanol was evaporated from reaction mixture and the residue was acidified to *p*H ~ 3 using 5% HCl (5% volume in water) at cold conditions after diluting with 50 mL cold water. Product was extracted with ethyl acetate (3 × 20 mL). Combined organic layer was washed with brine (40 mL) and dried over anhydrous Na_2SO_4.

Organic layer was concentrated under reduced pressure to give gummy product with quantitative yield 98% (1.17 mmol, 0.439 g).

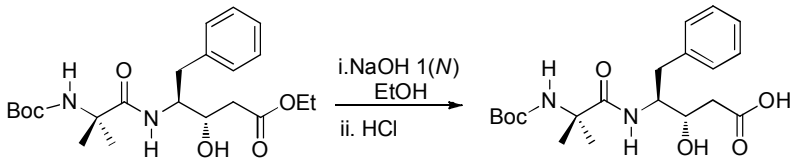

NH_2-Aib-(*S, S*)-γPhe-OEt: Boc-Aib-(*S, S*)-γPhe-OEt (1.46 mmol, 0.585 g) was dissolved in DCM (3 mL) and cooled the solution in ice bath. Then 3 mL neat TFA was added to the solution. After completion of the reaction (~ 30 min), TFA was removed from reaction mixture under vacuum. The residue was dissolved in water and the pH was adjusted to ~ 10 by the slow addition of solid Na_2CO_3 in ice cold conditions. Then Boc deprotected dipeptide was extracted with ethyl acetate (3 × 20 mL). Combined organic layer was washed with brine (30 mL), dried over Na_2SO_4 and concentrated under vacuum to *ca*. 2 mL and used for coupling reaction in the next step.

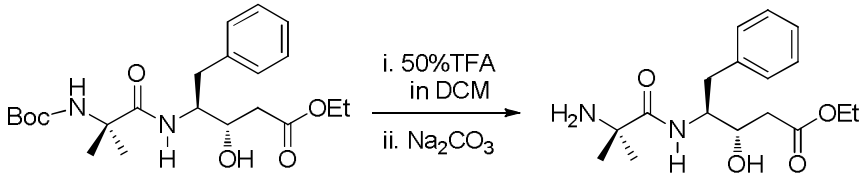

Boc-Aib-(*S, S*)-γPhe-OH (1.17 mmol, 0.439 g) and NH_2-Aib-(*S, S*)-γPhe-OEt were dissolved together in DMF (5 mL) followed by HBTU (1.28 mmol, 0.500 g) was added. The reaction mixture was cooled to 0 ^oC for 5 min. Then DiEPA (1.40 mmol, 0.250 mL) was added to the reaction mixture and it was allowed to come in room temperature at constant stirring. The progress of the reaction was monitored by TLC. After completion of the reaction (roughly 4hrs), reaction mixture was diluted with 200 mL of ethyl acetate and washed with 5% HCl (5 % by vol. in water, 2 × 80 mL), 10% sodium carbonate solution in water (2 × 80 mL) and followed by brine (80 mL). The organic layer was dried over Na_2SO_4 and evaporated under reduced pressure to give gummy yellowish product, which was purified on silica gel column chromatography using EtOAc/Petether (60-80 ^oC) solvent system to get gummy product,

which was further crystallized using EtOAc/Hexane. Overall yield 72% (0.83 mmol, 0.585 g).

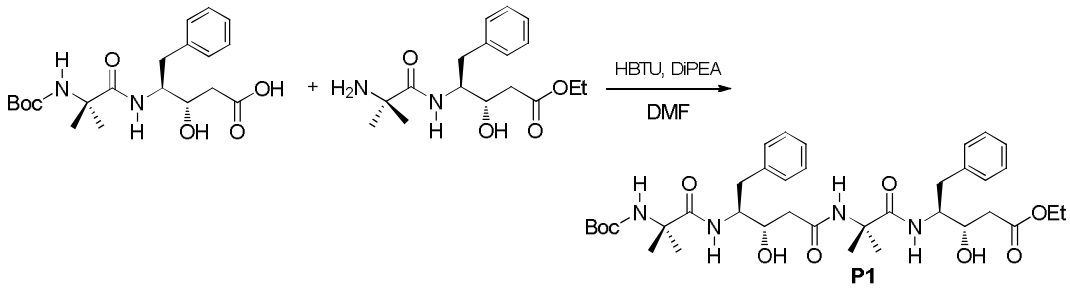

Boc-Aib-(*S*, *S*)-γPhe-Aib-(*S*, *S*)-γPhe-OEt (P1)

Physical state **:** white crystalline powder

Mol. Formula **:** $C_{37}H_{54}N_4O_9$

Yield **:** 72%

^{1}H NMR (500 MHz, $CDCl_3$) **:** δ_H 7.41 (b, 1H, 4NH), 7.39-7.15 (m, 10H, -Ph), 7.12 (b, 1H, 3NH), 6.65-6.63 (d, *J* = 9.15, 1H, 2NH), 5.03 (s, 1H, 1NH), 4.29-4.21 (m, 2H, -γ & βCH of (*S*, *S*) γPhe2, -γCH of (*S*, *S*) γPhe4), 4.16-4.11 (m, 3H, -OC*H*$_2$, βCH of (*S*, *S*) γPhe4), 3.85 (b, 1H, -OH of (*S*, *S*) γPhe4), 2.75-2.72 (m, 4H, C*H*$_2$-Ph), 2.89-2.70 (m, 2H, αCH$_2$ of (*S*, *S*) γPhe4), 2.59-2.37 (m, 2H, αCH$_2$ of (*S*, *S*) γPhe2), 1.41 (s, 12H, -$(CH_3)_3$ Boc, -$(CH_3)_2$ for Aib), 1.38 (s, 3H, -$(CH_3)_2$ for Aib), 1.29 (s, 3H, -$(CH_3)_2$ for Aib), 1.26-1.23 (t, *J* = 7, 3H, -OCH$_2$C*H*$_3$,), 1.12 (s, 3H, -$(CH_3)_2$ for Aib), 1.06 (s, 3H, -$(CH_3)_2$ for Aib).

MALDI TOF/TOF m/z **:** Calcd. $[M+Na]^+$ 721.3788, observed 721.6497.

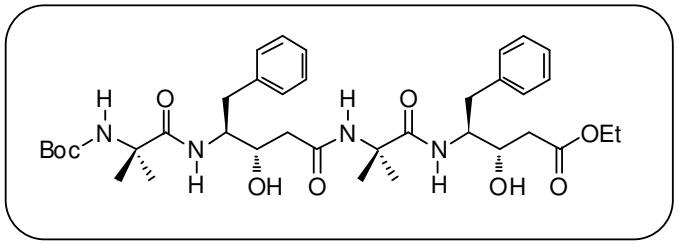

Synthesis of Pentapeptide Boc-Aib-(S, S)-γPhe-Aib-(S, S)-γPhe-Aib-OEt

Boc-Aib-*(S, S)*-γPhe-Aib-*(S, S)*-γPhe-OH: Boc-Aib-(*S, S*)-γPhe-Aib-(*S, S*)-γPhe-OEt (0.57 mmol, 0.400 g) was dissolved in ethanol (4 mL). Then 5 mL of 1(N) NaOH was added slowly to this solution. After completion of the reaction (~ 2 hrs), ethanol was evaporated from reaction mixture and the residue was acidified to *p*H ~ 3 using 5% HCl (5% volume in water) at cold conditions after diluting with 50 mL cold water. Product was extracted with ethyl acetate (3 × 25 mL). Combined organic layer was washed with brine (40 mL) and dried over anhydrous Na_2SO_4. Organic layer was concentrated under reduced pressure to give gummy product with quantitative yield 98% (0.558 mmol, 0.373 g).

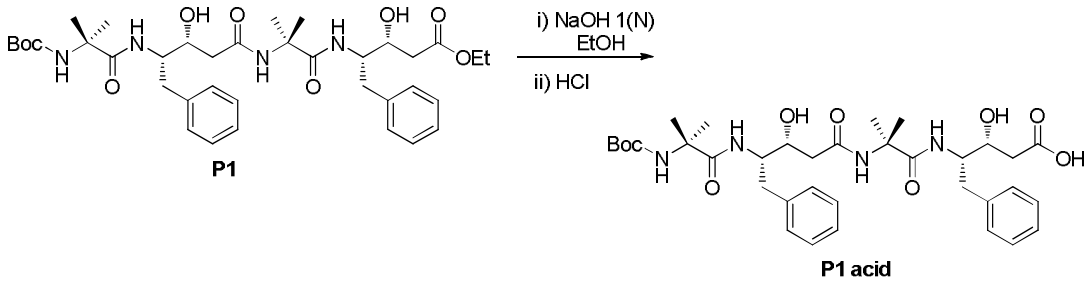

Boc-Aib-(*S, S*)-γPhe-Aib-(*S, S*)-γPhe-OH (0.558 mmol, 0.373 g) and HCl.NH_2-Aib-OMe (0.725 mmol, 0.11 g) were dissolved together in DMF (1.5 mL) followed by HBTU (0.613 mmol, 0.238 g) was added. The reaction mixture was cooled to 0 ^oC for 5 min. Then DiEPA (1.4 mmol, 0.260 mL) was added to the reaction mixture and it was allowed to come to room temperature at constant stirring. The progress of the reaction was monitored by TLC. After completion of the reaction (roughly 4hrs), reaction mixture was diluted with 200 mL of ethyl acetate and washed with 5% HCl (5 % by vol. in water, 2 × 80 mL), 10% sodium carbonate solution in water (2 × 80 mL) and followed by brine (80 mL). The organic layer was dried over Na_2SO_4 and evaporated under reduced pressure to give gummy yellowish product, which was purified on silica gel column chromatography using DCM/MeOH solvent system to get gummy product, which was further crystallized using EtOAc/Hexane. Overall yield 70% (0.39 mmol, 0.572 g).

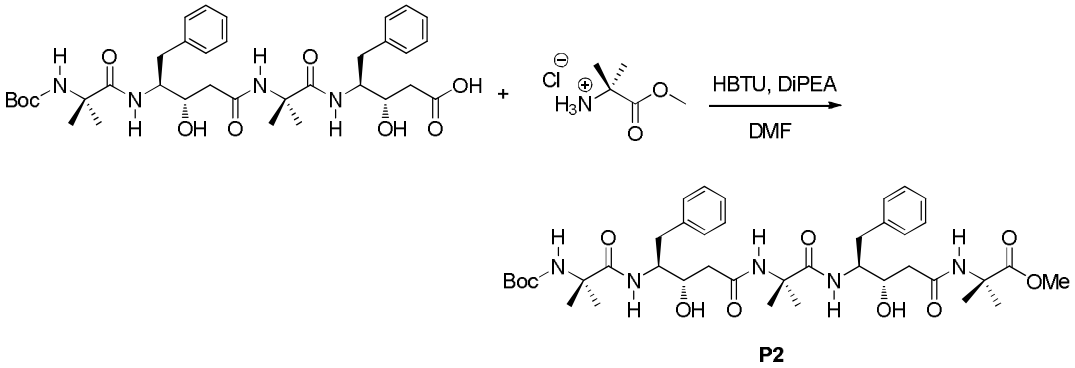

P2

Boc-Aib-(S, S)-γPhe-Aib-(S, S)-γPhe-Aib-OMe (P2)

Physical state **:** white crystalline powder

Mol. Formula **:** $C_{40}H_{59}N_5O_{10}$

Yield **:** 70%

^{1}H NMR (500 MHz, $CDCl_3$) **:** δ_H 7.44 (b, 2H, 5NH and 4NH), 7.29-7.12 (m, 11H, -Ph, NH), 6.64-6.62 (d, *J* = 8.9, 1H, NH), 4.96 (s, 1H, NH), 4.35-4.32 (m, 1H, -βCH of (*S*, *S*) γPhe2), 4.25-4.23 (m, 2H, -γCH of (*S*, *S*) γPhe2, -βCH of (*S*, *S*) γPhe4), 4.07-4.05 (m,1H, -γCH of (*S*, *S*) γPhe4), 3.70 (s, 3H,-OMe), 2.99-2.90 (m, 4H, C*H*$_2$-Ph), 2.59-2.42 (m, 4H, αC*H*$_2$ of (*S*, *S*) γPhe), 1.54 (s, 3H, -$(CH_3)_2$ for Aib5), 1.51 (s, 3H, -$(CH_3)_2$ for Aib5), 1.42 (s, 12H, -$(CH_3)_3$ Boc, -$(CH_3)_2$ for Aib1), 1.38 (s, 3H, -$(CH_3)_2$ for Aib3), 1.12 (s, 3H, -$(CH_3)_2$ for Aib3), 1.07 (s, 3H, -$(CH_3)_2$ for Aib1).

MALDI TOF/TOF m/z **:** Calcd. $[M+Na]^+$ 792.4160, observed 792.6137.

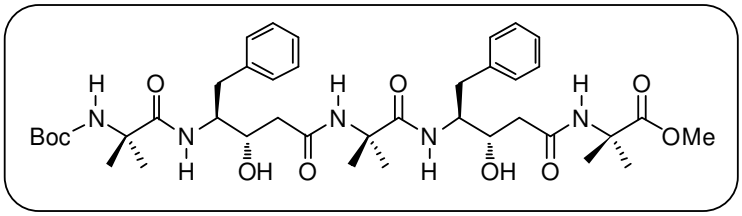

SPPS peptide synthesis of (Ac-Ala-(*R, S*)-γPhe-Aib-(*R, S*)-γPhe-Ala-(*R, S*)-γPhe-Aib-NH_2 (P3)

P3 peptide was synthesized at 0.2 mmol scales on Rink Amide resin using standard Fmoc-chemistry. HBTU/HOBT was used as coupling agents for alpha amino acids and only HBTU was used as coupling agent for Fmoc-(*R, S*)-γPhe-OH amino acids. Fmoc deprotections were facilitated using 20% piperidine in DMF. *N*-terminal of peptide was capped with acetyl group. The coupling reactions were monitored by Kaiser Test. After completion of the synthesis, peptide was cleaved from the resin using 15 mL of TFA/thioanisole/H_2O (98:1.5:0.5) cocktail mixture. After cleavage, the resin was filtered and washed with TFA. The cleavage mixture was evaporated under reduced pressure to give gummy product. Peptide was further recrystallized using EtOAc/Hexane. Peptide was filtered and finally it was purified on reverse phase HPLC (Waters 600), with C_{18} column (XBridge^{TM} Prep BEH 130, C_{18} 5µm, dimension 10 × 250 mm column) using MeOH/H_2O (system MeOH/H_2O 65:35- 95:5 as gradient, 1.25 mL flow per min)gradient system. Homogeneity of peptide was further confirmed using analytical (XBridge^{TM} BEH 130, C_{18} 5µm, dimension 4.6 × 250 mm column) C_{18} column in same MeOH/H_2O (system MeOH/H_2O 65:35- 95:5 as gradient, 0.75 mL flow per min) gradient system. The mass of the peptide was confirmed using **MALDI TOF/TOF** Mass Calcd. for $C_{49}H_{68}N_8O_{11}$ $[M+Na]^+$ 967.4905 Da, observed 967.3572 Da.

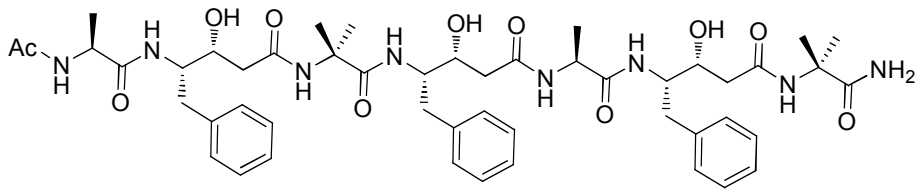

Crystal data analysis of Boc-(R, S)-γPhe (2d")

Crystals were grown by slow evaporation from a solution of methanol. A single crystal (0.21 × 0.14 × 0.11 mm) was mounted on loop with a small amount of the paraffin oil. The X-ray data were collected at 200K temperature on a Bruker APEX DUO CCD diffractometer using Mo K_α radiation (λ = 0.71073 Å), *ω*-scans (2*θ* = 56.56), for a total of 3404 independent reflections. Space group P21, *a* = 13.914(12), *b* = 5.145(4), *c* = 13.914(12), β = 107.40, V =

950.5(14) Å^3, Monoclinic, Z = 2 for chemical formula $C_{18}H_{24}NO_5$, with one molecule in asymmetric unit; ρ calcd. = 1.168 gcm^{-3}, μ = 0.085 mm^{-1}, F(000) = 358, R_{int} = 0.0390. The final R value was 0.0524 (wR2 = 0.1061) 1611 observed reflections ($F_0 \geq 4\sigma$ (|F_0|)) and 223 variables, S = 0.660. The structure was obtained by direct methods using SHELXS-97.[42] All non-hydrogen atoms were refined anisotropically. The hydrogen atoms were fixed geometrically in the idealized position and refined in the final cycle of refinement as riding over the atoms to which they are bonded. The largest difference peak and hole were 0.134 and -0.129 eÅ^3, respectively.

Crystal data analysis of Boc-Aib-(S, S)-γPhe-Aib-(S, S)-γPhe-OEt (P1)

Crystals were grown by slow evaporation from a solution of methanol. A single crystal (0.23 × 0.16 × 0.10 mm) was mounted on loop with a small amount of the paraffin oil. The X-ray data were collected at 100K temperature on a Bruker APEX DUO CCD diffractometer using Mo K_α radiation (λ = 0.71073 Å), ω-scans (2θ = 56.64), for a total of 15158 independent reflections. Space group P2, a = 13.6287(14), b = 10.3904(10), c = 29.171(3), β = 102.281(3), V = 4036.4(7) Å^3, Monoclinic, Z = 2 for chemical formula $C_{74}H_{108}N_8O_{18}$. 3(H_2O), with two molecule in asymmetric unit; ρ calcd. = 1.189 gcm^{-3}, μ = 0.087 mm^{-1}, F(000) = 1552, R_{int} = 0.0990. The final R value was 0.0881 (wR2 = 0.1911) 7215 observed reflections ($F_0 \geq 4\sigma$ (|F_0|)) and 936 variables, S = 1.025. The structure was obtained by direct methods using SHELXS-97.[42] All non-hydrogen atoms were refined anisotropically. The hydrogen atoms were fixed geometrically in the idealized position and refined in the final cycle of refinement as riding over the atoms to which they are bonded. The largest difference peak and hole were 0.884 and -0.554 eÅ^3, respectively.

Crystal data analysis of Boc-Aib-(S, S)-γPhe-Aib-(S, S)-γPhe-Aib-OEt (P2)

Crystals were grown by slow evaporation from a solution of methanol. A single crystal (0.35 × 0.32 × 0.14 mm) was mounted on loop with a small amount of the paraffin oil. The X-ray data were collected at 100K temperature on a Bruker APEX DUO CCD diffractometer using Mo K_α radiation (λ = 0.71073 Å), ω-scans (2θ = 56.54), for a total of 10296 independent reflections. Space group C2, a = 23.242(4), b = 10.6100(19), c = 18.879(3), β = 104.706(2),

V = 4503.1(14) Å^3, Monoclinic, Z = 4 for chemical formula $C_{40}H_{59}N_5O_{10}$. (C_2H_6O), with one molecule in asymmetric unit; ρ calcd. = 1.204 gcm^{-3}, μ = 0.087 mm^{-1}, F(000) = 1760, R_{int} = 0.0276. The final R value was 0.0472 (wR2 = 0.1312) 9461 observed reflections ($F_0 \geq 4\sigma$ ($|F_0|$)) and 537 variables, S = 0.834. The structure was obtained by direct methods using SHELXS-97.[42] All non-hydrogen atoms were refined anisotropically. The hydrogen atoms were fixed geometrically in the idealized position and refined in the final cycle of refinement as riding over the atoms to which they are bonded. The largest difference peak and hole were 0.547 and -0.621 eÅ^3, respectively.

4.3 Reference

1. a) Williams, P. G.; Moore, R. E.; Paul, V. J. *J. Nat. Prod*. **2003**, *66,* 1356-1363. b) Simmons, T. L.; Nogle, L. M.; Media, J.; Valeriote, F. A.; Mooberry, S. L.; Gerwick, W. H. *J. Nat. Prod.* **2009**, *72*, 1011-1106. c) Mynderse, J. S.; Hunt, H. A.; Moore, R. E. *J. Nat. Prod*. **1988**, *51*, 1299-1301. d) Golakoti, T.; Yoshida, W. Y.; Chaganty, S.; Moore, R. E. *J. Nat. Prod*. **2001**, *64*, 54-59. e) Golakoti, T.; Yoshida, W. Y.; Chaganty, S.; Moore, R. E. *Tetrahedron*, **2000**, *56*, 9093-9120.
2. a) Hoffmann, D.; Hevel, J. M.; Moore, R. E.; Moore, B. S. *Gene,* **2003**, *311*, 171-180. b) Pettit, G. R.; Kamano, Y.; Kizu, H.; Dufresne, C.; Herald, C. L.; Bontems, R. J.; Schmidt, J. M.; Boettner, F. E.; Nieman, R. A. *Heterocycles* **1989**, *28*, 553-558. c) Pettit, G. R.; Smith, T. H.; Feng, S.; Knight, J. C.; Tan, R.; Pettit, R. K.; Hinrichs, P. A. *J. Nat. Prod*. **2007**, *70*, 1073-1083.
3. a) Maibaum, J.; Rich, D. H. *J. Org. Chem.* **1988**, *53*, 869-875. b) Preciado, A.; Williams, P. G. *J. Org. Chem.* **2008**, *73*, 9228-9234. c) Hoffman, R.V.; Kim. H. –O. *J. Org. Chem.* **1995,** *60*, 5107-5113. d) Meloni, M. M.; Taddei, M. *Org. Lett.* **2001**, *3*, 337-345. e) Gasparski, C. M.; Ghosh, A.; Miller, M. J. *J. Org. Chem*. **1992**, *57*, 3546-3550. f) Durham, T. B.; Miller, M. J. *J. Org. Chem.* **2003**, *68,* 35-42. g) Bagley, M. C.;

Xiong, X. *Org. Lett.* **2004**, *6*, 3401-3404. h) Burn, M. P.; Bischoff, L.; Garbay, C. *Angew. Chem. Int. Ed.* **2004**, *43*, 3432-3436. i) Wang, J.; Xie, J.; Schultz, P. G. *J. Am. Chem. Soc.* **2006**, *128*, 8738-8739. j) Muñoz-Ruiz, P,; García-López, M. T.; Cenarruzabeitia, E.; Del Río, J.; Dufresne, M.; Foucaud, M.; Fourmy, D.; Herranz, R. *J. Med. Chem.* **2004**, *47*, 5318-5329. k) Baxter, J. M.; Steinhuebel, D.; Palucki, M.; Davies, I. W. *Org. Lett*, **2005**, *7*, 215-218. l) Moyer, M. P.; Feldman, P. L.; Rapoport, H. *J. Org. Chem.* **1985**, *50*, 5223-5230.

4. Patiño-Molina, R.; Martín-Martínez, M.; Herranz, R.; Garcia Lopez, M. T.; González-Muñiz, R. *Lett. Pept. Sci*. **2000**, *7*, 143-148.

5. a)Yurek-George, A.; Habens, F.; Brimmell, M.; Packham, G.; Ganesan, A. *J. Am. Chem. Soc.* **2004**, *126*, 1030-1031. b) Kim. H. –O.; Olsen, R. K.; Choi, O.-S. *J. Org. Chem*. **1987**, *52*, 4531-4536. c) Harris, B. D.; Bhat, K. L.; Joullie, M. M. *Tetrahedron Lett*, **1987**, *28*, 2837-2840. d) Schuda, P. F.; Greenlee, W. J.; Chakravarty, P. K.; Eskola, P. *J. Org. Chem*. **1988**, *53*, 873-878.
6. Paul, R.; Anderson, G. W. *J. Am. Chem. Soc.* **1960**, *82*, 4596-4600.

7. (a) Palomo, C.; Cossio, F. P.; Rubiales, G.; Aparicio, D. *Tetrahedron Lett.* **1991**, *32*, 3115-3118. (b) Paris, M.; Fehrentz, J. –A.; Heitz, A.; Martinez, J. *Tetrahedron Lett*. **1998**, *39*, 1569-1572.

8. Li, B.; Franck R.W. *Bioorg. Med. Chem. Lett*. **1999**, *9*, 2629-2634.

9. Gutjche, C. D. *Org. React*. **1954**, *8*, 364-429.

10. a) Ye, T.; Mckervey, M. C. *Chem. Rev*. **1994**, *94*, 1091-1160. b) Doyle, M. P.; Duffy, R.; Ratnikov, M.; Zhou, L. Chem. *Rev*. **2010**, *110*, 704-724. c) Zhang, Y.; Wang, J. *Chem. Commun*. **2009**, 5350-5361. d) Doyle, M. P. *J. Org. Chem*. **2006**, *71*, 9253-9260. e) Padwa, A. M.; Weingarten, D. *Chem. Rev.* **1996**, *96*, 223-269. f) Peng, C.; Cheng, J.; Wang, J. *J. Am. Chem. Soc*. **2007***,129,* 8708-8709. g) Peng, L.; Zhang, X.; Ma, M.; Wang, J. *Angew. Chem. Int. Ed.* **2007**, *46*, 1905-1908. h) Liao, M.; Peng, L.; Wang, J. *Org. Lett*, **2008**, *10*, 693-696.

11. a) Trost, B. M.; Malhotra, S.; Fried, B. A. *J. Am. Chem. Soc*. **2009**, *131*, 1674-1675. b) Yao, W.; Wang, J. *Org. Lett*. **2003**, *5*, 1527-1530. c) Zhou, L.; Doyle, M. P. *Org.*

Lett. **2010**, *12*, 796-799. d) Wang, F.; Liu, X.; Zhang, Y.; Lin, L.; Feng, X. *Chem Commun*. **2009**, 7297-7299. e) Benfatti, F.; Yilmaz, S.; Cozzi, P. G. *Adv. Synth. Catal,* **2009***, 351,* 1763-1767. f) Xiao, F.; Liu Y.; Wang, J. *Tetrahedron Lett.* **2007**, *48*, 1147-1149.

12. Hashimoto, T.; Maruoka, K. *J. Am. Chem. Soc*. **2007**, *129*, 10054-10055.

13. a) Liu, W. J.; Lv, B. D.; Gong, L. Z. *Angew. Chem. Int. Ed.* **2009**, *48*, 6503-6506. b) Valdez, S. C.; Leighton, J. L. *J. Am. Chem. Soc,* **2009***, 131,* 14638-14639. c) Akiyama, T.; Suzuki, T.; Mori, K. *Org. Lett*, **2009**, *11*, 2445-2447.

14. Hashimoto, T.; Uchiyama, N.; Maruoka, K. *J. Am. Chem. Soc.* **2008***, 130*, 14380-14381.

15. Holmquist, C. R.; Roskamp, E. J. *J. Org. Chem.* **1989**, *54*, 3258-3260.

16. Fehrentz, J.-A.; Castro, B. *Synthesis*, **1983**, 676-678.

17. Zhou, L.; Doyle, M. P. *Org. Lett.* 2010, **12**, 796-799.

18. Padwa, A.; Hornbuckle, S. F.; Zhang, Z.; Zhi, L. *J. Org. Chem*. **1990**, *55*, 5297-5299.

19. Werner, R. M.; Shokek, O.; Davis, J. T. *J. Org. Chem*.**1997**, *62*, 8243-8246.

20. Dondoni, A.; Massi, A.; Aldhoun, M. *J. Org. Chem*. 2007, **72**, 7677-7687.

21. Wen. J. J.; Crews, C. M. *Tetrahedron Asymm*. 1998, **9**, 1855-1858.

22. Rodriguez, M.; Llinares, M.; Doulut, S.; Heitz, A.; Martinez, J. *Tetrahedron Lett.* **1991**, *32*, 923-926.

23. Dess, D. B.; Martin, J. C. *J. Org. Chem.* **1983,** *43*, 4155-4156.

24. a) Hoult, J. R. S.; Paya, M. *Gen. Pharmacol*. **1996**, *27*, 713-722. b) *Coumarins: Biology, Applications, and Mode of Action*; O'Kennedy, R., Thornes, R. D., Eds.; John Wiley & Sons: New York, 1997. c) Riveiro, M. E.; Kimpe N. D.; Moglioni, A.; Vazquez, R.; Monczor, F.; Shayo, C.; Davio, C. *Curr. Med. Chem.* **2010**, *17*, 1325-1338.

25. a) Riveiro, M. E.; Moglioni, A.; Vazquez, R.; Gomez, N.; Facorro, G.; Piehl, L.; de Celis, E. R.; Shayo, C.; Davio, C. *Bioorg. Med. Chem.* **2008**, *16*, 2665-2675. b) Feuer, G.; Kellen, J. A.; Kovacs, K. *Oncology* **1976**, *33*, 35-39. c) Belluti, F.; Fontana, G.;

Dal Bo, L.; Carenini, N.; Giommarelli, C.; Zunino, F. *Bioorg. Med. Chem*. **2010**, *18*, 3543-3550. d) Gage, B. F. *Hematol. Am. Soc. Hematol. Educ. Program.* **2006**, 467-473. f) Ostrov, D. A.; Hernandez Prada, J. A.; Corsino, P. E.; Finton, K. A.; Le, N.; Rowe, T. C. *Antimicrob. Agents Chemother*. **2007**, *51*, 3688-3698. g) Fylaktakidou, K. C.; Hadjipavlou-Litina, D. J.; Litinas, K. E.; Nicolaides, D. N. *Curr. Pharm. Des.* **2004**, *10*, 3813-3333.

26. Burlison, J. A.; Avila, C.; Vielhauer, G.; Lubbers, D. J.; Holzbeierlein, J.; Blagg, B. S. J. *J. Org. Chem*, **2008**, *73*, 2130-2137.
27. Sekar, N. *Colourage* **2003**, *50*, 55-56.
28. Clark, G. S. *Perfum. Flavor.* **1995**, *20*, 23-24.
29. a) Brun, M.-P.; Bischoff, L.; Garbay, C. *Angew. Chem., Int. Ed.* **2004**, *43*, 3432-3436. b) Zahradnik, M. *The Production and Application of Fluorescent Brightening Agents*; Wiley: New York, 1982.
30. a) Yavari, I.; Hekmatshoar, R.; Zonouzi, A. *Tetrahedron Lett*. **1998**, *39*, 2391-2392. b) Cairns, N.; Harwood, L. M.; Astles, D. P. *J. Chem. Soc., Perkin Trans.1,* **1994**, 3101-3107. c) Pisani, L.; Catto, M.; Giangreco, I.; Leonetti, F.; Nicolotti, O.; Stefanachi, A. A.; Cellamare, S.; Carotti, A. *ChemMedChem,* **2010**, *5*, 1616-1630. d) Henry C. E.; Kwon, O. *Org. Lett.* **2007**, *9*, 3069-3072 and references sited therein
31. Sun, W. C.; Gee, K. R.; Haugland, R. P. *Bioorg. Med. Chem. Lett,* **1998**, *8*, 3107-3110.
32. a) Bandyopadhyay, A.; Agarwal, N.; Mali, S. M.; Jadhav S. V.; Gopi, H. N. *Org. Biomol. Chem,* **2010**, *8*, 4855-4860 and references sited therein.
33. We carried out the Pachmann condensation using different organic acids including trifluoromethanesulfonic acid and found that MSA was better than other acids.
34. a) Hobza, P.; Havlas, Z. *Chem. Rev*. **2000**, *100*, 4253. b) Desiraju, G. R. *Angew. Chem. Int. Ed.* **2007**, *46*, 8342-8356.
35. An extra lysine was incorporated at the position 5 of the HIV-1 TAT peptide ^{1}GRKKRRQRRRPPQ^{13} to further increase the solubility in aqueous buffer.
36. Gante, J. *Angew. Chem., Int. Ed. Engl*., **1994**, *33*, 1699-1720.
37. Aoyagi, Y.; Williams, R. M. *Tetrahedron*, **1998**, *54*, 10419-10433 and reference therein.
38. a) Hossain, H. B.; Van der Helm, D.; Antel, J.; Sheldrick, G. M.; Sanduja, S. K.; Weinheimer, A. J. *Proc. Natl. Acad. Sci. U.S.A.*, **1988**, *85*, 4118-4122. b) Banaigs, B.;

Jeanty, G.; Francisco, C.; Jouin, P.; Poncet, J.; Heitz, A.; Cave, A.; Prome, J. C.; Wahl, M.; Lafargue, F. *Tetrahedron*,**1989**, *45*, 181-190. c) Jouin, P.; Poncet, J.; Dufour, M.; Pantaloni, A.; Castro, B.; *J. Org. Chem.* **1989**, *54*, 617-627.

39. Vervoort, H.; Fenical, W.; de Epifanio, R. *J. Org. Chem.* **2000**, *65*, 782–792.
40. Stratmann, K.; Burgoyne, D. L.; Moore, R. E.; Patterson, G. M. L. *J. Org. Chem.* **1994**, *59*, 7219-7226.
41. a) Bandyopadhyay, A.; *Org, Lett.* **2012**, 14, 2770-2773. b) Bandyopadhyay, A.; Jadhav, S. V.; Gopi, H. N. *Chem. Commun.* **2012**, *48*, 7170-7172.

42. a) SHELXS-97: Sheldrick, G. M. *Acta Crystallogr. Sect A* **1990,** *46,* 467-473. b) Sheldrick, G. M. SHELXL-97, Universitat Gottingen (Germany) **1997.**

1.7 Appendix I: Characterization Data of Synthesized Compounds

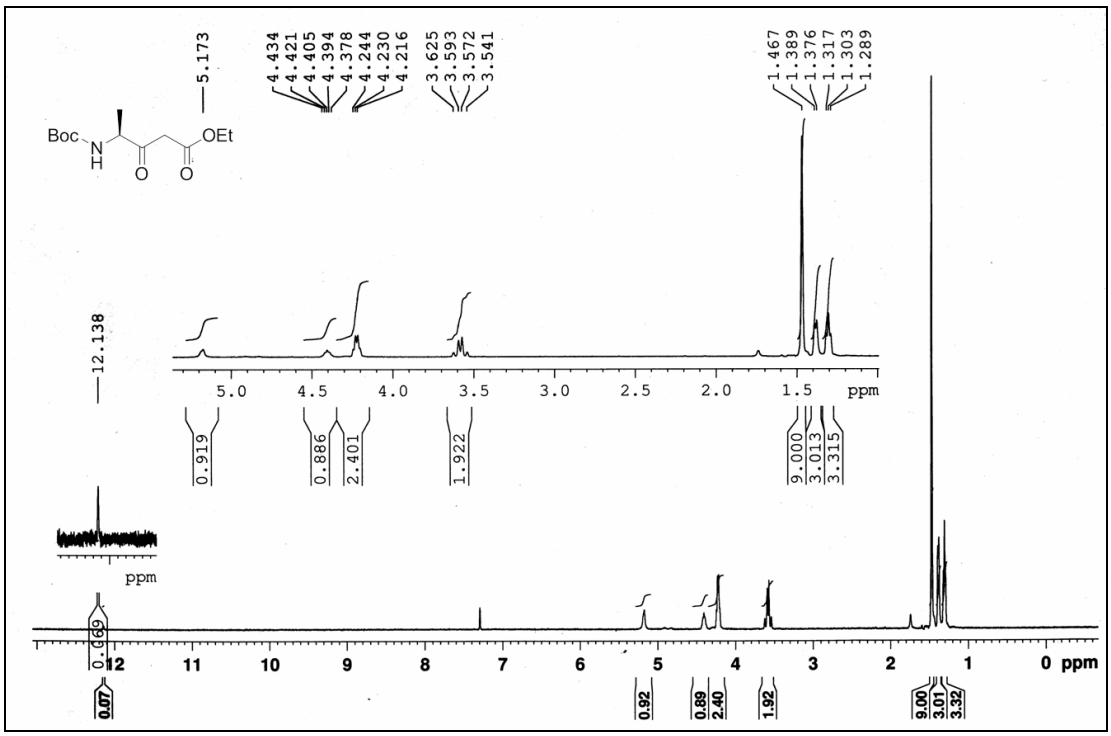
Boc
N
H
O
O
OEt
5.173
4.434
4.421
4.405
4.394
4.378
4.244
4.230
4.216
3.625
3.593
3.572
3.541
1.467
1.389
1.376
1.317
1.303
1.289
12.138
0.919
0.886
2.401
1.922
9.000
3.013
3.315
ppm
0.669
0.07
0.92
0.89
2.40
1.92
9.00
3.01
3.32

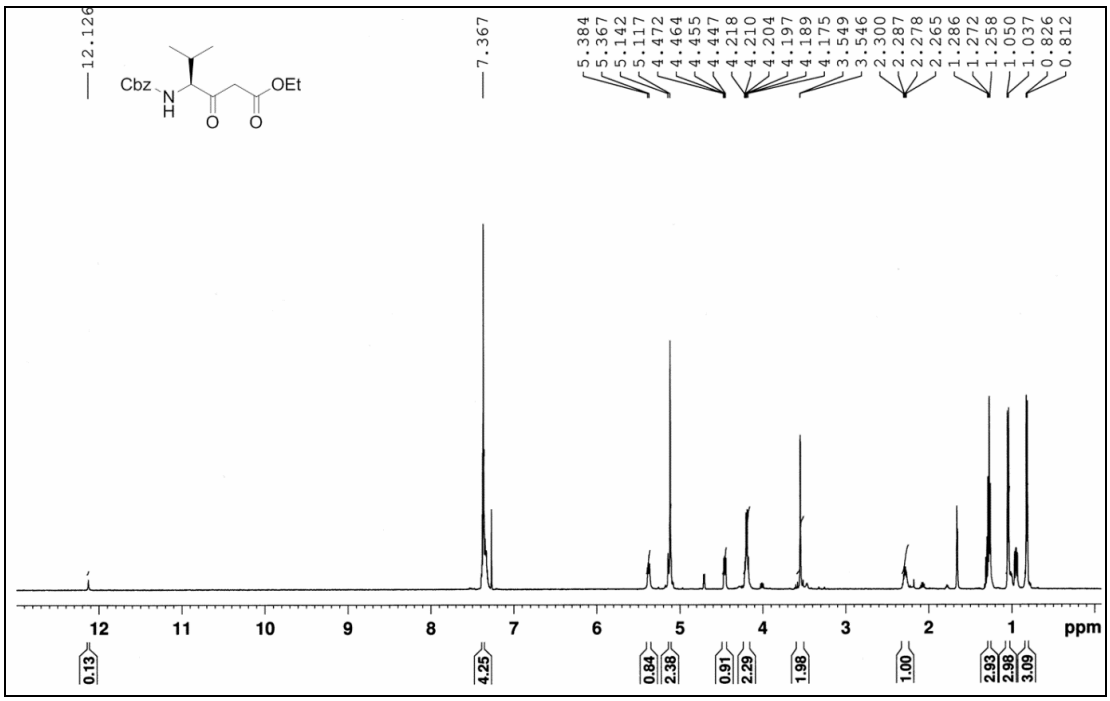
12.126
Cbz
N
H
O
O
OEt
7.367
5.384
5.367
5.142
5.117
4.472
4.464
4.455
4.447
4.218
4.210
4.204
4.197
4.189
4.175
3.549
3.546
2.300
2.287
2.278
2.265
1.286
1.272
1.258
1.050
1.037
0.826
0.812
0.13
4.25
0.84
2.38
0.91
2.29
1.98
1.00
2.93
2.98
3.09

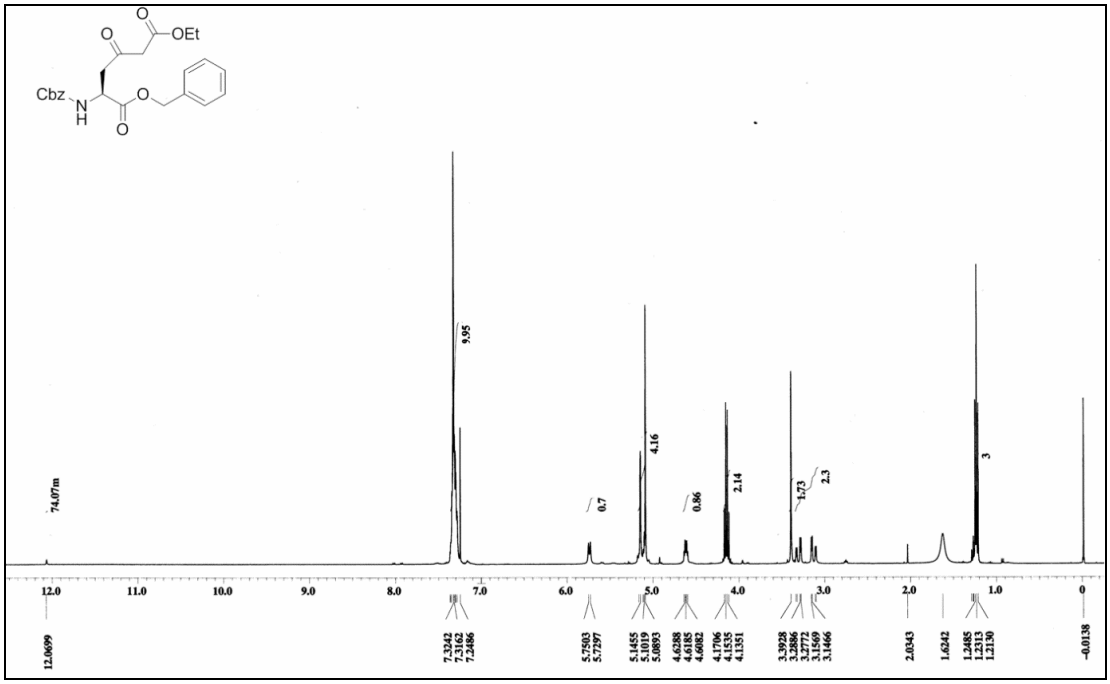
O
OEt
Cbz
N
H
O
O
O
74.07m
9.95
0.7
4.16
0.86
2.14
1.73
2.3
3
12.0
11.0
10.0
9.0
8.0
7.0
6.0
5.0
4.0
3.0
2.0
1.0
0
12.0699
7.3342
7.3162
7.2486
5.7503
5.7397
5.1455
5.1019
5.0693
4.6288
4.6185
4.6082
4.1706
4.1535
4.1351
3.8928
3.2886
3.2772
3.1569
3.1466
2.0343
1.6342
1.2485
1.2311
1.2130
−0.0138

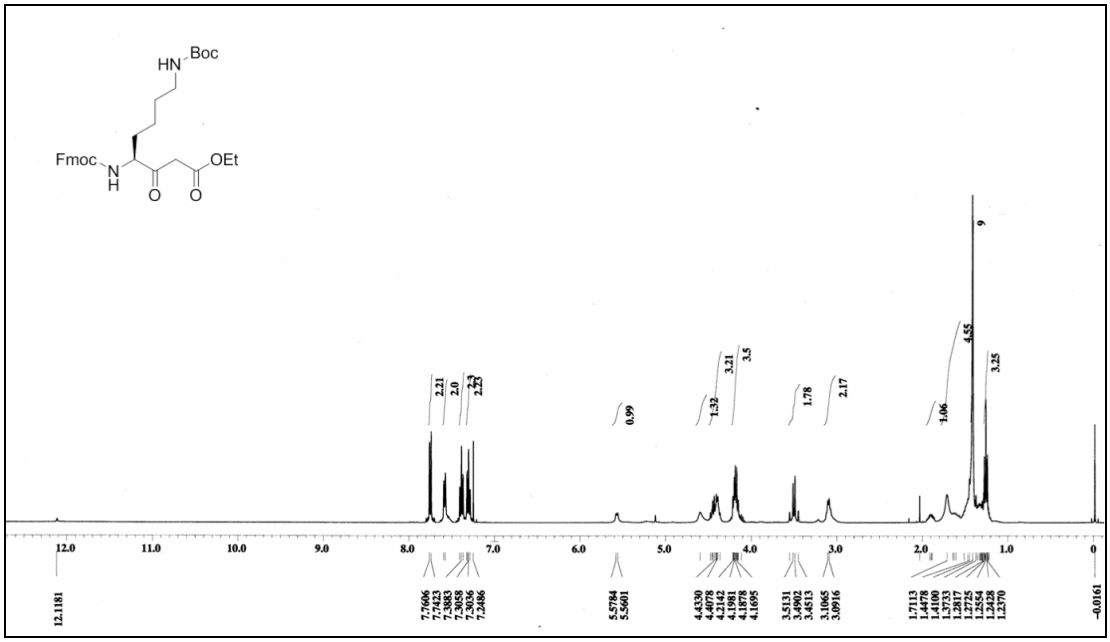
HN
Boc
Fmoc
N
H
O
O
OEt
2.21
2.0
2.25
0.99
1.32
3.21
3.5
1.78
2.17
1.06
4.55
9
3.25
12.0
11.0
10.0
9.0
8.0
7.0
6.0
5.0
4.0
3.0
2.0
1.0
0
12.1181
7.7606
7.7423
7.3983
7.3036
7.2486
5.5784
5.5601
4.4330
4.4078
4.2142
4.1981
4.1878
4.1695
3.5131
3.4972
3.4451
3.1065
3.0916
1.7113
1.4478
1.4180
1.3733
1.2817
1.2725
1.2564
1.2428
1.2370
−0.0161

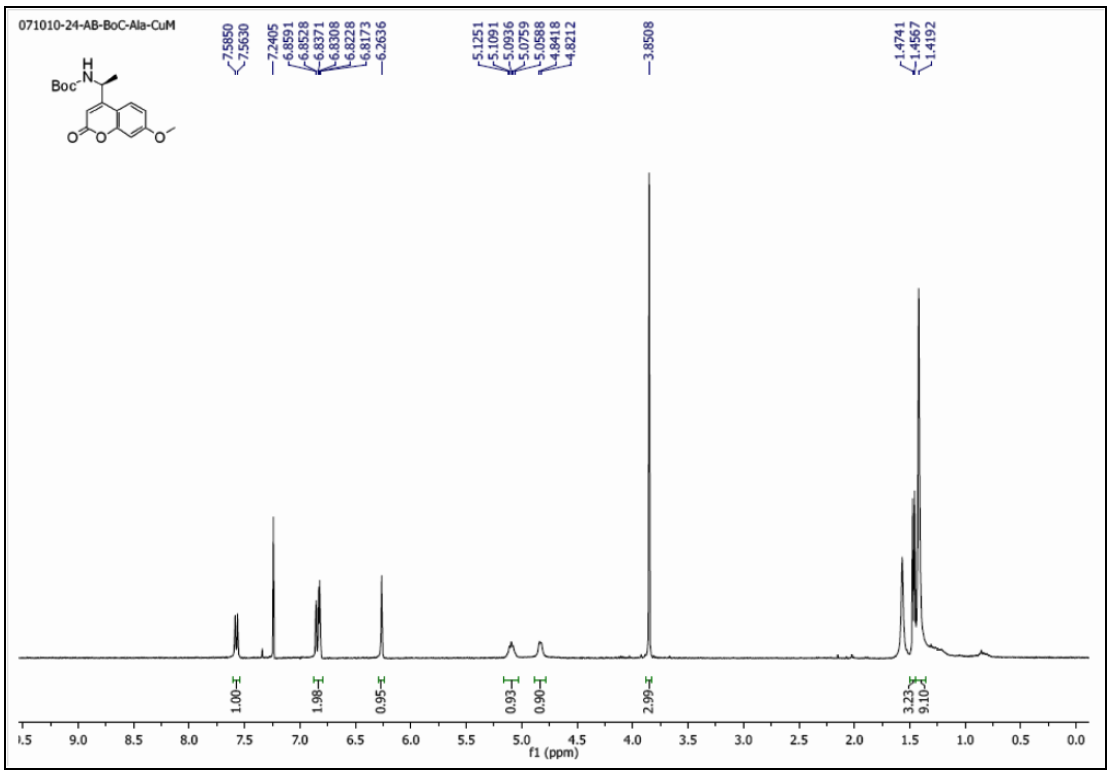
071010-24-AB-BoC-Ala-CuM
Boc
7.5850
7.5630
7.2405
6.8591
6.8528
6.8371
6.8308
6.8228
6.8173
6.2636
5.1251
5.1091
5.0936
5.0759
5.0588
4.8418
4.8212
3.8508
1.4741
1.4567
1.4192
1.00
1.98
0.95
0.93
0.90
2.99
3.23
9.10
f1 (ppm)

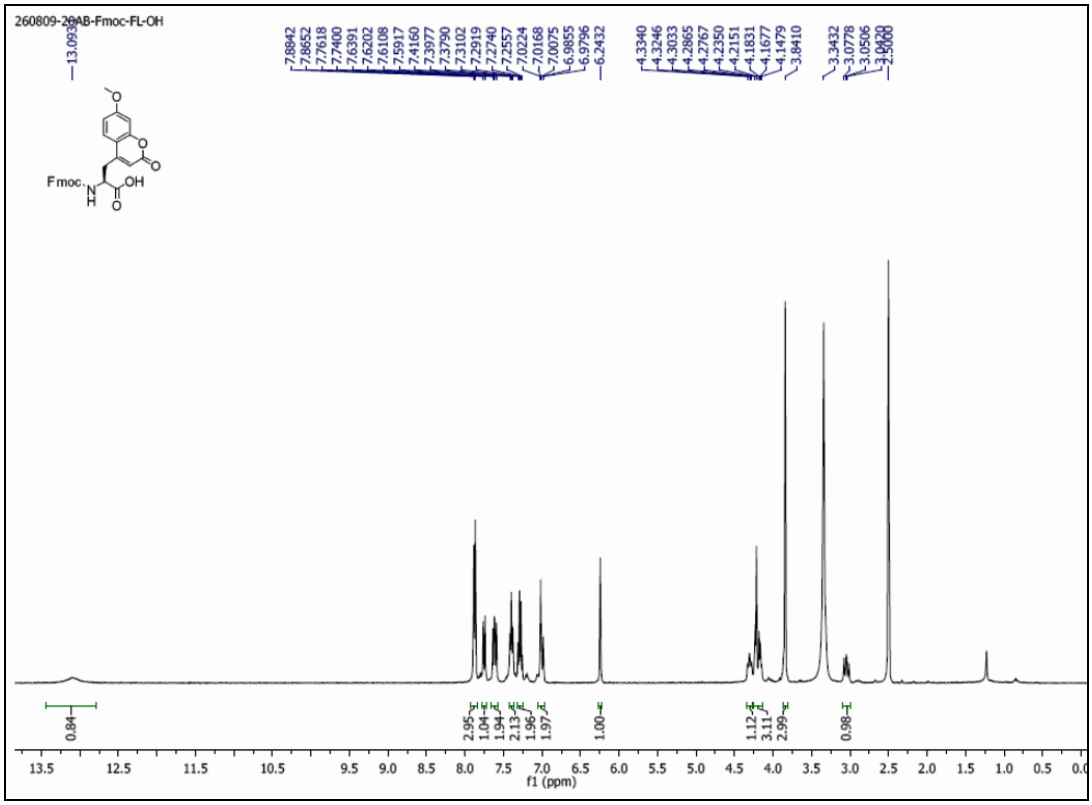
260809-2AB-Fmoc-FL-OH
13.0938
7.8842
7.8652
7.7618
7.7400
7.6391
7.6202
7.6108
7.5917
7.4160
7.3977
7.3790
7.3102
7.2919
7.2740
7.2557
7.0224
7.0168
7.0075
6.9855
6.9796
6.2432
4.3340
4.3246
4.3033
4.2865
4.2767
4.2350
4.2151
4.1831
4.1677
4.1479
3.8410
3.3432
3.0778
3.0506
Fmoc
OH
0.84
2.95
1.04
1.94
2.13
1.96
1.97
1.00
1.12
3.11
2.99
0.98
f1 (ppm)

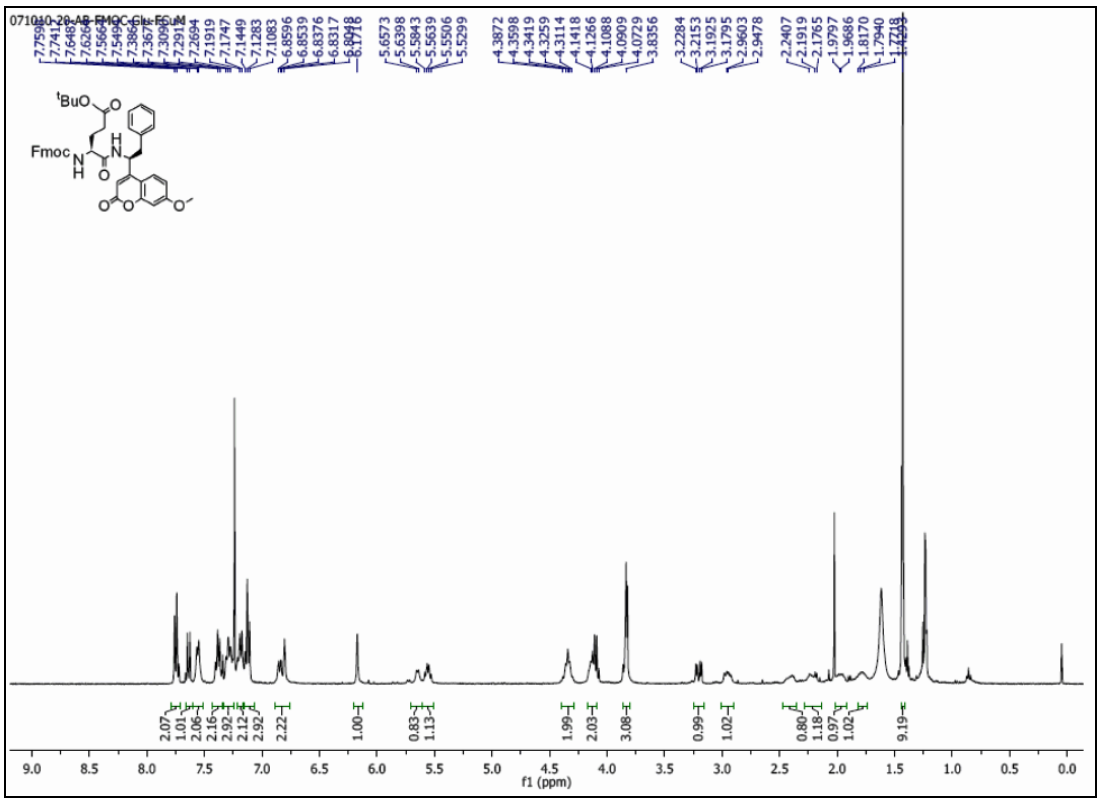
tBuO
Fmoc
N
H
O
f1 (ppm)

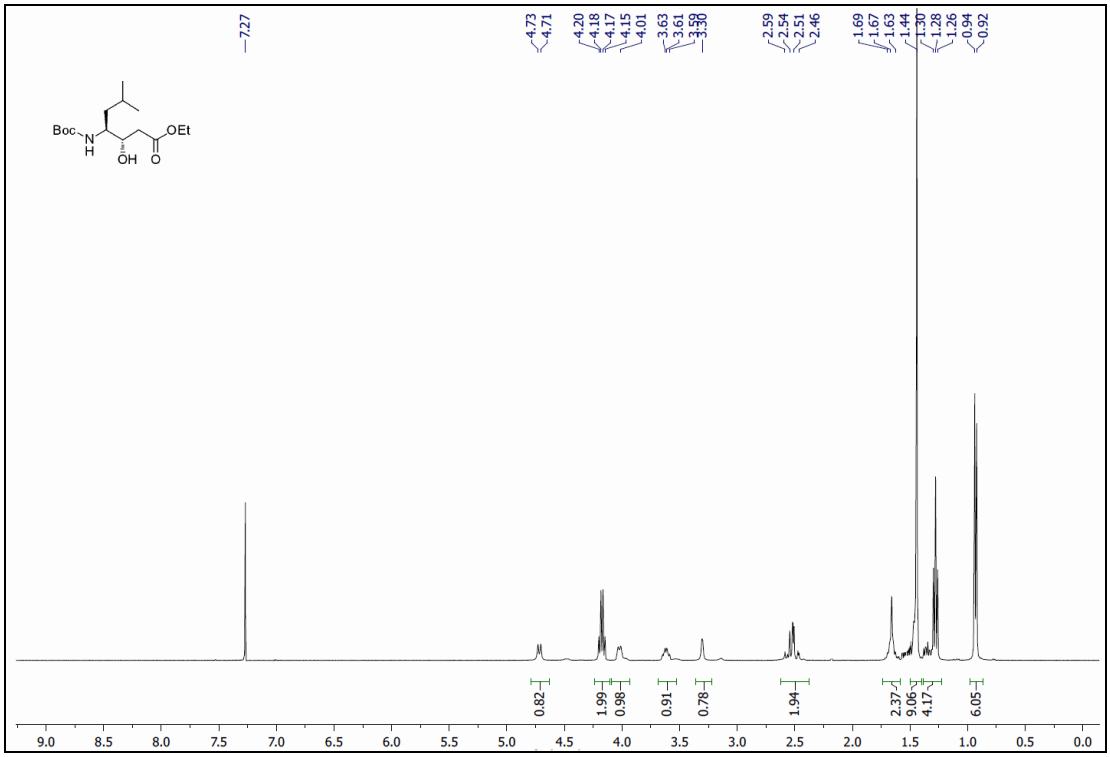
Boc
N
H
OH
OEt
O

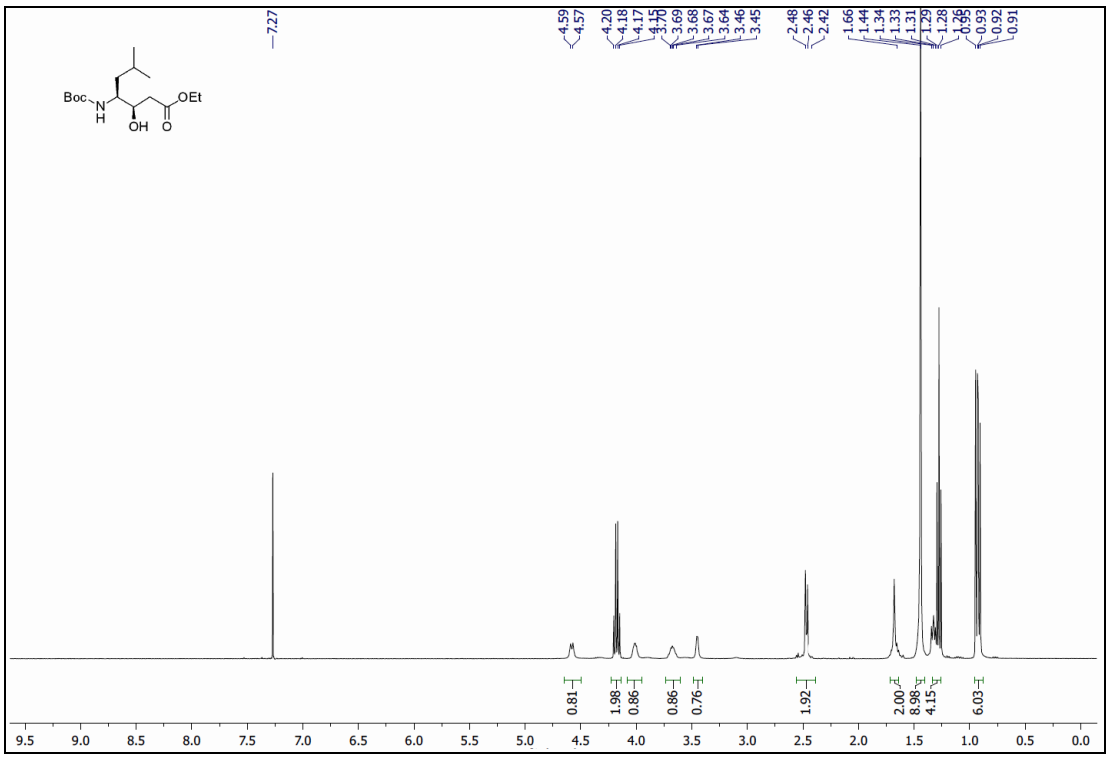
Boc
N
H
OH
O
OEt
7.27
4.59
4.57
4.20
4.18
4.17
4.15
3.70
3.69
3.68
3.67
3.64
3.46
3.45
2.48
2.46
2.42
1.66
1.44
1.34
1.33
1.31
1.29
1.28
0.95
0.93
0.92
0.91
0.81
1.98
0.86
0.86
0.76
1.92
2.00
8.98
4.15
6.03

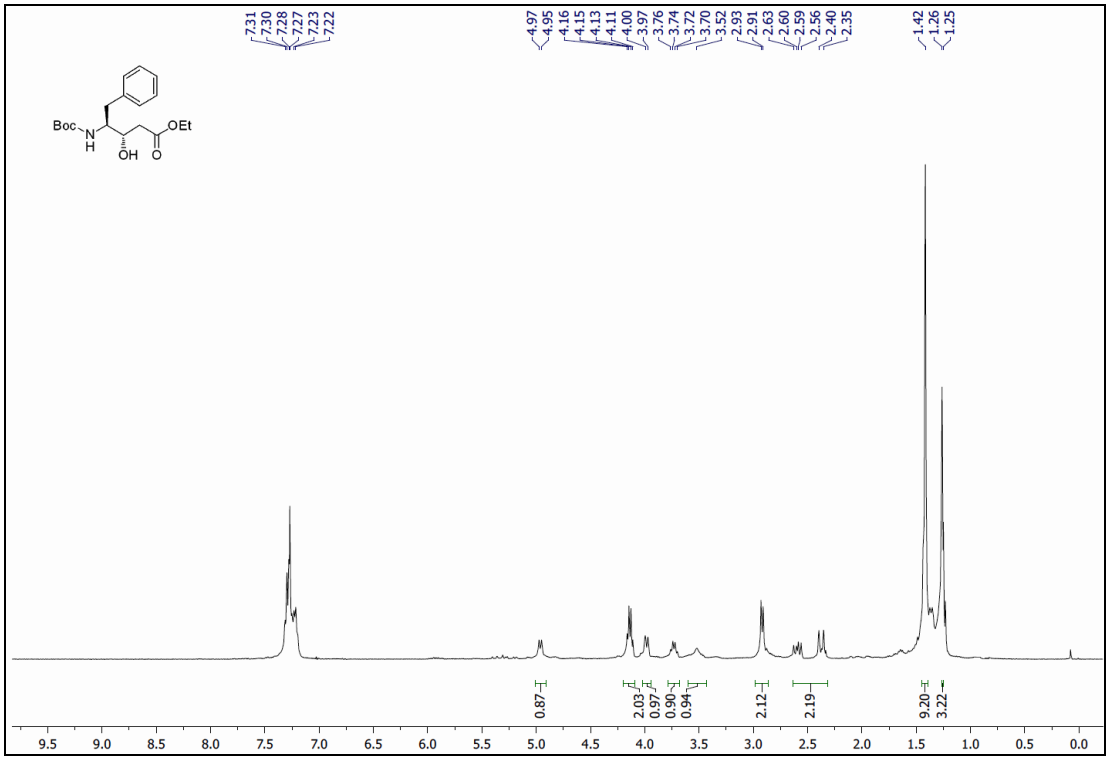
Boc
N
H
OH
O
OEt
7.31
7.30
7.28
7.27
7.23
7.22
4.97
4.95
4.16
4.15
4.13
4.11
4.00
3.97
3.76
3.74
3.72
3.70
3.52
2.93
2.91
2.63
2.60
2.59
2.56
2.40
2.35
1.42
1.26
1.25
0.87
2.03
0.97
0.90
0.94
2.12
2.19
9.20
3.22

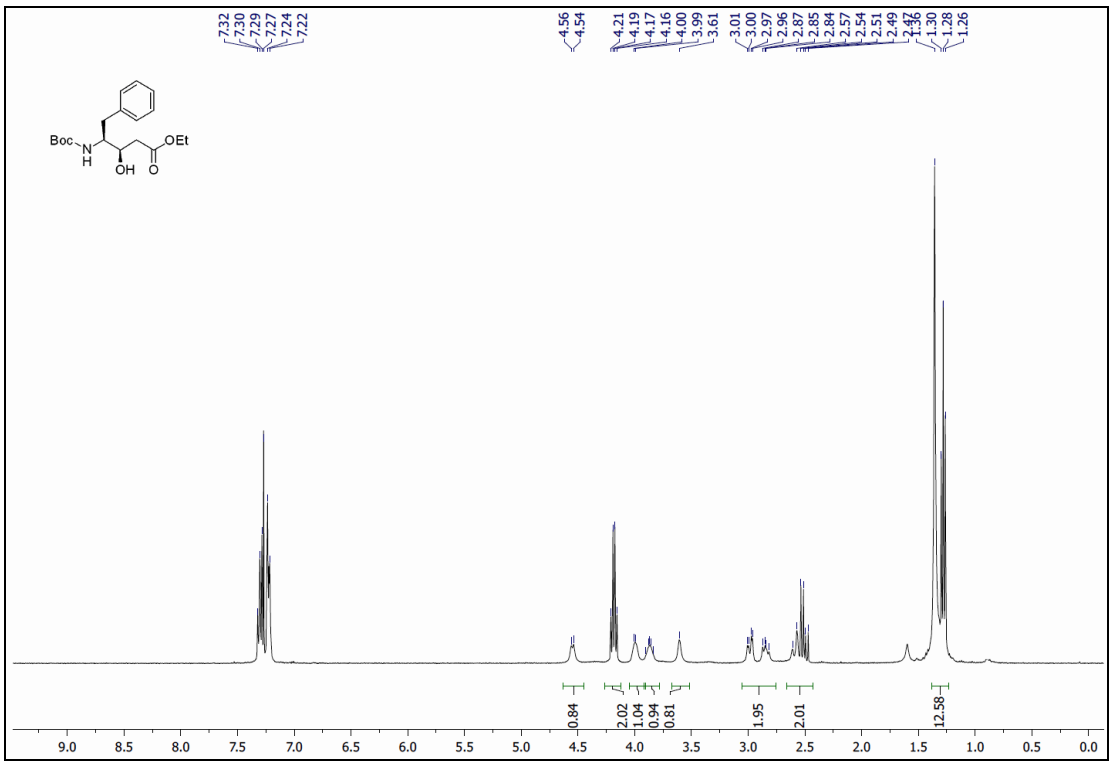
7.32
7.30
7.29
7.27
7.24
7.22
4.56
4.54
4.21
4.19
4.17
4.16
4.00
3.99
3.61
3.01
3.00
2.97
2.96
2.87
2.85
2.84
2.57
2.54
2.51
2.49
2.47
1.36
1.30
1.28
1.26
Boc
N
H
OH
O
OEt
0.84
2.02
1.04
0.94
0.81
1.95
2.01
12.58
9.0
8.5
8.0
7.5
7.0
6.5
6.0
5.5
5.0
4.5
4.0
3.5
3.0
2.5
2.0
1.5
1.0
0.5
0.0

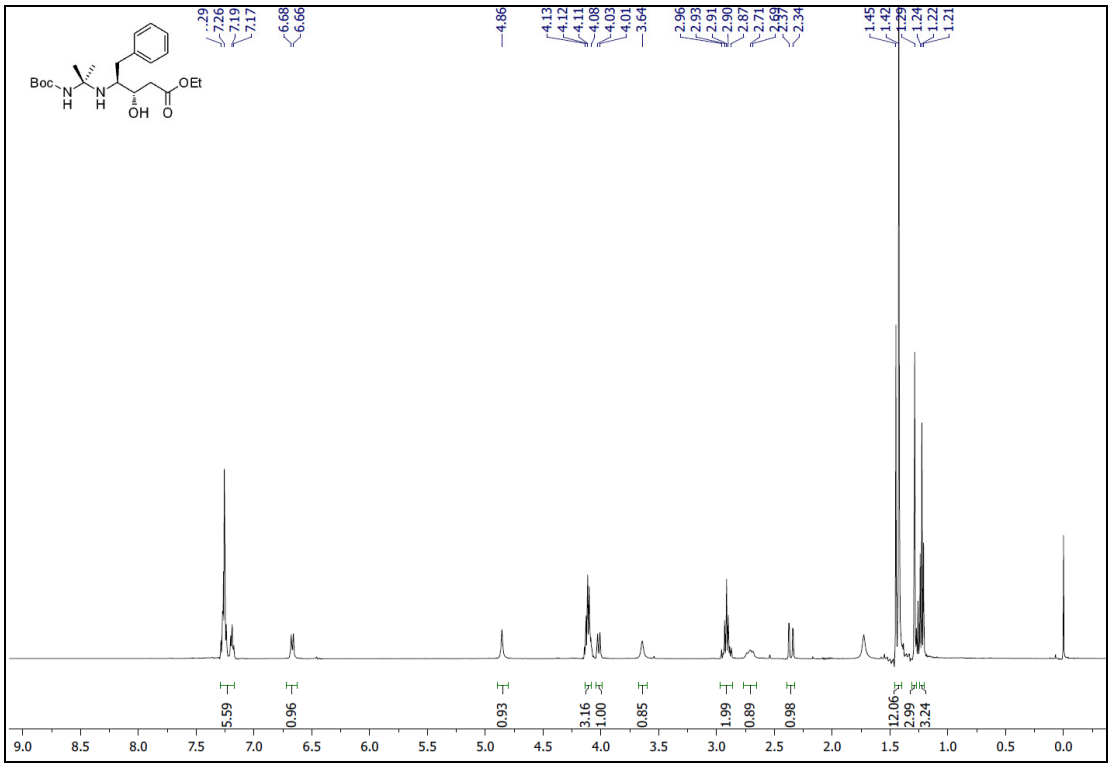
7.29
7.26
7.19
7.17
6.68
6.66
4.86
4.13
4.12
4.11
4.08
4.03
4.01
3.64
2.96
2.93
2.91
2.90
2.87
2.71
2.69
2.37
2.34
1.45
1.42
1.29
1.24
1.22
1.21
Boc
N
H
N
H
OH
O
OEt
5.59
0.96
0.93
3.16
1.00
0.85
1.99
0.89
0.98
12.06
2.99
3.24
9.0
8.5
8.0
7.5
7.0
6.5
6.0
5.5
5.0
4.5
4.0
3.5
3.0
2.5
2.0
1.5
1.0
0.5
0.0

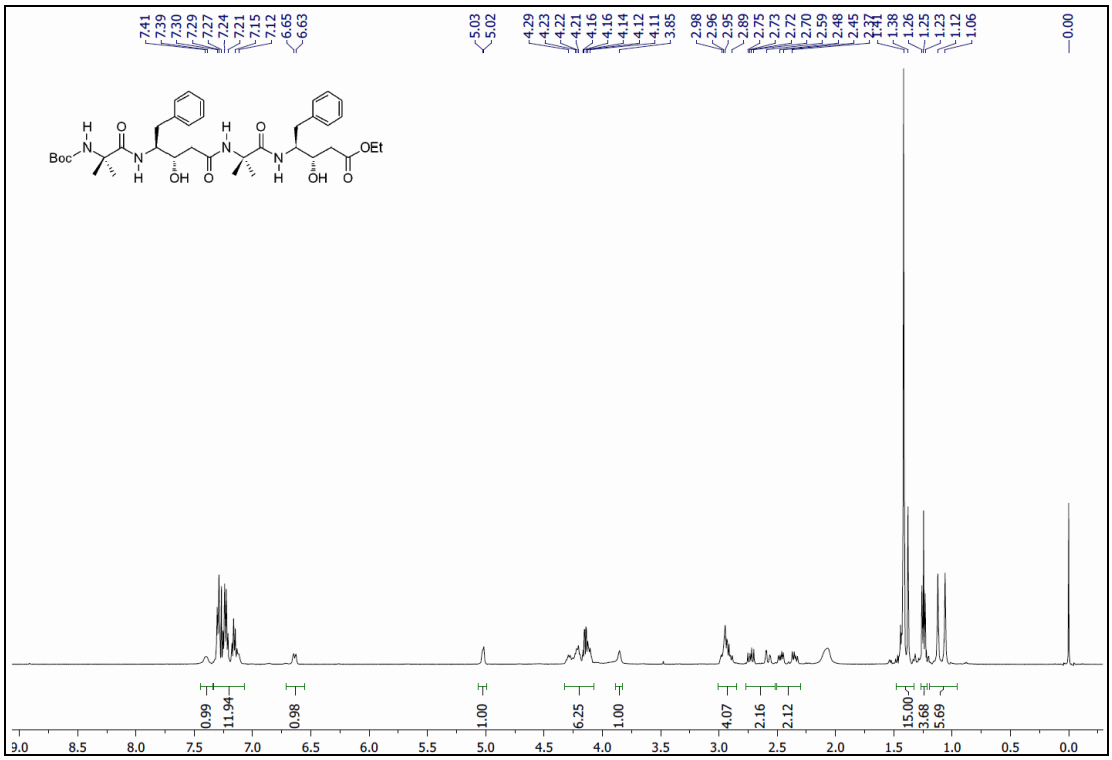
7.41
7.39
7.30
7.29
7.27
7.24
7.21
7.15
7.12
6.65
6.63
5.03
5.02
4.29
4.23
4.22
4.21
4.16
4.14
4.12
4.11
3.85
2.98
2.96
2.95
2.89
2.75
2.73
2.72
2.70
2.59
2.48
2.45
1.38
1.26
1.25
1.23
1.12
1.06
0.00
Boc
OEt
OH
0.99
11.94
0.98
1.00
6.25
1.00
4.07
2.16
2.12
15.00
3.68
5.69

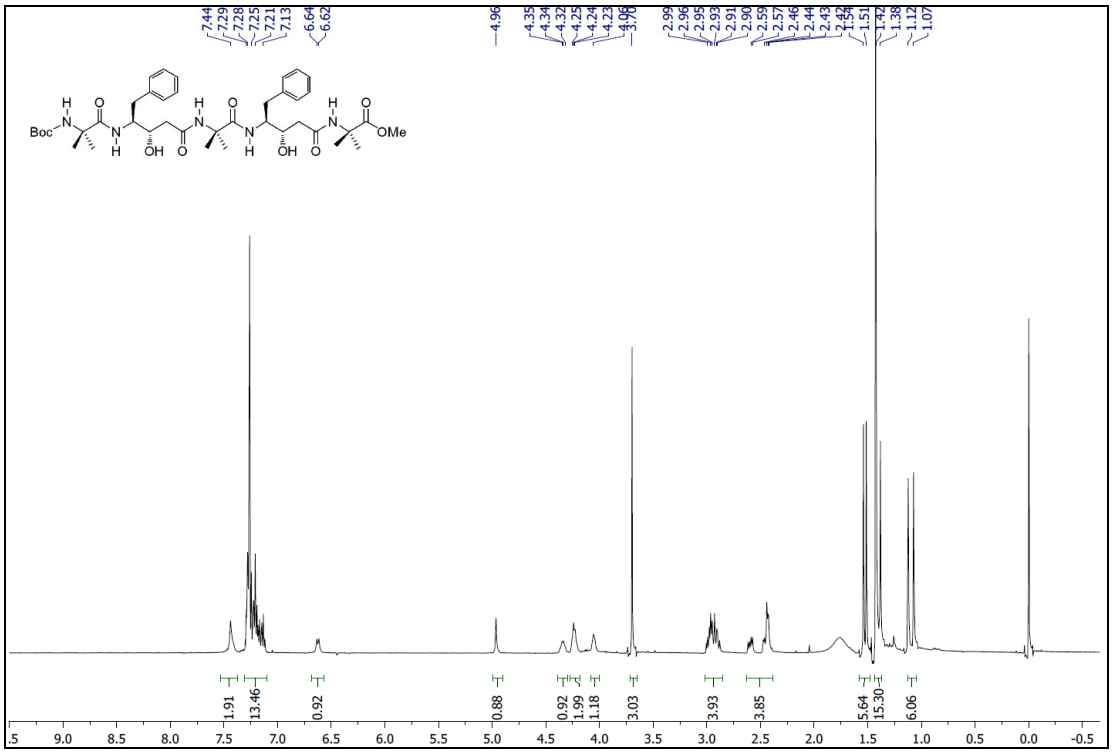
7.44
7.29
7.28
7.25
7.21
7.13
6.64
6.62
4.96
4.35
4.34
4.32
4.25
4.24
4.23
4.06
3.70
2.99
2.96
2.95
2.93
2.91
2.90
2.59
2.57
2.46
2.44
2.43
1.51
1.42
1.38
1.12
1.07
Boc
OMe
OH
1.91
13.46
0.92
0.88
0.92
1.99
1.18
3.03
3.93
3.85
5.64
15.30
6.06